ANNUAL REPORTS ON NMR SPECTROSCOPY

Volume 23

ANNUAL REPORTS ON

NMR SPECTROSCOPY

This Page Intentionally Left Blank

ANNUAL REPORTS ON

NMR SPECTROSCOPY

Edited by

G. A. WEBB

Department of Chemistry, University of Surrey, Guildford, Surrey, England

VOLUME 23

ACADEMIC PRESS

Harcourt Brace Jovanovich, Publishers

London • San Diego • New York
Boston • Sydney • Tokyo • Toronto

ACADEMIC PRESS LIMITED
24–28 Oval Road,
LONDON NW1 7DX

U.S. Edition Published by

ACADEMIC PRESS INC.
San Diego, CA 92101

This book is printed on acid free paper

Copyright © 1991 ACADEMIC PRESS LIMITED

All Rights Reserved

No part of this book may be reproduced or transmitted in any form or by any means, electronic or mechanical, including photocopying, recording, or any information storage and retrieval system without permission in writing from the publisher

A catalogue record for this book is available from the British Library.

ISBN 0-12-505323-1
ISSN 0066-4103

Phototypesetting by Thomson Press (I) Limited, New Delhi
Printed in Great Britain by St Edmundsbury Press Limited
Bury St Edmunds, Suffolk

List of Contributors

G. Binsch, *Institute of Organic Chemistry, University of Munich, Federal Republic of Germany.*

R. Garth Kidd, *Department of Chemistry, The University of Western Ontario, London, Ontario N6A 5B7, Canada.*

Jozef Kowalewski, *Division of Physical Chemistry, Arrhenius Laboratory, University of Stockholm, S-106 91 Stockholm, Sweden.*

B.E. Mann, *Department of Chemistry, The University, Sheffield S3 7HF, UK.*

Wolfgang Meiler, *Sektion Physik, Universität Leipzig, Linnestrasse 5, O-7010 Leipzig, Federal Republic of Germany.*

Reinhard Meusinger, *Sektion Physik, Universität Leipzig, Linnestrasse 5, O-7010 Leipzig, Federal Republic of Germany.*

William P. Power, *Department of Chemistry, Dalhousie University, Halifax, Nova Scotia B3H 4J3, Canada.*

S. Szymański, *Institute of Organic Chemistry, Polish Academy of Sciences, Warsaw, Poland.*

Roderick E. Wasylishen, *Department of Chemistry, Dalhousie University, Halifax, Nova Scotia B3H 4J3, Canada.*

This Page Intentionally Left Blank

Preface

In line with previous volumes in this series, Volume 23 of *Annual Reports on NMR Spectroscopy* consists of contributions from many scientific areas. Taken together they help to explain both the ever increasing popularity and the quiddity of NMR.

The topics in question relate to NMR studies of isolated spin pairs in the solid state, the oxidation-state dependence of transition metal shieldings, the Cinderella nuclei, permutation symmetry in NMR relaxation and exchange, nuclear spin relaxation in organic systems and solutions of macromolecules and aggregates and NMR of coals and coal products.

It is with great pleasure that I take this opportunity to express my sincere gratitude to the contributors for their understanding and cooperation during the preparation of this series of reports.

University of Surrey
Guildford

G.A. WEBB

This Page Intentionally Left Blank

Contents

The Cinderella Nuclei

B. E. MANN

Permutation Symmetry in NMR Relaxation and Exchange

S. SZYMAŃSKI and G. BINSCH

Nuclear Spin Relaxation in Diamagnetic Fields
Part 2. Organic Systems and Solutions of Macromolecules and Aggregates

JOZEF KOWALEWSKI

NMR of Coals and Coal Products

WOLFGANG MEILER and REINHARD MEUSINGER

This Page Intentionally Left Blank

NMR Studies of Isolated Spin Pairs in the Solid State

WILLIAM P. POWER and RODERICK E. WASYLISHEN*

Department of Chemistry, Dalhousie University, Halifax, Nova Scotia B3H 4J3, Canada

1. INTRODUCTION

One of the pioneering applications of NMR spectroscopy involved the determination of the hydrogen–hydrogen internuclear separation for the water molecules of hydration in $CaSO_4 \cdot 2H_2O$.[1] Pake was able to account for the orientation dependence of the ^{1}H NMR frequency in single crystals of $CaSO_4 \cdot 2H_2O$ by suggesting that the two hydrogen nuclei in a given water molecule interact via a magnetic dipole–dipole coupling. The local magnetic

ANNUAL REPORTS ON NMR SPECTROSCOPY
VOLUME 23 ISBN 0-12-505323-1

Copyright © 1991 Academic Press Limited
All rights of reproduction in any form reserved

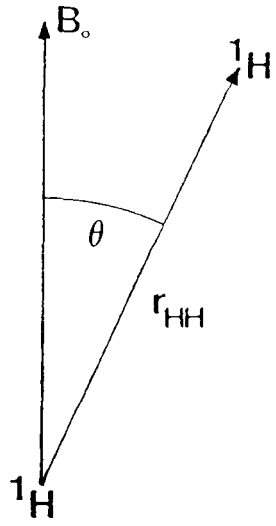

Fig. 1. The angle θ describes the orientation of the ^1H–^1H internuclear vector, $\mathbf{r}_{HH}$, in the applied magnetic field, $\mathbf{B}_0$.

field at one nucleus of the pair was described using the following equation,

$$B_{eff} = B_0 \pm \tfrac{3}{4}(\mu_0/4\pi)r_{HH}^{-3}\gamma_H\hbar(3\cos^2\theta - 1) \quad (1)$$

where γ_H is the magnetogyric ratio for hydrogen (protons), r_{HH} is the ^1H–^1H separation, and θ is the angle between the ^1H–^1H internuclear vector and the applied magnetic field, $\mathbf{B}_0$ (see Fig. 1). At any given orientation of the water proton–proton internuclear vector in $\mathbf{B}_0$, two ^1H NMR transitions are allowed. Analysis of the NMR single-crystal data indicated that the ^1H–^1H separation in each water of hydration was 1.58 Å. This was an important experimental result in 1948.

Pake also examined and analysed the ^1H NMR line shape of a powder sample of $CaSO_4 \cdot 2H_2O$. The observed line shape (Fig. 2) was explained by adding the intensities of the two allowed orientation-dependent transitions due to the intramolecular dipolar interaction over the spherical polar angles, θ and ϕ, that describe the orientation of the ^1H–^1H internuclear vector in $\mathbf{B}_0$. The line broadening of the observed powder spectrum resulted from dipolar interactions with protons in neighbouring water molecules. The success of Pake's experiment can in part be attributed to the presence of relatively isolated proton spin pairs in $CaSO_4 \cdot 2H_2O$.

Following Pake's study, ^1H NMR line shapes were calculated for triangular arrangements of nuclei which interact by the dipole–dipole interaction.[2] Nuclei at the apices of an equilateral triangle result in a more complex but

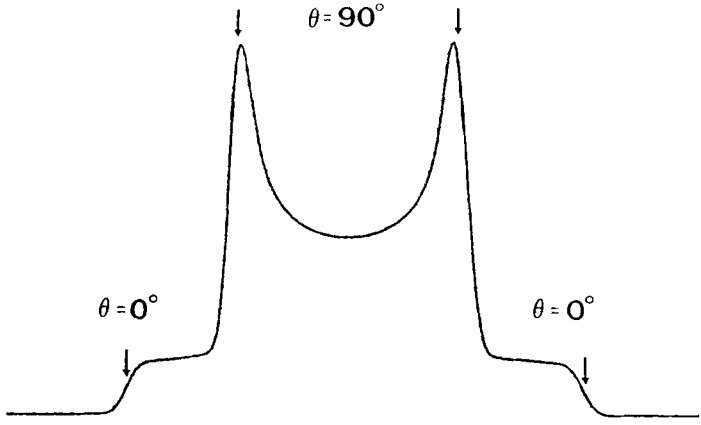

Fig. 2. The "Pake pattern" arising from dipolar coupling between two isolated spin-$\frac{1}{2}$ nuclei. The characteristic features of the powder line shape correspond to $\theta = 0°$ and $\theta = 90°$ orientations of the internuclear vector in $\mathbf{B}_0$.

symmetric NMR line shape that has a triplet structure when broadened. Such line shapes were observed for $HNO_3 \cdot H_2O$, $HClO_4 \cdot H_2O$ and $H_2SO_4 \cdot H_2O$, and provided evidence for the existence and structure of the hydronium ion (H_3O^+).[3] A tetrahedral arrangement of nuclei leads to a rather structureless powder line shape.[4–6] For systems containing four or more nuclei with more general arrangements, the calculation of the NMR line shape becomes exceedingly difficult. However, Van Vleck[7] showed that the moments of the powder pattern can be readily calculated, providing information similar to that obtained with exact line shape calculations. Powder ^1H NMR line shapes of the ammonium halides[8–11] and alkali metal borohydrides[12] yielded early estimates of the N–H and B–H bond lengths of 1.035 ± 0.01 Å and 1.255 ± 0.02 Å, respectively, in these salts.

In the 1950s, many simple systems in addition to those mentioned above were investigated using solid-state ^1H NMR and some specific questions were answered. For example, ^1H NMR was used to help distinguish between two proposed structures of diketene in the solid state.[13] In addition, the amino group in urea was found to be planar and not pyramidal.[14]

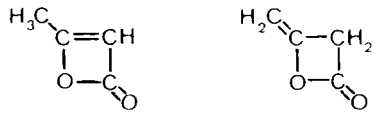

Early in the study of solids, it was recognized that ^1H dipolar NMR line shapes are narrowed by molecular motion.[15,16] During the 1950s and early

1960s, ^{1}H NMR was acknowledged as one of the most important techniques in characterizing molecular motion in solids. One of the points that became apparent from these studies was that if one was going to use dipolar NMR to obtain accurate structural information, it generally would be necessary to work at low temperature where motional averaging of the dipolar interactions would be minimal.[17] Also, in simple systems, such as salt hydrides, efforts were made to correct apparent dipolar splittings for averaging resulting from molecular vibrations and librations.[11,18,19]

Early applications of dipolar NMR have been summarized in a textbook by Andrew,[20] the first textbook devoted entirely to NMR spectroscopy. In addition, early reviews of the literature have been provided by Gutowsky[17] and Richards.[21] The importance of NMR in studying molecular motion in solids is nicely summarized in an important monograph by Parsonage and Stavely entitled *Disorder in Crystals*, published in 1978.[22] Also, Boden[23] has reviewed the applications of NMR in studying molecular motion in the plastic crystalline state.

Improvements in NMR instrumentation, the development of pulse Fourier-transform NMR[24,25] and techniques such as cross-polarization[26,27] made it possible to study rare or dilute spins such as ^{13}C in the solid state. In the 1970s, the most common solid-state NMR experiment for rare spins involved a transfer of magnetization from abundant spins (invariably ^{1}H) followed by high-power decoupling of the abundant spins during acquisition of the rare-spin spectrum. Under these conditions, experimentalists were able to characterize magnetic shielding parameters for rare spins from both single-crystal and powder samples. Shielding parameters obtained using these techniques have been summarized in a text by Mehring[27] and in several reviews.[28–34]

A rare spin, in the context of the above experiments, is defined as one in which homonuclear dipolar broadening is suppressed by magnetic dilution. For example, in the case of ^{13}C the natural abundance is only 1.1%; thus, in any given organic molecule, only a small fraction of these spins will have a neighbour that is also ^{13}C. It is important to recognize that, although the natural abundance of ^{31}P is 100%, broadening due to ^{31}P–^{31}P dipolar interactions is generally small unless two ^{31}P nuclei are directly bonded or in close proximity to one another. For example, two ^{31}P nuclei separated by more than 5 Å will have a homonuclear dipolar coupling constant of less than 160 Hz. We define the dipolar coupling constant, R, between two nuclei I and S in SI units (Hz) as $(\mu_0/4\pi)\gamma_I\gamma_S r_{IS}^{-3}(\hbar/2\pi)$, where γ_i denotes the magnetogyric ratio of each nucleus and r_{IS} is the internuclear separation.

The developments in the early 1970s made it possible to measure ^{13}C–^{14}N dipolar couplings in single crystals of the tetracyanoplatinate(II) anion[35] and glycine,[36] and in powders of acetonitrile.[37] Using single crystals of oxalic acid dihydrate and diammonium oxalate monohydrate doped with 2–5%

$^{13}C_2O_4^{2-}$, van Willigen *et al.*[38] were able to determine the ^{13}C–^{13}C dipolar tensor, and hence obtain the C–C bond lengths in these compounds from NMR spectra. In 1975 and 1976, separated local field (SLF) spectroscopy of ^{13}C nuclei in solids was introduced by Waugh and coworkers[39,40] to measure ^{13}C–^{1}H dipolar interactions. The two-dimensional character of this experiment displayed the ^{13}C–^{1}H dipolar spectrum along one axis and the ^{13}C shielding along the other axis.

The purpose of this chapter is to review the literature in which dipolar couplings in solid compounds are reported and comment on the information provided by these experiments. After a brief summary of the essential theoretical background, dipolar couplings in homonuclear spin pairs are discussed. This is followed by a section on heteronuclear spin pairs. The section on homonuclear spin pairs is by no means complete in that we do not discuss every paper in which abundant spin–abundant spin (e.g. ^{1}H–^{1}H and ^{19}F–^{19}F) dipolar interactions are reported. We have concentrated on systems which contain "isolated spin-pairs" such as ^{13}C–^{13}C, ^{15}N–^{15}N and ^{31}P–^{31}P. In general, the review focuses on literature published in the 1980s. Earlier work has been described in a number of texts and reviews, some of which we have already mentioned. Dipolar NMR experiments on solids have been discussed in two excellent monographs on solid-state NMR by Mehring[27] and Fyfe.[41] Some experimental aspects of solid-state NMR are described by Fukushima and Roeder,[42] Axelson[43] and Jelinski and Melchior.[44] Publications concerning the study of solids by NMR are reviewed annually in a publication of The Chemical Society (*Specialist Periodical Reports—Nuclear Magnetic Resonance*, edited by G. A. Webb). We have not reviewed the literature dealing with NMR studies of liquid-crystal systems; again, this topic is reviewed biennially in the *Specialist Periodical Reports—Nuclear Magnetic Resonance.*

2. BACKGROUND THEORY

2.1. Introduction

Most of the experimental NMR studies described in this review have involved observation of spin-$\frac{1}{2}$ nuclei in a strong magnetic field. Typically, the spin-$\frac{1}{2}$ nucleus is dipolar coupled to at least one other nucleus of spin I. If the second nucleus is a spin-$\frac{1}{2}$ nucleus and also has the same magnetogyric ratio, the spin pair is known as a homonuclear spin pair. If the two spin-$\frac{1}{2}$ nuclei have different magnetogyric ratios, they form a heteronuclear spin pair. In addition to being coupled by the direct dipolar interaction, the two spins in a spin pair may be coupled by an indirect spin–spin coupling interaction, J coupling.

Furthermore, the magnetic field at each nucleus will be modified by fields arising from the motion of surrounding electrons, a phenomenon known as chemical shielding. Thus, in general, it will be sufficient to express the Hamiltonian of a spin-$\frac{1}{2}$ nucleus in an isolated spin pair I–S as the following sum,

$$H = H_Z + H_{rf} + H_\sigma + H_D^{IS} + H_J^{IS} \tag{2}$$

where the subscripts denote the relevant interactions: Z, Zeeman; rf, radiofrequency pulse; σ, chemical shielding; D, direct dipolar coupling; and J, indirect spin–spin coupling. In general, we maintain the convention that S is a dilute or rare nucleus, often the one under observation, and I denotes the nucleus, often abundant, which is the other member of the spin pair. The fact that NMR measurements are carried out in strong magnetic fields ensures that the various interactions in (2) are only perturbations to the dominant Zeeman term. In heteronuclear spin systems, the high-field approximation may not be strictly valid if the I spin is a quadrupolar nucleus, particularly if the magnitude of the I spin quadrupolar coupling constant, $\chi(I)$, is comparable with or greater than its Larmor frequency, $\nu_0(I)$.

2.2. The NMR interactions

We now briefly outline the important features of each of the interactions described in (2). For completeness, the quadrupolar interaction is also included. There are many treatments available that are more detailed and quite varied in approach, and we refer here to a comprehensive, though certainly not exhaustive, set of monographs by Abragam,[45] Haeberlen,[46] Slichter,[47] Spiess,[34] Mehring,[27] Gerstein and Dybowski,[48] Ernst *et al.*[49] and Munowitz,[50] as well as to reviews by Taylor *et al.*,[51] Vaughan,[52] Duncan and Dybowski[53] and Gerstein.[54]

2.2.1. The Zeeman interaction

In the presence of a strong magnetic field, a nucleus possessing spin ($I > 0$) will be in one of $2I + 1$ equally spaced energy levels. Transitions between these levels are the basis of the NMR experiment. The energy difference between levels depends on the magnetic moment of the nucleus, $\boldsymbol{\mu}$, and the external magnetic field, $\mathbf{B}_0$,

$$H_Z = -\hbar^{-1}\boldsymbol{\mu}\cdot\mathbf{B}_0 = -\gamma_n\mathbf{B}_0\cdot\mathbf{I}$$

where γ_n is the characteristic magnetogyric ratio for a nuclear isotope, n, and $\mathbf{I}$ is the nuclear spin. The magnetic-field vector, $\mathbf{B}_0$, is usually chosen such

that it lies along the z axis of the laboratory frame, i.e. $\mathbf{B}_0 = (0, 0, B_0)$. This allows one to express the nuclear spin $\mathbf{I}$ in terms of I_z, the component along its axis of quantization, the magnetic field. The frequency of a pure Zeeman transition is called the Larmor frequency, and is given by

$$\nu_0 = \gamma_n B_0 / 2\pi \tag{4}$$

where ν_0 is in Hz.

2.2.2. *The radiofrequency interaction*

Transitions between the Zeeman energy levels are usually induced by radiofrequency (rf) fields, B_{rf}, applied perpendicular to the magnetic field direction, taken as the x direction of the laboratory frame. It is a time-dependent field,

$$\mathbf{B}_{rf}(t) = ([B_1(t) \cos \omega t], 0, 0) \tag{5}$$

where B_1 is the amplitude of the radiofrequency field and $\omega/2\pi$ is the carrier frequency. The nuclear spin interacts with the radiofrequency field in a similar fashion as it does with the static magnetic field, i.e.

$$H_{rf} = -\gamma_n \mathbf{B}_{rf} \cdot \mathbf{I} \tag{6}$$

2.2.3. *The chemical shielding interaction*

As mentioned in Section 2.1, the motion of electrons in a molecule generates magnetic fields which modify the applied field, B_0, at a nucleus. The induced fields are proportional to the strength of the external field and they generally shield the nucleus from the applied field,

$$H_\sigma = \gamma_n \mathbf{I} \cdot \boldsymbol{\sigma} \cdot \mathbf{B}_0 \tag{7}$$

where $\boldsymbol{\sigma}$ is the chemical shielding tensor of the observed nucleus. This tensor describes the three-dimensional nature of the electronic "screening" of the nucleus, which in general will vary with the orientation of the molecule in the magnetic field. In practice, only the symmetric part of the shielding tensor contributes to the NMR spectrum.[46] In its principal-axis system (PAS), the diagonalized tensor is described by three orthogonal principal components, σ_{11}, σ_{22} and σ_{33}, designating the directions of least, intermediate and greatest shielding, respectively. The values of these shielding components are absolute values with respect to the bare nucleus. In NMR, it is common to observe signals with respect to that of a reference, where the difference between the sample and the reference signals is called the chemical shift, symbolized by δ and expressed in units of parts per million (ppm), as

$$\delta_{sample} = 10^6(\nu_{sample} - \nu_{ref})/\nu_{ref} \simeq 10^6(\sigma_{ref} - \sigma_{sample}) \tag{8}$$

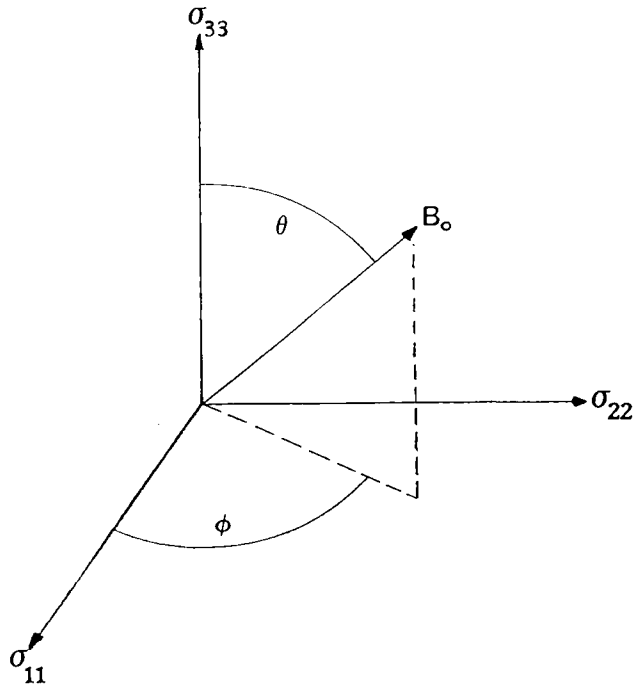

Fig. 3. The orientation dependence of the chemical shielding is described by the angles θ and ϕ according to (9).

The principal components of $\boldsymbol{\sigma}$ can also be expressed as chemical shifts, with δ_{11}, δ_{22} and δ_{33} corresponding to σ_{11}, σ_{22} and σ_{33}, respectively. It is important to recognize the difference between absolute chemical shielding and relative chemical-shift values; this distinction is preserved throughout this review.

In a solid, the chemical shielding experienced by a particular nucleus varies with the orientation of the molecule in the magnetic field B_0, according to

$$\nu_\sigma = \nu_0[1 - (\sigma_{11}\sin^2\theta\cos^2\phi + \sigma_{22}\sin^2\theta\sin^2\phi + \sigma_{33}\cos^2\theta)] \qquad (9)$$

where θ and ϕ are the polar and azimuthal angles orienting the applied magnetic field direction in the principal-axis system of the chemical-shielding tensor, as shown in Fig. 3. In a single crystal, this leads to a variation in the chemical shift of a nucleus as a function of orientation of the crystal in the magnetic field. In a powder, all possible orientations of the molecule contribute to the observed signal, and a powder line shape results, with limits marked by inflection points at δ_{11} and δ_{33} and a discontinuity at δ_{22}. Examples of axially symmetric and nonaxially symmetric chemical shift

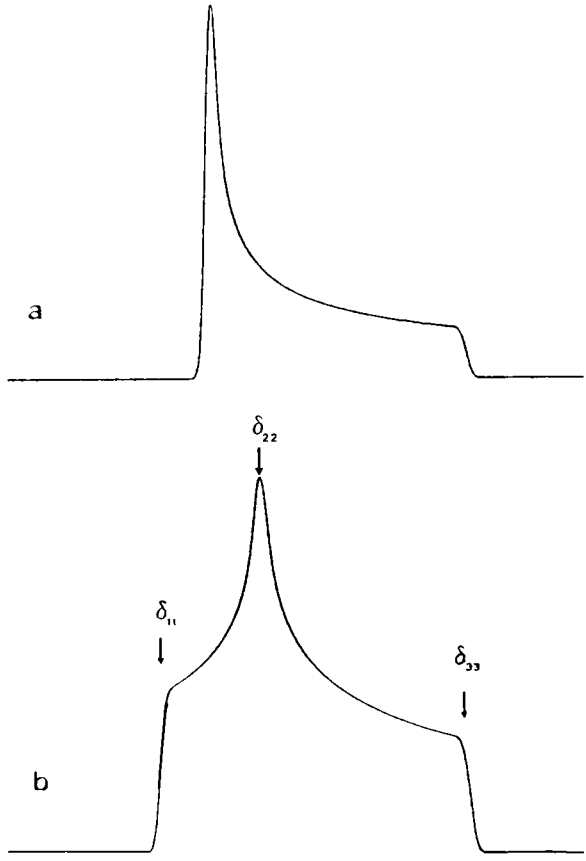

Fig. 4. Powder line shapes due to anisotropic chemical shift for (a) axial symmetry ($\eta_\sigma = 0$), and (b) nonaxial symmetry ($\eta_\sigma = 0.6$ in this example).

powder patterns are given in Fig. 4. In high-resolution NMR experiments, where the chemical-shift tensor is often averaged by rapid magic angle spinning (MAS), all anisotropic information is generally lost and only the isotropic average, δ_{iso}, is measured, where $\delta_{iso} = (\delta_{11} + \delta_{22} + \delta_{33})/3$. The width of the static powder line shape is called the chemical-shielding anisotropy, $\Delta\sigma = \delta_{11} - \delta_{33}$, and the asymmetry parameter, η_σ, denotes the departure from axial symmetry in a range from 0 to 1. For the case of nonaxial symmetry, more elaborate definitions of these parameters are available elsewhere.[29,34,46]

2.2.4. The direct dipolar interaction

This is the through-space coupling of two nuclear spins I and S. It can be

expressed as

$$H_D = \gamma_I \gamma_S \hbar^2 r^{-3}[\mathbf{I}\cdot\mathbf{S} - 3(\mathbf{I}\cdot\mathbf{r})(\mathbf{S}\cdot\mathbf{r})r^{-2}](\mu_0/4\pi) \tag{10}$$

where **I** and S may be like or unlike spins. The Hamiltonian may be expressed in polar coordinates as a sum of six terms, the so-called "dipolar alphabet",

$$H_D = \gamma_I \gamma_S \hbar^2 r^{-3}[A + B + C + D + E + F](\mu_0/4\pi) \tag{11}$$

where

$$A = -I_z S_z (3\cos^2\theta - 1)$$

$$B = (1/4)[I_+ S_- + I_- S_+](3\cos^2\theta - 1)$$

$$C = -(3/2)[I_z S_+ + I_+ S_z]\sin\theta\cos\theta\exp(-i\phi)$$

$$D = -(3/2)[I_z S_- + I_- S_z]\sin\theta\cos\theta\exp(i\phi)$$

$$E = -(3/4) I_+ S_+ \sin^2\theta\exp(-2i\phi)$$

$$F = -(3/4) I_- S_- \sin^2\theta\exp(2i\phi)$$

For heteronuclear spin pairs, normally only term A contributes to the observed spectra, while both terms A and B contribute to the spectra of homonuclear spin pairs, due to the "flip-flop" operator in term B. Consequently, the equations describing the resonance frequencies for dipolar coupled spins are different for hetero- and homo-nuclear cases. For two isolated spin-$\frac{1}{2}$ nuclei, the dipolar interaction leads to an orientation-dependent splitting,

$$\nu_D(\text{hetero}) = \nu_0 \pm \tfrac{1}{2} R(3\cos^2\theta - 1) \tag{12a}$$

$$\nu_D(\text{homo}) = \nu_0 \pm \tfrac{3}{4} R(3\cos^2\theta - 1) \tag{12b}$$

where θ is the angle between the I–S internuclear vector **r** and the magnetic field direction, and R is the dipolar coupling constant, expressed in SI units as

$$R = [(\gamma_I \gamma_S \hbar)/(2\pi)]\langle r_{IS}^{-3}\rangle(\mu_0/4\pi) \tag{12c}$$

Typical values of R are given in Table 1. When a spin-$\frac{1}{2}$ nucleus is coupled to a quadrupolar nucleus with spin I, there are $2I + 1$ transitions which arise due to the possible values of m_I. The frequency of each transition is given by

$$\nu_D(\text{hetero}) = \nu_0 + m_I R(3\cos^2\theta - 1) \tag{12d}$$

In a powder sample, the dipolar NMR spectrum of an isolated spin pair will appear as a characteristic "Pake doublet" (Fig. 2). In the case of a heteronuclear spin pair, the splitting between the discontinuities is R ($\theta = 90°$) and between the outer shoulders is $2R$ ($\theta = 0°$). For homonuclear systems containing a magnetically equivalent spin pair, the corresponding splittings are $3R/2$ and $3R$, respectively. For an AB spin system, where the two coupled

Table 1. Direct dipolar coupling constants for various isolated spin pairs, based on the typical internuclear separations indicated.

Spin pair	Example	Separation (Å)	R (kHz)
^{1}H–^{1}H	H_2O	1.51	34.888
^{2}H–^{1}H	HDO	1.51	5.356
^{2}H–^{2}H	D_2O	1.51	0.822
^{31}P–^{1}H	P–H bond length	1.41	17.365
^{31}P–^{2}H	P–H bond length	1.41	2.666
^{31}P–^{13}C	P–C single bond	1.85	1.934
^{31}P–^{35}Cl	P–Cl bond length	2.04	0.562
^{31}P–^{63}Cu	P–Cu bond length	2.30	1.061
^{31}P–^{103}Rh	P–Rh bond length	2.32	0.123
^{13}C–^{1}H	C–H bond length	1.09	23.328
^{13}C–^{2}H	C–H bond length	1.09	5.681
^{13}C–^{13}C	C–C single bond	1.54	2.080
^{13}C–^{13}C	C–C double bond	1.34	3.158
^{13}C–^{14}N	C–N peptide bond	1.32	0.949
^{13}C–^{15}N	C–N peptide bond	1.32	1.332
^{13}C–^{19}F	C–F bond length	1.38	10.820
^{13}C–^{35}Cl	C–Cl bond length	1.77	0.534
^{15}N–^{1}H	N–H bond length	1.01	11.819

nuclei are like spins but are not magnetically equivalent, the situation is more complex.[38,55] The four observed transitions are not split according to the limits given above, but are somewhere in between, depending on the degree of mixing of the spin states. Such mixing will occur whenever the difference in resonance frequencies for the two nuclei is on the order of, or smaller than, the strength of the coupling between them.

The dipolar interaction is directed along the internuclear vector, **r**, and, in the absence of oriented librations, is both axially symmetric (C_{∞} symmetry) and traceless. Therefore, the value of R is sufficient to describe the dipolar coupling completely. Note that R depends on the separation between the two nuclei; in principle, measurement of R can provide internuclear distances. The observed dipolar coupling vanishes whenever the internuclear vector is undergoing rapid isotropic motion. Averaging of the dipolar interaction can also be accomplished in spin space.

2.2.5. The indirect spin–spin interaction

This interaction involves a coupling between two nuclear spins, mediated by the electronic environment between the nuclei, rather than behaving as a

through-space interaction. It can be expressed as

$$H_J = \mathbf{I}\cdot\mathbf{J}\cdot\mathbf{S} \tag{13}$$

where **J** is the indirect spin–spin coupling tensor. This tensor describes the variation in the indirect spin–spin coupling with the orientation of the molecule in the magnetic field. In solution, only the isotropic average, J_{iso}, is observed. In principle, one can measure both the anisotropy and asymmetry of the **J** tensor in rigid solids. However, the anisotropy, ΔJ, transforms similarly to the direct dipolar coupling, thus, the two interactions cannot be easily separated via experiment. In practice, this leads to an effective dipolar coupling constant, R_{eff},

$$R_{eff} = R - \Delta J/3 \tag{14}$$

where $\Delta J = J_{\parallel} - J_{\perp}$, assuming that **J** is axially symmetric, with $J_{\parallel}$ designating the component oriented along the internuclear vector and $J_{\perp}$ the component that is perpendicular. This characteristic can complicate the interpretation of dipolar spectra, leading to erroneous results for internuclear separations derived from the observed dipolar splitting. Reliable experimental values of ΔJ are scarce in the literature; however, for any given spin pair, theoretical calculations indicate that the magnitude of ΔJ is of the same order of magnitude as, or smaller than, values for J_{iso}.[56] Furthermore, on the basis of calculations, the anisotropy in J is predicted to become more important for coupling constants involving heavier nuclei.[57]

2.2.6. The quadrupolar interaction

This interaction is important for all nuclei possessing a nuclear quadrupole moment, i.e. all nuclei with nuclear spin $I > \frac{1}{2}$. It is an electrostatic interaction between the quadrupole moment, eQ, and the electric-field gradient (EFG) at the nucleus, and is described by

$$H_Q = eQ\mathbf{I}\cdot\mathbf{V}\cdot\mathbf{I}/[6I(2I-1)] \tag{15}$$

where **I** and **V** are the nuclear spin vector and EFG tensor, respectively. The principal components of **V** ($V_{ii} = eq_{ii}$, $i = 1,2,3$) are defined such that $|V_{33}| \geq |V_{11}| \geq |V_{22}|$. The EFG tensor is traceless; therefore, the quadrupolar interaction is not observed directly in solution. The strength of this interaction is usually expressed in terms of the quadrupolar coupling constant, χ, where $\chi = e^2Qq_{33}/h$ (in Hz), and the magnitudes of the minor components are expressed via the asymmetry parameter, $\eta_Q = (V_{22} - V_{11})/V_{33}$. The orientation dependence of the quadrupolar interaction leads to a perturbation of the NMR transition of the quadrupolar nucleus, which, to first order, is given by

$$\nu_Q = [3\chi(m_I - \tfrac{1}{2})/4I(2I-1)][(3\cos^2\theta - 1) - \eta_Q \sin^2\theta \cos 2\phi] \tag{16}$$

where m_I is the spin state of the quadrupolar nucleus which can vary from $+I$ to $-I+1$, and θ and ϕ are the angles orienting the magnetic-field vector in the EFG tensor frame.

Equation (16) is only valid in the high-field limit, where $H_Z \gg H_Q$. If this condition is not satisfied, the axis of quantization for the quadrupolar nucleus will be tipped away from B_0. In such cases, the eigenfunctions for the quadrupolar nucleus become linear combinations of the pure Zeeman states, and the dipolar interaction between a spin-$\frac{1}{2}$ nucleus and a quadrupolar nucleus is no longer given by the simple truncated heteronuclear dipolar Hamiltonian; that is, terms of the dipolar alphabet other than term A contribute to the observed dipolar splitting.

2.3. Separation of internal Hamiltonians

When characterizing a system using NMR, one would like to be able to separate the various interactions that influence the NMR spectrum. A variety of "tricks" have been developed that allow the effects of these interactions to be turned "on" and "off". This possibility is contained in the different spatial, spin and field dependencies of the interactions acting on the nucleus, given in Table 2. Rapid magic angle spinning (MAS) can be used to obtain high-resolution spectra of solids, by removing the effects of the anisotropic terms.[58] These terms, in general, have a $(3\cos^2\theta - 1)$ dependence; the so-called magic angle, $\theta_m = 54.74°$, is that angle for which $(3\cos^2\theta - 1)$ equals zero. In practice, MAS is accomplished by spinning the sample about an axis inclined at $\cos^{-1}(1/\sqrt{3})$ with respect to the magnetic field. Manipulation in spin space can also be performed. Foremost among these techniques is homonuclear multiple-pulse decoupling,[27,46] such as WAHUHA,[59] where coupling between like nuclei is suppressed while chemical shift and heteronuclear coupling interactions remain, albeit scaled. This has been particularly useful in the NMR study of abundant spins in solids.[46] A variety of pulse sequences have been developed to suppress or eliminate the effect of the different interactions, a representative sample of which is included in Fig. 5, and will be discussed in more detail later.

It is obvious that the experimentalist has some control over the Hamiltonians which govern the system under observation. The effects of the interactions can be tailored to act separately, simultaneously, and even consecutively by applying the principles of two-dimensional NMR spectroscopy.[49] The latter technique is particularly advantageous as it allows the effects of the different interactions to be simultaneously resolved from, and related to, each other via the two-dimensional spectrum. This highly informative approach has been widely used in the study of solids by NMR,

Table 2. The NMR interactions arising from local fields and their various spatial, spin and field dependencies.

Interaction	Isotropic average	Spatial dependence	Spin dependence	Field Dependence
Chemical shift	$\delta_{iso}, \sigma_{iso}$	$\Delta\sigma[(3\cos^2\theta - 1) + \eta_\sigma \sin^2\theta \cos 2\phi]$	S_z	Linear
Homonuclear dipolar	0	$(3R/2)(3\cos^2\theta - 1)$	$3I_zS_z - \mathbf{I}\cdot\mathbf{S}$	None
Heteronuclear dipolar	0	$R(3\cos^2\theta - 1)$	I_zS_z	None
Indirect spin–spin	J_{iso}	$\Delta J(3\cos^2\theta - 1)$	$3I_zS_z - \mathbf{I}\cdot\mathbf{S}$ (homo) I_zS_z (hetero)	None
Quadrupolar	0	$[\chi/2I(2I-1)][(3\cos^2\theta - 1) - \eta_Q \sin^2\theta \cos 2\phi]$	$3S_z^2 - \mathbf{S}^2 + \eta(S_x^2 - S_y^2)$	None

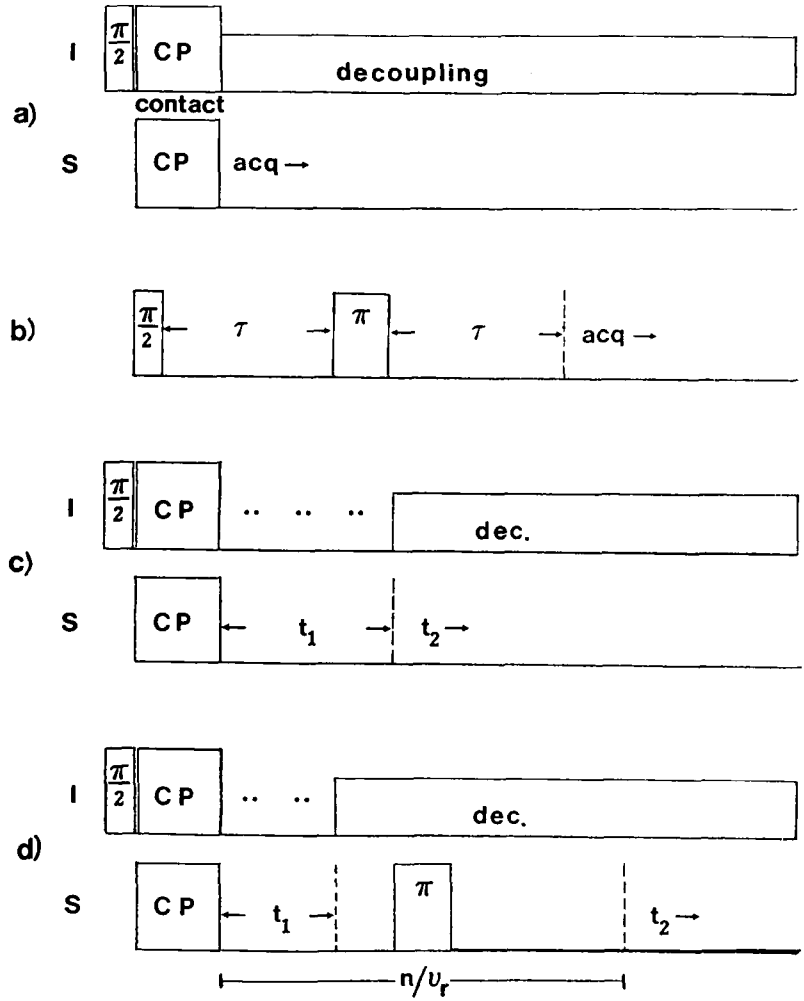

Fig. 5. Some basic NMR pulse sequences for acquiring spectra of nuclei that are members of isolated spin pairs. The relative phases of the pulses are omitted for convenience; the interested reader should consult the original literature. (a) Standard cross-polarization sequence, transferring polarization from abundant I spins to rare S spins. (b) Spin-echo sequence, where S spin interactions linear in the spin operator S_z (e.g. chemical shifts and heteronuclear couplings) are refocused at 2τ. (c) Typical SLF sequence. The evolution period t_1 may or may not include homonuclear I spin multiple-pulse decoupling, designated by "··". (d) MAS/SLF sequence. Note that the experiment is timed such that anisotropic and isotropic chemical shift evolution is refocused at $t_2 = 0$, by beginning t_2 at the peak of simultaneous rotational and spin echoes.

including isolated spin-pair systems, as will become evident in this review.

In dipolar NMR studies, it is advantageous to work with an "isolated" spin pair. For example, if one is studying a heteronuclear spin pair, I–S, it is important to ensure that the influence of H_D^{II} and H_D^{SS} are minimal. Also, if a third spin is present in the sample, e.g. ^1H, it is important to remove dipolar couplings to this spin. Dipolar couplings to abundant spins such as ^1H and ^{19}F are generally removed by high-power decoupling. The Hamiltonians H_D^{II} and H_D^{SS} can be suppressed by dilution of the I–S spin pair in unenriched samples of the compound of interest or by matrix-isolation techniques. In addition to the above techniques, several others have been devised to isolate the spin pair; these methods are discussed later in this chapter.

2.4. NMR response for isolated spin-pairs

For an isolated spin pair involving first-row elements, it is usually sufficient to consider only H_Z, H_σ and H_D^{IS} in (2). Under these conditions, the orientation-dependent NMR response is described by

$$\begin{aligned} \nu(\theta,\phi) &= \nu_0 - \nu_\sigma - m_I \nu_D \\ &= (\gamma_S B_0/2\pi)[1 - (\sigma_{11}\sin^2\theta\cos^2\phi + \sigma_{22}\sin^2\theta\sin^2\phi + \sigma_{33}\cos^2\theta)] \\ &\quad - m_I R(3\cos^2\theta - 1) \end{aligned} \tag{17}$$

where ν_0, ν_σ and ν_D are defined in (4), (9) and (12d), with $m_I = -I, -I+1, \ldots, +I$. Examples of line shapes due to chemical shielding and dipolar coupling for an isolated pair of spin $-\frac{1}{2}$ nuclei are shown in Fig. 6. However, the orientation dependence of ν_σ may not be the same as that of ν_D, i.e. they may not be defined in the same axis system. This would make a simple superposition of the two spectra (shown in Fig. 6) invalid. It then becomes necessary to interpret the orientation dependence of one of the tensorial interactions in terms of the other.

For dipolar–chemical shift powder NMR spectra, this is performed by expressing the orientation of the dipolar coupling with respect to the chemical-shift tensor. A rotational transformation can be applied to obtain a relation between the two interaction reference frames in terms of the Euler angles, α and β, which are the azimuthal and polar angles, respectively, that describe the fixed difference in orientation between the dipolar vector and the chemical-shift tensor (see Fig. 7). These angles are determined by the electronic environment around the nucleus and are a distinct physical property of a spin pair in any particular molecule. The splitting due to dipolar coupling is given by

$$\nu_D(\text{hetero}) = \pm\tfrac{1}{2}R\{3[\sin\beta\sin\theta\cos(\alpha-\phi) + \cos\beta\cos\theta]^2 - 1\} \tag{18a}$$

$$\nu_D(\text{homo}) = \pm\tfrac{3}{4}R\{3[\sin\beta\sin\theta\cos(\alpha-\phi) + \cos\beta\cos\theta]^2 - 1\} \tag{18b}$$

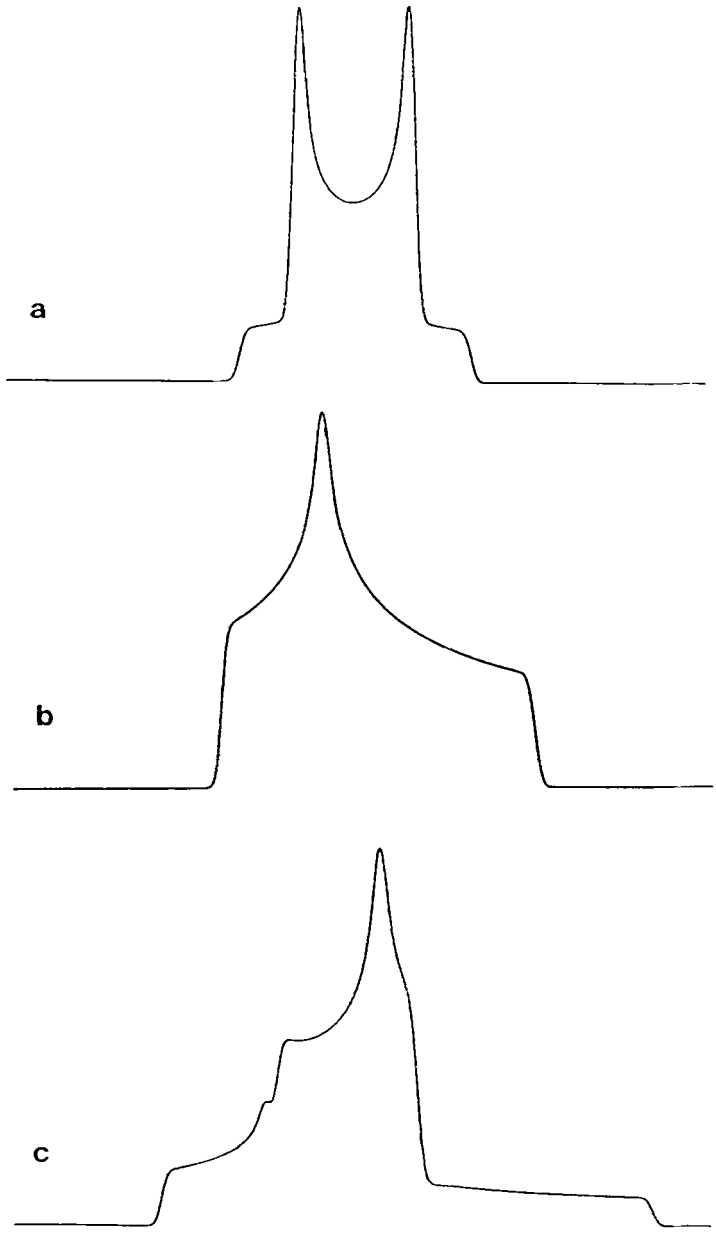

Fig. 6. Typical powder line shapes arising from (a) dipolar coupling ($R = 1000$ Hz) between two spin-$\frac{1}{2}$ nuclei, (b) anisotropic chemical shielding of a spin-$\frac{1}{2}$ nucleus ($\nu_{11} = 1200$ Hz, $\nu_{22} = 300$ Hz, $\nu_{33} = -1500$ Hz), and (c) both chemical shielding of a spin-$\frac{1}{2}$ nucleus and dipolar coupling to an adjacent spin-$\frac{1}{2}$ nucleus (assuming r_{IS} lies along δ_{33}).

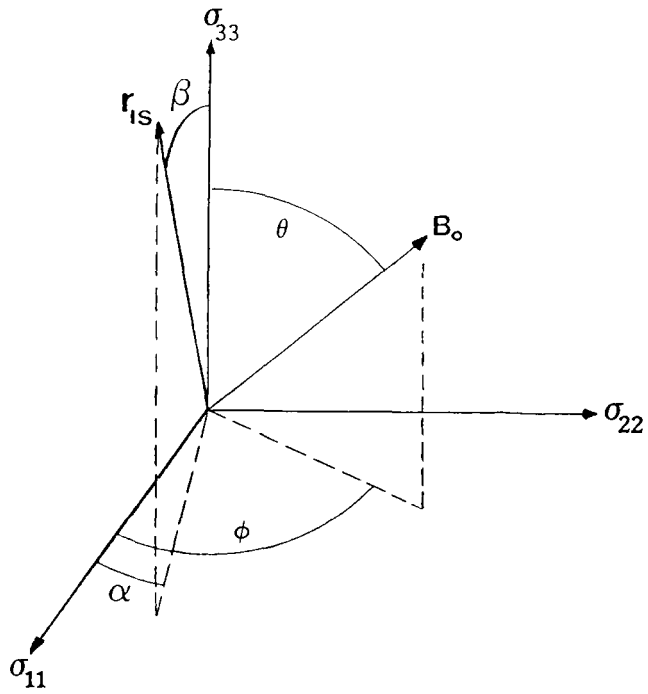

Fig. 7. The Euler angles α and β describe the orientation of the internuclear vector, $\mathbf{r}_{IS}$, with respect to the chemical-shift tensor. The angles θ and ϕ are defined in Fig. 3.

(cf. (12)), where the angles θ and ϕ orient the magnetic-field vector in the principal-axis system of the chemical-shift tensor. Equation (18) is now substituted into (17) in order to describe properly the effect of dipolar coupling. The experimental line shape is analysed, usually by fitting to spectra calculated using (17), in order to obtain R, α and β for that particular system, as well as the chemical-shift-tensor components. The value of R can be used to derive internuclear separations from polycrystalline samples. Determination of the angles α and β provides the orientation of the chemical-shift tensor with respect to the dipolar vector. The dipolar vector usually corresponds to a chemical bond, allowing the orientation of the chemical-shift tensor in the molecular frame to be determined. The line shape is quite sensitive to the values of the angles α and β, as illustrated in Fig. 8. Obviously, such experiments can prove useful in determining magnetic shielding as well as structural information from powder spectra.

Similar approaches can be envisaged for the analysis of spectra from systems involving other combinations of interactions, and applied to the

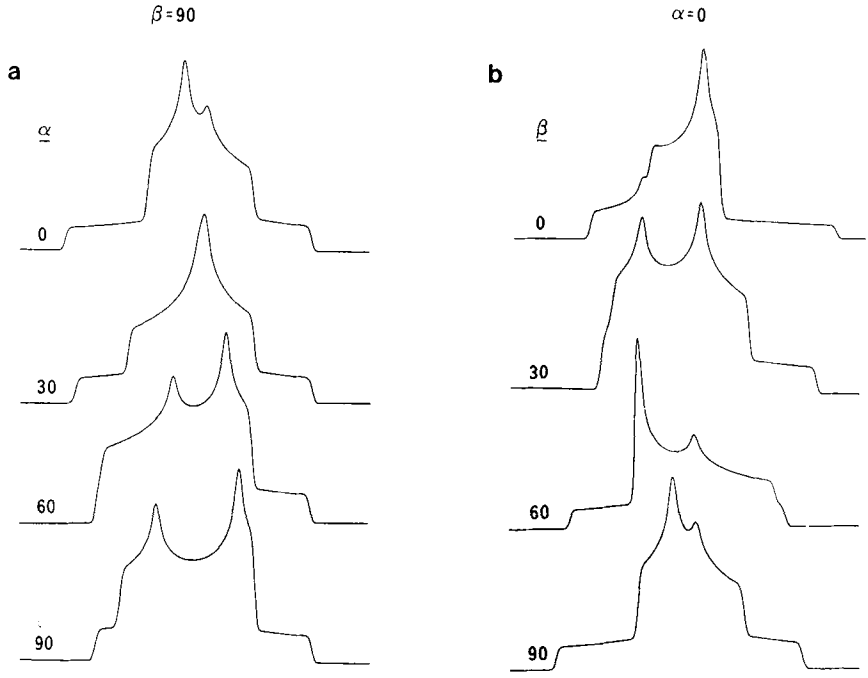

Fig. 8. The effect on the dipolar–chemical shift powder line shape of varying the orientation of $\mathbf{r}_{IS}$ with respect to the chemical-shift tensor. (a) $\beta = 90°$, $\alpha = 0°$, 30°, 60°, 90°, (b) $\alpha = 0°$. $\beta = 0°$, 30°, 60°, 90°. The spin pair consists of two spin-$\frac{1}{2}$ nuclei in these simulations.

interpretation of spectra obtained for single-crystal, powder and rotating samples. With the manipulation of Hamiltonians now possible using modern experimental techniques, one can tailor the investigation to extract very precise and valuable information for a variety of materials.

3. HOMONUCLEAR SPIN PAIRS

3.1. ^1H–^1H spin pairs

Many of the early dipolar NMR experiments discussed in the introduction were performed on ^1H–^1H spin pairs in static fields which were small enough that perturbations due to H_σ could be ignored. Much of the recent work has been performed at higher magnetic fields using more sophisticated techniques available with modern instrumentation or sample preparation. For example,

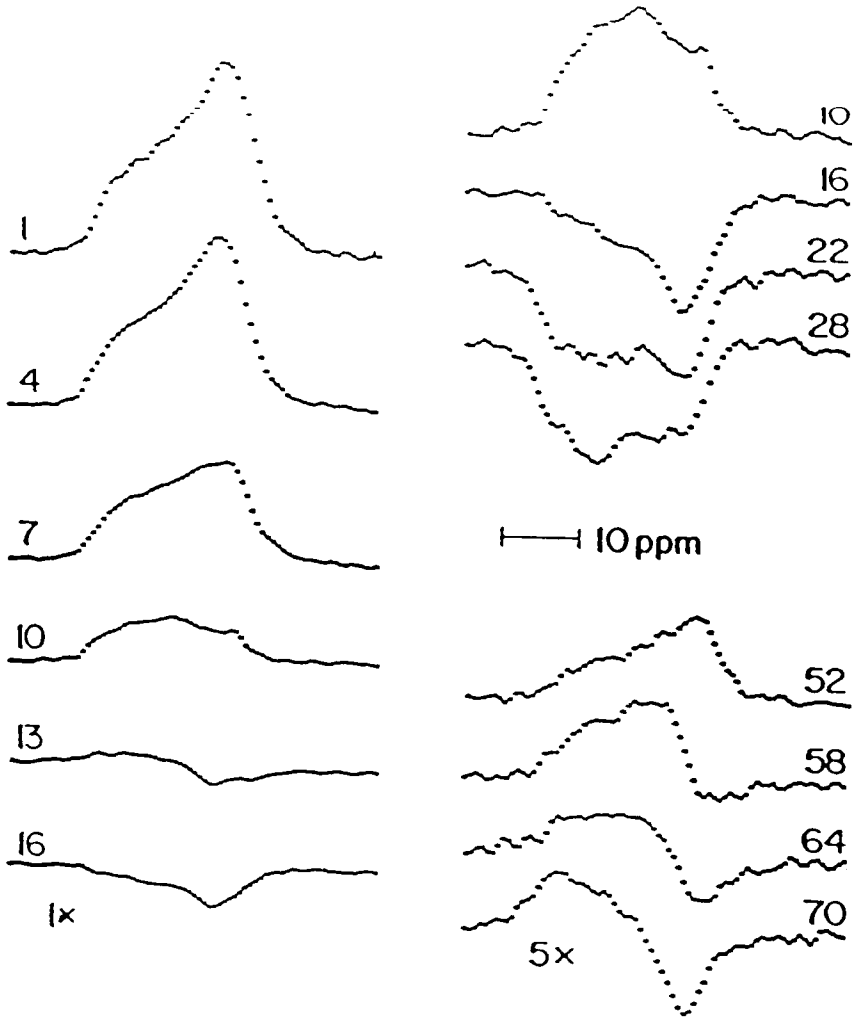

Fig. 9. Homonuclear dipole-modulated ^1H chemical shift powder spectra of CCl_3COOH, as a function of t_1, the dipolar evolution time, where one unit of t_1 corresponds to 4.17 μs. Spectra were obtained at 56.4 MHz. (Reproduced with permission from Stoll *et al.*[62])

Kohl *et al.*[60] used matrix isolation to dilute the ^1H–^1H spin pairs in a study of HCl and $(HCl)_2$. Analysis of the ^1H Pake pattern for the dimer in the argon matrix showed that the two HCl molecules form an angle of 122°. Together with the work of Grant's group,[61] this represented the first application of matrix isolation to the investigation of volatile or reactive species by solid-state NMR.

A two-dimensional experiment was applied to the proton–proton pair in trichloroacetic acid dimers.[62] The orientation of the ^1H chemical-shift tensor was determined via homonuclear dipole-modulated chemical-shift NMR spectra of a powder sample. The ^1H magnetization was allowed to evolve for a variable time t_1 under the influence of both ^1H–^1H dipolar coupling and ^1H chemical shift; during t_2, homonuclear multiple-pulse decoupling, such as WAHUHA[59] or MREV-8[63] (used in this particular experiment), was applied while the magnetization was detected. Fourier transformation of the t_2 dimension yielded chemical-shift spectra that were modulated by the dipolar interaction as a function of t_1. These spectra, shown in Fig. 9, could be analysed as a function of t_1 to obtain the ^1H–^1H dipolar coupling constant, hence, yielding $\mathbf{r}_{HH}$, and two angles which orient $\mathbf{r}_{HH}$ with respect to the principal components of the ^1H chemical-shift tensor. This approach removed ambiguities from a previous single-crystal study of this compound.[64]

The ^1H–^1H spin pair in carboxylic acid dimers has been a popular choice of investigators. For example, *p*-toluic acid (**I**),[65] malonic acid (**II**)[66] and tetrafluoroterephthalic acid (**III**)[67] have been studied, at least in part, in terms

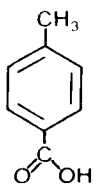

I

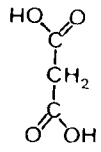

II

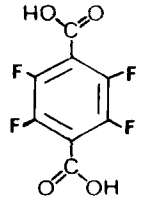

III

of the ^1H–^1H dipolar coupling between the two acidic protons. Meier *et al.*[65] used single-crystal ^1H NMR as well as ^1H relaxation measurements to determine the nature of the disorder for these protons in solid *p*-toluic acid-d_7 (i.e. all protons with the exception of the acidic protons were replaced by deuterium). At low temperature (26 K), one of the two tautomers of the dimer was frozen out. The observed dipolar coupling gave a ^1H–^1H separation of 2.33 Å, from which the static dimer structure, illustrated in Fig. 10, was obtained. The disorder was determined to be dynamic. The potential of the

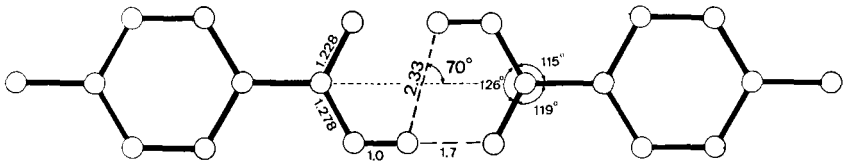

Fig. 10. The structure of *p*-toluic acid dimer at 26 K, determined from the ^1H–^1H dipolar coupling. Distances indicated are in Å. (Reproduced with permission from Meier *et al.*[65])

proton motion was asymmetric with a free-energy difference between the two sites of 1.0 kJ mol^{-1} and an activation energy of 4.8 kJ mol^{-1}.

Single-crystal ^1H NMR spectra of malonic acid (**II**) were obtained by Schuff and Haeberlen[66] using a two-dimensional technique similar to that used for trichloroacetic acid[62] with two important differences. First, Fourier transformation was applied to both time dimensions. This necessitated the second difference, a modified MREV-8 decoupling sequence to allow quadrature sensitivity in ω_1 by preserving the t_1 phase information at $t_2 = 0$. The result was a spectrum with homonuclear dipolar couplings in ω_1 resolved by isotropic chemical shifts in ω_2 for each crystallographically distinct ^1H. Previous ^1H chemical-shift tensor assignments for malonic acid[68] were confirmed in this manner.

Finally, precise crystal-structure information for tetrafluoroterephthalic acid (**III**) was obtained by considering the ^1H–^1H dipolar, ^1H and ^{19}F chemical-shift and ^2H quadrupolar interactions.[67] The orientation dependence of each of these interactions provided the spatial orientation of the phenyl ring plane, carboxyl group plane and the long axis of the molecule within the unit cell, in excellent agreement with neutron-diffraction results. Homonuclear and heteronuclear decoupling techniques were required to eliminate ^1H–^1H, ^1H–^{19}F and ^{19}F–^{19}F dipolar broadening of the various abundant spin spectra. For example, to allow observation of the ^1H–^1H dipolar splittings, the ^{19}F nuclei were decoupled by a train of π pulses. One point that unfortunately was not discussed in detail was the observed asymmetry in the ^1H–^1H dipolar coupling ($\eta_D = 0.19$). Presumably, this was due to the anisotropic libration of the protons in the dimer structure of **III**.

Recently, other investigators have considered asymmetric dipolar coupling tensors in detail. Sodium nitroprusside ($Na_2Fe(CN)_5NO{\cdot}2H_2O$) has two

molecules of water of hydration per molecular unit in its crystal lattice. The ^1H NMR spectra of a single crystal of this compound were measured at temperatures between 200 and 300 K.[69] Analysis of the dipolar splittings as a function of crystal orientation indicated that the dipolar coupling was nonaxially symmetric. Detailed treatment of the librational averaging of the ^1H–^1H dipolar coupling indicated that twisting motion (about the C_2 axis of H_2O) through an angle of 11.5° to 16.5° was responsible. The ^1H–^1H separation was 1.53 Å, corresponding to a H–O–H bond angle of 106.5°.

A metal dihydrogen complex, $(\eta^2\text{-}H_2)W(CO)_3(PCy_3)_2$ (Cy = cyclohexyl), was recently investigated by Zilm *et al.*[70] using ^1H NMR spectroscopy. The ^1H–^1H separation was determined to be 0.89 ± 0.01 Å. The internuclear vector between the protons was found to undergo an in-plane torsion of about 16°. The effect of this torsion was clearly evident in the ^1H powder NMR line shape, given in Fig. 11 with the molecular structure for this class of compounds. Contributions to the ^1H spectrum from the cyclohexyl protons were removed by applying a weak saturating pulse to the sample followed by a solid echo sequence, or, alternatively, by obtaining spectra of a sample with 95% perdeuterated PCy_3 ligands.

Asymmetry in dipolar NMR line shapes has also been noted in zero-field NMR spectra of barium chlorate monohydrate,[71] and a theoretical approach to the interpretation of these line shapes has been developed.[72] Zax *et al.*[73] have provided a complete description of the theory and practice of zero-field NMR, to which those interested should refer for details.

3.2. Rare spin homonuclear spin pairs

The observation of homonuclear dipolar couplings is not limited to abundant nuclei such as ^1H. Through isotopic enrichment, there has been a wide range of studies, particularly for ^2H, ^{13}C and ^{15}N, and also for 100% natural abundance dilute nuclei such as ^{31}P. When abundant spins are present, the rare spins are frequently isolated from them by high-power abundant-spin decoupling.

Haeberlen and coworkers[74,75] have used the homonuclear dipolar interaction between two ^2H nuclei as a reference, enabling them to obtain the absolute sign of the ^2H quadrupolar interactions. In a single crystal of malonic acid-d_4,[74] small line splittings appeared in the ^2H NMR spectrum when the crystal was oriented in the magnetic field such that the dipolar coupling was on the order of or larger than the splitting due to the quadrupolar interaction. Such a situation was possible because the internuclear vector was at an orientation close to the magic angle with respect to the principal component of

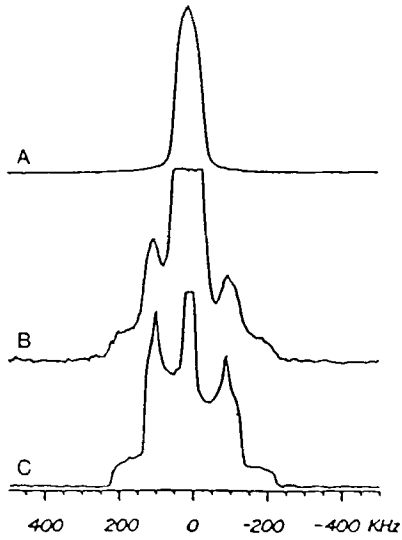

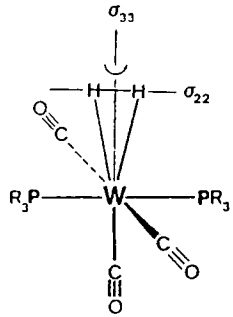

Fig. 11. Powder ^1H NMR spectra of $(\eta^2\text{-}H_2)\text{-}W(CO)_3(PCy_3)_2$ (structure indicated below) obtained at 300.1 MHz. (a) Experimental spectrum without suppression of ligand proton signal; (b) spectrum obtained by applying a soft ^1H pulse before a solid echo sequence; (c) spectrum of sample in which the PCy_3 ligands were 95% deuterated. The slight asymmetry in the intensities of the Pake doublet is due to chemical-shift anisotropy; asymmetry in the frequencies of the singularities is due to the librational motion of the H_2 ligand about the axis indicated in the structure. (Reproduced with permission from Zilm *et al.*[70])

the ^2H EFG tensor. The pattern of splittings was observed to depend on the sign of the ^2H quadrupolar coupling constant, $\chi(^2H)$, relative to the sign of the dipolar coupling, which was known. In malonic acid, the $^2H-^2H$ vector of the methylene-d_2 group was oriented at an angle of 6° with respect to the normal to the C–C–C backbone. In a similar study,[75] the application of a pulse sequence analogous to COSY provided the sign of $\chi(^2H)$ with respect to the dipolar coupling. The only modification of the COSY sequence was a change in the mixing pulse flip angle from 90° to 54.7°. The exact form of the resulting spectra depended on the relative signs of the dipolar and the two quadrupolar interactions. This technique was applied to the ^2H nuclei of the water molecule in a single-crystal study of $K_2C_2O_4 \cdot {}^2H_2O$.

Single crystals of oxalic acid dihydrate, $(COOH)_2 \cdot 2H_2O$, and diammonium oxalate monohydrate, $(NH_4)_2(COO)_2 \cdot H_2O$, have been studied using ^{13}C NMR.[38] The $^{13}C-^{13}C$ dipolar spectra of these doubly labelled compounds were used to obtain information about the dipolar and chemical-shift tensors of these ^{13}C nuclei. Oxalic acid was found to have a peculiar ^{13}C chemical-shift tensor orientation, with δ_{33}, the most shielded component, 26° away from the normal to the carboxyl plane. Diammonium oxalate is unusual in that the two ^{13}C nuclei of one oxalate anion are not generally equivalent. Thus, at various orientations of the crystal, the ^{13}C spectra exhibit A_2, AB and AX character, as is evident in Fig. 12. This was the first observation of AB spectra in solids, and the analysis appropriate to such spectra was described. For both compounds, the C–C bond lengths derived from the observed dipolar couplings agreed well (within 0.02 Å) with X-ray diffraction values.

The first comprehensive study of powder line shapes arising from $^{13}C-^{13}C$ dipolar interactions was that of Zilm and Grant.[55] These authors detailed the theory and analysis of spectra arising from AX, AB and A_2 spin systems, as well as heteronuclear spin pairs, in systems where the rare spins have been isotopically enriched. In order to reduce intermolecular dipolar interactions and ensure that they were studying an "isolated spin pair", Zilm and Grant carried out their measurements on samples in an argon matrix at 20 K. Dipolar couplings to protons were eliminated by high-power proton decoupling. A full treatment of the powder line shape, and the variables involved for each type of spin system, was provided, as well as a consideration of the effects of motional averaging, important to their matrix isolation studies. The ^{13}C chemical shift and dipolar tensors in methyl fluoride ($^{13}C-^{19}F$ spin pair, AX spin system), acetylene ($^{13}C-^{13}C$, A_2), ethylene ($^{13}C-^{13}C$, A_2) and acetaldehyde ($^{13}C-^{13}C$, AB) were obtained by analysis of the ^{13}C NMR powder line shapes. The dipolar vector, along with symmetry arguments, was used to orient the principal components of the ^{13}C chemical-shift tensor in the molecular frame without resorting to single-crystal analyses. In all cases, the bond lengths derived from the dipolar NMR data were approximately 0.02 Å

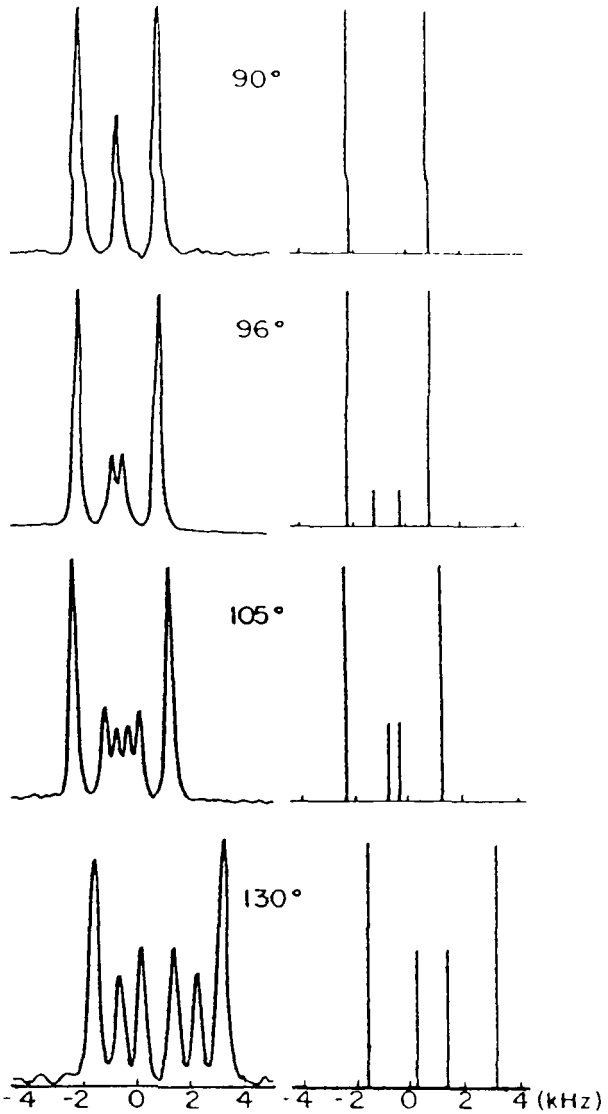

Fig. 12. Experimental and calculated ^{13}C NMR spectra of a single crystal of diammonium oxalate monohydrate at 73.9 MHz. Rotation of the crystal is about the crystallographic *a* axis, which lies perpendicular to B_0. The extra lines apparent at the centre of the splittings are due to natural abundance ^{13}C nuclei that are not bonded to another ^{13}C. (Reproduced with permission from van Willigen *et al.*[38])

longer than diffraction or microwave results. These discrepancies were probably due to inadequacies in the model used to correct for librational averaging of the dipolar interaction. Anisotropy in the indirect coupling tensor (ΔJ) could not be determined reliably because of uncertainties in the direct dipolar couplings.

Grant and coworkers have continued to use dipolar–chemical shift NMR to study various matrix-isolated species. The results for [1,2-$^{13}C_2$]cyclopropane[76] indicated that the most shielded component of the methylene ^{13}C chemical shift tensor, δ_{33}, was unusual in both its low value (-36 ppm from TMS) and its orientation (perpendicular to the ring plane). Similarly, the magnitudes and orientations of the principal components of the chemical-shift tensors for [1,2-$^{13}C_2$]cyclobutane[77] and [1,2-$^{13}C_2$]cyclobutadiene[78] were examined. The experimental results appear to be consistent with theoretical results obtained from molecular-orbital calculations. Unfortunately, in these latter two systems, the line shapes were broadened considerably, leading to some ambiguity in the experimental results.

The ^{13}C NMR spectra of *trans*-poly(acetylene-$^{13}C_2$) were also analysed in the same fashion to determine the ^{13}C chemical shift tensor and the C–C bond length in this polymer.[79,80] A dynamic nuclear polarization–cross-polarization (DNP-CP) experiment[81] was used to increase sensitivity by Overhauser enhancement of the ^1H magnetization through Larmor irradiation of the free electron, which was then transferred to ^{13}C by Hartmann–Hahn matching.[82] The presence of two distinct dipolar couplings, corresponding to C–C bond lengths of 1.38 ± 0.01 Å and 1.45 ± 0.01 Å, indicated that the bonds were non-alternating on the time scale of the dipolar coupling ($\simeq 10^{-3}$ s) (see also the discussion in Section 3.3).

Recently, Engelsberg and Yannoni[83] have used a modified Carr- Purcell–Meiboom–Gill (CPMG) sequence[84] (see Fig. 5(b)) which incorporates cross-polarization and proton decoupling to measure Pake doublet splittings in isolated homonuclear spin pairs. Under ideal circumstances, the observed dipolar splitting, Δ, corresponding to the $\theta = 90°$ singularities, depends linearly on the duty factor, D,

$$\Delta = (3/2)R(1 - D) \tag{19}$$

where $D = t_w/(2\tau + t_w)$, 2τ denotes the interval between the end of a π pulse and the beginning of the next one and t_w is the pulse width. In a study of acetic acid, $^{13}CH_3{}^{13}COOH$, at 80 K, (19) was found to be applicable for D values in the range 0.125 ($2\tau = 67.2$ μs) to 0.35 ($2\tau = 17.8$ μs) with $t_w = 9.6$ μs. Thus a plot of Δ vs. D was linear; extrapolation to $D = 0$ indicated $\Delta_0 = 3R/2 = 3192 \pm 15$ Hz, hence $r_{CC} = 1.52$ Å.[83] Analogous experiments on benzene-$^{13}C_1$, $^{13}C_2$ led to $r_{CC} = 1.42$ Å after correcting the measured Δ_0 for motional averaging (rapid

reorientation about the hexad axis).[83] Note that the Carr–Purcell sequence suppresses the chemical-shift anisotropy broadening.

The Carr–Purcell sequence[84] has also been used to suppress heteronuclear dipolar interactions in the study of $^{13}C_2H_4$ and ^{13}CO molecules adsorbed on catalytic surfaces, such as Pt,[85,86] and Ru and Rh.[87] As the spin-echo amplitude is sensitive to homonuclear ^{13}C–^{13}C dipolar coupling, it can be used to determine the separation between the carbon nuclei on a metal surface. For ethylene chemisorbed on Pt, this was found to be 1.49 Å, which corresponds to the bond length expected for ethylidyne (C–CH_3) species.[85] The homonuclear ^{13}C–^{13}C dipolar coupling provided a probe of the surface density of the CO layer on the metal particles. For Pt, the ^{13}C NMR results indicated that, at low surface coverages, the CO molecules adsorbed initially in clusters, possibly to the small Pt [100] crystal faces.[86] Various morphologies of Ru and Rh particles on oxide supports were described from similar ^{13}C experiments.[87] The influence of the homonuclear ^{13}C–^{13}C dipolar interaction on the ^{13}C magnetization decay in a CPMG experiment[84] for $Rh(^{13}CO)_2$ species on a Rh/Y-zeolite catalyst was used to determine the separation between the two carbonyl carbons (2.58 Å).[88] Further applications of this sequence can be anticipated.

Homonuclear ^{15}N dipolar-chemical shift NMR spectra have been reported for powder samples of $^{15}N_2$[89] and *trans*-azobenzene-$^{15}N_2$.[90] For $^{15}N_2$, spectra obtained at various field strengths at 4.2 K yielded $\Delta\sigma = \sigma_{\parallel} - \sigma_{\perp} = 603 \pm 28$ ppm after correction for the orientational order parameter for α-N_2, known from other techniques. The N–N bond length was determined to be 1.101 ± 0.003 Å. Crystalline *trans*-azobenzene contains two crystallographically nonequivalent molecules in the unit cell; however, the ^{15}N MAS spectrum of this compound indicated only one resonance with a half-width of less than 20 Hz (1 ppm). Close inspection of the static powder pattern (Fig. 13) revealed subtle differences in the overall ^{15}N chemical-shift tensors of the two sites, i.e. the identical value of δ_{iso} was fortuitous. Analysis indicated a large ^{15}N chemical shift anisotropy of 925 and 880 ppm for the two sites, much larger than that observed for $^{15}N_2$. The slightly smaller value of $\Delta\sigma$ at one site was attributed to the disorder reported for one site in the crystal structure. The values of the splittings due to dipolar coupling at frequencies corresponding to the three principal components of the ^{15}N chemical-shift tensor were used to determine the orientation of the shift tensor. For *trans*-azobenzene, the orientation was found to be similar to that observed for other ^{15}N nuclei in π-bonded systems (see Section 4.1), and calculated using IGLO methods,[91] with δ_{33} perpendicular to the molecular plane and δ_{22} approximately along the direction of the nitrogen lone pair.

Homonuclear ^{31}P–^{31}P spin pairs have also received considerable attention in the literature. Several investigators have found that the ^{31}P–^{31}P dipolar

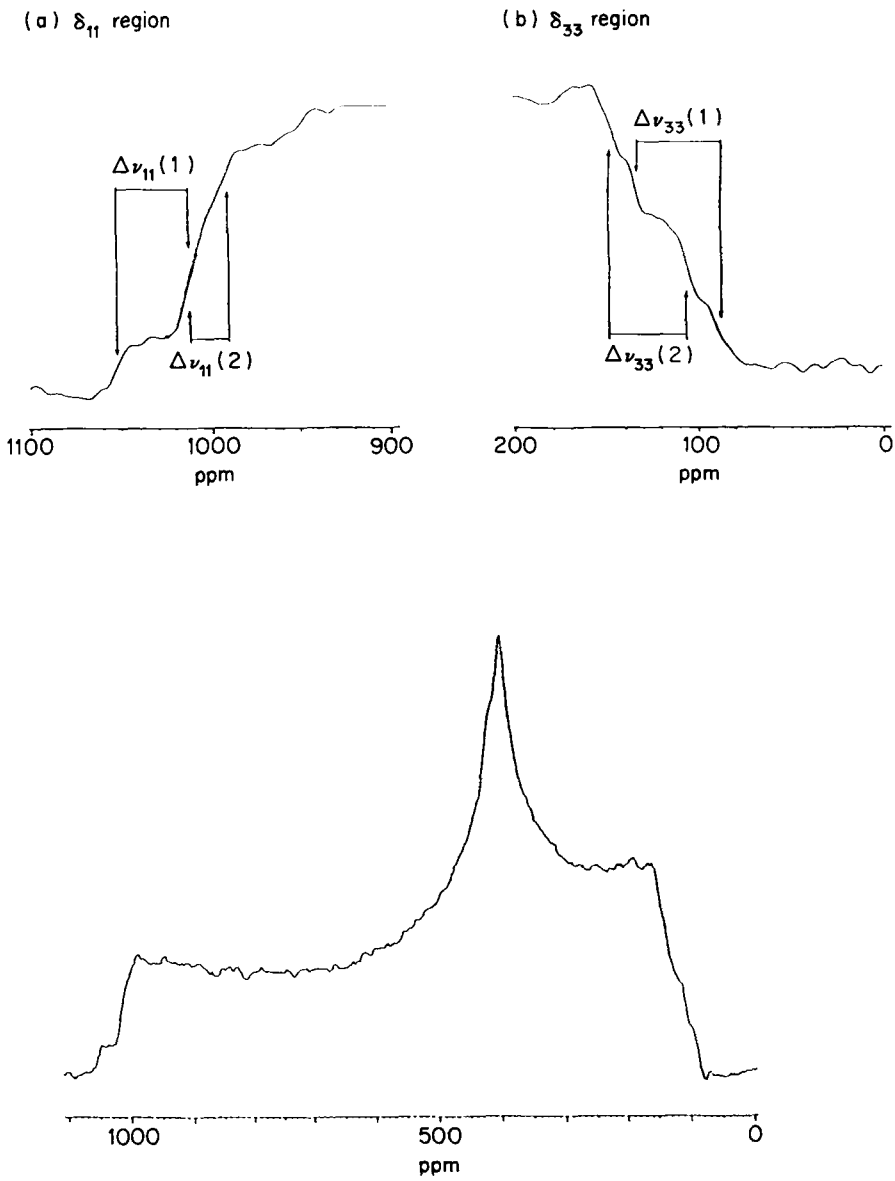

Fig. 13. Powder ^{15}N NMR spectra of *trans*-azobenzene-$^{15}N_2$ at 20.3 MHz. The expanded regions are (a) the high frequency shoulder, and (b) the low frequency shoulder, with the splittings due to dipolar coupling indicated for the crystallographic sites 1 and 2. (Reproduced with permission from Wasylishen *et al.*[90])

coupling constants derived from dipolar–chemical shift spectra yield bond lengths that are inconsistent with those obtained with X-ray diffraction. These discrepancies have been attributed to errors in the apparent values of R which arise because of neglect of contributions from the anisotropy in the indirect ^{31}P–^{31}P spin–spin couplings (see (14)). In order to obtain estimates of $\Delta J(^{31}P–^{31}P)$ in $Ag_4P_2O_6$, Grimmer *et al.*[92] calculated $R(^{31}P–^{31}P)$ from the value of r_{PP} obtained by X-ray diffraction. Assuming axial symmetry in the **J** tensor, a value for ΔJ of 800 ± 80 Hz was calculated for the $P_2O_6^{4-}$ ion using (20),

$$\Delta J = 3(R_{calc} - R_{eff}) \tag{20}$$

where R_{calc} is the dipolar coupling constant calculated using the bond length from diffraction experiments and R_{eff} is the value obtained directly from the NMR spectrum. Note that any error in the difference in R values is multiplied by 3 in obtaining ΔJ, and that this equation neglects the fact that R_{eff} corresponds to a motionally averaged dipolar coupling constant.[18,19,93]

Subsequently, Tutunjian and Waugh[94] analysed the ^{31}P single-crystal NMR rotation patterns of tetraethyldiphosphine disulphide at room temperature and, using the value of r_{PP} from X-ray diffraction experiments to calculate the direct dipolar coupling constant, $R(^{31}P–^{31}P)$, determined that $\Delta J(^{31}P–^{31}P) = +1491 \pm 30$ Hz or $+5860 \pm 30$ Hz. They established that the anisotropy in J was essentially axially symmetric in this σ-bonded system, which has been a common assumption in most of the ensuing studies of ΔJ.

The ^{31}P NMR spectra of Mes*P = PMes* (Mes* = (2,4,6-tri-t-butyl)-phenyl) were analysed to characterize the ^{31}P chemical-shielding tensor of a diphosphene.[95] Due to the extreme breadth of the spectrum (ca. 60 kHz), a CPMG pulse sequence[84] was applied. Since homonuclear dipolar couplings are not refocused in a spin-echo experiment, a two-dimensional experiment using a range of τ values was necessary. The resulting spectrum, illustrated in Fig. 14, contained pure homonuclear dipolar coupling information along ω_1, and both homonuclear dipolar coupling and ^{31}P anisotropic chemical-shift information along ω_2. The observed dipolar coupling constant, $R(^{31}P, ^{31}P)$, was 2800 Hz, much larger than predicted (2340 Hz) based on the P–P bond length (2.034 Å) from an X-ray diffraction study. The authors attributed this discrepancy to anisotropy in the indirect coupling, -920 Hz or $+10\,280$ Hz. The ^{31}P chemical-shift anisotropy was large, 1239 ppm; the extremely high frequency value of δ_{11} was ascribed to the low-lying $n \rightarrow \pi^*$ transition in this compound. The principal components of the chemical-shift tensor were found to be oriented such that δ_{33} was perpendicular to the molecular plane and δ_{22} was approximately along the phosphorus lone pair.

Eckert and coworkers[96,97] have used ^{31}P NMR to characterize the phosphorus sites in various phosphorus chalcogenide compounds.

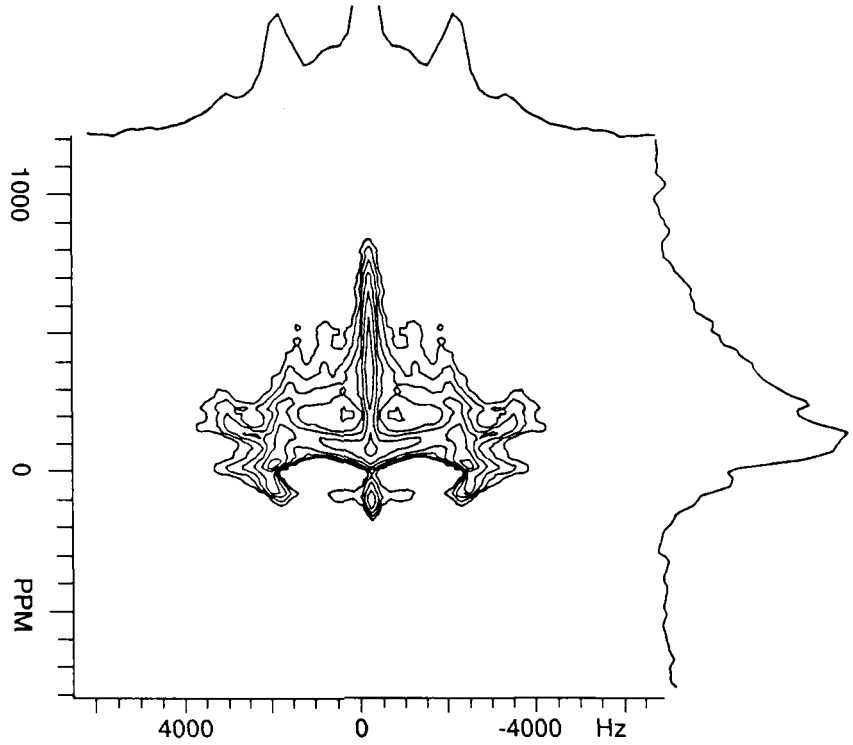

Fig. 14. Two-dimensional ^{31}P spin-echo spectrum of Mes*P = PMes* obtained at 40.466 MHz. The horizontal axis corresponds to homonuclear dipolar coupling alone, the summation of which is given at the top. The vertical axis contains both homonuclear dipolar coupling and chemical shift information, summed along the side. Note that there is no dipolar splitting apparent at the high-frequency end of the dipolar-chemical shift line shape (vertical axis), indicating δ_{11} is oriented close to the magic angle with respect to the P–P bond. (Reproduced with permission from Zilm *et al.*[95])

Phosphorus-31 MAS NMR of different phosphorus sulphides[96] was used to correlate ^{31}P chemical-shielding tensors with their local environment. Some AB character was evident in the spectrum of P_4S_7 but was not analysed due to the small value of the dipolar coupling compared with the chemical-shift anisotropy. A more detailed treatment of the ^{31}P–^{31}P dipolar coupling was performed in the study of phosphorus–selenium glasses.[97] The distribution of phosphorus in glasses of varying composition (10–50 atom% P) was determined via ^{31}P spin-echo measurements. The second moment due to ^{31}P–^{31}P homonuclear dipolar coupling was obtained by observing the modulation of the spin-echoes for various delays, because, as mentioned previously, these

couplings are not refocused. The variation in the second moment as a function of phosphorus concentration indicated that the phosphorus distribution was random, with P–Se bond formation favoured over that of P–P bonds at all concentrations. Only at phosphorus concentrations higher than 25 atom% was there evidence that P–P bonds were present.

3.3. Nutation NMR

As indicated in the introduction, second moments of abundant spin NMR line shapes are capable of providing important structural and dynamical information. In molecules where heteronuclear spins contribute to the abundant spin second moment, it is desirable to have procedures available to separate the homonuclear and heteronuclear dipolar interactions.[98] The Hamiltonian for the abundant spins describing this general problem is given by

$$H = H_Z + H_{rf} + H_D^{II} + H_D^{IS} \tag{21}$$

where all symbols are standard.

Although a number of techniques are available to effect this separation, problems arise when the heteronuclear spin, S, is a quadrupolar nucleus with a large quadrupolar coupling constant.[99,100] Under these conditions, the quantization axis of the quadrupolar nucleus is neither along B_0 nor along the principal axis of the EFG tensor. A technique applicable under these circumstances was proposed by Yannoni and Wind.[98] By subjecting the abundant I spins to a strong resonant field using an on-resonant nutation scheme, the I–S dipolar interaction is completely eliminated because I_z is effectively averaged to zero. The on-resonant I-spin excitation (Nut(I)) reduces the contribution of H_D^{II} to the I spin linewidth by a factor of two and the I spin second moment by a factor of 4.[101]

$$H^{Nut(I)} = \tfrac{1}{2} H_D^{II} \tag{22}$$

Since the line shape and second moment following Fourier transformation of the standard FID resulting from a single pulse excitation are determined by both homonuclear and heteronuclear dipolar interactions, it is possible to separate H_D^{II} and H_D^{IS} using (22) and (23),

$$H^{FID} = H_D^{II} + H_D^{IS} \tag{23}$$

In their ^1H NMR study of iodic acid (HIO_3), Yannoni and Wind[98] also carried out a third experiment to confirm that H_D^{II} and H_D^{IS} had been successfully separated (i.e. the homonuclear ^1H–^1H dipolar contribution and the heteronuclear ^1H–^{127}I dipolar contribution). They applied an off-resonance line narrowing (LN) sequence designed to remove homonuclear

dipolar coupling.[102] The sequence used also attenuated interactions linear in I_z (heteronuclear dipolar coupling and the I spin chemical shielding anisotropy) so that

$$H^{LN} = \delta H_D^{IS} \tag{24}$$

where δ is a scaling factor, $0 < \delta < 1$. For HIO_3 at 170 K, application of the above pulse sequences indicated $M_2^{H-H} = 16.2$ kHz (Nut), $M_2^{H-H} + M_2^{H-I} = 28.1$ kHz (FID), implying $M_2^{H-I} = 11.9$ kHz. The line-narrowing experiment confirmed successful separation of M_2^{H-H} and M_2^{H-I}, giving $M_2^{H-I} = 12.3$ kHz.

The nutation experiment was subsequently applied to measure the ^{13}C–^{13}C dipolar coupling constant in an isolated spin pair, acetic acid ($^{13}CH_3{}^{13}CO_2H$ in $^{12}CH_3{}^{12}CO_2H$; 1:40).[103] The nutation pulse train, applied while the protons were decoupled, was preceded by the standard cross-polarization pulse sequence (Fig. 15). This experiment allows one to measure the homonuclear dipolar splitting, reduced by a factor of two, in the absence of anisotropic chemical-shift effects. For acetic acid at 80 K, the C–C bond length determined from the CP-nutation experiment was 1.49 ± 0.02 Å, which is in good agreement with the X-ray result obtained at the same temperature (1.478 Å) and the value obtained from neutron diffraction (1.501 Å at 133 K).

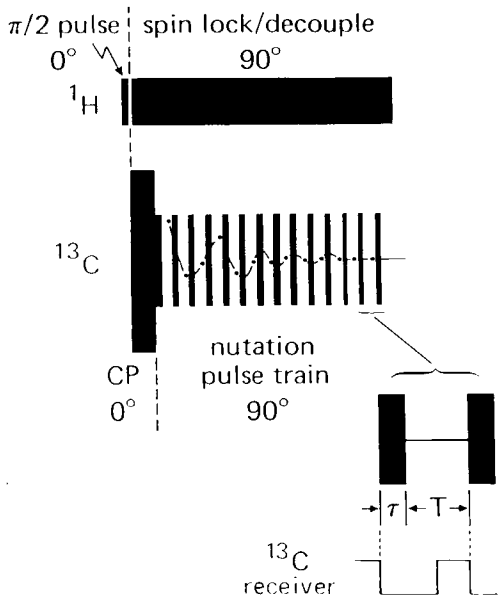

Fig. 15. Pulse sequence for the cross-polarization–nutation NMR experiment. The times τ and T were 8 and 17 μs, respectively, and the free induction decay was sampled during the windows, T, 6 μs after τ. (Reproduced with permission from Horne *et al.*[103b])

After establishing the accuracy of the CP nutation experiment, Yannoni and coworkers applied this technique to a number of interesting chemical systems where it was either impossible or difficult to apply diffraction techniques. For example, a 4% mixture of doubly ^{13}C-enriched acetylene ($\geqslant 99\%$ ^{13}C) in doubly ^{13}C-depleted acetylene was polymerized by a Ziegler–Natta catalyst at 196 K to provide the *cis*-transoid isomer of polyacetylene (**IV**).[104,105] Interestingly, the best fit to the observed Pake NMR powder pattern which arose from direct ^{13}C,^{13}C dipolar coupling between adjacent ^{13}C nuclei, indicated $r(^{13}C, ^{13}C) = 1.37$ Å.[104] This bond length implies that the Ziegler–Natta reaction leaves the original ^{13}C-labelled pair doubly bonded to one another. On the basis of this result, the authors were able to propose a four-centre acetylene insertion mechanism for polymerization of acetylene and concluded that a metallacycle mechanism was not operative under the conditions employed. The latter mechanism would have resulted in the ^{13}C-enriched sites being separated by a typical C–C single-bond distance.

IV

The *trans* isomer of polyacetylene, prepared by heating the *cis*-$(CH)_x$ sample, **IV**, clearly displayed two overlapping Pake powder patterns of comparable intensity.[104,105] Analysis of the powder patterns indicated C–C bond lengths of 1.44 Å and 1.36 Å, confirming a bond-alternated structure (**V**). Since motion of neutral solitons along the polymer chain would lead to the interchange of the single and double bond in *trans*-polyacetylene, the authors were able to conclude that such a process is either slow ($\leqslant 10^3\ s^{-1}$) or not operative.[105]

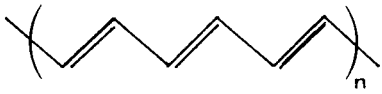

V

Subsequently, Yannoni and coworkers studied the polymerization of phenylacetylene using two different initiators.[106] In this case, the isolated spin pairs were found mainly in a double bond (reaction 1) or a single bond (reaction 2), as indicated below, depending on the catalyst used.

Two symmetrically substituted hexaphenylethanes, **VI** and **VII**, have been examined using nutation NMR spectroscopy in order to establish the C–C bond length of the ethane fragment.[107] On the basis of the NMR studies at 77 K, Yannoni *et al.*[107] were able to conclude that r_{CC} was between 1.64 and 1.65 Å in both compounds. An earlier X-ray structure of **VI** indicated an

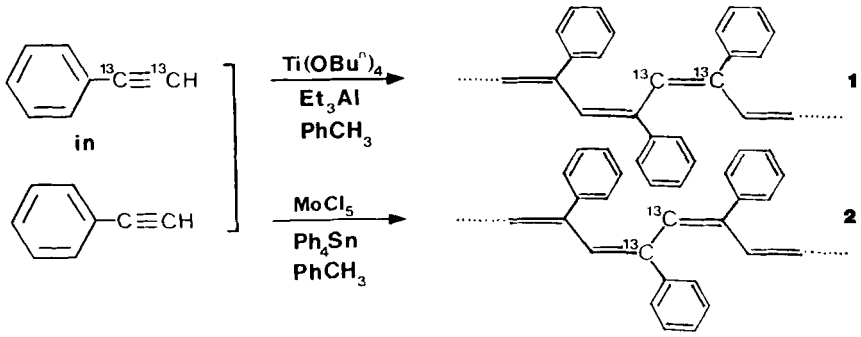

abnormally short central C–C bond length of 1.47 Å, in marked contrast to the corresponding X-ray value for **VII** of 1.67 Å. Thus, the dipolar NMR results, together with MM2 calculations, led the authors to conclude that the short C–C bond length reported for **VI** was grossly in error.

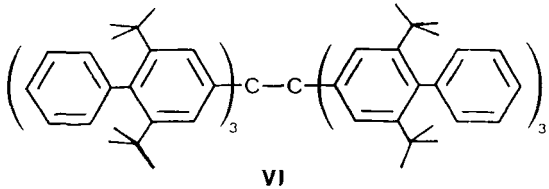

VI

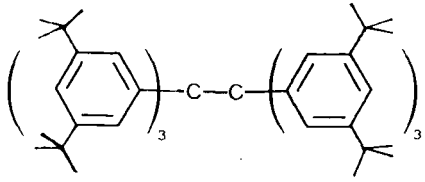

VII

The power of dipolar NMR studies of isolated spin pairs was nicely illustrated by the following recent example.[108] Examination of the ^{13}C CP-nutation NMR spectra of two separate samples of doubly labelled t-butyl cations, $[^{13}CH_3{}^{13}C(CH_3)_2]^+$ and $[CH_3C(^{13}CH_3)_2]^+$ (see Fig. 16), revealed ^{13}C–^{13}C separations of 1.46 Å and 2.51 Å, respectively. These separations indicated that the C–C–C bond angle was 120° (i.e. the carbon skeleton of the t-butyl cation in $C_4H_9^+$ $Sb_2F_{10}X^-$ was planar). This example clearly demonstrated that in situations where single crystals of reactive carbocations are unavailable, valuable structural information could be obtained from dipolar NMR.

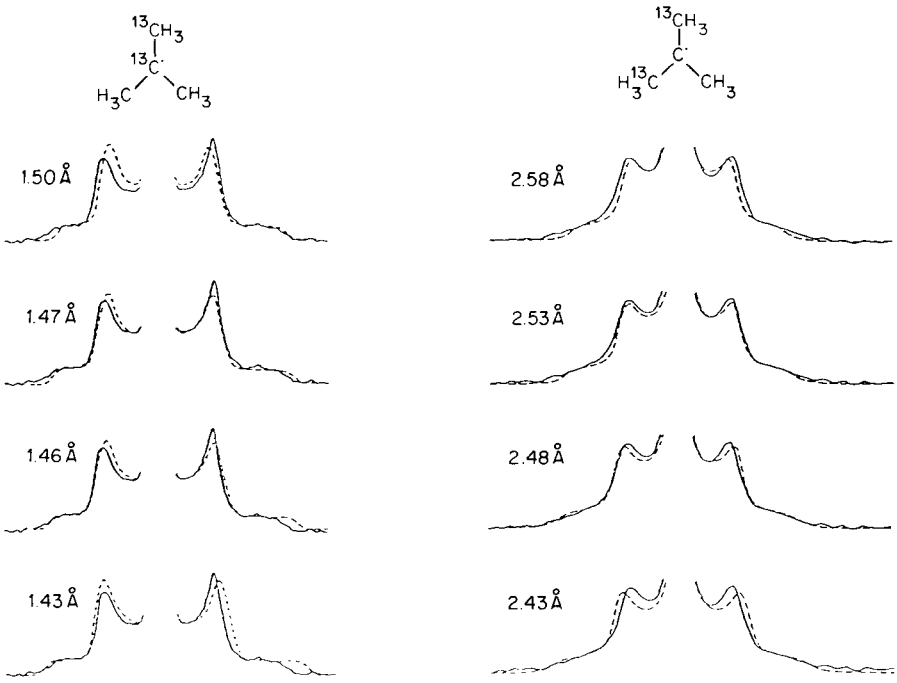

Fig. 16. Experimental ^{13}C nutation NMR spectra of $[^{13}CH_3{}^{13}C(CH_3)_2]^+$ and $[CH_3C(^{13}CH_3)_2]^+$, with overlaying simulations corresponding to the various ^{13}C–^{13}C distances indicated. The best fits are between 1.46 Å and 1.47 Å for $[^{13}CH_3{}^{13}C(CH_3)_2]^+$, and between 2.48 Å and 2.53 Å for $[CH_3C(^{13}CH_3)_2]^+$. (Reproduced with permission from Yannoni *et al.*[108])

3.4. Selective detection of ^{13}C–^{13}C connectivities

One of the primary goals of solid-state NMR has been to obtain precise structural information from the spectra of, if possible, natural abundance samples. The increase in sensitivity achieved by applying cross-polarization between ^1H nuclei and rare spins[26] has satisfied this to some extent. VanderHart illustrated this in 1976 when he observed ^{13}C–^{13}C dipolar satellites in the natural-abundance ^{13}C NMR spectrum of ultraoriented polyethylene.[109] From the variable-temperature spectra, it was possible to discern couplings to ^{13}C nuclei one, two and three bonds away. The splittings induced by ^{13}C nuclei separated by one and three bonds agree well with those anticipated based on X-ray diffraction results. However, the coupling between ^{13}C nuclei separated by two bonds was smaller than expected. Less than a year later, Garroway also showed the influence of ^{13}C–^{13}C dipolar coupling in spectra of natural abundance samples.[110] Proton-decoupled ^{13}C NMR

spectra of static powder samples of adamantane exhibit rather large line widths (40 Hz) considering the high degree of molecular motion these molecules undergo at room temperature. The origin of this broadening was investigated by observing the averaging effects of various pulse sequences (Carr–Purcell, CPMG and solid-echo) as well as MAS. The results indicated that natural-abundance ^{13}C–^{13}C intermolecular dipolar coupling was responsible.

One possible application of ^{13}C homonuclear dipolar NMR is the establishment of ^{13}C–^{13}C connectivities in natural-abundance samples, in parallel to various solution experiments utilizing coherence transfer.[49] Incorporating only one ^{13}C label provided the first step towards achieving this goal. Specific ^{13}C labelling was used to assign resonances in ^{13}C CP/MAS spectra of α-D-glucose.[111] Not only did the intensity of the labelled ^{13}C resonance greatly increase, the directly bonded natural-abundance ^{13}C nuclei could also be identified, since their signals were extensively broadened. Under MAS, the ^{13}C–^{13}C dipolar interaction behaves homogeneously; as a result it does not split into sidebands, rather it gives rise to a severely broadened line with a concomitant drop in signal intensity.[58]

Experiments on natural-abundance samples of several amino acids and peptides established which carbon sites were in close proximity to each other by ^{13}C spin exchange.[112] These ^{13}C nuclei may have been near one another due to direct bonding or by the conformation of the molecule bringing different fragments together. The two-dimensional ^{13}C CP/MAS experiment identified exchange pairs by the presence of off-diagonal cross-peaks in the spectrum, as illustrated in Fig. 17.

Bork and Schaefer[113] have also proposed an experiment to establish connectivities in organic compounds which is based on spin diffusion. In their experiment, a DANTE pulse sequence was applied at a particular ^{13}C resonance frequency in order to invert it selectively. By introducing a "diffusion delay", connectivities to other ^{13}C sites could be detected by observing enhanced intensities for particular signals in the difference spectra which combined the results of experiments with and without the DANTE sequence. This technique was illustrated using [1,2-$^{13}C_2$]glycine samples. Application to natural-abundance samples has not yet been demonstrated and may require higher sensitivity.

One problem in detecting ^{13}C–^{13}C connectivities in natural-abundance samples is that the normal one-quantum signal from an isolated ^{13}C nucleus is much larger than any signals due to natural-abundance ^{13}C–^{13}C dipolar coupling. It is essential to filter out these one-quantum signals from the coupled resonances. This has been accomplished using multiple quantum (MQ) NMR techniques,[114–116] which have been developed in recent years. A double-quantum filter would allow ^{13}C–^{13}C spin pairs to be observed free of

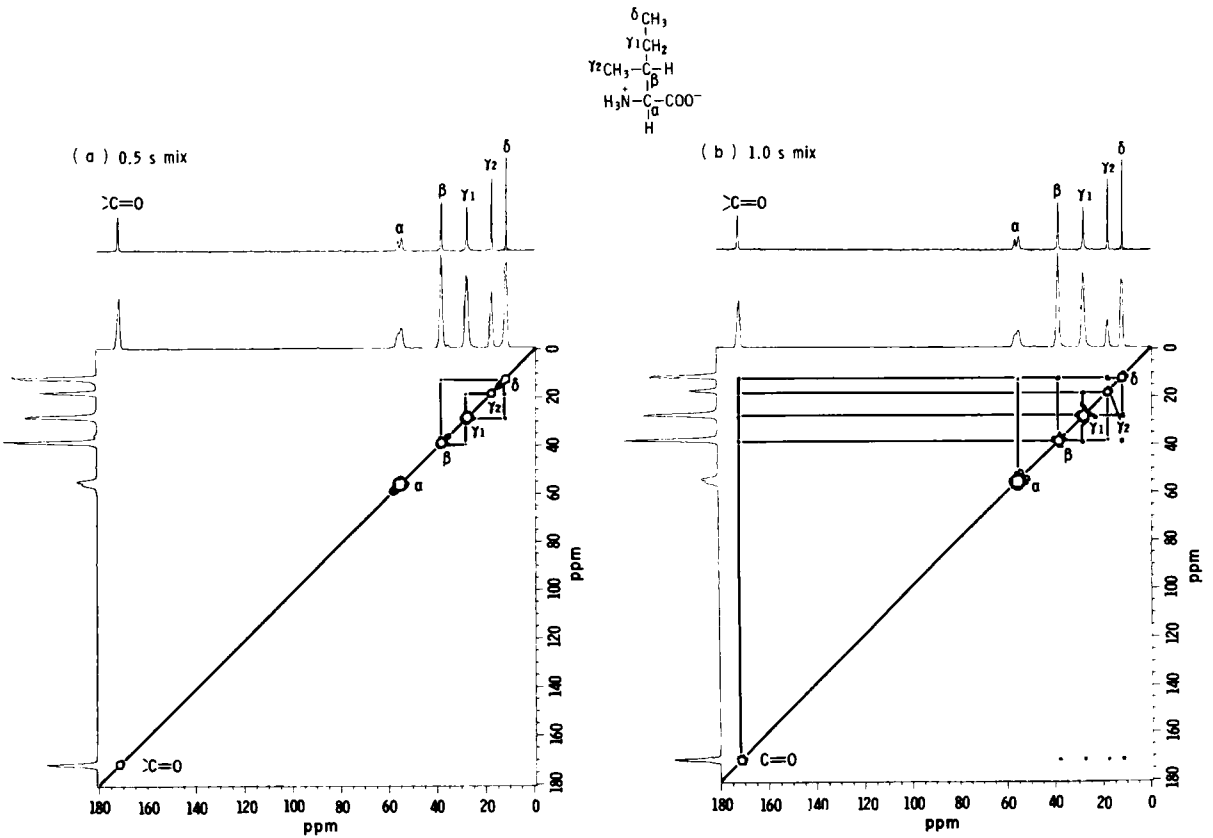

Fig. 17. ^{13}C CP/MAS spin exchange spectra of L-isoleucine·HCl powder for two different mix times to allow spin exchange between carbon sites to occur. The signals are assigned according to the structure given. (Reproduced with permission from Frey and

the influence of any isolated ^{13}C nuclei. This has been performed experimentally by two groups,[117,118] and the MAS applications they propose will probably prove the most useful. Two types of MAS experiment have been described; one simply indicates the presence of connectivities in a one-dimensional spectrum, while the other, a two-dimensional experiment, maps out the specific connectivities. Synchronization of pulses with sample rotation is important in this latter MAS experiment, as it ensures that all anisotropic information is refocused whenever manipulation or detection of the nuclear magnetization occurs. To date, only labelled compounds have been used as examples to illustrate the technique. Low-temperature or DNP techniques may be required in order to obtain the sensitivity necessary for natural-abundance samples.[117]

3.5. Rotational resonance

In the course of their work on a double-quantum filtered detection of ^{13}C spectra, Meier and Earl[118] noticed an interesting effect at certain spinning rates. Significant broadening of the centre bands and side bands of two different ^{13}C resonances of doubly labelled zinc acetate-$^{13}C_2$ occurred when an integer multiple of the spinning rate matched the difference in their chemical shifts (in Hz). This phenomenon was observed concurrently by Raleigh *et al.*[119] It was first described by Andrew and coworkers[120,121] over 20 years previously, who found that cross-relaxation was enhanced and line broadening was introduced when the spinning rate, or some integer multiple of it, matched the difference in ^{31}P isotropic chemical shifts of PCl_4^+ and PCl_6^- ions in solid PCl_5. When this condition was met, the B or "flip-flop" term of the dipolar interaction (see (11)) was introduced, promoting communication between the two spins and producing homogeneous broadening of their resonances.

A more quantitative treatment of this "rotational resonance" effect was provided by Raleigh *et al.*[122] and Gan and Grant.[123] In the first treatment,[122] the splittings of the centre bands that occur when $\Delta\nu_{iso} = n\nu_r$, where $n = 1, 2, 3, \ldots$, etc., and ν_r is the spinning rate (in Hz), were shown to depend on the chemical-shift anisotropies and asymmetries for the two nuclei involved, the dipolar and indirect coupling between them and, when $n \geqslant 3$, the relative orientations of the tensors involved. The MAS line shapes could, in principle, be simulated to derive this information. The oscillatory transfer of magnetization from an inverted resonance to another resonance $n\nu_r$ Hz away could also be used to obtain dipolar couplings, hence internuclear separations, from variable-delay experiments. However, such applications require precise knowledge of the chemical-shift tensors for the two nuclei. Gan and Grant[123]

have used a "pseudo-spin" model to describe rotational resonance, where the near-degenerate levels of the homonuclear spin system are expressed in terms of the two levels of a pseudo-spin. In this formalism, $\Delta\nu_{iso}$ behaves like the static magnetic field, and the flip-flop terms, reintroduced by the sample rotation, act analogous to radiofrequency fields. Thus, resonance is achieved when $\Delta\nu_{iso} = n\nu_r$. This theory was presented for the fast and slow spinning forms of rotational resonance without specific experimental examples.

One application of rotational resonance has been the measurement of weak dipolar interactions in solids.[124] It has been used to follow the magnetization transfer between two ^{13}C-labelled sites in tyrosine ethyl ester (**VIII**).[125] The two sites are not directly bonded but are in close proximity as a result of the conformation that molecule adopts in the solid state. By following the magnetization transfer for $n = 1, 2, 3$ conditions of $\Delta\nu_{iso} = n\nu_r$, the internuclear distance was determined to be 5.0 ± 0.5 Å via simulation. The dipolar coupling is only on the order of 50 Hz in this case, indicating the potential of this technique for observing such small interactions, and, hence, large spin–spin separations.

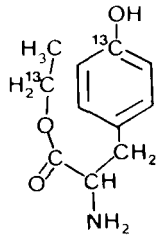

VIII

4. HETERONUCLEAR SPIN PAIRS

4.1 One-dimensional NMR studies of single-crystal and powder samples

The first rigorous treatment of NMR powder patterns due to isolated heteronuclear spin pairs was detailed by VanderHart and Gutowsky[126] in 1968. They proposed both moment and full line-shape methods of analysis to determine chemical shift, dipolar coupling and indirect coupling information from rigid-lattice NMR line shapes. In particular, the line-shape analysis was described in detail for three different isolated spin pairs:

(i) a heteronuclear spin pair ($S = \frac{1}{2}$, $I = n/2$) with overall axial symmetry and the unique chemical shielding component $\sigma_{\parallel}$ along r_{IS};

(ii) a heteronuclear spin pair ($S = \frac{1}{2}$, $I = n/2$) with axial symmetry at spin S, but also with an angle $\beta > 0°$ (designated χ by VanderHart and Gutowsky[126]) between r_{IS} and $\sigma_{\|}$; and
(iii) a homonuclear spin pair (A_2 spin system, $S_1 = S_2 = \frac{1}{2}$) with axial symmetry along r_{12}.

This approach included the effects of direct dipolar coupling and anisotropic chemical shielding, indirect spin–spin coupling and anisotropy in the indirect coupling. Analytical expressions were developed for cases (i) and (iii); for case (ii), simulations of line shapes required an iterative procedure. Most importantly, this represented the first treatment where $\beta \neq 0°$ i.e. $\sigma_{\|}$ and r_{IS} were not coincident. This theory was subsequently applied to ^{19}F and ^{31}P NMR powder spectra of $BaFPO_3$,[127] obtained at different field strengths, and provided information on the sign of $^1J(^{19}F, ^{31}P)$, the chemical-shift anisotropy for each nucleus and the F–P bond length. A moment analysis of the ^{19}F NMR spectrum yielded a ^{19}F chemical-shift anisotropy of 182 ± 22 ppm, and also indicated substantial intermolecular ^{19}F–^{19}F dipolar broadening. Phosphorus-31 line shape analysis gave a value for $\Delta\sigma$ of -145 ± 20 ppm, and indicated that the P–F internuclear distance was 1.63 ± 0.035 Å. The sign of $^1J(^{19}F, ^{31}P)$ was unambiguously determined to be negative by its influence on the ^{31}P NMR line shape.

Proton and ^{19}F NMR spectra of the FHF^- anion in a single crystal of KHF_2 displayed very large splittings due to the large dipolar interactions in this system.[128] The very short H–F separation allowed the dipolar couplings to be observed in the ^1H spectra without multiple-pulse line-narrowing techniques.[46] The variation in the splitting as a function of crystal orientation in the magnetic field yielded a ^1H–^{19}F separation of 1.153 ± 0.005 Å, in excellent agreement with neutron-diffraction results.

Dipolar-chemical shift powder NMR spectra were obtained for ^{13}C in $CH_3{}^{13}C^{14}N$ and for ^{13}C and ^{15}N in $CH_3{}^{13}C^{15}N$ at 83 K.[37] Although a theoretical treatment was not presented, simulations were included which provided values for the ^{13}C and ^{15}N chemical-shift anisotropies, as well as a C–N bond length of 1.182 ± 0.04 Å, approximately 0.03 Å larger than the value determined by microwave experiments. A later study of acetonitrile in a β-quinol clathrate[129] gave an unacceptably long bond length derived from the dipolar coupling; this was attributed to anisotropy in J coupling on the order of 430 Hz.

For $^{13}CH_3{}^{19}F$ isolated in an argon matrix, Zilm and Grant[55] derived a C–F bond length of 1.40 ± 0.02 Å from the ^{13}C NMR powder spectrum, only slightly longer (0.01 Å) than the values obtained from microwave and electron-diffraction experiments. One noted feature of the ^{13}C NMR spectrum was the presence of a small hump near the centre of the line shape, as shown in Fig. 18.

Fig. 18. ^{13}C NMR spectrum of $^{13}CH_3{}^{19}F$ in an argon matrix at 20 K and 20.12 MHz. (Reproduced with permission from Zilm and Grant.[55])

Zilm and Grant[55] observed that the intensity of this hump was reduced if the contact time for cross-polarization was carefully chosen. Recently, Gan *et al.*[130] have attributed this feature to transverse cross-relaxation between ^{13}C and ^{19}F nuclei, which arises from slowly oscillating non-secular components of the relaxation matrix. This effect is most significant for dipole-coupled pairs in which the internuclear vector is oriented at or near the magic angle with respect to $\mathbf{B}_0$. It also causes a small reduction in the observed dipolar splittings. However, as it has only been noted in spectra where dipolar coupling dominates, and no physical origin has been given, it is unlikely to be a principal source of error in measuring the dipolar coupling constant, R. The presence of the hump in the line shape at frequencies corresponding to orientations near the magic angle should indicate those cases where it must be considered. This should be distinguished from another distortion recognized by Zilm and Grant.[55] In an argon matrix, the CP ^{13}C NMR spectrum of acetylene-$^{13}C_2$ was observed to have reduced intensity at frequencies corresponding to orientations of the C–H vector in $\mathbf{B}_0$ at or near the magic angle, because of extremely inefficient cross-polarization at these orientations. Situations such as this may occur whenever one rare spin–abundant spin dipolar interaction dominates the polarization transfer.

Other distortions in the observed dipolar spectra of spin-$\frac{1}{2}$ nuclei were found to be introduced by neighbouring quadrupolar nuclei, as first

noticed by Casabella.[131] The ^{19}F NMR powder spectrum of BF_3 exhibited an asymmetric splitting due to dipolar coupling to ^{11}B, a quadrupolar $I = 3/2$ nucleus (80.42% natural abundance). Any effects due to dipolar coupling to the other boron isotope, ^{10}B ($I = 3$), were not apparent in the spectrum. The asymmetry was attributed to the perturbations of the ^{11}B Zeeman energy levels by the quadrupolar interactions, resulting in uneven separations between the four levels. Using a perturbation approach, Casabella succeeded in simulating the ^{19}F line shape and determined both the B–F bond length, 1.29 ± 0.04 Å, and the sign of the ^{11}B quadrupolar coupling constant, positive. This absolute-sign information was determined from the NMR spectrum; it is usually not available from NQR experiments.[132]

Several years later, VanderHart *et al.*[133] obtained unreasonably short metal–hydrogen bond lengths by moment analysis of the ^1H NMR powder line shapes of $HCo(CO)_4$ and $HMn(CO)_5$. To account for the effects of the quadrupolar interactions of ^{59}Co ($I = 7/2$) and ^{55}Mn ($I = 5/2$), they diagonalized the metal nuclei Zeeman-quadrupolar spin Hamiltonians to describe better the metal spin energy levels. Use of these results in calculating the dipolar ^1H NMR spectrum resulted in longer bond lengths. For example, the Co–H bond length as derived from the NMR spectrum increased from 1.42 Å to 1.57 Å when quadrupolar effects were included. For the Mn–H bond, the increase was from 1.28 Å to 1.42 Å. Curiously, this value is still substantially less than that determined by using neutron-diffraction experiments (1.60 Å).[134]

A single-crystal study involving a spin-$\frac{1}{2}$ nucleus dipolar coupled to a quadrupolar nucleus was performed by Spiess *et al.*[135] It was found that the effect of ^1H–^{127}I dipolar coupling on the ^1H NMR spectrum of *trans*-diiodoethylene was masked at some orientations of the single crystal, due to orientation-dependent self-decoupling of the quadrupolar ^{127}I ($I = 5/2$) nucleus. Such self-decoupling of the chlorine nuclei in matrix-isolated $(HCl)_2$ removed most of the effects of ^1H–$^{35/37}Cl$ ($I = 3/2$) dipolar coupling, resulting only in broadening of the ^1H spectrum.[60]

One of the clearest examples of the influence of the quadrupolar interaction on dipolar splittings was provided by a single-crystal ^{13}C NMR study of $K_2Pt(CN)_4Br_{0.3}\cdot 3H_2O$.[35] The variation in the ^{14}N Zeeman energy levels, and the accompanying variation in the ^{13}C–^{14}N dipolar splitting, as a function of crystal orientation in $\mathbf{B}_0$ was calculated (see Fig. 19). The C and D terms of the dipolar alphabet contribute to the observed coupling and were responsible for the asymmetric splittings. The dipolar splitting is unaffected when the principal component of $\chi(^{14}N)$ is directed along $\mathbf{B}_0$.

Powder line shapes of spin-$\frac{1}{2}$ nuclei are also influenced when the high-field approximation breaks down for a neighbouring quadrupolar nucleus. For example, in a ^{13}C NMR study of matrix-isolated nitromethane, Solum

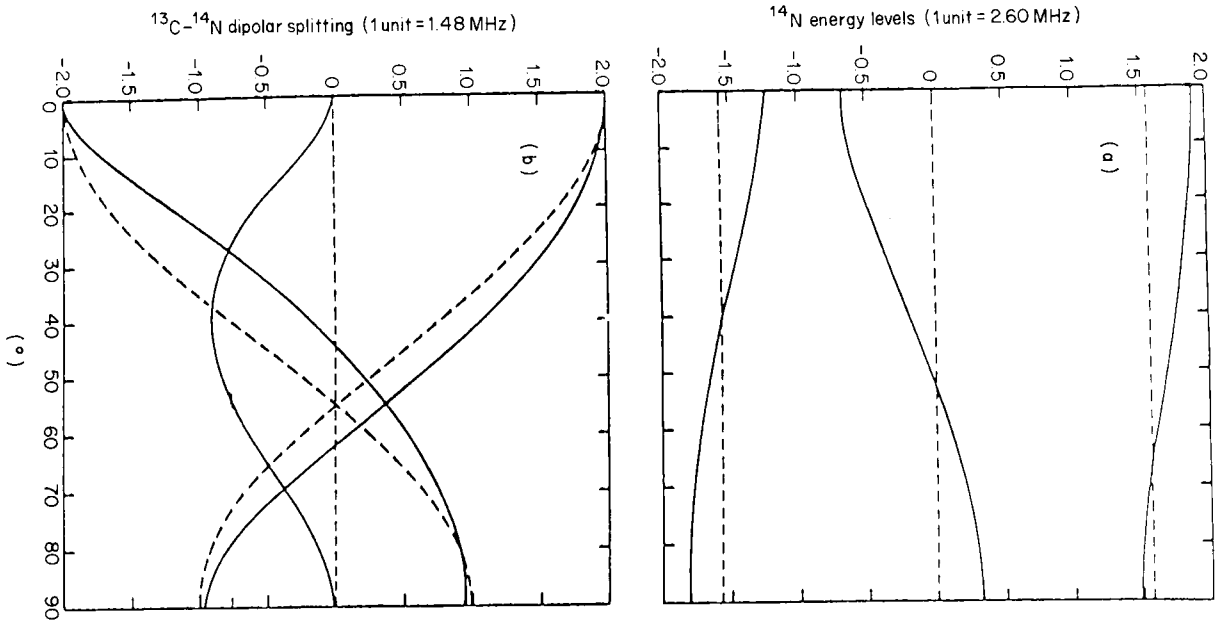

Fig. 19. (a) ^{14}N Zeeman-quadrupolar spin energy levels and (b) $^{13}C-^{14}N$ dipolar splittings as a function of orientation of the symmetry axis of the C≡N bond with respect to $\mathbf{B}_0$. The dashed lines in (a) and (b) correspond to the energy levels and splittings, respectively, that would be observed if the high-field approximation was valid. (Reproduced with permission from Stoll *et al.*[35])

et al.[136] were able to determine approximate information regarding the magnitude and orientation of the ^{14}N EFG tensor. However, the observed ^{13}C–^{14}N dipolar coupling was found to have an apparent trace, possibly arising from some molecular libration, which complicated the analysis and made definitive conclusions difficult. In ammonium thiocyanate,[137] the magnitude of the ^{13}C–^{14}N dipolar splitting along the unique axis of the linear $N{=}C{=}S^-$ ion is unaffected by the ^{14}N quadrupolar interaction. The C–N bond length (1.19 Å) obtained from this splitting (Fig. 20) is in excellent agreement with neutron and X-ray diffraction results. The dynamics of the cyanide ion in a solid solution KCN–KBr have also been investigated by using variable-temperature solid-state ^{13}C and ^{15}N NMR.[138] Although the ^{14}N quadrupolar coupling constant was quite large (ca. 4 MHz) compared with $\nu_0(^{14}N)$ (6 MHz), Doverspike *et al.*[135] were able to interpret the ^{13}C–^{14}N splittings in the ^{13}C spectra of ^{13}C-enriched KCN–KBr without considering the breakdown of the high-field approximation. Their results indicated a C–N bond length for the cyanide anion of 1.21 Å, derived from the ^{13}C NMR spectrum.

Quadrupolar distortions to the ^{13}P–^{14}N dipolar coupling in a series of monophosphazenes[139] were found to be minimal at $B_0 = 4.7$ T. The

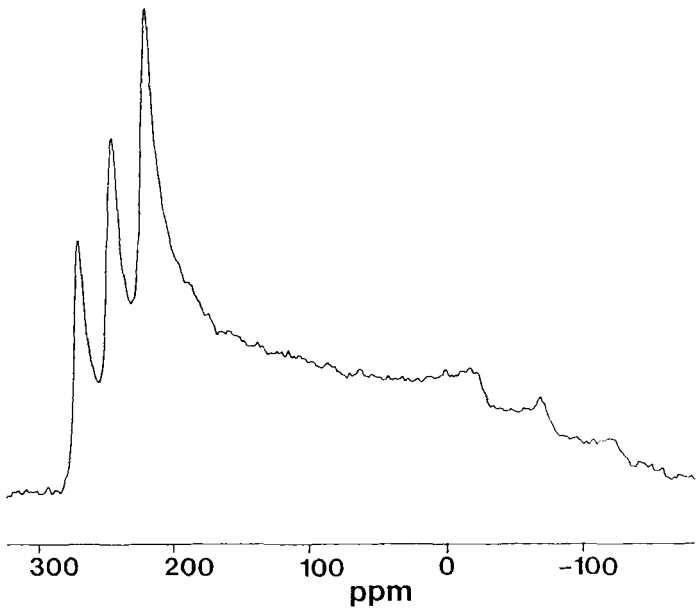

Fig. 20. ^{13}C NMR powder spectrum of NH_4SCN at $B_0 = 4.7$ T. The ^{13}C chemical shielding anisotropy is split into three subspectra due to dipolar coupling between ^{13}C and ^{14}N. (Reproduced with permission from Dickson *et al.*[137])

P–N bond length (1.60 ± 0.02 Å) in one of the monophosphazenes, *N*-(triphenyl)phosphoranylideneaniline ($Ph_3P{=}NPh$), was determined before diffraction values for this compound were available;[140] when this information was reported, the two values were found to be in excellent agreement. The orientation of the ^{31}P chemical shielding tensor in this P(V) compound, with the most shielded component directed along the P=N bond, was in marked contrast to that observed for the P(III) compound, diphosphene,[95] where the most shielded component lies perpendicular to the molecular plane.

The ^{14}N quadrupolar interaction appeared to have little effect on the ^{13}C–^{14}N dipolar coupling in the ^{13}C powder NMR spectrum of (*E*)-acetophenone oxime[141] at 4.7 T. However, the ^{13}C NMR powder line shape in benzylideneaniline[142] at the same field strength could only be simulated by considering the effect of the ^{14}N quadrupolar interaction on the ^{13}C–^{14}N dipolar coupling. In this case, it was found that the ^{13}C NMR spectrum was quite sensitive to the relative orientations of the ^{14}N EFG tensor, the ^{13}C chemical-shift tensor and the ^{13}C–^{14}N internuclear vector. Double isotopic enrichment with ^{13}C and ^{15}N at the C–N double bond in both the oxime[141] and the imine[142] permitted measurement of the principal components and orientation of the ^{15}N and ^{13}C chemical-shift tensors. As anticipated for carbon nuclei involved in π-bonding, the most shielded direction is perpendicular to the molecular plane. The ^{15}N NMR results indicated that the nitrogen shielding in these compounds was similar to that observed for azobenzene-$^{15}N_2$,[90] with the most shielded component, σ_{33}, oriented perpendicular to the molecular plane and σ_{22} lying approximately along the direction of the nitrogen lone pair.

By far the most popular application of one-dimensional dipolar–chemical shift NMR spectroscopy has been to the study of compounds of biological interest, particularly peptides.[143] The principal components of the ^{13}C chemical shielding tensors, their orientation and C–N bond lengths have been determined from dipolar NMR studies of several amino acid single crystals. Griffin and coworkers[36] were able to analyse the single-crystal NMR data for glycine without accounting for the ^{14}N quadrupolar interaction. The C–N bond length was 1.509 ± 0.009 Å, in agreement with neutron-diffraction results. Naito *et al.*[144] have characterized a number of amino acids in detail using ^{13}C NMR of single-crystal samples of L-alanine, L-serine, L-asparagine and L-histidine. Information on the ^{14}N EFG tensor was accessible by analysis of the effect it had on the ^{13}C–^{14}N dipolar splitting. In general, the principal component of the ^{14}N EFG tensor for peptide nitrogens is approximately 1.0 to 1.2 MHz, with η_Q close to 0.2. In glycine, however, the asymmetry is much higher, $\eta_Q = 0.54$.[36] The influence of ^{14}N on the ^{13}C NMR spectra of a single crystal of L-threonine[145] proved to be a useful assignment technique of the various ^{13}C chemical-shift tensors.

Isotopic enrichment with both ^{13}C and ^{15}N in a peptide bond provides an isolated spin pair at this chemically and biologically important site and avoids any complications arising from ^{14}N quadrupolar interactions. Such studies have focused on determination of the magnitudes and orientation of the principal components of the ^{13}C and ^{15}N chemical shift tensors. Single-crystal studies of [1-^{13}C]glycyl[^{15}N]glycine·HCl·H_2O have been used to characterize the ^{13}C and ^{15}N chemical-shift tensors at the peptide linkage. From the ^{13}C NMR study,[146] the ^{13}C–^{15}N bond length was found to be 0.06 Å longer than that obtained by X-ray diffraction; the subsequent ^{15}N analysis[147] yielded a lower value (1.340 Å) which is close to neutron (1.33 Å) and X-ray (1.325 Å) diffraction results. The principal components and orientation of the ^{13}C chemical-shielding tensor were found to be analogous to reported values for carbonyl and carboxyl ^{13}C nuclei in related molecules, with σ_{33}, the most shielded component, perpendicular to the carbonyl plane and σ_{22} close to the C=O bond, leading the authors to propose that the ^{13}C shielding parameters should be similar in all peptide bonds. Analysis of the ^{15}N NMR spectrum indicated that the least shielded component, σ_{11}, of the ^{15}N chemical-shielding tensor was oriented 21.3° from the N–H bond. The near-axial symmetry of this tensor precluded orienting the other components in the molecular frame. The nitrogen shielding parameters were also proposed to be general for all peptide bonds. Typical orientations of peptide ^{13}C and ^{15}N chemical-shift tensors are given in Fig. 21, and a variety of ^{15}N chemical-shift-tensor components and orientations derived from ^{13}C dipole-coupled ^{15}N powder NMR spectra of ^{13}C, ^{15}N-labelled peptides are given in Table 3.

One-dimensional dipole-coupled chemical shift powder spectra of a series of ^{13}C- and ^{15}N-labelled dipeptides were used to determine the principal components of the ^{13}C and ^{15}N chemical-shift tensors, as well as their orientations relative to the ^{13}C–^{15}N bond.[148] Representative ^{13}C and ^{15}N

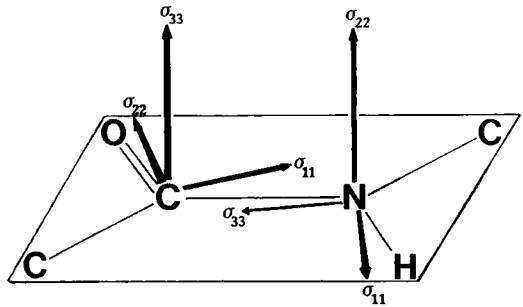

Fig. 21. Typical orientations of chemical-shielding tensors for carbon and nitrogen nuclei involved in a peptide bond.

Table 3. ^{15}N NMR parameters for nitrogen nuclei involved in peptide bonds. The parameters include the principal components of the chemical shift tensor, the ^{15}N–^{13}C dipolar coupling constants, R (and the corresponding C–N separation), and the relative orientation of the nitrogen shift tensor with respect to the internuclear vector, as illustrated in Fig. 7. In some cases, the data has been modified to conform to the convention outlined in Section 2.

System	$\delta_{11}, \delta_{22}, \delta_{33}$[a]	R(Hz)(r_{CN}(Å))	α, β (°)	Ref.
GlyGly·HCl	216, 71, 60	1273(1.340)	0.9, 8.6	147
GlyAla	229, 85, 45	1150–1250 (1.39–1.35)	0, 10	148b
GlyTyr	209, 77, 52	"	0, 8	148b
GlyGly·HCl	210, 60, 57	"	0, 9	148b
GlyGly	211, 64, 41	"	0, 10	148b
AlaAla	216, 78, 65	1260(1.34)	5, 16	148c
AlaPro	226, 130, 29	1210(1.36)	0, 20	150
Gramicidin A				
Gly^2Ala^3	—	1275(1.34)	0, 14	153
Ala^3Leu^4	—	1275(1.34)	0, 15	

[a]Chemical shifts are in ppm relative to external $^{15}NH_3$(l).

powder NMR spectra of these samples are shown in Fig. 22. The ^{13}C chemical-shift tensors were found to differ significantly in orientation through the homologous series of dipeptides, as did the magnitude of the intermediate shielding component. For the carbonyl carbon of the peptide fragment, σ_{33} was consistently perpendicular to the peptide plane, with σ_{22} along or close to the C=O bond. The orientation of the principal components of the nitrogen chemical-shift tensor was relatively constant. In all compounds investigated, the peptide ^{15}N chemical-shift tensor was oriented such that σ_{22} was perpendicular to the peptide plane and σ_{33} was close to the $^{13}C(O)$–^{15}N bond. The differences in chemical shielding in the series, as well as the differences between the solution and solid-state isotropic-shift values, were attributed to lattice effects, such as the geometry of the hydrogen-bonding networks. The use of a standard chemical-shift tensor for ^{13}C and ^{15}N nuclei in all peptide bonds based on the previous single-crystal studies[146,147] was questioned as a result of the variations in shielding observed in this study. The ^{13}C and ^{15}N spectra in this series of dipeptides were simulated by least-squares fitting of particular regions of the spectra in the derivative mode.[149] In order to obtain reasonable fits from the somewhat distorted spectra, analysis was limited in most cases to the areas of maxima and inflection points of the absorption line shape. The use of first- and second-derivative plots of these regions increased the sensitivity of the fitting procedure. However, it is important to recognize

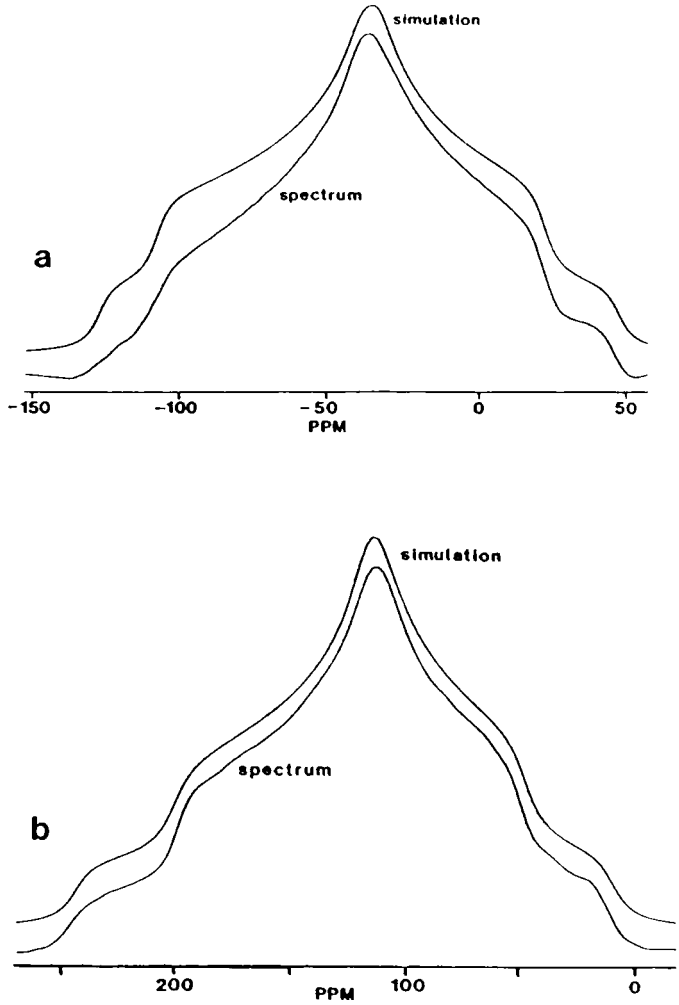

Fig. 22. (a) ^{13}C and (b) ^{15}N NMR powder spectra of L-[1-^{13}C]alanyl-L-[^{15}N]alanine at $B_0 = 4.7$ T. (Reproduced with permission from Hartzell *et al.*[1480])

that a very high signal-to-noise ratio is required to obtain satisfactory derivative spectra.

One important aspect of the least-squares fitting was the observation of the high covariance between the value of the dipolar coupling constant and the angles α and β, which orient the internuclear vector in the principal-axis system of the chemical-shift tensor.[149] In other words, small changes in R

could be accommodated by small changes in the values of the angles, resulting in identical calculated powder spectra for a range of R, α and β values. Consequently, it is often necessary either to assume a value for R based on internuclear separations reported from other techniques and derive the orientation of the chemical-shift tensor, or to assume an orientation for the chemical-shift tensor and determine the internuclear separation.

The ^{15}N chemical-shift tensor of the imide nitrogen of proline was determined by analysis of the ^{13}C-dipole-coupled ^{15}N NMR powder line shape of Boc-L-[1-^{13}C]alanyl-L-[^{15}N]prolyl-OBz.[150] The principal components of this tensor and its orientation were similar to those reported earlier for other peptide nitrogens. The C–N bond length (1.36 Å) was within the range expected for peptide bonds.

The orientation and principal components of the ^{15}N chemical-shift tensor were determined for Boc-glycylglycyl [^{15}N, ^{2}H]glycine benzyl ester, using the ^{15}N–^{2}H spin pair.[151] Two crystalline forms of this compound could be obtained; one exhibited a typical peptide ^{15}N chemical-shift tensor, with almost no asymmetry, while the other possessed a significantly asymmetric chemical-shift tensor with $\eta_\sigma = 0.44$. The ^{2}H-coupled ^{15}N powder NMR spectra indicated no apparent difference in the shift-tensor orientations, while the ^{2}H NMR spectra indicated both no difference in hydrogen bonding, and, together with ^{15}N relaxation measurements, no appreciable motion. It was suggested that the asymmetry was due to a non-planar peptide bond, although this could not be confirmed. The spectra from the ^{15}N–^{2}H spin pairs for peptides appeared to be of better quality than those of the ^{13}C–^{15}N spin pairs for peptides, and may prove attractive due to the ease with which ^{2}H enrichment can be achieved, as the amide hydrogen is exchangeable. However, the quality of the powder line shapes for ^{13}C, ^{15}N-enriched peptides has been improved by application of COMARO-2 broad-band decoupling.[152]

The orientation dependence of the ^{13}C and ^{15}N chemical shift and the ^{13}C–^{15}N dipolar coupling has been used to orient the peptide planes within Gramicidin A, a polypeptide.[153] In these dipolar–chemical shift NMR powder spectra, the splittings about the chemical-shift tensor principal components were analysed to provide estimates of the orientation of the ^{15}N chemical-shift tensor, much the same as was described for homonuclear spin pairs.[90] The estimates were then refined further by simulation of the full line shape. The claim by Oas and coworkers[148] of an invariant orientation of the peptide ^{15}N chemical-shift tensor was disputed in light of the results of this investigation. Cross has determined the torsional angles ϕ and ψ for the amino acid sequence, D-Val-8–L-Trp-9–D-Leu-10, using the ^{13}C–^{15}N and ^{15}N–^{1}H dipolar couplings.[154] Opella and coworkers have developed a computer routine to determine relative orientations of peptide planes in a protein backbone from such data.[155] Orientation dependence of the ^{15}N–^{1}H, ^{14}N–^{1}H, ^{13}C–^{15}N and

^{13}C–^{1}H dipolar couplings, as well as chemical-shift or quadrupolar interactions were used to derive the torsion angles ϕ and ψ, which were then checked on a Ramachandran plot to obtain the secondary structure, e.g. α-helix and β-sheet.

Another biologically important species, the choline cation, $[(CH_3)_3{}^{15}N{}^{13}CH_2CH_2OH]^+$, has been investigated by ^{13}C powder NMR.[156] The principal components of the ^{13}C chemical-shift tensor and their orientation were determined with respect to the ^{13}C–^{15}N bond, although dipolar coupling to chloride and bromide counterions led to severe line broadening.

Dipolar couplings are also evident in the NMR spectra of quadrupolar nuclei. Stark *et al.*[157] first observed splittings due to the ^{1}H–^{14}N dipolar interaction in the ^{14}N NMR spectrum of a single crystal of *N*-acetylvaline, and derived a N–H bond length of 1.06 Å. Overtone ^{14}N NMR spectra[158] were also found to be sensitive to ^{14}N–^{13}C and ^{14}N–^{1}H dipolar coupling. These spectra have been used to derive bond lengths and orientational information for amino acids and peptides. Scheubel *et al.*[159] determined the C–O bond length in a single crystal of benzophenone to be 1.213 ± 0.005 Å from the effect of ^{13}C–^{17}O dipolar coupling on the ^{17}O NMR spectrum. Dipolar coupling between ^{14}N and ^{2}H in urea-d_4 was also found to influence the ^{2}H NMR powder spectra.[160]

Spin pairs in inorganic compounds have also been studied. Cadmium(II) acetate dihydrate single crystals have been investigated via ^{13}C and ^{113}Cd NMR.[161,162] The ^{113}Cd–^{13}C dipolar interaction was evident in the carboxyl ^{13}C resonance, and corresponded to C–Cd distances of 2.822 Å and 2.783 Å for each distinct acetate ligand.[161] The ^{13}C–^{1}H and ^{13}C–^{113}Cd dipolar interactions were used to differentiate between the crystallographically distinct sites.

The ^{13}C–^{11}B dipolar interaction in boron carbide was used to identify the site occupancies for carbon.[163] Due to the different strengths of this coupling for different carbon sites, ^{13}C spin-echo NMR experiments were able to show that the carbon was present exclusively as C_3 chains. The two types of carbon environment (terminal and central) exhibited spectra indicative of their site symmetry.

The structure of fluorophosphate glasses has been studied using ^{19}F and ^{31}P NMR.[164] The second moment of the observed line shapes was interpreted using the theory of VanderHart *et al.*[126,127] Due to the low applied magnetic field strength, the influence of anisotropic chemical shifts was negligible. The ^{19}F–^{31}P dipolar coupling corresponded to a F–P separation of approximately 1.6 Å. Recent analysis by Grimmer *et al.*[165] of the ^{31}P powder line shapes of a series of polycrystalline fluorophosphates has determined substantial anisotropies in the *J* coupling for the ^{31}P–^{19}F spin pair, on the

order of 3 kHz. The P–F bond lengths from X-ray diffraction studies were used to calculate a value for the direct dipolar coupling constant.

Theoretical calculations by Pyykkö and Wiesenfeld[57] indicate that the indirect couplings involving heavier nuclei of the periodic table are substantially anisotropic. This is supported by several experimental NMR studies of solids. In a series of tellurides, Nolle and coworkers[166] found ΔJ between ^{125}Te and a metal nucleus to increase as one moves down group 12 of the periodic table, e.g. ZnTe, CdTe and HgTe. A large anisotropy in J has been reported for the ^{31}P–^{199}Hg spin pair in $[HgP(o\text{-tolyl})_3(NO_3)_2]_2$.[167] From the ^{31}P powder NMR spectrum illustrated in Fig. 23, with the assumption of a bond length from diffraction studies, a value of $\Delta J(^{31}P, ^{199}Hg) = +5170 \pm 250$ Hz was obtained, and the sign of $J_{iso}(^{31}P, ^{199}Hg)$ was determined to be positive in a single experiment. The large value of $^1J(^{31}P, ^{199}Hg)$, +9660 Hz, compared with $R(^{31}P, ^{199}Hg)$, 634 Hz, provided a well-resolved separation of the two subspectra in the ^{31}P spectrum from the central line shape. This feature, due to ^{31}P nuclei which are bonded to Hg nuclei possessing no nuclear

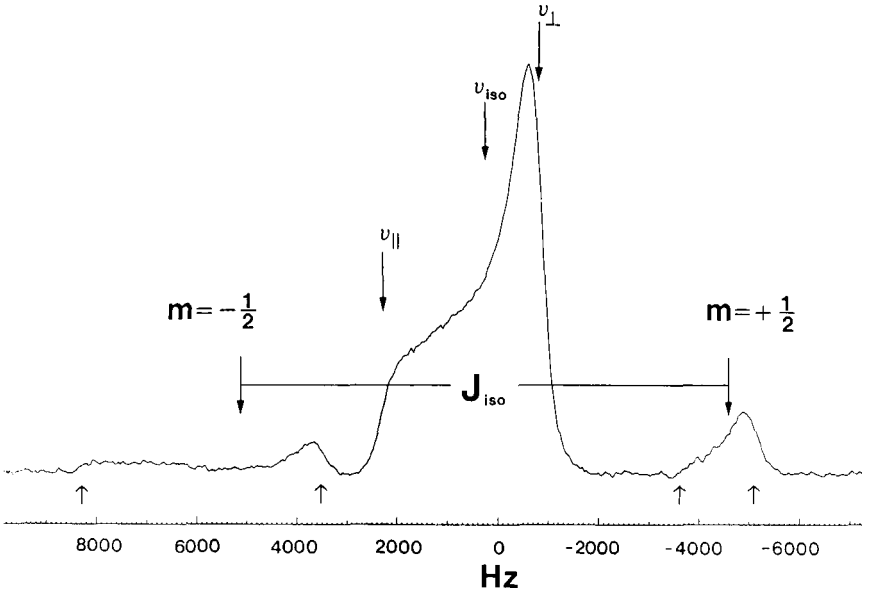

Fig. 23. ^{31}P NMR powder spectrum of $[HgP(o\text{-tolyl})_3(NO_3)_2]_2$ at $B_0 = 4.7$ T. The satellites are due to ^{31}P nuclei which are bonded directly to ^{199}Hg (16.84% natural abundance) and are split by $^1J_{iso}(^{31}P, ^{199}Hg)$. The central feature of the ^{31}P spectrum is due to phosphorus sites which are adjacent to Hg nuclei other than ^{199}Hg. (Reproduced with permission from Penner *et al.*[167])

spin, allowed unambiguous values for the ^{31}P chemical-shift-tensor principal components to be derived.

The influence of dipolar coupling on NMR spectra has also been utilized to study small molecules on surfaces by NMR, and has been reviewed recently by Slichter and coworkers.[168,169] The surface species have been characterized using spin-echo[84] and spin-echo double-resonance (SEDOR)[170] experiments. The spin-echo experiment permits measurement of homonuclear dipolar couplings by removing the effects of anisotropic chemical shielding, heteronuclear coupling and magnetic susceptibility interactions from the magnetization at the echo maximum. The SEDOR experiment performs the identical function for a heteronuclear spin pair, and depends on the observation of dipolar modulation of echo formation after π pulses are applied to both of the dipolar-coupled nuclei. The variation in the echo amplitudes as a function of pulse spacing depends on the strength of the heteronuclear dipolar coupling, which corresponds to the internuclear distance. SEDOR has been used to determine dispersions, or particle sizes, in supported Pt catalysts, by distinguishing between surface and bulk Pt on the basis of dipolar coupling to chemisorbed ^{13}CO.[171] This technique has also been applied to the ^{13}C–^{1}H spin pair in acetylene chemisorbed on Pt[111][172] and in ethylene on small Pt clusters,[85] as well as the ^{13}C–^{17}O spin pair in carbon monoxide chemisorbed on Pd.[173] For acetylene on Pt, SEDOR results, as well as ^{13}C spin-echo spectra and ^{1}H multiple-quantum NMR, were used to identify 77% of the surface species as $C{=}CH_2$, while 23% existed as HCCH. In this study, the C–C bond length for the predominant species was 1.44 Å, halfway between that accepted for a C–C double bond and a C–C single bond. For ethylene chemisorbed on Pt, the SEDOR experiment indicated that only approximately half of the ^{13}C nuclei were attached to ^{1}H, giving further evidence of the ethylidyne structure[85] (see also the discussion in Section 3.2). The ^{13}C isotropic chemical shift of CO adsorbed on Pd was + 540 ppm, about 310 ppm to high frequency of the ^{13}C shift in metal carbonyls. This was attributed to a Knight shift promoted by the conduction band of the Pd particles. ^{17}O SEDOR analysis provided a value for the C–O bond length of 1.20 ± 0.03 Å, indicating the carbonyls were in bridging positions over Pd atoms.

4.2. Separated local field spectroscopy of static samples

One is faced with various problems when attempting to derive dipolar and anisotropic chemical shielding information from NMR experiments on static samples, particularly when the spin pair of interest consists of rare spins coupled to ^{1}H nuclei. These difficulties include overlap of spectra arising from spin pairs in crystallographically or magnetically nonequivalent sites, spin

diffusion among the abundant spins and the relatively long range of the dipolar interactions. These difficulties can be circumvented by using a two-dimensional experiment which separates the dipolar and the anisotropic chemical shifts, enabling one to measure each independently. One way of accomplishing this is to use separated local field (SLF) spectroscopy, a two-dimensional technique proposed in 1976 by Waugh[40] to resolve rare spin (S)–abundant spin (I) dipolar couplings from rare spin chemical shielding parameters. In one dimension, I–S dipolar evolution occurs under homonuclear spin I multiple-pulse decoupling, and in the other dimension, spin S signals are separated via their chemical shifts. Such an experiment, illustrated in Fig. 5(c), was suggested as a means of obtaining structural information about the abundant spins (specifically ^1H) in solid samples. The symmetry of the dipolar interactions allowed spectra to remain relatively simple despite the influence of surrounding I spins. Implementation of homonuclear multiple-pulse decoupling schemes scales the size of the I–S dipolar interaction. This proves useful for ^{13}C–^1H spin pairs as it results in the ^{13}C chemical shielding and ^{13}C–^1H dipolar interaction being comparable in magnitude, rather than having the dipolar coupling completely dominate the spectra.

Single-crystal SLF spectra of calcium tartrate and calcium formate illustrated how the dipolar information was resolved via chemical-shift differences.[39] It appears that this technique is limited to cases where there is no overlap in the chemical-shift dimension (ω_2), as would be provided by a single crystal or MAS experiment. The SLF technique was also applied to carbon atoms with zero to three protons attached, and the resulting single-crystal ^{13}C NMR spectra displayed the patterns predicted by theory.[174] The problem of overlapping spectra was apparent in the ^{13}C SLF spectra of ammonium hydrogen malonate, illustrated in Fig. 24, as the two CH_2 groups in the asymmetric unit possessed identical chemical shifts but different dipolar couplings at particular crystal orientations. However, this technique does provide an alternative to neutron diffraction in determining proton positions in solids. Carbon–hydrogen bond lengths of 1.09 Å in diacetylene[175] and 1.10 Å in oriented polyethylene[176] have been reported along with the ^{13}C chemical-shielding-tensor data. A similar type of experiment suited to observation of ^{14}N–^1H splittings in ^{14}N single-crystal spectra of L-histidine was developed[177] that separated the quadrupolar and dipolar splittings onto orthogonal axes in a two-dimensional SLF experiment.

In 1976, Stoll *et al.*[178] proposed a powder experiment similar to Waugh's SLF technique that differed in two respects. First of all, a spin-echo was used to refocus the chemical shift of the S spin, thus removing its effects from the dipolar dimension (ω_1), and second, only the chemical-shift time dimension was Fourier transformed. This resulted in a I dipole-modulated S chemical-shift spectrum, providing information on the internuclear I–S separation and

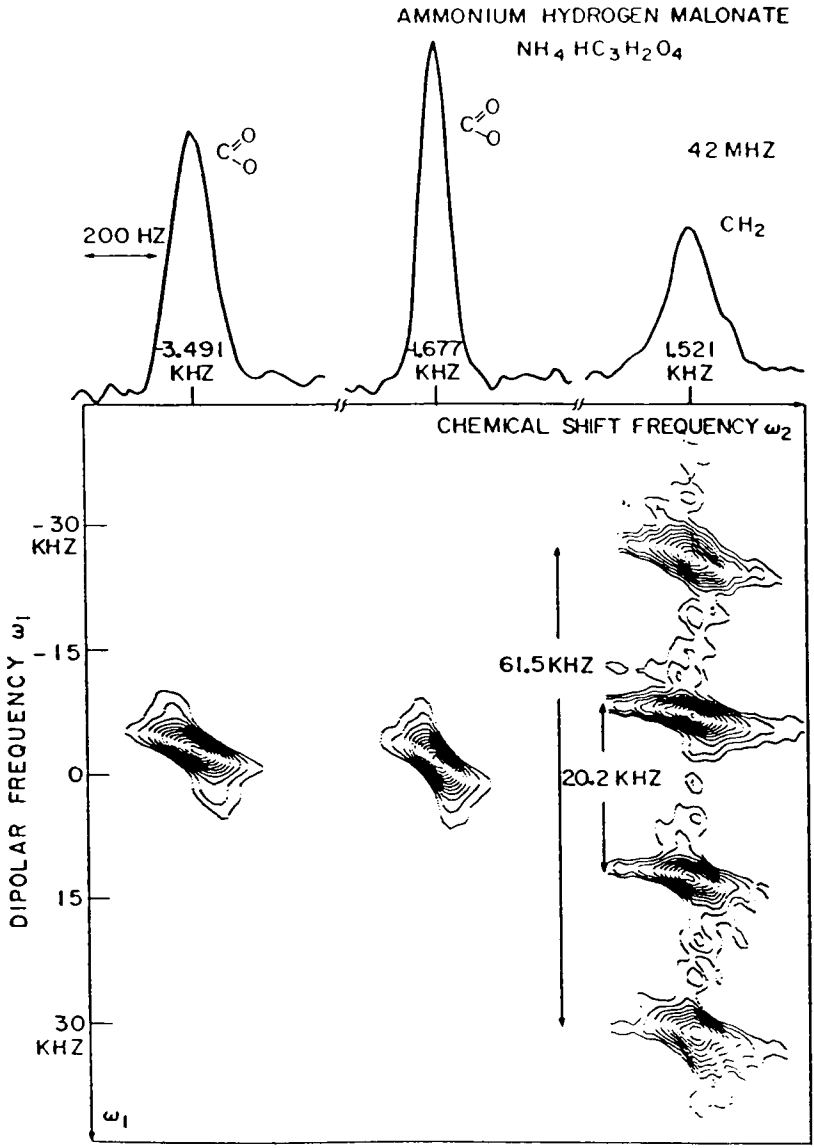

Fig. 24. ^{13}C SLF single-crystal spectrum of $NH_4O_2CCH_2CO_2H$. Note that there are two distinct splittings due to ^{13}C–^{1}H dipolar coupling. (Reproduced with permission from Rybaczewski *et al.*[174])

the orientation of the S chemical-shift tensor with respect to the I–S bond. The homonuclear analogue of this experiment was also described by Stoll *et al.*[62] (see Section 3.1).

Linder *et al.*[177] used a full two-dimensional frequency spectrum to provide separated dipolar coupling and anisotropic chemical shielding information from powder samples. Fourier transformation in both dimensions of the signal array resulted in more conventional two-dimensional powder patterns, where the point of greatest width in the dipolar dimension, i.e. the I–S bond direction, could be easily related to the S chemical-shift-tensor orientation. "Ridge plots" were proposed as a rapid technique to provide estimates of the various parameters. However, both these powder techniques are limited to samples containing only one dominant I–S spin pair; any spectral contribution from other nuclei or interactions may lead to spectra which are too complicated to interpret.

Studies of $^{13}C-^{1}H$ and $^{15}N-^{1}H$ spin pairs by SLF spectroscopy have been performed mainly on amino acids and peptides. Cross and Opella[180,181] have used SLF spectra to determine the orientation of particular amino acid residues or peptide planes with respect to the protein backbone of the bacteriophage *fd* coat protein. Both the ^{15}N chemical shift and the $^{15}N-^{1}H$ dipolar splitting provided orientation information for a particular ^{15}N enriched amino acid in this protein in solution, when compared with the powder spectra.[180] The *fd* coat protein self-oriented in solution due to the magnetic susceptibility induced by the large number of similarly oriented carbonyl groups; thus, solid-state NMR experiments could be performed on a "solution" sample. The three-dimensional structure of one section of this protein was also determined in this manner.[181] The $^{15}N-^{1}H$ and $^{15}N-^{13}C$ dipolar and ^{15}N chemical-shift spectra of *fd* coat protein with isotopically labelled amino acid residues 40–45 provided the orientation of the amino acids and the helical axis with respect to the protein filament axis. Detailed analysis indicated a bend in the α-helix at Lys-43, presumably to promote protein–DNA interactions. These techniques were also applied to compare the amount of mobility in membrane-bound and virus-bound forms of the *fd* coat protein.[182] The $^{15}N-^{1}H$, SLF, ^{15}N chemical shift and ^{2}H NMR spectra all showed that there was substantially more motion in the membrane-bound form at both the N and C termini.

Application of $^{15}N-^{1}H$ SLF spectroscopy allowed the determination of the orientation of [^{15}N]-Ala-3 in Gramicidin A embedded in a membrane.[183] The β-helix was found to be tilted less than 10° from the bilayer normal, indicating that this helix may be right handed rather than left handed, as assumed. In order to avoid miscalibration of the multiple-pulse scaling factor, homonuclear decoupling was not applied during the dipolar evolution period.

The $^{13}C_\alpha$–^1H bond length in a single crystal of L-alanine was found to be 1.073 Å from SLF spectra,[184] 0.018 Å longer than that determined by neutron diffraction. In this experiment, it was possible to separate the $^{13}C_\alpha$–^1H dipolar splittings from the $^{13}C_\alpha$–^{14}N splittings, resulting in six lines for each magnetically unique $^{13}C_\alpha$.

The ^{13}C–^1H spin pair in dimedone (5,5-dimethyl-1,3-cyclohexanedione) has been studied by Takegoshi and McDowell[185] in order to determine the extent of flip-flop spin exchange between the ^{13}C-coupled proton and the surrounding bath of ^1H nuclei. This was performed both with and without perturbing proton radiofrequency fields. A new experiment, EXSLF (exchange-SLF), was used to study the ^1H spin dynamics in the absence of radiofrequency fields. Analyses with perturbing radiofrequency fields were performed by studying ^{13}C–^1H cross-polarization dynamics. The results indicated that the ^{13}C–^1H spin pair in dimedone was indeed isolated.

Two-dimensional dipole-correlated ^{13}C chemical shift NMR was used to determine the principal values and orientation of the ^{13}C chemical-shift tensor in polyoxymethylene.[186] The ^{13}C–^1H dipolar interaction provided an internal reference frame for this powder experiment, the results of which were used to study molecular motion in this polymer.

Another two-dimensional dipole-modulated chemical-shift NMR experiment has been described that can be used to study isolated I_2S systems,[187] such as $^{13}CH_2$ or $^{15}NH_2$ groups. In the first time dimension, the system was allowed to develop under the I–S dipolar interaction alone; multiple-pulse homonuclear decoupling and spin echoes were used to eliminate the effects of I–I coupling and S chemical shifts. In the second time dimension, under broadband I spin decoupling, only S chemical shift effects were allowed to evolve. This experiment was performed on the $N_\gamma H_2$ group of L-asparagine·H_2O, providing information on N–H bond lengths, the H–N–H bond angle and the ^{15}N chemical-shift-tensor components and orientation. Fourier transformation of t_1 data was unnecessary, as only three or four t_1 values were required in the analysis.

This approach has been expanded to a three spin IRS system, such as ^1H–^{13}C–^{15}N, by Hartzell *et al.*[188] The ^{15}N chemical-shift tensor in L-[1-^{13}C]alanyl-L-[^{15}N]alanine was unambiguously oriented by means of ^1H dipole-modulated ^{13}C dipole-coupled ^{15}N powder NMR. This two-dimensional experiment was similar to the SLF technique, as the ^{15}N–^1H dipolar interaction alone evolved during t_1 with multiple-pulse decoupling. In t_2, under ^1H decoupling, the system evolved according to the ^{15}N chemical shift and ^{15}N–^{13}C dipolar coupling, both of which were refocused at $t_2 = 0$ by a ^{15}N π pulse during t_1. This resulted in spectra such as that shown in Fig. 25. The angular relations for both sets of dipolar couplings allowed only one consistent orientation for the ^{15}N chemical-shift tensor. Deviations of the

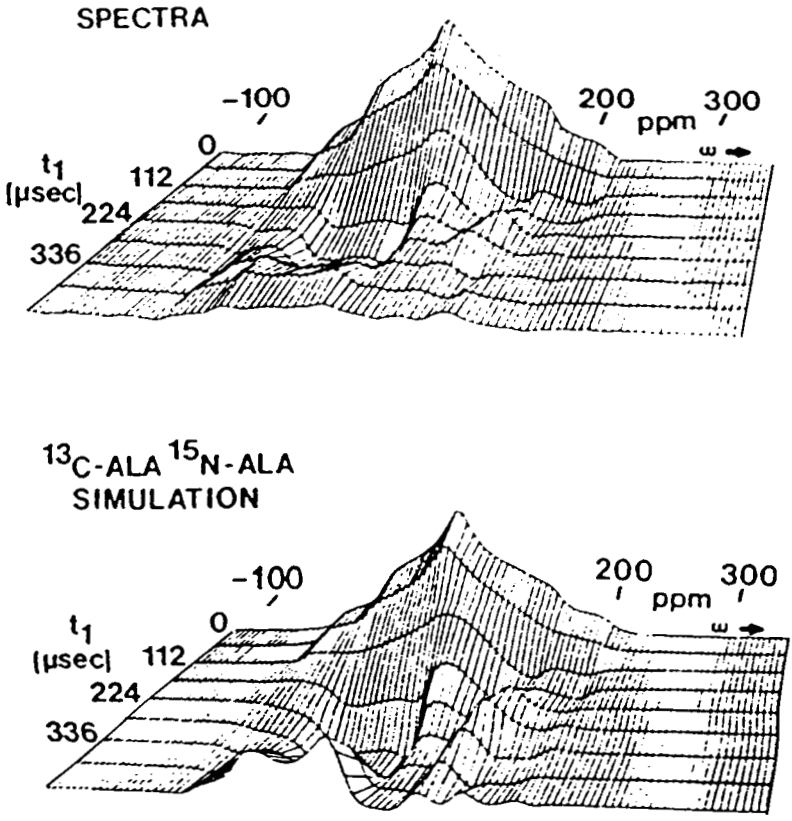

Fig. 25. ^{1}H dipole-modulated ^{13}C dipole-coupled ^{15}N powder NMR spectra of L-[1-^{13}C]alanyl-L-[^{15}N]alanine: (a) experimental and (b) calculated. The time scale t_1 corresponds to ^{15}N–^{1}H dipolar evolution, and the frequency axis ω contains the ^{13}C–^{15}N dipolar coupling and ^{15}N anisotropic chemical-shift information. (Reproduced with permission from Hartzell *et al.*[188])

peptide linkage from planarity can, in principle, be investigated using this technique.

The dipolar interaction can be used to obtain spectra of solids analogous to solution COSY spectra.[189,190] The limited resolution afforded by one-dimensional ^{1}H solid-state NMR spectra was improved by correlating the ^{1}H signals with the chemical shifts of the ^{13}C nuclei to which they were bonded, in both single crystals[189] and rotating solids.[190] Coherence transfer between the ^{1}H and ^{13}C spins was effected via the heteronuclear dipolar interaction between them.

4.3. One-dimensional MAS studies

The combined effects of chemical shielding, dipolar coupling and indirect coupling on the spinning sidebands in slow-spinning MAS spectra of two isolated heteronuclear spin-$\frac{1}{2}$ nuclei, such as the ^{13}C–^{31}P spin pair in phosphonium iodides, have been described by Harris *et al.*[191] Their method relies on the presence of a significant isotropic indirect coupling constant, $^1J_{iso}(^{13}C, ^{31}P)$, to separate the $m_I = +\frac{1}{2}$ and $m_I = -\frac{1}{2}$ subspectra due to coupling in the MAS spectrum. Making a number of reasonable assumptions, the sign of J_{iso} was assigned by simple inspection of the spinning side-band patterns for the subspectra. Stable spinning speeds and a high signal-to-noise ratio are essential to derive information by this side-band analysis. The theory of Zilm and Grant[55] was recast into a different set of equations and was applied following analysis of the side-bands, such as is accomplished by using a Herzfeld–Berger analysis.[192] These equations may also be applied to powder spectra, and can be used to determine, among other things, the orientation of the chemical-shift tensor from a single slow-MAS spectrum. However, on the basis of the experimental spectra presented, the errors in the derived parameters were quite large. This analysis could not be extended to the AX_2 spin system tributyltin fluoride, where each ^{119}Sn nucleus was coordinated to two ^{19}F, due to a low signal-to-noise ratio and the presence of impurities also containing tin.[193] Three subspectra in a 1:2:1 ratio were apparent in the MAS spectra, with $J(^{119}Sn, ^{19}F) = 1291$ Hz. It was possible, however, to derive a ^{119}Sn chemical shift anisotropy of 355 ppm, with $\eta_\sigma = 0.42$, from the MAS side-band pattern.

Recently, Grimmer and Neels[194] have analysed the ^{31}P MAS spectra of $K_3Na(PO_3F)_2$ via Herzfeld–Berger analysis[192] of the spinning side-bands. The isotropic J coupling between the ^{31}P and ^{19}F nuclei (795 Hz) separated the side-bands arising from each subspectrum. They obtained a value of 14 735 $\pm$ 320 Hz for the ^{31}P–^{19}F dipolar coupling, which corresponds to a P–F separation of 1.46 Å, assuming no anisotropy in J.

^{15}N CP/MAS spectra of the platinum complex, *cis*-di(ammine-^{15}N)bis(thiocyanato-S)-platinum(II), were used to determine the ^{15}N chemical-shift tensor as well as dipolar and indirect coupling tensors for the ^{15}N–^{195}Pt spin pair system.[195] The value of $J(^{195}Pt, ^{15}N)$, approximately 270 Hz, was large enough to separate the $m_I = +\frac{1}{2}$ and $-\frac{1}{2}$ subspectra. The components of the ^{15}N chemical-shift tensor perpendicular to the Pt–N bond were shifted substantially to higher frequency, and this was attributed to the "heavy-atom" shift. The authors reported that the ^{15}N shielding tensor resembled those of peptide nitrogens more closely than those of ammonium or amine nitrogens.

VanderHart has observed field-dependent ^{13}C chemical shifts in rotating

solids.[196] While small in magnitude at low magnetic field, e.g. less than 1 ppm at 1.4 T, they were negligible at higher field strengths. This effect originates in the C and D terms of the $^{13}C-^{1}H$ dipolar interaction. Strong proton irradiation (continuous wave (CW) decoupling) causes the ^{1}H spin to be quantized along the radiofrequency field in the ^{1}H rotating frame. The proton spin precesses about B_1, causing a sinusoidal variation in the z component of the ^{1}H magnetization, and dipolar coupling terms which are not averaged by MAS contribute to the observed spectrum. The second-order shifts are proportional to B_0^{-2}. For the polymers studied, these shifts varied according to the type of carbon: CH_2, 0.70 ppm; CH, 0.34 ppm; CH_3 (rotating), 0.07 ppm; and C (quaternary), -0.04 ppm. Restricted motion reduced these shifts according to the angle of the rotation axis with respect to the C–H vector, while isotropic motion averaged these shifts to zero.

4.4. Quadrupolar effects in MAS spectra

Soon after the acquisition of ^{13}C CP/MAS spectra from natural abundance samples became routine, it was pointed out by Lippmaa and coworkers[197] that there were field-dependent splittings in the spectra of carbons which were directly bonded to nitrogen, of which 99.635% is the quadrupolar $I = 1$ ^{14}N nuclear isotope. These splittings did not result in an equally spaced triplet, as one might intuitively expect for J coupling to an $I = 1$ nucleus, but in asymmetric doublets (see Fig. 26), with a characteristic 2:1 intensity ratio.[198] Upon substitution with ^{15}N, these splittings disappeared;[199] the magnitude of the splitting decreased as the magnetic field strength was increased.[144a] These facts indicated that the quadrupolar nature of ^{14}N is responsible for this effect.

Several theoretical treatments for the calculation of these MAS line shapes followed, using both perturbation theory[200,201] and diagonalization procedures[202,203] to calculate the ^{14}N spin eigenfunctions. Recently, Olivieri *et al.*[204] have proposed a simple expression that can be used to interpret the asymmetric splitting. As the ^{14}N quadrupolar interaction is often of the same order as its Zeeman interaction, the ^{14}N spins are not fully quantized along the magnetic field, but along some superposition of $\mathbf{B}_0$ and the principal component of the ^{14}N EFG tensor. As a result, the C and D terms of the dipolar interaction contribute somewhat to the overall dipolar coupling between ^{13}C and ^{14}N; these terms are not averaged by MAS, thus they give rise to the observed asymmetric doublet. The line shapes depend on a number of factors: the sign and magnitude of the quadrupolar coupling constant, the applied magnetic field strength, the dipolar coupling constant, and the relative orientations of the quadrupolar and dipolar interactions. The contribution of indirect $J(^{13}C, ^{14}N)$ coupling was not included in the above-mentioned papers

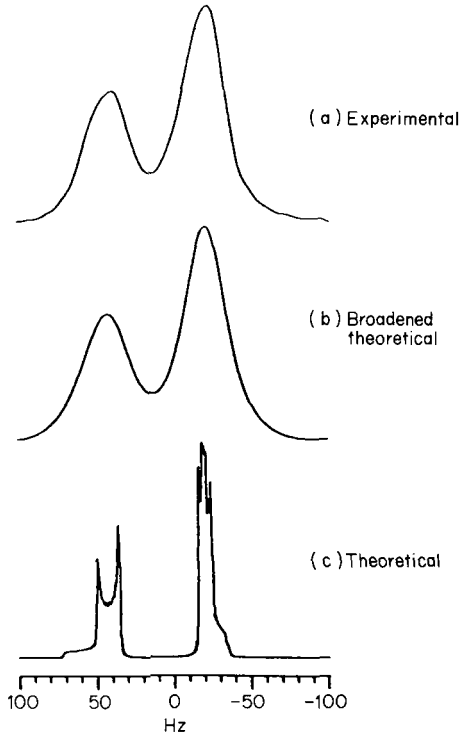

Fig. 26. ^{13}C MAS spectra for the $^{13}C_{\alpha}$ nucleus of glycine that is dipolar coupled to an adjacent ^{14}N nucleus: (a) experimental, (b) calculated with line broadening and (c) without line broadening. (Reproduced with permission from Hexem *et al.*[199])

since the magnitude of these couplings in isotropic systems are generally less than 15 Hz.[205]

The study of ^{13}C–^{14}N spin pairs by ^{13}C MAS NMR has provided a wide range of applications. For example, it has been demonstrated that one can readily distinguish between neutral (**IX**) and zwitterionic (**X**) forms of the tetracycline antibiotics (only the "A" ring of a general tetracycline is shown).[206] In the non-ionized form, **IX**, the $N(CH_3)_2$ is not protonated and $\chi(^{14}N)$ is large (ca. 5 MHz), whereas in **X** the symmetry about the ^{14}N nucleus is much greater and χ is relatively small (ca. 1 MHz). Thus, as expected, one observes relatively large ^{13}C–^{14}N residual dipolar splittings in the ^{13}C MAS spectrum of anhydrous oxytetracycline, which exists in the non-ionized form (**IX**), and negligible splittings in oxytetracycline dihydrate, which exists as a zwitterionic species (**X**).

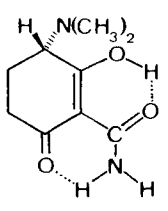

IX

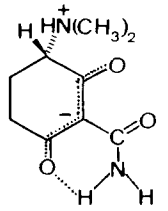

X

The ^{14}N quadrupolar coupling constant in crystalline morphine has been determined to be -1.5 MHz from the asymmetric splittings observed in the ^{13}C MAS spectra of the three directly bonded carbon nuclei.[207] Harris and coworkers[208] have used the magnitudes of the asymmetric splittings to gain some knowledge of the electronic structure in a variety of nitrogen containing aromatic compounds. Frey and Opella[209] have followed the changes in the ^{14}N quadrupolar interaction of the nitrogen sites in histidine as a function of pH by observing the changes in the ^{13}C asymmetric doublets. These splittings have also been observed for ^{13}C nuclei which were not directly bonded to ^{14}N, but are in close proximity to it by the conformation of the molecule in the solid state.[210] Presumably this type of information could provide some clues regarding the structure of the molecule in the crystal lattice.

As with quadrupolar nuclei in solution, there is the possibility that the effects of the quadrupolar interaction may be reduced or eliminated by "self-decoupling". Okazaki *et al.*[211] noted a reduction in the magnitude of the ^{14}N-induced splitting of the nitrile ^{13}C resonance in stearonitrile when this compound was in the channel of a urea inclusion complex. The splitting was reduced from 330 Hz in the crystalline compound to 92 Hz in the inclusion complex; this was explained in terms of a rapid rotation of the stearonitrile molecule within the urea channel. Jonsen[212] recently proposed a theoretical approach to account for ^{14}N self-decoupling based on the theory of Hexem *et al.*[202], while Olivieri[213] has extended his perturbation treatment to include the effect on the ^{13}C MAS line shape of self-decoupling of the quadrupolar ^{14}N nucleus.

The observation of quadrupolar effects on spin-$\frac{1}{2}$ MAS spectra have not been restricted to ^{13}C–^{14}N spin pairs. Asymmetric splittings have also been reported for ^{13}C–^{2}H systems in carbohydrates,[241,215] somewhat surprising when one considers the much smaller size of typical ^{2}H quadrupolar coupling constants compared with those for ^{14}N. Quadrupolar effects have also been observed for ^{13}C nuclei dipolar coupled to ^{75}As in cacodylic acid[216] and to $^{35/37}Cl$ in fluoropolymers containing chlorine.[217]

One of the first reports of the influence of quadrupolar nuclei on MAS spectra concerned the ^{31}P–$^{63/65}Cu$ spin pair in triphenylphosphine

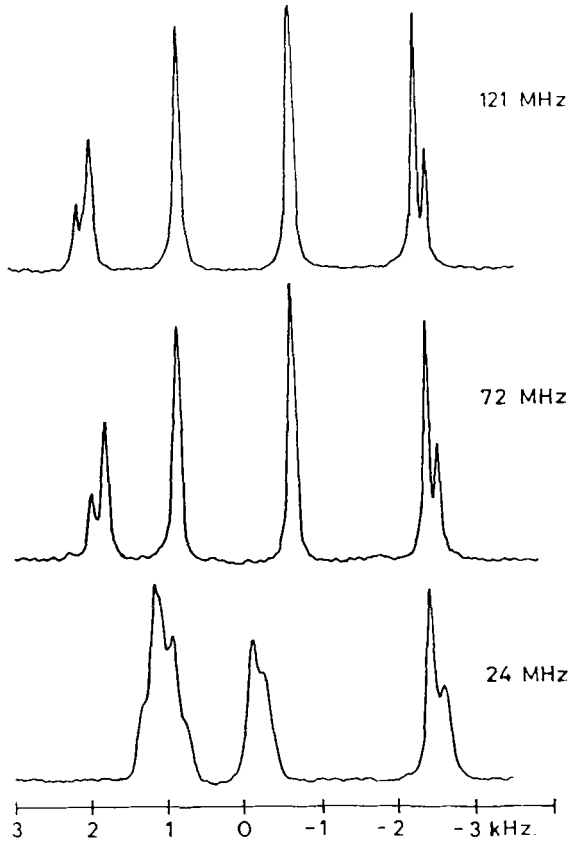

Fig. 27. ^{31}P MAS spectra of bis(triphenylphosphine) copper(I) nitrate at three field strengths corresponding to the ^{13}P NMR frequencies indicated. (Reproduced with permission from Menger and Veeman.[219])

copper(I) complexes.[218,219] In their analysis of these systems, Menger and Veeman[219] also had to consider the influence of the sizeable indirect coupling, $J(^{31}P, ^{63/65}Cu)$, on the ^{31}P line shape. ^{31}P MAS spectra of bis(triphenylphosphine)copper(I) nitrate were examined at three different applied magnetic fields corresponding to ^{31}P NMR Larmor frequencies of 24, 72 and 121 MHz (Fig. 27). At 121 MHz, the ^{31}P signal is split into two overlapping quartets; both ^{63}Cu (natural abundance 69.1%) and ^{65}Cu (natural abundance 30.9%) are spin 3/2 nuclei and possess similar magnetogyric ratios ($\gamma(^{65}Cu)/\gamma(^{63}Cu) = 1.071$). A comparison of observed and calculated spectra led the authors to conclude that $J_{iso}(^{31}P, ^{63}Cu)$ is approximately + 1450 Hz and $R(^{31}P, ^{63}Cu) \simeq 725$ Hz (i.e. $r_{CuP} \simeq 2.6$ Å). The ^{63}Cu quadrupolar coupling

constant was taken to be 30 MHz with $\eta_Q = 0$. Recently, Olivieri[220] has suggested that large anisotropies in $J(^{31}P, ^{63}Cu)$ are necessary in order to simulate the ^{31}P MAS spectra of $(PPh_3)_2CuNO_3$, shown in Fig. 27. Finally, it is interesting to point out that, in solution, one generally cannot measure $J_{iso}(^{31}P, ^{63/65}Cu)$ in copper phosphines because of very efficient $^{63/65}Cu$ quadrupolar relaxation.

In a ^{119}Sn MAS NMR study of several organotin compounds, Komoroski *et al.*[221] observed two broad ^{119}Sn resonances in diethyltin chloride that were separated by ca. 770 Hz at 33.56 MHz. Since this splitting was much smaller at higher applied magnetic field strengths, the authors concluded that $^{35/37}Cl$ quadrupolar effects must be important. A complicated ^{119}Sn MAS spectrum whose centre band spanned some 1.2 kHz was observed for triphenyltin chloride at 111.9 MHz. Although this spectrum was not explained by the authors, Harris[222] later showed that the origin of the complex MAS line shape observed by Komoroski *et al.*[221] was in part due to the breakdown of the high-field approximation. In simulating these spectra, one must include the effect of $^1J_{iso}(^{119}Sn, ^{35}Cl)$, which is of the order of 250 Hz in these compounds.[222,223] Olivieri[220] has suggested that it is necessary to invoke an anisotropy in the indirect Sn–Cl coupling constant, $\Delta J \simeq -350$ Hz, in order to simulate correctly the ^{119}Sn MAS spectrum of Ph_3SnCl. More recently, Apperley *et al.*[223] have examined the ^{119}Sn MAS spectrum of (acetylacetonato)tin(IV) dichloride at two fields and extended perturbation theory to deal with systems in which a spin-$\frac{1}{2}$ nucleus is coupled to two equivalent spin-$\frac{3}{2}$ nuclei (e.g. $^{119}Sn\,^{35}Cl_2$). These authors also suggest that ΔJ may be significant in these systems, -400 to -800 Hz.[223]

^{29}Si CP/MAS spectra of tri-*p*-toluenechlorosilane at 17.88 MHz also show characteristic spin-$\frac{1}{2}$, spin-$\frac{3}{2}$ splittings that result from the breakdown of the high-field approximation.[203] Simulation of the experimental spectrum indicated a Si–Cl bond length of 2.02 Å. ^{31}P MAS spectra of the phosphonitrilic chloride cyclic trimer (**XI**) show an extremely broad pattern ($\geqslant 3$ kHz) that appears to be consistent with heteronuclear dipole–dipole coupling to quadrupolar nuclei (^{14}N, ^{35}Cl and ^{37}Cl).[224]

Interestingly, the linear chloropolymer (**XII**) derived from **XI** shows a relatively narrow ^{31}P MAS spectrum. This probably results from self-decoupling of the quadrupolar nuclei as a result of molecular motion in this

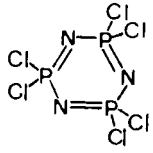

XI

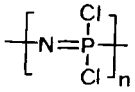

XII

elastomeric material. Finally, it has been suggested that ^{13}C–^{59}Co ($I = 7/2$) dipolar interactions may be responsible for the complex variable field and temperature ^{13}C MAS spectra observed for $Co_4(CO)_{12}$.[225]

In ^{125}Te MAS spectra of $(CH_3)_3TeCl \cdot H_2O$, distortions due to the quadrupolar interaction of the chlorine nuclei were absent.[226] A symmetric pattern due only to $^1J_{iso}(^{125}Te, ^{35/37}Cl)$ was observed, an example of the extreme high-field limit expected for spin-$\frac{1}{2}$ nuclei coupled to quadrupolar nuclei. The absence of dipolar contributions to the spectrum was ascribed to either a long Te–Cl distance or a small quadrupolar coupling constant for the chlorine nuclei.

In a recent series of papers, Olivieri and coworkers[204,213,220,227] have used first-order perturbation theory to calculate spin-$\frac{1}{2}$ MAS line shapes influenced by neighbouring quadrupolar nuclei, and have expressed the magnitude of the asymmetric splitting in terms of one convenient and simple equation. The method outlined in these publications merits some attention and should be applicable to most of the systems discussed in this section.

4.5. Dipolar dephasing and MAS/SLF spectroscopy

Opella and Frey[228] have shown how the ^{13}C–^1H dipolar interaction can be used to simplify and partially edit ^{13}C CP/MAS spectra. By placing a "window" in the ^1H decoupling between cross-polarization and acquisition, the ^{13}C magnetization rapidly decays for any carbon with strong ^{13}C–^1H dipolar couplings due to dipolar dephasing of the signal. This is similar to the SLF technique by Waugh,[39,40] except that the length of this dipolar-dephasing period is not incremented, but fixed based on the best discrimination of the different types of carbon atoms. Carbon atoms with directly bonded ^1H nuclei are obviously more susceptible to dipolar dephasing than quaternary carbons, which are relatively unaffected. In addition, any carbon sites undergoing a high degree of motion (e.g. rapidly rotating methyl groups) have reduced ^{13}C–^1H dipolar couplings, thus their signals are also not greatly affected by the dephasing period. Consequently, methylene, methine and static methyl group carbon atoms would disappear from a spectrum under dipolar dephasing, while quaternary and rotating methyl group carbons remain, providing a useful solid-state assignment technique. A detailed investigation of the influence of the ^{13}C–^1H dipolar interaction on cross-polarization and dipolar dephasing has been performed.[229] Methylene and methine ^{13}C nuclei dephase quickly ($< 55\ \mu s$), whereas quaternary and rotating methyl ^{13}C nuclei preserve their magnetization much longer. In some cases, the quaternary ^{13}C nuclei have been observable after a 135–180 μs dephasing period.[230]

One potentially useful extension of the dipolar dephasing experiment is to

perform it for various dephasing periods, and acquire a two-dimensional MAS spectrum analogous to the SLF-type experiments. In 1981, a MAS/SLF experiment was outlined[231] that successfully separated the ^{13}C–^{1}H dipolar and ^{13}C chemical-shift information for $Ca(H^{13}COO)_2$ in the two dimensions. Rotationally synchronized pulses and spin-echoes were used, as well as homonuclear multiple-pulse decoupling (see Fig. 5(d)). The advantages of the MAS/SLF experiment are two-fold:

(i) MAS experiments require less time than static or single-crystal experiments; and
(ii) the spinning side bands due to nuclei with different chemical shifts can be separated by a careful choice of spinning speed, resolving the anisotropic information.

The rotationally synchronized pulses were essential to avoid phase problems, since spin manipulation and sampling had to occur at the peak of a rotational echo where the anisotropic part of the chemical shift was refocused. The spin-echo refocused the isotropic shifts, thus permitting analysis of samples with nonequivalent ^{13}C nuclei and avoiding frequency-dependent phase shifts. The authors noted that the dipolar "slice" of a given chemical shift side band was

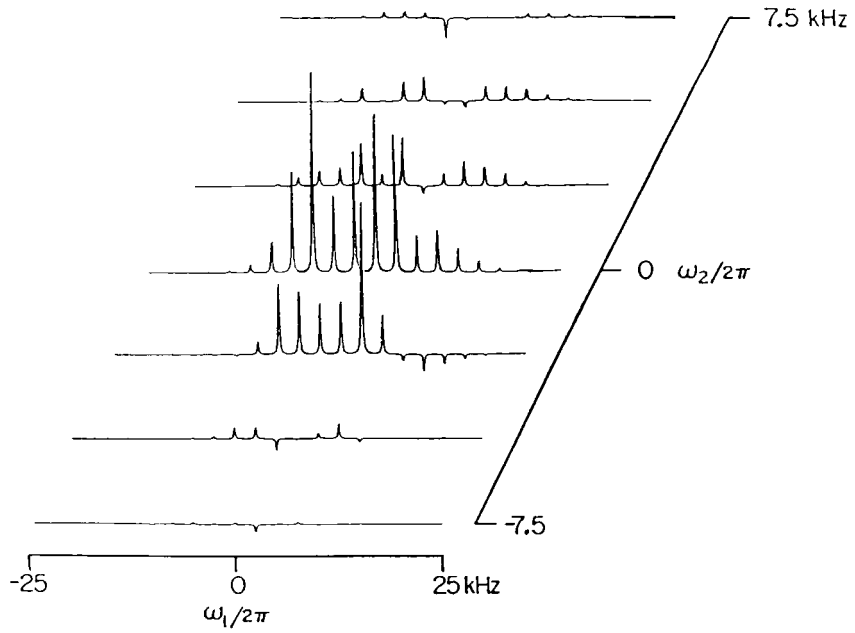

Fig. 28. Calculated ^{13}C MAS/SLF spectra of a model ^{13}C–^{1}H spin pair. (Reproduced with permission from Munowitz and Griffin.[232])

not necessarily symmetric, as illustrated in Fig. 28. Munowitz and Griffin[232] later showed that this asymmetry in the dipolar dimension arose because only certain crystallite orientations contribute to a given chemical-shift side band due to phase variations in the orientationally dependent signals. However, the sum of dipolar slices for all chemical-shift side bands of a given nucleus did result in a symmetric pattern. This was illustrated for the $^{31}P-^{1}H$ spin pair of the HPO_3^{2-} ion in $MgHPO_3 \cdot 6H_2O$. Application of the MAS/SLF technique to a mixture of $Na^{13}CH_3COO$ and $NaCH_3{}^{13}CH_2{}^{13}COO$ demonstrated the usefulness of this technique in resolving dipolar–chemical shift information from systems containing more than one type of nucleus, ^{13}C in this case. The spectral resolution obtained in this study depends on resolution in the chemical shift or ω_2 domain; the two-dimensional nature of the experiment does not improve the resolution, as it does in correlated spectra. The authors suggested that the MAS/SLF technique would be most useful in the study of rare spins dipolar coupled to abundant spins, particularly to systems where isotopic enrichment of the rare spins is not feasible.

The analysis of the side bands of MAS/SLF spectra yields very useful information, such as the rare-spin chemical-shift tensor, the dipolar coupling constant (hence the internuclear distance, r_{IS}), and the relative orientation of the chemical-shift tensor with respect to the dipolar vector. One method of obtaining this information has been presented[233] where it has also been shown that the I–S–I bond angle of an I_2S system can be derived. This was performed on ^{15}N MAS/SLF spectra of the side chain $^{15}N_\gamma H_2$ group of L-asparagine-$[^{15}N_\gamma] \cdot H_2O$. The N–H bond length (1.093 Å) was somewhat longer than that reported by neutron diffraction, while the H–N–H bond angle (114°) was smaller. The dipolar side-bands corresponding to each frequency in the chemical-shift side-band dimension were used to orient the ^{15}N chemical-shift tensor. The results obtained in this experiment were confirmed with a subsequent powder SLF-type experiment.[187]

In some cases, the only information that is required from the NMR experiment is the $^{13}C-^{1}H$ or $^{15}N-^{1}H$ bond lengths in a particular system. In such circumstances, it would be useful to collapse the dipolar information into one slice corresponding to the isotropic chemical shift in ω_2. This was accomplished[234] by sampling in t_2 at the peaks of the rotational echoes, thus removing anisotropic chemical-shift information. Scaling in t_2 was required to avoid aliasing of the chemical-shift dimension due to the reduced sampling frequency, which was achieved by a rotationally synchronized multiple-pulse technique. However, the small spectral window for ω_2 could be problematic for compounds with a large chemical-shift difference between two signals of a given rare spin.

One popular application of this MAS/SLF experiment has been to study various compounds of biological and chemical interest,[235,236] such as the

Table 4. Comparison of N–H bond lengths for four peptide systems, derived from MAS/SLF experiments and neutron diffraction. Original references can be found in Roberts *et al.*[239]

	r_{NH}(Å)	
Compound	NMR	Neutron
GlyGly·H_2O	1.061	1.0200 1.0240
GlyGly·HCl·H_2O	1.063	1.034 1.038
L-His·HCl·H_2O	1.093	1.070
L-Trp·HCl	1.058	0.995

measurement of N–H bond lengths in DNA,[237] peptides[238,239] and ammonium salts.[239] DiVerdi and Opella[237] modified the MAS/SLF experiment, using off-resonance decoupling rather than the multiple-pulse methods during t_1. Rapid spinning collapsed all the ^{15}N–^{1}H dipolar information into one slice at the ^{15}N isotropic shift for each nitrogen in DNA. The solid-state structures of three cyclic pentapeptides were investigated using ^{15}N–^{1}H MAS/SLF as well as ^{13}C CP/MAS and ^{2}H NMR experiments.[238] The N–H bond lengths were determined to be 1.07 Å and 1.10 Å, identical within experimental error, for the two nitrogen sites involved in intramolecular hydrogen bonding. A series of compounds analysed using ^{15}N–^{1}H MAS/SLF NMR[239] gave N–H bond lengths that were consistently 0.035 Å longer than the corresponding neutron-diffraction results, presumably due to the differences in averaging resulting from molecular motion for the two experiments. However, it is apparent that accurate N–H bond lengths can be obtained from NMR experiments of this type, as evident from the data in Table 4.[239] Considerable experimental detail was included in this article on the multiple-pulse decoupling and determination of the scaling factor. This care for experimental detail was reflected in the high precision (within 0.005 Å for N–H bond lengths, 3° for ^{15}N chemical-shift-tensor orientations) of the results.

Dipolar rotational spin-echo NMR was a technique proposed by Schaefer *et al.*[240] that resembled MAS/SLF spectroscopy,[231,232] although there were some slight differences. The ^{13}C π pulse was applied before t_1 began, and the experiment was performed at low field (1.4 T) to reduce the number of spinning side bands due to the chemical-shift anisotropy. A third time period was added immediately after cross-polarization between ^{1}H and ^{13}C, during which the ^{13}C magnetization was spin-locked permitting $T_{1\rho}$ decay. This allowed the rigid and mobile ^{13}C sites in various polymers, such as polystyrene, to be

identified. High-frequency molecular motion decreased the value of the multiple-pulse scaling factor to 0.44 from the theoretical value of 0.58.

The effects of such motions on the dipolar interaction can be traced with MAS/SLF or dipolar rotational spin-echo experiments. Both $^{13}C-^{1}H$ dipolar MAS and slow-spinning MAS ^{13}C spectra were used to characterize the ring motion in phenylalanine.[241] Two crystalline forms were investigated. When recrystallized from a water–ethanol mixture, the NMR spectra indicated that no phenyl ring motion was occurring. Phenylalanine recrystallized from aqueous solution had only about 50% of the sample in which the rings were rigid. The other 50% corresponded to rings undergoing both 180° flips and

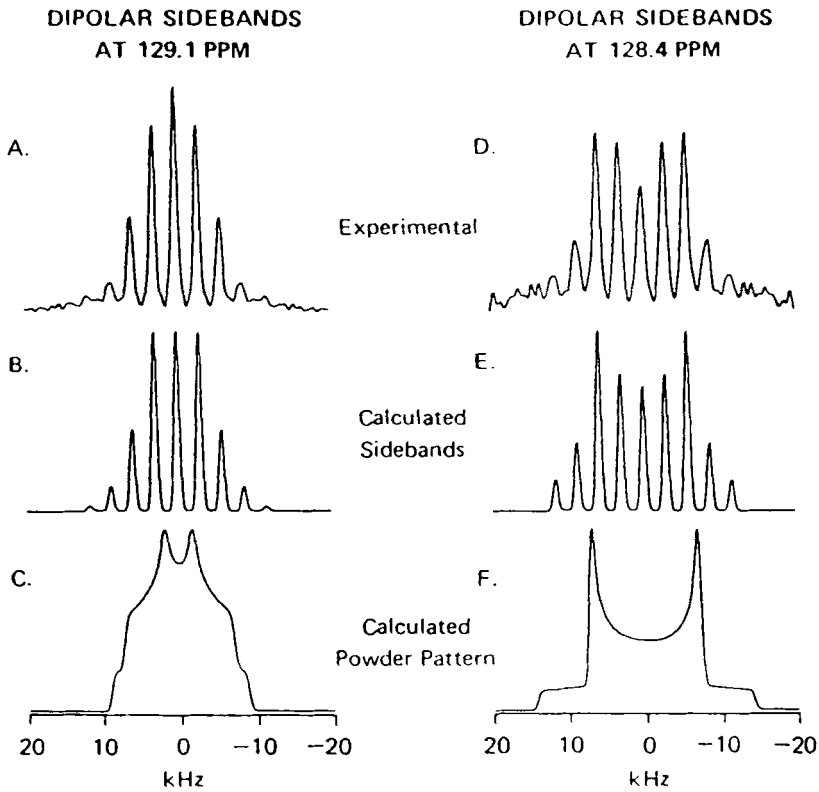

Fig. 29. Experimental and calculated dipolar side bands of $^{13}C-^{1}H$ MAS/SLF spectra of phenylalanine recrystallized from water, as well as the static dipolar line shape to which the spinning spectrum corresponds. The pattern at 129.1 ppm is due to the *meta* carbon atoms of the phenyl rings undergoing rapid flipping, and the pattern at 128.4 ppm is due to the *meta* carbon atoms of the phenyl rings which are rigid. (Reproduced with permission from Frey *et al.*[242])

ring wiggling (small-angle libration). Similar information was obtained by Frey *et al.*[242] by applying MAS/SLF spectroscopy to the aromatic C–H spin pairs of phenylalanine. The effects of motional averaging are clearly manifested in the dipolar sideband distribution, shown in Fig. 29. Deuterium NMR line-shape analysis and ^{13}C and ^{2}H relaxation measurements were used to provide complimentary information on the time-scales of the motional processes in the various samples. In the zwitterionic form of phenylalanine, obtained by recrystallization from H_2O at neutral pH, two crystallographically distinct molecules were evident, one exhibiting rapid ring flips (ca. 10^9 Hz), while the rings were rigid in the other form. These are the two spectra shown in Fig. 29. Phenylalanine recrystallized from ethanol–water solution also had two distinct molecules in the crystal, both of which possessed immobile phenyl rings. Finally, in phenylalanine hydrochloride recrystallized from H_2O one type of molecule was present in which motion of the rings was very slow, i.e. on the order of 10–100 Hz for a ring-flipping rate.

The ^{13}C–^{1}H MAS/SLF spectra of glassy polystyrene[243] showed slight averaging of the ^{13}C–^{1}H dipolar interaction. Together with ^{13}C relaxation measurements, this provided evidence of small-amplitude low-frequency ring and main-chain motion. However, the exact degree of motion was unclear due to difficulties in determining the proper multiple-pulse scaling factor to be used in interpreting the dipolar side bands. Ring flips and librations were apparent in studies of bisphenol-A polycarbonate, with flips occurring via a lattice distortion affecting the main chains as well,[244] while studies of poly(2,6-dimethylphenylene oxide) indicated that this polymer was rigid. Finally, ^{13}C–^{1}H MAS/SLF spectra and ^{13}C relaxation measurements were used to compare the motional characteristics of quenched and annealed poly(butylene)terephthalate.[245] Annealing above the glass transition temperature, T_g, appeared to improve the packing of this polymer in the amorphous regions of the sample, as the degree of motion decreased.

Several modifications and improvements to the original MAS/SLF experiment have been proposed. Early[246] has used BLEW-12 homonuclear multiple-pulse decoupling[247] instead of WAHUHA[59] or MREV-8[63] to obtain ^{13}C–^{1}H MAS/SLF spectra of phenylalanine hydrochloride and *p*-dimethoxybenzene. The application of this sequence is advantageous due to its more moderate radiofrequency field demands, i.e. a 90° pulse of up to 6 μs could be accommodated, compared with the 3 μs maximum required by the other multiple-pulse sequences.

Webb and Zilm[248] have described an experiment that does not require rotational synchronization. The principal goal of their sequence was to permit spectral assignment of ^{13}C in solid samples on the basis of the number of attached protons. The spinning speeds were high enough to prevent side bands appearing in the chemical-shift dimension, ω_2, removing the requirement of

rotational synchronization. The large $^{13}C-^{1}H$ dipolar coupling constant ensured that this interaction survived in spite of spinning in ω_1 even under scaling due to the homonuclear multiple-pulse decoupling. The different types of carbon atoms were distinguished by their dipolar spectra. A graphical technique for determining ratios of the types of carbons in overlapping signals appears useful, although it consistently underestimated the proportion of methylene carbon atoms due to broadening of the high-order ^{13}C spinning sidebands.

Another approach that removed the need for the experimentally demanding conditions of rotational synchronization and refocusing pulses has been described by Kolbert *et al.*[249] Sensitivity was increased by removing the delay between the end of the evolution period and the beginning of acquisition. During t_1, the spins evolved according to heteronuclear dipolar coupling and chemical-shift effects under homonuclear decoupling. Acquisition (t_2) began immediately after t_1, with broad-band decoupling removing all but chemical-shift effects. A shearing transformation[49] was then applied to the two-dimensional data matrix, resolving dipolar and chemical-shift information onto orthogonal axes. The resulting spectra were identical to those obtained with the original MAS/SLF sequence, and with an increased signal-to-noise ratio.

It is often difficult to obtain precise measurements of small anisotropies by MAS due to the small number of spinning side bands. Two-dimensional spin-echo MAS NMR has been used to avoid this problem.[250] The application of a π pulse at $t_1/2$ to a sample rotating at ν_r results in the appearance of side bands in ω_1 at multiples of $\nu_r/2$ instead of ν_r. This pulse interferes with the formation of rotational echoes, thus rotor period τ_r is doubled. The greater number of side bands should permit more precise determination of small dipolar couplings in MAS/SLF experiments or chemical-shift anisotropies in normal CP/MAS experiments.[251,252]

Of course, another way to increase the number of side bands in ω_1 of a MAS/SLF spectrum is simply to spin the sample more slowly. Switched-speed spinning NMR[253] provided slow-spinning MAS conditions during the evolution period while maintaining high resolution fast-MAS conditions during acquisition for a MAS/SLF experiment. During t_1, the sample is spun slowly while multiple-pulse decoupling is applied. This time period is an integer multiple of τ_r so that all anisotropic chemical-shift effects are removed from the dipolar dimension. At the end of t_1, the magnetization is stored along $\mathbf{B}_0$, and the spinning rate is increased. At $t_2 = 0$, the magnetization is flipped back into the transverse plane and the isotropic shift is detected under fast-MAS conditions. The change in the spinning rate is controlled by the pulse programmer via a voltage-driven controller that switches the drive air flow between two preset levels.

Another type of sample spinning NMR experiment that maintains the anisotropic information content of the spectrum has been performed by setting the axis of rotation a few degrees away from the magic angle. Such off-magic-angle spinning (off-MAS) results in a series of "side patterns", spinning side bands anisotropically broadened due to any inhomogeneous interaction.[254] Using slow spinning and homonuclear decoupling, the ^{13}C off-MAS spectrum has been interpreted in terms of the principal components of the ^{13}C chemical-shift tensor, the ^{13}C–^{1}H dipolar coupling, and, particularly for the "isotropic" side pattern, the relative orientation of these two interactions. This experiment was performed on the ^{13}C–^{1}H spin pair in $Ca(HCOO)_2$. A normal ^{13}C MAS spectrum obtained with ^{1}H homonuclear decoupling exhibited splitting of the side bands due to $J(^{13}C, ^{1}H)$, confirming the positive sign of this coupling constant.

Heteronuclear dipolar information has been obtained from rotating samples using dipolar switched-angle sample spinning (SASS) NMR.[255] This two-dimensional technique combines the anisotropic conditions of off-MAS in one dimension with the high resolution of normal MAS in the other. Thus the anisotropic powder pattern for each crystallographically distinct ^{13}C is resolved by its isotropic chemical shift. During the evolution period, off-MAS and homonuclear decoupling introduce scaling factors, S_θ due to the angle of rotation and S_{rf} due to the radiofrequency fields. A rotationally synchronized spin-echo is used to remove chemical shifts from t_1. After t_1, the rotor axis is stepped back to the magic angle and detection (t_2) is initiated. After two-dimensional Fourier-transformation, the ω_1 dimension contains J(IS) couplings scaled by S_{rf} and I–S dipolar couplings scaled by $S_{rf} \times S_\theta$. These different scaling factors allow the two interactions to be determined easily. The scaling of the dipolar coupling also reduces the spectral window required for ω_1, relaxing the instrumental requirements for measuring large dipolar couplings. The maximum angular departure of the rotation axis from the magic angle was 4°. ^{13}C spectra of the ^{13}C–^{1}H spin pair in several compounds, such as calcium formate, β-quinol–methanol clathrate and the urea–*trans*-4-octene inclusion complex, showed the influence of any molecular motion and the orientation of this motion on the resulting line shapes. The instrumental methodology has been described separately.[256]

The off-MAS experiment has been combined with SLF-type techniques, yielding scaled two-dimensional dipolar–chemical shift powder patterns.[257,258] The experiment has been conducted in the same manner as other rotating sample SLF methods, with rotational synchronization and homonuclear decoupling. The scaling of the dipolar interaction by both the radio-frequency fields and the angle of rotation is important, as is the width of the resulting scaled dipolar line shape (in Hz), which has to be less than the

spinning rate. The scaled patterns are similar to those obtained by using other static two-dimensional techniques[179] with improved sensitivity and resolution. Line shapes due to different sites were resolved by correct choice of the angle of rotation. One interesting addition to this experiment was a third time dimension, t_3, during which an isotropic MAS spectrum was obtained, immediately after the off-MAS/SLF spectrum, by switching the angle back to the magic angle.[258] The result was a three-dimensional spectrum where each isotropic shift in ω_3 resolved a two-dimensional powder pattern in ω_1 and ω_2 containing the anisotropic dipolar and chemical shift information.

Several compounds have been analysed using off-MAS/SLF spectroscopy. Careful choice of the scaling factors allowed resolution of several ^{13}C patterns in one two-dimensional spectrum of a sample containing both *cis*- and *trans*-polyacetylene[257] and of the methine, methylene and methyl ^{13}C patterns in isotactic polypropylene.[259] The three-dimensional technique has been used to resolve the two crystallographically nonequivalent ^{13}C sites in $Ca(HCOO)_2$.[258] Small-amplitude motions in calcium formate have also been investigated.[260] Anisotropic vibrations were found to introduce asymmetry in the ^{13}C–^{1}H dipolar line shape, which is clearly evident in the two-dimensional off-MAS/SLF powder patterns (see Fig. 30). The orientation of these vibrations is also indicated in the two-dimensional spectra, whereas in the one-dimensional line shapes the asymmetry in the Pake pattern may not have been apparent due to line broadening. By applying a Morse potential for the C–H bond stretch in the formate ion, the bending amplitudes were estimated from the off-MAS/SLF spectra.

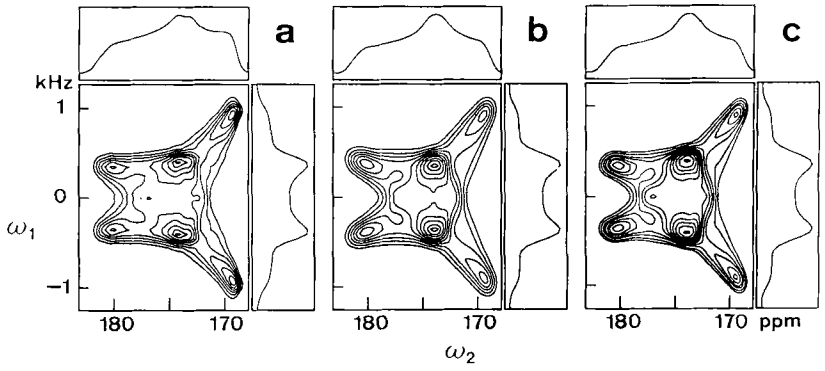

Fig. 30. ^{13}C–^{1}H off-MAS/SLF spectra of $Ca(^{1}H^{13}COO)_2$: (a) experimental; (b) calculated neglecting the effect of anisotropic C–H vibrations; and (c) calculated including these vibrations. (Reproduced with permission from Nakai *et al.*[260])

4.6. Triple-resonance NMR studies

The final few techniques to be discussed rely on triple-resonance NMR, utilizing probes tuned simultaneously to three nuclei (typically ^{1}H, ^{13}C and ^{15}N). Double cross-polarization (DCP) NMR[261,262] has been used to detect the proportion of ^{13}C–^{15}N bonds in a sample by observing the "drain" of ^{15}N magnetization induced by a matched contact to a ^{13}C spin bath. Any build-up of ^{13}C magnetization was limited by phase modulation of the ^{13}C radiofrequency field. The difference in ^{15}N signal intensity for spectra obtained with and without the $^{15}N \rightarrow {}^{13}C$ drain could be analysed, giving the fraction of directly bonded ^{15}N–^{13}C pairs. In order to interpret the DCP spectra, it is important to know the $^{15}N \rightarrow {}^{13}C$ drain rates for different carbon–nitrogen functionalities,[263] which depend mainly on the strength of the ^{13}C–^{15}N dipolar coupling. Other important experimental parameters are the radiofrequency field amplitudes and the MAS rates, both of which have to be closely controlled.[262]

As DCP NMR can be used to selectively detect labelled carbon–nitrogen functionalities, it has been applied predominantly to peptide and protein systems. Double cross-polarization NMR has been applied to studies of the metabolism of ^{15}N, ^{13}C-asparagine in developing plants,[261] the rate of protein turnover in soybean leaves,[264] and the polymerization of proteins and chitin in the strengthening of insect cuticles.[265] Together with dipolar rotational spin-echo NMR,[240] DCP NMR has been used to follow the polymerization of HCN,[266,267] proposed as one of the original reactions leading to primordial proteins. However, polarization pathways other than ^{1}H–^{15}N–^{13}C are possible, permitting identification of many bonding networks. Hagaman[268] has used DCP NMR to assign ^{13}C MAS spectra of organophosphorus compounds by draining ^{13}C magnetization to a ^{31}P bath in a ^{1}H–^{13}C–^{31}P pathway.

Rotational-echo double-resonance (REDOR)[269] has been used as an alternative to the demanding DCP NMR technique for detection of isolated ^{13}C–^{15}N spin pairs, and has been reviewed recently by Gullion and Schaefer.[270] This experiment relies on the dephasing of the ^{13}C rotational echoes in a MAS experiment by ^{13}C–^{15}N dipolar coupling, analogous to the effect of dipolar coupling on spin-echoes in SEDOR experiments by Slichter *et al.*[171–173] The coupling is not allowed to refocus after each rotational period by the application of ^{15}N π pulses at various times before or after rotational echoes occur, and before acquisition begins. Although similar to MAS/SLF techniques for ^{13}C–^{1}H and ^{15}N–^{1}H systems (see Section 4.5), the much weaker ^{13}C–^{15}N dipolar interaction necessitates that π pulses be used rather than ^{15}N decoupling. This removes any additional dephasing due to off-resonance Bloch–Siegert effects and isotropic indirect coupling. Various

one- and two-dimensional derivatives of the basic REDOR experiment have been proposed,[270] all with the principal aim of maximizing the evolution due to the weak ^{13}C–^{15}N dipolar interaction. When performed with synchronous sampling, REDOR results in a "Pake-spun" powder pattern, the width of which corresponds to the ^{13}C–^{15}N dipolar coupling constant.[270]

Various triple-resonance NMR experiments have been proposed by Schneider *et al.*[271] for amplification, modification or elimination of splittings in ^{13}C spectra due to ^{13}C–^{15}N dipolar coupling. Simple gated ^{15}N decoupling during ^{13}C acquisition removes the effects of dipolar coupling. A two-dimensional experiment with ^{15}N decoupling during the evolution period resolves pure ^{13}C chemical-shift signals by means of dipolar–chemical shift splittings in the other dimension. Gated ^{15}N decoupling during detection in a two-dimensional SLF-type experiment results in ^{13}C–^{15}N splittings that were resolved via the isotropic ^{13}C chemical shifts. Finally, a variation of the previous sequence is described that preferentially detects ^{13}C signals from ^{13}C–^{15}N spin pairs. All these experiments have been performed on single crystals or oriented samples, but should also be applicable to powder samples. Another method for selective detection of ^{13}C–^{15}N spin pairs has been proposed recently.[272] Similar to REDOR,[269] application of π pulses to one spin of a spin pair modulates the spin-echo of the other spin, to which a π pulse is also applied, but not necessarily simultaneously. This experiment was performed on single crystals, and the presence of ^{13}C–^{15}N spin pairs was manifested in difference spectra. Experiments on a powder sample would probably require variable delays, i.e. a two-dimensional experiment, due to the effect of the orientation dependence of the dipolar interaction on the pulse spacings.

One final technique for studying heteronuclear I–S dipolar coupling is rotary resonance recoupling.[273] Application of a weak radiofrequency field, B_{1I}, at the Larmor frequency of the coupling partners I of an IS spin pair has an interesting effect on the S spin MAS NMR line shape when $\nu_{1I} = n\nu_r$, where $\nu_{1I} = -\gamma_I B_{1I}/2\pi$ is the nutation frequency of the I spin and n is a small integer (1, 2, 3). Under these conditions, dramatic changes in the S spin NMR spectrum are observed, which depend on the I–S dipolar coupling constant, the I and S spin chemical shielding tensor and the integer n. Note that, if applied separately, either MAS or I-spin nutation would decouple the I–S dipolar coupling; however, when used in combination under particular matching conditions, the spins may be recoupled. This effect is closely related to the rotational resonance effects which may be observed in homonuclear spin pairs when a multiple of the spinning frequency matches the separation between a pair of isotropic chemical shifts (see Section 3.5). The heteronuclear experiment has been demonstrated for the ^{31}P–^{15}N spin pair in ^{31}P NMR spectra of *N*-methyldiphenylphosphoramidate ($(C_6H_5O)_2$ $^{31}P(O)$

$^{15}N(H)CH_3$).[273] This method was proposed as a useful means of measuring weak heteronuclear dipolar couplings.[251]

5. CONCLUDING REMARKS

In this chapter we have attempted to describe the basis of dipolar NMR experiments. In particular, we have made an effort to relate the developments that have taken place in this field over the last 40 years. Many new tricks have evolved over this time expanding the potential applications.

The applications described here vary from obtaining fundamental structural information, such as bond lengths, identifying small molecules on surfaces and describing the conformation of peptides in membranes, to characterizing magnetic shielding tensors, J coupling tensors and, in some cases, nuclear quadrupolar coupling tensors. These latter parameters are of great interest, especially with the development of ever-improving theoretical calculations. Theoreticians must have reliable experimental data with which to test their calculations and theoretical models.

In the future, more effort will probably be devoted to attempting to recover dipolar (structural) and other anisotropic information from high-resolution spectra. The thrust of much recent work has been to detect and characterize weaker interactions, such as $^{13}C-^{15}N$ dipolar couplings, or couplings between nuclei which are not directly bonded. Three-spin systems will also be a likely focus, due to both the possibility of obtaining unambiguous structural information, and the commercial availability of triple-resonance NMR probes and spectrometers which can deliver the required radiofrequency fields. Variable- or low-temperature studies will be important in correcting for bond vibrations and molecular librations. Improvements in these corrections should also allow more detailed experimental study of the anisotropy in the indirect coupling tensor.

The sensitivity of the solid-state NMR experiment to internuclear separations, electronic environments and molecular motions has made it a useful and powerful probe of microscopic structure, and it can be expected to provide even more detailed and exciting information in the future.

ACKNOWLEDGEMENTS

We wish to thank several authors and publishers for permission to reproduce some of the figures appearing in this review. The comments of many of our co-workers are also appreciated. Finally, we wish to acknowledge the financial

assistance of NSERC of Canada for supporting our research in the area covered by this review.

REFERENCES

1. G.E. Pake, *J. Chem. Phys.*, 1948, **16**, 327.
2. E.R. Andrew and R. Bersohn, *J. Chem. Phys.*, 1950, **18**, 159.
3. R.E. Richards and J.A.S. Smith, *Trans. Faraday Soc.*, 1951, **47**, 1261.
4. (a) J. Itoh, R. Kusaka, Y. Yamagata, R. Kiriyama and H. Ibamoto, *J. Chem. Phys.*, 1952, **20**, 1503; **21**, 190.
   (b) J. Itoh, R. Kusaka, Y. Yamagata, R. Kiriyama and H. Ibamoto, *J. Phys. Soc. Japan*, 1953, **8**, 287.
5. (a) K. Tomita, *Progr. Theor. Phys.*, 1952, **8**, 138.
   (b) K. Tomita, *Phys. Rev.*, 1953, **89**, 429.
6. R. Bersohn and H.S. Gutowsky, *J. Chem. Phys.*, 1954, **22**, 651.
7. J.H. Van Vleck, *Phys. Rev.*, 1948, **74**, 1168.
8. H.S. Gutowsky, G.B. Kistiakowsky, G.E. Pake and E.M. Purcell, *J. Chem. Phys.*, 1949, **17**, 972.
9. H.S. Gutowsky, G.E. Pake and R. Bersohn, *J. Chem. Phys.*, 1954, **22**, 643.
10. L.E. Drain, *Discuss. Faraday Soc.*, 1955, **19**, 201.
11. J.A. Ibers and D.P. Stevenson, *J. Chem. Phys.*, 1958, **28**, 929.
12. P.T. Ford and R.E. Richards, *Discuss. Faraday Soc.*, 1955, **19**, 230.
13. P.T. Ford and R.E. Richards, *Discuss. Faraday Soc.*, 1955, **19**, 193.
14. E.R. Andrew and D. Hyndman, *Discuss. Faraday Soc.*, 1955, **19**, 195.
15. (a) N.L. Alpert, *Phys. Rev.*, 1947, **72**, 637.
   (b) N.L. Alpert, *Phys. Rev.*, 1949, **75**, 398.
16. H.S. Gutowsky and G.E. Pake, *J. Chem. Phys.*, 1950, **18**, 162.
17. H.S. Gutowsky, in *Physical Methods of Organic Chemistry*, Vol. 1, Part 4, 3rd edn (ed. A. Weissberger), p. 2663. Interscience, New York, 1960.
18. B. Pedersen, *J. Chem. Phys.*, 1964, **41**, 122.
19. L.W. Reeves, *Prog. Nucl. Magn. Reson. Spectrosc.*, 1969, **4**, 193.
20. E.R. Andrew, *Nuclear Magnetic Resonance*. Cambridge University Press, Cambridge, 1955.
21. R.E. Richards, in *Determination of Organic Structures by Physical Methods* (ed. F.C. Nachod and W.D. Phillips), pp. 537–562. Academic Press, New York, 1962.
22. N.G. Parsonage and L.A.K. Stavely, *Disorder in Crystals*. Clarendon Press, Oxford, 1978.
23. N. Boden, in *The Plastically Crystalline State* (ed. J.N. Sherwood), pp. 147–214. Wiley, New York, 1979.
24. R.R. Ernst and W.A. Anderson, *Rev. Sci. Instrum.*, 1966, **37**, 93.
25. T.C. Farrar and E.D. Becker, *Pulse and Fourier Transform NMR*. Academic Press, New York, 1971.
26. A. Pines, M.G. Gibby and J.S. Waugh, *J. Chem. Phys.*, 1973, **59**, 569.
27. M. Mehring, *High Resolution NMR in Solids*, 2nd edn. Springer-Verlag, Berlin. 1983.
28. W.S. Veeman, *Prog. Nucl. Magn. Reson. Spectrosc.*, 1984, **16**, 193.
29. (a) T.M. Duncan, *J. Phys. Chem. Ref. Data*, 1987, **16**, 125.
   (b) T.M. Duncan, *A Compilation of Chemical Shift Anisotropies*. Farragut Press, Chicago, 1990.
30. J.C. Facelli and D.M. Grant, in *Topics in Stereochemistry*, Vol. 19 (ed. E.L. Eliel and S.H. Wilen), pp. 1–61. Wiley, New York, 1989.
31. J.B. Robert and L. Wiesenfeld, in *Phosphorus-31 NMR Spectroscopy in Stereochemical*

Analysis (ed. J.G. Verkade and L.D. Quin), p. 151. VCH Publishers, Deerfield Beach, FL, 1987.
32. J. Mason, in *Multinuclear NMR* (ed. J. Mason), p. 335. Plenum Press, New York, 1987.
33. C.J. Jameson, in *Specialist Periodical Reports—Nuclear Magnetic Resonance*, Vols. 10–18 (ed. G.A. Webb), Chap. 1, p. 1. The Chemical Society, London, 1981–1989.
34. H.W. Spiess, *NMR Basic Principles and Progress*, Vol. 15 (ed. P. Diehl, E. Fluck and R. Kosfeld), pp. 55–214. Springer-Verlag, Berlin, 1978.
35. M.E. Stoll, R.W. Vaughan, R.B. Saillant and T. Cole, *J. Chem. Phys.*, 1974, **61**, 2896.
36. (a) R.G. Griffin, A. Pines and J.S. Waugh, *J. Chem. Phys.*, 1975, **63**, 3676.
(b) R.A. Haberkorn, R.E. Stark, H. van Willigen and R.G. Griffin, *J. Am. Chem. Soc.*, 1981, **103**, 2534.
37. S. Kaplan, A. Pines, R.G. Griffin and J.S. Waugh, *Chem. Phys. Lett.*, 1974, **25**, 78.
38. H. van Willigen, R.G. Griffin and R.A. Haberkorn, *J. Chem. Phys.*, 1977, **67**, 5855.
39. (a) R.K. Hester, J.L. Ackerman, V.R. Cross and J.S. Waugh, *Phys, Rev. Lett.*, 1975, **34**, 993.
(b) R.K. Hester, J.L. Ackerman, B.L. Neff and J.S. Waugh, *Phys. Rev. Lett.*, 1976, **36**, 108.
40. J.S. Waugh, *Proc. Natl. Acad. Sci. USA*, 1976, **73**, 1394.
41. C.A. Fyfe, *Solid State NMR for Chemists*. C.F.C. Press, Guelph, Ontario, 1983.
42. E. Fukushima and S.B.W. Roeder, *Experimental Pulse NMR—A Nuts and Bolts Approach*, Chap. 4. Addison-Wesley, Reading, MA, 1981.
43. D.E. Axelson, *Solid State Nuclear Magnetic Resonance of Fossil Fuels*, Multiscience Publications, Montreal, 1985.
44. L.W. Jelinski and M.T. Melchior, in *NMR Spectroscopy Techniques* (ed. C. Dybowski and R.L. Lichter), pp. 253–329. Marcel Dekker, New York, 1987.
45. A. Abragam, *Principles of Nuclear Magnetism*. Oxford University Press, Oxford, 1963.
46. (a) U. Haeberlen, *Adv. Magn. Reson.*, Suppl. 1 (ed. J.S. Waugh). Academic Press, New York, 1976.
(b) U. Haeberlen, *Magn. Reson. Rev.*, 1985, **10**, 81.
47. C.P. Slichter, *Principles of Magnetic Resonances*, 2nd edn. Springer-Verlag, Berlin, 1978.
48. B.C. Gerstein and C.R. Dybowski, *Transient Techniques in NMR of Solids*. Academic Press, Orlando, FL, 1985.
49. R.R. Ernst, G. Bodenhausen and A. Wokaun, *Principles of Nuclear Magnetic Resonance in One and Two Dimensions*. Oxford University Press, Oxford, 1987.
50. M. Munowitz, *Coherence and NMR*. Wiley-Interscience, New York, 1988.
51. P.C. Taylor, J.F. Baugher and H.M. Kriz, *Chem. Rev.*, 1975, **75**, 203.
52. R.W. Vaughan, *Ann. Rev. Phys. Chem.*, 1978, **29**, 397.
53. T.M. Duncan and C. Dybowski, *Surf. Sci. Rep.*, 1981, **1**, 157.
54. (a) B.C. Gerstein, *Anal. Chem.*, 1983, **55**, 782A.
(b) B.C. Gerstein, in *Topics in Carbon-13 NMR Spectroscopy*, Vol. 4 (ed. G.C. Levy), p. 123. Wiley, New York, 1984.
(c) B.C. Gerstein. *Adv. Coll. Interface Sci.*, 1985, **23**, 45.
55. K.W. Zilm and D.M. Grant, *J. Am. Chem. Soc.*, 1981, **103**, 2913.
56. C.J. Jameson, in *Multinuclear NMR* (ed. J. Mason), p. 93. Plenum Press, New York, 1987.
57. P. Pyykkö and L. Wiesenfeld, *Mol. Phys.*, 1981, **43**, 557.
58. M.M. Maricq and J.S. Waugh, *J. Chem. Phys.*, 1979, **70**, 3300.
59. J.S. Waugh, L.M. Huber and U. Haeberlen, *Phys. Rev. Lett.*, 1968, **20**, 180.
60. J.E. Kohl, M.G. Semack and D. White, *J. Chem. Phys.*, 1978, **69**, 5378.
61. K.W. Zilm, R.T. Conlin, D.M. Grant and J. Michl, *J. Am. Chem. Soc.*, 1978, **100**, 8038.
62. M.E. Stoll, A.J. Vega and R.W. Vaughan, *J. Chem. Phys.*, 1978, **69**, 5458.
63. W.-K. Rhim, D.D. Elleman and R.W. Vaughan, *J. Chem. Phys.*, 1973, **59**, 3740.
64. C.R. Dybowski, B.C: Gerstein and R.W. Vaughan, *J. Chem. Phys.*, 1977, **67**, 3412.
65. B.H. Meier, F. Graf and R.R. Ernst, *J. Chem. Phys.*, 1982, **76**, 767.

66. N. Schuff and U. Haeberlen, *J. Magn. Reson.*, 1983, **52**, 267.
67. W. Schajor, H. Post, R. Grosescu, U. Haeberlen and G. Blockus, *J. Magn. Reson.*, 1983, **53**, 213.
68. S.F. Sagnowski, S. Aravamudhan and U. Haeberlen, *J. Magn. Reson.*, 1977, **28**, 271.
69. J. Tritt-Goc, N. Piślewski and U. Haeberlen, *Chem. Phys.*, 1986, **102**, 133.
70. K.W. Zilm, R.A. Merrill, M.W. Kummer and G.J. Kubas, *J. Am. Chem. Soc.*, 1986, **108**, 7837.
71. J.M. Millar, A.M. Thayer, D.B. Zax and A. Pines, *J. Am. Chem. Soc.*, 1986, **108**, 5113.
72. P. Meier, G. Kothe, P. Jonsen, M. Trecoske and A. Pines, *J. Chem. Phys.*, 1987, **87**, 6867.
73. D.B. Zax, A. Bielecki, K.W. Zilm, A. Pines and D.P. Weitekamp, *J. Chem. Phys.*, 1985, **83**, 4877.
74. C. Müller, S. Idziak, N. Piślewski and U. Haeberlen, *J. Magn. Reson.*, 1982, **47**, 227.
75. H. Schlemmer and U. Haeberlen, *J. Magn. Reson.*, 1986, **70**, 436.
76. K.W. Zilm, A.J. Beeler, D.M. Grant, J. Michl, T.-C. Chou and E.L. Allred, *J. Am. Chem. Soc.*, 1981, **103**, 2119.
77. J.C. Facelli, A.M. Orendt, A.J. Beeler, M.S. Solum, G. Depke, K.D. Malsch, J.W. Downing, P.S. Murthy, D.M. Grant and J. Michl, *J. Am. Chem. Soc.*, 1985, **107**, 6749.
78. A.M. Orendt, B.R. Arnold, J.G. Radziszewski, J.C. Facelli, K.D. Malsch, H. Strub, D.M. Grant and J. Michl, *J. Am. Chem. Soc.*, 1988, **110**, 2648.
79. A. Manenschijn, M.J. Duijvestijn, J. Smidt, R.A. Wind, C.S. Yannoni and T.C. Clarke, *Chem. Phys. Lett.*, 1984, **112**, 99.
80. M.J. Duijvestijn, A. Manenschijn, J. Smidt and R.A. Wind, *J. Magn. Reson.*, 1985, **64**, 461.
81. R.A. Wind, M.J. Duijvestijn, C. van der Lugt, A. Manenschijn and J. Vriend, *Prog. Nucl. Reson. Spectrosc.*, 1985, **17**, 33.
82. S.R. Hartmann and E.L. Hahn, *Phys. Rev.*, 1962, **128**, 2042.
83. M. Engelsberg and C.S. Yannoni, *J. Magn. Reson.*, 1990, **88**, 393.
84. (a) H.Y. Carr and E.M. Purcell, *Phys. Rev.*, 1954, **94**, 630.
    (b) S. Meiboom and D. Gill, *Rev. Sci. Instrum.*, 1958, **29**, 688.
85. P.-K. Wang, C.P. Slichter and J.H. Sinfelt, *J. Phys. Chem.*, 1985, **89**, 3606.
86. J.P. Ansermet, C.P. Slichter and J.H. Sinfelt, *J. Chem. Phys.*, 1988, **88**, 5963.
87. T.M. Duncan and T.W. Root, *J. Phys. Chem.*, 1988, **92**, 4426.
88. P.F. Molitor, R.K. Shoemaker and T.M. Apple, *J. Phys. Chem.*, 1989, **93**, 2891.
89. L.M. Ishol and T.A. Scott, *J. Magn. Reson.*, 1977, **27**, 23.
90. R.E. Wasylishen, W.P. Power, G.H. Penner and R.D. Curtis, *Can. J. Chem.*, 1989, **67**, 1219.
91. M. Schindler, *J. Am. Chem. Soc.*, 1987, **109**, 5950.
92. A.R. Grimmer, R. Peter and E. Fechner, *Z. Chem.*, 1978, **18**, 109.
93. E.R. Henry and A. Szabo, *J. Chem. Phys.*, 1985, **82**, 4753.
94. (a) P.N. Tutunjian and J.S. Waugh, *J. Chem. Phys.*, 1982, **76**, 1223.
    (b) P.N. Tutunjian and J.S. Waugh, *J. Magn. Reson.*, 1982, **49**, 155.
95. K.W. Zilm, G.G. Webb, A.H. Cowley, M. Pakulski and A. Orendt, *J. Am. Chem. Soc.*, 1988, **110**, 2032.
96. H. Eckert, C.S. Liang and G.D. Stucky, *J. Phys. Chem.*, 1989, **93**, 452.
97. D. Lathrop and H. Eckert, *J. Am. Chem. Soc.*, 1989, **111**, 3536.
98. C.S. Yannoni and R.A. Wind, *J. Magn. Reson.*, 1980, **38**, 493.
99. P. Mansfield, *Phys. Rev.*, 1965, **137**, 961.
100. M. Engelsberg and R.E. Norberg, *Phys. Rev., Ser. B*, 1972, **5**, 3395.
101. D. Barnaal and I.J. Lowe, *Phys. Rev. Lett.*, 1963, **11**, 258.
102. C.S. Yannoni and R.D. Kendrick, *Phys. Rev. Lett.*, 1976, **37**, 1230.
103. (a) C.S. Yannoni and R.D. Kendrick, *J. Chem. Phys.*, 1981, **74**, 747.
    (b) D. Horne, R.D. Kendrick and C.S. Yannoni, *J. Magn. Reson.*, 1983, **52**, 299.
104. (a) C.S. Yannoni and T.C. Clarke, *Phys. Rev. Lett.*, 1983, **51**, 1191.
    (b) T.C. Clarke, R.D. Kendrick and C.S. Yannoni, *J. Physique Colloque*, 1983, **44**, C3-369.
    (c) T.C. Clarke, C.S. Yannoni and T.J. Katz, *J. Am. Chem. Soc.*, 1983, **105**, 7787.

105. J.R. Lyerla, in *High Resolution NMR Spectroscopy of Synthetic Polymers in Bulk* (ed. R.A. Komoroski). VCH Publishers, Deerfield Beach, FL, 1987.
106. T.J. Katz, S.M. Hacker, R.D. Kendrick and C.S. Yannoni, *J. Am. Chem. Soc.*, 1985, **107**, 2182.
107. N. Yannoni, B. Kahr and K. Mislow, *J. Am. Chem. Soc.*, 1988, **110**, 6670.
108. C.S. Yannoni, R.D. Kendrick, P.C. Myhre, D.C. Bebout and B.L. Peterson, *J. Am. Chem. Soc.*, 1989, **111**, 6440.
109. D.L. VanderHart, *J. Magn. Reson.*, 1976, **24**, 467.
110. A.N. Garroway, *J. Magn. Reson.*, 1977, **28**, 365.
111. P.E. Pfeffer, K.B. Hicks, M.H. Frey, S.J. Opella and W.L. Earl, *J. Magn. Reson.*, 1983, **55**, 344.
112. M.H. Frey and S.J. Opella, *J. Am. Chem. Soc.*, 1984, **106**, 4942.
113. V. Bork and J. Schaefer, *J. Magn. Reson.*, 1988, **78**, 348.
114. G. Bodenhausen, *Prog. NMR Spectrosc.*, 1981, **14**, 137.
115. G.P. Drobny, *Ann. Rev. Phys. Chem.*, 1985, **36**, 451.
116. M. Munowitz and A. Pines, *Adv. Chem. Phys.*, 1987, **66**, 1.
117. (a) E.M. Menger, S. Vega and R.G. Griffin, *J. Magn. Reson.*, 1984, **56**, 338.
(b) E.M. Menger, S. Vega and R.G. Griffin, *J. Am. Chem. Soc.*, 1986, **108**, 2215.
118. B.H. Meier and W.L. Earl, *J. Am. Chem. Soc.*, 1987, **109**, 7937.
119. D.P. Raleigh, G.S. Harbison, T.G. Neiss, J.E. Roberts and R.G. Griffin, *Chem. Phys. Lett.*, 1987, **138**, 285.
120. E.R. Andrew, A. Bradbury, R.G. Eades and V.T. Wynn, *Phys. Lett.*, 1963, **4**, 99.
121. E.R. Andrew, S. Clough, L.F. Farnell, T.D. Gledhill and I. Roberts, *Phys. Lett.*, 1966, **21**, 505.
122. D.P. Raleigh, M.H. Levitt and R.G. Griffin, *Chem. Phys. Lett.*, 1988, **146**, 71.
123. Z.-H. Gan and D.M. Grant, *Mol. Phys.*, 1989, **67**, 1419.
124. D.P. Raleigh, A.C. Kolbert, M.H. Levitt and R.G. Griffin, *Isr. J. Chem.*, 1988, **28**, 263.
125. D.P. Raleigh, F. Cruezet, S.K. Das Gupta, M.H. Levitt and R.G. Griffin, *J. Am. Chem. Soc.*, 1989, **111**, 4502.
126. D.L. VanderHart and H.S. Gutowsky, *J. Chem. Phys.*, 1968, **49**, 261.
127. D.L. VanderHart, H.S. Gutowsky and T.C. Farrar, *J. Chem. Phys.*, 1969, **50**, 1058.
128. P. Van Hecke, H.W. Spiess, U. Haeberlen and S. Haussühl, *J. Magn. Reson.*, 1976, **22**, 93.
129. J.A. Ripmeester, J.S. Tse and D.W. Davidson, *Chem. Phys. Lett.*, 1982, **86**, 428.
130. Z.-H. Gan, J.C. Facelli and D.M. Grant, *J. Chem. Phys.*, 1988, **89**, 5542.
131. P.A. Casabella, *J. Chem. Phys.*, 1964, **41**, 3793.
132. C.R. Brett and D.T. Edmonds, *J. Magn. Reson.*, 1982, **49**, 304.
133. D.L. VanderHart, H.S. Gutowsky and T.C. Farrar, *J. Am. Chem. Soc.*, 1967, **89**, 5056.
134. F.A. Cotton and G. Wilkinson, *Advanced Inorganic Chemistry*, 5th edn. p. 1098. Wiley, New York, 1988.
135. H.W. Spiess, U. Haeberlen and H. Zimmermann, *J. Magn. Reson.*, 1977, **25**, 55.
136. M.S. Solum, J.C. Facelli, Z. Gan and D.M. Grant, *Mol. Phys.*, 1988, **64**, 1031.
137. R.M. Dickson, M.S. McKinnon, J.F. Britten and R.E. Wasylishen, *Can. J. Chem.*, 1987, **65**, 941.
138. M.A. Doverspike, M.-C. Wu and M.S. Conradi, *Phys. Rev. Lett.*, 1986, **56**, 2284.
139. W.P. Power, R.E. Wasylishen and R.D. Curtis, *Can. J. Chem.*, 1989, **67**, 454.
140. W.P. Power, B.Sc. Honours Thesis, Dalhousie University, 1988.
141. R.E. Wasylishen, G.H. Penner, W.P. Power and R.D. Curtis, *J. Am. Chem. Soc.*, 1989, **111**, 6082.
142. R.D. Curtis, G.H. Penner, W.P. Power and R.E. Wasylishen, *J. Phys. Chem.*, 1990, **94**, 4000.
143. S.J. Opella, P.L. Stewart and K.G. Valentine, *Q. Rev. Biophys.*, 1987, **19**, 7.
144. (a) A Naito, S. Ganapathy, K. Akasaka and C.A. McDowell, *J. Chem. Phys.*, 1981, **74**, 3190.
(b) A. Naito, S. Ganapathy, P. Raghunathan and C.A. McDowell, *J. Chem. Phys.*, 1983, **79**, 4173.

(c) A. Naito and C.A. McDowell, *J. Chem. Phys.*, 1984, **81**, 4795.
(d) C.A. McDowell, A. Naito, D.L. Sastry and K. Takegoshi, *J. Magn. Reson.*, 1986, **69**, 283.
145. N. Janes, S. Ganapathy and E. Oldfield, *J. Magn. Reson.*, 1983, **54**, 111.
146. R.E. Stark, L.W. Jelinski, D.J. Ruben, D.A. Torchia and R.G. Griffin, *J. Magn. Reson.*, 1983, **55**, 266.
147. G.S. Harbison, L.W. Jelinski, R.E. Stark, D.A. Torchia, J. Herzfeld and R.G. Griffin, *J. Magn. Reson.*, 1984, **60**, 79.
148. (a) T.G. Oas, C.J. Hartzell, T.J. McMahon, G.P. Drobny and F.W. Dahlquist, *J. Am. Chem. Soc.*, 1987, **109**, 5956.
(b) T.G. Oas, C.J. Hartzell, F.W. Dahlquist and G.P. Drobny, *J. Am. Chem. Soc.*, 1987, **109**, 5962.
(c) C.J. Hartzell, M. Whitfield, T.G. Oas and G.P. Drobny, *J. Am. Chem. Soc.*, 1987, **109**, 5966.
149. T.G. Oas, G.P. Drobny and F.W. Dahlquist, *J. Magn. Reson.*, 1988, **78**, 408.
150. K.G. Valentine, A.L. Rockwell, L.M. Gierasch and S.J. Opella, *J. Magn. Reson.*, 1987, **73**, 519.
151. Y. Hiyama, C.-H. Niu, J.V. Silverton, A. Bavoso and D.A. Torchia, *J. Am. Chem. Soc.*, 1988, **110**, 2378.
152. D. Suter, A. Pines, J.H. Lee and G. Drobny, *Chem. Phys. Lett.*, 1988, **144**, 324.
153. Q. Teng and T.A. Cross, *J. Magn. Reson.*, 1989, **85**, 439.
154. T.A. Cross, *Biophys. J.*, 1986, **49**, 124.
155. (a) P.L. Stewart, K.G. Valentine and S.J. Opella, *J. Magn. Reson.*, 1987, **71**, 45.
(b) P.L. Stewart, R. Tycko and S.J. Opella, *J. Chem. Soc., Faraday Trans. 1*, 1988, **84**, 3803.
156. D. Wemmer, V. Petrouleas, N. Panaglotopoulos, S.E. Filippakis and R.M. Lemmon, *J. Phys. Chem.*, 1983, **87**, 999.
157. R.E. Stark, R.A. Haberkorn and R.G. Griffin, *J. Chem. Phys.*, 1978, **68**, 1996.
158. (a) R. Tycko, P.L. Stewart and S.J. Opella, *J. Am. Chem. Soc.*, 1986, **108**, 5419.
(b) R. Tycko and S.J. Opella, *J. Chem. Phys.*, 1987, **86**, 1761.
(c) K.V. Ramanathan and S.J. Opella, *J. Magn. Reson.*, 1988, **78**, 367.
159. W. Scheubel, H. Zimmermann and U. Haeberlen, *J. Magn. Reson.*, 1985, **63**, 544.
160. N.J. Heaton, R.R. Vold and R.L. Vold, *J. Chem. Phys.*, 1989, **91**, 56.
161. S. Ganapathy, V.P. Chacko and R.G. Bryant, *J. Chem. Phys.*, 1984, **81**, 661.
162. P.S. Marchetti, R.S. Honkonen and P.D. Ellis, *J. Magn. Reson.*, 1987, **71**, 294.
163. T.M. Duncan, *J. Am. Chem. Soc.*, 1984, **106**, 2270.
164. M. Dubiel and D. Ehrt, *Phys. Stat. Sol (a)*, 1987, **100**, 415.
165. (a) A.-R. Grimmer, D. Müller and J. Neels, *Z. Chem.*, 1983, **23**, 140.
(b) U. Haubenreisser, U. Sternberg and A.-R. Grimmer, *Mol. Phys.*, 1987, **60**, 151.
166. (a) A. Nolle, *Z. Physik B: Condens. Matter*, 1979, **34**, 175.
(b) R. Balz, M. Haller, W.E. Hertler, O. Lutz, A. Nolle and R. Schafitel, *J. Magn. Reson.*, 1980, **40**, 9.
167. G.H. Penner, W.P. Power and R.E. Wasylishen, *Can. J. Chem.*, 1988, **66**, 1821.
168. C.P. Slichter, *Ann. Rev. Phys. Chem.*, 1986, **37**, 25.
169. P.-K. Wang, J.-P. Ansermet, S.L. Rudaz, Z. Wang, S. Shore, C.P. Slichter and J.H. Sinfelt, *Science*, 1986, **234**, 35.
170. D.E. Kaplan and E.L. Hahn, *J. Phys. Radium*, 1958, **19**, 821.
171. (a) C.D. Makowka, C.P. Slichter and J.H. Sinfelt, *Phys. Rev. Lett.*, 1982, **49**, 379.
(b) C.D. Makowka, C.P. Slichter and J.H. Sinfelt, *Phys. Rev. B: Condens. Mat.*, 1985, **31**, 5663.
172. P.-K. Wang, C.P. Slichter and J.H. Sinfelt, *Phys. Rev. Lett.*, 1984, **53**, 82.
173. S.E. Shore, J.-P. Ansermet, C.P. Slichter and J.H. Sinfelt, *Phys. Rev. Lett.*, 1987, **58**, 953.
174. E.F. Rybaczewski, B.L. Neff, J.S. Waugh and J.S. Sherfinski, *J. Chem. Phys.*, 1977, **67**, 1231.
175. V.R. Cross and J.S. Waugh, *J. Magn. Reson.*, 1977, **25**, 225.
176. S.J. Opella and J.S. Waugh, *J. Chem. Phys.*, 1977, **66**, 4919.

177. G. Bodenhausen, R.E. Stark, D.J. Ruben and R.G. Griffin, *Chem. Phys. Lett.*, 1979, **67**, 424.
178. M.E. Stoll, A.J. Vega and R.W. Vaughan, *J. Chem. Phys.*, 1976, **65**, 4093.
179. M. Linder, A. Höhener and R.R. Ernst, *J. Chem. Phys.* 1980, **73**, 4959.
180. T.A. Cross and S.J. Opella, *J. Am. Chem. Soc.*, 1983, **105**, 306.
181. T.A. Cross and S.J. Opella, *J. Mol. Biol.*, 1985, **182**, 367.
182. K.G. Valentine, D.M. Schneider, G.C. Leo, L.A. Colnago and S.J. Opella, *Biophys. J.*, 1986, **49**, 36.
183. P.V. LoGrasse, L.K. Nicholson and T.A. Cross, *J. Am. Chem. Soc.*, 1989, **111**, 1910.
184. A. Naito, P.B. Barker and C.A. McDowell, *J. Chem. Phys.*, 1984, **81**, 1583.
185. K. Takegoshi and C.A. McDowell, *J. Chem. Phys.*, 1987, **86**, 6077.
186. W.E.J.R. Maas, A.P.M. Kentgens and W.S. Veeman, *J. Chem. Phys.*, 1987, **87**, 6854.
187. M. Munowitz, T.-H. Huang and R.G. Griffin, *J. Chem. Phys.*, 1987, **86**, 4362.
188. C.J. Hartzell, T.K. Pratum and G. Drobny, *J. Chem. Phys.*, 1987, **87**, 4324.
189. P. Caravatti, G. Bodenhausen and R.R. Ernst, *Chem. Phys. Lett.*, 1982, **89**, 363.
190. P. Caravatti, L. Braunschweiler and R.R. Ernst, *Chem. Phys. Lett.*, 1983, **100**, 305.
191. R.K. Harris, K.J. Packer and A.M. Thayer, *J. Magn. Reson.*, 1985, **62**, 284.
192. J. Herzfeld and A. Berger, *J. Chem. Phys.*, 1980, **73**, 6021.
193. R.K. Harris, K.J. Packer and P. Reams, *Chem. Phys. Lett.*, 1985, **115**, 16.
194. A.-R. Grimmer and J. Neels, *Z. Anorg. Allg. Chem.*, 1989, **576**, 117.
195. R.A. Santos, W.-J. Chien, G.S. Harbison, J.D. McCurry and J.E. Roberts, *J. Magn. Reson.*, 1989, **84**, 357.
196. D.L. VanderHart, *J. Chem. Phys.*, 1986, **84**, 1196.
197. E. Lippmaa, M. Alla, H. Roude, R. Teeäär, I. Heinmaa and E. Kundla, *Magn. Reson. Relat. Phenom., Proc. Cong. Ampere 20th*, 1979, 87.
198. S.J. Opella, M.H. Frey and T.A. Cross, *J. Am. Chem. Soc.*, 1979, **101**, 5856.
199. J.G. Hexem, M.H. Frey and S.J. Opella, *J. Am. Chem. Soc.*, 1981, **103**, 224.
200. (a) A. Naito, S. Ganapathy and C.A. McDowell, *J. Chem. Phys.*, 1981, **74**, 5393.
(b) A. Naito, S. Ganapathy and C.A. McDowell, *J. Magn. Reson.*, 1982, **48**, 367.
201. N. Zumbulyadis, P.M. Henrichs and R.H. Young, *J. Chem. Phys.*, 1981, **75**, 1603.
202. J.G. Hexem, M.H. Frey and S.J. Opella, *J. Chem. Phys.*, 1982, **77**, 3847.
203. J. Böhm, D. Fenzke and H. Pfeifer, *J. Magn. Reson.*, 1983, **55**, 197.
204. A.C. Olivieri, L. Frydman and L.E. Diaz, *J. Magn. Reson.*, 1987, **75**, 50.
205. M. Witanowski, L. Stefaniak, and G.A. Webb, *Ann. Rep. NMR Spectrosc.*, 1986, **18**, 1–761.
206. S. Mooibroek and R.E. Wasylishen, *Can. J. Chem.*, 1987, **65**, 357.
207. J.G. Hexem, M.H. Frey and S.J. Opella, *J. Am. Chem. Soc.*, 1983, **105**, 5717.
208. (a) R.K. Harris, P. Jonsen and K.J. Packer, *Magn. Reson. Chem.*, 1984, **22**, 784.
(b) R.K. Harris, P. Jonsen and K.J. Packer, *Magn. Reson. Chem.*, 1985, **23**, 565.
(c) R.K. Harris, P. Jonsen, K.J. Packer and C.D. Campbell, *Magn. Reson. Chem.*, 1986, **24**, 977.
209. M.H. Frey and S.J. Opella, *J. Magn. Reson.*, 1986, **66**, 144.
210. C.G. Moreland, E.O. Stejskal, S.C.J. Sumner, J.D. Memory, F.I. Carroll, G.A. Brine and P.S. Portoghese, *J. Magn. Reson.*, 1989, **83**, 173.
211. M. Okazaki, A. Naito and C.A. McDowell, *Chem. Phys. Lett.*, 1983, **100**, 15.
212. (a) P. Jonsen, *J. Magn. Reson.*, 1988, **77**, 348.
(b) P. Jonsen, *J. Magn. Reson.*, 1989, **83**, 663.
213. A.C. Olivieri, *J. Magn. Reson.*, 1989, **82**, 342.
214. S.D. Swanson, S. Ganapathy and R.G. Bryant, *J. Magn. Reson.*, 1987, **73**, 239.
215. P. Jonsen, S.F. Tanner and A.H. Haines, *Chem. Phys. Lett.* 1989, **164**, 325.
216. D.L. Sastry, A. Naito and C.A. McDowell, *Chem. Phys. Lett.*, 1988, **146**, 422.
217. W.W. Fleming, C.A. Fyfe, J.R. Lyerla, H. Vanni and C.S. Yannoni, *Macromolecules*, 1980, **13**, 460.

218. J.W. Diesveld, E.M. Menger, H.T. Edzes and W.S. Veeman, *J. Am. Chem. Soc.*, 1980, **102**, 7936.
219. E.M. Menger and W.S. Veeman, *J. Magn. Reson.*, 1982, **46**, 257.
220. A.C. Olivieri, *J. Magn. Reson.*, 1989, **81**, 201.
221. R.A. Komoroski, R.G. Parker, A.M. Mazany and T.A. Early, *J. Magn. Reson.*, 1987, **73**, 389.
222. R.K. Harris, *J. Magn. Reson.*, 1988, **78**, 389.
223. D.C. Apperley, B. Haiping and R.K. Harris, *Mol. Phys.*, 1989. **68**, 1277.
224. R.C. Crosby and J.F. Haw, *Macromolecules*, 1987, **20**, 2324.
225. S. Aime, M. Botta, R. Gobetto and B.E. Hanson, *Inorg. Chem.*, 1989, **28**, 1196.
226. M.J. Collins, J.A. Ripmeester and J.F. Sawyer, *J. Am. Chem. Soc.*, 1987, **109**, 4113.
227. (a) A.C. Olivieri, L. Frydman, M. Grasselli and L.E. Diaz, *Magn. Reson. Chem.*, 1988, **26**, 281. (b) A. Olivieri, L. Frydman, M. Grasselli and L. Diaz, *Magn. Reson. Chem.*, 1988, **26**, 615.
228. S.J. Opella and M.H. Frey, *J. Am. Chem. Soc.*, 1979, **101**, 5854.
229. L.B. Alemany, D.M. Grant, T.D. Alger and R.J. Pugmire, *J. Am. Chem. Soc.*, 1983, **105**, 6697.
230. G.S. Harbison, P.P.J. Mulder, H. Pardoen, J. Lugtenburg, J. Herzfeld and R.G. Griffin, *J. Am. Chem. Soc.*, 1985, **107**, 4809.
231. M.G. Munowitz, R.G. Griffin, G. Bodenhausen and T.H. Huang, *J. Am. Chem. Soc.*, 1981, **103**, 2529.
232. M.G. Munowitz and R.G. Griffin, *J. Chem. Phys.*, 1982, **76**, 2848.
233. J. Herzfeld, J.E. Roberts and R.G. Griffin, *J. Chem. Phys.*, 1987, **86**, 597.
234. M. Munowitz, W.P. Auc and R.G. Griffin, *J. Chem. Phys.*, 1982, **77**, 1686.
235. M.G. Munowitz, T.H. Huang, C.M. Dobson and R.G. Griffin, *J. Magn. Reson.*, 1984, **57**, 568.
236. S.O. Smith and R.G. Griffin, *Ann. Rev. Phys. Chem.*, 1988, **39**, 511.
237. J.A. DiVerdi and S.J. Opella, *J. Am. Chem. Soc.*, 1982, **104**, 1761.
238. M.H. Frey, S.J. Opella, A.L. Rockwell and L.M. Gierasch, *J. Am. Chem. Soc.*, 1985, **107**, 1946.
239. J.E. Roberts, G.S. Harbison, M.G. Munowitz, J. Herzfeld and R.G. Griffin, *J. Am. Chem. Soc.*, 1987, **109**, 4163.
240. J. Schaefer, R.A. McKay, E.O. Stejskal and W.T. Dixon, *J. Magn. Reson.*, 1983, **52**, 123.
241. J. Schaefer, E.O. Stejskal, R.A. McKay and W.T. Dixon, *J. Magn. Reson.*, 1984, **57**, 85.
242. M.H. Frey, J.A. DiVerdi and S.J. Opella, *J. Am. Chem. Soc.*, 1985, **107**, 7311.
243. J. Schaefer, M.D. Sefcik, E.O. Stejskal, R.A. McKay, W.T. Dixon and R.E. Cais, *Macromolecules*, 1984, **17**, 1107.
244. J. Schaefer, E.O. Stejskal, D. Perchak, J. Skolnick and R. Yaris, *Macromolecules*, 1985, **18**, 368.
245. J.R. Garbow and J. Schaefer, *Macromolecules*, 1987, **20**, 819.
246. T.A. Early, *J. Magn. Reson.*, 1987, **75**, 129.
247. D.P. Burum, M. Linder and R.R. Ernst, *J. Magn. Reson.*, 1981, **44**, 173.
248. G.G. Webb and K.W. Zilm, *J. Am. Chem. Soc.*, 1989, **111**, 2455.
249. A.C. Kolbert, M.H. Levitt and R.G. Griffin, *J. Magn. Reson.*, 1989, **85**, 42.
250. A.C. Kolbert, D.P. Raleigh, M.H. Levitt and R.G. Griffin, *J. Chem. Phys.*, 1989, **90**, 679.
251. D.P. Raleigh, A.C. Kolbert, T.G. Oas, M.H. Levitt and R.G. Griffin, *J. Chem. Soc., Faraday Trans. 1*, 1988, **84**, 3691.
252. D.P. Raleigh, A.C. Kolbert, M.H. Levitt and R.G. Griffin, *Isr. J. Chem.*, 1988, **28**, 263.
253. A.C. Kolbert, H.J.M. de Groot and R.G. Griffin, *J. Magn. Reson.*, 1989, **85**, 60.
254. H. Miura, T. Terao and A. Saika, *J. Chem. Phys.*, 1986, **85**, 2458.
255. T. Terao, H. Miura and A. Saika, *J. Chem. Phys.*, 1986, **85**, 3816.
256. T. Terao, *Trends Anal. Chem.*, 1987, **6**, 182.
257. T. Nakai, T. Terao and H. Shirakawa, *Chem. Phys. Lett.*, 1988, **145**, 90.
258. T. Nakai, J. Ashida and T. Terao, *J. Chem. Phys.*, 1988, **88**, 6049.
259. T. Nakai, J. Ashida and T. Terao, *Magn. Reson. Chem.*, 1989, **27**, 666.
260. T. Nakai, J. Ashida and T. Terao, *Mol. Phys.*, 1989, **67**, 839.

261. J. Schaefer, T.A. Skokut, E.O. Stejskal, R.A. McKay and J.E. Varner, *Proc. Natl. Acad. Sci. USA*, 1981, **78**, 5978.
262. (a) J. Schaefer, R.A. McKay and E.O. Stejskal, *J. Magn. Reson.*, 1979, **34**, 443.
(b) J. Schaefer, E.O. Stejskal, J.R. Garbow and R.A. McKay, *J. Magn. Reson.*, 1984, **59**, 150.
263. E.O. Stejskal, J. Schaefer and R.A. McKay, *J. Magn. Reson.*, 1984, **57**, 471.
264. J. Schaefer, T.A. Skokut, E.O. Stejskal, R.A. McKay and J.E. Varney, *J. Biol. Chem.*, 1981, **256**, 11574.
265. J. Schaefer, K.J. Kramer, J.R. Garbow, G.S. Jacob, E.O. Stejskal, T.L. Hopkins and R.D. Speirs, *Science*, 1987, **235**, 1200.
266. R.A. McKay, J. Schaefer, E.O. Stejskal, R. Ludicky and C.N. Matthews, *Macromolecules*, 1984, **17**, 1124.
267. J.R. Garbow, J. Schaefer, R. Ludicky and C.N. Matthews, *Macromolecules*, 1987, **20**, 305.
268. E.W. Hagaman, *J. Am. Chem. Soc.*, 1988, **110**, 5594.
269. (a) T. Gullion, M.D. Poliks and J. Schaefer, *J. Magn. Reson.*, 1988, **80**, 553.
(b) T. Gullion and J. Schaefer, *J. Magn. Reson.*, 1989, **81**, 196.
270. T. Gullion and J. Schaefer, in *Advances in Magnetic Resonance*, Vol. 13 (ed., W.S. Warren), pp. 57–83. Academic Press, San Diego, 1989.
271. D.M. Schneider, R. Tycko and S.J. Opella, *J. Magn. Reson.*, 1987, **73**, 568.
272. T.G. Oas, C.J. Hartzell, G.P. Drobny and F.W. Dahlquist, *J. Magn. Reson.*, 1989, **81**, 395.
273. (a) T.G. Oas, R.G. Griffin and M.H. Levitt, *J. Chem Phys.*, 1988, **89**, 692.
(b) M.H. Levitt, T.G. Oas and R.G. Griffin, *Isr. J. Chem.*, 1988, **28**, 271.

The Oxidation-State Dependence of Transition-Metal Shieldings

R. GARTH KIDD

Department of Chemistry, The University of Western Ontario, London, Ontario N6A 5B7, Canada

1. INTRODUCTION

It is now a third of a century since Freeman, Murray and Richards[1] published their classic paper on ^{59}Co, establishing for the first time—and for all time—that electron density integrated over some localized volume of a molecule is not the only cause of magnetic shielding at a particular nucleus.

ANNUAL REPORTS ON NMR SPECTROSCOPY
VOLUME 23 ISBN 0-12-505323-1

Copyright © 1991 Academic Press Limited
All rights of reproduction in any form reserved

The correlation between the ^{59}Co shift and the wavelength of the lowest-energy d–d transition in octahedral complexes of the d^6 cobalt(III) system is linear, and it spans a large fraction of the total ^{59}Co shielding range. The correlation was so striking it led to the discovery of analogous correlations in other systems, and a paradigm of nuclear deshielding caused by low-lying electronically excited states gained ready acceptance among NMR spectroscopists.

In 1950, Ramsey[2] had developed a general model for the shielding of nuclei in molecules and within weeks of the Freeman, Murray and Richards discovery, Griffith and Orgel[3] obtained a quantitative fit of the cobalt chemical shifts and the molecular excitation energies to the Ramsey model. Thereafter, there developed a school of thinking about nuclear shielding generally in which an electronic excitation energy is the dominant *variable*.

In this chapter I survey and summarize for the transition metals the experimental evidence bearing on the question of what causes a chemical shift. I conclude that *variation* in the radial size of valence-shell atomic orbitals, caused by variation in effective nuclear charge with change in oxidation state, is the causative factor with the greatest generality. Furthermore, while excitation energy is certainly a major influence on nuclear shielding in some molecules, oxidation state operating through the $\langle r^{-3} \rangle$ factor in the paramagnetic term of Ramsey's model influences the nuclear shielding in all molecules.

The pattern of chemical shifts to higher frequencies—lower shieldings—with increases in oxidation state is not restricted to the transition metals. It is seen among the alkali metals where the ^{23}Na shielding of sodium(−I) is 60 ppm greater than that of sodium(I), and in ^{87}Rb spectroscopy the corresponding difference is 150 ppm. In ^{205}Tl spectroscopy, the centre of the thallium(I) shielding range is more highly shielded than that of the thallium(III) range by 2800 ppm, and the regular shielding increase along the series Xe(VIII) < Xe(VI) < Xe(IV) < Xe(II) is shown in Fig. 16. Even in proton spectroscopy, hydridic hydrogen(−I) is more highly shielded than hydrogen(I), but for a different reason.

The ^{59}Co shieldings whose original correlation[3] with optical wavelengths generated the excitation-energy paradigm have in the past decade been reanalysed in greater depth[4,5] to reveal the instrumentality of causative factors other than excitation energy; orbital size in particular. What the deeper analysis reveals is that, together with and coupled to changes in excitation energy, there are changes in both orbital size and orbital angular momentum when one ligand is substituted for another in the octahedral array. The magnitudes of these changes indicate that the shielding picture for ^{59}Co,

dominated by the excitation-energy factor, is not inconsistent with the oxidation-state paradigm that is broadly applicable to all atoms.

1.1. The literature of transition-metal shieldings

The NMR literature dealing with the transition metals is reviewed annually, and the reports[6] prepared by Hawkes until 1985 and by Forster since then are comprehensive. These reports greatly facilitate the search for patterns of behaviour that extend beyond a narrow region of the periodic table.

Reviews of the literature covering all the transition metals have appeared at regular intervals. These have been prepared by Kidd and Goodfellow in 1978,[7] by Kidd in 1978,[8] by Dechter in 1985,[9] by Rehder in 1986,[10] by Mason in 1987,[11] and by Rehder and Goodfellow in 1987.[12] In addition to these reviews covering all the transition metals including the copper and zinc triads, there have been a number of transition metal reviews with more limited scope but correspondingly greater detail. In 1979 Wehrli[13] reviewed the quadrupolar transition metals. In 1984 Rehder[14] reviewed the first-row transition metals in great detail and drew many theoretical correlations. Pregosin[15] in 1982 reviewed the ^{195}Pt literature. Minelli *et al.*[16] in 1985 reviewed the chromium, molybdenum, and tungsten NMR literature. In 1986 von Philipsborn[17] reviewed the members, primarily in their low oxidation states, of the iron, cobalt, and nickel triads with the potential for catalytic activity.

In preparing this chapter I have drawn heavily upon these reviews and am indebted to their authors for the work they have invested in abstracting, collating, and analysing from a body of literature that is very large the salient numbers, comparisons, and correlations from which a general pattern of shielding behaviour can be elucidated.

2. THE DISPOSITION OF VALENCE ELECTRONS IN MOLECULES

The chemist for whom NMR spectroscopy is a well-used instrument is conversant with two different sets of scientific theory: the theory of chemical bonding; and the theory of nuclear magnetic shielding, coupling, and relaxation. When one is familiar with both, the NMR effects observed in the laboratory point, through one or other bonding theory, to the structural characteristics of a molecule.

The chemist specializing in compounds of the transition metals faces a considerably larger body of theory on both fronts. On the bonding front, one has not just valence-bond theory and molecular-orbital theory, but ligand-

field theory as well. On the NMR front one faces not just chemical shifts caused by variations in bonds with *s*- and *p*-type electrons only. One discovers that *d*-electron participation in the bonding picture introduces a shielding perturbation of major dimensions, even in molecules where all the *d* electrons are spin paired.

Transition-metal compounds with unpaired electrons and spin angular momentum are paramagnetic and not generally amenable to NMR characterization. But those diamagnetic compounds of the transition metals with low-lying electronic excited states containing large increments of *orbital* angular momentum exhibit Van Vleck or temperature-independent paramagnetism (TIP), something not observed in compounds of the representative atoms. While the orbital angular momentum may be viewed as originating in the transition-metal molatom, it is ultimately a molecular parameter not restricted to any one molatom, and its effect is to deshield all parts of the molecule.

The ultimate purpose of bonding theories is the explanation of two things: how the unique chemical behaviour of a pure substance is determined by the unique topological arrangement of molatoms in its molecule; and how the valence electrons distribute themselves within a molecule so as to favour that particular topology over the feasible alternatives.

The first of these explanations forges the link between macroscopic chemistry seen in the laboratory and microscopic chemistry seen in the imagination. The other uses NMR evidence to place the molatoms and their bonding electrons within the imagination's picture. The definitive evidence on molecular topology comes from X-ray diffractometry, but NMR and other spectroscopies usually provide—in far less time— preliminary evidence that may be close to definitive.

2.1. Theories of chemical bonding

Providing an explanation about the location of electrons within a molecule is what generates theories of chemical bonding. Out of Lewis's early speculation about the electron-pair bond have grown the two families of bonding theory that inform chemistry today: one based on the principle of *equal shares* in bonding electrons, and the other based on the principle of *unequal shares* generating positive and negative oxidation states.

On the one hand we have the valence-bond (VB) and the molecular-orbital (MO) theories, both of which start with bond-free, electrically neutral atoms, each species being extremely high in bond-forming potential. The bonding theory that emerges is an explanation of why, starting with that particular set of atoms, the valence electrons redistribute themselves into bonds of various

types among the nuclear centres in a molecule so that the particular molatom arrangement observed is the energetically favoured one.

On the other hand we have the crystal-field (CF) and ligand-field (LF) theories, developed since 1950 to alleviate the problem created for the earlier bonding theories by transition-metal complexes with their seemingly anomalous "coordinate" bonds. What was needed was a theory that would explain why ligands (originally, stable molecules in which the bonding potentials of the free atoms have been largely requited) such as NH_3, H_2O, CO, N_2, cyclopentadiene, benzene, phosphines, arsines and others should react with transition-metal halides (also stable molecules), sometimes relegating the bonded halide to a secondary role in satisfying the bonding requirements of the transition metal.

A crystal-field/ligand-field theory analysis of bonding begins at the opposite end of the electron-sharing spectrum from where a valence bond/molecular orbital analysis begins. At the metal end of a bond, one starts with an n^+ cation that is hundreds of kilojoules (per 6.02×10^{23}) higher in energy than the metal atom. At the ligand end, one starts with chemically bonded molatoms hundreds of kilojoules lower in energy than the atoms from which the molatoms were formed. The theoretical analysis consists of transferring negative charge from the ligand to the metal by gradually moving the bonding electron pair or pairs along the bond axis from the ligand towards the metal until the point of minimum energy is reached.

Some less-than-definitive NMR thinking today about transition-metal compounds occurs through a failure to acknowledge this salient difference between the two families of bonding theory. Both theory sets start with all nuclear centres fixed in their equilibrium positions defining the topology of the molecule. However, to locate the valence electrons within this fixed framework, one begins in the covalent limit of equal sharing and polarizes the valence electrons in the directions of the more electronegative atoms. The other theory begins in the ionic limit of unequal sharing, recognizes through the electroneutrality principle[18] that this overstates the inequality in sharing, and depolarizes the valence electrons towards the less electronegative atoms, in the direction of more equal sharing.

Regardless of the theoretical limit in which one starts thinking about the disposition of valence electrons in a real molecule, the end result is one of unequal sharing in which the "gives and takes" of each molatom during molecule formation are accounted for by positive and negative oxidation states that sum to zero over the uncharged molecule. But the way in which one describes the chemical bonds after they are formed is entirely dependent on the theoretical starting point because, of course, every actual chemical bond is more ionic than one theoretical starting point and more covalent than the other.

2.2. Electron locations and chemical shifts

Along with the surprising discovery of the chemical-shift phenomenon in 1951 came the realization that NMR provides, in raw form, the most sensitive evidence yet about the disposition of valence electrons in molecules. The interpretive task is one of deciding in which cases a positive chemical shift indicates:

(i) a reduction in the integrated electron density assigned to that particular nucleus;
(ii) in which cases it indicates an increase in the $d{:}p$ or $p{:}s$ ratio at constant integrated density (i.e. a redistribution of electrons among orbitals resulting in increased orbital angular momentum);
(iii) in which cases it indicates merely the proximity of low-lying electronic excited states having greater orbital angular momentum about the particular nucleus than has the ground state molecule under study.

These decisions are made on the basis of correlations within a structurally related series of molecules between chemical shifts observed and independent measures of causes (i)–(iii) above. Because these three causes are coupled to one another, more strongly in one series than in another, it has been difficult to decide upon cases in which one cause dominates to the point that its chemical shift can be taken as a definitive measure of valence-electron disposition. Many of the correlations observed are found to hold over a fairly wide range of molecules, but fail when tested with molecules of different characteristics. The correlations that are lacking in generality are discussed in Section 3.

The oxidation state of a particular molatom is the most primitive but also the most general measure of integrated electron density associated with various nuclear centres within a molecule. Every chemically bonded atom has an oxidation state, and for electrically neutral molecules it is a zero-sum parameter easily computed in terms of the electronegativity differences between the parts of a molecule. Of all the chemical-shift correlations that have been studied, the one with a molatom's oxidation state has the fewest exceptions. The generality of the nuclear shielding/oxidation state correlation among the transition metals is discussed in Section 3.

3. SHIELDING CORRELATIONS LACKING IN GENERALITY

Theoretical commentary about chemical shifts falls into one of two categories. The first is *numerical analysis*, the outcome of which is a set of additive substituent constants for systems amenable to a first-order analysis, and pairwise additive constants for systems requiring a second-order analysis. In

transition-metal NMR the object of numerical analysis is to quantify the shielding change at the metal when one substituent replaces another. This type of analysis can be useful in predicting the position of a new resonance and in making spectral assignments for complex mixtures, but substituent constants provide only limited structural insight.

Correlation analysis of NMR shieldings is the type of theoretical commentary used to gain structural insight. The objective is to find another structurally significant observable with which to correlate the chemical shift and then see whether chemical shifts can be used to identify the disposition of valence electrons. Correlations provide the greatest chemical insight and it is with these that this chapter is concerned.

The Ramsey $\{\sigma_d + \sigma_p\}$ model for nuclear shielding is the only comprehensive one that has stood the test of time,[2] and it is an angular-momentum model. Although the absolute magnitudes of the diamagnetic and paramagnetic terms are comparable, 90% of the variation in nuclear shielding that is manifested as a chemical shift is attributable to the variation in the orbital angular momentum of the valence electrons associated with the nucleus, a shielding variation that is modelled in the paramagnetic term. Somewhat less than 10% of the variation, modelled in the diamagnetic term, is attributable to the variation in the integrated electron density associated with the nucleus.

Because it is concerned with orbital angular momentum, this Ramsey model does not account for the chemical shifts observed in (some) paramagnetic molecules, and it does not work particularly well for those solids where antiferromagnetic interactions are present. The number of chemical-shift comparisons between solution-state and solid-state spectra is not large, but where the comparisons have been made the solution shift and the solid shift are usually similar. Where there is reason to believe the solid may be antiferromagnetic, and semiconductors are prime candidates, the solid-state shifts are significantly different from those observed for comparable coordination in solution. The ^{51}V shieldings in the Cu_3VE_4 (E = S, Se or Te) system are good examples and are discussed in detail in Section 5.

3.1. The excitation-energy correlation

In the earliest ^{59}Co studies[1] a strong correlation was noted between deshielded extremes and sample colour, leading to the belief that low-lying electronic excited states somehow cause nuclear deshielding. This connection was not restricted to the *d–d* excitations of transition-metal complexes and the effect of excited states associated with charge-transfer bands was noted in the deshielding of $^{17}O^{19}$ in organic carbonyl compounds.

The paramagnetic term in Ramsey's shielding model takes the form

$$\sigma_p = (\text{constant}/\Delta E)(L\text{-factor})\langle r^{-3}\rangle_{\text{valence}}$$

and the facile association of longest-wavelength absorption energy with ΔE in the paramagnetic term led to an early belief that in transition-metal compounds generally, and probably in most other compounds as well, both the orbital angular momentum factor and the factor describing the average radius of the valence electrons remain essentially constant from molecule to molecule while variations in ΔE only cause the observed variations in nuclear shielding.

Constancy of all factors except ΔE is only one circumstance in which chemical shift and ΔE will be linearly correlated. If there are significant changes in one or both of the other two factors accompanying the independently observed change in ΔE, there will still be a linear correlation between σ_p and ΔE provided that the changes in the other two factors are proportional to the changes in ΔE.

If, except for minor exceptions, the vast majority of all chemical systems studied followed the excitation-energy correlation, one would opt for the "other factors constant" interpretation of the Ramsey model. But the totality of all evidence from 30 years of NMR spectroscopy goes against this interpretation. While there are many systems that follow the excitation-energy correlation there are at least as many, if not more, that go against it.

The Cl vs. I shielding effect upon the molatom to which the halogen is bonded has been studied for most of the atoms in the periodic table. While there are a number of well-documented cases (discussed below) that show inverse behaviour, in the majority of cases the iodide causes the highest shielding of any substituent, despite the fact that the electronic excited states of the iodide lie lower than those of the analogous chloride compound which is related to a weaker hold upon non-bonding electrons exerted by the iodide. In other words, in the many systems that follow the pattern of normal halogen dependence, a dependence that has been rationalized through the $\langle r^{-3}\rangle$ factor, the observed shielding runs counter to the ΔE predictions of the Ramsey model.

With the "other factors constant" interpretation out of the way, the existence of many excitation-energy correlations can mean only one thing. Except for a few limiting cases in which the substitution of one molatom for another happens to have a dominating influence on only one of the three variables in the paramagnetic term, a substitution affects all three variables. Furthermore, since the variables are not independent of each other, a change in one correlates with changes in the others and the chemical shift observed depends upon a blended change in each of the three factors.

Scientists generally and chemists in particular have an aversion to multi-cause effects. They much prefer single-variable models and indeed the

philosophical underpinning of modern science is one of minimum complexity in theoretical models consistent with the facts being modelled—the principle known as Occam's razor. We cannot, however, escape the fact that the only model to account adequately for nuclear shieldings generally contains at least three variables.[20] The preference for models of minimum complexity can be satisfied only when, over a broad region of the landscape, one of the variables is dominant.

Before moving on, let us be quite clear on this matter of low-lying excited states (LLESs) and their influence on nuclear shielding. Their influence is invoked only when one observes a deshielding that cannot be explained in terms of some feature of the ground-state molecule. When this occurs we must be aware that we are no longer dealing with just a ground-state molecule, but are measuring an NMR frequency that depends on both electronic ground and excited states—effectively, an effect dependent jointly on two different structures.

When chemists trace the variation in some chemical aspect of bonding along a series of related molecules, it is the ground-state molecules that are being compared unless there is some very definite indication to the contrary. Photochemists, for example, would not compare the ground states of several molecules with the excited states of different molecules in the same series. Ideally, an NMR spectrum would give us information only about ground-state molecules or only about excited-state molecules, information that could be used to make valid comparisons among one or the other along a series. For molecules without low-lying excited states, this is essentially what an NMR spectrum provides.

However, for those molecules with LLESs below about $30\,000\,cm^{-1}$, an NMR spectrum provides information that is not comparable with that obtained from ground-state molecules. The spectrum cannot be obtained without putting the molecule into a magnetic field, and as soon as we do the ground state changes in the degree to which there were LLESs in the molecule unperturbed by the magnetic field. The change does not occur because the molecule has been electronically excited, but because a magnetic field has been applied. The spectrum obtained when the resonance condition is satisfied provides information about a new molecule that is effectively a hybrid of the old ground and excited molecules. An uncritical comparison of shielding in these hybrids with that in ground-state molecules can lead to conclusions that are essentially meaningless.

3.2. Normal/inverse halogen dependence

The shieldings of all atoms are particularly sensitive to halogen substitution. In the spectroscopies of ^{11}B, ^{27}Al, ^{69}Ga, ^{115}In, ^{13}C, ^{29}Si, and ^{73}Ge, the

tetraiodo molecule marks (or is very close to) the high-shielded limit of the atom's chemical shift range. By contrast, the tetrachloro molecule is on the deshielded side of the range centre, and the tetrabromo one lies about one-third of the way up the shielding range from the chloride, so that halogen substituents alone account for the major part of an atom's shielding range. This shielding order $Cl < Br \ll I$ with a (Br–Cl)/(I–Cl) shielding ratio of around 0.3 has been called *normal halogen dependence* (NHD).[8]

Beyond this localized region of the periodic table, NHD has been noted in the spectroscopies of other atoms as well, to the point where it represents the majority and, therefore, the normal behaviour. This majority includes: Mg, Ca, Sr, Ba; W; Mn, Tc; Ru; Co, Rh; Pt; Zn, Cd, Hg; B, Al, Ga, In; C, Si, Ge, Sn, Pb; and Sb—a total of 24.

In the spectroscopies of nuclei with low receptivity, an F–Cl series may be the only one available and it is tempting to try and establish the nature of the halogen dependence by extrapolating from the F–Cl experience. However, among systems where data for all four halogens are available and where the chloride, bromide, and iodide data reflect the normal shielding pattern, the shielding in the fluoride can be anomalous. In ^{11}B spectroscopy the shielding order is $Cl < F < Br$, and in ^{27}Al, ^{29}Si and ^{119}Sn spectroscopies the order is $Br < F < I$. Similar anomalies are seen among the transition metals, sufficient to preclude the possibility of using fluoride shieldings to predict NHD; and vice versa.

The reason for the F anomaly can be found in the bond enthalpies of the I_2, Br_2, Cl_2, and F_2 molecules of 151, 193, 255 and 160 kJ, respectively, upon which their Pauling electronegativities are, in part, based. With electronegativities of 2.7 for I, 3.0 for Br, 3.2 for Cl and 4.0 for F, there is obviously some additional factor—a large one—beyond electronegativity that is present in the bonds formed by fluorine. Whatever this factor is, and it has been variously referred to as a lone-pair effect, a long-bond effect, a low-bond-energy effect, or just simply "the fluoride effect", it is probably the same factor that causes the shielding anomaly seen with fluoride substituents.

Throughout the periodic table the availability of a Cl–Br–I series of compounds with which to test the response of nuclear shielding to substitution is far higher than that of any comparable series, but it has recently been observed[11] that where shielding data for a S–Se–Te series is available it tends to mirror the pattern seen in the Cl–Br–I series; i.e. shielding increases in the order $S < Se \ll Te$. Since NHD is widespread among the 100-plus species of molatom, and since it is an effect that spans over half the total shielding range for most molatoms, a comprehensive theory of nuclear shielding has to provide an explanation, and this the Ramsey theory does.

The valence-orbital size factor $\langle r^{-3} \rangle$ in the Ramsey model, because it is a cubed factor, indicates that chemical shifts are unusually sensitive to changes

in orbital size when one bonded molatom is substituted for another at the resonant molatom. According to the model, a substitution that enlarges the valence orbital(s) will reduce the paramagnetic term and enhance the shielding. In a ^{27}Al study of the tetrahaloaluminates,[29] a parallel was drawn between the appearance of iodide at the high-shielded extreme and the appearance of iodide at the top of the *nephelauxetic* or cloud-expanding series of substituents. The nephelauxetic mechanism operating within the Ramsey shielding model provides the rationale for normal halogen dependence.

Several commentators have suggested that an *electronegativity* mechanism operating through the $\langle r^{-3} \rangle$ factor also explains NHD, and while the electronegativity mechanism is qualitatively plausible, it is quantitatively less appealing. Qualitatively, substitution of a more electronegative molatom diminishes the valence-orbital size, enhances the paramagnetic term, and deshields the resonant molatom. But the ubiquitous 1/3:2/3 split in the Cl < Br ≪ I NHD ordering—calculated by taking the ratio of *d*-value differences (Cl–Br/Cl–I) and referred to as the regular Br/I ratio of 0.33—matches the Cl < Br ≪ I split for the nephelauxetic *h* parameters rather than the split in electronegativities closer to 1/2:1/2.

The early transition metals found in the Sc, Ti and V triads are noteworthy for a halogen dependence that is the exact opposite of the Cl < Br ≪ I shielding norm. In the spectroscopies of ^{45}Sc, ^{89}Y, ^{139}La and ^{181}Ta shielding increases in the order of Br < Cl, and in the spectroscopies of ^{47}Ti, ^{91}Zr, ^{51}V and ^{93}Nb, the shielding order is I ≪ Br < Cl. This ordering has been termed *inverse halogen dependence* (IHD) and there are two other regions of the periodic table where this inverted ordering is observed. Among the alkali metals of the Li group and in the spectroscopies of ^{63}Cu and ^{109}Ag of the Cu triad, inverse halogen dependence is also observed.

Some investigators working primarily among the early transition metals have taken issue with the "inverse" designation for a halogen dependence in which the bromide and the iodide are less and a lot less shielded than is the chloride.[21] Even after a satisfactory theoretical model (as opposed to speculative hypotheses) for the inversion has been provided (and I will argue below that it has not), the fact remains that unambiguous examples of IHD have been documented in the spectroscopies of Na, K, Rb, Cs; Sc, Y, La; Ti, Zr; V, Nb, Ta; Ag—13 at most.

There is a third class containing examples whose halogen dependence is ambivalent and it includes ambivalence of three types:

(i) an irregular halogen sequence in which Br does not lie between Cl and I—copper(I) and phosphorus(III) appear to be of this type;
(ii) molatoms exhibiting NHD in one oxidation state and IHD in another—thallium and molybdenum fall into this category; and

(iii) examples of both NHD and IHD can be found in one oxidation state of the same molatom—technetium presently belongs with the majority, but further work could easily reveal that it belongs in this category.

In this context, *normal* carries implications neither of orthodoxy nor of heterodoxy and serves only to designate majority behaviour, regardless of oxidation state. It does carry a historical implication in that the Cl < Br ≪ I shielding pattern was widely recognized in 1973 when the first examples of the opposite behaviour were discovered.[22,23]

As for the factor or factors causing the inversion in halogen dependence, there are two schools of thought and it is still very much an open question. According to the earlier school, there is a spin–orbit coupling term not presently represented in the Ramsey model the sign of which changes according to whether the electron configuration *for the free atom* ends in a valence orbital set that is more or less than half filled.[24] The more recent school of thought sees no need for a spin–orbit coupling term and attributes the crossover from NHD to IHD to a crossover in the Ramsey model from domination by the $\langle r^{-3} \rangle$ factor—called the nephelauxetic effect—to domination by the ΔE factor called the spectrochemical effect.[11]

Table 1 provides a summary listing arranged by periodic table grouping of the halogen dependence of a particular atom's nuclear shielding. The data is presented for each atom in the form of two numbers: the first giving the strength and direction of the halogen dependence in parts per million, and the second (in square brackets) giving the chloride–bromide separation as a fraction of the chloride–iodide separation—the so-called Br/I ratio. The strength figure represents the iodide minus chloride shielding difference (i.e. the chloride minus iodide *d*-value difference) *per bonded halogen* and the strength value is positive for NHD and negative for IHD. In those cases where no iodide shielding value is available, a Br/I ratio of 0.3 has been assumed and an imputed chloride–iodide separation obtained by dividing the chloride–bromide separation by 0.3. Imputed strength values are identified by the lack of an accompanying Br/I ratio.

It is an implicit rule of theory construction in science that the simplest model, the one with the fewest independent variables, is preferable provided it explains all the salient facts. From this point of view, it would be preferable if alternation between nephelauxetic and spectrochemical dominance alone could account for the alternation between normal and inverse halogen dependence without the need for spin–orbit coupling, but there are just too many facts that do not sit comfortably within the simpler model.

It has been suggested[14] that the presence of low-lying magnetically active states are sufficient to account for the inverse dependence, and low-lying *p* orbitals are cited to explain IHD among the alkali metal halides. But the

Table 1. Halogen shielding dependencies of metals, by oxidation state.

Li(I)	−ve		Na(I)	−ve		K(I)	−ve		Rb(I)	−ve
Be(II)	+2.3		Mg(II)	?		Ca(II)	+ve		Sr(II)	+ve
	Sc(III)	−79		Y(III)	?		La(III)	−133		
	Ti(IV)	−320[0.4]								
	Ti(II)	−128[0.4]		Zr(II)	−124[0.3]					
	V(V)	−480		Nb(V)	−366[0.4]					
				Mo(VI)	−147		W(II)	+590[0.3]		
	Mn(I)	+481[0.3]		Tc(I)	+247					
	Fe(II)	+958[0.3]		Ru(II)	+235					
	Co(III)	+90[0.3]		Rh(III)	+504					
	Co(−I)	+860[0.3]		Rh(I)	+187[0.3]					
							Pt(IV)	+1008[0.3]		
							Pt(II)	+974[0.3]		
				Ag(I)	−295[0.3]					
	Zn(II)	+71[0.3]		Cd(II)	+98[0.2]		Hg(II)	+451[0.3]		
B(III)	+34[0.2]		Al(III)	+33[0.2]		Ga(III)	+181[0.3]		In(III)	+256[0.3]
C(IV)	+97[0.3]		Si(IV)	+83[0.2]		Ge(IV)	+279[0.3]		Sn(IV)	+391[0.3]
									Sb(V)	+1350

alkaline earth halides have the same *p* orbitals at roughly the same levels and their halogen dependence appears normal. It is true that the vanadium and niobium sequences exhibiting inverse behaviour have low-lying excited states, but so do the high oxidation state cobalt(III) and the low oxidation state cobalt(−I) sequences in both of which the halogen dependence is normal; weak and regular in the former and strong and regular in the latter.

Among molecules alike in other respects, iodides have lower-energy charge-transfer excitations than chlorides, and tellurides have lower-energy ones than sulphides. This is a generally observable pattern related to the lower ionization energy of bonded iodine which is not restricted to any region or group within the periodic table. The absolute magnitude of the excitation energies varies from region to region, being generally smaller among the transition metal halides and chalcogenides in high oxidation states, but the relative ordering in excitation energies I < Br < Cl and Te < Se < S remains uniform throughout. In particular, there is no well-documented evidence of a reversal in relative orderings where the reversal from inverse to normal shielding dependence occurs.

If (and only if) it can be demonstrated that the absolute magnitude of the charge transfer energies is systematically lower among all groups of molecules showing IHD, then a reversal in relative ordering is not a necessary requirement of the spectrochemical mechanism for IHD. If the incidence of IHD were limited to systems having lower than normal excitation energies, then the excited-state hypothesis would be very appealing. But there is no experimental evidence pointing to such a limitation.

It may be purely fortuitous that all three episodes of inverse halogen dependence occur in a region of the periodic table where free atoms have insufficient valence electrons to half fill (or only enough to half fill) an *s* or *d* subshell that subsequently contributes to the highest occupied molecular orbital (HOMO) in the halide compound under investigation. But in the absence of an alternative explanation that rationalizes all three episodes, the spin–orbit coupling mechanism has considerable appeal.

If the sign change in spin–orbit coupling observed at the half-filled subshell in some way marks a crossover from one type of shielding influence to another, then the question as to why there is no well-documented episode of a shielding anomaly associated with a half-filled *p* subshell can and should be asked. Asking the question draws one's attention to ^{31}P NMR[25] where there is in fact another example of inverse halogen dependence. In phosphorus(V) both OPX_3 and SPX_3 are strongly IHD, while in the lower oxidation state the halogen dependence of PX_3 is weak and irregular like that of ^{63}Cu with shielding increasing in the order I < Cl < Br.

Irregular halogen dependence persists into the next group where in ^{77}Se NMR the higher oxidation state $SeOX_2$ is IHD but Se_2X_2 and Me_2SeX_2 are

NHD and where in ^{125}Te NMR the higher oxidation state is IHD in TeX_4 but NHD in H_2TeX_6 and the lower oxidation state Me_2TeX_2 is NHD.[26] A shielding irregularity of this sort is characteristic of molatoms in periodic table groups with and immediately to the right of a group with a half-filled subshell. This "to-the-right" incidence of irregularity is seen most dramatically in ^{95}Mo NMR where NHD and IHD are equally frequent.[16]

The reason why crossover behaviour is observed to the right and not to the left of the half-filled subshell has to do with the fact that free-atom s^1, p^3 and d^5 configurations are only limiting approximations to the electron arrangement shielding a molatom nucleus, and electronegative ligands pull an $n+1$ configuration in the direction of a half-filled shell.

Two features of the IHD associated with a half-filled *p* subshell call for further comment. Why is it much less pronounced; and why does it occur after rather than before the half-filled subshell? Both features, I think, are related to the fact that *p* orbitals are antisymmetric to inversion but *s* and *d* orbitals both have a symmetrical inversion centre. Among the early transition metals at a point where each subshell is less than half full, there is *s* orbital/*d* orbital energy crossing when a free transition metal atom becomes a molatom through bond formation, and it is among the early transition metals that inverse halogen dependence is most pronounced.

Mendeleev's periodic law of the atom/molatom relationship is underwritten by crossover points on one side of which bond-forming potential is driven by negative electrons in search of a positive centre (which happens to have an unpaired electron with which it can reduce its spin and orbital momenta); on the other side of which bond-forming potential is driven by positive orbital vacancies in search of an electron (with which it can reduce its spin and orbital momenta). This is the physical principle underlying the chemical principle of metals on the left, halogens on the right; electropositive on the left, electronegative on the right; positive oxidation states on the left, negative oxidation states on the right.

It is the same physical principle that underlies the negative electron/positive hole formalism of ligand-field theory and is, of course, the one responsible for the sign change in spin–orbit coupling at a half-filled subshell.

4. A GENERALIZED PATTERN OF SHIELDING DEPENDENCE

In his *Traité* of 1789,[27] Lavoisier introduced three revolutionary ideas that continue to influence our understanding of chemicals today. The first was the idea that combustible substances do not contain phlogiston. The second was a new system of chemical nomenclature, compositionally based and giving

emphasis to the oxidation rather than the dephlogistication paradigm of combustion. It was the third of Lavoisier's ideas that was to have a profound influence on the way we look at substances today and on the way we interpret their NMR spectra, particularly the spectra of metallic compounds.

By introducing for metals forming more than one oxide what he called "different degrees of oxygenation", Lavoisier invented the idea which today goes under the name of oxidation state. On a philosophical level, the oxidation state describes not a chemical attribute that is intrinsic to an unbonded atom but one which is created in that atom by the neighbours to which it is chemically attached. The oxidation state is a molecular and not an atomic property even though it is associated with one constituent part of a molecule. An atom freed of chemical bonds may have an ionic charge, but it does not have an oxidation state. Only the chemically bonded components of a molecule have oxidation states, and they are referred to hereafter as molatoms to avoid confusing them with the transitory building blocks of chemistry that have no oxidation state and no chemical properties as such.

Although oxidation states have been an integral part of the IUPAC-approved nomenclature for inorganic compounds since 1958, chemists have tended to regard them as merely a numerical convenience, useful for balancing redox reactions, but having little chemical significance beyond that. What the accumulated evidence of NMR shieldings, particularly among the transition metals, now tells us is that oxidation state, far from being a mere convenience, is a primary parameter of molecular structure. It is the one that generates a first-order picture of unequal electron sharing within a molecule, the picture upon which the bonding subtleties such as the *cis* effect, the *trans* effect, π back-bonding and so on are overlaid as perturbations.

When the NMR spectroscopy of transition metals was reviewed 10 years ago,[8] only ^{59}Co, ^{51}V, ^{111,113}Cd, and ^{55}Mn had been studied over a sufficiently wide range of ligands that the shielding limits of each had been mapped out, however tentatively. Now the shielding range of each oxidation state of each transition metal has been mapped to the point where, despite range overlaps, a uniform trend in the range centres from high to low shielding with increase in oxidation state is evident. This trend is summarized in Table 2. The details for each transition metal are given in Section 5 where most of the shielding ranges are presented diagrammatically.

Among the compounds of transition metals, we encounter a rich variety of oxidation states such as is seen in Mo molatoms with eight and in Tc molatoms with nine. Among the 30 transition metals, Hf, Ir, Pd and Au have yielded no solution NMR spectra at all, and La(III), Ni(0), Ag(I), Zn(II), Cd(II) and Hg(II) have been observed in only one oxidation state. For the remainder, the sensitivity of nuclear shielding to a change in oxidation state has been tested, and the picture that emerges is summarized in Table 3.

Table 2. The σ shielding (in ppm) at the centre of the oxidation state range with reference to $\delta 0$.

Sc(I)	−29	Y(I)	166		
Sc(III)	−67	Y(III)	−54		
		Zr(0)	355		
Ti(II)	−386	Zr(II)	−2		
Ti(IV)	−1220	Zr(IV)	−342		
V(−I)	1825	Nb(−I)	2095	Ta(−I)	3450
V(0)	1205	Nb(I)	1830		
V(V)	50	Nb(V)	−565	Ta(V)	0
Cr(0)	1749	Mo(0)	1358	W(0)	3065
		Mo(II)	770	W(II)	2585
		Mo(IV)	−945		
Cr(VI)	0	Mo(VI)	−1425	W(VI)	−1325
Mn(−I)	2740	Tc(0)	2477		
Mn(0)	2050	Tc(I)	1765	Re(I)	3400
Mn(I)	900				
Mn(VII)	0	Tc(VII)	−198	Re(VII)	−1750
Fe(0)	−700	Ru(0)	1208		
Fe(II)	−6883	Ru(II)	−3250	Os(II)	2562
				Os(VIII)	0
Co(−I)	2532				
Co(0)	1115	Rh(0)	1208		
Co(I)	−2245	Rh(I)	−1190		
Co(III)	−7403	Rh(III)	−4985		
				Pt(0)	270
				Pt(II)	−1780
				Pt(IV)	−5161

Without exception, the molatoms in their lowest oxidation states are the most highly shielded. The progression from high to low shielding with increase in oxidation state is fairly uniform. Furthermore, the shielding sensitivity or "shiftability" of each molatom species, expressed in ppm per oxidation state unit, coincides rather well with other measures of "shiftability" observed in the past; things such as total chemical-shift range and slopes of δ(A) vs. δ(B) plots for molatoms A and B in identically or similarly bonded environments. The overall picture of oxidation state dependencies among the transition metals is illustrated in Fig. 1.

This chapter documents the fact that among the 10 transition-metal triads and well beyond them in other regions of the periodic table as well, the most general correlation of all is one of nuclear shielding becoming uniformly lower with increase in oxidation state. Unit change in oxidation state has an incremental effect on effective nuclear charge, which in turn has a calculable effect on the radius variable of the valence electrons, the point at which the

Table 3. Shielding increments (in ppm per OSU) with reference to the highest oxidation state.

Sc(I)	20	Y(I)	110		
Sc(III)	Base	Y(III)	Base		
		Zr(0)	180		
Ti(II)	420	Zr(II)	170		
Ti(IV)	Base	Zr(IV)	Base		
V(−I)	300	Nb(−I)	450	Ta(−I)	660
V(0)	290	Nb(I)	600		
V(V)	Base	Nb(V)	Base	Ta(V)	Base
Cr(0)	300	Mo(0)	470	W(0)	730
		Mo(II)	550	W(II)	980
		Mo(IV)	240		
Cr(VI)	Base	Mo(VI)	Base	W(VI)	Base
Mn(−I)	340	Tc(0)	380		
Mn(0)	290	Tc(I)	330	Re(I)	860
Mn(I)	150				
Mn(VII)	Base	Tc(VII)	Base	Re(VII)	Base
Fe(0)	3090	Ru(0)	2230		
Fe(II)	Base	Ru(II)	Base	Os(II)	430
				Os(VIII)	Base
Co(−I)	2480				
Co(0)	2840	Rh(0)	2060		
Co(I)	2580	Rh(I)	1900		
Co(III)	Base	Rh(III)	Base		
				Pt(0)	1360
				Pt(II)	1690
				Pt(IV)	Base

oxidation state cause plugs into the paramagnetic term of the Ramsey shielding model.

4.1. The orbital-size factor

Shortly after the ΔE variable in the Ramsey model was highlighted in 1957, Jameson and Gutowsky[28] highlighted the significant role played by the $\langle r^{-3} \rangle$ variable—the inverse cube radius of the local valence electrons. It was shown that the observed periodicity in the range of chemical shifts experienced by different nuclei is correlated with the periodicity in free-atom $\langle r^{-3} \rangle$ values for valence-shell p and d electrons. Later, it was also shown[29] that a nephelauxetic mechanism operating through $\langle r^{-3} \rangle$ accounts for the extremely high shielding (i.e. extremely low deshielding resulting from an extremely small paramagnetic term) exerted by iodide in NHD.

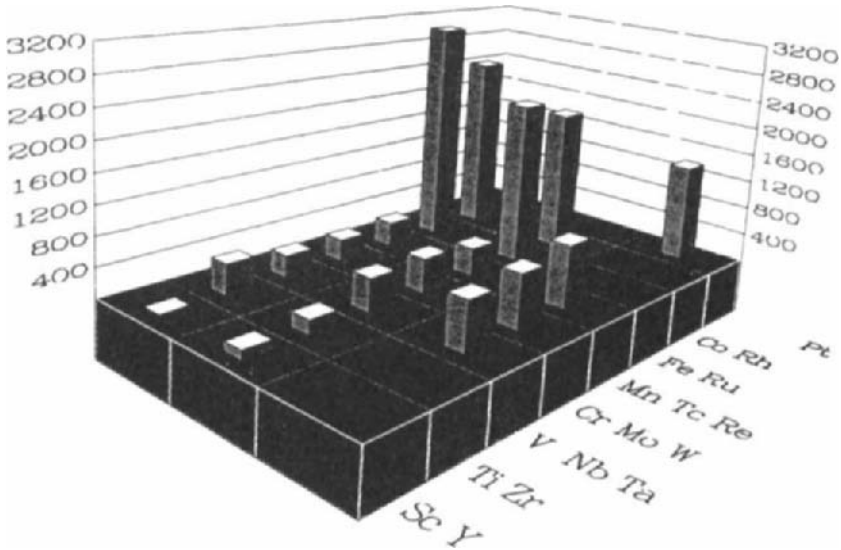

Fig. 1. Oxidation-state dependence of transition-metal shieldings.

Regardless of the sort of wavefunction one uses to describe valence orbitals, the radial part of the function is dependent on an effective nuclear charge (Z^{eff}) seen as the actual nuclear charge (Z) less a screening constant (S).

$$Z^{\text{eff}} = Z - S$$

Screening constants can be estimated in a number of different ways, but the Slater method in which a one-electron decrement in the valence shell increases Z^{eff} by 0.35 has become the standard when designing the wavefunctions for calculations of nuclear shielding.

In calculations of ^{13}C shieldings, Pople[30] used the charge-dependent relationship

$$\langle r^{-3} \rangle_{2p} = 34.33 a_0^{-3} (1 - 0.323 q^-)$$

to represent the decrease in $\langle r^{-3} \rangle$ when the net (negative) charge on a C molatom increases by q^- due to substitution by atoms or groups of lower electronegativity. The $0.323q^-$ represents the increase in screening constant and the $(1 - 0.323q^-)$ factor represents the proportional decrease in $\langle r^{-3} \rangle$ that it engenders.

Being of intermediate electronegativity, carbon is as likely to be found in negative as in positive oxidation states, and Pople's modelling of $\langle r^{-3} \rangle$ variations focuses on the screening constant enhanced by increases in net

negative charge. Negative oxidation states are the exception for metals and the oxidation state terminology represents a focusing on net positive charge enhanced by decreases in the screening constant. When studying metal molatoms, the $(1 - 0.323q^-)$ factor can be recast as $(1 + 0.323q^+)$, and the problem reduces to one of deciding the magnitude of q^+ corresponding to a unit increase in oxidation state.

The exact increment of charge associated with one unit of oxidation state has always been a matter of some debate among chemists, but the general conclusion in Pauling's postulate of essential electrical neutrality[18] has never been seriously challenged. The principle states that, in molecules, molatoms seek to achieve net charges as close to zero as is consistent with electronegativity differences, and that only in molecules with large electronegativity differences and maximum electron polarization will localized net charges approach their limiting maxima of about $+0.5$ at metals and about -0.5 at non-metals.

In the terminology of oxidation states this means that in its highest oxidation state a metal molatom has a net charge of roughly $+0.5$. When the oxidation state is incremented by one oxidation state unit (OSU), the net positive charge increases by roughly $+1/2n$, where n is the integer designating the molatom's highest oxidation state. Thus, in the scandium triad one OSU represents 0.17^+ while in the manganese triad one OSU represents 0.071^+.

A simple replacement of Pople's $-0.323q^-$ screening factor for carbon with $+0.323q^+$ for the metal, plus replacement of 34.33 with the appropriate orbital-size constant allows one to estimate the increase in the $\langle r^{-3} \rangle$ factor as a metal molatom assumes higher oxidation states. Based on Pauling's electroneutrality postulate, the magnitude of the q^+ increment accompanying a unit increase in oxidation state is simply 0.5 divided by the maximum positive oxidation state adopted by the molatom.

4.2. The theoretical basis for oxidation-state dependence

When a metal molatom is oxidized, it loses a half-share in one or more of its valence electrons, and few things are more sensitive to this loss than the magnetic shielding of the metal's nucleus. Mossbauer, Electron Spectroscopy for Chemical Analysis (ESCA) and similar spectroscopies also respond to variations in oxidation state, but the response is less marked and none of them covers as large a fraction of the chemical landscape as does NMR spectroscopy.

Why is the nuclear shielding parameter so sensitive to what must be extremely small variations in total electronic charge "belonging to" a particular molatom? The sign of the oxidation-state dependence is consistent

with a mechanism based on simple Lenz's law diamagnetism, and in early days of NMR when the bulk of experience was with a proton-shielding range of 10 ppm, it was just assumed that variations in the nuclear shielding of heavier molatoms could also be explained in terms of Lamb's diamagnetic term evaluated by Dickinson.[31]

This satisfying state of theoretical simplicity was short-lived. A more elaborate but more reliable model for nuclear shielding appeared in a classic trio of papers published by Ramsey in the early 1950s.[32]

In the Ramsey model for nuclear shielding as it is applied to all atoms heavier than He, variations in nuclear shielding are localized in the paramagnetic term, σ_p, and chemical shifts to higher frequencies (lower fields) are seen not simply as the lack of diamagnetic shielding but as an actively paramagnetic influence introduced by the orbital motion of the valence electrons. The occurrence of NMR lines to high frequency of the bare nucleus position confirms this view.

In the electronic ground state of a molecule, only two variables affect the σ_p of its molatoms: the intrinsic orbital angular momentum of the electrons around that nucleus, $\langle 0|L|0\rangle$, and the average radial distance of these electrons from that nucleus, $\langle 1/r^3\rangle$. The first of these is analogous to the moving mass in classical angular momentum, and the second is a weighting factor analogous to r^2. Classical angular momentum is more sensitive to the length of the string than to the mass of the stone. Electronic excitation energies have no bearing on the magnetic shielding of a molecule in its electronic ground state, and if NMR spectra could be captured without placing the molecule in a magnetic field they would have no bearing on the chemical shifts observed.

Qualitatively, the effect of molatom oxidation on each of these two factors is fairly obvious. The $\langle 0|L|0\rangle$ factor is proportional to the number of electrons whose momentum it quantifies, and when that number is reduced through oxidation, the $\langle 0|L|0\rangle$ factor is also reduced; and so also is σ_p. Because the magnitude of this reduction is judged to be minor and is difficult to quantify, it is usually neglected in detailed calculations.

The effect of molatom oxidation on σ_p through the $\langle 1/r^3\rangle$ factor is more marked. Removal of electrons from a molatom's valence shell increases the effective nuclear charge experienced by those remaining and draws them closer to the nucleus. In $\langle 1/r^3\rangle$ even small contractions are cubed and transformed into the major factor that causes nuclear shieldings to become uniformly lower with increase in oxidation state.

And how do excitation energies get into the shielding picture? In each of its electronic excited states, a molecule's orbital magnetism and hence σ_p is influenced by the same two factors affecting the ground state. As long as the molecule is unperturbed by a magnetic field this excited-state orbital

magnetism has no effect on the ground-state molecule. However, during the taking of an NMR spectrum, the magnetic field creates a new electronic ground state for the molecule, similar to the old one, but with small amounts of (old) excited-state character mixed in. The degree of mixing is inversely proportional to the energy separation between the ground and excited states. The reciprocal of electronic excitation energy is, therefore, the weighting factor which determines the degree of excited-state mixing.

If the excited state mixed in has less angular momentum than the ground state, then of course the mixing dilutes the angular momentum and low-lying excited states of this type would be the cause of increased shielding. But the probability of finding an excited state with less angular momentum than the ground state is not high. The chemical-binding force that drives free atoms inexorably toward molatoms in ground-state molecules is one that seeks to minimize both spin and orbital momenta.

Electronic excited states generally have more angular momentum than the ground state and where the excitation energy is low enough—in the near-ultraviolet or visible region—σ_p is likely to be near the deshielded end of the range for that particular oxidation state. There does appear, however, to be a maximum ΔE threshold around $30\,000\,\mathrm{cm}^{-1}$ beyond which excitation energies are so large that, regardless of orbital magnetism resident in the excited state, the state does not become admixed to the point of enhancing σ_p beyond that determined by the ground-state factors.[33]

In summary, the $1/\Delta E$ factor to which prominent examples of deshielding are commonly attributed is not a third shielding factor beyond the $\langle 0|L|0\rangle$ orbital angular momentum factor and its $\langle 1/r^3\rangle$ weighting factor. Rather, $1/\Delta E$ is a mixing coefficient determining the extent to which orbital angular momentum resident in an electronic excited state augments that in the ground state to deshield a nucleus further.

5. THE EXPERIMENTAL EVIDENCE

5.1 The scandium triad

Scandium is named after Scandinavia where it was discovered by Nilson in 1879. Scandium shieldings (Table 4) range from a low of $\delta + 249$ in $ScCl_6^{3-}$ to a high of $\delta - 116$ in $Sc(OH)_4^-$, referenced to aqueous $Sc(ClO_4)_3$ at high dilution whose signal falls two-thirds of the way up the scale.

Practically all the available data pertain to scandium(III) spanning 365 ppm centred on $\delta + 67$. The McGlinchey group has, however, carried out several studies on cyclopentadienyls containing scandium(I) whose shielding spans a range of 78 ppm centred on $\delta + 29$. This oxidation-state dependence of 20 ppm per OSU is shown in Fig. 2.

Table 4. Nuclear properties of the scandium triad isotopes.

Nucleus	Spin	Abundance (%)	Quadrupole moment 10^{28} (m^2)	Usual shift reference	Receptivity[a]
^{45}Sc	7/2	100	−0.22	Sc^{3+}(aq)	1710
^{89}Y	1/2	100	0	Y^{3+}(aq)	0.67
^{138}La	5	0.09	0.51	La^{3+}(aq)	0.48
^{139}La	7/2	99.9	0.22	La^{3+}(aq)	340
^{171}Yb	1/2	14.3	0	—	4.4
^{175}Lu	7/2	97.4	(5)	—	170

[a]With reference to ^{13}C.

Yttrium is named after Ytterby in Sweden, source of the oxide from which the Finnish chemist Gadolin isolated the element. Yttrium shieldings range from a low of $\delta + 126$ to a high of $\delta - 371$ referenced to aqueous $Y(ClO_4)_3$ at high dilution whose signal falls only one-third of the way up a scale more heavily influenced by the lower oxidation state than is that of scandium.

Yttrium(III) shieldings span 144 ppm centred on $\delta + 54$. EDTA-complexed yttrium is least shielded and ligand substitution causes shielding to increases in the order: EDTA < acetate < Cl < Br < nitrate. The yttrium(I) compounds studied all contain cyclopentadiene (Cp) or methyl substituted Cp and span

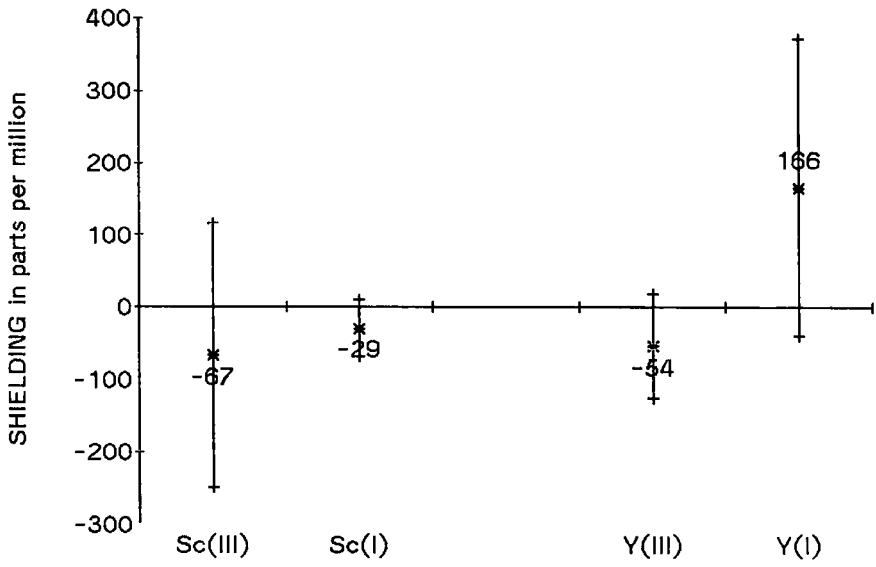

Fig. 2. Scandium and yttrium shielding ranges.

411 ppm centred on $\delta - 166$. The highest value of this range (268 ppm) is achieved when $MeCp^-$ replaces Cl^- in $(MeCp)_2$ YCl and illustrates the dramatic shielding increase when Cp^- acts as a Lewis base. The oxidation state dependence for yttrium of 110 ppm per OSU is shown in Fig. 2.

The name **lanthanum** comes from the Greek *lanthano* meaning "to conceal", and it is so named because the Swedish chemist Mosander in 1839 extracted a new oxide from impure cerium nitrate. Lanthanum shieldings range from a low of $\delta + 1090$ in $LaBr_6^{3-}$ to a high of $\delta - 129$ in $La(MeCN)_6^{3+}$, referenced to aqueous $La(ClO_4)_3$ (0.5 M) whose signal falls nine-tenths of the way up the scale near the highly shielded end.

Lanthanum(I) is an unstable oxidation state that has yet to be observed. Lanthanum(III) shieldings span 1219 ppm centred on $\delta + 480$. Where the coordination is six identical ligands generating octahedral symmetry, narrowest linewidths in the range 200–600 Hz are observed. In $La(SCN)_7^{4-}$, however, the linewidth balloons to 4400 Hz and linewidths approaching 8000 Hz are not uncommon. The quadrupole moment of 0.21 barns is virtually identical with that of ^{45}Sc, and it is not entirely clear why the ^{139}La lines should be so much wider. Both cations exchange ligands readily in solution, and perhaps the larger La^{3+} finds it difficult to limit the coordination number to six, after which the symmetry deteriorates. It may also be that, coming just before the lanthanide contraction in the periodic table, lanthanum complexes are a lot bigger than the corresponding scandium ones and have rotational correlation times that are a lot longer. The true reason is probably a combination of both factors.

All three members of the scandium triad tend toward inverse halogen dependence. The evidence is strongest in the case of La, and weaker for Y and Sc. Although there is little evidence to indicate the effect of I^- upon these metals, $Br^- < Cl^-$ shielding comparisons are available. With lanthanum, $LaBr_6^{3-}$ demarcates the lower end of the shielding range and $LaCl_6^{3-}$ is more shielded by 239 ppm; 20% of the total La shielding range. In non-aqueous solvents, La shielding increases in the order: en < DMSO < HMPA < DMF < MeCN, the order of solvent donor number which is also seen in the alkali-metal cations which are unambiguously inverse halogen dependent.

5.2. The titanium triad

Discovered by Gregor in 1791, **titanium** was named by Klaproth in 1795 after Titanes, one of the six primeval sons of Earth in Greek mythology. Titanium shieldings (Table 5) range from a low of $\delta + 2440$ in TiI_4 to a high of $\delta 0$ in TiF_6^{2-}, referenced to aqueous $[NH_4]_2TiF_6$ whose signal demarcates the shielded end of the range.

Table 5. Nuclear properties of the titanium triad isotopes.

Nucleus	Spin	Abundance (%)	Quadrupole moment 10^{28} (m^2)	Usual shift reference	Receptivity[a]
^{47}Ti	5/2	7.3	0.29	$TiCl_4$(l)	0.86
^{49}Ti	7/2	5.5	0.24	$TiCl_4$(l)	1.2
^{91}Zr	5/2	11.2	−0.21	Cp_2ZrBr_2	6.0
^{177}Hf	7/2	18.5	3.3	—	1.5
^{179}Hf	9/2	13.8	3.7	—	0.43

[a]With reference to ^{13}C.

The few data that are available are pretty evenly divided between titanium(IV) and titanium(II) compounds. The chemical shifts for titanium(IV) span a range of 2440 ppm centred on $\delta + 1220$. Those for titanium(II) span 520 ppm centred on $\delta + 386$, for an oxidation-state dependence of 420 ppm per OSU (see Fig. 3).

Both the higher and the lower oxidation states of titanium exhibit inverse halogen dependence. In titanium(IV) the intensity is −320 ppm per halogen with a Br/I ratio of 0.38. In titanium(II) the intensity is 128 ppm per halogen with a Br/I ratio 0.41.

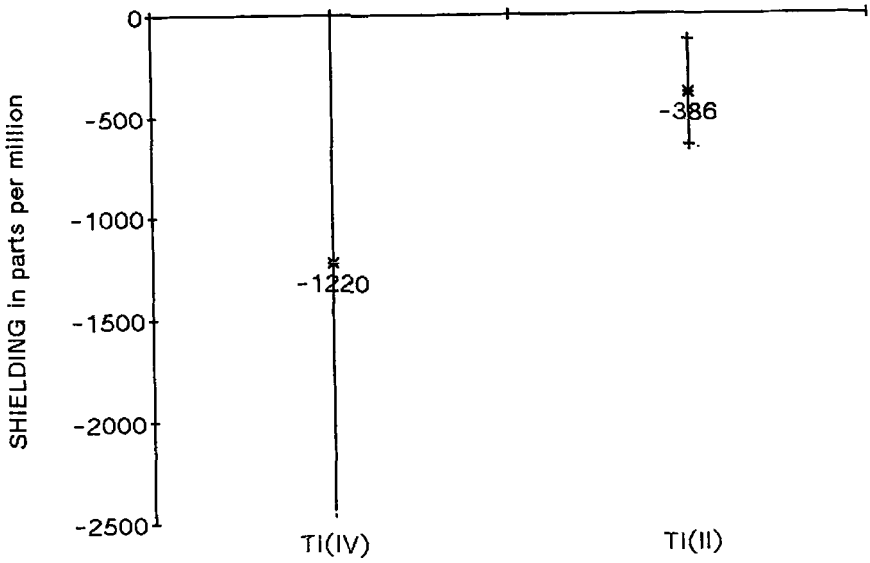

Fig. 3. Titanium shielding ranges.

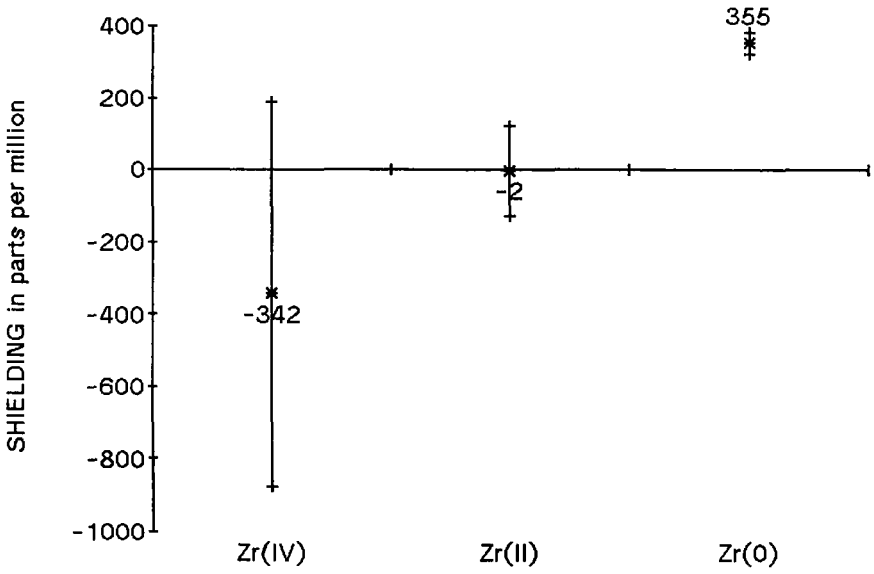

Fig. 4. Zirconium shielding ranges.

Zirconium was discovered by Klaproth in 1789 and was probably named after the Arabic *zargun* or *jargon* describing the colour of the gemstone now known as zircon. Zirconium shieldings range from a low of $\delta + 875$ in $Zr(NEt_2)_4$ to a high of $\delta - 384$ in $ZrCp_2$ ($\nu^4 - C_4H_6$), referenced to $ZrCp_2Br_2$ whose signal falls about two-thirds of the way up the range.

Although NMR data on zirconium is still sparse, three different oxidation states have been studied and they show a regular progression from higher to lower shieldings with increase in oxidation state. Zirconium(IV) shieldings span a range of 1066 ppm centred on $\delta + 340$, those for zirconium(II) span 248 ppm centred on $\delta + 2$, and those for zirconium (0) span 60 ppm centred on $\delta - 355$. As shown in Fig. 4, the oxidation-state dependence of zirconium is 175 ppm per OSU.

The shielding effects of Br and I substitution at Zr(IV) are not presently known, but Zr(II) shows inverse halogen dependence with an intensity of 124 ppm per halogen, comparable with that found in Ti(II).

Hafnium, named after the Latin for Copenhagen, honours the city in which it was discovered in 1923. There are two magnetically active isotopes of hafnium, but large quadrupole moments for each taken together with receptivities that are not high provide sufficient reason for the absence of any solution data to date.

5.3. The vanadium triad

Vanadium was first discovered by del Rio in 1801 and then rediscovered in 1830 by the Swedish chemist Sefstrom who named it after the Scandinavian goddess Vanadis with reference to its multicoloured display of chromatic virtuosity.

Vanadium shieldings (Table 6) range from a low of $\delta + 1457$ in $V_2S_7^{4-}$ to a high of $\delta - 2054$ in $CpV(SnPh_3)(CO)_3^-$, referenced to $VOCl_3$ neat liquid that occurs just below the midpoint in the shielding range. With vanadium NMR, the dilemma of whether or not to include in the analysis the results of solid-state studies is highly problematical. Semiconductors of the type Cu_3VE_4 containing vanadium(V) tetrahedrally coordinated by S, Se and Te have been studied. In the Te compound, the vanadium resonance occurs at $\delta + 3950$ and, if included, it would quadruple the range for vanadium(V) and would almost double the range of all vanadium shieldings.

Two factors indicate that this particular system is not comparable with vanadium systems studied in solution. In $Cu_3VS_4(s)$ the vanadium is more highly shielded by 1345 ppm than in aqueous VS_4^{3-}, suggesting there is something different about the solid. The fact that the solid is a semiconductor and, therefore, not magnetically dilute, confirms this view. There are antiferromagnetic interactions in the solid with the potential to perturb in a major way the magnetic shielding observed in isolated vanadium centres.

Vanadium(V) shieldings span 2300 ppm centred on $\delta + 306$. Thiovanadates dominate the bottom of the range. $VOBr_3$ at $\delta + 450$ and $VOCl_3$ at $\delta 0$, showing the IHD characteristic of vanadium(V), occur in the middle of the range. Oxyvanadates and heteropolyvanadates occur in the band from $\delta - 400$ to $\delta - 600$. The peroxide ligands in $VO(O_2)_3^{3-}$ push the vanadium(V) up to $\delta - 845$.

Vanadium(III) has the d^2 configuration and, like d^7 cobalt(II) with which it is spectroscopically and magnetically comparable, it is paramagnetic. The nitrosyl complexes which have been regarded as complexes of NO^- and

Table 6. Nuclear properties of the vanadium triad isotopes.

Nucleus	Spin	Abundance (%)	Quadrupole moment 10^{28} (m^2)	Usual shift reference	Receptivity[a]
^{51}V	7/2	99.8	−0.052	$VOCl_3$(l)	2160
^{93}Nb	9/2	100	−0.22	$NbCl_6^-$(MeCN)	2740
^{181}Ta	7/2	99.9	3	$TaCl_6^-$(MeCN)	204

[a]With reference to ^{13}C.

classed with true vanadium(III) compounds[8] are here regarded as complexes of NO^+ and classed with the d^4 vanadium(I) compounds.

Vanadium(I) shieldings span 800 ppm centred on $\delta - 1200$. All compounds belong to the system $CpV(CO)_nL$ in which the variable ligand is $Ph_2PCH_2PPh_2$ at the low end and PF_3 at the high end.

Vanadium(−I) shieldings span 500 ppm centred on $\delta - 1775$. Most compounds belong to the system $V(CO)_{6-n}L_n^-$ in which the variable ligand is 2-NH_2-pyridine at the low end and the high end is demarcated by $VCp(CO)_3SnPh_3^-$.

The regular increase in shielding that accompanies a lowering in oxidation state is shown in Fig. 5. The oxidation-state dependence between vanadium(V) and vanadium(−I) is 350 ppm per OSU. The vanadium(V) range is positioned at $\delta + 306$ by the electronegativities of the ligands determining the oxidation state. Within the 2300-ppm range for vanadium(V), relative shieldings are determined by a second factor the origin of which will be known when the cause of alternation between normal and inverse halogen dependency has been resolved.

Vanadium(V) exhibits an inverse halogen dependence of 500 ppm between $VOBr_3$ and $VOCl_3$ which, when extended to include the unobserved VOI_3 by scaling to 1667 ppm with the usual (I–Cl)/(Br–Cl) ratio, represents 70% of the 2300-ppm span of the oxidation state.

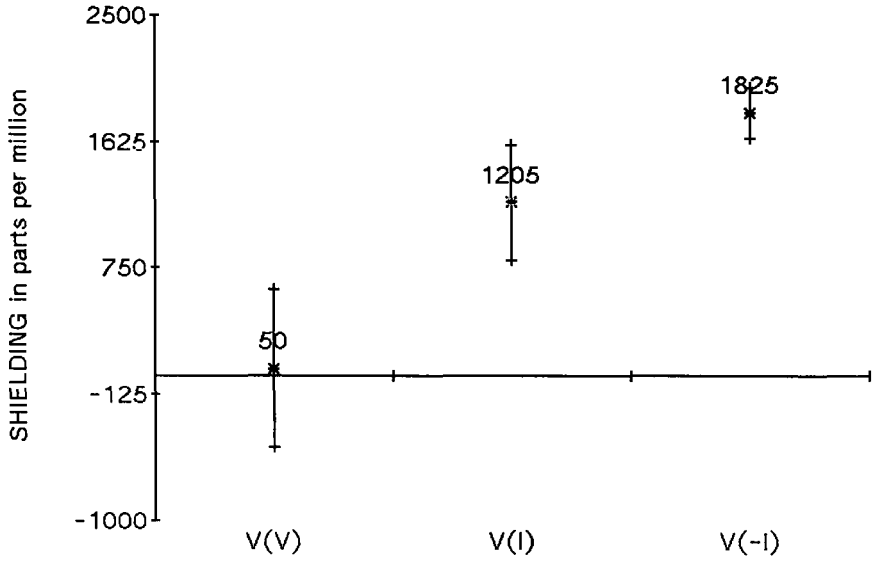

Fig. 5. Vanadium shielding ranges.

Niobium was noted by Hatchett in an ore sent to England from Connecticut in 1801. Named after Niobe, the daughter of Tantalus in Greek mythology, it has also gone under the names of pelopium and columbium at various times in the past. Niobium shieldings range from a low $\delta + 1910$ in $ScNbBr_3$ to a high of $\delta - 2120$ in $Nb(CO)_6^-$, referenced to $NbCl_6^-$ near the middle of the scale. Chemical shifts in semiconductors containing niobium have been measured and they have been excluded from this analysis for the reason cited above in the case of vanadium, even though the inclusion of $Cu_3NbTe_4(s)$ at $\delta + 2590$ (extending the low end of the shielding range by 600 ppm) would not introduce a similarly overwhelming perturbation in the solution picture.

There is some merit in referencing niobium shifts to $NbOCl_3$, making them comparable with vanadium shifts.[14] This advantage is offset by a linewidth of up to 1000 Hz, making uncertainty in the $NbOCl_3$ resonance frequency unacceptably high for a reference, and the niobium chemical shifts in this chapter have been referenced to $NbCl_6^-$.

The niobium(V) range spans 3370 ppm centred on $\delta + 565$. The ligands are Se^{2-}, S^{2-} and O^{2-}, and Br^-, Cl^- and F^-, and the shielding increases uniformly with substitution of a lighter ligand in the $ENbCl_3$, $ONbX_3$, and NbX_6^- systems. The pattern of IHD observed previously for niobium(V) has its counterpart in the Te < Se < S shieldings of the chalcogens.

Niobium(I) shieldings in a small series of $Cp_nNb(CO)_m(PEt_3)_x$ compounds spans 371 ppm centred on $\delta - 1830$. $Nb(PF_3)_6^-$ at $\delta - 2067$ and $Nb(CO)_6^-$ at $\delta - 2120$ demarcate the range for an even smaller series of niobium(−I) compounds centred at $\delta - 2095$. The dependence of niobium shielding upon oxidation state follows the regular pattern at a rate of 440 ppm per OSU and is illustrated in Fig. 6.

Tantalum was discovered in Sweden by Ekeberg in 1802 and was named after the Greek god Tantalus forced to sit thirsty in a pool of water that receded whenever he attempted to drink. While extremely sparse, the solution data available for ^{181}Ta are sufficient to establish that tantalum obeys both a regular oxidation-state dependence and an IHD.

Relative to $TaCl_6^-$ in MeCN, adopted as the reference at present, TaF_6^- in aqueous HF/HNO_3 is shielded by 2376 ppm, thus delineating IHD for tantalum(V). Tantalum(−I) in $Ta(CO)_6^-$ at $\delta - 3450$ represents the upper end of the shielding range for tantalum and indicates a regular oxidation-state dependence.

When included in the tantalum picture, the $\delta + 3344$, $\delta + 1354$, and $\delta + 376$ shifts for $Cu_3TaE_4(s)$ semiconductors, E = Te, Se and S, respectively, bring the shielding range for tantalum(V) to 5700 ppm; 3700 ppm if the Te compound is excluded leaving $TaSe_4^{3-}$ to delineate the range. The corresponding range of 4900 ppm for tungsten(VI) delimited by WS_4^{2-} and WF_6 (see below) suggest it is not unreasonable to group the semiconductor and solution data for

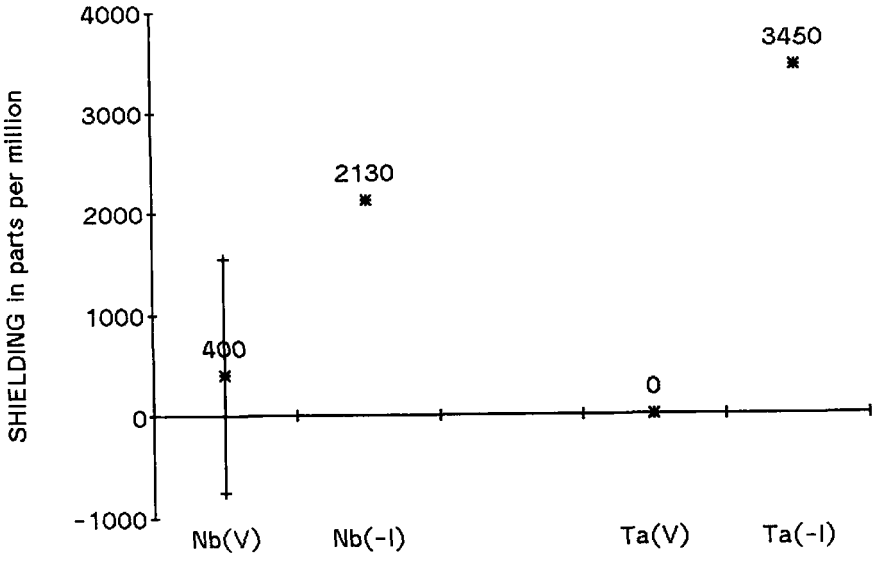

Fig. 6. Niobium and tantalum shielding ranges.

tantalum. It is probable that the antiferromagnetic factor in vanadium compounds that is anomalous in the first transition series is

(i) attenuated by the larger spacings in the analogous tantalum compounds; and
(ii) not particularly prominent among the complicated mix of magnetic factors that operates in the third transition series.

Thus, with the extended data set included, Fig. 6 shows a shielding range of 5700 ppm for tantalum(V) centred at $\delta + 2376$, and an oxidation-state dependence of 655 ppm per OSU.

From vanadium to niobium to tantalum, the oxidation-state dependence increases uniformly from 350 to 440 to 655 ppm per OSU. Among the various comparisons that can be made to quantify the relative shielding sensitivities of different molatoms, these parameters reflecting the extent to which the shielding responds to a change in oxidation state are the most reliable. They have two advantages over comparisons between equivalently substituted molecules:

(i) the effect of differences in the oxidation state difference from comparison to comparison are eliminated; and
(ii) the possibility of overstating the factor by selecting molecules from

Table 7. Nuclear properties of the chromium triad isotopes.

Nucleus	Spin	Abundance (%)	Quadrupole moment 10^{28} (m^2)	Usual shift reference	Receptivity[a]
^{53}Cr	3/2	9.6	−0.15	CrO_4^{2-}(aq)	0.49
^{95}Mo	5/2	15.7	−0.015	MoO_4^{2-}(aq)	2.88
^{97}Mo	5/2	9.5	0.17	MoO_4^{2-}(aq)	1.84
^{183}W	1/2	14.4	0	WO_4^{2-}(aq)	0.059

[a]With reference to ^{13}C.

opposite ends of two ranges, or understating the factor by selecting from adjacent ends of two ranges is eliminated.

5.4. The chromium triad

It is the chromium triad (Table 7) that has seen the most dramatic growth over the past 10 years, and out of this growth has emerged not only new oxidation states previously undocumented by NMR but also systematic evidence of massive deshieldings introduced by metal–metal π bonds and δ bonds. The NMR spectroscopy of chromium, molybdenum, and tungsten compounds has been comprehensively reviewed in an international joint undertaking by the La Trobe and Arizona groups responsible for much of the growth.[16]

Chromium named after the Greek *chroma* meaning "colour" was discovered by the French chemist Vauquelin in 1797. The NMR of ^{53}Cr in solution remains stalled at CrO_4^{2-} and $Cr(CO)_6$ only, with the chromium(0) compound at $\delta - 1795$ relative to the chromium(VI) compound for an oxidation-state dependence of 300 ppm per OSU as shown in Fig. 7.

Molybdenum named after the Greek *molybdos* meaning "lead" was discovered by Scheele in 1778 and was isolated as an impure metal by the Swedish chemist Hjelm in 1782. Shielding ranges for four oxidation states are available and molybdenum shieldings span a total range of 5000 ppm from $MoSe_4^{2-}$ at $\delta + 3145$ to $Mo(CO)_6$ at $\delta - 1856$ referenced to aqueous MoO_4^{2-} whose signal falls six-tenths of the way up the scale.

Molybdenum(VI) shieldings span 3440 ppm centred on $\delta + 1425$. $MoSe_4^{2-}$ marks the deshielded limit and shielding increases with substitution in the order Se < S < O < = NPh. Molybdenum(IV) shieldings span 4510 ppm overlapping all the molybdenum(VI) range but extending to significantly higher shielding marked by $Mo(CN)_8^{4-}$ at $\delta - 1309$, the range being centred at $\delta + 945$. The $CpMo(CO)_mL_n$ system comprises most of the

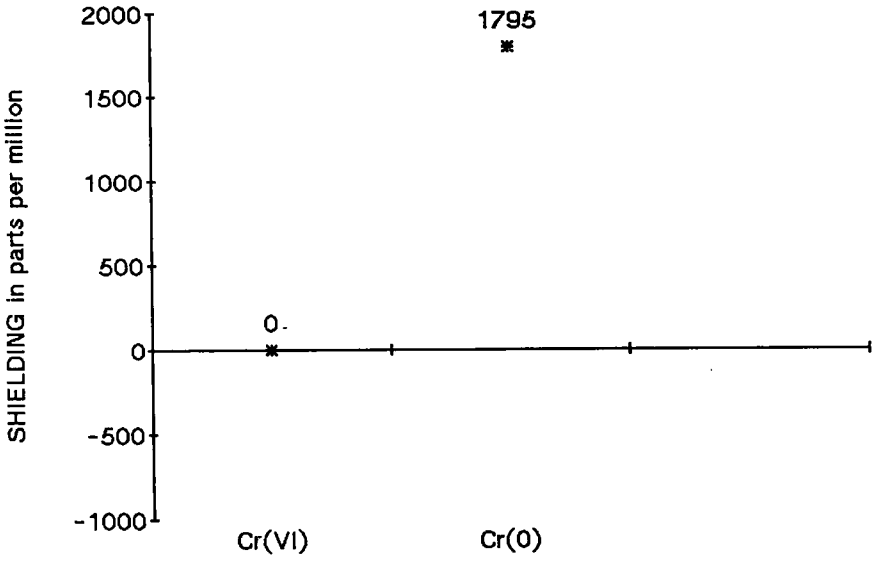

Fig. 7. Chromium shielding ranges.

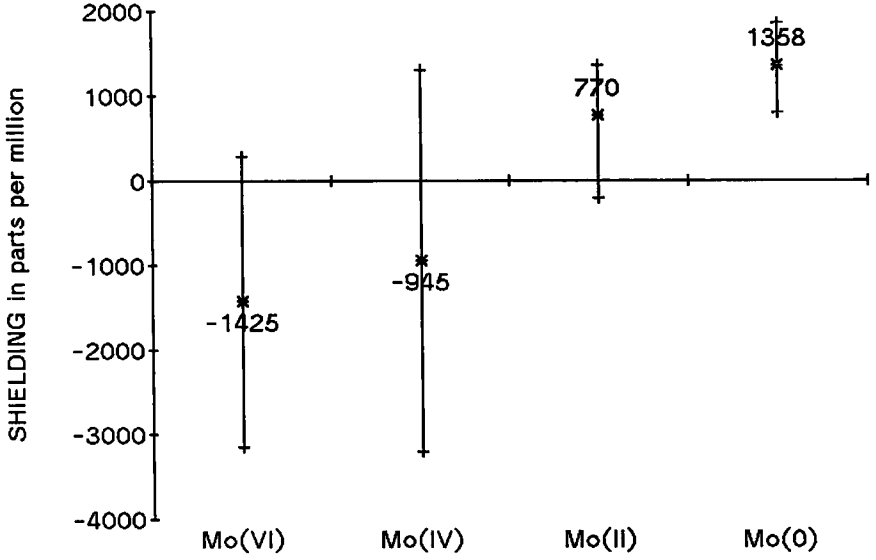

Fig. 8. Molybdenum shielding ranges.

molybdenum(II) class whose shieldings span 2000 ppm centred on $\delta - 770$. The $Mo(CO)_mL_n$ system comprises the molybdenum(0) class and its shieldings span a range of 1500 ppm centred on $\delta - 1358$.

These four shielding ranges are illustrated in Fig. 8 where, although the higher oxidation states cover more ground than do the lower ones, there is nevertheless a steady progression from low to high shielding with decrease in oxidation state. Taken between oxidation states VI and 0, the overall rate of the oxidation-state dependence is 465 ppm per OSU.

Interspersed between these four even oxidation states are three odd-numbered oxidation states representing sizeable classes of molybdenum compounds all of which are paramagnetic. In the past decade Mo(V) and Mo(III) compounds have appeared which are diamagnetic because of single and triple Mo–Mo bonds, respectively. With the oxidation-state dependence of molybdenum shifts now quantified, it is possible to interpolate imputed values of $\delta + 1185$ for Mo(V) and $\delta + 90$ for Mo(III) with which to compare the metal–metal bonded molecules. The comparison casts some light on the metal–metal bond anomaly in NMR spectroscopy.

The Mo(V)–Mo(V) molecule with only a single σ bond between metal centres is shielded by 520 ppm above the imputed Mo(V) position, suggesting an anomalous shielding contribution from a σ bond between two metals of the same species. The Mo(III)–Mo(III) interaction is a triple bond and the resonance occurs at $\delta + 3020$. After applying the 520 ppm shielding contribution from the σ component, the π bonds are seen to introduce an anomalous deshielding component of 1800 ppm each.

The ^{95}Mo signal for Mo(II)–Mo(II) quadruply bonded molecule is observed 500 ppm beyond the most deshielded molybdenum(VI) position. This is deshielded by 4460 ppm from the centre of the molybdenum(II) range, and when the anomalies for one σ bond and two π bonds evaluated above are taken into account, it indicates that the δ bond deshields by a further 1500 ppm.

Tungsten, named after the Swedish *tung sten* meaning "heavy stone" was isolated from tungstic acid by the Spanish d'Elhuyar brothers in 1783. Shielding ranges for tungsten(VI), tungsten(II) and tungsten(0) have been investigated and they are illustrated in Fig. 9. Leaving aside two compounds with high-frequency shifts at $\delta + 6760$ and $\delta + 4408$ attributable to tungsten–tungsten quadruple and triple bonds, respectively, and one compound with a very low-frequency shift attributable to the anomalous effect of hydride ligands, tungsten shieldings span a range of 7250 ppm from WS_4^{2-} at $\delta + 3769$ to $W(CO)_6$ at $\delta - 3486$, all relative to aqueous WO_4^{2-} whose signal falls almost exactly half-way up the present scale.

As found with molybdenum where Mo(VI) systems span two-thirds of the total shielding range, tungsten(VI) shieldings span almost 5000 ppm from

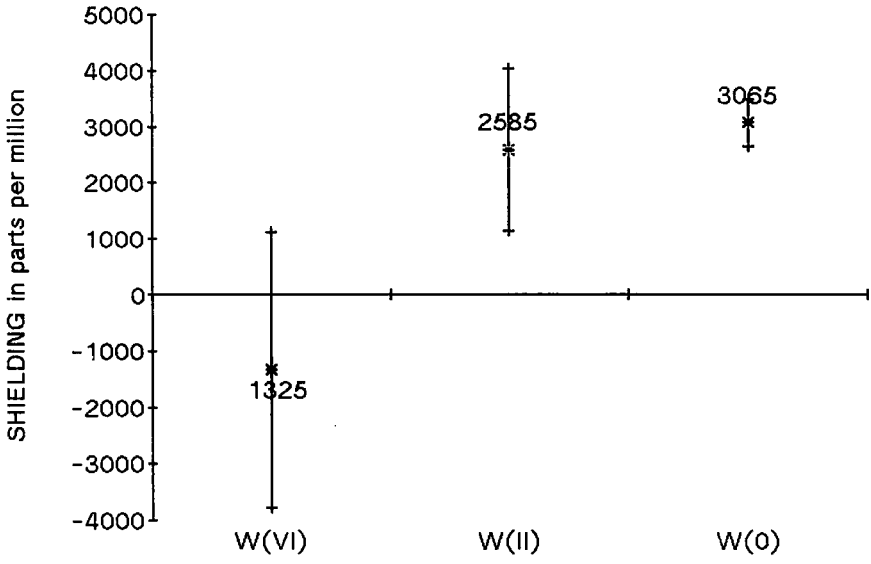

Fig. 9. Tungsten shielding ranges.

WS_4^{2-} at $\delta + 3769$ to WCl_6 at $\delta + 2184$ to WF_6 at $\delta - 1117$. The isopolytungstates cover a range of 200 ppm just above $\delta 0$, and the heteropolytungstates stretch to lower shieldings by about 200 ppm before paramagnetic ones are encountered. The W(VI) shielding range is centred on $\delta + 1325$.

Tungsten does not have a well-developed tungsten(IV) chemistry analogous to that of molybdenum. Tungsten(II) shieldings span 2900 ppm centred on $\delta - 2585$. At the low end of the range are compounds in the system $W(CNCMe_3)_5L^+$ and at the high end those in the system $CpW(CO)_3L$. Tungsten(0) compounds belong to the system of substituted carbonyls and span a range of 900 ppm centred on $\delta - 3065$. The regular trend to higher shieldings with progressive reduction of the metal is seen again in tungsten, with an oxidation-state dependence of 730 ppm per OSU.

With tungsten's oxidation-state dependence quantified, the metal–metal bond anomaly and the hydride anomaly can both be evaluated. There is no W–W single-bond example available with which to obtain a shielding anomaly for the σ bond, but scaling the 520 ppm value for molybdenum by the 730/465 ratio in oxidation-state dependencies gives a putative 800 ppm. Using this to account for the σ bond in each case, each of the π bonds in the W(III)–W(III) triple bond deshields by 3000 ppm, and the δ component in the W(II)–W(II) quadruple bond deshields by a further 3000 ppm.

In Cp_2WH_2 there is more than the usual amount of uncertainty in assigning

Table 8. Nuclear properties of the manganese triad isotopes.

Nucleus	Spin	Abundance (%)	Quadrupole moment 10^{28} (m^2)	Usual shift reference	Receptivity[a]
^{55}Mn	5/2	100	0.4	MnO_4^-	994
^{99}Tc	9/2	[10^5 years]	−0.13	TcO_4^-	2130
^{185}Re	5/2	37	2.8	ReO_4^-	280
^{187}Re	5/2	48	2.6	ReO_4^-	490

[a]With reference to ^{13}C.

an oxidation state. If it is classed as a tungsten(II) compound belonging to the group whose shielding range is centred on $\delta - 2585$, then its chemical shift of $\delta - 4663$ suggests a shielding anomaly of 1039 ppm for each hydrogen. If it is classed as a tungsten(0) compound bearing acidic hydrogens, then the shielding anomaly is only 800 ppm per hydrogen.

5.5. The manganese triad

Manganese was first isolated by the Swedish chemist Gahn in 1774 using carbon to reduce the dioxide in pyrolusite, and it was named after the Latin *magnes* for magnet because of the magnetic properties associated with pyrolusite. Manganese shieldings (Table 8) range from a low of $\delta + 500$ in $Mn(CO)_3(MeCN)_3^+$ to a high of $\delta - 3458$ in $(CO)_3[P(OPh)_3]_2Mn\text{-}SnMe_3$, referenced to the aqueous permanganate ion whose signal is found near the low end of the shielding range.

Of the 10 oxidation states in which manganese has been identified, four are diamagnetic and have been characterized by NMR. The regular progression from highest shielding in Mn(−1) to lowest shielding in Mn(VII) is shown in Fig. 10. The chemical shifts for Mn(−1) compounds span 1434 ppm centred on $\delta - 2740$, those for Mn(0) compounds span 450 ppm centred on $\delta - 2050$, those for Mn(I) compounds span 2800 ppm centred on $\delta - 900$, and the permanganate ion at $\delta 0$ is the only Mn(VII) compound to have been studied. Between the lowest and highest oxidation states, the oxidation-state dependence is 340 ppm per OSU.

The iodide in the Cl, Br, I series $Mn(CO)_5X$ of manganese(I) compounds is the most shielded, giving manganese a normal halogen dependence with an intensity of 481 ppm per halogen with a Br/I ratio of 0.32.

Technetium (known previously as masurium) is named after the Greek *technetos* meaning "artificial", and was first manufactured (rather than

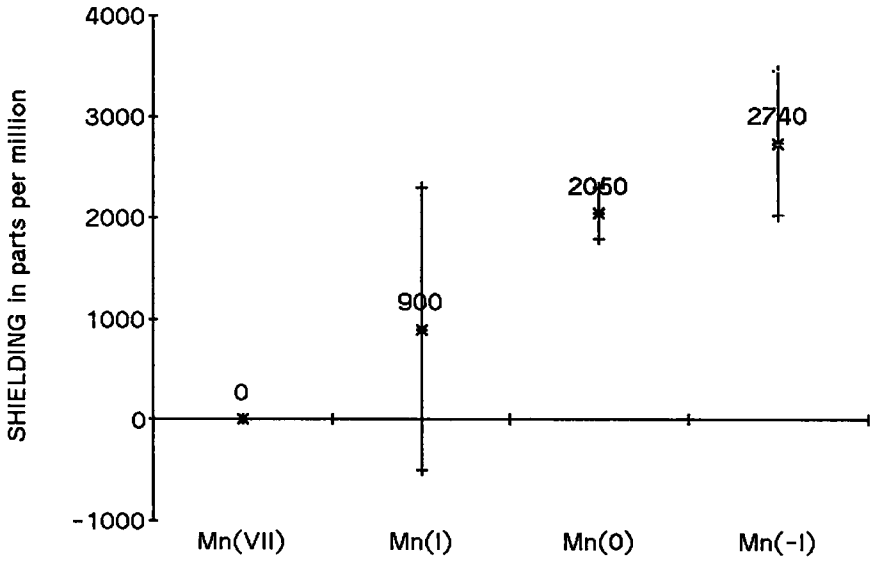

Fig. 10. Manganese shielding ranges.

discovered) by Segre working on the Berkeley cyclotron in 1937. It is a weak β emitter with a half-life of 212 000 years and the only one among the first 60 species of atom with no naturally occurring isotope. Technetium shieldings range from a low of $\delta + 806$ in $TcO_2(CN)_4^{3-}$ to a high of $\delta - 3517$ in $Tc(CO)_3(MeCN)(diphos)^+$, referenced to the aqueous pertechnetate ion whose signal occurs near the low end of the shielding range.

The shielding ranges for Tc(0), Tc(I) and Tc(VII) form a regular progression from high to low with increase in oxidation state illustrated in Fig. 11. The chemical shift for $Tc_2(CO)_{10}$ at $\delta - 2477$ is the only Tc(0) one measured to date. The shifts for Tc(I) compounds span a range of 3504 ppm centred at $\delta - 1765$, and those for Tc(VII) compounds span a range of 396 ppm centred at $\delta + 198$. Between the outer two oxidation states of these three the oxidation-state dependence in 380 ppm per OSU.

One Tc(V) resonance has been reported to date and its position is anomalous. According to the 380 ppm per OSU trend, Tc(V) should appear in the region of $\delta - 560$ but in fact the Tc in $TcO_2(CN)_4^{3-}$ occurs at $\delta + 806$.

Although no technetium iodides have been studied, the bromides and chlorides of both *trans*-$TcX(CO)_3(PPh_3)_2$ and *cis*-$TcX(CO)_3(PMe_2Ph)_2$ have been measured. The per halogen Cl–Br separations have been divided by 0.3—the normal Br/I ratio—scaling them up to obtain imputed Cl, cf. the I dependencies of + 247 ppm and + 173 ppm for the *trans* and the *cis* series,

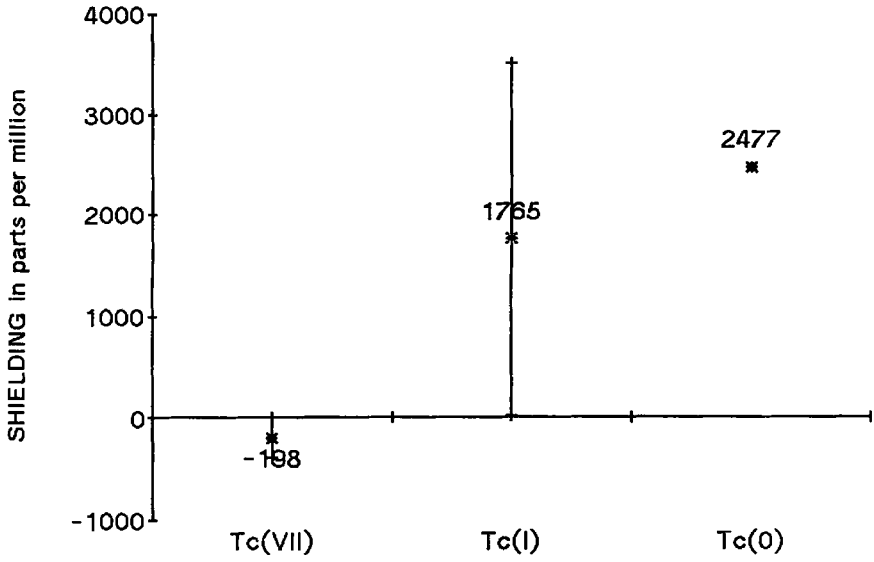

Fig. 11. Technetium shielding ranges.

respectively. These normal halogen dependencies seen in Tc(I) are significantly weaker than the + 481 ppm normal halogen dependence seen in Mn(I).

Rhenium was discovered in 1924 by Noddack, Tacke (Frau Noddack), and Berg and was named after the Rhine River of their native Germany. Only three rhenium compounds have been reported, two of them by Rehder's group in Hamburg, and their shieldings range from a low of $\delta + 3500$ in ReS_4^- to a high $\delta - 3400$ in $Re(CO)_6^+$, relative to aqueous ReO_4^- near the middle of the range.

The two rhenium(VII) compounds span a range of 3500 ppm centred on $\delta + 1750$. The welcome fact that the third compound contains rhenium(I) enables a calculation of the oxidation-state dependence for rhenium: 860 ppm per OSU.

5.6. The iron triad

Iron is one of the half-dozen metals dating from the pre-Christian era, and its Old English *iren* precursor is not parallelled in any other language. Iron shieldings (Table 9) range from a low of $\delta + 11\,269$ in tris (bipyridyliron(II)) to a high of $\delta - 583$ in (cyclobutadiene)iron(0)tricarbonyl, relative to neat iron pentacarbonyl near the high end of the shielding range.

Table 9. Nuclear properties of the iron triad isotopes.

Nucleus	Spin	Abundance (%)	Quadrupole moment 10^{28} (m^2)	Usual shift reference	Receptivity[a]
^{57}Fe	1/2	2.2	0	Neat $Fe(CO)_5$	0.004
^{99}Ru	5/2	12.7	0.076	$Ru(CN)_6^{4-}$	0.82
^{101}Ru	5/2	17.1	0.44	$Ru(CN)_6^{4-}$	1.5
^{187}Os	1/2	1.64	0	OsO_4	0.001
^{189}Os	3/2	16.1	0.91	OsO_4	2.2

[a]With reference to ^{13}C.

Iron-57 has the highest oxidation-state dependence of any nucleus, with the result that the 8800-ppm range for Fe(II) centred on $\delta + 6883$ is separated from the 2500-ppm range for Fe(0) centred on $\delta + 700$ by a gap of 500 ppm as shown in Fig. 12. The iron(II) compounds are mainly porphyrin and similar macrocyclic complexes, low-spin d^6 systems comparable with the cobalt(III) complexes long recognized as deshielded extremes. The lower fifth of the iron(0) range is occupied by the substituted ferrocenes covering 500 ppm, while the upper four-fifths is occupied by various diene complexes of $Fe(CO)_3$ for which von Philipsborn has provided an elegant theoretical analysis.[17]

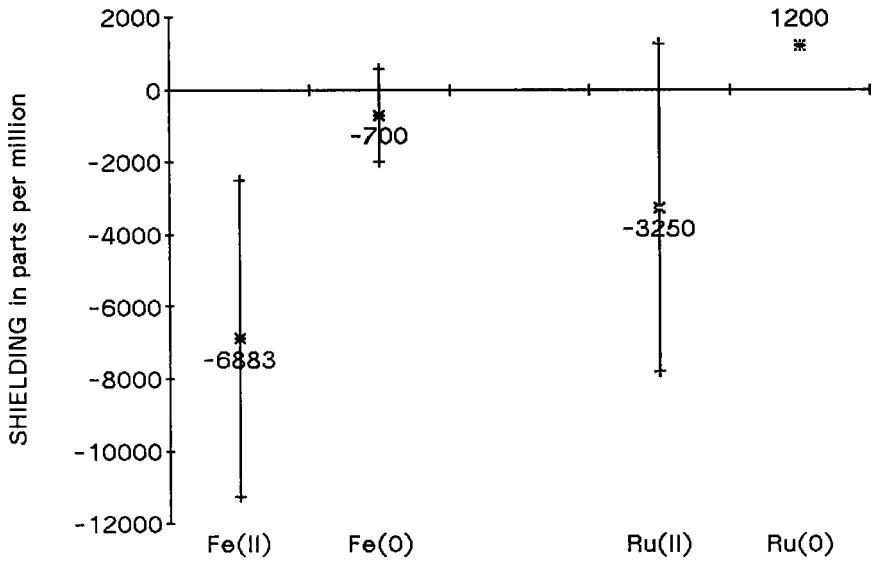

Fig. 12. Iron and ruthenium shielding ranges.

Halogen substitution is probably incompatible with the low oxidation state iron(0), but the chloride, bromide and iodide in the $Fe(C_5H_5(CO))_2X$ system have all been reported. The halogen dependence is normal with the iodide being the most highly shielded and a Br/I ratio of 0.31. The intensity of 958 ppm per halogen is the largest among the first-row transition metals, and is exceeded only by mercury at 977 ppm, platinum at 1017 ppm, thallium at 1465 ppm and antimony at 1353 ppm; all of which have normal halogen dependencies.

Ruthenium, named after the Latin *Ruthenia* for Russia, was isolated by Klaus in 1844 from platinum ore brought from the Ural Mountains. Ruthenium shieldings range from a low of $\delta + 7800$ in $Ru(NH_3)_6^{2+}$ to a high of $\delta - 1270$ in ruthenocene, relative to aqueous $Ru(CN)_6^{4-}$ near the shielded end of the range and the most highly shielded Ru(II) environment to date.

Ruthenium(II) shieldings span a range of 8000 ppm centred on $\delta + 3825$ and, as with iron(II), the deshielded end of the range is dominated by N bonded environments. $Ru(C_5H_5)_2$ and $Ru_3(CO)_{12}$ are the only Ru(0) compounds reported and their separation of 62 ppm defines a Ru(0) range centred on $\delta - 1239$. These oxidation states provide an oxidation-state dependence for ruthenium of 2530 ppm per OSU.

Ruthenium tetroxide is the only Ru(VIII) compound to be reported, and its resonance position of $\delta + 1931$ is anomalous. In an oxidation state much higher than all the others, the Ru(VIII) shielding should be much lower than all the Ru(II) environments, but it is not. There is no obvious explanation for this anomaly.

The chloride and iodide compounds in the *fac*-$Ru(CO)_3X_3^-$ system have been reported, showing a normal halogen dependence of 235 ppm per halogen.

Osmium, named after the Greek *osme* meaning "a smell", was discovered by Tennant in 1803 in the residue left after dissolving impure platinum with aqua regia. Its tetroxide is highly toxic, a powerful oxidizing agent, and has a strong smell.

An arene compound of osmium(II) has been reported to be 2562 ppm more highly shielded than the Os(VIII) in OsO_4. While the trend to lower shielding with increasing oxidation state is normal, the magnitude of the dependence is anomalously low for a third-row atom in this region of the periodic table, suggesting an OsO_4 anomaly similar to that associated with RuO_4 above.

5.7. The cobalt triad

Cobalt was discovered by the Swedish chemist Brandt in 1735, and it derives its name from the German *Kobold* for the goblin or evil spirit thought to inhabit mines. In 1951 the chemical-shift phenomenon in NMR spectroscopy was

Table 10. Nuclear properties of the cobalt triad isotopes.

Nucleus	Spin	Abundance (%)	Quadrupole moment 10^{28} (m^2)	Usual shift reference	Receptivity[a]
^{59}Co	7/2	100	0.4	$Co(CN)_6^{3-}$	1570
^{103}Rh	1/2	100	0	$\Xi = 3.16$ MHz	0.18
^{191}Ir	3/2	37.3	0.9	—	0.55
^{193}Ir	3/2	62.7	0.8	—	0.12

[a]With reference to ^{13}C.

discovered when the resonance frequencies in different cobalt compounds, resolvable to the nearest 1 ppm, were found to differ by as much 2%.[34] Forty years later, the total span of cobalt shieldings observed is still roughly 20 000 ppm, the largest range of any nucleus.

Cobalt shieldings (Table 10) range from a low of $\delta + 15\,110$ in aqueous $Co(H_2O)_6^{3+}$ to a high of $\delta - 4220$ in $Co(PF_3)_4^-$, relative to aqueous $Co(CN)_6^{3-}$ three-quarters of the way up the range. The regular progression from higher to lower shieldings with increase in oxidation state is seen in cobalt spectroscopy without any anomalies.

The shieldings in cobalt(III) compounds span 15 400 ppm centred on $\delta + 7403$, with O bonding ligands at the low end and $P(OR)_3$ alkyl phosphite ligands at the high end. In cobalt(I) compounds, the shieldings span a much narrower range of 2790 ppm centred on $\delta + 2245$ ppm, in cobalt(0) compounds they span a range of 1490 ppm centred on $\delta - 1115$, and in cobalt ($-$ I) compounds they span a range of 3376 ppm centred on $\delta - 2532$. Between the highest and lowest oxidation states, the oxidation-state dependence is 2480 ppm per OSU, second only to ^{57}Fe in magnitude. The relationships of these overlapping ranges to one another are all shown in Fig. 13.

The chloride, bromide and iodide compounds in the cobalt(III) series $Co(NH_3)_5X^{2-}$ have all been reported and they show a normal halogen dependence with an intensity of 90 ppm per halogen and a Br/I ratio of 0.30. Three cobalt($-$ I) series in which the halogen dependence is also normal and an order of magnitude stronger have also been reported. In $[Co(NO)_2X]_2$, $Co(NO)_2X(PMe_2Ph)$, and $Co(NO)_2X[P(OEt)_2Ph]$ the halogen dependencies and Br/I ratios are + 850 and 0.29, + 750 and 0.28, and + 860 and 0.29, respectively.

Rhodium was discovered by Wollaston in 1803 and is named after the Greek *rhodon* for "rose" whose deep-red colour is adopted by many rhodium salts. Rhodium shieldings range from a low of $\delta + 9931$ in $Rh(H_2O)_6^{3+}$ to a high of $\delta - 2050$ in $Rh(C_5H_5)$ (cyclooctadiene). Spectroscopists have found it more

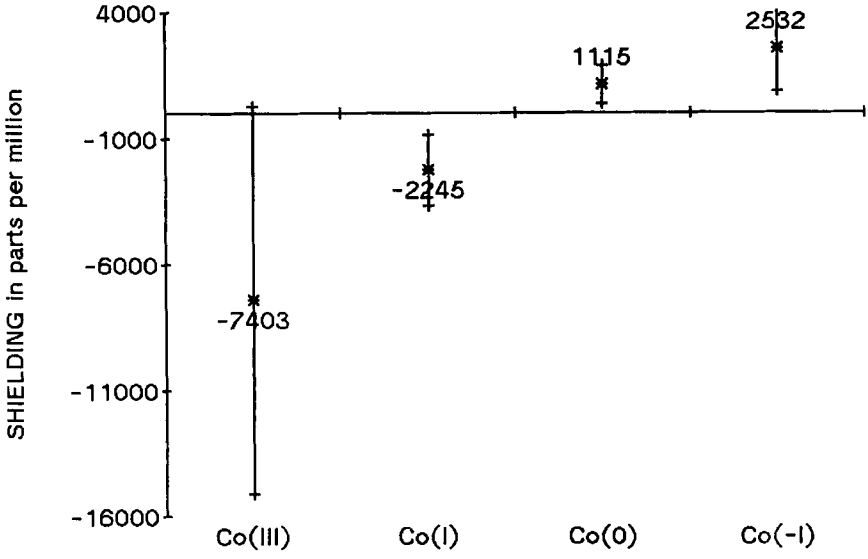

Fig. 13. Cobalt shielding ranges.

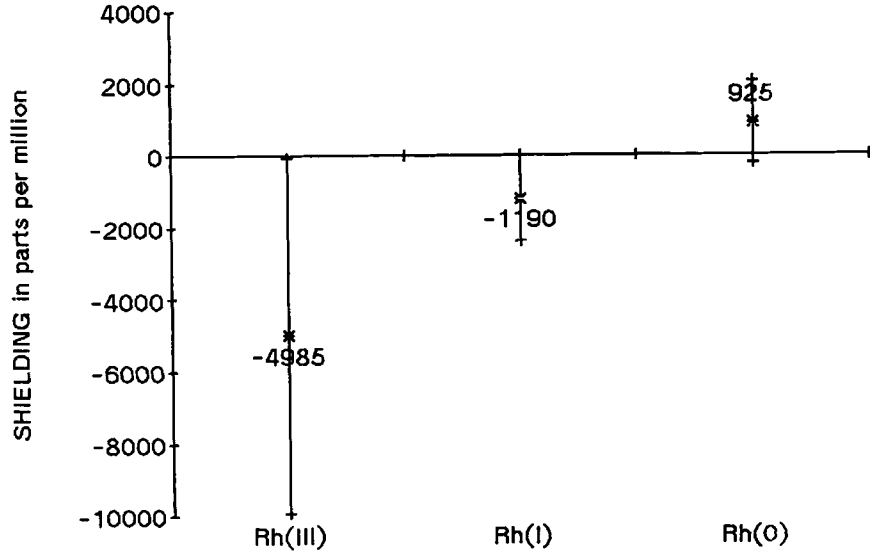

Fig. 14. Rhodium shielding ranges.

convenient to reference rhodium chemical shifts against an absolute field/frequency standard rather than against a specific rhodium compound, and the frequency of 3.16 MHz in the field where TMS protons resonate at 100 MHz was adopted by Kidd and Goodfellow in an early review of rhodium NMR.[7]

The shielding ranges for Rh(0), Rh(I) and Rh(III) form a regular progression from high to low with increase in rhodium oxidation state. The shifts for rhodium(0) compounds span a range of 2500 ppm centred on $\delta - 1200$, those for rhodium(I) compounds span 3400 ppm centred on $\delta + 1650$, and those for rhodium(III) span 9900 ppm centred on $\delta + 4985$. Between the highest and lowest, the oxidation state dependence for rhodium is 1970 ppm/OSU.

In two series of rhodium(III) compounds—$RhX_2Me(CO)(PMe_2Ph)_2$ and $RhXMe(CNBu^t)_4^+$—the chlorides, bromides and iodides have all been observed and the halogen dependencies and Br/I ratios (+ 224 and 0.33; and + 419 and 0.38, respectively) are both normal.

Iridium was discovered in 1803 and was named after the Latin *iris* for "*rainbow*", again because of the brilliant array of colours displayed in many of its salts. While there are two magnetically active isotopes of iridium shown in Table 10, the low receptivity and large quadrupole moment for each are sufficient to account for the lack of NMR observation to date.

5.8. The nickel triad

Nickel was discovered by the Swedish chemist Cronstedt in 1751 and was named after the German *Nickel* for Satan or "Old Nick", a reference to *kupfernickel* or Old Nick's copper. Nickel shieldings (Table 11) range from a low of $\delta + 267$ in $Ni(PCl_3)_4$ to a high of $\delta - 929$ in $Ni(PF_3)_4$, relative to $Ni(CO)_4$ a quarter of the way up the range.

Nickel(0) is the only oxidation state to have been studied and, since most nickel(II) compounds are paramagnetic, the possibility of obtaining either an

Table 11. Nuclear properties of the nickel triad isotopes.

Nucleus	Spin	Abundance (%)	Quadrupole moment 10^{28} (m^2)	Usual shift reference	Receptivity[a]
^{61}Ni	3/2	1.2	0.2	$Ni(CO)_4$	0.24
^{105}Pd	5/2	22.2	0.7	$PdCl_6^{2-}$	1.4
^{195}Pt	1/2	33.8	0	$PtCl_6^{2-}$	19.1

[a] With reference to ^{13}C.

oxidation-state dependence or a halogen dependence for nickel shieldings is remote. Some of the d^6 nickel(IV) compounds are diamagnetic, but are not particularly stable and are very difficult to maintain free of paramagnetic impurities.

Palladium, like rhodium, was discovered by Wollaston in 1803 and was named after the asteroid Pallus discovered about the same time, Pallus being a Greek goddess of wisdom. We do not yet have a shielding range for palladium. It takes at least two compounds to establish a range, and $PdCl_6^{2-}$ is the only compound to have been studied in solution. The unexpectedly large linewidth of 25 kHz is unusual for a six-coordinate d^6 complex and suggests a geometry other than octahedral.

Platinum was discovered in South America in 1841 and was named after the Spanish *plata* meaning "silver", to which the native metal bears a strong resemblance. Platinum shieldings range from a low of $\delta + 11\,847$ in PtF_6^{2-} to a high of $\delta - 1528$ in PtI_6^{2-}, relative to $PtCl_6^{2-}$ nine-tenths of the way up the range.

The shielding ranges for Pt(0), Pt(II) and Pt(IV) form a regular progression from high to low with increase in platinum oxidation state. The shifts for platinum(IV) span 13 375 ppm centred on $\delta + 5160$, those for platinum(II) span 5553 ppm centred on $\delta + 1780$, and those for platinum(0) span 2056 ppm centred on $\delta - 270$. Between the highest and the lowest states, the oxidation-state dependence for platinum is 1360 ppm per OSU.

The halogen dependence for platinum shieldings (Fig. 15) is normal and is astonishingly insensitive to a change in oxidation state. For both the platinum(IV) series PtX_6^{2-} and the platinum(II) series PtX_4^{2-} the chlorides, bromides and iodides have all been studied. In the Pt(IV) case, the shielding dependence is + 1008 ppm per halogen with a Br/I ratio of 0.31. In the Pt(II) case it is + 974 ppm per halogen with a Br/I ratio of 0.27. This insensitivity of halogen dependence in the case of platinum to a change in oxidation state can only cast doubt on an earlier suggestion that oxidation-state change is the primary cause of the change from IHD to NHD along the series of transition metals.

5.9. The copper triad

The number of copper NMR recordings is not large. The copper(II) oxidation state which represents the majority of copper compounds is paramagnetic, and the linewidths of the copper(I) compounds studied are much larger than is to be expected for a nucleus with a quadrupole moment of only 0.2 barns; half that of ^{55}Mn. A good explanation for this anomaly based on the kinetic lability of copper(I) in solution has been provided by Rehder.[14]

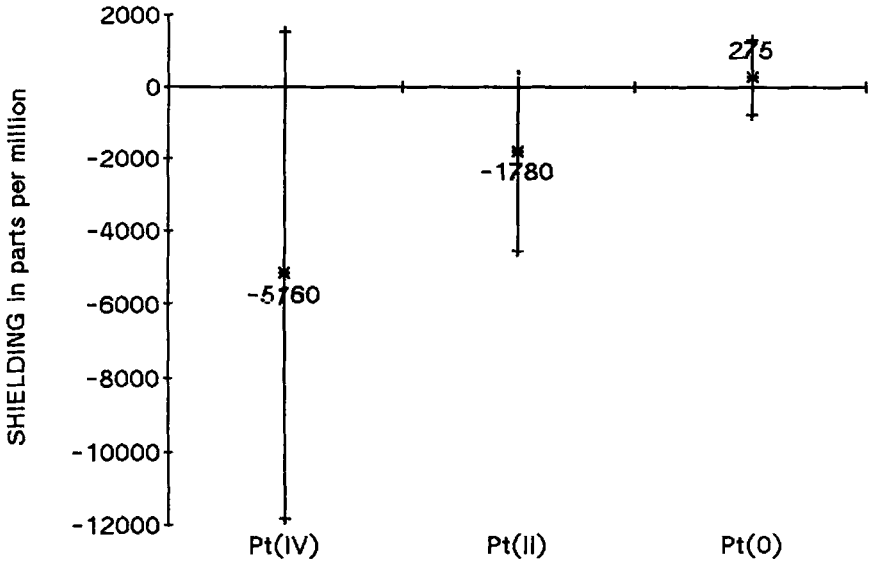

Fig. 15. Platinum shielding ranges.

Copper is another of the half-dozen metals dating from the pre-Christian era and it derives its name from *cuprum*, the Latin designation for the island of Cyprus where much ancient copper was obtained. Copper shieldings (Table 12) range from a low of $\delta + 501$ in $Cu(CN)_4^{3-}$ to a high of $\delta - 381$ in powdered CuBr, relative to $Cu(MeCN)_4^+$ in acetonitrile solution just up from the middle of the range. (Shieldings in solids may not be strictly comparable with those in solution and they must be used with caution.)

The halogen dependence of copper shieldings is interesting. All the available evidence comes from the cuprous halide solids where the shielding of Cu(I)

Table 12. Nuclear properties of the copper triad isotopes.

Nucleus	Spin	Abundance (%)	Quadrupole moment 10^{28} (m^2)	Usual shift reference	Receptivity[a]
^{63}Cu	3/2	69.1	−0.21	$Cu(MeCN)_4^+$	365
^{65}Cu	3/2	30.9	−0.19	$Cu(MeCN)_4^+$	201
^{107}Ag	1/2	51.8	0	$Ag^+(aq)$	0.20
^{109}Ag	1/2	48.2	0	$Ag^+(aq)$	0.28
^{197}Au	3/2	100	0.55	—	0.14

[a]With reference to ^{13}C.

occupying tetrahedral sites in the zinc blende structure increases in the order $Cl \simeq I < Br$, an ordering that is not normal. In $Cu_2HgI_4(s)$ where Cu is also coordinated by iodides the copper is even more deshielded, and if one calculates the dependence using CuI and CuBr the resulting IHD (normalized to a Cl–I difference) has an intensity of 21 ppm per halogen.

Silver tailings in Asia Minor suggest people were separating it from lead as early as 3000 B.C. Known as *argentum* in Latin, its English name comes from the Anglo-Saxon *seolfor* or *siolfur*. Silver shieldings range from a low of $\delta + 841$ in $Ag(S_2O_3)_3^{5-}$ to a high of $\delta - 100$ in AgF(s), relative to aqueous Ag^+ down by one-tenth from the top of the range.

In solution, the chloride, bromide and iodide in the system $AgX(NH_2Et)_2$ have all been studied and they show a marked inverse halogen dependence of 295 ppm per halogen with a regular Br/I ratio of 0.31.

Gold (from the Latin *aurum*) is an old Anglo-Saxon word related to the Sanskrit *Jval* and it names a metal that has been highly valued from the earliest of times. To the NMR spectroscopist it is ironic that the same quality giving value to gold inhibits the formation of symmetrical compounds with lines narrow enough to be observed above the background noise. The combination of low receptivity and a moderately large quadrupole moment make ^{197}Au an unlikely source of NMR spectra.

5.10. The zinc triad

Zinc is named after the German *zink* and, although used for alloying in ancient times, was rediscovered and recognized as an element in 1746 by the German chemist Marggraf. Zinc shieldings (Table 13) range from a low of $\delta + 418$ in $Zn(SCH_2CH_2S)_2^{2-}$ to a high of $\delta - 36$ in an aqueous ZnI_2/12 M HI solution (probably ZnI_4^{2-}), relative to $Zn^{2+}(aq)$ very near the top of the range.

Aqueous solutions of zinc chloride, bromide and iodide loaded with the

Table 13. Nuclear properties of the zinc triad isotopes.

Nucleus	Spin	Abundance (%)	Quadrupole moment 10^{28} (m^2)	Usual shift reference	Receptivity[a]
^{67}Zn	5/2	4.1	0.15	$Zn^{2+}(aq)$	0.67
^{111}Cd	1/2	12.9	0	$Cd^{2+}(aq)$	6.98
^{113}Cd	1/2	12.3	0	$Cd^{2+}(aq)$	7.60
^{199}Hg	1/2	16.8	0	$Hg^{2+}(aq)$	5.42
^{201}Hg	3/2	13.2	0.4	$Hg^{2+}(aq)$	1.08

[a]With reference to ^{13}C.

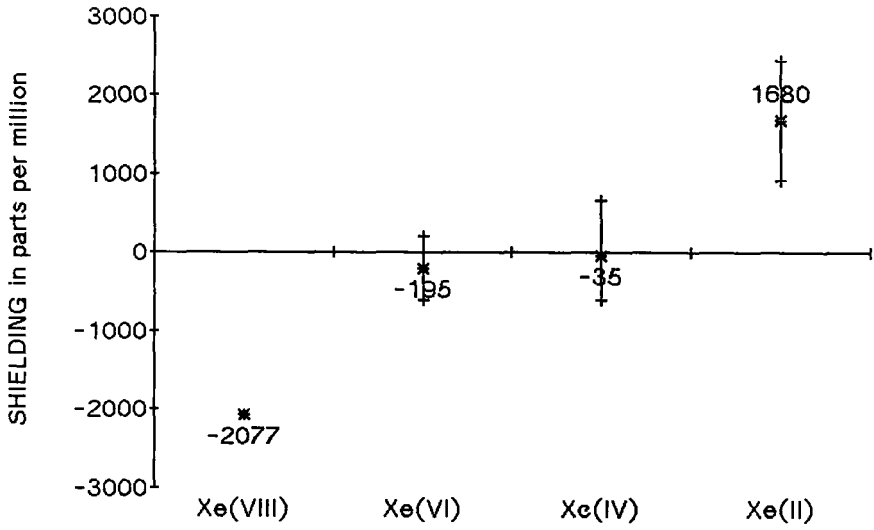

Fig. 16. Xenon shielding ranges.

corresponding hydrogen halide have all generated ^{67}Zn spectra, but because of the kinetic lability of the complexes there is some uncertainty as to the stoichiometry of the species producing the signal. Making the most likely assumption that it is ZnX_4^{2-} that produces the signal in each case, the halogen dependence of zinc shieldings is normal with an intensity of 71 ppm per halogen and a Br/I ratio of 0.30.

Cadmium was discovered by Stromeyer in 1817 and its name derives from the Latin *cadmia*, the ancient name for calamine or zinc carbonate. Cadmium shieldings range from a low of $\delta + 829$ in $Cd(SCH_2CH_2S)_2^{2-}$ to a high of $\delta - 27$ in a bis(diketonate) where the Cd is coordinated by six oxygens, all relative to Cd^{2+} (aq) near the top of the shielding range.

The chloride, bromide and iodide in the CdX_4^{2-} system exhibit a normal halogen dependence with an intensity of 98 ppm per halogen and a Br/I ratio of 0.22. In solid CdX_4 environments the dependence is + 98 ppm per halogen, and in solid CdX_6 environments it is + 147 ppm per halogen.

Mercury is named after the planet Mercury; it was known to the ancient Chinese and Hindus, and was found in Egyptian tombs dating from 1500 B.C. Mercury shieldings range from a low of $\delta + 3080$ in $Hg(SiEt_3)_2$ to a high of $\delta - 1185$ in HgI_2, relative to Hg^{2+}(aq) three-quarters of the way up the range.

There are a number of systems from which the halogen dependence of mercury shieldings can be assessed. In the HgX_4^{2-} system the dependence is

+ 551 ppm per halogen and in the $HgX_2(PR_3)_2$ system it is + 451 ppm per halogen; NHD in both cases.

5.11. A non-metal

Xenon is named after the Greek *xenos* for "stranger" and is one of the rare gases isolated from the atmosphere by Ramsey and Travers in 1898. It is one of the few molatoms outside the transition metals whose chemistry is also marked by a rich variety of oxidation states, and it has been included here at the end as evidence that the pattern of oxidation-state dependencies created out of transition-metal chemical shifts is not restricted to the transition metals. The shielding ranges for Xe(VIII), Xe(VI), Xe(IV) and Xe(II) are given in Fig. 16, showing the same regular progression from low to high shielding with decline in oxidation state that is typical of the transition metals.

REFERENCES

1. R. Freeman, G.R. Murray, and R. Richards, *Proc. R. Soc., Ser. A*, 1957, **242**, 455.
2. N.F. Ramsey, *Phys. Rev.*, 1950, **78**, 699.
3. J.S. Griffith and L.E. Orgel, *Trans. Faraday Soc.*, 1957, **53**, 601.
4. N. Juranic, *Inorg. Chem.*, 1983, **22**, 521.
5. R. Bramley, M. Brorson, A.M. Sargeson, and C.E. Schaeffer, *J. Am. Chem. Soc.*, 1985, **107**, 2780.
6. Applications of Nuclear Shieldings, in *Specialist Periodical Reports NMR* (ed. G.A. Webb). Royal Society of Chemistry, London.
7. R.G. Kidd and R.J. Goodfellow, in *NMR and the Periodic Table* (ed. R.K. Harris and B.E. Mann). Academic Press, London, 1978.
8. R.G. Kidd, in *Annual Reports on NMR Spectroscopy*, Vol. 10A (ed. G.A. Webb), p. 1. Academic Press, London, 1978.
9. J.J. Dechter, in *Progress in Inorganic Chemistry* Vol. 33 (ed. S.J. Lippard), p. 393. Wiley-Interscience, New York, 1985.
10. D. Rehder, *Chimia*, 1986, **40**, 1896.
11. J. Mason, *Chem. Rev.*, 1987, **87**, 1299.
12. D. Rehder and R.J. Goodfellow, in *Multinuclear NMR* (ed. J. Mason). Plenum Press, New York, 1987.
13. F. Wehrli, in *Annual Reports on NMR Spectroscopy*, Vol. 9 (ed. G.A. Webb) p. 125. Academic Press, London, 1979.
14. D. Rehder, *Magn. Reson. Rev.*, 1984, **9**, 125.
15. P.S. Pregosin, *Coord. Chem. Rev.*, 1982, **44**, 247.
16. M. Minelli, J.H. Enemark, R.T.C. Brownlee, M.J. O'Connor and A.G. Wedd, *Coord. Chem. Rev.*, 1985, **68**, 169.
17. W. von Philipsborn, *Pure Appl. Chem.*, 1986, **58**, 513.
18. L. Pauling, *J. Chem. Soc.*, 1948, 1461.
19. B.N. Figgis, R.G. Kidd and R.S. Nyholm, *Proc. R. Soc., Ser. A*, 1962, **269**, 469.

20. To account for the inversion in halogen dependence of nuclear shieldings, a spin–orbit coupling variable is likely to be required. Hartree–Fock wavefunctions are not normally corrected for spin–orbit coupling.
21. F. Naumann, D. Rehder and V. Pank, *Inorg. Chim. Acta*, 1984, **84**, 117.
22. Yu. A. Buslaev, V.D. Kopanev and V.P. Tarasov, *Chem. Commun.*, 1971, 1175.
23. R.G. Kidd, R.W. Matthews and H.G. Spinney, *J. Am. Chem. Soc.*, 1972, **94**, 6686.
24. Ref. 8, p. 8.
25. K.R. Dixon, in *Multinuclear NMR* (ed. J. Mason). Plenum Press, New York, 1987.
26. H.C.E. McFarlane and W. McFarlane, in *Multinuclear NMR* (ed. J. Mason). Plenum Press, New York, 1987.
27. A. Lavoisier, *Traité élémentaire de Chimie*, Paris, 1789. (*Elements of Chemistry*, Dover, New York, 1965, p. 179.)
28. C.J. Jameson and H.S. Gutowsky, *J. Chem. Phys.*, 1964, **40**, 1714.
29. R.G. Kidd and D.R. Truax, *J. Am. Chem. Soc.*, 1968, **90**, 6867.
30. J.A. Pople, *Mol. Phys.*, 1964, **7**, 301.
31. W.C. Dickinson, *Phys. Rev.*, 1950, **80**, 563.
32. N.F. Ramsey, *Phys. Rev.*, 1950, **78**, 699; 1952, **86**, 243; 1953, **91**, 303.
33. Ref. 8, p. 46.
34. W.G. Proctor and F.C. Yu, *Phys. Rev.*, 1951, **81**, 20.

BIBLIOGRAPHY

The scandium triad

Scandium

P. Bougeard, M. Mancini, B.G. Sayer and M.J. McGlinchey, *Inorg. Chem.*, 1985, **24**, 93.
Yu.A. Buslaev, G.A. Kirakosyan and V.P. Tarasov, *Dokl. Akad. Nauk SSSR*, 1982, **264**, 1405.
P.G. Gassman, W.H. Cambell and D.W. Macomber, *Organometallics*, 1984, **3**, 385.
M. Mancini, P. Bougeard, R.C. Burns, M. Mlekuz, B.G. Sayer, J.I.A. Thompson and M.J. McGlinchey, *Inorg. Chem.*, 1984, **23**, 1072.
G.A. Melson, D.J. Olzanski and A.Z. Rahimi, *Spectrochim. Acta, Part A*, 1977, **33**, 301.
A.R. Thompson and E. Oldfield, *J. Chem. Soc. Chem. Commun.*, 1987, 27.
D. Rehder and M. Speh, *Inorg. Chim. Acta*, 1987, **135**, 73.

Yttrium

R.M. Adam, G.V. Fazakerly and D.G. Reid, *J. Magn. Reson.*, 1979, **33**, 655. (Questionable shift directions.)
W.J. Evans, J.H. Meadows, A.G. Kostka and G.L. Closs, *Organometallics*, 1985, **4**, 324.
C.E. Holloway, A. Mastracci and I.M. Walker, *Inorg. Chim. Acta*, 1986, **113**, 187.

Lanthanum

J.C.G. Buenzli, A.E. Merbach and R.M. Nielson, *Inorg. Chim. Acta*, 1987, **139**, 151.
S.H. Eggers and R.D. Fisher, *J. Organomet. Chem.*, 1986, **315**, C61.
D.F. Evans and P.H. Missen, *J. Chem. Soc., Dalton Trans.*, 1982, 1929.

V.P. Tarasov, G.A. Kirakosyan, S.V. Trots, Yu. A. Buslaev and V.T. Panyushkin, *Koord. Khim.*, 1983, **9**, 205.

The titanium triad

Titanium

K.M. Chi, S.R. Frerichs, S.B. Philson and J.E. Ellis, *J. Am. Chem. Soc.*, 1988, **110**, 303.
A. Dormond, M. Fauconet, J.C. Leblanc and C. Mose, *Polyhedron*, 1984, **8**, 897.
W.C. Finch, E.V. Anslyn and R.H. Grubbs, *J. Am. Chem. Soc.*, 1988, **110**, 2406.
N. Hao, B.G. Sayer, G. Denes, D.G. Bickley, C. Detellier and M.J. McGlinchey, *J. Magn. Reson.*, 1982, **50**, 50.

Zirconium

R. Benn and A. Rufinska, *J. Organomet. Chem.*, 1984, **273**, C51.
P. Bougeard, J.J. McCullough, B.G. Sayer and M.J. McGlinchey, *Inorg. Chim. Acta*, 1984, **89**, 133.
B.G. Sayer, N. Hao, G. Denes, D.G. Bickley and M.J. McGlinchey, *Inorg. Chim. Acta*, 1981, **48**, 53.
B.G. Sayer, J.I.A. Thompson, N. Hao, T. Birchall, D.R. Eaton and M.J. McGlinchey, *Inorg. Chem.*, 1981, **20**, 3748.

The vanadium triad

Vanadium

K.D. Becker and U. Berlage, *J. Magn. Reson.*, 1983, **54**, 272.
A.T. Harrison and O.W. Howarth, *J. Chem. Soc., Dalton Trans.*, 1986, 1405.
M. Herberhold and H. Trampisch, *Inorg. Chim. Acta*, 1983, **70**, 143.
M. Hoch, D. Rehder and C. Weidemann, *Inorg. Chim. Acta*, 1984, **92**, L5.
M. Hoch, A. Duch and H. Rehder, *Inorg. Chem.*, 1986, **25**, 2907.
K. Ihmels and D. Rehder, *Chem. Ber.*, 1985, **118**, 895.
K. Ihmels and D. Rehder, *Organometallics*, 1985, **4**, 1340.
N. Juranic, *J. Chem. Soc., Dalton Trans.*, 1988, 79.
M.A. Leparulo-Loftus and M.T. Pope, *Inorg. Chem.*, 1987, **26**, 2112.
R.I. Maskimovskaya and N.N.Chumachenko, *Polyhedron*, 1987, **6**, 1813.
F. Naeumann and D. Rehder, *Z. Naturforsch., Teil B*, 1984, **39**, 1654.
F. Naumann, D. Rehder and V. Pank, *Inorg. Chim. Acta*, 1984, **84**, 117.
W. Priebsch and D. Rehder, *Inorg. Chem.*, 1985, **24**, 3058.
D. Rehder, *Bull. Magn. Reson.*, 1982, **4**, 33.
D. Rehder and K. Ihmels, *Inorg. Chim. Acta*, 1983, **76**, L313.
D. Rehder and P. Jaitner, *J. Organomet. Chem.*, 1987, **329**, 337.
D. Rehder, P. Oltmanns and M. Hoch, *J. Organomet. Chem.*, 1986, **308**, 19.
R. Talay and D. Rehder, *Inorg. Chim. Acta*, 1983, **77**, L175.
A.S. Tracey, M.J. Gresser and B. Galeffi, *Inorg. Chem.*, 1988, **27**, 157.
G.F.P. Warnock and J.E. Ellis, *J. Am. Chem. Soc.*, 1984, **110**, 5016.
C. Weidemann and D. Rehder, *Inorg. Chim. Acta*, 1986, **120**, 15.

Niobium

K. Bachmann and D. Rehder, *J. Organomet. Chem.*, 1984, **276**, 177.
Yu.A. Buslaev, V.P. Tarasov, S.M. Sinitsyna, V.G. Khlebodarov and V.D. Kopanev, *Koord. Khim.*, 1979, **5**, 189.
M. Hoch and D. Rehder, *Z. Naturforsch. Teil B*, 1983, **38**, 446.
F. Naumann, D. Rehder and V. Pank, *J. Organometal. Chem.*, 1982, **240**, 362.
D. Rehder, H.Ch. Bechthold and K. Paulsen, *J. Magn. Reson.*, 1980, **40**, 305.
D. Rehder, H.Ch. Bechthold, A. Kecici, H. Schmidt and M. Siewing, *Z. Naturforsch., Teil B*, 1982, **37**, 631.
J. Sola, Y. Do, J.M. Berg and R.H. Holm, *J. Am. Chem. Soc.*, 1983, **105**, 7784.
V.P. Tarasov, S.M. Sinitsyna, V.D. Kopanev, V.G. Khlebodarov and Yu.A. Buslaev, *Koord. Khim.*, 1980, **6**, 1568.

Tantalum

K.D. Becker and U. Berlage, *J. Magn. Reson.*, 1983, **54**, 272.
D. Rehder and W. Basler, *J. Magn. Reson.*, 1986, **68**, 172.
V.V. Skopenko, V.M. Amirkhanov and V.V. Trachevskii, *Chem. Abs.*, 1987, **106**, 94709.

The chromium triad

Chromium

B.W. Epperlein, H. Kruger, O. Lutz, A. Nolle and W. Mayr, *Z. Naturforsch.*, Teil A, 1975, **30**, 1237.
E. Haid, D. Kohnlein, G. Kossler, O. Lutz and W. Schich, *J. Magn. Reson.*, 1983, **55**, 145.
V.P. Tarasov, V.I. Privalov and Yu.A. Buslaev, *Z. Naturforsch., Teil B*, 1984, **39**, 1230.

Molybdenum

E.C. Alyea and A. Somogyvari, *Magn. Reson. Chem.*, 1986, **24**, 357.
E.C. Alyea and A. Somogyvari, *Trans. Met. Chem.*, 1987, **12**, 310.
E.C. Alyea, A. Malek and J. Malito, *Inorg. Chim. Acta*, 1985, **101**, 147.
R.T.C. Brownlee, M.J.O'Connor, B.P. Shehan and A.G. Wedd, *J. Magn. Reson.*, 1985, **64**, 124.
R.T.C. Brownlee, M.J.O'Connor, P.B. Shehan and A.G. Wedd, *Aust. J. Chem.*, 1986, **39**, 931.
C.J. Casewit, M.R. Dubois, R.A. Grieves and J. Mason, *Inorg. Chem.*, 1987, **26**, 1889.
J.W. Faller and B.C. Whitmore, *Organometallica*, 1986, **5**, 752.
S.F. Gheller, P.A. Gazzana, A.F. Masters, R.T.C. Brownlee, M.J.O'Connor and A.G. Wedd, *Inorg. Chim. Acta*, 1981, **54**, L131.
J.C. Green, R.A. Grieves and J. Mason, *J. Chem. Soc., Dalton Trans.*, 1986, 1313.
R.A. Grieves and J. Mason, *Polyhedron*, 1986, **5**, 415.
O. Lutz, A. Nolle and P. Kroneck, *Z. Naturforsch., Teil A*, 1976, **31**, 454.
A.F. Masters, R.T.C. Brownlee, M.J.O.'Connor and A.G. Wedd, *Inorg. Chem.*, 1981, **20**, 4183.
M. Minelli, T.W. Rockway, J.H. Enemark, H. Brunner and M. Muschiol, *J. Organomet. Chem.*, 1981, **217**, C34.
M. Minelli, J.L. Hubbard, D.L. Lichtenberger and J.H. Enemark, *Inorg. Chem.*, 1984, **23**, 2721.
M. Minelli, K. Yamanouchi, J.H. Enemark, P. Supramanian, B.B. Kaul and J.T. Spence, *Inorg. Chem.*, 1984, **23**, 2554.
M. Minelli, E.J.H. Martin, A. Bell and R.A. Walton, *J. Organomet. Chem.*, 1985, **284**, 25.

B. Piggott, S.F. Wong and R.N. Sheppard, *Inorg. Chim. Acta*, 1985, **107**, 97.
B.P. Shehan, M. Kony, R.T.C. Brownlee, M.J.O'Connor and A.G. Wedd, *J. Magn. Reson.*, 1985, **63**, 343.
M.J. Toohey, C.D. Scatterwood and C.D. Garner, *Inorg. Chim. Acta*, 1987, **129**, L19.
C.G. Young and J.H. Enemark, *Inorg. Chem.*, 1985, **24**, 4416.
C.G. Young and J.H. Enemark, *Aust. J. Chem.*, 1986, **39**, 997.
C.G. Young, E.M. Kober and J.H. Enemark, *Polyhedron*, 1987, **6**, 255.

Tungsten

J. Banck and A. Schwenk, *Z. Phys., Ser. B*, 1975, **20**, 75.
V. Chauveau, *Bull. Soc. Chim. Fr.*, 1986, 199.
R.G. Finke, B. Rapko and P.J. Domaille, *Organometallics*, 1986, **5**, 175.
S.F. Gheller, M. Sidney, A.F. Masters, R.T.C. Brownlee, M.J.O'Connor and A.G. Wedd, *Aust. J. Chem.*, 1984, **37**, 1825.
M. Kozic, C.F. Hamer and L.C.W. Baker, *J. Am. Chem. Soc.*, 1986, **108**, 2748.
W. Malisch, R. Maisch, I.J. Colquhoun and W. McFarlane, *J. Organomet. Chem.*, 1981, **220**, C1.
A.C. McDonell, S.G. Vasudevan, M.J.O'Connor and A.G. Wedd, *Aust. J. Chem.*, 1985, **38**, 1017.
W. McFarlane, A.M. Noble and J.M. Winfield, *J. Chem. Soc. A*, 1971, 948.
H.C.E. McFarlane, W. McFarlane and D.S. Rycroft, *J. Chem. Soc., Dalton Trans.*, 1976, 1616.
A. Nagasawa, Y. Sasaki, B. Wang, S. Ikari and T. Ito, *Chem. Lett.*, 1987, 1271.
K. Piepgrass and M.T. Pope, *J. Am. Chem. Soc.*, 1987, **109**, 1586.
D.J. Santure, K.W. McLaughlin, J.C. Huffman and P.P. Sattelberger, *Inorg. Chem.*, 1983, **22**, 1877.

The manganese triad

Manganese

F. Calderazzo, E.A.C. Lucken and D.F. Williams, *J. Chem. Soc.*, 1967, 154.
A. Kececi and D. Rehder, *Z. Naturforsch., Teil B*, 1981, **36**, 20.
U. Kunze, A. Bruno and D. Rehder, *J. Organomet. Chem.*, 1984, **268**, 213.
W.J. Miles, B.B. Garnett and R.J. Clark, *Inorg. Chem.*, 1969, **8**, 2817.
R.M. Nielson and S. Wherland, *Inorg. Chem.*, 1985, **24**, 3458.
P. Oltmanns and D. Rehder, *J. Organometal. Chem.*, 1985, **281**, 263.
S. Onaka, *Bull. Chem. Soc. Jpn*, 1986, **59**, 3079.
D. Rehder, H.Ch. Bechthold, A. Kececi, H. Schmidt and M. Siewing, *Z. Naturforsch., Teil B*, 1982, **37**, 631.
D. Rehder, V. Pank, U. Kunze and A. Bruns, *Inorg. Chim. Acta*, 1985, **99**, L35.

Technetium

M.J. Buckingham, G.E. Hawkes and J.R. Thornback, *Inorg. Chim. Acta*, 1981, **56**, L41.
M. Findeisen, L. Kaden, B. Lorenz, S. Rummel and M. Wahren, *Inorg. Chim. Acta*, 1987, **128**, L15.
M. Findeisen, L. Kaden, B. Lorenz and M. Wahren, *Inorg. Chim. Acta*, 1988, **142**, 3.
K.J. Franklin, C.J. Lock, B.G. Sayer and G.J. Schrobilgen, *J. Am. Chem. Soc.*, 1982, **104**, 5303.
L. Mathieu, P. Thivolle, G. Galy and M. Berger, *J. Biophys. Biomec.*, 1985, **9**, 95. (*Chem. Abs.*, 1985, **103**, 209313.)
D.I. Spitsyn, V.P. Tarasov, K.E. German, S.A. Petrushkin, A.F. Kuzina and S.V. Kryuchkov, *Dokl. Akad. Nauk SSSR*, 1986, **290**, 1411.

J.L. Vanderheyden, A.R. Ketring, K. Libson, M.J. Heeg, L. Roecker, P. Motz, R. Whittle, R.C. Elder and E. Deutsch, *Inorg. Chem.*, 1984, **23**, 3184.
D.W. Wester, D.H. White, F.W. Miller and R.T. Dean, *Inorg. Chem.*, 1984, **23**, 1501.

Rhenium

R.E. Dwek, Z. Luz and M. Shporer, *J. Phys. Chem.*, 1970, **74**, 2232.
A. Kececi and D. Rehder, *Z. Naturforsch., Teil B*, 1981, **36**, 20.
A. Mueller, I. Krickmeyer, H. Boegge, M. Penk and D. Rehder, *Chimia*, 1986, **40**, 50.

The iron triad

Iron

L. Baltzer, *J. Am. Chem. Soc.*, 1987, **109**, 3479.
L. Baltzer and O.A. Gansow, *Congr. AMPERE Magn. Reson. Relat. Phenom., Proc. 22nd*, 1984, 343.
L. Baltzer and M. Landergren, *J. Chem. Soc., Chem. Commun.*, 1987, 32.
R. Benn and C. Brevard, *J. Am. Chem. Soc.*, 1986, **108**, 5622.
T. Jenny, W. von Philipsborn, J. Kronenbitter and A. Schwenk, *J. Organomet. Chem.*, 1981, **205**, 211.
W. von Philipsborn, *Pure Appl. Chem.*, 1986, **58**, 513.

Ruthenium

C. Brevard and P. Granger, *Inorg. Chem.*, 1983, **22**, 532.
R.W. Dykstra and A.M. Harrison, *J. Magn. Reson.*, 1982, **46**, 338.
N. Juranic, *J. Magn. Reson.*, 1987, **71**, 144.
C. Marzin, F. Budde, P.J. Steel and D. Lerner, *New J. Chem.*, 1987, **11**, 33.
P.J. Steel, F. LaHousse, S. Lerner and C. Marzin, *Inorg. Chem.*, 1983, **22**, 1488.

Osmium

J.A. Cabeza, B.E. Mann, C. Brevard and P.M. Maitlis, *J. Chem. Soc., Chem. Commun.*, 1985, 65.
A.A. Koridze, *Chem. Abs.*, 1986, **104**, 60826.

The cobalt triad

Cobalt

R. Benn, K. Cibura, P. Hofmann, K. Jones and A. Rufinska, *Organometallics*, 1985, **4**, 2214.
A.M. Bond, R. Colton, J.E. Moir and D.R. Page, *Inorg. Chem.*, 1985, **24**, 1298.
R. Bramley, M. Brorson, A.M. Sargeson and C.E. Schaeffer, *J. Am. Chem. Soc.*, 1985, **107**, 2780.
J. Bultitude, L.F. Larkworthy, J. Mason, D.C. Povey and B. Sandell, *Inorg. Chem.*, 1984, **23**, 3629.

M.G. Fitzpatrick, L.R. Hanton, W. Levason and M.D. Spicer, *Inorg. Chim. Acta*, 1987, **142**, 17.
K.I. Hagen, C.M. Schwab, J.O. Edwards and D.A. Sweigart, *Inorg. Chem.*, 1986, **25**, 978.
C.J. Hawkins, E. Horn, J. Martin, J.A.L. Palmer and M.R. Snow, *Aust. J. Chem.*, 1986, **39**, 1213.
H.C. Jewiss, W. Levason and M. Webster, *Inorg. Chem.*, 1986, **25**, 1997.
H.C. Jewiss, W. Levason, M.D. Spicer and M. Webster, *Inorg. Chem.*, 1987, **26**, 2102.
N. Juranic, *Inorg. Chim. Acta*, 1984, **87**, L37.

Rhodium

H. Adams, N.A. Bailley, B.E. Mann, B.F. Taylor, C. White and P. Yavari, *J. Chem. Soc., Dalton Trans.*, 1987, 1947.
C. Arz, P.S. Pregosin and C. Anklin, *Magn. Reson. Chem.*, 1987, **25**, 158.
R. Benn, H. Brenneke and A. Rufinska, *J. Organomet. Chem.*, 1987, **320**, 115.
R. Bonnaire, D. Davoust and N. Platzer, *Org. Magn. Reson.*, 1984, **22**, 80.
C. Carr, J. Glaser and M. Sandstrom, *Inorg. Chim. Acta*, 1987, **131**, 153.
M.J. Fernandez, P.M. Bailey, P.O. Bentz, J.S. Ricci, T.F. Koetzle and P.M. Maitlis, *J. Am. Chem. Soc.*, 1984, **106**, 5458.
C.D. Garner, M. Berry and B.E. Mann, *Inorg. Chem.*, 1984, **23**, 1500.
S.M. Socol and D.W. Meek, *Inorg. Chim. Acta*, 1985, **101**, L45.

The nickel triad

Nickel

N. Hao, M.J. McLinchey, B.G. Sayer and G.J. Schrobilgen, *J. Magn. Reson.*, 1982, **46**, 158.
H. Schumann, M. Meissner and H.J. Kroth, *Z. Naturforsch., Teil B*, 1980, **35**, 639.

Palladium

M.A. Fedotov and V.A. Likholobov, *Chem. Abs.*, 1984, **101**, 162447.

Platinum

H.G. Alt, W.D. Mueller, J. Unsin and H.A. Brune, *J. Organomet. Chem.*, 1986, **307**, 121.
T.G. Appleton, J.R. Hall, D.W. Neale and S.F. Ralph, *Inorg. Chim. Acta*, 1983, **77**, L149.
T.G. Appleton, J.R. Hall, S.F. Ralph and C.S.M. Thompson, *Inorg. Chem.*, 1984, **23**, 3521.
R. Benn, R.D. Reinhardt and A. Rufinska, *J. Organometal. Chem.*, 1985, **282**, 291.
J.P. Farr, F.E. Wood, and A.L. Balch, *Inorg. Chem.*, 1983, **22**, 3387.
J.A. Galbraith, K.A. Menzel, E.M.A. Ratilla and N.M. Kostic, *Inorg. Chem.*, 1987, **26**, 2073.
L.M. Green, A. Par and D.W. Meek, *Inorg. Chem.*, 1988, **27**, 1658.
E.G. Hope, W. Levason and N.A. Powell, *Inorg. Chim. Acta*, 1986, **115**, 187.
S.J.S. Kerrison and P.J. Sadler, *Inorg. Chim. Acta*, 1985, **104**, 197.
G.E. Kirvan and D.W. Margerum, *Inorg. Chem.*, 1985, **24**, 3017.
L.G. Marzelli, Y. Hayden and M.D. Reily, *Inorg. Chem.*, 1986, **25**, 974.
O.J. Scherer, R. Konrad, E. Guggolz and M.L. Ziegler, *Chem. Ber.*, 1985, **118**, 1.

The copper triad

Copper

J.A. Connor and R.J. Kennedy, *Polyhedron*, 1988, **7**, 161.
G. Doyle, B.T. Heaton and E. Occhiello, *Organometallics*, 1985, **4**, 1224.
K. Endo, K. Yamamoto and K. Deguchi, *Bull. Chem. Soc. Jpn.*, 1987, **60**, 2803.
S. Kitagawa and M. Munakata, *Inorg. Chem.*, 1984, **23**, 4388.
S. Kitagawa, M. Munakata and M. Sasaki, *Inorg. Chim. Acta*, 1986, **120**, 77.

Silver

L. Guinand, K.L. Hobt, E. Mittermaier, E. Roessler, A. Schwenk and H. Schneider, *Z. Naturforsch., Teil A*, 1984, **39**, 83.
H. Looser and D. Brinkmann, *J. Magn. Reson.*, 1985, **64**, 76.
G.C. VanStein, G. VanKoten, B. DeBok, L.C. Taylor, K. Vrieze and C. Brevard, *Inorg. Chim. Acta*, 1984, **89**, 29.
C.G. VanStein, G. VanKoten, K. Vrieze, C. Brevard and A.L. Spek, *J. Am. Chem. Soc.*, 1984, **106**, 4486.
G.C. VanStein, G. VanKoten, K. Vrieze and C. Brevard, *Inorg. Chem.*, 1984, **23**, 4269.
C. VanStein, G. VanKoten, F. Blank, L.C. Taylor, K. Vrieze, A.L. Spek, A.J.M. Duisenberg, A.M.M. Screurs, B. Kojic-Prodic and C. Brevard, *Inorg. Chim. Acta*, 1985, **98**, 107.

The zinc triad

Zinc

K.J. Cain, C.A. Melendres and V.A. Maroni, *J. Electrochem. Soc.*, 1987, **134**, 519.
D. Kohnlein, O. Lutz and P. Ruppert, *J. Magn. Reson.*, 1984, **57**, 486.
G.E. Maciel, L. Simeral and J.H. Ackerman, *J. Phys. Chem.*, 1977, **81**, 263.

Cadmium

M.J.B. Ackerman and J.J.H. Ackerman, *J. Am. Chem. Soc.*, 1985, **107**, 6413.
E.C. Alyea and K.J. Fisher, *Polyhedron*, 1986, **5**, 695.
D. Dakterniaeks, *Inorg. Chim. Acta*, 1984, **89**, 209.
P.A.W. Dean and J.J. Vittal, *Inorg. Chem.*, 1985, **24**, 3722.
P.A.W. Dean and J.J. Vittal, *Inorg. Chem.*, 1985, **25**, 514.
P.G. Mennitt, M.P. Shatlock, V.J. Bartuska and G.E. Maciel, *J. Phys. Chem.*, 1981, **85**, 2087.
H. Nakatsuuji, T. Nakao and K. Kanda, *Chem. Phys.*, 1987, **118**, 25.
A. Nolle, *Z. Naturforsch., Teil A*, 1978, **33**, 666.

Mercury

S.S. Al-Showiman, *Inorg. Chim. Acta*, 1988, **141**, 263.
T. Allman and R.G. Goel, *Can. J. Chem.*, 1984, **62**, 615.

R.D. Bach, H.B. Vardhan, A.F.M.M. Rahman and J.P. Oliver, *Organometallics*, 1984, **4**, 846.
A.M. Bond, R. Colton, M.L. Dillon, J.E. Moir and D.R. Page, *Inorg. Chem.*, 1984, **23**, 2883.
C. Cauletti, C. Furlani, M.N. Piancastelli, A. Sebald and B. Wrackmeyer, *Inorg. Chem.*, 1984, **23**, 1113.
R. Colton and D. Dakternieks, *Aust. J. Chem.*, 1980, **33**, 955.
P.A.W. Dean and R.S. Srivastava, *Can. J. Chem.*, 1985, **63**, 2829.
R.J. Gillespie, P. Granger, K.R. Morgan and G.J. Schrobilgen, *Inorg. Chem.*, 1984, **23**, 887.
P. Peringer and D. Obendorf, *Inorg. Chim. Acta*, 1983, **77**, L147.

This Page Intentionally Left Blank

The Cinderella Nuclei

B.E. MANN

Department of Chemistry, The University, Sheffield S3 7HF, UK

1. INTRODUCTION

At the time of writing *NMR and the Periodic Table* in 1977,[1] a number of $I = \frac{1}{2}$ nuclei, which pose considerable difficulties, were identified.[2] These nuclei were ^{57}Fe, ^{89}Y, ^{103}Rh, ^{107}Ag, ^{109}Ag, ^{183}W and ^{187}Os. The problems associated with these nuclei are apparent from Table 1.

The sensitivity of these nuclei is low. All the nuclei are less sensitive than ^{13}C, with ^{187}Os having only 1/877 the sensitivity of ^{13}C. They resonate at low frequency, and the purchase of additional probe(s) had to be justified. Many of the nuclei have negative gyromagnetic ratios, possibly leading to negative nuclear Overhauser enhancements when ^{1}H decoupling is used. Many of the nuclei have, or were believed to have, long relaxation times. All these problems

ANNUAL REPORTS ON NMR SPECTROSCOPY
VOLUME 23 ISBN 0-12-505 323-1

Copyright © 1991 Academic Press Limited
All rights of reproduction in any form reserved

Table 1. NMR parameters of the nuclei ^{57}Fe, ^{89}Y, ^{103}Rh, ^{107}Ag, ^{109}Ag, ^{169}Tm, ^{183}W and ^{187}Os.

Isotope	Natural abundance $N(\%)$	Magnetic moment $\mu(\mu_N)$	Magnetogyric ratio $\gamma(10^7\,\mathrm{rad\,T^{-1}\,s^{-1}})$	NMR frequency Ξ(MHz)	Relative receptivity D^P	D^C
^{57}Fe	2.19	0.1563	0.8644	3.231	7.39×10^{-7}	4.19×10^{-3}
^{89}Y	100	−0.2370	−1.3106	4.899	1.18×10^{-4}	0.668
^{103}Rh	100	−0.1522	−0.8420	3.16	3.12×10^{-5}	0.177
^{107}Ag	51.82	−0.1957	−1.0828	4.047649	3.44×10^{-5}	0.195
^{109}Ag	48.18	−0.2251	−1.2449	4.653623	4.86×10^{-5}	0.276
^{169}Tm	100	−0.400	−2.21	8.272	5.66×10^{-4}	3.21
^{183}W	14.40	0.2013	1.1131	4.161733	1.04×10^{-5}	5.89×10^{-2}
^{187}Os	1.64	0.1114	0.6161	2.282343	2.00×10^{-7}	1.14×10^{-3}

combine to make the observation of these nuclei difficult. As a consequence, up to 1977, very few direct observations had been made of these nuclei in solution, with one observation of ^{57}Fe,[3] two observations of ^{89}Y,[4,5] no observations of ^{103}Rh, six observations of ^{107,109}Ag,[6–11] three observations of ^{183}W,[3,11,12] and one observation of ^{187}Os.[11] Most of the observations involved using 'Quadriga' pulsed Fourier transform technique (Section 2.3,[3] but there were a few direct observations. When coupling to a more sensitive nucleus was observed, INDOR was used to observe the insensitive nucleus (see Section 2.1). This technique was used to observe ^{57}Fe,[13] ^{103}Rh, [14–20] and ^{183}W.[15,21,22]

Over recent years, NMR techniques have developed, and these nuclei can now be readily observed. A number of general reviews have appeared which include these nuclei, and several reviews on a limited selection of reviews have been published. The principal general reviews are *NMR and the Periodic Table*,[1] *NMR of Newly Accessible Nuclei*,[23] which contains descriptions of ^{103}Rh and ^{109}Ag, *Multinuclear NMR*,[24] *NMR of the First Transition Series Nuclei (Sc to Zn)*,[25] and *Transition Metal NMR Spectroscopy*.[26] In addition, there are some reviews covering part of the material in this chapter. They include *The Nuclear Magnetic Resonance Properties of Chromium, Molybdenum, and Tungsten Compounds*,[27] and *NMR Spectroscopy of the Early Transition Metals*.[28] There are also several reviews of the experimental techniques, namely *High-Resolution Metal-NMR Spectroscopy of Organometallic Compounds*,[29] and *Indirect Two-Dimensional Heteronuclear NMR Spectroscopy of Low-γ Metal Nuclei* ($M = ^{183}W$, ^{57}Fe, ^{103}Rh, ^{61}Ni).[30] Within this chapter, the techniques and then the results are examined.

2. EXPERIMENTAL TECHNIQUES

Many of the early observations of these insensitive nuclei were performed using INDOR. This technique required coupling to the insensitive nuclei, and spectra were produced either by observing the sensitive nucleus, and decoupling the insensitive nucleus, in a A-{X} experiment, e.g. ^{1}H-{^{183}W}, or by using a triple resonance relay, where sensitive nucleus is observed, a less sensitive nucleus is irradiated, and the insensitive nucleus in irradiated, e.g. ^{1}H-{^{31}P, ^{183}W}. This technique uses continuous-wave observation. It is as sensitive as the observed nucleus, but is difficult to use with signal averaging. INDOR became disused as continuous-wave NMR spectrometers were displaced by Fourier-transform NMR spectrometers, which are not amenable to this technique, but are preferable for most other NMR experiments. Direct observation of these insensitive nuclei is difficult. The observation of these nuclei by Fourier-transform NMR spectroscopy has become much easier over the past few years with the development of inverse detection methods, analogous to INDOR.

2.1. INDOR

The original method for observing insensitive nuclei was INDOR. This technique involves the use of a continuous-wave NMR spectrometer, which has virtually become an extinct species. This is unfortunate as INDOR is probably the easiest way to detect an NMR signal arising from an insensitive nuclei. A ^{1}H NMR signal, which is split by the insensitive nuclei, is chosen, and the ^{1}H frequency adjusted so that an outer line of the multiplet is on resonance. A decoupling frequency is applied to the sample and the frequency swept through the insensitive nuclei frequency range. When the insensitive nucleus frequency is irradiated the insensitive nucleus is decoupled and the ^{1}H signal collapses to a singlet. When this happens, the intensity of the ^{1}H NMR signal decreases as the intensity is transferred from one arm of the doublet to a central singlet. This provides an easy and sensitive way to detect signals from insensitive nuclei.

2.2. Direct observation

The direct observation used to be believed to be extremely difficult. This is despite the observation of ^{107}Ag and ^{109}Ag from a concentrated solution of $Ag(NO_3)$ as early as 1954![6,7] The problem of observing these nuclei appears to

have arisen from the presumed long T_1 values which are caused by the small γ characteristic of these nuclei. Attempts to reduce T_1 by the addition of paramagnetic ions have not been very successful. At the motional narrowing limit, the paramagnetic contribution to the relaxation is given by

$$T_1^{-1} = \frac{\mu_0^2 \gamma_I^2 \gamma_S^2 \hbar S(S+1)\tau_c}{12\pi^2 r^6} + \frac{\mu_0^2 \gamma_S^2 a_N^2 S(S+1)\tau_e}{24\pi^2} \quad (1)$$

where μ_0 is the permeability of a vacuum, γ_I is the gyromagnetic ratio of the observed nucleus, γ_S is the gyromagnetic ratio of the electron, τ_c and τ_e are the correlation times of the nucleus and the electron, r is the distance between the electron and the nucleus, and a_N is the hyperfine electron–nucleus interaction. The first term represents the dipolar contribution, and is normally the only significant term when relaxation reagents are used. The second term is the contact term, which arises from the delocalization of the unpaired electron(s) onto the atom, whose nucleus is being observed. If the application of relaxation reagents to ^{13}C and ^{183}W are compared, the efficiency for ^{183}W is far lower. $\gamma(^{183}W)^2$ is only 0.0274 that of $\gamma(^{13}C)^2$. In addition, due to the larger size of tungsten, compared with carbon, the relaxation reagent cannot approach the tungsten nucleus as closely as it can the carbon nucleus. These two factors reduce the efficiency of relaxation reagents by approximately two orders of magnitude for the insensitive nuclei discussed in this review. There have been a couple of reports of using tanol, 2,2,6,6-Me_4-4-HO-piperidine-1-oxyl, as a relaxation agent for ^{109}Ag.[31,32] The tanol appears to coordinate to silver, producing relaxation, but also a significant coordination shift. In the presence of 0.05 M tanol, 1.0 M $AgNO_3$ has a chemical shift of δ 24.5 rather than 0, but the T_1 is only 0.083 s, making observation far easier.

The direct observation of ^{13}C NMR signals benefits from nuclear Overhauser enhancements (NOE). Where measurements have been made on these insensitive nuclei, no significant NOE has been observed (see Section 2.6).

Subsequent investigations have shown chemical-shift anisotropy to be the dominant relaxation mechanism in asymmetric compounds, and spin rotation to be the dominant mechanism in the symmetric complexes. Many early investigations involved symmetric compounds, where the inefficient spin rotation mechanism was the only available relaxation route. As a consequence, considerable difficulties were encountered in the direct observation of these nuclei. Provided compounds with large chemical shift anisotropy are chosen, and high magnetic fields are used to observe the nuclei, then direct observation is easy. This is illustrated in Fig. 1 for the ^{103}Rh NMR spectrum of a 0.25 M solution of [Rh(acac)$(CO)_2$] which was obtained in less than 1 min.

In a more symmetric environment, ^{103}Rh NMR spectra can be considerably more difficult to record. Figure 2 shows the 12.65 MHz ^{103}Rh NMR spectrum

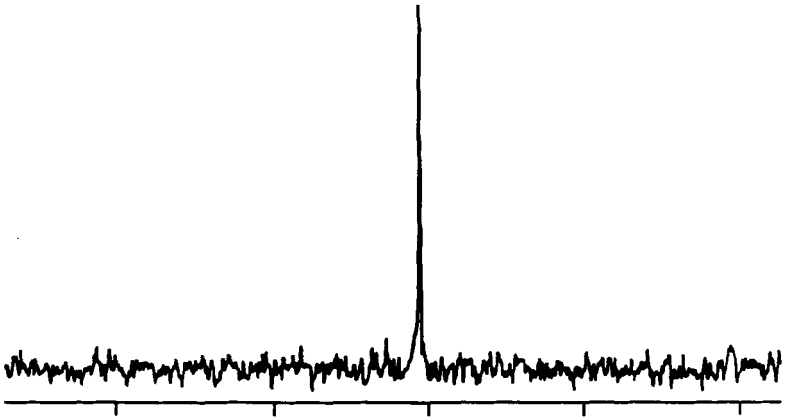

Fig. 1. 12.65 MHz ^{103}Rh NMR spectrum of an 0.25 M solution of [Rh(acac)$(CO)_2$] in $CDCl_3$ in a 10 mm tube at 25°C. (Reproduced with permission from Cocivera *et al.*[64])

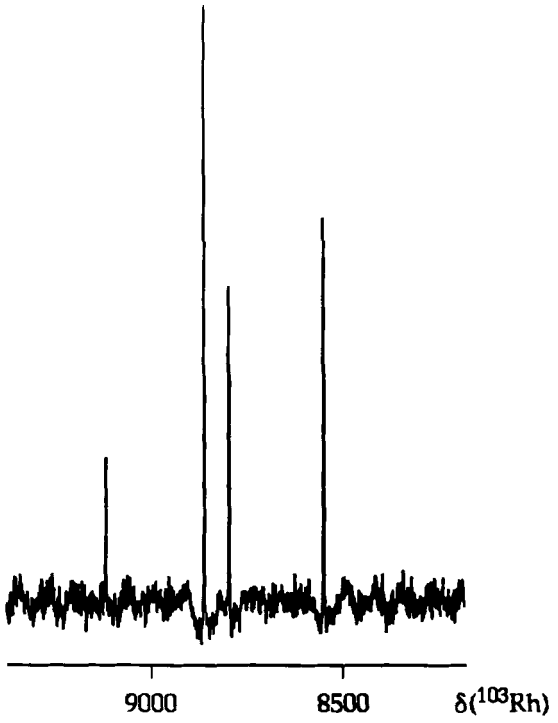

Fig. 2. 12.65 MHz ^{103}Rh NMR spectrum of an 0.80 M solution of commercial $RhCl_3 \cdot 3H_2O$ after 14 h in a 10-mm tube. The recording conditions were *ca.* 10^5 pulses, with a repetition time of 0.3 s. (Reproduced with permission from Mann.[214])

of an 0.75 M solution of commercial $RhCl_3 \cdot 3H_2O$. For such symmetric compounds, the overnight detection limit is *ca.* 0.1 M. Very symmetric compounds such as $[Rh(OH_2)_6]^{3+}$ are even more difficult to detect.

In order to carry out direct observation of these insensitive nuclei, there are a number of problems about which the spectroscopist must be aware.

(i) For many measurements it is important to know approximately the $\pi/2$ pulse. It is possible to determine this using a relatively easy sample such as $[Rh(CO)_2(acac)]$. Alternatively, as most NMR spectra of these insensitive nuclei are recorded using a broad band probe, the $\pi/2$ pulse length can be determined for an easier nucleus with a similar frequency. Often, the $\pi/2$ pulse is relatively insensitive to frequency, and it can be determined on a sensitive nuclei. There are two convenient nuclei, ^{73}Ge as $GeCl_4$, which has $\Xi = 3.488$, and ^{39}K as saturated KCl in D_2O, which has $\Xi = 4.666$. In both cases, the inherent sensitivity is relatively low, but the short T_1 values of these quadrupolar nuclei make observation easy.

(ii) It appears that for most compounds of these insensitive nuclei, T_1 values are dominated by chemical-shift-anisotropy relaxation. The relaxation time is given by

$$\frac{1}{T_{1sa}} = \frac{\mu_0 \gamma_I^2 B_0^2 \Delta\sigma^2 \tau_c}{30\pi} \tag{2}$$

where μ_0 is the permeability of a vacuum, γ_I is the gyromagnetic ratio of the nucleus, B_0 is the magnetic flux density, $\Delta\sigma$ is the chemical-shift anisotropy, and τ_c is the correlation time for molecular tumbling. This equation only applies in the rapid tumbling limit, i.e. when $\omega^2 \tau_c^2 \ll 1$, where ω is the NMR frequency in radians per second. As T_1 is proportional to B_0^{-2}, high magnetic fields reduce T_1 and make the observation of the NMR signal easier. It is therefore of no surprise that most of the direct observations of the NMR spectra of these insensitive nuclei have been reported using spectrometers with magnetic fields in excess of 8.4 T.

(iii) If the sample has an unknown chemical shift, it is necessary to cover the complete chemical-shift range, which is 12 000 ppm for ^{103}Rh; at 9.4 T, this corresponds to 150 kHz. In order to excite uniformly over this whole range, the observing pulse must be less than 3.3 μs. It is therefore advantageous to be able to estimate where a signal will come. If a narrower range is used, then it is possible that the signal could be folded. It is therefore often necessary to run two spectra; one on a wide sweep width to locate the signal, and a second on a narrower sweep width to make sure that the first observed signal was not folded.

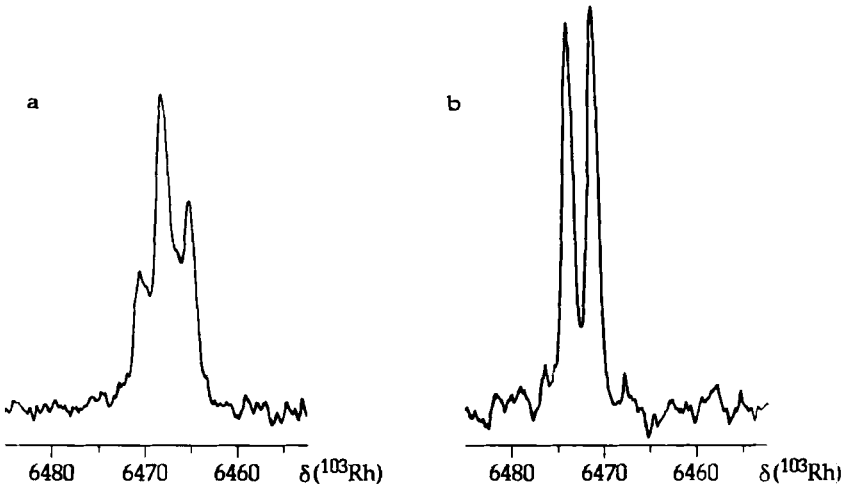

Fig. 3. A partial ^{103}Rh NMR spectrum of $[Rh_2(O_2CCF_3)_2$ (*p*-tol-*N*-CHN-*p*-tol)$_2$(PMe_2Ph)]. (a) Recorded without instrumental temperature control. (b) Recorded with instrumental temperature control. (Reproduced with permission from Mann.[26])

(iv) As metal chemical shifts are extremely temperature dependent, accurate temperature control is essential. It is not normally satisfactory to rely on the room's air conditioning, and it is usually preferable to use the spectrometer's variable-temperature controller. Room-temperature changes can produce signal broadening or multiplicity (see Fig. 3). Spectrum (b) in Fig. 3 is the true spectrum and was recorded with temperature control. Spectrum (a) was recorded using only the room-temperature control. Part of the signal was recorded while the building's central heating was on and the rest during the night while the central heating was off. The room's air-conditioning could not cope with the temperature change and produced somewhat different daytime and night-time temperatures.

(v) There have been no significant observations of a NOE between ^1H and these insensitive nuclei. Small NOEs, *ca.* 0.15, have been reported for ^{183}W,[33] but these values are negligible when compared with the theoretical maximum ^{183}W NOE of 12. The relaxation is dominated by chemical-shift anisotropy and not by dipole–dipole interaction. Any small residual enhancement can be unhelpful as the γ values of ^{89}Y, ^{103}Rh, ^{107}Ag and ^{109}Ag are negative leading to negative "enhancement".

2.3. Quadriga NMR spectroscopy

Quadriga[3,34–36] is a pulse technique which is used to detect very weak NMR signals with relaxation times T_1 and T_2 which are long compared with the decay time T_2^* of the free induction decay signals. This technique is therefore used where the linewidth of the signal is dominated by processes other than T_2 relaxation, e.g. magnetic field inhomogeneity. Four measurements with different observation frequencies, ν_ρ, are used, where

$$\nu_\rho = \nu_E - \frac{\rho}{4T}, \quad \rho = 0, 1, 2, \text{ or } 3 \tag{3}$$

T is the time between the observation pulses, and ν_E is the basic observation frequency. The experiment is

$$\{\theta(\nu_0) - \text{acquire}(0) - \theta(\nu_1) - \text{acquire}(1) - \theta(\nu_2) - \text{acquire}(2) - \theta(\nu_3) - \text{acquire}(3)\}_n \tag{4}$$

where $\theta(\nu_\rho)$ means a pulse of angle θ at frequency ν_ρ as defined above. Acquire(ρ) means acquiring the data in memory location ρ, i.e. four separate computer memory locations are used. This technique gives rise to distorted signals (see Fig. 4).

2.4. INEPT and DEPT

Both INEPT[37] and DEPT[38] use polarization transfer to enhance the sensitivity of the insensitive nucleus. When the polarization transfer is between ^{1}H and X, the signal is enhanced by γ_H/γ_X (see Table 2). As a consequence, it is, in principle, very easy to observe NMR spectra from the insensitive nuclei when there is significant coupling between them. The technique can be used for other nuclei, e.g. including polarization transfer between ^{31}P and ^{183}W.[39]

The simplest version of the INEPT pulse sequence is

$$\begin{array}{ll} ^1\text{H} & D_1 - \dfrac{\pi_x}{2} - \tau - \pi_x - \tau - \dfrac{\pi_y}{2} \\ \text{X} & \pi_x - \tau - \dfrac{\pi_x}{2} \text{ acquire} \end{array} \tag{5}$$

where D_1 is a relaxation delay which is typically $2T_1$ for the proton(s) which is(are) coupled to the X nucleus. For most purposes, it is this sequence that is preferred since it takes the shortest possible time. The delay, τ is $1/[4J(^{103}\text{Rh}, ^1\text{H})]$. When $J(^{103}\text{Rh}-^1\text{H})$ is substantial, e.g. in a hydride, it is very easy to use this pulse sequence to obtain ^{103}Rh NMR spectra on very

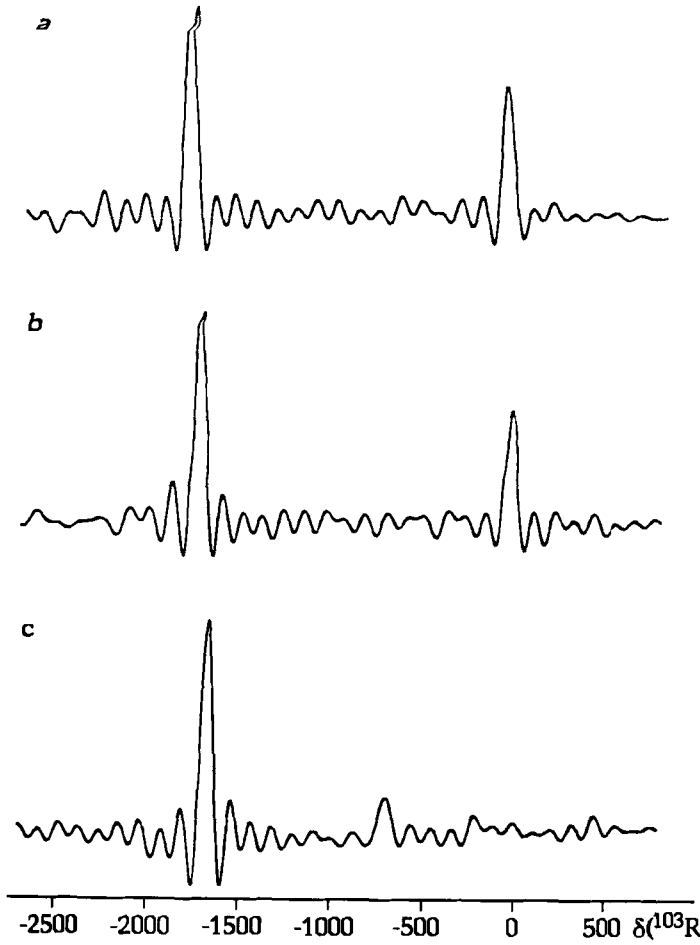

Fig. 4. ^{103}Rh NMR spectra of three rhodium complexes, recorded with the Quadriga Fourier-transform technique. (a) $[(\eta^5\text{-}C_5H_5)Rh(\eta^4\text{-}C_8H_8\text{-}\eta^4)Rh(\eta^5\text{-}C_7H_8)]^+$; (b) $[(\eta^5\text{-}C_5H_5)Rh(\eta^4\text{-}C_8H_8\text{-}\eta^4)Rh(\eta^4\text{-}C_8H_{12})]^+$; (c) $[(\eta^5\text{-}C_5H_5)Rh(\eta^4\text{-}C_8H_8\text{-}\eta^4)Rh(CO)_2]^+$. To minimize double-resonance effects, a pulse repetition rate, $1/T = 166$ Hz was chosen. Measuring times were in the range 4 × 1 h to 4 × 4 h, depending on the concentration of the sample. Note that shielding increases from right to left. (Reproduced with permission from Maurer *et al.*[211])

little compound, but when $J(^{103}Rh-^1H)$ is small, relaxation during the pulse sequence causes the signal to be weak. This problem becomes worse if the more sophisticated INEPT or DEPT pulse sequences are used. This pulse sequence produces multiplets which do not follow the usual intensity patterns. Thus a doublet is a $-1:1$ doublet, a triplet is a $-1:0:1$ triplet, and a quartet is a

Table 2. Values of optimum delay, Δ_{opt}, for different numbers of protons coupling equally to the less sensitive nuclei to give the maximum decoupled enhancement, E_{dopt} as a function of the number of scalar coupled protons, n. τ is set equal to $1/4J(X-^1H)$.

	n					
	1	2	3	6	9	12
	Δ_{opt}					
E_{dopt}	$\frac{1}{2J}$	$\frac{1}{4J}$	$\frac{1}{5J}$	$\frac{1}{8.4J}$	$\frac{1}{9J}$	$\frac{0.093}{J}$
^{57}Fe	30.9	30.9	32.7	47.3	57.8	66.5
^{89}Y	20.4	20.4	21.6	31.2	38.2	43.9
^{103}Rh	31.8	31.8	33.7	48.7	59.5	68.4
^{107}Ag	24.7	24.7	26.2	37.8	46.2	53.1
^{109}Ag	21.5	21.5	22.8	32.9	40.2	46.2
^{183}W	24.0	24.0	25.4	36.8	44.9	51.6
^{187}Os	43.4	43.4	46.0	66.5	81.2	93.4

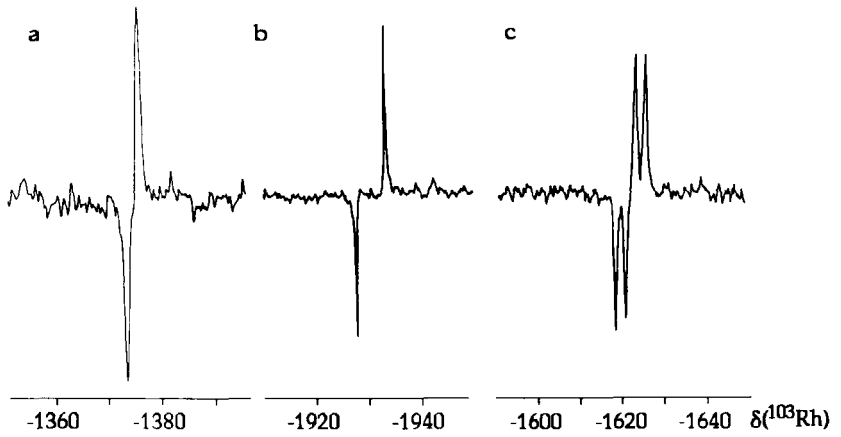

Fig. 5. The 12.62 MHz ^{103}Rh NMR spectra obtained using the INEPT pulse sequence with $D_2 = 0.0074$ s, corresponding to $^1J(^{103}Rh-^1H) = 34$ Hz. The spectra are referenced to $\Xi = 3.16$ MHz. (a) $[(\eta^5\text{-}C_5Me_5)RhH(SiEt_3)(\eta^2\text{-}C_2H_4)]$ in $CD_3C_6D_5$, showing a $-1{:}1$ doublet. (b) $[(\eta^5\text{-}C_5Me_5)(RhH_2(SiEt_3)_2]$ in C_6D_6, showing a $-1{:}0{:}1$ triplet. (c) $[(\eta^5\text{-}C_5Me_5)RhH_3(SiEt_3)]$ in $CD_3C_6D_5$, showing a $-1{:}-1{:}1{:}1$ quartet. (Reproduced with permission from Mann.[215])

$-1:-1:1:1$ quartet. This is illustrated in Fig. 5. It is quite easy to differentiate between the $-1:1$ doublet and the $-1:0:1$ triplet, as the separation of the lines in the doublet is $J(^{103}\text{Rh}-^{1}\text{H})$, but in triplet it is $2J(^{103}\text{Rh}-^{1}\text{H})$, with $J(^{103}\text{Rh}-^{1}\text{H})$ already being known from the ^{1}H NMR spectrum.

In order to measure an INEPT spectrum, it is necessary to know the $\pi/2$ pulse for both ^{1}H and X. The problem of determining the $\pi/2$ pulse for X has already been discussed (see Section 2.2). If a broad-band probe is used, the $\pi/2$ pulse for ^{1}H can be determined when the probe is tuned to another nucleus such as ^{13}C. The major problem is the length of the $\pi/2$ pulse for X. On the broad-band probe in Sheffield, this pulse is 90 μs for ^{103}Rh! As the INEPT pulse sequence uses π ^{103}Rh pulses, this means an effective spectral width of ± 1389 Hz, or ± 110 ppm at 9.4 T. This is very small compared with the complete ^{103}Rh chemical-shift range and, as a consequence, INEPT is only successful if the X nucleus chemical shift is reasonably accurately known. It is often necessary to record a series of spectra where the carrier frequency is changed by 3000 Hz between spectra to locate the signal. The importance of this frequency search is illustrated in Fig. 6, where the ^{183}W NMR spectrum is recorded using INEPT, on-resonance, 1000 Hz off-resonance and 10 000 Hz off-resonance. Clearly, when the ^{183}W frequency is 10 000 Hz off-resonance, no signal is detected. These results should be compared with those obtained on the same compound using reverse two-dimensional $^{1}\text{H}\{^{183}\text{W}\}$ spectroscopy in Section 2.5, where

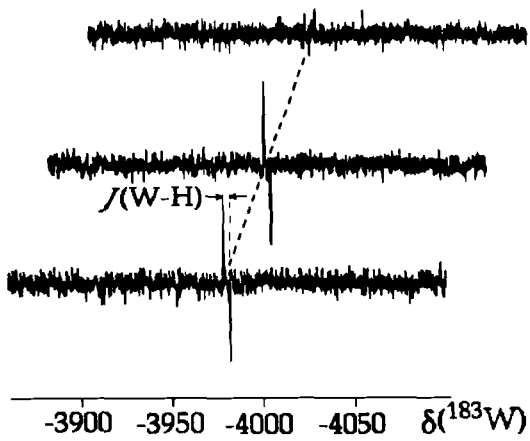

Fig. 6. The 16.61 MHz $^{183}\text{W}\{^{1}\text{H}\}$ INEPT spectrum of $[Me_2Si\{(\eta^5\text{-}C_5H_4)W(CO)_3H\}_2]$ showing the dependence of the signal on the ^{183}W pulse frequency. (a) On-resonance ^{183}W pulse. (b) 1000 Hz off-resonance ^{183}W pulse. (c) 10 000 Hz off-resonance ^{183}W pulse. Note that the 90° ^{183}W pulse was 22 μs, and the recording time for each experiment was 6 h. (Reproduced with permission from Benn *et al.*[145])

having the ^{183}W pulse 10000 Hz off-resonance has little effect on signal intensity.

If a decoupled X NMR spectrum is required, then the extended INEPT pulse sequence is used:

$$\begin{aligned} &^1H \quad D_1\text{–}\frac{\pi_x}{2}\text{–}\tau\text{–}\pi_x\text{–}\tau\text{–}\frac{\pi_y}{2}\text{–}\Delta\text{–}\pi\text{–}\Delta\text{–decouple} \\ &X \quad \pi_x\text{–}\tau\text{–}\frac{\pi_x}{2}\text{–}\Delta\text{–}\pi\text{–}\Delta\text{–acquire} \end{aligned} \tag{6}$$

where Δ is chosen depending on the multiplicity of the X NMR signal (see Table 2). As with the simple INEPT sequence, τ is $1/4J(X\text{–}^1H)$.

The DEPT pulse sequence is not normally used where there is a single NMR signal. It was developed for ^{13}C NMR spectroscopy, where there is considerable variation in $^1J(^{13}C\text{–}^1H)$, leading to discrepancies between the signals. Usually, there is only one X nucleus environment, and $J(X\text{–}^1H)$ is known from the ^1H NMR spectrum. The major problem with the DEPT pulse sequence:

$$\begin{aligned} &^1H \quad D_1\text{–}\frac{\pi_x}{2}\text{–}\tau\text{–}\pi_x\text{–}\tau\text{–}\theta_y\text{–}\tau\text{–(decouple)} \\ &X \quad \frac{\pi_x}{2}\text{–}\tau\text{–}\frac{\pi_x}{2}\text{–}\tau\text{–acquire} \end{aligned} \tag{7}$$

is that it takes a time 3τ, where $\tau = 1/2J(X\text{–}^1H)$, giving a total time of $3/2J(X\text{–}^1H)$ which can be compared with the total time of $1/2J(X\text{–}^1H)$ required for the basic INEPT pulse sequence. $J(X\text{–}^1H)$ can be small, especially when it is over two or three bonds, leading to very long preparation times before acquiring the signal. During this time, relaxation reduces the signal strength. As a consequence, polarization transfer is most successful when $J(X\text{–}^1H)$ is large, as in a metal hydride. This problem of the loss of intensity during a DEPT experiment is illustrated in Fig. 7. Figure 7a shows the INEPT ^{109}Ag NMR spectrum of $[AgRu_4(\mu_3\text{-}H)_3(CO)_{12}(PPh_3)]$ with proton coupling. The signals are all positive as the data were converted into a magnitude spectrum. Figure 7(b) shows the refocused and decoupled INEPT ^{109}Ag NMR spectrum. The corresponding DEPT spectra are given in Fig. 7(d) and 7(c) and clearly show the poorer signal-to-noise ratio resulting from the longer time required for the pulse sequence.

INEPT and DEPT are not restricted to polarization transfer between ^1H and X. Any nucleus which couples to X can be used. This experiment has been performed for polarization transfer between ^{31}P and ^{109}Ag (see Fig. 8).[40] This is a very powerful experiment, which is rarely used as it requires the purchase of a $X\text{–}\{^1H, ^{31}P\}$ probe, a second frequency synthesizer and an amplifier with phase shifting.

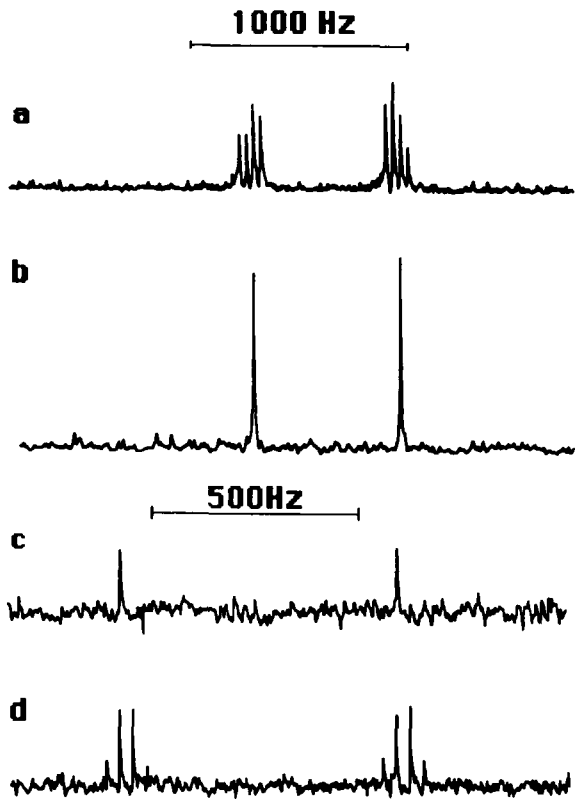

Fig. 7. The ^{109}Ag NMR spectra at 4.17 MHz of $[AgRu_4(\mu_3\text{-}H)_3(CO)_{12}(PPh_3)]$ in $CDCl_3$ at $-30°C$. (a) INEPT spectrum with no refocusing in the absolute-intensity mode. (b) As (a) with refocusing and ^{1}H decoupling. (c) DEPT spectrum without ^{1}H decoupling. (d) DEPT spectrum without ^{1}H decoupling. (Reproduced with permission from Brown *et al.*[99])

2.5. Two-dimensional inverse INEPT

This is the most sensitive technique for observing NMR spectra of insensitive nuclei, giving an enhancement of $(\gamma_H/\gamma_X)^{5/2}$. The result of this enhancement is given in Table 3.

The NMR frequency is first determined approximately, using the pulse sequence

$$\begin{array}{ll} {}^1H & D_1\text{–}\dfrac{\pi}{2}\text{–}\tau\text{–}\pi\text{–}\tau\text{–acquire} \\ X & \pi \end{array} \qquad (8)$$

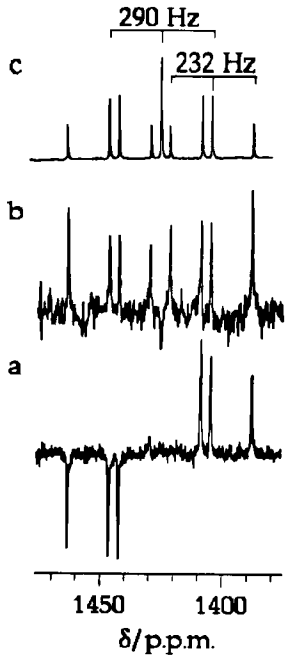

Fig. 8. The 13.97 MHz $^{109}Ag\{^{31}P\}$ spectra of 65 mM $[Ag(Et_2PCH_2CH_2PPh_2)_2][NO_3]$ in $CDCl_3$ at 223 K. (a) INEPT spectrum (3107 transients, with $\tau = 0.90$ ms). (b) DEPT spectrum (4000 transients, with $\tau = 1.75$ ms, 90° pulse = 22 μs). (c) Spectrum of the X region simulated as an AA'BB'X spectrum). (Reproduced with permission from Berners Price *et al.*[39])

Table 3. The theoretical enhancement produced by inverse shift correlation between ^1H and the insensitive nucleus.

Nucleus	^{57}Fe	^{103}Rh	^{107}Ag	^{109}Ag	^{183}W
Enhancement	5328	5689	3033	2140	2831

In the case of reverse INEPT, D_1 is estimated as $2T_1$ for the insensitive nucleus, and τ is $1/2J(X-^1H)$. This X nucleus frequency is stepped through the expected range to produce an inversion of the doublet in the ^1H NMR spectrum. This gives the approximate frequency to be used for the two-dimensional experiment. The pulse sequence

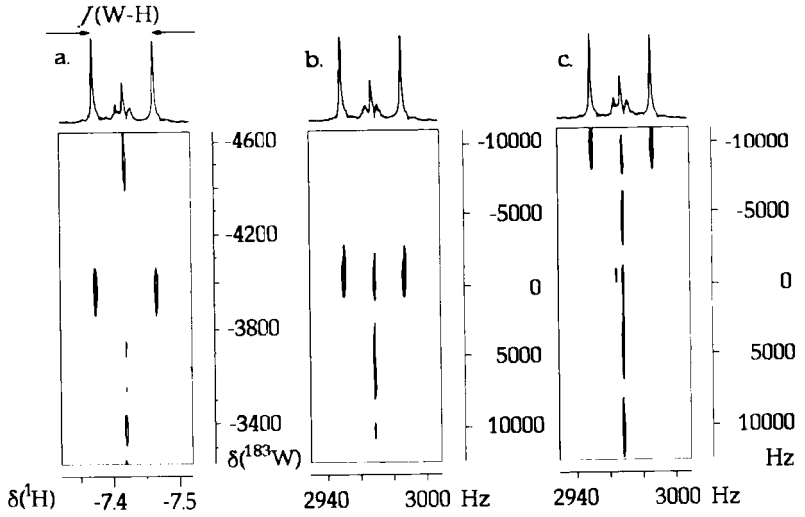

Fig. 9. Contour diagrams and projection of the indirect two-dimensional 400.13 MHz $^{1}H\{^{183}W\}$ NMR spectrum of $[Me_2Si\{(\eta^5\text{-}C_5H_4)W(CO)_3H\}_2]$. (a) On-resonance ^{183}W pulse. (b) 1000 Hz off-resonance ^{183}W pulse. (c) 10 000 Hz off-resonance ^{183}W pulse. (Reproduced with permission from Benn *et al.*[145])

$$\begin{array}{lll} ^{1}H & D_1 - \dfrac{\pi}{2} - \tau - & -t-\pi-t-\text{acquire} \\ X & \dfrac{\pi}{2} & \dfrac{\pi}{2} \end{array} \qquad (9)$$

is then used, where τ is $1/2J(X-^{1}H)$ and t is the delay for the second dimension. The spectrum obtained for $[Me_2Si\{(\eta^5\text{-}C_5H_4)W(CO)_3H\}_2]$ is shown in Fig. 9. The ^{183}W spectra were obtained in only 13 min, and a frequency off-set of 10 000 Hz had little or no effect on the sensitivity.

This experiment can provide extra information from a sample. Figure 10 shows the indirect two-dimensional $^{1}H\{^{109}Ag\}$ NMR spectrum of $[(Ph_3P)Ag(\mu\text{-}H)IrH_2(PPh_3)_3]$ (**1**).[41] The ^{1}H NMR spectrum of the hydride signals (Fig. 10(a)) are multiplets due to $J(^{1}H-^{1}H)$, $J(^{31}P-^{1}H)$, $J(^{107}Ag-^{1}H)$, and $J(^{109}Ag-^{1}H)$. The ^{109}Ag NMR spectrum (Fig. 10(c)) is a doublet of doublets due to $^{1}J(^{109}Ag-^{31}P)$ and $2J(^{109}Ag-^{31}P)$. The contour plot immediately identifies the $J(^{109}Ag-^{1}H)$ coupling constant. Examination of the contour plot shows that correlations between the ^{109}Ag and H^1 and H^3 lean in the opposite direction to those due to the correlation between ^{109}Ag and H^2. The lean of the correlation shows that $^{2}J(^{109}Ag-^{1}H^2)$ is of opposite sign to $^{1}J(^{109}Ag-^{1}H^1)$ and $^{2}J(^{109}Ag-^{1}H^3)$. The projection of the ^{1}H NMR spectrum gives the hydride signal of the ^{109}Ag isotopomer, and is free from ^{107}Ag coupling.

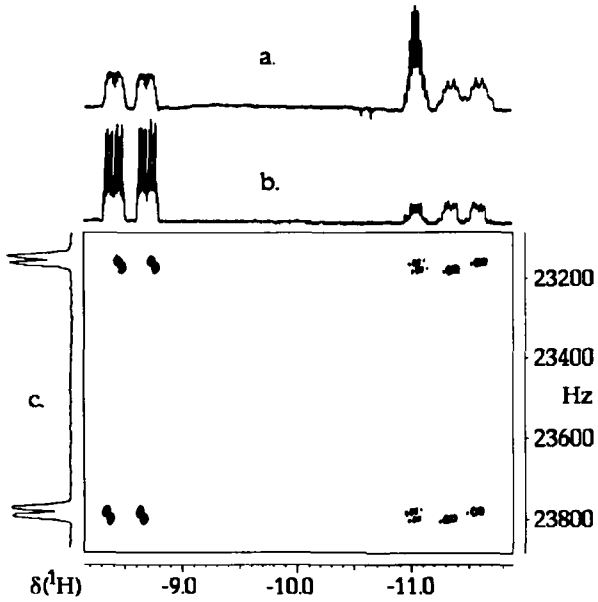

Fig. 10. The $^{1}H\{^{109}Ag\}$ NMR spectrum of $[(Ph_3P)Ag(\mu\text{-}H)IrH_2(PPh_3)_3]$ (**1**). (a) Normal ^{1}H NMR spectrum. (b) ^{1}H NMR spectrum without couplings due to ^{107}Ag nuclei. (c) Two-dimensional inverse ^{1}H decoupled $^{1}H\{^{109}Ag\}$ NMR spectrum. (Reproduced with permission from Albinati *et al.*[41])

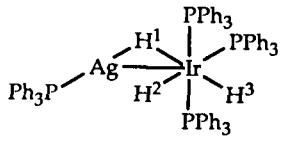

1

This is a very powerful technique and is likely to become the method of choice for observing NMR spectra from the less-sensitive nuclei. The gains in signal-to-noise ratio are not as substantial as for experiments involving ^{1}H, but they are significant (see Table 4). Figure 11(b) and 11(c) shows the application of reverse two-dimensional $^{31}P\{^{183}W\}$ NMR spectroscopy to $[Me_2Si(\eta^5\text{-}C_5H_4)_2W_2(CO)_4(\mu\text{-}H)(\mu\text{-}PMe_2)]$. The enhancement is shown in Table 4. Examination of the lean of the contours in Fig. 11(a) shows that $J(^{183}W\text{–}^{1}H)$ and $J(^{183}W\text{–}^{31}P)$ are of opposite sign, while Fig. 11(b) shows that $J(^{183}W\text{–}^{1}H)$ and $J(^{31}P\text{–}^{1}H)$ are of opposite sign.

Table 4. The theoretical enhancement produced by inverse shift correlation between ^{31}P and the insensitive nucleus.

Nucleus	^{57}Fe	^{103}Rh	^{107}Ag	^{109}Ag	^{183}W
Enhancement	556	593	316	223	295

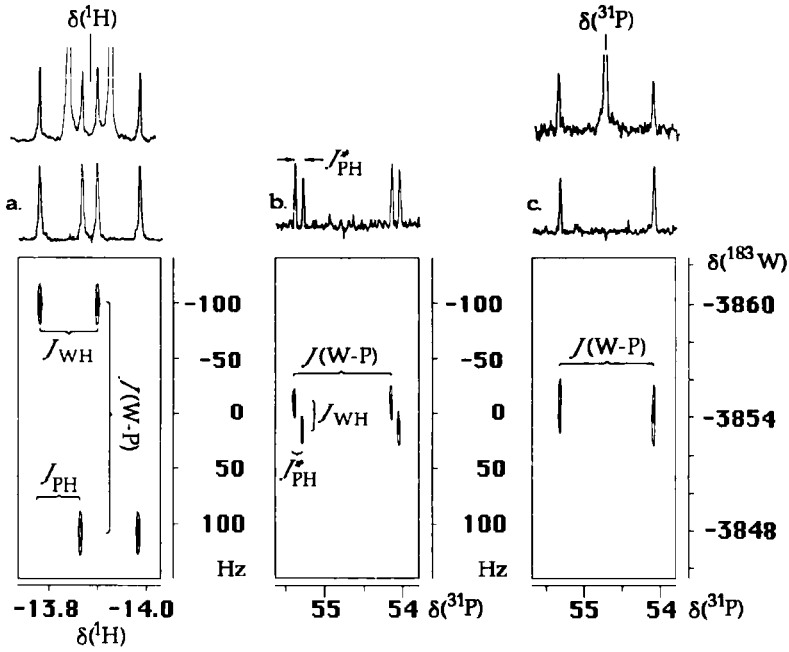

Fig. 11. Reverse two-dimensional $^{1}H\{^{183}W\}$ and $^{31}P\{^{183}W\}$ NMR spectra of $[Me_2Si(\eta^5\text{-}C_5H_4)_2W_2(CO)_4(\mu\text{-}H)(\mu\text{-}PMe_2)]$ at 9.4 T. (a) The $^{1}H\{^{183}W\}$ NMR spectrum (recording time 1 h). (b) The $^{31}P\{^{183}W\}$ NMR spectrum with continuous-wave decoupling of the PMe_2 protons; note that J^*_{PH} denotes the scaled $J(^{31}P-^{1}H)$ coupling, resulting from the continuous-wave decoupling of the PMe_2 group (recording time 21 h). (c) As (b) but with complete ^{1}H decoupling (recording time 5 h). (Reproduced with permission from Benn *et al.*[145])

2.6. COSY

The majority of metal complexes give rise to only one signal and assignment presents no problem. However, when NMR spectroscopy is applied to polymetallic compounds, then assignment can be a problem. Provided the sensitivity is adequate, COSY can be used to determine the connectivity

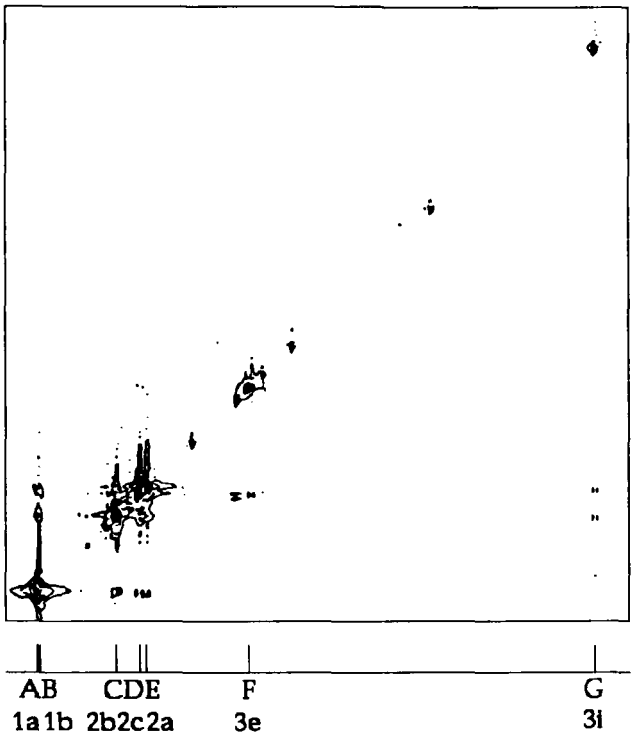

Fig. 12. A COSY NMR spectrum of $Na_4H_2[P_2W_{21}O_{71}(OH_2)_3]$ in D_2O–H_2O (*ca.* 4:1) at 303 K (Reproduced with permission from Tourné *et al.*[107])

through J(M–M). This technique has been applied to $[P_2W_{21}O_{71}(OH_2)_3]^{2-}$ (see Fig. 12). Examination of Fig. 12 shows cross-peaks between the signals C and G, E and G, and F and D. Such information can assist in assignment, because such coupling in this type of compound arises from W–O–W linkages.

2.7. INADEQUATE

COSY suffers from the disadvantage that the signals without homonuclear coupling occur on the diagonal. For isotopically dilute nuclei such as ^{183}W, this signal on the diagonal is strong, because the probability of having two ^{183}W nuclei occurring close together in one molecule is low. As a result, the strong diagonal signal can mask cross-peaks close to the diagonal. The problem is removed by using INADEQUATE, which rejects signals without homonuclear coupling. This technique has been applied to a number of

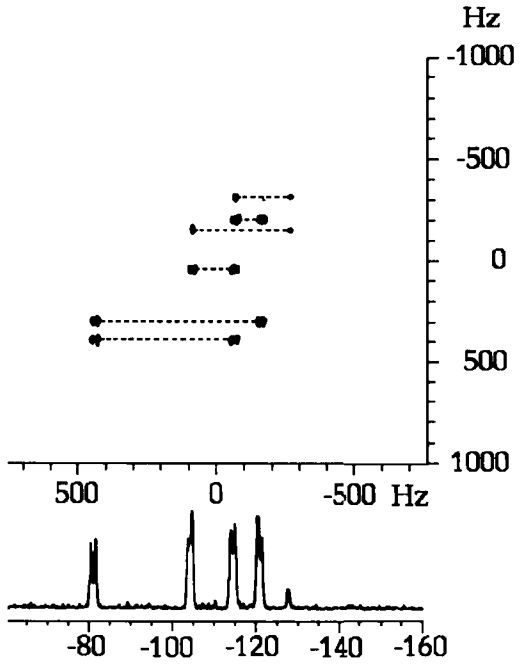

Fig. 13. The two-dimensional INADEQUATE ^{183}W NMR spectrum of ^{51}V decoupled $Li_5[SiVW_{11}O_{40}]$, 0.6 M, 30°C, 1536 transients, 128 × 2k files, 115 h, 20 mm sideways tube. (Reproduced with permission from Domaille.[119])

polytungstates. The two-dimensional INADEQUATE spectrum of $[SiVW_{11}O_{40}]^{5-}$ is shown in Fig. 13. There are five ^{183}W signals in the intensity ratio 2:2:2:2:1. The INADEQUATE spectrum shows which ^{183}W nuclei are coupled to each other, and hence which are adjacent in the molecule.

The major difficulty with this experiment is that it is inherently insensitive. The spectrum shown in Fig. 13 was recovered in just under 5 days using approximately 10 g of compound, a wide bore 8.45 T magnet and a 20 mm sideways spinning solenoidal probe. Clearly, it is a technique which has some limitations.

3. CHEMICAL-SHIFT REFERENCES

Before a chemical shift can be determined, a satisfactory referencing method has to be found. Three approaches have been adopted for metal nuclei:

(i) referencing to a readily available compound;

(ii) referencing to the metal; and
(iii) referencing to a frequency based on the ^1H frequency of Me_4Si being at $\Xi = 100.000\,000$ MHz.

Referencing to a readily available compound is unsatisfactory as metal chemical shifts are temperature, concentration, and medium dependent. It is therefore necessary to work with a reference in a standard state. Frequently measurements are made at different temperatures, and it is therefore necessary to calibrate the reference with respect to a reference with a known chemical-shift dependence, usually ^{129}Xe gas. This has been done for the ^1H and ^{13}C frequency of Me_4Si.[42] The chosen compound normally has to be used as an external reference. This results in the need to apply susceptibility corrections.

Referencing to the metal has the advantage that all the chemical shifts of compounds should be positive, but suffers from the major disadvantage that the reference signal is not accurately measured and will be subject to future revision. As a consequence, all the measured chemical shifts will change in the future; this is clearly unsatisfactory.

Referencing to the ^1H chemical shift of Me_4Si has many advantages. Firstly, the concentration and temperature dependence of this reference is low, typically less than 0.1 ppm over a normal working conditions. This chemical-shift variation is negligible compared with the temperature and solvent dependence of the metal chemical shift. Consequent upon errors in temperature and concentration measurements, chemical shifts are normally only good to 1 ppm at best. Internal Me_4Si can be observed on the same probe as the metal nucleus using the decoupling coil. The major difficulty about this approach is that instead of a chemical shift in ppm involving, typically, four significant figures, a frequency involving at least six significant figures is generated. For convenience it is easiest to choose a frequency as the metal reference and then to quote the chemical shift in ppm with respect to this reference frequency. This has now been accepted by most workers as the mode to adopt when referencing ^{103}Rh. In most cases, these are the frequencies for references relative to Me_4Si, and these have become the *de facto* references.

4. CHEMICAL SHIFTS

The chemical shifts of Cinderella nuclei are believed to be dominated by the paramagnetic term, σ_p. This term is of opposite sign to the chemical shift δ. The theory has been discussed elsewhere,[43] and will not be examined here. The chemical-shift range is dominated by the presence of a small energy gap between the highest filled and lowest empty molecular orbital. This gap is particularly small for atoms with a partially filled *d*-shell, as is found for ^{57}Fe, ^{103}Rh, ^{183}W and ^{187}Os, where a large range of chemical shifts has been found.

Table 5. Chemical-shift ranges observed for ^{57}Fe, ^{89}Y, ^{103}Rh, ^{107}Ag, ^{109}Ag, ^{183}W and ^{187}Os.

Nucleus	Oxidation state	Chemical shift range (ppm)
^{57}Fe	0	849– – 337
^{57}Fe	2	11197–305
^{89}Y	3	449– – 371
^{103}Rh	1	2344– – 1224
^{103}Rh	2	7644– – 1395
^{103}Rh	3	9931– – 1839
^{103}Rh	5	– 1573– – 1931
^{109}Ag	1	1468– – 1261
^{183}W	0	– 2647– – 3630
^{183}W	2	6760– – 4044
^{183}W	4	848– – 4671
^{183}W	6	3769– – 915
^{187}Os	2	– 1185– – 4889
^{187}Os	8	0

The chemical-shift range for ^{107}Ag and ^{109}Ag is small. The present chemical-shift ranges are given in Table 5.

It has been fashionable to equate the chemical shift with the oxidation state of the metal. This erroneous belief arose in the early days of transition-metal NMR spectroscopy when high oxidation states were associated with hard O and N ligands which produce high-frequency chemical shifts, and low oxidation states were associated with soft carbon ligands which produce low-frequency chemical shifts. The fallacy of this belief is well illustrated for ^{103}Rh, where the Rh(V) shift range is from – 1573 to – 1931 ppm, the Rh(III) shift range is from 9931 to – 1839 and the Rh(I) shift range is from 2344 to – 1224. Clearly, there is no correlation between oxidation state and chemical shift. It is the coordination sphere that is dominant.[26] The effects of substituents on octahedral d^6 transition-metal complexes have been discussed.[44]

Chemical shifts of metal nuclei are very temperature dependent. A selection of the temperature dependences of nuclei is given in Table 6. The values do not follow any pattern, but a temperature dependence of 1–2 ppm $^{\circ}C^{-1}$ is common. It is therefore useless to quote a metal chemical shift to an accuracy of greater than 1 ppm unless the temperature is accurately known. There are similar solvent and concentration dependencies, so these should be stated whenever accurate chemical shifts are required.

Secondary isotope effects have been noted for $^{1}H/^{2}H$, $^{12}C/^{13}C$ and $^{35}Cl/^{37}Cl$. The ^{103}Rh chemical-shift difference between [Rh[η^5-C_5Me_5)H_3(SiEt_3)] and [Rh(η^5-C_5Me_5)H_2D(SiEt_3)] has been determined

Table 6. A selection of temperature coefficients for the chemical shift of ^{57}Fe, ^{103}Rh, and ^{183}W.

Compound	Nucleus	Temperature coefficient of the chemical shift (ppm °C^{-1})	Ref.
Carbonyl myoglobin	^{57}Fe	−1.6	61
$[(\eta^5\text{-}C_5H_5)(\eta^5\text{-}C_5H_4Bu^n)Fe]$	^{57}Fe	+0.7	61
$[Fe(bipy)_3]^{2+}$	^{57}Fe	+2.1	61
$[Fe(CN)_6]^{4-}$	^{57}Fe	+2.3	61
Cytochrome *c*	^{57}Fe	+3.0	61
$[Rh(\eta^5\text{-}C_5H_4CO_2Me)(\eta^2\text{-}C_2H_4)_2]$ in $(CD_3)_2CO$	^{103}Rh	0.25	62
trans-$[RhCl(CO)(PMe_2Ph)_2]$	^{103}Rh	0.26	63
$[Rh(\eta^5\text{-}C_5H_4CO_2Me)(\eta^2\text{-}C_2H_4)_2]$ in $CDCl_3$	^{103}Rh	0.32	62
$[RhH(CO)(PPh_3)_3]$	^{103}Rh	0.44	20
mer-$[RhCl_3(SMe_2)_3]$	^{103}Rh	1.0	17
$[RhCl_2(MeSCH_2CH_2SMe)_2]^+$	^{103}Rh	1.0	64
$[Rh(acac)_3]$	^{103}Rh	1.6	36
$[Rh(OH_2)_{6-n}Cl_n]^{3-n}$	^{103}Rh	*ca* 2	47
$[WO_4]^{2-}$	^{183}W	0.16	12
$[WCl_6]$	^{183}W	0.34	12

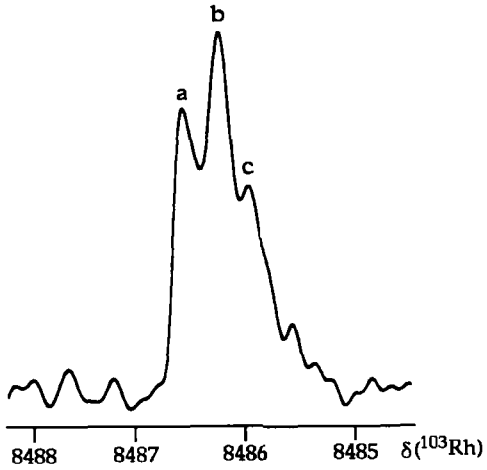

Fig. 14. The observed isotopic splitting of the ^{103}Rh NMR signal of *cis*-$[RhCl_4(OH_2)_2]^-$. The calculated natural abundances are $[Rh^{35}Cl_4(OH_2)_2]^- = 32\%$, $[Rh^{35}Cl_3{}^{37}Cl(OH_2)_2]^- = 42\%$, $[Rh^{35}Cl_2{}^{37}Cl_2(OH_2)_2]^- = 21\%$, $[Rh^{35}Cl^{37}Cl_3(OH_2)_2]^- = 4.5\%$, in fair agreement with the peak-height ratios obtained from the spectrum. (Reproduced with permission from Carr.[47])

using INEPT as -9 ppm.[45] Similarly, by analysing the ABX ^{13}C NMR spectrum of $[Rh_2(\eta^5\text{-}C_5Me_5)_2(\mu\text{-}^{13}CH_2)(\mu\text{-}CH_2)\{\mu\text{-}CH_2CH(CH_2CH{=}CH_2)CH_2\}]$ a $^{12}C/^{13}C$ secondary isotope effect of ± 0.36 ppm has been determined.[46] $^{35}Cl/^{37}Cl$ isotope shift have proven useful in the assignment of compounds in the $[RhCl_n(OH_2)_{6-n}]^{3-n}$ compounds (see Fig. 14). An isotope effect of -0.3 ppm has been observed.[47] These large isotope effects reflect the sensitivity of ^{103}Rh chemical shifts to the environment.

4.1. ^{57}Fe chemical shifts

The Fe(0) complexes only cover a range of 1200 ppm. In contrast, Fe(II) complexes fall within the range δ 11197 to 305. Most of the compounds examined are organometallic derivatives, and fall relatively close to $\delta 0$. Part of the limitation arises from the fact that many of the Fe(II) coordination compounds are paramagnetic. The ^{57}Fe chemical shifts are collected in Table 7–9.

4.2. ^{89}Y chemical shifts

Very few observations have been made of ^{89}Y NMR signals. There have been several reports of the use of ^{89}Y NMR spectroscopy to investigate the solvation of Y^{3+}.[4,5,48,49] Most of the studies have involved oxygen containing ligands, where the chemical-shift changes are small. However, when Cl^- is used as the ligand, substantial shifts occur, but exchange broadening is a problem.[48] A number of stable complexes have been studied, which give chemical shifts ranging from δ 449 to -371 (see Table 10).

4.3. ^{103}Rh chemical shifts

^{103}Rh NMR spectroscopy has been reviewed recently.[26] As extensive tables of ^{103}Rh chemical shifts are given in the review by Mann,[26] these tables are only updated here (see Tables 11–14).

4.4. ^{107}Ag and ^{109}Ag chemical shifts

There have been relatively few observations of ^{107}Ag and ^{109}Ag NMR spectra. When measured, ^{109}Ag is strongly preferred, due to its slightly higher sensitivity (see Table 1). The major difficulty is the limited availability of stable

Table 7. ^{57}Fe chemical shifts of some Fe(II) compounds, referenced to $[Fe(CO)_5]$.

Compound	Chemical shift (ppm)	Ref.
$[(\eta^5\text{-}C_5H_5)Fe(CO)_2I]$	305	65
$[(\eta^5\text{-}C_5H_5)_2FeH]^+$	460	66
$[(\eta^5\text{-}C_5H_5)(F_3P)_2FeCH_2CH{=}CH_2]$	594	67
$[(\eta^5\text{-}C_5H_5)(Pr^i_2PCH_2CH_2PPr^i_2)_2FeH]$	596	30
$[(\eta^5\text{-}C_5H_5)Fe(CO)_3]^+$	686	68
$[(\eta^3\text{-}1\text{-}syn\text{-}EtC_3H_4)Fe(CO)_4]^+$	785	68
$[(\eta^3\text{-}C_3H_5)Fe(CO)_4]^+$	796	68
$[(\eta^3\text{-}1\text{-}syn\text{-}3\text{-}syn\text{-}Me_2C_3H_3)Fe(CO)_4]^+$	803	68
$[(\eta^3\text{-}1\text{-}syn\text{-}MeC_3H_4)Fe(CO)_4]^+$	807	68
$[(\eta^5\text{-}C_5H_5)FeH(dppe)]$	823	67
$[(\eta^5\text{-}C_5H_5)FeH(dppe)]$	832	69
$[(\eta^3\text{-}1\text{-}syn\text{-}Me\text{-}3\text{-}anti\text{-}EtC_3H_3)Fe(CO)_4]^+$	835	68
$[(\eta^3\text{-}1\text{-}anti\text{-}MeC_3H_4)Fe(CO)_4]^+$	837	68
$[(\eta^3\text{-}1\text{-}syn\text{-}3\text{-}anti\text{-}Me_2C_3H_3)Fe(CO)_4]^+$	847	68
$[(\eta^3\text{-}1\text{-}syn\text{-}Pr^i\text{-}2\text{-}MeC_3H_3)Fe(CO)_4]^+$	861	68
$[(\eta^3\text{-}1\text{-}syn\text{-}3,3\text{-}Me_3C_3H_2)Fe(CO)_4]^+$	863	68
$[(\eta^5\text{-}MeC_5H_4)FeH(dppe)]$	868	67
$[(\eta^3\text{-}2\text{-}MeC_3H_4)Fe(CO)_4]^+$	868	68
$[(\eta^3\text{-}1\text{-}syn\text{-}2\text{-}3\text{-}anti\text{-}Me_3C_3H_2)Fe(CO)_4]^+$	884	68
$[(\eta^3\text{-}1,1\text{-}Me_2C_3H_3)Fe(CO)_4]^+$	896	68
$endo\text{-}[(\eta^5\text{-}C_5H_5)(\eta^3\text{-}1\text{-}syn\text{-}MeC_3H_4)FePF_3]$	906	67
$[(\eta^5\text{-}C_7H_9)Fe(CO)_3]^+$	926	66, 68
$[(\eta^5\text{-}C_5H_5)Fe(CO)_2CH_2CMe{=}CH_2]$	959	66
$[(\eta^5\text{-}C_5H_5)Fe(CO)_2Br]$	962	65
$exo\text{-}[(\eta^5\text{-}C_5H_5)(\eta^3\text{-}C_3H_5)FePF_3]$	997	67
$[(\eta^3\text{-}1,1,3,3\text{-}Me_4C_3H)Fe(CO)_4]^+$	998	68
$[(\eta^5\text{-}C_5H_5)Fe(\eta^5\text{-}C_5H_4CH_2)]^+$	1014	70
$[(\eta^5\text{-}C_5H_5)Fe(\eta^5\text{-}C_5H_4CH_2)]^+$	1015	71
$[(\eta^5\text{-}1\text{-}syn\text{-}Me\text{-}C_5H_6)Fe(CO)_3]^+$	1018	68
$[(\eta^5\text{-}C_5H_5)Fe(\eta^5\text{-}C_5H_4)CH_2]^+$	1036	66
$exo\text{-}[(\eta^5\text{-}C_5H_5)(\eta^3\text{-}1\text{-}syn\text{-}MeC_3H_4)FePF_3]$	1039	67
$[(\eta^5\text{-}C_5H_5)(Pr^i_2PCH_2CH_2CH_2PPr^i_2)_2FeH]$	1089	30, 67
$[(\eta^5\text{-}C_6H_7)Fe(CO)_3]^+$	1125	68
$[(\eta^5\text{-}C_6H_7)Fe(CO)_3]^+$	1128	66
$[(\eta^5\text{-}C_6H_7)(Pr^i_2PCH_2CH_2PPr^i_2)_2FeH]$	1225	67
$[(\eta^5\text{-}EtC_6H_6)(Pr^i_2PCH_2CH_2PPr^i_2)_2FeH]$	1233	67
$[(\eta^3\text{-}C_3H_5)Fe(CO)_3I]$	1235	68
$[OCF(CH_2)_2(\eta^5\text{-}C_5H_4)_2Fe]_2$	1310	72
$[CHOH(CH_2)_2(\eta^5\text{-}C_5H_4)_2Fe]$	1311	72
$[(\eta^5\text{-}C_5H_5)Fe(CO)_2Cl]$	1263	65
$[(\eta^5\text{-}C_5H_4CH_2CH_2CH_2C_5H_4\text{-}\eta^5)Fe]$	1279	73
$[(\eta^5\text{-}C_5H_5)(Me_3P)_2FeH]$	1309	30, 67
$[(\eta^5\text{-}C_5H_5)Fe(\eta^5\text{-}C_5H_4CHMe)]^+$	1315	70
$[(\eta^5\text{-}C_5H_5)Fe(\eta^5\text{-}C_5H_4CHMe)]^+$	1319	71
$[(\eta^5\text{-}C_5H_5)Fe(\eta^5\text{-}C_5H_4)CMeH]^+$	1341	66
$[(\eta^5\text{-}C_5H_5)(MePh_2P)_2FeH]$	1354	67
$[(\eta^3\text{-}C_3H_5)Fe(CO)_3I]$	1356	68

Table 7. (*Continued*)

Compound	Chemical shift (ppm)	Ref.
$[HC(CH_2)_2(\eta^5\text{-}C_5H_4)_2Fe]^+$	1377	72
$[(\eta^5\text{-}C_5H_5)(Pr^i_2PCH_2PPr^i_2)_2FeD]$	1395	30
$[(\eta^5\text{-}C_5H_5)(Pr^i_2PCH_2PPr^i_2)_2FeH]$	1415	30
$[OC(CH_2)_2(\eta^5\text{-}C_5H_4)_2Fe]$	1415	72
$[(\eta^5\text{-}C_7H_7)Fe(CO)_3]^+$	1435	68
$[(CH_2)(CO)(CH_2)_2(\eta^5\text{-}C_5H_4)_2Fe]$	1449	72
$[(\eta^5\text{-}C_5H_5)FeH\{Ph_2P(CH_2)_4PPh_2\}]$	1452	67
$[(CH_2)(HOCH)(CH_2)_2(\eta^5\text{-}C_5H_4)_2Fe]$	1456	72
$[(\eta^5\text{-}C_5Me_5)(\eta^2\text{-}C_2H_4)FeH(PMe_3)]$	1480	67
$[(CH_2)_4(\eta^5\text{-}C_5H_4)_2Fe]$	1481	72
$[(\eta^5\text{-}C_5H_5)Fe(\eta^5\text{-}C_5H_4CH_2Br)]$	1524	73
$[(\eta^3\text{-}C_3H_5)Fe(CO)_3Br]$	1528	66, 68
$[(\eta^5\text{-}C_5H_5)_2Fe]$	1531	74
$[(\eta^5\text{-}C_5H_5)Fe(\eta^5\text{-}C_5H_4CH_2OMe)]$	1536	73
$[(\eta^5\text{-}C_5H_5)Fe(\eta^5\text{-}C_5H_4CH_2Cl)]$	1537	73
$[(\eta^5\text{-}C_5H_5)Fe(\eta^5\text{-}C_5H_4CH_2OH)]$	1537	73, 75
$[(\eta^5\text{-}C_5H_5)Fe(\eta^5\text{-}C_5H_4C{\equiv}N)]$	1537	73
$[(\eta^5\text{-}C_5H_5)_2Fe]$	1538	71
$[(\eta^5\text{-}C_5H_5)Fe(\eta^5\text{-}C_5H_4CH_2NMe_2)]$	1539	73, 75
$[\{(\eta^5\text{-}C_5H_5)Fe(\eta^5\text{-}C_5H_4CH_2)\}_2O]$	1541	73, 75
$[(\eta^5\text{-}C_5H_5)Fe(\eta^5\text{-}C_5H_4CHMeOH)]$	1546	73, 75
$[(\eta^5\text{-}C_5H_5)(Ph_3P)_2FeH]$	1564	67
$[(\eta^5\text{-}C_5H_5)Fe(\eta^5\text{-}C_5H_4Pr^i)]$	1571	73
$[(\eta^5\text{-}C_5H_5)Fe(\eta^5\text{-}C_5H_4Et)]$	1573	73, 75
$[(\eta^5\text{-}C_5H_5)Fe(\eta^5\text{-}C_5H_4Bu^t)]$	1577	73
$[(\eta^5\text{-}C_5H_5)Fe(\eta^5\text{-}C_5H_4Me)]$	1582	73
$[(\eta^5\text{-}C_5H_4Et)_2Fe]$	1608	73, 75
$[(\eta^5\text{-}C_5H_5)\{(MeO)_3P\}_2FeCH_2CH(CMe{=}CH_2)(CH_2CMe{=}CH_2)]$	1608	67
exo-$[(\eta^5\text{-}C_5H_5)(\eta^3\text{-}1\text{-}syn\text{-}MeC_3H_4)Fe\{P(OMe)_3\}]$	1622	67
$[(\eta^5\text{-}C_6H_7)(Pr^i_2PCH_2CH_2CH_2PPr^i_2)_2FeH]$	1659	67
$[(\eta^5\text{-}C_5H_5)Fe(\eta^5\text{-}C_5H_4C{\equiv}N)]$	1660	73, 75
exo-$[(\eta^5\text{-}C_5H_5)(\eta^3\text{-}2\text{-}MeC_3H_4)Fe\{P(OMe)_3\}]$	1667	67
$[(\eta^5\text{-}C_5H_5)Fe(\eta^5\text{-}C_5H_4C{\equiv}CH)]$	1680	73, 75
$[(\eta^5\text{-}C_5H_4CH_2CH_2COC_5H_4\text{-}\eta^5)Fe]$	1687	73, 75
$[(\eta^5\text{-}C_5H_5)\{(MeO)_3P\}_2FeCH_2CH{=}CH_2]$	1691	67
$[(\eta^5\text{-}C_5H_5)Fe(\eta^5\text{-}C_5H_4CH{=}CH_2)]$	1704	73, 75
$[(\eta^3\text{-}C_3H_5)Fe(CO)_3Cl]$	1708	68
$[(\eta^5\text{-}C_5H_5)Fe(\eta^5\text{-}C_5H_4Ph)]$	1727	73, 75
$[(\eta^5\text{-}C_5H_5)Fe(\eta^5\text{-}C_5H_4CO_2CH_3)]$	1733	73, 75
$[(\eta^5\text{-}C_5H_5)\{(MeO)_3P\}_2FeCH_2CMe{=}CH_2]$	1744	67
$[(\eta^5\text{-}C_5H_5)Fe(\eta^5\text{-}C_5H_4CHPh)]^+$	1760	71
$[(\eta^5\text{-}C_5H_5)Fe(\eta^5\text{-}C_5H_4CHO)]$	1771	73, 75
$[(\eta^5\text{-}C_5H_5)Fe(\eta^5\text{-}C_5H_4CMeO)]$	1773	73, 75
$[(\eta^5\text{-}C_5H_5)Fe(\eta^5\text{-}C_5H_4CMeO)]$	1776	66
$[(\eta^5\text{-}C_5H_5)Fe\{\eta^5\text{-}1,3\text{-}C_5H_4(CH_2OH)(CHO)\}]$	1806	73, 75
$[(\eta^5\text{-}C_5H_5)Fe(CH{=}CH_2)(dppe)]$	1807	67

Table 7. (*Continued*)

Compound	Chemical shift (ppm)	Ref.
$[(\eta^5\text{-}C_5H_5)Fe(\eta^5\text{-}C_5H_4CPhO)]$	1808	66
$[(\eta^5\text{-indenyl})(Pr^i_2PCH_2CH_2CH_2PPr^i_2)_2FeH]$	1825	67
$[(\eta^5\text{-}C_5H_5)Fe(\eta^5\text{-}C_5H_4CMe_2)]^+$	1827	71
$[(\eta^5\text{-}C_5H_5)Fe(\eta^5\text{-}C_5H_4CPhO)]$	1828	73
$[(\eta^5\text{-}C_5H_5)FeCH_3(dppe)]$	1833	67
$[(\eta^5\text{-}C_5H_5)Fe(\eta^5\text{-}C_5H_4CHPh)]^+$	1859	70
exo-$[(\eta^5\text{-}C_5H_5)(\eta^3\text{-2-}MeC_3H_4)Fe\{P(OPh)_2(menthyl)\}]$	1871	67
$[\{(\eta^5\text{-}C_5H_5)Fe(\eta^5\text{-}C_5H_4)\}_3C_3]$	1901	66
$[(\eta^5\text{-}C_5H_5)Fe(\eta^5\text{-}C_5H_4CHC_5H_4\text{-}\eta^5)Mn(CO)_3]^+$	1904	70
$[(\eta^5\text{-}C_5H_5)Fe(\eta^5\text{-}C_5H_4CHC_5H_4\text{-}\eta^5)Mn(CO)_3]^+$	1907	71
$[(\eta^5\text{-}C_5H_4CO_2CH_3)_2Fe]$	1918	73, 75
$[(\eta^5\text{-}C_5H_5)Fe(\eta^5\text{-}C_5H_4)CH(\eta^5\text{-}C_5H_4)Ru(\eta^5\text{-}C_5H_5)]^+$	1934	70
$[(\eta^5\text{-}C_5H_5)Fe(\eta^5\text{-1,3-}C_5H_3(CHO)_2\}]$	1940	73, 75
$[(\eta^5\text{-}C_5H_5)Fe(\eta^5\text{-}C_5H_4CHC_5H_4\text{-}\eta^5)Ru(\eta^5\text{-}C_5H_5)^+$	1944	71
$[(\eta^5\text{-}C_5H_4CMeO)_2Fe]$	1975	73, 75
$[(\eta^5\text{-}C_5H_4CMeO)_2Fe]$	1986	66
$[(\eta^5\text{-}C_5H_4CBu^tO)_2Fe]$	2065	73, 75
$[\{(\eta^5\text{-}C_5H_5)Fe(\eta^5\text{-}C_5H_4)\}_2CH]^+$	2230	70
$[\{(\eta^5\text{-}C_5H_5)Fe(\eta^5\text{-}C_5H_4)\}_2CH]^+$	2238	71
exo-$[(\eta^5\text{-}C_5Me_5)(\eta^3\text{-}C_3H_5)FePMe_3]$	2246	67
$[\{(\eta^5\text{-}C_5H_5)Fe(\eta^5\text{-}C_5H_4)\}_2CH]^+$	2274	66
$[(\eta^5\text{-}MeC_5H_4)(Me_3P)_2FeCH_3]$	2318	67
$[(\eta^5\text{-}C_5H_5)(Me_3P)_2FeCH_3]$	2342	30, 67
$[(\eta^5\text{-}C_5H_5)(Me_3P)_2FeCH{=}CH_2]$	2350	67
$[(\eta^5\text{-}C_5H_5)(MePh_2P)_2FeCH_3]$	2427	67
$[(\eta^5\text{-}MeC_5H_4)(MePh_2P)_2FeCH_3]$	2451	67
$[(\eta^5\text{-}MeC_5H_4)(MePh_2P)_2FeEt]$	2487	67
$[Fe(CN)_6]^{4-}$	2495	74
$[Fe(CN)_6]^{4-}$	2497	66
$[(\eta^5\text{-}C_5H_5)(MePh_2P)_2FeCH{=}CH_2]$	2524	67
$[(\eta^5\text{-}MeC_5H_4)(MePh_2P)_2FeEt]$	2542	67
$[(\eta^5\text{-}Me_5C_5)(Me_3P)_2FeCH_3]$	2679	67
$[(\eta^5\text{-}C_5Me_5)(1,2,5\text{-}\eta^{1,2}\text{-}C_5H_9)FePMe_3]$	2896	67
$[(\eta^5\text{-}C_5Me_5)(1\text{-}C_6H_4\text{-}2\text{-}\eta^{2,3}\text{-}C_3H_5)FePMe_3]$	2997	67
$[(\eta^5\text{-}MeC_5H_4)\{Pr^i_2P(CH_2)_3PPr^i_2\}FeEt]$	2999	67
$[(\eta^5\text{-}C_5H_5)(Me_3P)_2FeI]$	4287	30, 67
$[(\eta^5\text{-}C_5H_5)(Me_2PhP)_2FeCl]$	5070	30
$[Fe(tetraphenylporphine)(HNC_5H_{10})]$	7258	74
$[Fe(tetra\text{-}p\text{-}tolylporphine)(HNC_5H_{10})]$	7341	74
$Fe(protoporphyrin\text{-}IX)(CO)(4\text{-}Me_2NC_5H_4N)$	8137	76
Fe(protoporphyrin-IX)(CO)(imidazole)	8145	76
Fe(protoporphyrin-IX)(CO)(2-Me-imidazole)	8146	76
$Fe(protoporphyrin\text{-}IX)(CO)(4\text{-}MeC_5H_4N)$	8180	76
$Fe(protoporphyrin\text{-}IX)(CO)(C_5H_5N)$	8183	76
$Fe(protoporphyrin\text{-}IX)(CO)(4\text{-}MeCOC_5H_4N)$	8204	76
$Fe(protoporphyrin\text{-}IX)(CO)(4\text{-}NCC_5H_4N)$	8209	76
Carbonylmyoglobin	8227	77
Carbonylmyoglobin	8234	61
Cytochrome c	11197	78

Table 8. ^{57}Fe chemical shifts of some Fe(I) compounds, referenced to $[Fe(CO)_5]$.

Compound	Chemical shift (ppm)	Ref.
$[(\eta^3,\eta^{3'}\text{-}C_7H_8)Fe_2(CO)_6]$	228	66
$[\{\eta^1,\eta^2,\eta^{1'},\eta^{2'}\text{-}(C_3H_5)_2C_4(C_3H_5)_2\}Fe_2(CO)_6]$	480	66

Table 9. ^{57}Fe chemical shifts of some Fe(0) compounds, referenced to $[Fe(CO)_5]$.

Compound	Chemical shift (ppm)	Ref.
$[(OC)_3(Pr^i_2PCH_2CH_2PPr^i_2)Fe]$	−337	30
$[OC)_3(Pr^i_2PCH_2CH_2CH_2PPr^i_2)Fe]$	−102	30
$[(\eta^4\text{-}C_4H_6)Fe(CO)_3]$	−77	66
$[(\eta^4\text{-}C_6H_8)Fe(CO)_3]$	−73	66
$[(\eta^2\text{-PhCH=CHCHO})Fe(CO)_4]$	9	66
$[(\eta^4\text{-}C_4H_6)Fe(CO)_3]$	0	66
$[(\eta^4\text{-}C_4H_6)Fe(CO)_3]$	4	68
$[(\eta^4\text{-1-}syn\text{-}MeC_4H_5)Fe(CO)_3]$	33	68
$[(\eta^4\text{-2-}MeC_4H_5)Fe(CO)_3]$	37	68
$[(\eta^4\text{-1-}syn\text{-2-}Me_2C_4H_4)Fe(CO)_3]$	51	68
$[(\eta^4\text{-1-}syn\text{-3-}Me_2C_4H_4)Fe(CO)_3]$	65	68
$[(\eta^4\text{-2,3-}Me_2C_4H_4)Fe(CO)_3]$	69	68
$[(\eta^4\text{-}C_7H_{10})Fe(CO)_3]$	86	66
$[(\eta^4\text{-1-}syn\text{-Me-4-}syn\text{-}MeC_4H_4)Fe(CO)_3]$	86	68
$[(\eta^4\text{-1-}anti\text{-}MeC_4H_5)Fe(CO)_3]$	105	68
$[(\eta^4\text{-1-}anti\text{-2-}Me_2C_4H_4)Fe(CO)_3]$	130	68
$[(\eta^4\text{-1-}syn\text{-Me-4-}anti\text{-}MeC_4H_4)Fe(CO)_3]$	165	68
$[(\eta^4\text{-1,3-}C_8H_{12})Fe(CO)_3]$	169	66
$[(\eta^4\text{-}C_7H_8)Fe(CO)_3]$	170	66
$[(\eta^4\text{-1,1-}Me_2C_4H_4)Fe(CO)_3]$	179	68
$[(\eta^4\text{-1,1,3-}Me_3C_4H_3)Fe(CO)_3]$	216	68
$[Fe(CO)_2(PMe_3)_2(CS_2)]$	220	40
$[(\eta^4\text{-}C_4H_4O)Fe(CO)_3]$	274	68
$[(\eta^4\text{-1-}syn\text{-2-}Me_2C_4H_2O)Fe(CO)_3]$	277	68
$[(\eta^4\text{-1-}syn\text{-}MeC_4H_3O)Fe(CO)_3]$	279	68
$[(\eta^4\text{-2-}MeC_4H_3O)Fe(CO)_3]$	279	68
$[\{\eta^4\text{-}C_6H_4(=CH_2)_2\}Fe(CO)_3]$	293	66
$[(\eta^4\text{-}C_8H_8)Fe(CO)_3]$	301	66
$[\{\eta^4\text{-1-Me-4-}(EtO_2C)C_4H_4\}Fe(CO)_3]$	312	68
$[(\eta^4\text{-3-}EtC_4H_3O)Fe(CO)_3]$	318	68
$[(\eta^4\text{-3-}MeC_4H_3O)Fe(CO)_3]$	325	68
$[(\eta^4\text{-1-}syn\text{-}MeC(O)C_4H_5)Fe(CO)_3]$	335	68
$[(\eta^4\text{-1-}syn\text{-3-}Me_2C_4H_2O)Fe(CO)_3]$	335	68
$[(\eta^4\text{-2,3-}Me_2C_4H_2O)Fe(CO)_3]$	349	68

Table 9. (*Continued*)

Compound	Chemical shift (ppm)	Ref.
$[(\eta^4\text{-1-}syn\text{-Me-4-}syn\text{-NCCH=CHC}_4\text{H}_5)\text{Fe(CO)}_3]$	359	68
$[\{\eta^4\text{-1-}anti\text{-MeC(O)C}_4\text{H}_5\}\text{Fe(CO)}_3]$	359	68
$[\{\eta^4\text{-1-}syn\text{-Me-4-}syn\text{-(MeCO)}_2\text{C=CHC}_4\text{H}_5\}\text{Fe(CO)}_3]$	374	68
$[\{\eta^4\text{-1-}syn\text{-Me-4-}syn\text{-HC(O)C}_4\text{H}_5\}\text{Fe(CO)}_3]$	378	68
$[(\eta^4\text{-1,5-C}_8\text{H}_{12})\text{Fe(CO)}_3]$	380	66
$[(\eta^4\text{-norbornadiene})\text{Fe(CO)}_3]$	382	66
$[(\eta^4\text{-C}_4\text{H}_6)_2\text{Fe(CO)}]$	412	66
$[(\eta^4\text{-C}_4\text{H}_6)(\text{OC})(\text{Pr}^i_2\text{PCH}_2\text{CH}_2\text{PPr}^i_2)\text{Fe}]$	502	30
$[(\eta^4\text{-1-}syn\text{-PhC}_4\text{H}_3\text{O})\text{Fe(CO)}_3]$	504	68
$[(\eta^4\text{-1-}syn\text{-NC-4-}syn\text{-MeCH=CHC}_4\text{H}_5)\text{Fe(CO)}_3]$	527	68
$[(\eta^4\text{-1-}syn\text{-Ph-3-MeC}_4\text{H}_2\text{O})\text{Fe(CO)}_3]$	559	68
$[(\eta^4\text{-PhCH=CHCMe=O})\text{Fe(CO)}_3]$	562	66
$[\{\eta^4\text{-1-}syn\text{-Me-4-}syn\text{-(NC)}_2\text{C=CHC}_4\text{H}_5\}\text{Fe(CO)}_3]$	589	68
$[(\eta^4\text{-C}_5\text{H}_4\text{=CPh}_2)\text{Fe(CO)}_3]$	589	66
$[(\eta^4\text{-1-}syn\text{-3-Ph}_2\text{C}_4\text{H}_2\text{O})\text{Fe(CO)}_3]$	688	68
$[(\eta^4\text{-C}_4\text{H}_6)(\text{OC})(\text{Pr}^i_2\text{PCH}_2\text{CH}_2\text{PPr}^i_2)\text{Fe}]$	838	30
$[(\eta^4\text{-tropone})\text{Fe(CO)}_3]$	849	66

Table 10. ^{89}Y Chemical shifts of some Y(III) compounds, referenced to $[\text{Y(OH}_2)_6]^{3+}$.

Compound	Chemical shift (ppm)	Ref.
$[(\eta^5\text{-C}_5\text{H}_4\text{Me})_3\text{Y(THF)}]$	−371	79
$[(\eta^5\text{-C}_5\text{Me}_5)_2\text{Y}(\mu\text{-Cl})_2\text{K(THF)}_2]$	−324	79
$[(\eta^5\text{-C}_5\text{H}_4\text{Me})_2\text{YCl(THF)}]$	−103	79
$[(\eta^5\text{-C}_5\text{H}_4\text{Me})_2\text{YCl}]_2$	−97	79
$[(\eta^5\text{-C}_5\text{H}_4\text{Me})_2\text{Y}(\mu\text{-H})\text{(THF)}]_2$	−92	79
$[(\eta^5\text{-C}_5\text{H}_4\text{Me})_2\text{Y}(\mu\text{-C}\equiv\text{CBu}^t)]_2$	−74	79
$[(\eta^5\text{-C}_5\text{H}_5)_2\text{Y}(\mu\text{-H})\}_3]^+$	−67	79
$[(\eta^5\text{-C}_5\text{H}_4\text{Me})_2\text{Y}(\mu\text{-CH}_3)]_2$	−15	79
$[(\eta^5\text{-C}_5\text{H}_4\text{Me})_2\text{Y(CH}_3)\text{(THF)}]$	40	79
$[\text{YCl}\{\text{N(SiMe}_2\text{CH}_2\text{PMe}_2)_2\}_2]$	449	80

Table 11. ^{103}Rh chemical shifts for some Rh(III) complexes not included in an earlier review,[26] referenced to Ξ 3.16 MHz.

Compound	Chemical shift (ppm)	Ref.
$[MeC(CH_2AsPh_2)_3RhH_2\{Au(AsPh_3)\}_3]^{2+}$	96	51
$[RhEtCl\{C_6H_3(CH_2NMe_2)_2\text{-}2,6\}]$	3163	82
$[RhMeCl\{C_6H_3(CH_2NMe_2)_2\text{-}2,6\}]$	3165	82
$[RhMeI\{C_6H_3(CH_2NMe_2)_2\text{-}2,6\}]$	3179	82
$[RhEtI\{C_6H_3(CH_2NMe_2)_2\text{-}2,6\}]$	3201	82

Table 12. ^{103}Rh chemical shifts for some Rh(II) complexes not included in an earlier review,[26] referenced to Ξ 3.16 MHz.

Compound	Chemical shift (ppm)	Ref.
$[Rh_2(4\text{-}MeC_6H_4NCHNC_6H_4Me\text{-}4)_3(NO_3)(PPh_3)]$	3007	83
$[Rh_2(4\text{-}MeC_6H_4NCHNC_6H_4Me\text{-}4)_2(O_2CCF_3)_2(PPh_3)]$	3394	84
$[Rh_2(4\text{-}MeC_6H_4NCHNC_6H_4Me\text{-}4)_3(NO_3)(NC_5H_5)]$	4332	83
$[Rh_2(4\text{-}MeC_6H_4NCHNC_6H_4Me\text{-}4)_3(NO_3)(NC_5H_5)]$	6060	83
$[Rh_2(4\text{-}MeC_6H_4NCHNC_6H_4Me\text{-}4)_3(NO_3)(PPh_3)]$	6472	83
$[Rh_2(4\text{-}MeC_6H_4NCHNC_6H_4Me\text{-}4)_2(O_2CCF_3)_2(PPh_3)]$	7086	84

Table 13. ^{103}Rh chemical shifts for some Rh(I) complexes not included in an earlier review,[26] referenced to Ξ 3.16 MHz.

Compound	Chemical shift (ppm)	Ref.
$[Rh\{Ph_2P(CH_2)_2AsPh_2\}_2]^+$	−1224[a]	85
$[Rh\{Ph_2P(CH_2)_2AsPh_2\}_2]^+$	−1199[a]	85
$[Rh\{Ph_2P(CH_2)_2PPh_2\}\{Ph_2P(CH_2)_2AsPh_2\}]^+$	−1187	85
$[Rh\{Ph_2P(CH_2)_2PPh_2\}_2]^+$	−1167	85
$[(\eta^5\text{-}C_5H_5)Rh(\mu\text{-}CO)(\mu\text{-}Ph_2PC_5H_4N)Rh(CO)Cl]$	−1119	86
$[(\eta^4\text{-norbornadiene})Rh\{Ph_2P(CH_2)_2PPh_2\}]^+$	−390	85
$[(\eta^4\text{-norbornadiene})Rh\{Ph_2P(CH_2)_3PPh_2\}]^+$	−264	85
$[(\eta^4\text{-norbornadiene})Rh\{Ph_2P(CH_2)_4PPh_2\}]^+$	−210	85
$[(\eta^5\text{-}C_5H_5)Rh(\eta^4\text{-}MeNBEtCEtCMeSiMe_2)]$	−171	87
$[(\eta^5\text{-}C_5H_5)Rh(\mu\text{-}CO)(\mu\text{-}Ph_2PC_5H_4N)Rh(CO)Cl]$	472	86
$[(acac)Rh(\eta^4\text{-}MeNBEtCEtCMeSiMe_2)]$	2344	87

[a] *cis* and *trans* isomers.

Table 14. ^{103}Rh chemical shifts for some Rh cluster complexes not included in an earlier review,[26] referenced to Ξ 3.16 MHz.

Compound	Chemical shift (ppm)	Ref.
$[Rh_6(CO)_{15}I]^-$	−498	88
$[Rh_6(CO)_{15}(CN)]^-$	−481	88
$[Rh_6(CO)_{15}(CN)]^-$	−462	88
$[Rh_6(CO)_{15}(SCN)]^-$	−460	88
$[Rh_6(CO)_{15}(CN)]^-$	−430	88
$[Rh_6(CO)_{12}\{P(OPh)_3\}_4]$	−418	88
$[Rh_6(CO)_{15}I]^-$	−417	88
$[Rh_6(CO)_{15}I]^-$	−405	88
$[Rh_6(CO)_{15}(SCN)]^-$	−403	88
$[Rh_6(CO)_{10}(dppm)_3]$	−371	88
$[Rh_6(CO)_{15}(SCN)]^-$	−358	88
$[Rh_6(CO)_{12}\{P(OPh)_3\}_4]$	−296	88
$[Rh_6(CO)_{10}(dppm)_3]$	−152	88
$[Rh_6(CO)_{15}I]^-$	−104	88
$[Rh_6(CO)_{15}(CN)]^-$	−102	88
$[Rh_6(CO)_{15}(SCN)]^-$	148	88

compounds. Most complexes of silver are very labile, and it is difficult to know what is present in solution. This provides a challenge to use ^{109}Ag NMR spectroscopy to investigate solution equilibria, and to characterize the labile compounds, but this challenge has still to be taken. The presence of rapid exchange generally prevents the use of any of the INEPT/DEPT based pulse sequences to enhance the sensitivity. The limited reports of ^{109}Ag chemical shifts are listed in Table 15.

4.5. ^{183}W chemical shifts

Extensive attention has been paid to ^{183}W NMR spectroscopy of the polytungstates, driven by commercial interest in these compounds. As it is possible to use COSY and INADEQUATE to observe ^{183}W–^{183}W coupling, the assignment of the signals can be securely based. Table 16 contains extensive data for these compounds. The lower oxidation states of tungsten have received less attention, despite the relative ease with which a spectrum can be obtained. The available data are gathered together in Tables 16–22.

Table 15. ^{109}Ag chemical shifts of some Ag(I) compounds, referenced of $[Ag_{aq}]^+$.

Compound	Chemical shift (ppm)	Ref.
$[Ag_2Ru_4(\mu_3\text{-}H)_2(\mu\text{-}Ph_2AsCH_2AsPh_2)(CO)_{12}]$	−391[b]	89
$[AgRu_4(\mu_3\text{-}H)_3(CO)_{12}(PPh_3)]$	−250[b]	99
$[Ag_2Ru_4(\mu_3\text{-}H)_2\{Ph_2P(CH_2)_4PPh_2\}(CO)_{12}]$	−181[b]	89,97,99
$[Ag_2Ru_4(\mu_3\text{-}H)_2(dppm)(CO)_{12}]$	−153[b]	89,97,99
$[Ag_2Ru_4(\mu_3\text{-}H)_2(dppe)(CO)_{12}]$	−135[b]	89,97,99
$[Ag\{N(CH_2CH_2OH)_3\}_2]^+$	232	31,98
$[Ag\{NH(CH_2CH_2OH)_2\}_2]^+$	306	31,98
$[Ag_2(NO_3)_2\{P(OPh)_3\}_4]$	409	90
$[Ag\{NH_2(CH_2CH_2OH)\}_2]^+$	505	98
[{2,6-(Me$_2$NCH$_2$)$_2$C$_6$H$_3$}(4-tolNCHNPr^i)PtAgBr][a]	524	91
[{2,6-(Me$_2$NCH$_2$)$_2$C$_6$H$_3$}(4-tolNCHNtol-4)PtAgBr]	534	91
[{2,6-(Me$_2$NCH$_2$)$_2$C$_6$H$_3$}(4-tolNCHNEt)PtAgBr][a]	539	91
[{2,6-(Me$_2$NCH$_2$)$_2$C$_6$H$_3$}(4-tolNCHNMe)PtAgBr][a]	544	91
[{2,6-(Me$_2$NCH$_2$)$_2$C$_6$H$_3$}(4-tolNCHNMe)PtAgBr][a]	547	91
[{2,6-(Me$_2$NCH$_2$)$_2$C$_6$H$_3$}(4-tolNCHNEt)PtAgBr][a]	552	91
[{2,6-(Me$_2$NCH$_2$)$_2$C$_6$H$_3$}(4-tolNCHNPr^i)PtAgBr][a]	557	91
[1,2-(2-pyridylCH=N)$_2$C$_6$H$_{10}$}$_2$Ag$_2$]$^{2+}$	580	92
[1,2-{2-thiophenylCH=N)$_2$C$_6$H$_{10}$}$_2$Ag]$^+$	582	93
[1,2-{2-5-Me-thiophenylCH=N)$_2$C$_6$H$_{10}$}$_2$Ag]$^+$	583	93
[Ag{(*S*)(6-Me-2-C$_5$H$_3$N)CH=CHPhMe}$_2$]$^+$[a]	612	94
$[AgBr_4]^{3-}$	623	31,98
[Ag{(*S*)(6-Me-2-C$_5$H$_3$N)CH=CHPhMe}$_2$]$^+$[a]	636	94
[1,2-{(2-5-Me-thiophenylCH=N)$_2$C$_6$H$_{10}$}$_2$Ag]$^+$	659	95
[1,2-{(2-thiophenylCH=N)$_2$C$_6$H$_{10}$}$_2$Ag]$^+$	678	95
$[AgI_4]^{3-}$	739	31,98
$[Ag(S_2O_3)_4]^{3-}$	826	31,98
$[Ag(SCN)_4]^{3-}$	951	31,98
$[Ag(CN)_4]^{3-}$	1224	98
$[Ag(dppe)_2]^+$	1378	96
$[Ag(cis\text{-}Ph_2PCH{=}CHPPh_2)_2]^+$	1413	96
$[Ag(Et_2PCH_2CH_2PPh_2)_2]^+$	1432	96
$[Ag(Ph_2PCH_2CH_2CH_2PPh_2)_2]^+$	1468	96

[a]Two isomers.

[b]Relative to $[Ag\{P(OEt)_3\}_4]^+$.

Table 16. ^{183}W chemical shifts of some W(VI) compounds, referenced to 2 M Na_2WO_4.

Compound	Chemical shift[a] (ppm)	Ref.
$[WF_6]$	−1121	12
$[WF_5(OMe)]$	−1069	21
cis-$[WF_4(OMe)_2]$	−950	21
$[WF_5(OPh)]$	−920	21
$[Co^{II}W_{12}O_{40}]^{6-}$	−915	53
cis-$[WF_4(OPh)_2]$	−853	21
$[W_2O_3(O_2)_4(OH_2)_2]^{2-}$	−699	100
mer-$[WF_3(OMe)_3]$	−646	21
trans-$[WF_4OS(OMe)_2]$	−581	21
trans-$[WF_4OPMe(OMe)_2]$	−577	21
trans-$[WF_4O(OMe_2)]$	−544	21
cis-$[WF_2(OMe)_4]$	−506	21
$[WF_5O]^-$	−505	21
$[(WF_4O)_2F]^-$	−493	21
α-$[P_2W_{18}O_{62}]^{8-}$	−299 (6)	55
$[\{(\eta^5\text{-}C_5H_5)Fe(CO)_2Sn\}_2W_{10}PO_{38}]^{5-}$	−296.7 (1)	101
$[P_3W_{18}O_{66}]^{8-}$	−282.6 (12)	102
WO_3	−281	103
α-$[(D_2O)_2CoSiW_{11}O_{39}]^{6-}$	−280.2 (1)	52
β-$[(D_2O)_2Zn_4P_2W_{30}O_{112}]^{16-}$	−272.6	104
$[P_3W_{18}O_{66}]^{8-}$	−270.4 (12)	102
β-$[(D_2O)_2Zn_4P_2W_{30}O_{112}]^{16-}$	−269.0	104
β-$[(D_2O)_2Zn_4P_2W_{30}O_{112}]^{16-}$	−266.8	104
$\alpha[(D_2O)_2CoPW_{11}O_{39}]^{5-}$	−256.0 (1)	52
α_2-$[P_2W_{17}VO_{62}]^{7-}$	−244.8 (2)	105
α-$[(D_2O)_2Zn_4P_2W_{30}O_{112}]^{16-}$	−244.7 (4)	104
$[P_4(H_2O)_2Zn_4W_{30}O_{112}]^{16-}$	−244.7 (4)	106
β-$[(D_2O)_2Zn_4P_2W_{30}O_{112}]^{16-}$	−243.6	104
α-$[(D_2O)_2Zn_4P_2W_{30}O_{112}]^{16-}$	−243.4 (4)	104
$[P_4(H_2O)_2Zn_4W_{30}O_{112}]^{16-}$	−243.4 (4)	106
α_2-$[(D_2O)_2ZnP_2W_{17}O_{61}]^{8-}$	−242.7 (2)	52
β-$[(D_2O)_2Zn_4P_2W_{30}O_{112}]^{16-}$	−242.7	104
α_2-$[P_2W_{17}O_{61}]^{10-}$	−242.3 (2)	105
α-$[(D_2O)_2Zn_4P_2W_{30}O_{112}]^{16-}$	−238.2 (4)	104
$[P_4(H_2O)_2Zn_4W_{30}O_{112}]^{16-}$	−238.2 (4)	106
α-$[P_2Mo_3W_{15}O_{62}]^{8-}$	−238 (6)	55
β-$[(D_2O)_2Zn_4P_2W_{30}O_{112}]^{16-}$	−237.3	104
β-$[(D_2O)_2Zn_4P_2W_{30}O_{112}]^{16-}$	−236.9	104
α_2-$[(D_2O)_2CoP_2W_{17}O_{61}]^{8-}$	−230.5 (2)	52
α_2-$[(D_2O)_2NiP_2W_{17}O_{61}]^{8-}$	−230.5 (2)	52
α-$[P_2Mo_3W_{15}O_{62}]^{8-}$	−226 (6)	55
$[P_2W_{21}O_{71}(OH_2)_3]^{6-}$	−225.9 (3)	107
$[(O_5W)_3(W_9PO_{34})_2H_6]^{4-}$	−225.6 (2)	108
α_1-$[(D_2O)_2ZnP_2W_{17}O_{61}]^{8-}$	−225.5 (1)	52
α_2-$[P_2W_{17}VO_{62}]^{7-}$	−225.4 (2)	105

Table 16. (*Continued*)

Compound	Chemical shift[a] (ppm)	Ref.
α_2-$[P_2W_{17}O_{61}]^{10-}$	−225.0 (2)	105
α-$[(D_2O)_2NiSiW_{11}O_{39}]^{6-}$	−224.5 (1)	52
α_2-$[P_2W_{17}O_{61}]^{10-}$	−222.7 (2)	105
α-$[(D_2O)_2CoSiW_{11}O_{39}]^{6-}$	−222.2 (2)	52
α_2-$[P_2W_{17}VO_{62}]^{7-}$	−221.6 (2)	105
α_2-$[P_2W_{17}VO_{62}]^{7-}$	−220.0 (2)	105
$[(\eta^5\text{-}C_5H_4C_6H_9)TiP_2W_{17}O_{61}]^{7-}$	−219.1 (2)	109
$[(\eta^5\text{-}C_5H_4C_6H_9)TiP_2W_{17}O_{61}]^{7-}$	−219.1 (2)	110
$[(\eta^5\text{-}C_5H_4C_5H_{10}CHO)TiP_2W_{17}O_{61}]^{7-}$	−219.0 (2)	110
α_2-$[P_2W_{17}O_{61}]^{10-}$	−218.9 (2)	105
$[\{\eta^5\text{-}C_5H_4(CH_2)_3OC_6H_4CHO\text{-}4\}TiP_2W_{17}O_{61}]^{7-}$	−218.8 (2)	110
$[\{(\eta^5\text{-}C_5H_5)Fe(CO)_2Sn\}_2W_{10}PO_{38}]^{5-}$	−218.7 (2)	111
$[H_8P_8W_{48}O_{184}]^{32-}$	−216.6 (16)	112
$[(\eta^5\text{-}C_5H_5)TiP_2W_{17}O_{61}]^{7-}$	−215.9 (2)	109
$[(\eta^5\text{-}C_5H_5)TiP_2W_{17}O_{61}]^{7-}$	−215.9 (2)	110
α_2-$[(D_2O)_2ZnP_2W_{17}O_{61}]^{8-}$	−214.8 (6)	52
α_1-$[(D_2O)_2ZnP_2W_{17}O_{61}]^{8-}$	−214.6 (1)	52
$[P_2W_{15}Nb_3O_{62}]^{9-}$	−210.8 (6)	113
α_1-$[(D_2O)_2ZnP_2W_{17}O_{61}]^{8-}$	−210.3 (1)	52
$[\{(\eta^5\text{-}C_5H_5)Fe(CO)_2Sn\}_2W_{10}PO_{38}]^{5-}$	−209.0 (2)	111
$[Zn_2(O_2W)(W_9PO_{34})_2]^{12-}$	−208.8 (2)	108
α_2-$[(D_2O)_2ZnP_2W_{17}O_{61}]^{8-}$	−208.6 (2)	52
$[P_3W_{18}O_{66}]^{8-}$	−205.3 (6)	102
$[H_8P_8W_{48}O_{184}]^{32-}$	−204.4 (16)	112
$[H_8P_8W_{48}O_{184}]^{32-}$	−203.7 (16)	112
α_1-$[(D_2O)_2ZnP_2W_{17}O_{61}]^{8-}$	−203.7 (1)	52
$[P_3W_{18}O_{66}]^{8-}$	−203.2 (6)	102
$[HOTiP_2W_{17}O_{61}]^{7-}$	−202.6 (2)	110
α_2-$[(D_2O)_2CoP_2W_{17}O_{61}]^{8-}$	−202 (3)	52
α_2-$[(D_2O)_2NiP_2W_{17}O_{61}]^{8-}$	−202 (3)	52
α_1-$[D_2O)_2ZnP_2W_{17}O_{61}]^{8-}$	−200.1 (1)	52
α_2-$[(D_2O)_2CoP_2W_{17}O_{61}]^{8-}$	−200 (3)	52
α_2-$[(D_2O)_2NiP_2W_{17}O_{61}]^{8-}$	−200 (3)	52
$[\{\eta^5\text{-}C_5H_4(CH_2)_3OC_6H_4CHO\text{-}4\}TiP_2W_{17}O_{61}]^{7-}$	−197.2 (2)	110
$[(\eta^5\text{-}C_5H_4C_6H_9)TiP_2W_{17}O_{61}]^{7-}$	−197.0 (2)	109
$[(\eta^5\text{-}C_5H_4C_6H_9)TiP_2W_{17}O_{61}]^{7-}$	−197.0 (2)	110
α-$[D_2O)_2NiPW_{11}O_{39}]^{5-}$	−197.0 (1)	52
$[(\eta^5\text{-}C_5H_4C_5H_{10}CHO)TiP_2W_{17}O_{61}]^{7-}$	−196.7 (2)	110
$[\{\eta^5\text{-}C_5H_4(CH_2)_3OC_6H_4CHO\text{-}4\}TiP_2W_{17}O_{61}]^{7-}$	−196.2 (2)	110
$[(\eta^5\text{-}C_5H_4C_6H_9)TiP_2W_{17}O_{61}]^{7-}$	−196.1 (2)	109
$[(\eta^5\text{-}C_5H_4C_6H_9)TiP_2W_{17}O_{61}]^{7-}$	−196.1 (2)	110
$[(O_2W)_2(W_9PO_{34})_2]^{14-}$	−195.9 (2)	108
$[(\eta^5\text{-}C_5H_4C_5H_{10}CHO)TiP_2W_{17}O_{61}]^{7-}$	−195.8 (2)	110
$[(\eta^5\text{-}C_5H_5)TiP_2W_{17}O_{61}]^{7-}$	−195.4 (2)	109

(*Continued*)

Table 16. (*Continued*)

Compound	Chemical shift[a] (ppm)	Ref.
$[(\eta^5\text{-}C_5H_5)TiP_2W_{17}O_{61}]^{7-}$	−195.4 (2)	110
$[(\eta^5\text{-}C_5H_5)TiP_2W_{17}O_{61}]^{7-}$	−194.3 (2)	109
$[(\eta^5\text{-}C_5H_5)TiP_2W_{17}O_{61}]^{7-}$	−194.3 (2)	110
$[Zn_2(O_2W)(W_9PO_{34})_2]^{12-}$	−194.1 (1)	108
$\alpha_1\text{-}[(D_2O)_2ZnP_2W_{17}O_{61}]^{8-}$	−193.3 (1)	52
$[(\eta^5\text{-}C_5H_4C_6H_9)TiP_2W_{17}O_{61}]^{7-}$	−192.6 (2)	109
$[(\eta^5\text{-}C_5H_4C_6H_9)TiP_2W_{17}O_{61}]^{7-}$	−192.6 (2)	110
$\alpha\text{-}[(D_2O)_2CoPW_{11}O_{39}]^{5-}$	−192.4 (2)	52
$[(\eta^5\text{-}C_5H_4C_5H_{10}CHO)TiP_2W_{17}O_{61}]^{7-}$	−192.4 (2)	110
$[(\eta^5\text{-}C_5H_5)TiP_2W_{17}O_{61}]^{7-}$	−191.9 (2)	109
$[(\eta^5\text{-}C_5H_5)TiP_2W_{17}O_{61}]^{7-}$	−191.9 (2)	110
$[\{\eta^5\text{-}C_5H_4(CH_2)_3OC_6H_4CHO\text{-}4\}TiP_2W_{17}O_{61}]^{7-}$	−191.9 (2)	110
$\beta\text{-}[P_2W_{18}O_{62}]^{6-}$	−191.2 (6)	114
$\beta\text{-}[P_2W_{18}O_{62}]^{6-}$	−191.2 (6)	105
$\beta\text{-}[P_2W_{18}O_{62}]^{6-}$	−191.0	113
$[HOTiP_2W_{17}O_{61}]^{7-}$	−190.7 (2)	110
$[HOTiP_2W_{17}O_{61}]^{7-}$	−189.8 (2)	110
$[Si_2W_{18}Zr_3O_{71}H_n]^{n-14}$	−189 (6)	115
$\beta\text{-}[(D_2O)_2Zn_4P_2W_{30}O_{112}]^{16-}$	−186.8	104
$\alpha_2\text{-}[(D_2O)_2ZnP_2W_{17}O_{61}]^{8-}$	−186.7 (2)	52
$[P_2W_{18}O_{62}]^{6-}$	−186.6 (6)	116
$\alpha\text{-}[P_2W_{18}O_{62}]^{6-}$	−186.5 (6)	102
$[HOTiP_2W_{17}O_{61}]^{7-}$	−185.8 (2)	110
$[(\eta^5\text{-}C_5Me_5)RhP_2W_{15}Nb_3O_{62}]^{7-}$	−185.2 (6)	113
$\alpha\text{-}[(D_2O)_2Zn_4P_2W_{30}O_{112}]^{16-}$	−185.0 (4)	104
$[P_4(H_2O)_2Zn_4W_{30}O_{112}]^{16-}$	−185.0 (4)	106
$\beta\text{-}[(D_2O)_2Zn_4P_2W_{30}O_{112}]^{16-}$	−184.5	104
$\alpha_2\text{-}[P_2W_{17}VO_{62}]^{7-}$	−184.4 (1)	105
$[(\eta^6\text{-}C_6H_6)RuP_2W_{15}Nb_3O_{62}]^{7-}$	−183.0 (6)	113
$\alpha\text{-}[(D_2O)_2ZnSiW_{11}O_{39}]^{6-}$	−182.9 (2)	52
$\beta\text{-}[(D_2O)_2Zn_4P_2W_{30}O_{112}]^{16-}$	−182.7	104
$\alpha_2\text{-}[P_2W_{17}VO_{62}]^{7-}$	−182.5 (2)	105
$[HSiW_{10}O_{36}]^{7-}$	−181.5	117
$[(\eta^5\text{-}C_5H_4C_6H_9)TiP_2W_{17}O_{61}]^{7-}$	−180.9 (2)	109
$[(\eta^5\text{-}C_5H_4C_6H_9)TiP_2W_{17}O_{61}]^{7-}$	−180.9 (2)	110
$[(\eta^5\text{-}C_5H_4C_5H_{10}CHO)TiP_2W_{17}O_{61}]^{7-}$	−180.8 (2)	110
$\alpha\text{-}[P_2W_{15}Mo_3O_{62}]^{6-}$	−180.1 (6)	114
$[(\eta^5\text{-}C_5H_5)TiP_2W_{17}O_{61}]^{7-}$	−180.1 (2)	109
$[(\eta^5\text{-}C_5H_5)TiP_2W_{17}O_{61}]^{7-}$	−180.1 (2)	110
$\alpha\text{-}[(D_2O)_2Zn_4P_2W_{30}O_{112}]^{16-}$	−180.0 (4)	104
$[P_4(H_2O)_2Zn_4W_{30}O_{112}]^{16-}$	−180.0 (4)	106
$\alpha\text{-}[P_2Mo_3W_{15}O_{62}]^{6-}$	−180 (6)	55
$\alpha_2\text{-}[(D_2O)_2ZnP_2W_{17}O_{61}]^{8-}$	−180 (1)	52
$\alpha\text{-}[P_2W_{12}Mo_6O_{62}]^{6-}$	−179.9 (4)	114
$\beta\text{-}[(D_2O)_2Zn_4P_2W_{30}O_{112}]^{16-}$	−179.8	104

Table 16. (*Continued*)

Compound	Chemical shift[a] (ppm)	Ref.
α_2-$[P_2W_{17}O_{61}]^{10-}$	−179.6 (1)	105
$[\{\eta^5$-$C_5H_4(CH_2)_3OC_6H_4CHO$-4$\}TiP_2W_{17}O_{61}]^{7-}$	−179.4 (2)	110
α-$[P_2W_{15}Mo_3O_{62}]^{6-}$	−179.3 (6)	114
α-$[P_2Mo_3W_{15}O_{62}]^{6-}$	−179 (6)	55
$[W_7O_{24}]^{6-}$	−178.9 (2)	118
β-$[(D_2O)_2Zn_4P_2W_{30}O_{112}]^{16-}$	−178.9	104
α_1-$[(D_2O)_2ZnP_2W_{17}O_{61}]^{8-}$	−177.3 (1)	52
$[SiW_{11}O_{39}]^{8-}$	−176.2 (2)	105
$[SiW_{11}O_{39}]^{8-}$	−176.1 (2)	119
$[SiW_{11}O_{39}]^{8-}$	−176	102
$[(\eta^5$-$C_5H_5)TiP_2W_{17}O_{61}]^{7-}$	−175.9 (2)	109
$[(\eta^5$-$C_5H_5)TiP_2W_{17}O_{61}]^{7-}$	−175.9 (2)	110
α_2-$[P_2W_{17}O_{61}]^{10-}$	−175.8 (2)	105
α_1-$[(D_2O)_2ZnP_2W_{17}O_{61}]^{8-}$	−175.7 (1)	52
$[(\eta^5$-$C_5H_4C_5H_{10}CHO)TiP_2W_{17}O_{61}]^{7-}$	−175.4 (2)	110
$[HOTiP_2W_{17}O_{61}]^{7-}$	−175.4 (2)	110
$[(\eta^5$-$C_5H_4C_6H_9)TiP_2W_{17}O_{61}]^{7-}$	−174.7 (2)	109
$[(\eta^5$-$C_5H_4C_6H_9)TiP_2W_{17}O_{61}]^{7-}$	−174.7 (2)	110
$[P_2W_{15}Nb_3O_{62}]^{9-}$	−174.3 (6)	113
α_1-$[(D_2O)_2ZnP_2W_{17}O_{61}]^{8-}$	−174.2 (1)	52
α-$[P_2W_{18}O_{62}]^{6-}$	−173.8 (12)	114
α-$[P_2W_{18}O_{62}]^{6-}$	−173.8 (12)	105
$[Zn_2(O_2W)(W_9PO_{34})_2]^{12-}$	−173.3 (4)	108
α-$P_2W_{18}O_{62}]^{6-}$	−173 (12)	55
$[\{\eta^5$-$C_5H_4(CH_2)_3OC_6H_4CHO$-4$\}TiP_2W_{17}O_{61}]^{7-}$	−172.1 (2)	110
β-$[P_2W_{18}O_{62}]^{6-}$	−171.1 (6)	114
β-$[P_2W_{18}O_{62}]^{6-}$	−171.1 (6)	104
β-$[P_2W_{18}O_{62}]^{6-}$	−171.0	113
α-$[P_2W_{18}O_{62}]^{6-}$	−170.1	120
α-$[P_2W_{18}O_{62}]^{6-}$	−170.0	113
$[\{(\eta^5$-$C_5H_5)Fe(CO)_2Sn\}_3W_{18}P_2O_{68}]^{9-}$	−169.7 (12)	101
$[HOTiP_2W_{17}O_{61}]^{7-}$	−169.7 (2)	110
$[(\eta^5$-$C_5H_4C_6H_9)TiP_2W_{17}O_{61}]^{7-}$	−169.7 (1)	109
$[(\eta^5$-$C_5H_4C_6H_9)TiP_2W_{17}O_{61}]^{7-}$	−169.7 (1)	110
$[(\eta^5$-$C_5H_4C_5H_{10}CHO)TiP_2W_{17}O_{61}]^{7-}$	−169.0 (1)	110
$[\{\eta^5$-$C_5H_4(CH_2)_3OC_6H_4CHO$-4$\}TiP_2W_{17}O_{61}]^{7-}$	−168.7 (1)	110
$[P_2W_{18}O_{62}]^{6-}$	−168 (12)	102
α_1-$[(D_2O)_2ZnP_2W_{17}O_{61}]^{8-}$	−167.6 (1)	52
$[P_2W_{18}O_{62}]^{6-}$	−167.3 (6)	116
$[(\eta^5$-$C_5H_5)TiP_2W_{17}O_{61}]^{7-}$	−167.3 (1)	109
$[(\eta^5$-$C_5H_5)TiP_2W_{17}O_{61}]^{7-}$	−167.3 (1)	110
α-$[P_2W_{18}O_{62}]^{6-}$	−166.8 (6)	102
α-$[P_2W_{12}Mo_6O_{62}]^{6-}$	−166.6 (4)	114
$Zn_2(O_2W)(W_9PO_{34})_2]^{12-}$	−166.3 (8)	108

(*Continued*)

Table 16. (*Continued*)

Compound	Chemical shift[a] (ppm)	Ref.
α-$[(D_2O)_2ZnSiW_{11}O_{39}]^{6-}$	−166.3 (2)	104
γ-$[As_2W_{18}O_{62}]^{6-}$	−166.0 (12)	114
β-$[D_2O)_2Zn_4P_2W_{30}O_{112}]^{16-}$	−162.3	104
α-$[(D_2O)_2Zn_4P_2W_{30}O_{112})^{16-}$	−162.0 (4)	104
$[P_4(H_2O)_2Zn_4W_{30}O_{112}]^{16-}$	−162.0 (4)	106
α-$[(D_2O)_2Zn_4P_2W_{30}O_{112}]^{16-}$	−160.5 (4)	104
$[P_4(H_2O)_2Zn_4W_{30}O_{112}]^{16-}$	−160.5 (4)	106
$[W_{10}O_{32}]^{4-}$	−160 (8)	102
β-$[(D_2O)_2Zn_4P_2W_{30}O_{112}]^{16-}$	−159.8	104
$[(O_2W)_2(W_9PO_{34})_2]^{14-}$	−159.6 (4)	108
α_2-$[P_2W_{17}O_{61}]^{10-}$	−159.6 (2)	105
$[(O_2W)_2(W_9PO_{34})_2]^{14-}$	−159.2 (4)	108
$[HOTiP_2W_{17}O_{61}]^{7-}$	−157.9 (1)	110
α_1-$[(D_2O)_2ZnP_2W_{17}O_{61}]^{8-}$	−157.7 (1)	52
β-$[(D_2O)_2Zn_4P_2W_{30}O_{112}]^{16-}$	−157.4	104
α-$[(D_2O)_2ZnPW_{11}O_{39}]^{5-}$	−157.1 (2)	52
$[PZnW_{11}O_{40}]^{7-}$	−157.1 (2)	108
$[(PhPO_3)_3W_5O_{15}]^{4-}$	−155.9	121
$[HSiW_{10}O_{36}]^{7-}$	−155.2	117
$[BVW_{11}O_{40}]^{6-}$	−154.8 (2)	119
$[H_2W_{18}F_6O_{56}]^{8-}$	−154 (12)	102
$[(O_5W)_3(W_9PO_{34})_2H_6]^{4-}$	−153.6 (1)	108
$[PW_{11}O_{39}]^{7-}$	−153.5 (2)	105
$[(\eta^6\text{-}C_6H_6)RuP_2W_{15}Nb_3O_{62}]^{7-}$	−152.9 (6)	113
$[(\eta^5\text{-}C_5Me_5)RhP_2W_{15}Nb_3O_{62}]^{7-}$	−152.6 (6)	113
β-$[(D_2O)_2Zn_4P_2W_{30}O_{112}]^{16-}$	−152.6	104
$[PW_{11}O_{39}]^{7-}$	−152.4 (2)	122
$[P_2W_{21}O_{71}(OH_2)_3]^{6-}$	−152.3 (3)	107
$[PW_{11}O_{39}]^{7-}$	−152.2 (2)	119
α_1-$[(D_2O)_2ZnP_2W_{17}O_{61}]^{8-}$	−151.9 (1)	52
$[(\eta^5\text{-}C_5Me_5)RhSiW_9Nb_3O_{40}]^{5-}$	−151.1 (1)	123
α-$[(D_2O)_2Zn_4P_2W_{30}O_{112}]^{16-}$	−150.4 (2)	104
$[P_4(H_2O)_2Zn_4W_{30}O_{112}]^{16-}$	−150.4 (2)	106
β-$[(D_2O)_2Zn_4P_2W_{30}O_{112}]^{16-}$	−150.4	104
α-$[P_2Mo_3W_{15}O_{62}]^{8-}$	−149 (3)	55
$[P_2W_{15}Nb_3O_{62}]^{9-}$	−148.0 (3)	113
$[\{(\eta^5\text{-}C_5H_5)Fe(CO)_2Sn\}_2W_{10}PO_{38}]^{5-}$	−146.6 (2)	111
α-$[(D_2O)_2ZnSiW_{11}O_{39}]^{6-}$	−146.4 (2)	52
$[PPbW_{11}O_{39}]^{5-}$	−146.3 (2)	119
$[(\eta^5\text{-}C_5Me_5)RhSiW_9Nb_3O_{40}]^{5-}$	−146.3 (2)	123
α_1-$[(D_2O)_2ZnP_2W_{17}O_{61}]^{8-}$	−146.1 (1)	52
$[\{(\eta^5\text{-}C_5H_5)Fe(CO)_2Sn\}_2W_{10}PO_{38}]^{5-}$	−146.0 (1)	101
α_2-$[(D_2O)_2CoP_2W_{17}O_{61}]^{8-}$	−146.0 (4)	52
α_2-$[(D_2O)_2NiP_2W_{17}O_{61}]^{8-}$	−146 (4)	52
α-$[As_2W_{18}O_{62}]^{6-}$	−145.3 (12)	114

Table 16. (*Continued*)

Compound	Chemical shift[a] (ppm)	Ref.
$[BVW_{11}O_{40}]^{6-}$	−144.5 (2)	119
$[SiW_{11}O_{39}]^{8-}$	−143.2 (2)	119
$[SiW_{11}O_{39}]^{8-}$	−143.2 (2)	105
$[Ti_2W_{10}PO_{40}]^{7-}$	−143.0 (2)	111
$[SiW_{11}O_{39}]^{8-}$	−143	102
$[BVW_{11}O_{40}]^{6-}$	−142.8 (2)	119
$[Si_2W_{18}Nb_6O_{77}]^{8-}$	−142.6 (12)	123
α-1,2-$[SiV_2W_{10}O_{39}]^{6-}$	−142.5 (1)	119
$[SiV_2W_{10}O_{40}]^{6-}$	−142.5	102
$[(O_2W)_2(W_9PO_{34})_2]^{14-}$	−142.4 (4)	108
α_2-$[P_2W_{17}VO_{62}]^{7-}$	−142.08 (2)	105
α_2-$[(D_2O)_2CoP_2W_{17}O_{61}]^{8-}$	−142 (4)	52
α_2-$[(D_2O)_2NiP_2W_{17}O_{61}]^{8-}$	−142 (4)	52
$[H_2W_{12}O_{42}]^{10-}$	−141.4 (4)	124
α_2-$[P_2W_{17}O_{61}]^{10-}$	−140.8 (2)	105
$[BVW_{11}O_{40}]^{6-}$	−140.7 (1)	119
α-$[(D_2O)_2ZnPW_{11}O_{39}]^{5-}$	−140.4 (2)	52
$[PZnW_{11}O_{40}]^{7-}$	−140.4 (2)	108
$[Si_2W_{18}Zr_3O_{71}H_n]^{n-14}$	−140 (12)	115
α-$[(D_2O)_2ZnSiW_{11}O_{39}]^{6-}$	−139.9 (1)	52
$[H_2W_{18}F_6O_{56}]^{8-}$	−139.5 (6)	102
α_2-$[(D_2O)_2ZnP_2W_{17}O_{61}]^{8-}$	−138.7 (2)	52
$[\{(\eta^5\text{-}C_5H_5)Fe(CO)_2Sn\}_2W_{10}PO_{38}]^{5-}$	−136.8 (2)	101
α-1,2,3-$[SiV_3W_{10}O_{39}]^{7-}$	−136.7 (3)	119
$[SiV_3W_9O_{40}]^{7-}$	−136.7	102
$[(D_2O)_2Zn_4P_2W_{18}O_{68}]^{10-}$	−135.6 (4)	125
$[(D_2O)_2Zn_4P_2W_{18}O_{68}]^{10-}$	−134.9 (4)	104
$[\{(\eta^5\text{-}C_5H_5)Fe(CO)_2Sn\}_2W_{10}PO_{38}]^{5-}$	−134.5 (2)	101
$[(D_2O)_2Zn_4P_2W_{18}O_{68}]^{10-}$	−134.2 (4)	126
α-$[P_2W_{15}Mo_3O_{62}]^{6-}$	−134.1 (3)	114
α-$[P_2Mo_3W_{15}O_{62}]^{6-}$	−134 (3)	55
α-$[(D_2O)_2NiSiW_{11}O_{39}]^{6-}$	−133.9 (2)	52
$[PW_{11}O_{39}]^{7-}$	−133.6 (2)	105
$[PW_{11}O_{39}]^{7-}$	−132.4 (2)	119
$[(\eta^5\text{-}C_5H_5)TiSiW_9V_3O_{40}]^{4-}$	−132.2 (2)	127
β-$[(D_2O)_2Zn_4P_2W_{30}O_{112}]^{16-}$	−131.7	104
$[BW_{12}O_{40}H_6]^{5-}$	−131.6 (6)	128
$[P_2W_{21}O_{71}(OH_2)_3]^{6-}$	−131.2 (3)	107
β-$[P_2W_{18}O_{62}]^{6-}$	−131.1 (3)	114
β-$[P_2W_{18}O_{62}]^{6-}$	−131.1 (3)	105
β-$[P_2W_{18}O_{62}]^{6-}$	−131.0	113
$[B_2W_{12}O_{40}]^{5-}$	−130.8	105
β-$[H_2W_{12}O_{40}]^{6-}$	−130.6 (3)	102
α-$[(D_2O)_2ZnPW_{11}O_{39}]^{5-}$	−130.6 (2)	52

(*Continued*)

Table 16. (*Continued*)

Compound	Chemical shift[a] (ppm)	Ref.
$[PZnW_{11}O_{40}]^{7-}$	−130.6 (2)	108
$[(D_2O)_2Zn_4P_2W_{18}O_{68}]^{10-}$	−130.5 (4)	125
$[PW_{11}O_{39}]^{7-}$	−130.5 (2)	122
$[BW_{12}O_{40}]^{5-}$	−130.4	129
$[BW_{12}O_{40}]^{5-}$	−130.4	102
α-$[P_2W_{12}Mo_6O_{62}]^{6-}$	−130.3 (4)	114
$[(O_5W)_3(W_9PO_{34})_2H_6]^{4-}$	−130.3 (4)	108
$[(\eta^5\text{-}C_5H_4C_6H_9)TiP_2W_{17}O_{61}]^{7-}$	−130.2 (2)	109
$[(\eta^5\text{-}C_5H_4C_6H_9)TiP_2W_{17}O_{61}]^{7-}$	−130.2 (2)	110
α-1,2,3-$[PV_3W_{10}O_{39}]^{6-}$	−130.1 (3)	119
$[\{\eta^5\text{-}C_5H_4(CH_2)_3OC_6H_4CHO\text{-}4\}TiP_2W_{17}O_{61}]^{7-}$	−130.1 (2)	110
α-$[(D_2O)_2ZnPW_{11}O_{39}]^{5-}$	−130.1 (1)	52
$[PZnW_{11}O_{40}]^{7-}$	−130.1 (1)	108
$[HOTiP_2W_{17}O_{61}]^{7-}$	−130.0 (2)	110
$[BW_{12}O_{40}]^{5-}$	−130	53
$[(\eta^5\text{-}C_5H_4C_5H_{10}CHO)TiP_2W_{17}O_{61}]^{7-}$	−129.9 (2)	110
β-$[SiW_{12}O_{40}]^{4-}$	−129.8 (3)	102
β-$[SiW_{12}O_{40}]^{4-}$	−129.8 (3)	130
$[P_2W_{21}O_{71}(OH_2)_3]^{6-}$	−129.7 (3)	107
$[HW_{12}FO_{39}]^{6-}$	−129.7 (3)	102
$[(D_2O)_2Zn_4P_2W_{18}O_{68}]^{10-}$	−129.6 (4)	104
$[(\eta^5\text{-}C_5H_5)TiP_2W_{17}O_{61}]^{7-}$	−129.5 (2)	109
$[(\eta^5\text{-}C_5H_5)TiP_2W_{17}O_{61}]^{7-}$	−129.5 (2)	110
$[(\eta^5\text{-}C_5H_5)TiSiW_9V_3O_{40}]^{4-}$	−129.3 (2)	127
$[(O_5W)_3(W_9PO_{34})_2H_6]^{4-}$	−129.2 (4)	108
$[(D_2O)_2Zn_4As_2W_{18}O_{68}]^{10-}$	−129.0 (4)	125
$[(\eta^5\text{-}C_5Me_5)RhP_2W_{15}Nb_3O_{62}]^{7-}$	−128.9 (3)	113
α-1,2-$[PV_2W_{10}O_{39}]^{5-}$	−128.8 (1)	119
$[BW_{12}O_{40}]^{5-}$	−128.5	128
$[SiW_{11}O_{39}]^{8-}$	−128.5	102
$[(D_2O)_2Zn_4P_2W_{18}O_{68}]^{10-}$	−128.4 (4)	126
$[(\eta^6\text{-}C_6H_6)RuP_2W_{15}Nb_3O_{62}]^{7-}$	−128.2 (3)	113
α-$[P_2W_{18}O_{62}]^{6-}$	−128.1 (6)	114
α-$[P_2W_{18}O_{62}]^{6-}$	−128.1 (6)	105
$[SiVW_{11}O_{40}]^{5-}$	−128.0 (2)	119
$[SiVW_{11}O_{40}]^{5-}$	−128.0	102
$[SiW_{11}O_{39}]^{8-}$	−127.9 (2)	119
$[SiW_{11}O_{39}]^{8-}$	−127.9 (2)	105
α_2-$[P_2W_{17}O_{61}]^{10-}$	−127.9 (2)	105
$[\{(\eta^5\text{-}C_5H_5)Fe(CO)_2Sn\}_2W_{10}PO_{38}]^{5-}$	−127.8 (2)	111
$[P_2W_{18}O_{62}]^{6-}$	−127.4 (3)	116
$[PPbW_{11}O_{39}]^{5-}$	−127.4 (2)	119
α-$[P_2W_{18}O_{62}]^{6-}$	−127.2 (3)	102
$[HOTiP_2W_{17}O_{61}]^{7-}$	−127.2 (2)	110
$[Ti_2W_{10}PO_{40}]^{7-}$	−127.0 (2)	111

Table 16. (*Continued*)

Compound	Chemical shift[a] (ppm)	Ref.
α-$[P_2W_{18}O_{62}]^{6-}$	−127 (6)	55
$[BVW_{11}O_{40}]^{6-}$	−126.4 (2)	119
$[(D_2O)_2Zn_4As_2W_{18}O_{68}]^{10-}$	−126.1 (4)	125
$[Ti_2W_{10}PO_{40}]^{7-}$	−125.5 (2)	111
α-$[P_2W_{18}O_{62}]^{6-}$	−125.0	113
$[Fe^{III}W_{12}O_{40}]^{5-}$	−125	53
$[P_2W_{21}O_{71}(OH_2)_3]^{6-}$	−124.7 (3)	107
α-$[P_2W_{18}O_{62}]^{6-}$	−124.2	120
$[(O_5W)_3(W_9PO_{34})_2H_6]^{4-}$	−123.9 (2)	108
$[(\eta^5\text{-}C_5H_4C_5H_{10}CO_2H)TiPW_{11}O_{39}]^{4-}$	−123.8 (4)	110
$[(\eta^5\text{-}C_5H_4C_6H_9)TiPW_{11}O_{39}]^{4-}$	−123.8 (2)	110
$[(\eta^5\text{-}C_5H_4C_5H_{10}CHO)TiPW_{11}O_{39}]^{4-}$	−123.8 (1)	110
$[(\eta^5\text{-}C_5H_4C_6H_{12}OH)TiPW_{11}O_{39}]^{4-}$	−123.6 (4)	110
$[(\eta^5\text{-}(C_5H_4C_6H_{12}NH_2)TiPW_{11}O_{39}]^{4-}$	−123.4 (4)	110
$[\{(\eta^5\text{-}C_5H_5)Fe(CO)_2Sn\}_2W_{10}PO_{38}]^{5-}$	−123.4 (2)	101
$[(\eta^5\text{-}C_5H_4C_5H_{10}CHO)TiPW_{11}O_{39}]^{4-}$	−123.4 (2)	110
$[(\eta^5\text{-}C_5H_4C_6H_9)TiPW_{11}O_{39}]^{4-}$	−123.4 (2)	110
α_1-$[(D_2O)_2ZnP_2W_{17}O_{61}]^{8-}$	−123.0 (1)	52
$[P_2W_{18}O_{62}]^{6-}$	−123 (6)	102
$[PW_{11}O_{39}]^{7-}$	−122.9 (1)	105
α1,2-$[SiV_2W_{10}O_{39}]^{6-}$	−122.7 (2)	119
$[SiV_2W_{10}O_{40}]^{6-}$	−122.7	102
$[SiW_9Nb_3O_{40}]^{7-}$	−122.1 (3)	123
α-$[As_2W_{18}O_{62}]^{6-}$	−121.9 (6)	114
β-$[(D_2O)_2Zn_4P_2W_{30}O_{112}]^{16-}$	−121.8	104
$[PW_{11}O_{39}]^{7-}$	−121.4 (1)	119
$[SiW_{11}O_{39}]^{8-}$	−121.3 (1)	119
$(SiW_{11}O_{39})^{8-}$	−121.3 (1)	105
$[SiVW_{11}O_{40}]^{5-}$	−121.0 (2)	119
$[SiVW_{11}O_{40}]^{5-}$	−121.0	102
$[SiW_{11}O_{39}]^{8-}$	−121	102
β-$[H_2W_{12}O_{40}]^{6-}$	−120.6 (6)	102
α-$[(D_2O)_2NiPW_{11}O_{39}]^{5-}$	−120.6 (2)	52
$[HSiW_{10}O_{36}]^{7-}$	−120.5	117
$[D_2W_{12}O_{40}]^{6-}$	−120.0	105
1,4-$[PV_2W_{10}O_{40}]^{5-}$	−119.3 (2)	131
$[\{(\eta^5\text{-}C_5H_5)Fe(CO)_2Sn\}_2W_{10}PO_{38}]^{5-}$	−119.0 (2)	101
$[PTiW_{11}O_{39}]^{5-}$	−118.0 (2)	119
$[(D_2O)_2Zn_4P_2W_{18}O_{68}]^{10-}$	−117.8 (4)	125
$[ClTiPW_{11}O_{39}]^{4-}$	−117.4 (2)	132
α_1-$[(D_2O)_2ZnP_2W_{17}O_{61}]^{8-}$	−117.4 (1)	52
$[(\eta^5\text{-}C_5H_4C_6H_{10}NH_2)TiPW_{11}O_{39}]^{4-}$	−116.8 (2)	132
α-1,2-$[PV_2W_{10}O_{39}]^{5-}$	−116.7 (2)	119
$[(\eta^5\text{-}C_5H_4C_2H_4CH{=}CHCH{=}CH_2)TiPW_{11}O_{39}]^{4-}$	−116.6 (2)	132

(*Continued*)

Table 16. (*Continued*)

Compound	Chemical shift[a] (ppm)	Ref.
$[(D_2O)_2Zn_4P_2W_{18}O_{68}]^{10-}$	−116.5 (4)	104
$[\{\eta^5\text{-}C_5H_4C_5H_{10}CH(OMe)_2\}TiPW_{11}O_{39}]^{4-}$	−116.3 (2)	132
$[(\eta^5\text{-}C_5H_4C_6H_{12}OR)TiPW_{11}O_{39}]^{4-}$	−116.3 (2)	132
$[(\eta^5\text{-}C_5H_4C_5H_{10}CO_2Bu^t)TiPW_{11}O_{39}]^{4-}$	−116.2 (2)	132
$[SiW_{11}O_{39}]^{8-}$	−116.1 (2)	119
$[SiW_{11}O_{39}]^{8-}$	−116.1 (2)	105
$[SiW_{11}O_{39}]^{8-}$	−116	102
$\alpha\text{-}[(D_2O)_2ZnSiW_{11}O_{39}]^{6-}$	−115.1 (2)	52
$[H_2W_{12}O_{40}H_6]^{6-}$	−115.0 (6)	128
$[(D_2O)_2Zn_4P_2W_{18}O_{68}]^{10-}$	−115.0 (4)	126
$[HW_{12}FO_{39}]^{6-}$	−114.8 (6)	102
$\beta\text{-}[SiW_{12}O_{40}]^{4-}$	−114.7 (6)	102
$\beta\text{-}[SiW_{12}O_{40}]^{4-}$	−114.7 (6)	130
$1,4\text{-}[PV_2W_{10}O_{40}]^{5-}$	−114.7 (2)	131
$[PW_{11}O_{39}]^{7-}$	−114.7 (2)	122
$[SiVW_{11}O_{40}]^{5-}$	−114.6 (2)	119
$[SiVW_{11}O_{40}]^{5-}$	−114.6 (1)	119
$[SiVW_{11}O_{40}]^{5-}$	−114.6	102
$[H_2W_{12}O_{42}]^{10-}$	−114.5 (2)	118
$[PW_{11}O_{39}]^{7-}$	−114.3 (1)	122
$[Si_2W_{18}Nb_6O_{77}]^{8-}$	−114.3 (6)	123
$[BVW_{11}O_{40}]^{6-}$	−113.2 (2)	119
$[(\eta^5\text{-}C_5H_4C_5H_{10}CO_2H)TiPW_{11}O_{39}]^{4-}$	−113.0 (2)	110
$[H_2W_{12}O_{40}]^{6-}$	−113.0	105
$[HSiV_3W_9O_{40}]^{6-}$	−112.9 (2)	133
$[(\eta^5\text{-}C_5H_4C_6H_{12}OH)TiPW_{11}O_{39}]^{4-}$	−112.8 (2)	110
$[(\eta^5\text{-}C_5H_4C_6H_9)TiPW_{11}O_{39}]^{4-}$	−112.8 (2)	110
$[(\eta^5\text{-}C_5H_4C_6H_{12}NH_2)TiPW_{11}O_{39}]^{4-}$	−112.8 (2)	110
$1,4\text{-}[PV_2W_{10}O_{40}]^{5-}$	−112.7 (2)	131
$[(\eta^5\text{-}C_5H_4C_2H_4CH{=}CHCH{=}CH_2)TiPW_{11}O_{39}]^{4-}$	−112.6 (2)	110
$[(\eta^5\text{-}C_5H_4C_6H_{12}OR)TiPW_{11}O_{39}]^{4-}$	−112.5 (2)	110
$[Ti_2W_{10}PO_{40}]^{7-}$	−112.5 (2)	111
$[(\eta^5\text{-}C_5H_4C_6H_{10}NH_2)TiPW_{11}O_{39}]^{4-}$	−112.5 (2)	110
$[(\eta^5\text{-}C_5H_4C_5H_{10}CHO)TiPW_{11}O_{39}]^{4-}$	−112.4 (2)	110
$[(\eta^5\text{-}C_5H_4C_5H_{10}CO_2Bu^t)TiPW_{11}O_{39}]^{4-}$	−112.4 (2)	110
$[\{\eta^5\text{-}C_5H_4C_5H_{10}CH(OMe)_2\}TiPW_{11}O_{39}]^{4-}$	−112.4 (2)	110
$[(\eta^5\text{-}C_5H_5)TiSiW_9V_3O_{40}]^{4-}$	−112.3 (1)	127
$\beta\text{-}[P_2W_{18}O_{62}]^{6-}$	−112.0	113
$[SiW_9Nb_3O_{40}]^{7-}$	−112.0 (6)	123
$\alpha\text{-}1,2\text{-}[SiV_2W_{10}O_{39}]^{6-}$	−111.7 (2)	119
$\alpha\text{-}1,2\text{-}[SiV_2W_{10}O_{39}]^{6-}$	−111.7 (1)	119
$[SiV_2W_{10}O_{40}]^{6-}$	−111.7	102
$\beta\text{-}[P_2W_{18}O_{62}]^{6-}$	−111.6 (3)	114
$\beta\text{-}[P_2W_{18}O_{62}]^{6-}$	−111.6 (3)	105
$[PPbW_{11}O_{39}]^{5-}$	−111.5 (1)	119

Table 16. (*Continued*)

Compound	Chemical shift[a] (ppm)	Ref.
$[H_2W_{12}O_{40}]^{6-}$	−111.3	129
$[H_2W_{12}O_{40}]^{6-}$	−111.3	102
$[H_3SiV_3W_9O_{40}]^{4-}$	−110.1 (3)	133
γ-$[As_2W_{18}O_{62}]^{6-}$	−110.0 (6)	114
$[HW_{12}F_2O_{38}]^{5-}$	−110.0 (4)	102
$[H_2W_{12}O_{42}]^{10-}$	−110 (4)	134
$[H_2W_{12}O_{40}]^{6-}$	−110	53
β-$[SiW_{12}O_{40}]^{4-}$	−109.7 (3)	102
β-$[SiW_{12}O_{40}]^{4-}$	−109.7 (3)	130
$[H_2W_{12}O_{40}]^{6-}$	−109.5	128
$[\{(\eta^5\text{-}C_5H_5)Fe(CO)_2Sn\}_3W_{18}P_2O_{68}]^{9-}$	−109.2 (6)	101
$[PTiW_{11}O_{39}]^{5-}$	−109.2 (2)	119
$[PVW_{11}O_{40}]^{4-}$	−108.7 (2)	119
$[(O_5W)_3(W_9PO_{34})_2H_6]^{4-}$	−108.6 (6)	108
$[H_2W_{12}FO_{39}]^{5-}$	−108.6 (3)	102
$[H_2W_{12}FO_{39}]^{5-}$	−108.6 (3)	130
$[ClTiPW_{11}O_{39}]^{4-}$	−108.6 (2)	132
$[P_2W_{21}O_{71}(OH_2)_3]^{6-}$	−108.5 (3)	107
$[H_3SiV_3W_9O_{40}]^{4-}$	−108.4 (6)	133
$[P_2W_{21}O_{71}(OH_2]_3]^{6-}$	−108.3 (3)	107
$[H_2W_{12}O_{42}]^{10-}$	−108.2 (2)	134
$[\{(\eta^5\text{-}C_5H_5)Fe(CO)_2Sn\}_2W_{10}PO_{38}]^{5-}$	−108.1 (2)	111
1,4-$[PV_2W_{10}O_{40}]^{5-}$	−107.9 (2)	131
$[P_2W_{18}O_{62}]^{6-}$	−107.7 (3)	116
α-$[P_2W_{18}O_{62}]^{6-}$	−107.5 (3)	102
$[BW_{12}O_{40}H_6]^{5-}$	−107.4 (3)	128
β-$[H_2W_{12}O_{40}]^{6-}$	−107.2 (3)	102
$[PV_2W_{10}O_{40}]^{5-}$	−107.2 (2)	131
$[HW_{12}FO_{39}]^{6-}$	−107.0 (3)	102
$[PVW_{11}O_{40}]^{4-}$	−106.7 (2)	119
$[PTiW_{11}O_{39}]^{5-}$	−106.7 (2)	119
α-1,2-$[PV_2W_{10}O_{39}]^{5-}$	−106.7 (2)	119
$[SiW_{12}O_{40}H_6]^{4-}$	−106.6 (6)	128
α-$[(D_2O)_2ZnPW_{11}O_{39}]^{5-}$	−106.5 (2)	52
$[PZnW_{11}O_{40}]^{7-}$	−106.5 (2)	108
$[ClTiPW_{11}O_{39}]^{4-}$	−106.1 (2)	132
$[(D_2O)_2Zn_4P_2W_{18}O_{68}]^{10-}$	−105.8 (4)	125
$[(D_2O)_2Zn_4P_2W_{18}O_{68}]^{10-}$	−105.8 (4)	104
$[(\eta^5\text{-}C_5H_4C_5H_{10}CO_2H)TiPW_{11}O_{39}]^{4-}$	−105.6 (1)	110
$[(\eta^5\text{-}C_5H_4C_6H_{12}NH_2)TiPW_{11}O_{39}]^{4-}$	−105.6 (1)	110
$[HW_{12}F_6O_{37}]^{4-}$	−105.5 (3)	102
$[(D_2O)_2Zn_4P_2W_{18}O_{68}]^{10-}$	−105.4 (4)	126
$[(\eta^5\text{-}C_5H_4C_6H_{12}OH)TiPW_{11}O_{39}]^{4-}$	−105.3 (1)	110
$[(\eta^5\text{-}C_5H_4C_6H_9)TiPW_{11}O_{39}]^{4-}$	−105.3 (1)	110

(*Continued*)

Table 16. (*Continued*)

Compound	Chemical shift[a] (ppm)	Ref.
$[PW_{11}O_{39}]^{7-}$	−105.1 (2)	105
$[(\eta^5\text{-}C_5H_4C_5H_{10}CO_2H)TiPW_{11}O_{39}]^{4-}$	−105.0 (2)	110
$[(\eta^5\text{-}C_5H_4C_5H_{10}CHO)TiPW_{11}O_{39}]^{4-}$	−105.0 (1)	110
$[(\eta^5\text{-}C_5H_4C_6H_9)TiPW_{11}O_{39}]^{4-}$	−104.9 (2)	110
$[(\eta^5\text{-}C_5H_4C_6H_{12}OH)TiPW_{11}O_{39}]^{4-}$	−104.6 (2)	110
$[(\eta^5\text{-}C_5H_4C_5H_{10}CHO)TiPW_{11}O_{39})^{4-}$	−104.6 (2)	110
$[(\eta^5\text{-}C_5H_4C_6H_{12}NH_2)TiPW_{11}O_{39}]^{4-}$	−104.4 (2)	110
$[SiVW_{11}O_{40}]^{5-}$	−104.3 (2)	119
$[SiVW_{11}O_{40}]^{5-}$	−104.3	102
$[H_2W_{12}FO_{39}]^{5-}$	−104.1 (6)	130
$[H_2W_{12}FO_{39}]^{5-}$	−104.0 (6)	102
$[Zn_2(O_2W)(W_9PO_{34})_2]^{12-}$	−103.8 (4)	108
$[SiW_{12}O_{40}]^{4-}$	−103.8	129
$[SiW_{12}O_{40}]^{4-}$	−103.8	102
$[SiW_{12}O_{40}]^{4-}$	−103.8	105
$[PVW_{11}O_{40}]^{4-}$	−103.7 (1)	119
$[(O_2W)_2(W_9PO_{34})_2]^{14-}$	−103.6 (4)	108
$[PW_{11}O_{39}]^{7-}$	−103.6 (2)	119
$[HW_{12}F_2O_{38}]^{5-}$	−103.3 (2)	102
$[SiW_{12}O_{40}]^{4-}$	−103	55
$[PPbW_{11}O_{39}]^{5-}$	−102.8 (2)	119
$[SiW_{12}O_{40}]^{4-}$	−102.5	128
$[PTiW_{11}O_{39}]^{5-}$	−101.9 (1)	119
$[(\eta^5\text{-}C_5H_4C_6H_{10}NH_2)TiPW_{11}O_{39}]^{4-}$	−101.7 (2)	132
$[PVW_{11}O_{40}]^{4-}$	−101.2 (2)	119
$[ClTiPW_{11}O_{39}]^{4-}$	−101.2 (1)	132
$[(\eta^5\text{-}C_5Me_5)RhSiW_9Nb_3O_{40}]^{5-}$	−101.0 (2)	123
$[Cu^{II}W_{12}O_{40}]^{6-}$	−101	53
$[SiW_{11}O_{39}]^{8-}$	−101	102
$[SiW_{11}O_{39}]^{8-}$	−100.9 (2)	105
$[PW_{11}O_{39}]^{7-}$	−100.9 (2)	105
$[SiW_{11}O_{39}]^{8-}$	−100.8 (2)	119
$[(\eta^5\text{-}C_5H_4C_2H_4CH{=}CHCH{=}CH_2)TiPW_{11}O_{39}]^{4-}$	−100.7 (2)	132
$[(\eta^5\text{-}C_5H_4C_6H_{12}OR)TiPW_{11}O_{39}]^{4-}$	−100.6 (2)	132
$[\{\eta^5\text{-}C_5H_4C_5H_{10}CH(OMe)_2\}TiPW_{11}O_{39}]^{4-}$	−100.6 (2)	132
$[(\eta^5\text{-}C_5H_4C_5H_{10}CO_2Bu^t)TiPW_{11}O_{39}]^{4-}$	−100.5 (2)	132
$[H_2W_{12}F_2O_{38}]^{4-}$	−100.0 (4)	102
$[(D_2O)_2Zn_4As_2W_{18}O_{68}]^{10-}$	−99.6 (4)	125
$\alpha_1\text{-}[(D_2O)_2ZnP_2W_{17}O_{61}]^{8-}$	−99.4 (1)	52
$[PW_{12}O_{40}]^{3-}$	−99.4	105
$[HSiV_3W_9O_{40}]^{6-}$	−99 (2)	133
$[PW_{11}O_{39}]^{7-}$	−98.8 (2)	119
$[PW_{12}O_{40}]^{3-}$	−98.8	129
$[PW_{12}O_{40}]^{3-}$	−98.8	102
$[PVW_{11}O_{40}]^{4-}$	−98.6 (2)	119

Table 16. (*Continued*)

Compound	Chemical shift[a] (ppm)	Ref.
$[PW_{11}O_{39}]^{7-}$	−98.2 (2)	122
$[PW_{11}O_{39}]^{7-}$	−98.1 (2)	119
[(*N*,*N*′,*N*″-Me_3-1,4,7-triazacyclononane)WO_3]	−98	135
1,4-$[PV_2W_{10}O_{40}]^{5-}$	−97.5 (1)	131
$[HW_{12}F_2O_{38}]^{5-}$	−97 (6)	102
$[ZnW_{12}O_{40}]^{6-}$	−95.8	105
$[(\eta^5\text{-}C_5H_4C_2H_4CH{=}CHCH{=}CH_2)TiPW_{11}O_{39}]^{4-}$	−94.8 (3)	132
$[(\eta^5\text{-}C_5H_4C_6H_{10}NH_2)TiPW_{11}O_{39}]^{4-}$	−94.8 (3)	132
$[(\eta^5\text{-}C_5H_4C_6H_{12}OR)TiPW_{11}O_{39}]^{4-}$	−94.5 (3)	132
$[\{\eta^5\text{-}C_5H_4C_5H_{10}CH(OMe)_2\}TiPW_{11}O_{39}]^{4-}$	−94.5 (3)	132
$[H_2W_{12}FO_{39}]^{5-}$	−94.5 (3)	102
$[(\eta^5\text{-}C_5H_4C_5H_{10}CO_2Bu^t)TiPW_{11}O_{39}]^{4-}$	−94.4 (3)	132
$[PW_{11}O_{39}]^{7-}$	−94.4 (2)	122
$[H_2W_{12}FO_{39}]^{5-}$	−94.3 (3)	130
$[PV_2W_{10}O_{40}]^{5-}$	−94.0 (2)	131
$[(D_2O)_2Zn_4As_2W_{18}O_{68}]^{10-}$	−93.9 (4)	125
$[HSiV_3W_9O_{40}]^{6-}$	−93.3 (2)	133
$[PTiW_{11}O_{39}]^{5-}$	−92.6 (2)	119
$[(\eta^5\text{-}C_5H_4C_6H_9)TiP_2W_{17}O_{61}]^{7-}$	−92.3 (2)	109
$[(\eta^5\text{-}C_5H_4C_6H_9)TiP_2W_{17}O_{61}]^{7-}$	−92.3 (2)	110
$[(\eta^5\text{-}C_5H_4C_5H_{10}CHO)TiP_2W_{17}O_{61}]^{7-}$	−92.1 (2)	110
$[ClTiPW_{11}O_{39}]^{4-}$	−92.0 (2)	110
α-1,2-$[PV_2W_{10}O_{39}]^{5-}$	−91.9 (1)	119
$[W_7O_{24}]^{6-}$	−91.8 (4)	134
$[\{\eta^5\text{-}C_5H_4(CH_2)_3OC_6H_4CHO\text{-}4\}TiP_2W_{17}O_{61}]^{7-}$	−91.7 (2)	110
α-1,2,3-$[SiV_3W_{10}O_{39}]^{7-}$	−91.5 (6)	119
$[SiV_3W_9O_{40}]^{7-}$	−91.5	102
$[(D_2O)_2Zn_4P_2W_{18}O_{68}]^{10-}$	−90.7 (2)	125
$[(\eta^5\text{-}C_5H_5)TiP_2W_{17}O_{61}]^{7-}$	−90.7 (2)	109
$[(\eta^5\text{-}C_5H_5)TiP_2W_{17}O_{61}]^{7-}$	−90.7 (2)	110
$[(\eta^5\text{-}C_5Me_5)RhSiW_9Nb_3O_{40}]^{5-}$	−90.4 (2)	123
$[(D_2O)_2Zn_4P_2W_{18}O_{68}]^{10-}$	−90.3 (2)	104
$[HW_{12}F_6O_{37}]^{4-}$	−90 (9)	102
$[SiW_{12}O_{40}H_6]^{4-}$	−89.9 (3)	128
$[HSiV_3W_9O_{40}]^{6-}$	−88.1 (2)	133
α-1,2,3-$[PV_3W_{10}O_{39}]^{6-}$	−86.6 (6)	119
α-1,2-$[SiV_2W_{10}O_{39}]^{6-}$	−86.0 (2)	119
$[SiV_2W_{10}O_{40}]^{6-}$	−86.0	102
$[H_2W_{12}F_2O_{38}]^{4-}$	−85 (6)	102
α-1,2-$[SiV_2W_{10}O_{39}]^{6-}$	−83.5 (2)	119
$[SiV_2W_{10}O_{40}]^{6-}$	−83.5	102
$[HSiV_3W_9O_{40}]^{6-}$	−83.3 (1)	133
α_2-$[(D_2O)_2ZnP_2W_{17}O_{61}]^{8-}$	−83.2 (2)	52
$[PPbW_{11}O_{39}]^{5-}$	−82.7 (2)	119

(*Continued*)

Table 16. (*Continued*)

Compound	Chemical shift[a] (ppm)	Ref.
$[H_2W_{12}F_2O_{38}]^{4-}$	−82.6 (2)	102
α-1,2-$[PV_2W_{10}O_{39}]^{5-}$	−82.2 (2)	119
$[PV_2W_{10}O_{40}]^{5-}$	−82.2 (1)	131
$[H_2W_{12}O_{40}H_6]^{6-}$	−82.0 (3)	128
$[GeW_{12}O_{40}]^{4-}$	−81.9	105
$[SiVW_{11}O_{40}]^{5-}$	−81.1 (2)	119
$[SiVW_{11}O_{40}]^{5-}$	−81.1	102
α-1,2-$[PV_2W_{10}O_{39}]^{5-}$	−80.8 (2)	119
$[(\eta^5\text{-}C_5H_4C_5H_{10}CO_2H)TiPW_{11}O_{39}]^{4-}$	−80.7 (2)	110
$[(\eta^5\text{-}C_5H_4C_6H_9)TiPW_{11}O_{39}]^{4-}$	−80.7 (2)	110
$[(\eta^5\text{-}C_5H_4C_6H_{12}NH_2)TiPW_{11}O_{39}]^{4-}$	−80.7 (2)	110
$[(\eta^5\text{-}C_5H_4C_6H_{12}OH)TiPW_{11}O_{39}]^{4-}$	−80.4 (2)	110
$[(\eta^5\text{-}C_5H_4C_5H_{10}CHO)TiPW_{11}O_{39}]^{4-}$	−80.0 (2)	110
$[(D_2O)_2Zn_4As_2W_{18}O_{68}]^{10-}$	−79.7 (2)	125
$[(\eta^5\text{-}C_5H_4C_6H_{10}NH_2)TiPW_{11}O_{39}]^{4-}$	−78.6 (2)	110
$[(\eta^5\text{-}C_5H_4C_2H_4CH{=}CHCH{=}CH_2)TiPW_{11}O_{39}]^{4-}$	−77.0 (2)	110
$[(\eta^5\text{-}C_5H_4C_5H_{10}CO_2Bu^t)TiPW_{11}O_{39}]^{4-}$	−76.7 (2)	110
$[\{\eta^5\text{-}C_5H_4C_5H_{10}CH(OMe)_2\}TiPW_{11}O_{39}]^{4-}$	−76.7 (2)	110
$[(\eta^5\text{-}C_5H_4C_6H_{12}OR)TiPW_{11}O_{39}]^{4-}$	−76.6 (2)	110
$[(O_2W)_2(W_9PO_{34})_2]^{14-}$	−74.6 (2)	108
$[PPbW_{11}O_{39}]^{5-}$	−74.47 (2)	119
$[Ti_2W_{10}PO_{40}]^{7-}$	−73.4 (2)	111
α-$[(D_2O)_2ZnPW_{11}O_{39}]^{5-}$	−73.0 (2)	52
$[PZnW_{11}O_{40}]^{7-}$	−73.0 (2)	108
$[PVW_{11}O_{40}]^{4-}$	−72.2 (2)	119
α-$[(D_2O)_2ZnSiW_{11}O_{39}]^{6-}$	−71.6 (2)	52
$[(\eta^5\text{-}C_5H_5)TiSiW_9V_3O_{40}]^{4-}$	−71.5 (2)	127
$[(\eta^5\text{-}C_5H_5)TiSiW_9V_3O_{40}]^{4-}$	−71.5 (2)	127
$[PTiW_{11}O_{39}]^{5-}$	−57.2 (2)	119
$[ClTiPW_{11}O_{39}]^{4-}$	−56.9 (2)	132
α-$[P_2W_{18}O_{62}]^{8-}$	−51 (12)	55
$[(\eta^5\text{-}C_5Me_5)RhSiW_9Nb_3O_{40}]^{5-}$	−49.2 (2)	123
1,4-$[PV_2W_{10}O_{40}]^{5-}$	−48.8 (1)	131
$[SiW_{12}O_{40}]^{6-}$	−43	55
$[W_{10}O_{32}]^{4-}$	−20 (2)	102
$[ZrW_5O_{19}H_2]^{2-}$	34.6 (4)	136
$[ZrW_5O_{19}H_2]^{2-}$	45 (1)	136
$[Nb_2W_4O_{19}]^{4-}$	47.7 (2)	137
$[W_6O_{19}]^{2-}$	58 (1)	136
$[V_2W_4O_{19}]^{3-}$	69.4 (1)	119
$[V_2W_4O_{19}]^{3-}$	70.3 (4)	119
$[VW_5O_{19}]^{3-}$	75.9 (1)	119
$[VW_5O_{19}]^{3-}$	76.4 (4)	119
$[Nb_2W_4O_{19}]^{4-}$	80.3 (2)	137
$[W_7O_{24}]^{6-}$	269.2 (1)	134

Table 16. (*Continued*)

Compound	Chemical shift[a] (ppm)	Ref.
α-$[(D_2O)_2NiSiW_{11}O_{39}]^{6-}$	307.9 (2)	52
α-$[(D_2O)_2NiSiW_{11}O_{39}]^{6-}$	327.7 (2)	52
α_2-$[(D_2O)_2NiP_2W_{17}O_{61}]^{8-}$	338.7 (2)	52
α-$[(D_2O)_2CoSiW_{11}O_{39}]^{6-}$	390.2 (2)	52
α-$[(D_2O)_2CoSiW_{11}O_{39}]^{6-}$	437.6 (2)	52
α_2-$[(D_2O)_2NiP_2NiP_2W_{17}O_{61}]^{8-}$	468.3 (2)	52
α_2-$[(D_2O)_2CoP_2W_{17}O_{61}]^{8-}$	475.7 (2)	52
α_2-$[(D_2O)_2CoP_2W_{17}O_{61}]^{8-}$	533.7 (2)	52
α-$[(D_2O)_2NiPW_{11}O_{39}]^{5-}$	592.9 (2)	52
α-$[(D_2O)_2NiPW_{11}O_{39}]^{5-}$	642.3 (2)	52
α-$[(D_2O)_2CoPW_{11}O_{39}]^{5-}$	725 (2)	52
α-$[(D_2O)_2CoPW_{11}O_{39}]^{5-}$	817.8 (2)	52
$[WO_3S]^{2-}$	841	138
$[W_2OS_3\{S_2CNBu^i\}_2]$	881.8 (W=S)	139
$[W_3O_4(H_2O)_9]^{4+}$	1138.4	128
$[D_2W_{12}O_{40}H_6]^{6-}$	1354.3 (3)	128
$[HDW_{12}O_{40}H_6]^{6-}$	1354.8 (3)	128
$[H_2W_{12}O_{40}H_6]^{6-}$	1355.4 (3)	128
$[BW_{12}O_{40}H_6]^{5-}$	1452.8 (3)	128
$[SiW_{12}O_{40}H_6]^{4-}$	1544.6 (3)	128
$[WO_2S_2]^{2-}$	1787	138
$[(NC)CuS_2WOS]^{2-}$	1994	138
$[Co^{III}W_{12}O_{40}]^{5-}$	2000	53
$[W_2S_{12}]^{2-}$	2131.9	139
$[WCl_6]$	2181	12
$[W_2OS_3\{S_2CNBu^i\}_2]$	2239.7 (W=O)	139
$[W_2S_4\{S_2CNBu^i\}_2]$	2270.5	139
$[(NC)CuS_2WS_2Cu(CN)]^{2-}$	2641	138
$[WOS_3]^{2-}$	2760	138
$[Rh(WS_4)_3]^{3-}$	2948	140
$[(NC)CuS_2WS_2]^{2-}$	3084	138
$[(NC)AgS_2WS_2]^{2-}$	3184	138
$[WS_4]^{2-}$	3649.0	139
$[WS_4]^{2-}$	3769	138

[a] Numbers in parentheses are the number of equivalent W nuclei.

Table 17. ^{183}W chemical shifts of some W(V) compounds referenced to 2 M Na_2WO_4.

Compound	Chemical shift (ppm)	Ref.
$[MoW(O)_2(\mu\text{-}O)_2(\mu\text{-EDTA})]^{2-}$	549	141
$[W_2(O)_2(\mu\text{-}O)_2(\mu\text{-EDTA})]^{2-}$	793	141
$[W_2(O)_4(EDTA)]^{2-}$	798	142

Table 18. ^{183}W chemical shifts of some W(IV) compounds referenced to 2 M Na_2WO_4.

Compound	Chemical shift (ppm)	Ref.
$[(\eta^5\text{-}C_5H_5)_2WH_2]$	−4671	15
$[(\eta^3\text{-}C_3H_5)_4W]$	−3186	33
$[(\eta^3\text{-}C_3H_5)_3(Me_3P)WMe]$	−2999	30
$[(\eta^3\text{-}C_3H_5)_3(Me_3P)WCl]$	−2263	30
$[(\eta^3\text{-}C_3H_5)_3(Me_3P)WBr]$	−2244	30
$[(\eta^3\text{-}C_3H_5)_3(Me_3P)WI]$	−2172	30
$[Mo_2W(O)_2(O_2CCH_3)_6(OH_2)_3]^{2+}$	848	142
$[MoW_2(O)_2(O_2CCH_3)_6(OH_2)_3]^{2+}$	897	142
$[W_3(O)_2(O_2CCH_3)_6(OH_2)_3]^{2+}$	1005	142

Table 19. ^{183}W chemical shifts of some W(III) compounds referenced to 2 M Na_2WO_4.

Compound	Chemical shift (ppm)	Ref.
$[W_3O_4]^{4+}$	1116	143
$[W_3O_4Cl]^{3+}$	1157	143
$[W_3O_4Cl]^{3+}$	1165	143
$[W(OBu^t)_3(CPh)]$	2526	144
$[W_2(O_2CMe)_4(CH_2CMe_3)_2]$	2653	144
$[W(CH_2Bu^t)_3(CBu^t)]$	2867	144
$[W_2Cl_9]^{3-}$	3539	142
$[W(CH_2SiMe_3)_3(CSiMe_3)]$	3613	144
$[W_2(NMe_2)_6]$	4196	144
$[W_2(OBu^t)_6]$	4489	144
$[W_2(OPr^i)_6(MeNHCH_2CH_2NHMe)]$	4489	144
$[W_2(OPr^i)_6(DMPE)]$	4736	144

Table 20. ^{183}W chemical shifts of some W(II) compounds referenced to 2 M Na_2WO_4.

Compound	Chemical shift (ppm)	Ref.
$[(\eta^5\text{-}C_5H_5)W(CO)_3(SnMe_3)]$	−4044	15
$[(\eta^5\text{-}C_5H_5)W(CO)_3D]$	−4028	15
$[(\eta^5\text{-}C_5H_5)W(CO)_3D]$	−4017	15
$[\{W(CO)_3H\}_2[\mu\text{-}\{(\eta^5\text{-}C_5H_4)_2SiMe_2\}]]$	−3982	145
$[\{W_2(CO)_3\}_2(\mu\text{-}PMe_2)_2[\mu\text{-}\{(\eta^5\text{-}C_5H_4)_2SiMe_2\}]]$	−3945	145
$[(\eta^5\text{-}C_5H_5)W(CO)_2\{P(OMe)_3\}H]$	−3893	15
$[\{W(CO)_2\}_2(\mu\text{-}H)(\mu\text{-}PMe_2)[\mu\text{-}\{\eta^5\text{-}C_5H_4)_2SiMe_2\}]]$	−3854	145
$[(\eta^5\text{-}C_5H_5)W(CO)_2(PMePh_2)H]$	−3681	15
$[(\eta^5\text{-}C_5H_5)W(CO)_2(PMe_2Ph)H]$	−3679	15
$[(\eta^5\text{-}C_5H_5)W(CO)_3Me]$	−3549	15
$[(\eta^5\text{-}C_5H_5)W(CO)_3Et]$	−3467	15
$[\{W_2(CO)_3\}_2(\mu\text{-}PMe_2)_2[\mu\text{-}\{(\eta^5\text{-}C_5H_4)_2SiMe_2\}]]$	−3387	145
$[(\eta^5\text{-}C_5H_5)W(CO)_3I]$	−2996	15
$[(\eta^5\text{-}C_5H_5)W(CO)_3Br]$	−2584	15
$[(\eta^5\text{-}C_5H_5)W(CO)_3Cl]$	−2406	15
$[W(C_6H_4CH{=}NCH_2CH_2N{=}C_6H_4I\text{-}2)(CO)_3I]$	−1598	146
$[W(C_6H_4CH{=}NCH_2CH_2NH_2)(CO)_3F]$	−1576	146
$[W(C_6H_4CH{=}NC_6H_4NH_2)(CO)_3Cl]$	−1529	146
$[W(C_6H_4CH{=}NCH_2CH_2N{=}C_6H_4Br\text{-}2)(CO)_3Br]$	−1513	146
$[W(S_2CNEt_2)_2(CO)_3]$	−1500	146
$[W(C_6H_4CH{=}NCH_2CH_2N{=}C_6H_4Cl\text{-}2)(CO)_3Cl]$	−1488	146
$[W(C_6H_4CH{=}NC_6H_4NH_2)(CO)_3F]$	−1466	146
$[W(C_6H_4CH{=}NCH_2CH_2NMe_2)(CO)_3I]$	−1413	146
$[W(C_6H_4CH{=}NCH_2CH_2NMe_2)(CO)_3F]$	−1411	146
$[W(C_6H_4CH{=}NCH_2CH_2NMe_2)(CO)_3Br]$	−1357	146
$[W(C_6H_4CH{=}NCH_2CH_2NMe_2)(CO)_3Cl]$	−1351	146
$[W(S_2CNEt_2)_2(CO)_2\{P(OMe)_3\}]$	−1243	147
$[W(S_2CNEt_2)_2(CO)_2\{P(OEt)_3\}]$	−1208	147
$[W(S_2CNEt_2)_2(CO)_2\{P(OPh)_3\}]$	−1196	147
$[W(S_2CNEt_2)_2(CO)_2(PMe_3)]$	−1012	147
$[W(S_2CNEt_2)_2(CO)_2(PPh_2Me)]$	−1001	147
$[\{W(S_2CNEt_2)_2(CO)_2\}_2(dppe)]$	−990	147
$[W(S_2CNEt_2)_2(CO)_2(PPh_2Et)]$	−985	147
$[W(S_2CNEt_2)_2(CO)_2(PPh_3)]$	−966	147
$[\{W(S_2CNEt_2)_2(CO)_2\}_2(dppm)]$	−936	147
$[W(S_2CNEt_2)_2(CO)_2(AsPh_3)]$	−845	147
$[W_2(O_2CBu^t)_4]$	5954	148
$[W_2(O_2CCF_3)_4]$	6760	148

Table 21. ^{183}W chemical shifts of some W(I) compounds referenced to 2 M Na_2WO_4.

Compound	Chemical shift (ppm)	Ref.
$[(\eta^5\text{-}C_5H_5)W(CO)_3]_2$	−4040	15

Table 22. ^{183}W chemical shifts of some (WO) compounds referenced to 2 M Na_2WO_4.

Compound	Chemical shift (ppm)	Ref.
$[(\eta^4\text{-}C_4H_6)_3W]$	−3630	33
$[W(CO)_5\{P(OMe)_3\}]$	−3475	15
$[W(CO)_5\{P(OMe)\{(OCH_2)_2CMe\}]$	−3462	15
$[W(CO)_6]$	−3446	150
$[W(CO)_5\{PO(OMe)_2\}]^-$	−3437	15
$[W(CO)_5\{P(OMe)(OPh)_2\}]$	−3433	15
trans-$[W(CO)_4\{P(OMe)_3\}_2]$	−3433	15
$[W(CO)_5(PH_2Ph)]$	−3420	15
cis-$[W(CO)_4\{P(OMe)_3\}_2]$	−3407	15
$[W(CO)_5\{PPh(OMe)_2\}]$	−3392	15
$[W(CO)_5\{P(NMe_2)_3\}]$	−3391	15
$[W(CO)_5\{PPh_2(OMe)\}]$	−3346	15
$[W(CO)_5(PMe_2Ph)]$	−3326	15
$[W(CO)_5(PMePh_2)]$	−3313	15
trans-$[W(CO)_4(PBu^n_3)_2]$	−3305	22
$[W(CO)_5\{PPh(CH{=}CH_2)_2\}]$	−3301	150
$[W(CO)_5\{P(SnMe_3)_3\}]$	−3301	15
$[W(CO)_4(cis\text{-}Ph_2PCH{=}CHPPh_2)]$	−3296	151
$[W(CO)_5\{PPh(SnMe_3)_2\}]$	−3288	15
$[W(CO)_5\{PPh_2(SnMe_3)\}]$	−3281	15
$[(\eta^4\text{-}2\text{-}MeC_4H_5)_3W]$	−3277	33
$[W(CO)_5\{PPh_2(CH{=}CH_2)\}]$	−3274	150
$[W(CO)_5PPh_2CH(PPh_2)CH_2PPh_2]$	−3266	153
$[W(CO)_4(Ph_2PCH_2CH_2PPh_2)]$	−3255	151
cis-$[W(CO)_4(PBu^n_3)_2]$	−3249	22
$[W(CO)_5(PPh_3)]$	−3236	150
$[W(CO)_4PPh_2CH(PPh_2)CH_2PPh_2]$	−3219	153
$[W(CO)(CNC_6H_3Me_2\text{-}2,6)_5]$	−3139	154
$[W(CO)_5\{PCl_2(OMe)\}]$	−3139	15
$[W(CO)_4(Ph_2PCH_2CH_2CH_2PPh_2)]$	−3121	151
cis-$[W(CO)_4(PMe_2Ph)_2]$	−3117	15
$[W(CO)_4\{Ph_2PCH(CH_2PPh_2O)CH_2CH_2PPh_2\}]$	−3103	152
$[W(CO)_4\{Ph_2PCH(CH_2PPh_2)CH_2CH_2PPh_2\}]$	−3100	152
$[W(CO)_4(Ph_2PCH_2CH_2CH_2CH_2PPh_2)]$	−3080	151

Table 22. (*Continued*)

Compound	Chemical shift (ppm)	Ref.
$[W(CO)_3\{Ph_2PCH(CH_2PPh_2)CH_2CH_2PPh_2\}]$	−3066	152
$[(\eta^4\text{-}2,3\text{-}MeC_4H_4)_3W]$	−3021	33
$[W(CO)_4\{(Ph_2P)_2CHCH_2PPh_2\}]$	−3003	153
$[W(CO)_4\{(Ph_2P)_2C{=}CH_2\}]$	−2971	151
cis-$[W(CO)_4\{P(OMe)_3\}(NCPh)]$	−2968	15
$[W(CO)_4\{(Ph_2P)_2NH\}]$	−2966	151
$[W(CO)_3\{(Ph_2P)_2CHCH_2PPh_2\}]$	−2947	153
cis-$[W(CO)_4\{P(OMe)_3\}\{S(SnMe_3)_2\}]$	−2923	15
$[W(CO)_4\{(Ph_2P)_2CH_2\}]$	−2921	151
$[W(CNC_6H_3Me_2\text{-}2,6)_6]$	−2918	154
fac-$[W(CO)_3(PMe_2Ph)_3]$	−2818	15
cis-$[W(CO)_4\{P(OMe)_3(NC_5H_4Me\text{-}4)\}]$	−2660	15
cis-$[W(CO)_4\{P(OMe)_3(NC_5H_5)\}]$	−2647	15

Table 23. ^{187}Os chemical shifts of some Os compounds, referenced to OsO_4.

Compound	Chemical shift (ppm)	Ref.
$[(\eta^5\text{-}C_5Me_5)Os(\eta^4\text{-}1,5\text{-}C_8H_{12})H]$	−4889	155
$[(\eta^5\text{-}C_5H_5)Os(PMe_3)_2Me]$	−4779	155
$[(\eta^5\text{-}C_5H_5)Os(PPh_3)_2I]$	−3530	155
$[(\eta^5\text{-}C_5H_5)Os(PMe_3)_2Br]$	−3506	155
$[(\eta^5\text{-}C_5H_5)Os(PMe_3)(PPh_3)Br]$	−3324	155
$[(\eta^5\text{-}C_5H_5)Os(PPh_3)_2Br]$	−3008	155
$[(\eta^5\text{-}C_5H_5)Os(PPh_3)_2Cl]$	−2595	155
$[(\eta^6\text{-}1\text{-}Me\text{-}4\text{-}Pr^i\text{-}C_6H_4)_2Os_4(\mu\text{-}H)_3]^+$	−2526	156
$[(\eta^6\text{-}1\text{-}Me\text{-}4\text{-}Pr^i\text{-}C_6H_4)_4Os_4(\mu\text{-}H)_4]^{2+}$	−2171	156, 157
$[(\eta^6\text{-}1\text{-}Me\text{-}4\text{-}Pr^i\text{-}C_6H_4)_2Os_2(\mu\text{-}H)(\mu\text{-}Cl)Cl_2]$	−2037	156
$[(\eta^6\text{-}1\text{-}Me\text{-}4\text{-}Pr^i\text{-}C_6H_4)_2Os_2(\mu\text{-}H)(\mu\text{-}Cl)(\mu\text{-}O_2CCH_3)]^+$	−1951	156
$[(\eta^6\text{-}1\text{-}Me\text{-}4\text{-}Pr^i\text{-}C_6H_4)_2Os_2(\mu\text{-}H)_2(\mu\text{-}O_2CCH_3)]^+$	−1185	156

4.6. ^{187}Os chemical shifts

The very low sensitivity of ^{187}Os NMR spectroscopy provides a major difficulty for detection. However, inverse two-dimensional $^1H\{^{187}Os\}$ has been used to observe ^{187}Os on a few compounds (see Table 23) and Quadriga NMR spectroscopy has been used to observe OsO_4.[11,50]

4.7. Paramagnetic compounds

Paramagnetic compounds do not usually give satisfactory spectra, but two exceptions occur for these nuclei. There have been reports of the treatment of Ag^+ with the organic radical, tanol, 2,2,6,6-Me_4-4-HO-piperidine-1-oxyl. The unpaired electron density is slightly delocalized onto the silver nucleus and this produces shifts of up to 25 ppm.[31,32]

Very substantial ^{183}W chemical shifts are found for paramagnetic heteropolytungstates. These shifts arise either from incorporating a paramagnetic centre in the complex[51–54] or by reducing the complex.[55,56]

5. COUPLING CONSTANTS

Coupling constants involving low γ nuclei, such as those described in this chapter are generally small. This is directly related to the fact that coupling constants are proportional to γ for both the coupling nuclei. Nevertheless, useful coupling constants have been found and a selection is given in Tables 24–29.

6. RELAXATION TIMES

Spin-lattice relaxation times of these low-frequency nuclei were believed to be extremely long. Although in some cases this is true with T_1 values as large as $1000\,s^{-1}$,[57] measurements have shown that T_1 values can be quite short, especially at high field strengths. There are several relaxation measurements which can, in principle, contribute. Dipole–dipole relaxation, T_{1dd}, which is important for nuclei such as ^{13}C is generally unimportant. In the fast tumbling region, then equation

$$T_{1dd}^{-1} = \frac{\mu_0^2 \gamma_I^2 \gamma_S^2 \hbar^2 S(S+1)\tau_c}{12\pi^2 \sum_i r_{IS_i}^6} \tag{10}$$

applies, where μ_0 is the permeability of a vacuum, γ_X is the magnetogyric ratio of nucleus X, S is the nuclear spin, τ_c is correlation time for molecular tumbling, and r_{IS} is the distance between the nuclei. For nuclei with small magnetogyric ratio, such as those reviewed here, this term is very small and rarely contributes significantly. So far, significant values of T_{1dd}^{-1} have not been detected for these nuclei and, as a consequence, the nuclear Overhauser enhancement is negligible.

Chemical-shift anisotropy often makes a substantial contribution to the

Table 24. Some representative coupling constants for ^{57}Fe.

Compound	Coupling constant (Hz)	Ref.
$[(\eta^5\text{-}C_5H_5)FeH(dppe)]$	$^1J(^{57}Fe\text{–}^1H) = 9.3$	158
$[(\eta^5\text{-}C_5H_5)Fe(\eta^5\text{-}C_5H_4CH_2)]^+$	$^1J(^{57}Fe\text{–}^{13}C) = 0.8$ to 4.4	71, 158, 159
$[(\eta^5\text{-}C_6H_7)Fe(\eta^5\text{-}C_5H_5)]$	$^1J(^{57}Fe\text{–}^{13}C) = 1.4$ to 5.8	160
$[(\eta^5\text{-}C_5H_5)Fe(CO)_2(\eta^2\text{-}CH_2{=}CMe_2)]^+$	$^1J(^{57}Fe\text{–}^{13}C) = 1.5$ to 4.4, 27.9 (CO)	159
$[(\eta^5\text{-}C_5H_4CHCH_2CH_2C_5H_4\text{-}\eta^5)Fe]^+$	$^1J(^{57}Fe\text{–}^{13}C) = 1.8$ to 4.4	71, 72
$[\{(\eta^5\text{-}C_5H_5)Fe(\eta^5\text{-}C_5H_4)\}_2CH]^+$	$^1J(^{57}Fe\text{–}^{13}C) = 2.2$ to 4.4	71, 158
$[(\eta^5\text{-}C_5H_5)Fe(CO)_2(CH_2CMe{=}CH_2)]$	$^1J(^{57}Fe\text{–}^{13}C) = 2.3$ (Cp), 8.8 (CH_2), 27.9(CO)	159
$[(\eta^5\text{-}C_5H_5)Fe(CO)_2C{=}CPh)]$	$^1J(^{57}Fe\text{–}^{13}C) = 2.3$ (Cp), 19.5 (C≡), 27.8 (CO)	71
$[(\eta^5\text{-}C_5H_5)Fe(\eta^5\text{-}C_5H_4CHMe)]^+$	$^1J(^{57}Fe\text{–}^{13}C) = 2.5$ to 4.3	71, 158
$[(\eta^5\text{-}C_5H_5)Fe(\eta^5\text{-}C_5H_4CHPh)]^+$	$^1J(^{57}Fe\text{–}^{13}C) = 2.5$ to 4.3	71, 158
$[(\eta^5\text{-}C_5H_5)Fe(\eta^5\text{-}C_5H_4CMe_2)]^+$	$^1J(^{57}Fe\text{–}^{13}C) = 2.5$ to 4.3	71, 158
$[(\eta^5\text{-}C_5H_5)Fe(\eta^5\text{-}C_5H_4CHC_5H_4\text{-}\eta^5)Mn(CO)_3]^+$	$^1J(^{57}Fe\text{–}^{13}C) = 2.7$ to 4.4	71, 158
$[(\eta^5\text{-}C_6H_7)Fe(CO)_3]^+$	$^1J(^{57}Fe\text{–}^{13}C) = 2.7, 2.8,$ 25.7 (CO)	159,160
$[(\eta^4\text{-}C_6H_8)Fe(CO)_3]$	$^1J(^{57}Fe\text{–}^{13}C) = 2.8, 3.7,$ 28.0 (CO)	159
$[(\eta^6\text{-}C_6H_6)Fe(\eta^5\text{-}C_5H_5)]^+$	$^1J(^{57}Fe\text{–}^{13}C) = 3.3, 4.8$	71
$[(\eta^4\text{-}C_4H_4)Fe(CO)_3]$	$^1J(^{57}Fe\text{–}^{13}C) = 3.6, 28.7$	161
$[\{\eta^5\text{-}C_5H_4CH_2CH(OH)(CH_2)_2C_5H_4\text{-}\eta^5\}Fe]$	$^1J(^{57}Fe\text{–}^{13}C) = 4.0, 4.8$	72
$[(\eta^5\text{-}C_5H_5)Fe(\eta^5\text{-}C_5H_4CHC_5H_4\text{-}\eta^5)Ru(\eta^5\text{-}C_5H_5)]^+$	$^1J(^{57}Fe\text{–}^{13}C) = 4.1$ to 4.4	71, 158
$[\{\eta^5\text{-}C_5H_4CH_2C(O)(CH_2)_2C_5H_4\text{-}\eta^5\}Fe]$	$^1J(^{57}Fe\text{–}^{13}C) = 4.1, 4.7$	71, 72
$[O\{(CHC_5H_4\text{-}\eta^5)(CH_2(CH_2C_5H_4\text{-}\eta^5)Fe\}_2]$	$^1J(^{57}Fe\text{–}^{13}C) = 4.2$ to 5.6	72
$[(\eta^5\text{-}C_5H_5)Fe(\eta^5\text{-}C_5H_4CHO)]$	$^1J(^{57}Fe\text{–}^{13}C) = 4.4$ to 4.9	159
$[CH_2(CH_2C_5H_4\text{-}\eta^5)_2Fe]$	$^1J(^{57}Fe\text{–}^{13}C) = 4.4, 4.8$	71, 72
$[(\eta^5\text{-}C_5H_5)Fe(\eta^5\text{-}C_5H_4I)]$	$^1J(^{57}Fe\text{–}^{13}C) = 4.4, 5.2$	71
$[\{\eta^5\text{-}C_5H_4CH(OH)CH_2CH_2C_5H_4\text{-}\eta^5\}Fe]$	$^1J(^{57}Fe\text{–}^{13}C) = 4.5$ to 4.9	71, 72
$[(\eta^5\text{-}C_5H_4Me)_2Fe]$	$^1J(^{57}Fe\text{–}^{13}C) = 4.6$	161
$[(CH_2CH_2C_5H_4\text{-}\eta^5)_2Fe]$	$^1J(^{57}Fe\text{–}^{13}C) = 4.6, 4.7$	72
$[(\eta^5\text{-}C_5H_5)_2Fe]$	$^1J(^{57}Fe\text{–}^{13}C) = 4.7$	161
$[(\eta^5\text{-}C_5H_5)Fe(\eta^5\text{-}C_5H_4Me)]$	$^1J(^{57}Fe\text{–}^{13}C) = 4.7$	161
$[(\eta^5\text{-}C_5H_5)_2Fe]$	$^1J(^{57}Fe\text{–}^{13}C) = 4.8$	162
$[Fe_3(CO)_{12}]$	$^1J(^{57}Fe\text{–}^{13}C) = 8.3$	163
$[Fe_3(CO)_{12}]$	$^1J(^{57}Fe\text{–}^{13}C) = 8.3$	164
$[(\eta^2\text{-}CH_2{=}CHCHO)Fe(CO)_4]$	$^1J(^{57}Fe\text{–}^{13}C) = 23.0$	66
$[Fe(CO)_5]$	$^1J(^{57}Fe\text{–}^{13}C) = 23.3$	160
$[Fe(CO)_5]$	$^1J(^{57}Fe\text{–}^{13}C) = 23.4$	165
$[(\eta^4\text{-tropone})Fe(CO)_3]$	$^1J(^{57}Fe\text{–}^{13}C) = 24.5, 31.5$	66
cis-$[Fe(CO)_4(SiMe_3)_2]$	$^1J(^{57}Fe\text{–}^{13}C) = 25$	166
$[(\eta^4\text{-norbornadiene})Fe(CO)_3]$	$^1J(^{57}Fe\text{–}^{13}C) = 26.4$	66

(*Continued*)

Table 24. (*Continued*)

Compound	Coupling constant (Hz)	Ref.
$[\{(OC)_3Fe\}_2(\mu\text{-}SMe)_2]$	$^1J(^{57}Fe-^{13}C) = 27.0$	163
$[(\eta^4\text{-}C_4H_6)Fe(CO)_3]$	$^1J(^{57}Fe-^{13}C) = 27.7$	66
$[(\eta^4\text{-}C_4H_6)Fe(CO)_3]$	$^1J(^{57}Fe-^{13}C) = 27.9$	167
$[(\eta^4\text{-}1\text{-}MeC_4H_5)Fe(CO)_3]$	$^1J(^{57}Fe-^{13}C) = 28.0$	66
$[(\eta^4\text{-}C_6H_8)Fe(CO)_3]$	$^1J(^{57}Fe-^{13}C) = 28.0$	66
$[(OC)_3Fe(\eta^4\text{-}MeNBEtCEtCMeSiEt_2)]$	$^1J(^{57}Fe-^{13}CO) = 28$	87
$[(\eta^4\text{-}C_5H_6)Fe(CO)_3]$	$^1J(^{57}Fe-^{13}C) = 28.6$	66
$[(\eta^4\text{-}C_8H_8)Fe(CO)_3]$	$^1J(^{57}Fe-^{13}C) = 28.6$	66
$[\{\eta^4\text{-}C_6H_4(CH_2)_2\}Fe(CO)_3]$	$^1J(^{57}Fe-^{13}C) = 28.6, 32.0$	66
$[\{(OC)_3Fe\}_2(\mu\text{-}S_2)]$	$^1J(^{57}Fe-^{13}C) = 29.3$	163
$[Fe(CO)_4P(SnMe_3)_3]$	$^1J(^{57}Fe-^{31}P) = 20.5$	168
$[Fe(CO)_4PBu^t(SnMe_3)_2]$	$^1J(^{57}Fe-^{31}P) = 22.2$	168
$[Fe(CO)_4PEt_3]$	$^1J(^{57}Fe-^{31}P) = 25.9$	165
$[Fe(CO)_4PEt_2Ph]$	$^1J(^{57}Fe-^{31}P) = 26.5$	165
$[Fe(CO)_4PEtPh_2]$	$^1J(^{57}Fe-^{31}P) = 27.4$	165
$[Fe(CO)_4PBu^t_3]$	$^1J(^{57}Fe-^{31}P) = 29.8$	168
$[Fe(CO)_2(PMe_3)_2CS_2]$	$^1J(^{57}Fe-^{31}P) = 31$	169
$[Fe(CO)(NO)_2\{P(SiMe_3)_3\}]$	$^1J(^{57}Fe-^{31}P) = 47.2$	168
$[Fe(CO)(NO)_2\{P(SnMe_3)_3\}]$	$^1J(^{57}Fe-^{31}P) = 48.5$	168
$[(\eta^5\text{-}C_5H_5)(Pr^i_2PCH_2PPr^i_2)_2FeH]$	$^1J(^{57}Fe-^{31}P) = 50$	67
$[(\eta^5\text{-}C_6H_7)(Pr^i_2PCH_2CH_2CH_2PPr^i_2)_2FeH]$	$^1J(^{57}Fe-^{31}P) = 50$	67
$[Fe(CO)(NO)_2\{P(SiMe_3)_3\}]$	$^1J(^{57}Fe-^{31}P) = 50.1$	168
$[(\eta^5\text{-}C_5H_5)(Pr^i_2PCH_2PPr^i_2)_2FeD]$	$^1J(^{57}Fe-^{31}P) = 50.5$	30
$[Fe(CO)(NO)_2\{PBu^t(SiMe_3)_2\}]$	$^1J(^{57}Fe-^{31}P) = 51.1$	168
$[(\eta^5\text{-}EtC_6H_6)(Pr^i_2PCH_2CH_2PPr^i_2)_2FeH]$	$^1J(^{57}Fe-^{31}P) = 52$	67
$[Fe(CO)(NO)_2\{PBu^t(SnMe_3)_2\}]$	$^1J(^{57}Fe-^{31}P) = 52.3$	168
$[(\eta^5\text{-}C_5Me_5)(1\text{-}C_6H_4\text{-}2\text{-}\eta^{2,3}\text{-}C_3H_5)FePMe_3]$	$^1J(^{57}Fe-^{31}P) = 53$	67
$[Fe(CO)(NO)_2\{PBu^t(GeMe_3)_2\}]$	$^1J(^{57}Fe-^{31}P) = 54.1$	168
$[(\eta^5\text{-}C_5Me_5)(\eta^2\text{-}C_2H_4)FeH(PMe_3)]$	$^1J(^{57}Fe-^{31}P) = 55$	
$[Fe(CO)(NO)_2\{PBu^t_2(SiMe_3)\}]$	$^1J(^{57}Fe-^{31}P) = 56.2$	168
$[Fe(CO)(NO)_2\{PBu^t_2(SnMe_3)\}]$	$^1J(^{57}Fe-^{31}P) = 57.2$	168
$[(\eta^5\text{-}C_5H_5)(Pr^i_2PCH_2CH_2CH_2PPr^i_2)_2FeH]$	$^1J(^{57}Fe-^{31}P) = 58$	30, 67
$[(\eta^5\text{-}C_6H_7)(Pr^i_2PCH_2CH_2PPr^i_2)_2FeH]$	$^1J(^{57}Fe-^{31}P) = 58$	67
$[Fe(CO)(NO)_2\{PBu^t_2(GeMe_3)\}]$	$^1J(^{57}Fe-^{31}P) = 58.0$	168
$[(\eta^5\text{-}C_5H_5)(Me_3P)_2FeH]$	$^1J(^{57}Fe-^{31}P) = 59$	30, 67
$[(\eta^5\text{-}C_5Me_5)(1,2,5\text{-}\eta^{1,2}\text{-}C_5H_9)FePMe_3]$	$^1J(^{57}Fe-^{31}P) = 59$	67
$[(\eta^5\text{-}MeC_5H_4)\{Pr^i_2P(CH_2)_3PPr^i_2\}FeEt]$	$^1J(^{57}Fe-^{31}P) = 59$	67
$[(\eta^5\text{-}C_5H_5)(Pr^i_2PCH_2CH_2PPr^i_2)_2FeH]$	$^1J(^{57}Fe-^{31}P) = 59.5$	30
$[(\eta^5\text{-}C_5H_5)Fe(CH{=}CH_2)(dppe)]$	$^1J(^{57}Fe-^{31}P) = 60$	67
$[(\eta^5\text{-indenyl})(Pr^i_2PCH_2CH_2CH_2PPr^i_2)_2FeH]$	$^1J(^{57}Fe-^{31}P) = 60$	67
$[(\eta^5\text{-}C_5H_5)FeCH_3(DPPE)]$	$^1J(^{57}Fe-^{31}P) = 60$	67
$[(\eta^5\text{-}C_5H_5)(Me_3P)_2FeCH{=}CH_2]$	$^1J(^{57}Fe-^{31}P) = 60$	67
$[(\eta^5\text{-}Me_5C_5)(Me_3P)_2FeCH_3]$	$^1J(^{57}Fe-^{31}P) = 60$	67
$[(\eta^5\text{-}C_5H_5)(Me_2PhP)_2FeCl]$	$^1J(^{57}Fe-^{31}P) = 60.5$	30
$[(\eta^5\text{-}C_5H_5)(MePh_2P)_2FeH]$	$^1J(^{57}Fe-^{31}P) = 61$	67

Table 24. (*Continued*)

Compound	Coupling constant (Hz)	Ref.
$[(\eta^5\text{-}C_5H_5)FeH\{Ph_2P(CH_2)_4PPh_2\}]$	$^1J(^{57}Fe\text{–}^{31}P) = 61$	67
$[(\eta^5\text{-}C_5H_5)(Ph_3P)_2FeH]$	$^1J(^{57}Fe\text{–}^{31}P) = 61$	67
$[(\eta^5\text{-}MeC_5H_4)(Me_3P)_2FeCH_3]$	$^1J(^{57}Fe\text{–}^{31}P) = 61$	67
$[(\eta^5\text{-}C_5H_5)(Me_3P)_2FeCH_3]$	$^1J(^{57}Fe\text{–}^{31}P) = 61$	30, 67
$[(\eta^5\text{-}C_5H_5)(MePh_2P)_2FeCH_3]$	$^1J(^{57}Fe\text{–}^{31}P) = 61$	67
$[(\eta^5\text{-}MeC_5H_4)(MePh_2P)_2FeCH_3]$	$^1J(^{57}Fe\text{–}^{31}P) = 61$	67
$[(\eta^5\text{-}C_5H_5)(MePh_2P)_2FeCH{=}CH_2]$	$^1J(^{57}Fe\text{–}^{31}P) = 61$	67
$[(\eta^5\text{-}C_5H_5)(Me_3P)_2FeI]$	$^1J(^{57}Fe\text{–}^{31}P) = 61$	30, 67
$[(\eta^5\text{-}C_5H_5)FeH(DPPE)]$	$^1J(^{57}Fe\text{–}^{31}P) = 62$	67
$[(\eta^5\text{-}MeC_5H_4)FeH(DPPE)]$	$^1J(^{57}Fe\text{–}^{31}P) = 62$	67
$[(\eta^5\text{-}MeC_5H_4)(MePh_2P)_2FeEt]$	$^1J(^{57}Fe\text{–}^{31}P) = 62$	67
$[Fe(CO)(NO)_2(PBu^t_3)]$	$^1J(^{57}Fe\text{–}^{31}P) = 62.4$	168
$[(\eta^5\text{-}MeC_5H_4)(MePh_2P)_2FeEt]$	$^1J(^{57}Fe\text{–}^{31}P) = 63$	67
exo-$[(\eta^5\text{-}C_5Me_5)(\eta^3\text{-}C_3H_5)FePMe_3]$	$^1J(^{57}Fe\text{–}^{31}P) = 70$	67
exo-$[(\eta^5\text{-}C_5H_5)(\eta^3\text{-}2\text{-}MeC_3H_4)Fe\{P(OPh)_2(menthyl)\}]$	$^1J(^{57}Fe\text{–}^{31}P) = 93$	67
$[(\eta^5\text{-}C_5H_5)\{(MeO)_3P\}_2FeCH_2CH{=}CH_2]$	$^1J(^{57}Fe\text{–}^{31}P) = 102$	67
$[(\eta^5\text{-}C_5H_5)\{(MeO)_3P\}_2FeCH_2CMe{=}CH_2]$	$^1J(^{57}Fe\text{–}^{31}P) = 102$	67
$[(\eta^5\text{-}C_5H_5)\{MeO)_3P\}_2FeCH_2CH(CMe{=}CH_2)\text{-}(CH_2CMe{=}CH_2)]$	$^1J(^{57}Fe\text{–}^{31}P) = 103$	67
exo-$[(\eta^5\text{-}C_5H_5)(\eta^3\text{-}2\text{-}MeC_3H_4)Fe\{P(OMe)_3\}]$	$^1J(^{57}Fe\text{–}^{31}P) = 108$	67
exo-$[(\eta^5\text{-}C_5H_5)(\eta^3\text{-}1\text{-}syn\text{-}MeC_3H_4)Fe\{P(OMe)_3\}]$	$^1J(^{57}Fe\text{–}^{31}P) = 111$	67
$[(\eta^5\text{-}C_5H_5)(F_3P)_2FeCH_2CH{=}CH_2]$	$^1J(^{57}Fe\text{–}^{31}P) = 127$	67
endo-$[(\eta^5\text{-}C_5H_5)(\eta^5\text{-}1\text{-}syn\text{-}MeC_3H_4)FePF_3]$	$^1J(^{57}Fe\text{–}^{31}P) = 145$	67
exo-$[(\eta^5\text{-}C_5H_5)(\eta^3\text{-}C_3H_5)FePF_3]$	$^1J(^{57}Fe\text{–}^{31}P) = 147$	67
exo-$[(\eta^5\text{-}C_5H_5)(\eta^3\text{-}1\text{-}syn\text{-}MeC_3H_4)FePF_3]$	$^1J(^{57}Fe\text{–}^{31}P) = 149$	67

Table 25. Some representative ^{89}Y coupling constants for some yttrium complexes.

Compound	Coupling constant (Hz)	Ref.
$[(\eta^5\text{-}C_5H_4Me)_2Y(\mu\text{-}H)(THF)]_2$	$^1J(^{89}Y\text{–}^1H) = 27$	27
$[(Bu^tCH_2)_3Y\cdot 2THF]$	$^2J(^{89}Y\text{–}^1H) = 2.5$	170
$[(\eta^5\text{-}C_5H_5)_2Y(\mu\text{-}Me)_2AlMe_2]$	$^2J(^{89}Y\text{–}^1H) = 5$	171
$[(\eta^5\text{-}C_5H_5)_2Y(\mu\text{-}Me)_2AlMe_2]$	$^2J(^{89}Y\text{–}^{13}C) = 12.2$	172
$[(\eta^5\text{-}C_5Me_5)Y(\mu\text{-}H)Y(\eta^5\text{-}C_5Me_4CH_2)(\eta^5\text{-}C_5Me_5)]$	$^1J(^{89}Y\text{–}^{13}C) = 35.6$	173
$[YCl\{N(SiMe_2CH_2PMe_2)_2\}_2]$	$^1J(^{89}Y\text{–}^{31}P) = 52$	80
$[Y\{(OPPh_2)_2C(PPh_2O)\}_3]$	$^2J(^{89}Y\text{–}^{31}P) = 6.5$	174

Table 26. Some representative ^{103}Rh coupling constants.

Compound	Coupling constant (Hz)	Ref.
trans,trans-[$RhCl_2H(CO)(PMe_2Ph)_2$]	$^1J(^{103}Rh-^1H) = -17.3$	18
trans-[$Fe_4Rh_2(CO)_{16}B$]	$^1J(^{103}Rh-^{11}B) = 23.3$	175
[$RhH_2(PPh_3)_2(2\text{-}O_2CC_9H_5N_2\text{-}1,4)$]	$^1J(^{103}Rh-^{15}N) = 9.1$	176
[$RhH_2(PPh_3)_2(2\text{-}O_2CC_9H_6N)$]	$^1J(^{103}Rh-^{15}N) = 9.2$	176
[$RhH_2(PPh_3)_2(2\text{-}O_2CC_5H_3N_2\text{-}1,4)$]	$^1J(^{103}Rh-^{15}N) = 9.6$	176
[$RhH_2(PPh_3)_2(2\text{-}O_2CC_5H_4N)$]	$^1J(^{103}Rh-^{15}N) = 9.7$	176
[$RhH_2(PPh_3)_2(2\text{-}O_2C\text{-}6\text{-}MeC_5H_3N)$]	$^1J(^{103}Rh-^{15}N) = 9.7$	176
[$RhH_2(PPh_3)_2(1\text{-}O_2CC_9H_6N)$]	$^1J(^{103}Rh-^{15}N) = 10.1$	176
trans-[$RhF(CO)(PPh_3)_2$]	$^1J(^{103}Rh-^{19}F) = -52.5$	177
[(acac)(Rh(η^4-MeNBEtCEtCMeSiMe$_2$)]	$^1J(^{103}Rh-^{29}Si) = 1.2$	87
[(η^5-C_5H_5)Rh(η^4-MeNBEtCEtCMeSiMe$_2$)]	$^1J(^{103}Rh-^{29}Si) = 2.3$	87
[Rh(η^5-C_5Me_5)$H_3(SiEt_3)$]	$^1J(^{103}Rh-^{29}Si) = 16$	178
[Rh(η^5-C_5Me_5)H($SiEt_3$)(η^2-C_2H_4)]	$^1J(^{103}Rh-^{29}Si) = 17$	179
[Rh(η^5-C_5Me_5)H{$Si(OEt)_3$}(η^2-C_2H_4)]	$^1J(^{103}Rh-^{29}Si) = 45$	179
trans-[$RhCl(CO)(PMe_2Ph)_2$]	$^1J(^{103}Rh-^{31}P) = -118$	180
[Rh_2(4-$MeC_6H_4NCHNC_6H_4Me$-4)$_2(O_2CCF_3)_2(PPh_3)$]	$^1J(^{103}Rh-^{103}Rh) = 38.6$	182
[$Rh_2(\eta^5\text{-}C_5H_5)_2(CO)_3$]	$^1J(^{103}Rh-^{103}Rh) = 4.2$	182
[$Rh_2(\eta^5\text{-}C_5H_5)_2(CO)_2(\mu\text{-}CH_2)$]	$^1J(^{103}Rh-^{103}Rh) = 4.4$	182
[$Rh_2(\eta^5\text{-}C_5H_5)_2(NO)_2$]	$^1J(^{103}Rh-^{103}Rh) = 4.4$	182
[$Rh_2(O_2CCH_3)_4${$P(OMe)_3$}$_2$]	$^1J(^{103}Rh-^{103}Rh) = 7.9$	183
[$Rh_2(\eta^5\text{-}C_5H_5)_2(\mu\text{-}H)_3(PPr^i_3)_2]^+$	$^1J(^{103}Rh-^{103}Rh) = 11.4$	184
[$Rh_2(\eta^5\text{-}C_5Me_5)_2(\mu\text{-}CH_2)_2$(DPPE)]$^{2+}$	$^1J(^{103}Rh-^{103}Rh) = 11.9$	185
[$Rh_2(\eta^5\text{-}C_5Me_5)_2(\mu\text{-}CH_2)_2$(DPPM)]$^{2+}$	$^1J(^{103}Rh-^{103}Rh) = 12.4$	185
[$Rh_2(\eta^5\text{-}C_5Me_5)_2(\mu\text{-}CH_2)_2$-{$\mu$-$CH_2CH(CH_2CH{=}CH_2)CH_2$}]	$^1J(^{103}Rh-^{103}Rh) = 13.5$	185
[$Rh_2(\eta^5\text{-}C_5H_5)_2(\mu\text{-}CH_2)(\mu\text{-}CHCH_3)Br_2$]	$^1J(^{103}Rh-^{103}Rh) = 13.5$	186
[$Rh_2(C_2H_3)(C_2Me_3)(\eta^5$-indenyl)$_2$]	$^1J(^{103}Rh-^{103}Rh) = 17$	187
[Rh_2(4-$MeC_6H_4NCHNC_6H_4Me$-4)$_3(NO_3)(PPh_3)$]	$^1J(^{103}Rh-^{103}Rh) = 34$	188
[$Rh_2(MHP)_4$]	$^1J(^{103}Rh-^{103}Rh) = 35$	189
[Rh_2(4-$MeC_6H_4NCHNC_6H_4Me$-4)$_3(NO_3)(NC_5H_5)$]	$^1J(^{103}Rh-^{103}Rh) = 40$	188
[Rh(η^5-C_5Me_5)$H_2(SnBu^n_3)_2$]	$^1J(^{103}Rh-^{119}Sn) = 146$	190
[Rh(η^5-C_5Me_5)$H_2(SnMe_3)_2$]	$^1J(^{103}Rh-^{119}Sn) = 151$	190
[Rh(η^5-C_5Me_5)H($SnBu^n_3$)(CO)]	$^1J(^{103}Rh-^{119}Sn) = 210$	190
[Rh(η^5-C_5Me_5)H($SnMe_3$)(CO)]	$^1J(^{103}Rh-^{119}Sn) = 221$	190
mer-[$RhCl_3(TeMe_2)_3$]	$^1J(^{125}Te-^{103}Rh) = +71, +95$	191
[$Rh_5Pt(CO)_{15}]^-$	$^1J(^{103}Rh-^{195}Pt) = 24, 73$	192, 193
[$Rh_4Pt(CO)_{12}]^{2-}$	$^1J(^{103}Rh-^{195}Pt) = 44$	193
[$Rh_4Pt(CO)_{14}]^{2-}$	$^1J(^{103}Rh-^{195}Pt) = 55$	193
[$Rh_2Pt(CO)_x]^{n-}_n$	$^1J(^{103}Rh-^{195}Pt) = 69, 55$	192
[$RhCl_2(HgCl)(CO)(PEtPh_2)_2$]	$^1J(^{103}Rh-^{199}Hg) = 426$	194

Table 27. Some representative ^{109}Ag coupling constants for some Ag(I) complexes.

Compound	Coupling constant (Hz)	Ref.
$[1,2\text{-}(2\text{-}5\text{-}Me\text{-}thiophenylCH{=}N)_2(C_6H_{10})_2Ag]^+$	$^1J(^{109}Ag\text{–}^{15}N) = 57, 12$	93
$[Ag(DPPE)_2]^+$	$^1J(^{109}Ag\text{–}^{31}P) = 231$	96
$[Ag(cis\text{-}Ph_2PCH{=}CHPPh_2)_2]^+$	$^1J(^{109}Ag\text{–}^{31}P) = 235$	96
$[Ag(Et_2PCH_2CH_2PEt_2)_2]^+$	$^1J(^{109}Ag\text{–}^{31}P) = 226$	96
$[Ag(Ph_2PCH_2CH_2CH_2PPh_2)_2)^+$	$^1J(^{109}Ag\text{–}^{31}P) = 220$	96
$[Ag(PPh_3)(bipy)]$	$^1J(^{109}Ag\text{–}^{31}P) = 640$	195
$[Ag_2Ru_4(\mu_3\text{-}H)_3(CO)_{12}(PPh_3)]$	$^1J(^{109}Ag\text{–}^{31}P) = 678$	99
$[Ag_2Ru_4(\mu_3\text{-}H)_2(dppm)(CO)_{12}]$	$^1J(^{109}Ag\text{–}^{31}P) = 498.5$	97, 99
$[Ag_2Ru_4(\mu_3\text{-}H)_2(dppe)(CO)_{12}]$	$^1J(^{109}Ag\text{–}^{31}P) = 510.5$	97, 99
$[Ag_2Ru_4(\mu_3\text{-}H)_2\{Ph_2P(CH_2)_4PPh_2\}(CO)_{12}]$	$^1J(^{109}Ag\text{–}^{31}P) = 523.8$	97, 99
$[Ag_2Ru_4(\mu_3\text{-}H)_2(\mu\text{-}Ph_2AsCH_2AsPh_2)(CO)_{12}]$	$^1J(^{109}Ag\text{–}^{31}P) = 570$	89
$[Ag_2Ru_4(\mu_3\text{-}H)_2\{\mu\text{-}Ph_2As(CH_2)_2AsPh_2\}(CO)_{12}]$	$^1J(^{109}Ag\text{–}^{31}P) = 529$	89
$[Ag_2Ru_4(\mu_3\text{-}H)_2(\mu\text{-}Ph_2AsCH_2AsPh_2)(CO)_{12}]$	$^1J(^{109}Ag\text{–}^{107}Ag) = 40$	89
$[Ag_2Ru_4(\mu_3\text{-}H)_2\{Ph_2P(CH_2)_4PPh_2\}(CO)_{12}]$	$^1J(^{109}Ag\text{–}^{107}Ag) = 41$	97, 99
$[Ag_2Ru_4(\mu_3\text{-}H)_2(dppm)(CO)_{12}]$	$^1J(^{109}Ag\text{–}^{107}Ag) = 35$	97, 99
$[Ag_2Ru_4(\mu_3\text{-}H)_2(dppe)(CO)_{12}]$	$^1J(^{109}Ag\text{–}^{107}Ag) = 35$	97, 99
$[Ag\{TeO_4(OH)_2\}_2]^{5-}$	$^1J(^{109}Ag\text{–}^{125}Te) = 73$	196
$[PtMe_2(bipy)\{Ag(PPh_3)\}]^+$	$^1J(^{109}Ag\text{–}^{195}Pt) = 680$	197
$[\{2,6\text{-}(Me_2NCH_2)_2C_6H_3\}(4\text{-}tolNCHNtol\text{-}4)PtAgBr]$	$^1J(^{109}Ag\text{–}^{195}Pt) = 170$	91
$[\{2,6\text{-}(Me_2NCH_2)_2C_6H_3\}(4\text{-}tolNCHNMe)PtAgBr]^a$	$^1J(^{109}Ag\text{–}^{195}Pt) = 171$	91
$[\{2,6\text{-}(Me_2NCH_2)_2C_6H_3\}(4\text{-}tolNCHNMe)PtAgBr]^a$	$^1J(^{109}Ag\text{–}^{195}Pt) = 173$	91
$[\{2,6\text{-}(Me_2NCH_2)_2C_6H_3\}(4\text{-}tolNCHNEt)PtAgBr]^a$	$^1J(^{109}Ag\text{–}^{195}Pt) = 165$	91
$[\{2,6\text{-}(Me_2NCH_2)_2C_6H_3\}(4\text{-}tolNCHNPr^i)PtAgBr]^a$	$^1J(^{109}Ag\text{–}^{195}Pt) = 172$	91

[a] Two isomers.

relaxation of these nuclei. The spin lattice relaxation due to chemical shift anisotropy, $T_{1\,csa}$, is given by

$$T^{-1}_{1\,csa} = \frac{\mu_o \gamma_I^2 B_0^2 \Delta\sigma^2 \tau_c}{30\pi} \tag{11}$$

where B_0 is the magnetic field strength, and $\Delta\sigma$ is the chemical-shift anisotropy. For the nuclei reviewed here, this term is normally dominant, whenever the metal nucleus lies in an unsymmetric environment. As $T_{1\,csa}$ depends on B_0^2, its significance can be determined by determining T_1 as a function of B_0. Chemical-shift anisotropy is unusual. Usually $T_1 = T_2$, but $T_{1\,csa} = \frac{7}{6}T_{2csa}$.

Table 28. Representative coupling constants between ^{183}W and other nuclei.

Compound	Coupling constant (Hz)	Ref.
$[Me_2Si\{(\eta^5\text{-}C_5H_4)WH(CO)_3\}_2]$	$^1J(^{183}W\text{–}^1H) = 36.0$	198
$[Me_2Si\{(\eta^5\text{-}C_5H_4)W(CO)_2\}_2(\mu\text{-}H)(\mu\text{-}PMe_2)]$	$^1J(^{183}W\text{–}^1H) = +39.0$	198
$[(\eta^4\text{-}C_4H_6)_3W]$	$^1J(^{183}W\text{–}^{13}C) = 19.8$	33
$[(\eta^4\text{-}2\text{-}MeC_4H_5)_3W]$	$^1J(^{183}W\text{–}^{13}C) = 5$ to 25	33
$[(\eta^4\text{-}2,3\text{-}Me_2\text{-}C_4H_4)_3W]$	$^1J(^{183}W\text{–}^{13}C) = 25$	33
$[W(C_6H_4CH{=}NCH_2CH_2NH_2)(CO)_3F]$	$^1J(^{183}W\text{–}^{19}F) = 20$	146
$[W(C_6H_4CH{=}NC_6H_4NH_2)(CO)_3F]$	$^1J(^{183}W\text{–}^{19}F) = 20$	146
$[Me_2Si\{(\eta^5\text{-}C_5H_4)W(CO)_2\}_2(\mu\text{-}H)(\mu\text{-}PMe_2)]$	$^1J(^{183}W\text{–}^{31}P) = +200.6$	198
$[(\eta^3\text{-}C_3H_5)_3(Me_3P)WMe]$	$^1J(^{183}W\text{–}^{31}P) = 164$	30
$[(\eta^3\text{-}C_3H_5)_3(Me_3P)WCl]$	$^1J(^{183}W\text{–}^{31}P) = 173.5$	30
$[(\eta^3\text{-}C_3H_5)_3(Me_3P)WBr]$	$^1J(^{183}W\text{–}^{31}P) = 172$	30
$[(\eta^3\text{-}C_3H_5)_3(Me_3P)WI]$	$^1J(^{183}W\text{–}^{31}P) = 171$	30
$[W(CO)_4\{(Ph_2P)_2CH_2\}]$	$^1J(^{183}W\text{–}^{31}P) = +201.2$	199
$[W(CO)_4\{(Ph_2P)_2NH\}]$	$^1J(^{183}W\text{–}^{31}P) = +207.5$	199
$[W(CO)_4\{(Ph_2P)_2C{=}CH_2\}]$	$^1J(^{183}W\text{–}^{31}P) = +210.9$	199
$[W(CO)_3\{Ph_2PCH(CH_2PPh_2)CH_2CH_2PPh_2\}]$	$^1J(^{183}W\text{–}^{31}P) = 215.7, 212.2$	152
$[W(CO)_4(Ph_2PCH_2CH_2CH_2PPh_2)]$	$^1J(^{183}W\text{–}^{31}P) = +230.7$	199
$[W(CO)_4\{Ph_2PCH(CH_2PPh_2)CH_2CH_2PPh_2\}]$	$^1J(^{183}W\text{–}^{31}P) = 221.1, 226.5$	152
$[W(CO)_4\{Ph_2PCH(CH_2PPh_2O)CH_2CH_2PPh_2\}]$	$^1J(^{183}W\text{–}^{31}P) = 223.5, 225.6$	152
$[W(CO)_4(Ph_2PCH_2CH_2CH_2PPh_2)]$	$^1J(^{183}W\text{–}^{31}P) = +222.2$	199
$[W(CO)_4(Ph_2PCH_2CH_2PPh_2)]$	$^1J(^{183}W\text{–}^{31}P) = +229$	199
$[W(CO)_4(cis\text{-}Ph_2PCH{=}CHPPh_2)]$	$^1J(^{183}W\text{–}^{31}P) = +233$	199
$[Rh(WS_4)_3]^{3-}$	$^2J(^{183}W\text{–}^{103}Rh) = 4.8$	200
$[(\eta^5\text{-}C_5H_5)W(CO)_3(SnMe_3)]$	$^1J(^{183}W\text{–}^{119}Sn) = -150$	15
$[(D_2O)_2Zn_4As_2W_{18}O_{68}]^{10-}$	$^2J(^{183}W\text{–}^{183}W) = 5.8, 6.2, 9.0, 19.6, 25.0$	125
$[(D_2O)_2Zn_4P_2W_{18}O_{68}]^{10-}$	$^2J(^{183}W\text{–}^{183}W = 7.1, 7.3, 9.0,$ 18.6, 19.2, 19.6, 23.5, 23.7, 23.8	125

$[(\eta^5\text{-}C_5Me_5)RhSiW_9Nb_3O_{40}]^{5-}$	$^2J(^{183}W-^{183}W) = 12.8, 14.0, 15.9, 16.2, 29.3, 30.2$	123
$[(\eta^5\text{-}C_5Me_5)RhP_2W_{15}Nb_3O_{62}]^{7-}$	$^2J(^{183}W-^{183}W) = 18.2, 24.6$	113
$[BW_{12}O_{40}H_6]^{5-}$	$^2J(^{183}W-^{183}W) = 4.2, 14.4$	56
$[H_2W_{12}FO_{39}]^{5-}$	$^2J(^{183}W-^{183}W) = 5, 22$ Hz	130
$[H_2W_{12}O_{40}H_6]^{6-}$	$^2J(^{183}W-^{183}W) = 14.6$	56
$[H_3SiV_3W_9O_{40}]^{4-}$	$^2J(^{183}W-^{183}W) = 16.4$	133
$[HSiW_{10}O_{36}]^{7-}$	$^2J(^{183}W-^{183}W) = 4.6, 4.9, 23.8$	117
$[Nb_2W_4O_{19}]^{4}$	$^2J(^{183}W-^{183}W) = 5.5$ Hz	137
$[P_2W_{21}O_{71}(OH_2)_3]^{6-}$	$^2J(^{183}W-^{183}W) = 8.5, 9.6, 19.4, 21.5, 22.0, 25.2$	107
$[Si_2W_{18}Nb_6O_{77}]^{8-}$	$^2J(^{183}W-^{183}W) = 18.3$ Hz	123
$[SiW_9Nb_3O_{40}]^{7-}$	$^2J(^{183}W-^{183}W) = 15.3$ Hz	123
$[SiW_{12}O_{40}H_6]^{4-}$	$^2J(^{183}W-^{183}W) = 6.4, 15.1$	56
$[Ti_2W_{10}PO_{40}]^{7-}$	$^2J(^{183}W-^{183}W) = 6.4, 6.7, 7.8, 16.8, 17.5, 17.9, 20.8$	111
$\beta\text{-}[SiW_{12}O_{40}]^{4-}$	$^2J(^{183}W-^{183}W) = 8, 20$	130
$[P_2W_{15}Nb_3O_{62}]^{9-}$	$^2J(^{183}W-^{183}W) = 17.2, 21.3$	113
$[Si_2W_{18}Zr_3O_{71}H_n]^{n-14}$	$^2J(^{183}W\cdot{}^{183}W) = 14$	115

Table 29. Representative coupling constants between ^{187}Os and other nuclei.

Compound	Coupling constant (Hz)	Ref.
$[OsH_4(PEt_2Ph)_3]$	$^1J(^{187}Os-^1H) = 30.8$	201
$[OsH_4(AsEt_2Ph)_3]$	$^1J(^{187}Os-^1H) = 34.0$	201
$[OsH_6(AsEt_2Ph)_2]$	$^1J(^{187}Os-^1H) = 33.0$	201
$[Os_3H_3(CO)_9CC(CH_2)_2CH_2]^+$	$^1J(^{187}Os-^1H) = 28.8, 32.0$	202
$[Os_3H(CO)_{12}]^+$	$^1J(^{187}Os-^1H) = 30.5$	202
$[RuOs_2H(CO)_{12}]^+$	$^1J(^{187}Os-^1H) = 29.1$	202
$[Os_3H_2(CO)_{12}]$	$^1J(^{187}Os-^1H) = 47.0$	202
$[Os_3ReH(CO)_{16}]$	$^1J(^{187}Os-^1H) = 27.0, 34.9$	202
$[Os_3Re_2H(CO)_{20}]$	$^1J(^{187}Os-^1H) = 27.8, 29.3$	202
$[Os_3H(CO)_{10}C_2Ph]$	$^1J(^{187}Os-^1H) = 33.5$	202
$[Os_4H_4(CO)_{12}]$	$^1J(^{187}Os-^1H) = 14.6$	202
$[HOs_3Re(CO)_{14}(C_2Ph)_2]$	$^1J(^{187}Os-^1H) = 30.3, 34.5$	203
$[H_2Os_3Ru(CO)_{12}(PC_6H_{11})]$	$^1J(^{187}Os-^1H) = 30, 37$	204
$[HOs_3Mn(CO)_{14}(C_2Ph)_2]$	$^1J(^{187}Os-^1H) = 30.2, 34.6$	204
$[H_2Os_4(CO)_{12}(PPh)]$	$^1J(^{187}Os-^1H) = 19.4, 36.1$	204
$[H_2Os_4(CO)_{12}(PC_6H_{11})]$	$^1J(^{187}Os-^1H) = 29.6, 36.6$	204
$[HOs_{10}C(CO)_{24}]^-$	$^1J(^{187}Os-^1H) = 15.9, 26.6$	205
$[HOs_{10}C(CO)_{24}\{Au(PPh_3)\}]$	$^1J(^{187}Os-^1H) = 15.4, 26.2$	205
$[HOs_{10}C(CO)_{22}(NO)I]^-$	$^1J(^{187}Os-^1H) = 13.8, 25.9$	205
$[HOs_{11}C(CO)_{27}]^-$	$^1J(^{187}Os-^1H) = 14.1, 38.2, 49.9$	205
$[(\eta^6\text{-1-Me-4-Pr}^iC_6H_4)_4Os_4(\mu\text{-H})_4]^{2+}$	$^1J(^{187}Os-^1H) = 36$	156, 157
$[(\eta^6\text{-1-Me-4-Pr}^iC_6H_4)_2Os_2(\mu\text{-H})(\mu\text{-Cl})(Cl_2]$	$^1J(^{187}Os-^1H) = 61$	156
$[(\eta^6\text{-1-Me-4-Pr}^iC_6H_4)_2Os_2(\mu\text{-H})_3]^+$	$^1J(^{187}Os-^1H) = 84$	156
$[(\eta^6\text{-1-Me-4-Pr}^iC_6H_4)_2Os_2(\mu\text{-H})(\mu\text{-Cl})(O_2CCH_3)]^+$	$^1J(^{187}Os-^1H) = 66$	156
$[(\eta^6\text{-1-Me-4-Pr}^iC_6H_4)_2Os_2(\mu\text{-H})_2(O_2CCH_3)]^+$	$^1J(^{187}Os-^1H) = 76$	156
$[OsH_4(PEt_2Ph)_3]$	$^1J(^{187}Os-^{31}P) = 166$	206
cis-$[OsCl_2(CO)_2(PBu^tPr^n_2)_2]$	$^1J(^{187}Os-^{31}P) = 149.8$	206
$[Os(SnCl_3)_6]^{4-}$	$^1J(^{187}Os-^{119}Sn) = 1123$	207

When the metal nucleus is in a very symmetric environment, i.e. octahedral or tetrahedral, then T_{1csa} may not be dominant, and spin rotation becomes the only residual relaxation mechanism, giving rise to T_{1sr}, which is given by (12) in the fast tumbling limit

$$T_{1sr}^{-1} = \frac{IkTC^2\tau_{sr}}{3\hbar^2} \tag{12}$$

where I is the moment of inertia, C is the spin–rotation coupling constant and τ_{sr} is the correlation time for the spin–rotation interaction. Due to Hubbard's relationship,

$$\tau_c\tau_{sr} = \frac{I}{6kT} \tag{13}$$

T_{1sr} is unusual, decreasing with temperature, while all other relaxation pathways become less efficient at high temperature, with a resulting increase in T_1. This temperature dependence is used to identify contributions by T_{1sr} to the total relaxation.

The presence of a quadrupolar nucleus bonded to the metal nucleus can cause substantial broadening of the signal although it is unlikely to contribute to T_1. This results from scalar coupling. The contribution to T_1 due to scalar coupling, T_{1sc} is given by

$$T_{1sc}^{-1} = \frac{8\pi^2J^2S(S+1)T_1^S}{8[1+(\omega_I-\omega_S)^2(T_1^S)^2]} \tag{14}$$

where J is the coupling constant between the metal nucleus and the quadrupolar nucleus, T_1^S is the spin lattice relaxation time of the quadrupolar nucleus, and ω_I and ω_S are the resonance frequencies of the metal and quadrupolar nuclei. Unless $\omega_I - \omega_S$ is small, then scalar coupling does not contribute to T_1. However, T_{2sc} can be significant,

$$T_{2sc}^{-1} = \tfrac{1}{2}T_{1sc}^{-1} + \tfrac{4}{3}\pi^2J^2S(S+1)T_1^S \tag{15}$$

As the nuclei described in this review are relatively difficult to observe, the broadening of the signals due to scalar coupling can make the observation difficult.

There have been relatively few observations of T_1 for these insensitive nuclei, see Tables 30–33. It has been shown that, for $[(\eta^5\text{-}C_5H_5)_2Fe]$, $[(\eta^4\text{-}C_4H_6)Fe(CO)_3]$, $[(\eta^4\text{-}2\text{-}MeC_4H_5)Fe(CO)_3]$ and $[(\eta^4\text{-}1\text{-}MeC_4H_5)Fe(CO)_3]$, both chemical-shift anisotropy and spin rotation play a significant role, especially at low field.[58] Adsorption of the iron complex on particles arising from decomposition also produced significant relaxation. Similarly for $[(C_6H_4\text{-}1\text{-}NMe_2\text{-}2\text{-}NMe)Rh(\eta^4\text{-cod})]$, at 9.4 T, the dominant relaxation is due

Table 30. Spin lattice relaxation times of ^{57}Fe.

Compound	Field strength (T)	Temperature (K)	T_1 (s)	Ref.
[Fe(protoporphyrin-IX)(CO)(NC_5H_5)]	11.74		0.030	61
[(η^5-C_5H_5)(η^5-$C_5H_4Bu^n$)Fe]				208
Carbonyl myoglobin	8.45	300	0.017	209
[$Fe(CO)_5$], neat	2.114	300	81.1	58
[$Fe(CO)_5$], 6.4 M in C_6D_6	2.114	276.5	65.9	58
[$Fe(CO)_5$], 6.4 M in C_6D_6	2.114	300	65.9	58
[$Fe(CO)_5$], 6.4 M in C_6D_6	2.114	321	50.0	58
[$Fe(CO)_5$], 6.4 M in C_6D_6	9.39	278	87.1	58
[$Fe(CO)_5$], 6.4 M in C_6D_6	9.39	298	69.4	58
[$Fe(CO)_5$], 6.4 M in C_6D_6	9.39	320	56.4	58
[$Fe(CO)_5$], neat	7.05		80	
[(η^5-C_5H_5)$_2$Fe], 1.05 M in CS_2	2.114	298	20	58
[(η^5-C_5H_5)$_2$Fe], 1.05 M in C_6D_6	2.114	298	21.9	58
[(η^5-C_5H_5)$_2$Fe], 1.05 M in 95% CS_2/5% C_6D_6	2.114	278	20.6	58
[(η^5-C_5H_5)$_2$Fe], 1.05 M in 95% CS_2/5% C_6D_6	2.114	298	20.6	58
[(η^5-C_5H_5)$_2$Fe], 1.05 M in 95% CS_2/5% C_6D_6	9.39	278	2.85	58
[(η^5-C_5H_5)$_2$Fe], 1.05 M in 95% CS_2/5% C_6D_6	9.39	298	4.21	58
[(η^5-C_5H_5)$_2$Fe]	7.05		4	210
[(η^5-C_5H_5)$_2$Fe], 1.05 M in 95% CS_2/5% C_6D_6	9.395		4.21	58
[(η^4-C_4H_6)$Fe(CO)_3$], neat	2.114	300	70.9	58
[(η^4-C_4H_6)$Fe(CO)_3$], 4.4 M in C_6D_6	2.114	282	76.8	58
[(η^4-C_4H_6)$Fe(CO)_3$], 4.4 M in C_6D_6	2.114	300	84.0	58
[(η^4-C_4H_6)$Fe(CO)_3$], 4.4 M in C_6D_6	2.114	321	63.7	58
[(η^4-C_4H_6)$Fe(CO)_3$], 4.4 M in C_6H_6	9.395	295	23.3	58
[(η^4-C_4H_6)$Fe(CO)_3$], 4.4 M in C_6D_6	9.395	318	28.4	58
[(η^5-2-MeC_4H_5)$Fe(CO)_3$], 2.7 M in C_6D_6	2.114	295	89.3	58
[(η^4-2-MeC_4H_5)$Fe(CO)_3$], 2.7 M in C_6D_6	9.395	295	26.0	58
[(η^4-Z-1-MeC_4H_5)$Fe(CO)_3$], 3.4 M in C_6D_6	2.114	295	107	58
[(η^4-Z-1-MeC_4H_5)$Fe(CO)_3$], 3.4 M in C_6D_6	9.395	295	22.1	58
[(η^4-E-1-MeC_4H_5)$Fe(CO)_3$, 3.8 M in C_6D_6	2.114	295	87.6	58
[(η^4-E-1-MeC_4H_5)$Fe(CO)_3$], 3.8 M in C_6D_6	9.395	295	18.9	58

Table 31. Spin lattice relaxation times of ^{103}Rh.

Compound	Field strength (T)	Temperature (K)	T_1 (s)	Ref.
$[(C_6H_4\text{-}1\text{-}NMe_2\text{-}2\text{-}NMe)Rh(\eta^4\text{-cod})]$	9.39	310	1.53	29
$[(\eta^4\text{-cod})_2Rh_2(\mu\text{-Cl})_2]$	9.39	310	1.75	29
$[Rh(acac)_3]$	9.39	310	39	29
$[Rh(acac)_3]$	2.114	300	62.8	36
$[Rh(acac)_3]$	2.114	300	82 ± 3	211
$[Rh(\eta^5\text{-}C_5H_5)(\eta^4\text{-cod})]$	9.39	339	12.7	212
$[Rh(\eta^5\text{-}C_5H_5)(\eta^4\text{-cod})]$	9.39	309	8.6	212
$[Rh(\eta^5\text{-}C_5H_5)(\eta^4\text{-cod})]$	2.114	300	60 ± 4	211
$[Rh(\eta^5\text{-}C_5H_5)(\eta^4\text{-cod}]]$	9.39	271	5.2	212
$[Rh(\eta^5\text{-}C_5H_5)(\eta^4\text{-cod})]$	9.39	240	2.4	212
$[Rh(\eta^5\text{-}C_5Me_5)(\eta^4\text{-}2,3\text{-}C_4H_4)]$	9.39	296	6.5	213
$[Rh(\eta^5\text{-}C_5Me_5)(\eta^4\text{-}2,3\text{-}C_4H_4)]$	9.39	203	0.7	213
$[Rh(\eta^5\text{-}C_5Me_5)(\eta^4\text{-}1,1,2\text{-}Me_3C_3H_3)]^+$	9.39	296	5.6	213
$[Rh(\eta^5\text{-}C_5Me_5)(\eta^4\text{-}1,1,2\text{-}Me_3C_3H_3)]^+$	9.39	203	0.8	213
$[Rh(CO)_2(acac)]$	9.39	298	> 30	64
$[Rh(\eta^4\text{-dq})(Bpz_4)]$	9.39	298	0.62	64
$[Rh(\eta^4\text{-cod})(Bpz_4)]$	9.39	298	0.51	64
$[Rh(\eta^4\text{-cod})(Bpz_4)]$	9.39	213	0.060	64

Table 32. Spin lattice relaxation time of ^{183}W.

Compound	Field strength (T)	Temperature (K)	T_1 (s)	Ref.
WF_6		179	4.2	4
$[(\eta^4\text{-}2\text{-}MeC_4H_5)_3W]$[a]	9.39	253	5.4	33
$[(\eta^4\text{-}2\text{-}MeC_4H_5)_3W]$[a]	9.39	273	10.7	33
$[(\eta^4\text{-}2\text{-}MeC_4H_5)_3W]$[a]	9.39	253	5.5	33
$[(\eta^4\text{-}2\text{-}MeC_4H_5)_3W]$[a]	9.39	273	9.5	33
$[(\eta^3\text{-}C_3H_5)_4W]$	9.39	310	9.7	33
$[(\eta^3\text{-}C_3H_5)_4W]$	9.39	273	6.6	33

[a] Ref. 4.

Table 33. Spin lattice relaxation times of ^{187}Os.

Compound	Field strength (T)	T_1 (s)	Ref.
$[(\eta^5\text{-}C_5H_5)Os(PPh_3)_2H]$	9.39	1.6	155
$[(\eta^5\text{-}C_5H_5)Os(PMe_3)_2Br]$[a]	9.39	6.7	155

[a] Ref. 155.

to chemical-shift anisotropy, with $T_{1csa} = 1.59$ s and $T_{1sr} = 38$ s, while for [[η^4-cod)$_2$Rh$_2$(μ-Cl)$_2$] $T_{1csa} = 2.19$ s and $T_{1sr} = 8.8$ s. In contrast, for an octahedral geometry, T_{1sr} is dominant even at 9.4 T, with $T_{1csa} = 390$ s and $T_{1sr} = 43$ s.[59]

A detailed investigation of the mechanism relaxation of $[Ag]^+$ in aqueous solution has been performed.[60] It was concluded that the main relaxation mechanisms are due to rapid chemical-exchange processes in the solvation shell of the ^{109}Ag ion and the chemical-shift anisotropy of this solvate complex. Adsorption of the Ag^+ ions onto colloidal silver particles also presents an additional transverse relaxation mechanism. T_1 values of the order of 700 s were found.

REFERENCES

1. R.K. Harris and B.E. Mann, *NMR and the Periodic Table*. Academic Press, London, 1978.
2. R.K. Harris, Ref. 1, pp. 13–14.
3. A. Schwenk, *J. Magn. Reson.*, 1971, **5**, 376.
4. J. Kronenbitter and A. Schwenk, *J. Magn. Reson.*, 1977, **25**, 147.
5. C. Hassler, J. Kronenbitter and A. Schwenk, *Z. Phys. A*, 1977, **280**, 117.
6. E. Brun, J. Oeser, H.H. Staub and C.G. Telschow, *Phys. Rev.*, 1954, **93**, 172.
7. P.B. Sogo and C.D. Jeffries, *Phys. Rev.*, 1954, **93**, 174.
8. C.W. Burges, R. Koschmeider, W. Sahm and A. Schwenk, *Z. Naturforsch., Teil A*, 1973, **28**, 1753.
9. K. Jucker, W. Sahm and A. Schwenk, *Z. Naturforsch., Teil A*, 1976, **31**, 1532.
10. A.K. Rahimi and A.I. Popov, *Inorg. Nucl. Chem. Lett.*, 1976, **12**, 703.
11. W. Sahm and A. Schwenk, *Z. Naturforsch., Teil A*, 1974, **29**, 1763.
12. J. Banck and A. Schwenk, *Z. Phys. B*, 1975, **20**, 75.
13. A.A. Koridze, P.V. Petrovskii, S.P. Gubin, and E.I. Fedin, *J. Organomet. Chem.*, 1975, **93**, C26.
14. T.H. Brown and P.J. Green, *J. Am. Chem. Soc.*, 1970, **92**, 2359.
15. H.C.E. McFarlane, W. McFarlane and D.S. Rycroft, *J. Chem. Soc., Dalton Trans.*, 1976, 1616.
16. M. Arthurs, S.M. Nelson and M.G.B. Drew, *J. Chem. Soc., Dalton Trans.*, 1977, 779.
17. H.C.E. McFarlane, W. McFarlane and R.J. Wood, *Bull. Soc. Chim. Belg.*, 1977, **85**, 864.
18. E.M. Hyde, J.D. Kennedy, B.L. Shaw and W. McFarlane, *J. Chem. Soc., Dalton Trans.*, 1977, 1571.
19. S. Martinengo, B.T. Heaton, R.J. Goodfellow and P. Chini, *J. Chem. Soc., Chem. Commun.*, 1977, 39.
20. T.H. Brown and P.J. Green, *Phys. Lett., Ser. A*, 1970, **31**, 148.
21. W. McFarlane, A.M. Noble and J.M. Winfield, *J. Chem. Soc., A*, 1971, 948.
22. P.J. Green and T.H. Brown, *Inorg. Chem.*, 1971, **10**, 206.
23. P. Laszlo, *N.M.R. of Newly Accessible Nuclei*. Academic Press, London, 1983.
24. J. Mason, *Multinuclear N.M.R.* Plenum Press, New York, 1987.
25. D. Rehder, *Magn. Reson. Rev.*, 1984, **9**, 125.
26. B.E. Mann, in *Transition Metal NMR Spectroscopy* (ed. P.S. Pregosin). Elsevier, Amsterdam, in press.
27. M. Minelli, J.H. Enemark, R.T.C. Brownlee, M.J. O'Connor and A.G. Wedd, *Coord. Chem. Rev.*, 1985, **68**, 169.

28. J. Mason, *Polyhedron*, 1989, **8**, 1657.
29. R. Benn and A. Rufińska, *Angew. Chem. Int. Ed. Engl.*, 1986, **25**, 861.
30. R. Benn and A. Rufińska, *Magn. Reson. Chem.*, 1988, **26**, 895.
31. K. Endo, K. Matsushita, K. Deguchi, K. Yamamoto, S. Susuki and K. Futaki, *Chem. Lett.*, 1982, 1497.
32. K. Endo, K. Yamamoto, K. Matsushita, K. Deguchi, K. Kanda and H. Nakatsuji, *J. Magn. Reson.*, 1985, **65**, 268.
33. R. Benn, C. Brevard, A. Rufińska and G. Schroth, *Organometallics*, 1987, **6**, 938.
34. A. Schwenk, *Z. Phys.*, 1968, **213**, 482.
35. A Schwenk, *J. Magn. Reson.*, 1980, **37**, 55.
36. K.-D. Grüninger, A Schwenk and B.E. Mann, *J. Magn. Reson.*, 1980, **41**, 354.
37. G.A. Morris and R. Freeman, *J. Am. Chem. Soc.*, 1979, **101**, 760.
38. D.M. Doddrell, D.T. Pegg and M.R. Bendall, *J. Magn. Reson.*; 1982, **48**, 323; D.T. Pegg, D.M. Doddrell and M.R. Bendall, *J. Chem. Phys.*, 1982, **77**, 2745.
39. S.J. Berners Price, C. Brevard, A. Pagelot and P.J. Sadler, *Inorg. Chem.*, 1985, **24**, 4278.
40. C. Brevard and R. Schimpf, *J. Magn. Reson.*, 1982, **47**, 528.
41. A. Albinati, C. Anklin, P. Janser, H. Lehner, D. Matt, P.S. Pregosin and L.M. Venanzi, *Inorg. Chem.*, 1989, **28**, 1105.
42. C.J. Jameson, A.K. Jameson and S.M. Cohen, *J. Magn. Reson.*, 1975, **19**, 385. F.G. Morin, M.S. Solum, J.D. Withers, D.M. Grant and D.K. Dalling, *J. Magn. Reson.*, 1982, **48**, 138.
43. G.A. Webb, in *NMR and the Periodic Table* (ed. R.K. Harris and B.E. Mann), Chap. 3. Academic Press, London, 1978.
44. N. Juranić, *Coord. Chem. Rev.*, 1989, **96**, 253.
45. J. Ruiz, B.E. Mann, C.M. Spencer, B.F. Taylor and P.M. Maitlis, *J. Chem. Soc., Dalton Trans.*, 1987, 1963.
46. B.E. Mann, N.J. Meanwell, C.M. Spencer, B.F. Taylor and P.M. Maitlis, *J. Chem. Soc., Dalton Trans.*, 1985, 1374.
47. C. Carr, J. Glaser and M. Sandström, *Inorg. Chim. Acta*, 1987, **131**, 153.
48. C.E. Holloway, A. Mastracci and I.M. Walker, *Inorg. Chim. Acta*, 1986, **113**, 187.
49. A. Fratiello, V. Kubo-Anderson, T. Bolinger, C. Cordero, B. DeMerit, T. Flores, D. Matejka and R. Perrigan, *J. Magn. Reson.*, 1989, **83**, 358.
50. A. Schwenk and G. Zimmermann, *Phys. Lett.*, 1968, **26A**, 258.
51. L.P. Kazansky and M.A. Fedotov, *J. Chem. Soc., Chem. Commun.*, 1983, 417.
52. T.L. Jorris, M. Kozik, N. Casa-Pastor, P.J. Domaille, R.G. Finke, W.K. Miller and L.C.W Baker, *J. Am. Chem. Soc.*, 1987, **109**, 7402.
53. L.P. Kazansky and M.A. Fedotov, *Koord. Chim.*, 1988, **14**, 939.
54. R. Acerete, N. Casañ-Pastor, J. Bas-Serra and L.C.W. Baker, *J. Am. Chem. Soc.*, 1989, **111**, 6049.
55. M. Kozik, C.F. Hammer and L.C.W. Baker, *J. Am. Chem. Soc.*, 1986, **108**, 2748.
56. K. Piepgrass and M.T. Pope, *J. Am. Chem. Soc.*, 1987, **109**, 1586.
57. J. Kronenbitter, U. Schweizer and A. Schwenk, *Z. Naturforsch., Teil A*, 1980, **35**, 319.
58. A. Hafner and W. von Philipsborn, *J. Magn. Reson.*, 1987, **74**, 433.
59. R. Benn and A. Rufińska, *Angew. Chem., Int. Ed. Engl.*, 1986, **25**, 861.
60. H. Pfister, A. Schwenk and D. Zeller, *J. Magn. Reson.*, 1986, **68**, 138.
61. L. Baltzer, E.D. Becker, R.G. Tschudin and O.A. Gansow, *J. Chem. Soc., Chem. Commun.*, 1985, 1040.
62. R.J. Goodfellow, unpublished results, quoted in R.J. Goodfellow, *N.M.R. and the Periodic Table* (ed. R.K. Harris and B.E. Mann), p. 244. Academic Press, London, 1978.
63. E.M. Hyde, J.D. Kennedy, B.L. Shaw, and W. McFarlane, *J. Chem. Soc., Dalton Trans.*, 1977, 1571.

64. M. Cocivera, G. Ferguson, R.E. Lenkinski, P. Szczecinski, F.J. Lalor and D.J. O'Sullivan, *J. Magn. Reson.*, 1982, **46**, 168.
65. A.A. Koridze, I.M. Astakhova and P.V. Petrovskii, *Izv. Akad. Nauk, Ser. Khim.*, 1982, 956.
66. J. Jenny, W. von Philipsborn, J. Kronenbitter and A. Schwenk, *J. Organomet. Chem.*, 1981, **205**, 211.
67. R. Benn, H. Brenneke, A. Frings, H. Lehmkuhl, G. Mehler, A. Rufińska and T. Wildt, *J. Am. Chem. Soc.*, 1988, **110**, 5661.
68. C.M. Adams, G. Cerioni, A. Hafner, H. Kalchhauser, W. von Philipsborn, R. Prewo and A. Schwenk, *Helv. Chim. Acta*, 1988, **71**, 1116.
69. P. Benn and C. Brevard, *J. Am. Chem. Soc.*, 1986, **108**, 5622.
70. A.A. Koridze, I.M. Astakhova and P.V. Petrovskii, *Izv. Akad. Nauk, Ser. Khim.*, 1982, 957.
71. A.A. Koridze, N.M. Astakhova and P.V. Petrovskii, *J. Organomet. Chem.*, 1983, **254**, 345.
72. A.A. Koridze, P.V. Petrovskii, I.M. Astakhova and I.E. Kolobova, *Izv. Akad. Nauk, Ser. Khim.*, 1987, 1504.
73. E. Haslinger, K. Koci, W. Robien, and K. Schlögl, *Monatsch. Chem.*, 1983, **114**, 495.
74. T. Nozawa, M. Sato, M. Hatano, N. Kobayashi and T. Osa, *Chem. Lett.*, 1983, 1289.
75. E. Haslinger, W. Robien, K. Schlögl and W. Weissensteiner, *J. Organomet. Chem.*, 1981, **218**, C11.
76. L. Baltzer and M. Landergren, *J. Chem. Soc., Chem. Commun.*, 1987, 32.
77. H.C. Lee, J.K. Gard, T.L. Brown, and E. Oldfield, *J. Am. Chem. Soc.*, 1985, **107**, 4087.
78. L. Baltzer, *J. Am. Chem. Soc.*, 1987, **109**, 3479.
79. W.J. Evans, J.H. Meadows, A.G. Kostka and G.L. Closs, *Organometallics*, 1985, **4**, 324.
80. M.D. Fryzuk and T.S. Haddad, *J. Am. Chem. Soc.*, 1988, **110**, 8263.
81. A. Albinati *et al.*, *J. Am. Chem. Soc.*, 1989, **111**, 2115.
82. A.A.H. van der Zeijden, G. van Koten, J.M. Ernsting, C.J. Elsevier, B. Krijnen and C.H. Stam, *J. Chem. Soc., Dalton Trans.*, 1989, 317.
83. P. Piraino, G. Bruno, G. Tresoldi, S. Lo Schiavo and F. Nicolò, *Inorg. Chem.*, 1989, **28**, 139.
84. E. Rotondo, B.E. Mann, P. Piraino and G. Tresoldi, *Inorg. Chem.*, 1989, **28**, 3070.
85. C.J. Elsevier, J.M. Ernsting and W.G.J. de Lange, *J. Chem. Soc., Chem. Commun.*, 1989, 585.
86. G. Bruno, S. Lo Schiavo, E. Rotondo, C.G. Arena and F. Faraone, *Organometallics*, 1989, **8**, 886.
87. R. Köster, G. Seidel, B. Wrackmeyer and D. Schlosser, *Chem. Ber.*, 1989, **122**, 2055.
88. C. Allevi, S. Bordoni, C.P. Clavering, B.T. Heaton, J.A. Iggo, C. Serengi and L. Garlaschelli, *Organometallics*, 1989, **8**, 385.
89. S.S.D. Brown, P.J. McCarthy, I.D. Salter, P.A. Bates, M.B. Hursthouse, I.J. Colquhoun, W. McFarlane and M. Murray, *J. Chem. Soc., Dalton Trans.*, 1988, 2787.
90. M. Ahlgrén, T. Pakkanen and I. Tahvanainen, *Acta Chem. Scand., Ser. A.*, 1985, **39**, 651.
91. A.F.M.J. van der Ploeg, G. van Koten and C. Brevard, *Inorg. Chem.*, 1982, **21**, 2878.
92. C. Brevard, G.C. van Stein and G. van Koten, *J. Am. Chem. Soc.*, 1981, **103**, 6746.
93. G.C. van Stein, G. van Koten, K. Vrieze, A.L. Spek, E.A. Klop and C. Brevard, *Inorg. Chem.*, 1985, **24**, 1367.
94. G.C. van Stein, G. van Koten and C. Brevard, *J. Organomet. Chem.*, 1982, **226**, C27.
95. G.C. van Stein, G. van Koten, F. Blank, L.C. Taylor, K. Vrieze, A.L. Spek, A.J.M. Duisenberg, A.M.M. Scheurs, B. Kojić-Prodić and C. Brevard, *Inorg. Chim. Acta*, 1985, **98**, 107.
96. S.J.B. Price, C. Brevard, A. Pagelot and P.J. Sadler, *Inorg. Chem.*, 1985, **24**, 4278.
97. S.S.D. Brown, I.J. Colquhoun, W. McFarlane, M. Murray, I.D. Salter and V. Šik, *J. Chem. Soc., Chem. Commun.*, 1986, 53.
98. K. Endo, K. Yamamoto, K. Matsushita, K. Deguchi, K. Kanda and H. Nakatsuji, *J. Magn. Reson.*, 1985, **65**, 268.

99. S.S.D. Brown, I.D. Salter, V. Šik, I.J. Colquhoun, W. McFarlane, P.A. Bates, M.B. Hursthouse and M. Murray, *J. Chem. Soc., Dalton Trans.*, 1988, 2177.
100. N.J. Campbell, A.C. Dengel, C.J. Edwards and W.P. Griffith, *J. Chem. Soc. Dalton Trans.*, 1989, 1203.
101. W.H. Knoth, P.J. Domaille and R.D. Farlee, *Organometallics*, 1987, **4**, 62.
102. F. Chauveau, *Bull. Soc. Chim. Fr.*, 1986, 199.
103. A. Narath and D.C. Wallace, *Phys. Rev.*, 1962, **127**, 724.
104. R.G. Finke, M.W. Droege and P.J. Domaille, *J. Am. Chem. Soc.*, 1987, **109**, 3886.
105. R. Acerete, C.F. Hammer and L.C.W. Baker, *J. Am. Chem. Soc.*, 1982, **104**, 5384.
106. R.G. Finke and M.W. Droege, *Inorg. Chem.*, 1983, **22**, 1006.
107. C.M. Tourné, G.F. Tourné and T.J.R. Weakley, *J. Chem. Soc., Dalton Trans.*, 1986, 2237.
108. W.H. Knoth, P.J. Domaille and R.L. Harlow, *Inorg. Chem.*, 1986, **25**, 1577.
109. J.F.W. Keana, M.D. Ogan, Y. Lü, M. Beer and J. Varkey, *J. Am. Chem. Soc.*, 1985, **107**, 6714.
110. J.F.A. Keana and M.D. Ogan, *J. Am. Chem. Soc.*, 1986, **108**, 7951.
111. P.J. Domaille and W.H. Knoth, *Inorg. Chem.*, 1983, **22**, 818.
112. R. Contant and A. Tézé, *Inorg. Chem.*, 1985, **24**, 4610.
113. D.J. Edlund, R.J. Saxton, D.K. Lyon and R.G. Finke, *Organometallics*, 1988, **7**, 1692.
114. R. Acerete, C.F. Hammer and L.C.W. Baker, *Inorg. Chem.*, 1984, **23**, 1478.
115. R.G. Finke, B. Rapko and J.T.R. Weakley, *Inorg. Chem.*, 1989, **28**, 1573.
116. R.I. Maksimovskaya, M.A. Fedotov and G.M. Maksimov, *Izv. Akad. Nauk SSSR, Ser. Khim.*, 1983, 247.
117. J. Canny, A. Tézé, R. Thouvenot and G. Hervé, *Inorg. Chem.*, 1986, **25**, 2114.
118. R.I. Maksimovskaya and K.G. Burtseva, *Polyhedron*, 1985, **4**, 1559.
119. P. Domaille, *J. Am. Chem. Soc.*, 1984, **106**, 7677.
120. R. Acerete, S. Harmalher, M.T. Pope and L.C.W. Baker, *J. Am. Chem. Soc.*, 1979, **101**, 267.
121. P.R. Sethuraman, M.A. Leparulo, M.T. Pope, F. Zonnevijlle, C. Brevard and J. Lemerle, *J. Am. Chem. Soc.*, 1981, **103**, 7665.
122. C.M. Tourné and G.F. Tourné, *J. Chem. Soc., Dalton Trans.*, 1988, 2411.
123. R.G. Finke and M. Droege, *J. Am. Chem. Soc.*, 1984, **106**, 7274.
124. R.I. Maksimovskaya and K.G. Burtseva, *Polyhedron*, 1985, **4**, 1559.
125. H.T. Evans, C.M. Tourné, G.F. Tourné and T.J.R. Weakley, *J. Chem. Soc., Dalton Trans.*, 1986, 2699.
126. R.G. Finke, M. Droege, J.R. Hutchinson and O. Gansow, *J. Am. Chem. Soc.*, 1981, **103**, 1587.
127. R.G. Finke, B. Rapko and P.J. Domaille, *Organometallics*, 1986, **5**, 175.
128. K. Piepgrass and M.T. Pope, *J. Am. Chem. Soc.*, 1987, **109**, 1586.
129. R. Acerete, C.F. Hammer and L.C.W. Baker, *J. Chem. Soc., Chem. Commun.*, 1979, 777.
130. J. Lefebvre, F. Cauveau, P. Doppelt and C. Brevard, *J. Am. Chem. Soc.*, 1981, **103**, 4589.
131. P.J. Domaille and G. Watunya, *Inorg. Chem.*, 1986, **25**, 1239.
132. J.F.W. Keana and M.D. Ogan, *J. Am. Chem. Soc.*, 1986, **108**, 7951.
133. R.G. Finke, B. Rapko, R.J. Saxton and P.J. Domaille, *J. Am. Chem. Soc.*, 1986, **108**, 2947.
134. R.I. Maksimovskaya and K.G. Burtseva, *Polyhedron*, 1985, **4**, 1559.
135. P.S. Roy and K. Wieghardt, *Inorg. Chem.*, 1987, **26**, 1885.
136. F. Chauveau, J. Éberlé and J. Lefebvre, *Nouv. J. Chem.*, 1985, **9**, 315.
137. C.J. Besecker, V.W. Day, W.G. Klemperer and M.R. Thompson, *J. Am. Chem. Soc.*, 1984, **106**, 4125
138. S.F. Gheller, T.W. Hambley, J.R. Rodgers, R.T.C. Brownlee, M.J. O'Connor, M.R. Snow and A.G. Wedd, *Inorg. Chem.*, 1984, **23**, 2519.
139. S.A. Cohen and E.I. Steifel, *Inorg. Chem.*, 1985, **24**, 4657.
140. K.E. Howard, T.B. Rauchfuss and S.R. Wilson, *Inorg. Chem.*, 1988, **27**, 3561.
141. S. Ikari, Y. Sasaki, A. Nagasawa, C. Kabuto and T. Ito, *Inorg. Chem.*, 1989, **28**, 1248.

142. A. Nagasawa, Y. Sasaki, B. Wang, S. Ikari and T. Ito, *Chem. Lett.*, 1987, 1271.
143. C.G. Young, E.M. Kober, and J.H. Enemark, *Polyhedron*, 1987, **6**, 255.
144. A. Patel, M.R. McMahon and D.T. Richens, *Inorg. Chim. Acta*, 1989, **163**, 73.
145. R. Benn, H. Brenneke, J. Heck and A. Rufińska, *Inorg. Chem.*, 1987, **26**, 2826.
146. R. Benn, A. Rufińska, M.A. King, C.E. Osterberg and T.G. Richmond, *J. Organomet. Chem.*, 1989, **376**, 359.
147. C.G. Young and J.H. Enemark, *Aust. J. Chem.*, 1986, **39**, 997.
148. D.J. Santure, J.C. Huffman and A.P. Sattelberger, *Inorg. Chem.*, 1985, **24**, 371.
149. D.J. Santure, K.W. McLaughlin, J.C. Huffman and A.P. Sattelberger, *Inorg. Chem.*, 1985, **22**, 1877.
150. R.L. Keiter and D.G. Vander Velde, *J. Organomet. Chem.*, 1983, **258**, C34.
151. G.T. Andrews, I.J. Colquhoun and W. McFarlane, *Polyhedron*, 1983, **2**, 783.
152. I.J. Colquhoun, W. McFarlane and R.L. Keiter, *J. Chem. Soc. Dalton Trans.*, 1984, 455.
153. J.L. Bookham, W. McFarlane and I.J. Colquhoun, *J. Chem. Soc., Dalton Trans.*, 1988, 503.
154. M. Minelli and W.J. Maley, *Inorg. Chem.*, 1989, **28**, 2954.
155. R. Benn, E. Joussen, H. Lehmkuhl, F.L. Ortiz and A. Rufińska, *J. Am. Chem. Soc.*, 1989, **111**, 8754.
156. J.A. Cabeza, B.E. Mann, P.M. Maitlis and C. Brevard, *J. Chem. Soc., Dalton Trans.*, 1988, 629.
157. J.A. Cabeza, A. Nutton, B.E. Mann, C. Brevard and P.M. Maitlis, *Inorg. Chim. Acta*, 1986, **115**, L47.
158. R. Benn and C. Brevard, *J. Am. Chem. Soc.*, 1986, **108**, 5622.
159. A.A. Koridze, N.M. Astakhova, P.V. Petrovskii and A.I. Lusenko, *Dokl. Akad. Nauk SSSR*, 1979, **242**, 416.
160. A.A. Koridze, P.V. Petrovskii, N.M. Astakhova, N.A. Vol'kenau, V.A. Petrakova and A.I. Nesmeyanov, *Dokl. Akad. Nauk SSSR*, 1980, **255**, 117.
161. P.S. Nielsen, R.S. Hansen and H.J. Jakobsen, *J. Organomet. Chem.*, 1976, **114**, 145.
162. A.A. Koridze, P.V. Petrovskii, S.P. Gubin and E.I. Fedin, *J. Organomet. Chem.*, 1975, **93**, C26.
163. S. Aime and D. Osella, *J. Organomet. Chem.*, 1981, **214**, C27.
164. F.A. Cotton and B.E. Hanson, *Isr. J. Chem.*, 1977, **15**, 165.
165. B.E. Mann, *J. Chem. Soc., Chem. Commun.*, 1971, 1173.
166. L. Vancea, M.J. Bennett, C.E. Jones, R.A. Smith and W.A.G. Graham, *Inorg. Chem.*, 1977, **16**, 897.
167. L. Kruzynski and J. Takats, *Inorg. Chem.*, 1976, **15**, 3140.
168. H. Schumann, K.H. Köhricht and M. Meissner, quoted in D. Rehder, *Magn. Reson. Rev.*, 1984, **9**, 125.
169. S. Aime and D. Osella, *J. Organomet. Chem.*, 1981, **214**, C27.
170. M.F. Lappert and R. Pearce, *J. Chem. Soc., Chem. Commun.*, 1973, 126.
171. D.G.H. Ballard and R. Pearce, *J. Chem. Soc., Chem. Commun.*, 1975, 621.
172. J. Holton, M.F. Lappert, G.R. Scollary, D.G.H. Ballard, R. Pearce, J.L. Atwood and W.E. Hunter, *J. Chem. Soc., Chem. Commun.*, 1976, 425.
173. K.H. den Haan and J.H. Teuben, *J. Chem. Soc., Chem. Commun.*, 1986, 682.
174. S.O. Grim and S.A. Sangokoya, *J. Chem. Soc., Chem. Commun.*, 1984, 1599.
175. R. Khaltar *et al.*, *J. Am. Chem. Soc.*, 1989, **111**, 1877.
176. L. Carlton and M.-P. Belciug, *J. Organomet. Chem.*, 1989, **378**, 469.
177. I.J. Colquhoun and W. McFarlane, *J. Magn. Reson.*, 1982, **46**, 525.
178. J. Ruiz, B.E. Mann, C.M. Spencer, B.F. Taylor and P.M. Maitlis, *J. Chem. Soc., Dalton Trans.*, 1987, 1963.
179. J. Ruiz, P.O. Bentz, B.E. Mann, C.M. Spencer, B.F. Taylor and P.M. Maitlis, *J. Chem. Soc., Dalton Trans.*, 1987, 2709.

180. B.E. Mann, C. Masters and B.L. Shaw, *J. Chem. Soc., Dalton Trans.*, 1971, 1104.
181. E. Rotondo, B.E. Mann, P. Piraino and G. Tresoldi, *Inorg. Chem.*, 1989, **28**, 3070.
182. R.J. Lawson and J.R. Shapley, *Inorg. Chem.*, 1978, **17**, 2963.
183. E.B. Boyer and S.D. Robinson, *Inorg. Chim. Acta*, 1982, **64**, L193; *J. Chem. Soc., Dalton Trans.*, 1985, 629.
184. H. Werner, J. Wolf and A. Hohn, *J. Organomet. Chem.*, 1985, **287**, 395.
185. B.E. Mann, N.J. Meanwell, C.M. Spencer, B.F. Taylor and P.M. Maitlis, *J. Chem. Soc., Chem. Commun.*, 1985, 1374.
186. P.M. Maitlis and B.E. Mann, unpublished results.
187. P. Caddy, M. Green, L.E. Smart and N. White, *J. Chem. Soc., Chem. Commun.*, 1978, 839.
188. P. Piraino, G. Bruno, G. Tresoldi, S. Lo Schiavo and F. Nicolò, *Inorg. Chem.*, 1989, **28**, 139.
189. C.D. Garner, M. Berry and B.E. Mann, *Inorg. Chem.*, 1984, **23**, 1501.
190. J. Ruiz, C.M. Spencer, B.E. Mann, B.F. Taylor and P.M. Maitlis, *J. Organomet. Chem.*, 1987, **325**, 253.
191. J.R. Barnes, P.L. Goggin and R.J. Goodfellow, unpublished results.
192. A. Fumagalli *et al.*, *J. Chem. Soc., Chem. Commun.*, 1978, 195.
193. A. Fumagalli, S. Martinengo, P. Chini, D. Galli, B.T. Heaton and R. Pergola, *Inorg. Chem.*, 1984, **23**, 2947.
194. A.R. Sanger, *Can. J. Chem.*, 1984, **62**, 822.
195. T.S. Hor, *Inorg. Chim. Acta*, 1988, **149**, 157.
196. W. Levason, M.D. Spicer and M. Webster, *J. Chem. Soc., Dalton Trans.*, 1988, 1377.
197. G.J. Arsenault, C.M. Anderson and R.J. Puddephatt, *Organometallics*, 1988, **7**, 2094.
198. R. Benn, H. Brenneke, J. Heck and A. Rufińska, *Inorg. Chem.*, 1987, **26**, 2826.
199. G.T. Andrews, I.J. Colquhoun and W. McFarlane, *Polyhedron*, 1983, **2**, 783.
200. K.E. Howard, T.B. Rauchfuss and S.R. Wilson, *Inorg. Chem.*, 1988, **27**, 3561.
201. B.E. Mann, C. Masters and B.L. Shaw, *J. Chem. Soc., Chem. Commun.*, 1970, 1041.
202. A.A. Koridze, O.A. Kizas, N.E. Kolobova, P.V. Petrovskii and E.I. Fedin, *J. Organomet. Chem.*, 1984, **265**, C33.
203. A.A. Koridze, O.A. Kizas, N.E. Kolobova, V.N. Vinogradova, N.A. Ustynyuk, P.V. Petrovskii, A.I. Yanovsky and Yu. T. Struchkov, *J. Chem. Soc., Chem. Commun.*, 1984, 1158.
204. S.B. Colbran, B.F.G. Johnson, F.J. Lahoz, J. Lewis and P.R. Raithby, *J. Chem. Soc., Dalton Trans.*, 1988, 1199.
205. S.R. Drake, B.F.G. Johnson and J. Lewis, *J. Chem. Soc., Dalton Trans.*, 1988, 1517.
206. D.F. Gill, B.E. Mann, C. Masters and B.L. Shaw, *J. Chem. Soc., Chem. Commun.*, 1970, 1269.
207. H. Moriyama, P.S. Pregosin, Y. Saito and T. Yamakawa, *J. Chem. Soc., Dalton Trans.*, 1984, 2329.
208. L. Baltzer, E.D. Becker, B.A. Averill, J.M. Hutchinson and O.A. Gansow, *J. Am. Chem. Soc.*, 1984, **106**, 2444.
209. H.C. Lee, J.K. Gard, T.L. Brown and E. Oldfield, *J. Am. Chem. Soc.*, 1985, **107**, 4087.
210. T. Nozawa, M. Hatano, M. Sato, Y. Toida and E. Batholdi, *Bull. Chem. Soc. Jpn.*, 1983, **56**, 3837.
211. E. Maurer, S. Rieker, M. Schollbach, A. Schwenk, T. Egolf and W. von Phillipsborn, *Helv. Chim. Acta*, 1982, **65**, 26.
212. H. Adams, N. Bailey, B.E. Mann, B.F. Taylor, C. White and P. Yavari, *J. Chem. Soc., Dalton Trans.*, 1987, 1947.
213. B. Buchmann, U. Piantini, W. von Philipsborn and A. Salzer, *Helv. Chim. Acta*, 1987, **70**, 1487.
214. B.E. Mann, in *NMR of Newly Accessible Nuclei*, Vol. 2 (ed. P. Laszlo), p. 316. Academic Press, New York, 19xx.
215. B.E. Mann, *Adv. Organomet. Chem.*, 1988, **28**, 397.

This Page Intentionally Left Blank

Permutation Symmetry in NMR Relaxation and Exchange

S. SZYMAŃSKI

Institute of Organic Chemistry, Polish Academy of Sciences, Warsaw, Poland

G. BINSCH

Institute of Organic Chemistry, University of Munich, Munich, F.R.G.

ANNUAL REPORTS ON NMR SPECTROSCOPY
VOLUME 23 ISBN 0-12-505323-1

Copyright © 1991 Academic Press Limited
All rights of reproduction in any form reserved

1. INTRODUCTION

The issue of permutation symmetry entered NMR spectroscopy soon after the unravelling, in the early 1950s, of the origin of the fine structure observed in the high-resolution spectra of the liquids. The theory of permutation symmetry in static stick spectra of coupled-spin systems, first formulated by McConnel *et al.*[1] in 1955, was presented in detail by Corio[2] a decade later. Implemented on a computer, permutation symmetry option has become an inherent part of the numerical procedures used to analyse static spectra, affording substantial simplification of the problem when the spin system in question exhibits relatively high symmetry.

It is clear that the presence of symmetry can also bring about considerable simplifications in the quantitative interpretation of nuclear-spin relaxation and exchange effects in coupled-spin systems. A maximum exploitation of permutation symmetry to simplify the computations is even more desirable in this case than in the analysis of stick spectra. This is because the theoretical description of relaxation and exchange in coupled-spin systems requires the use of Liouville space[3,4] and, therefore, the size of the spectral matrices to be handled is much larger than that of the static-spin Hamiltonian. For a system of 6–7 tightly coupled nuclei of spin $-\frac{1}{2}$, the static stick spectrum can be analysed without invoking the possible symmetry present in the system. However, without proper exploitation of the symmetry in handling the spectral matrices involved, quantitative analysis of relaxation and/or exchange phenomena in systems of such size is far beyond the capacity of modern computers.

Unlike the static NMR, the problem of permutation symmetry in spin relaxation and exchange has long awaited a complete and general solution. For spin exchange, the first partial solution involving intramolecular processes was proposed by Kleier and Binsch[5] as early as 1970. Their method was then employed in a number of computer programs to simulate[6] and iteratively analyse[7–9] the dynamic NMR (DNMR) spectra of coupled-spin systems. In the early 1970s[10–12] further *ad hoc* solutions were reported and in 1982 there appeared an interesting work by Luz and Naor[13] who demonstrated for the first time how, for a certain specific class of intramolecular degenerate rearrangements, the possible simplifications resulting from non-Abelian symmetry can be exploited fully in practical DNMR lineshape calculations.

In the context of NMR relaxation, described in terms of the Wangsness–Bloch–Redfield (WBR) theory,[14–17] the first deeper assignment of the problem is that due to Pyper.[18–20]

A general theory of permutation symmetry, encompassing both relaxation and exchange, was formulated in a series of papers which have appeared only recently.[21–25] The basic idea of the theory works, described first for

intramolecular exchange[21] and then extended to relaxation[22,25] and intermolecular exchange,[22] is that the problem must be considered at two levels, i.e. macroscopic and microscopic. The macroscopic symmetry properties, having a general character, are essentially identical for all these phenomena. The microscopic symmetry properties, however, are contingent features of certain specific systems in which the underlying random processes have intramolecular character. The recent theory[21–25] provides a means of clarifying some inconsistent or even incorrect statements that are perpetuated in the literature. First of all, however, the theory offers a method for exploiting in full the computational simplifications that are implied by the permutation symmetry present in an exchanging or relaxing systems. In particular this involves non-Abelian symmetries for which, except for the specific class of systems described by Luz and Naor,[13] the previous approaches[5,10–12,18] are insufficient.

The main purpose of the present report is to give a concise exposition of the recent theory[21–25] and to point out its possible consequences for the interpretation of relaxation and exchange phenomena in coupled symmetric-spin systems. In addition a brief review is given of the previous approaches which can now be seen in a proper perspective. The considerations of the present work are essentially also valid for exchanging uncoupled-spin systems. However, this limiting case will not be addressed explicitly here since it can be treated separately using simpler theoretical tools, as described in the recent review by Willem.[26]

2. GENERAL OUTLOOK

In order to facilitate a more formal discussion, we give here a general picture of the entire permutation symmetry in NMR relaxation and exchange problem by explaining some fundamental concepts and presenting the main results of the theory quoted above[21–25] in a purely descriptive way. The considerations given in this section focus on the two aspects of the problem already mentioned, i.e. the macroscopic and microscopic symmetry properties of exchanging and relaxing systems.

2.1. Macroscopic and microscopic symmetry in exchange

As an example of exchange in a symmetric system we consider the hypothetic rotations of nitroso groups in the two planar rotamers, *S* (*syn*) and *A* (*anti*), of *p*-dinitrosobenzene (Fig. 1). If the exchange is frozen on the DNMR time-scale, the proton stick spectrum of this system will be a superposition of the spectra

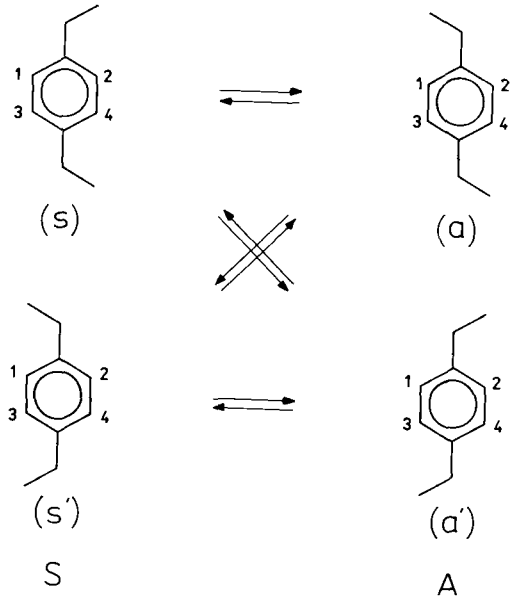

Fig. 1. Exchange network for rotations of single nitroso groups in 1,4-dinitrosobenzene as an illustration of the property of macroscopic symmetry invariance (see text).

of two symmetric-spin systems, AA'BB' and CC'DD' in the usual notation. The permutation symmetries of the spin Hamiltonians of both rotamers are isomorphic to the point group C_2. It follows from the theory of symmetry in static stick spectra[1,2] that the (static) spectrum of each rotamer can be decomposed into two independent "symmetry subspectra" which correspond to the two irreducible representations, A and B, of C_2. We now pass to the dynamic spectra and consider the permutation symmetry in the context of exchange. As depicted in Fig. 1, the exchange network includes four labelled molecules that represent four permutamers (also called "topomers"[27]): *s* and *s'* for rotamer *S*, and *a* and *a'* for rotamer *A*. Inspection of the molecular models in Fig. 1 shows that none of the symmetry of the nuclear system is conserved (in the usual sense of the notion of symmetry conservation) in the course of exchange. For instance, nuclei 1 and 3 are symmetry equivalent in a molecule belonging to permutamer *s*, but cease to be such on transforming the molecule to the form *a* or *a'*. Therefore there may arise the natural question: do any symmetry selection rules act in the DNMR spectra of the system? Do only those transitions that are symmetry allowed in the static spectrum participate in the DNMR spectra? Or can the exchange somehow also activate the symmetry-forbidden transitions?

At the earliest stages in the development of DNMR theory these questions are either passed over in silence or resolved in a purely practical way. Simply, in order to reduce the size of the spectral matrices involved, the symmetry-forbidden transitions were usually discarded in practical DNMR lineshape calculations. The validity of such a procedure was proved theoretically for the intramolecular mutual exchange in systems of Abelian symmetry.[11] For non-Abelian symmetries, it was believed that exchange does couple symmetry-allowed with symmetry-forbidden transitions.[11,13] A similar claim was formulated with respect to NMR relaxation.[18]

For a long time, no attempt was made to clarify the situation and, as already mentioned in the Introduction, the problem was solved only recently.[21-23] As far as exchange is concerned, the solution is based on an observation[21] that, under the condition of dynamic equilibrium, the permutation symmetry is always conserved in a certain macroscopic sense (see below) despite the fact that, as pointed out above, it may undergo breaking in individual exchange events. Consider again the permutamer *s* in Fig. 1. The symmetry group of the nuclear system involved comprises an identity permutation *e* and the permutation (13)(24). (The permutation $(ijk\ldots n)$ is effected as follows: put the label *j* in place of *i*, *k* in place of *j*, ..., and *i* in place of *n*.) Both these operations are *proper* operations on the labelled molecule concerned and, as such, they are *physically feasible*. In general, the feasible group of a permutamer is a group of all such operations that leave the permutamer unchanged. The feasible symmetries of non-planar (achiral) molecules can conveniently be described using permutation inversions which were introduced originally for the purposes of microwave spectroscopy.[28-30]

The property of macroscopic symmetry conservation involves only the feasible symmetries of individual permutamers. It can be formulated as follows: the set of product permutamers which are obtainable from a given substrate permutamer in elementary reactions compatible with the same mechanism (and thus characterized by the same rate constant) must be invariant under all operations from the feasible group of that substrate.[21] This is illustrated on Fig. 1. Namely, as is easy to see, performing the permutation (13)(24) from the feasible group of *s* on the product *a* gives *a'*, i.e. another permutamer obtainable from *s via* the same mechanism (rotation of a single nitroso group) as that transforming *s* into *a*.

The above property is a general one of rearranging molecular systems since it stems solely from the intrinsic symmetry properties of the underlying nuclear configuration space and can be derived from a purely kinematic analysis of the nuclear motions. This is better visualized from Figs. 5 and 6 which illustrate the discussions given in Sections 3.1 and 3.2, respectively. We now explain why such symmetry conservation it is termed "macroscopic".

One can reasonably speak of "conservation" of the substrate symmetry if,

invoking again the example given in Fig. 1, each molecule arriving at time t from permutamer s to permutamer a is accompanied by exactly one molecule leaving s for a' along the corresponding equivalent reaction path. In reality, such a matching takes place for macroscopic ensembles of molecules which rearrange not just in an instant t but during a finite (though very short) time interval $(t - dt, t)$. We therefore speak of *macroscopic* symmetry conservation bearing in mind that it involves macroscopic amounts of rearranging molecules considered on an appropriate macroscopic time-scale.

All that has been stated above refers to a "forward" effect. The corresponding "backward" property can be described as follows: the set of substrate permutamers, each of which can be transformed into the same product permutamer in an elementary reaction compatible with the same mechanism, is closed under the feasible group of that product.

The significance of the above conservation property of rearranging systems for DNMR theory becomes apparent if one realizes that the fundamental DNMR equation of motion describes the evolution of spin density matrices which are averaged over macroscopic ensembles of rearranging molecules. Indeed, as demonstrated in the papers already quoted,[21,23] the property of macroscopic symmetry conservation results in the appropriate macroscopic selection rule: the transitions (or, more generally, coherences) that are symmetry forbidden in the static stick spectra of individual components of a dynamic equilibrium remain forbidden in DNMR spectra. It must be stressed that the symmetries in question are feasible symmetries of the molecules involved. The rule is valid for Abelian as well as non-Abelian symmetries and, therefore, the claims mentioned above that in the latter case forbidden transitions may become allowed in DNMR spectra must be rejected.

A formal derivation of the macroscopic selection rule from the property of macroscopic symmetry conservation will not be reported here in full because of its length. The essential steps are reproduced in Sections 4 and 6. The reader is referred to the original papers[21,23] for more details. It is worth emphasizing, however, that a crucial point in the derivation is the writing of the general DNMR equation of motion in a compact form in which each of the exchanging species is described by only one spin density matrix, regardless of how many permutamers of the species are involved in the exchange network. This is at variance with the early formulation of the equation[5] in which separate density matrices were attributed to individual permutamers of the same species. The compact form of the DNMR equation requires the use of an additional system of labels (the skeleton-site labels) which, however, need not be introduced explicitly unless intermolecular processes are considered. The derivation of the DNMR equation of motion in the skeleton-site representation is described in Section 4.

Turning back to the example given in Fig. 1, we can now state that, owing to

the macroscopic selection rule, in calculating the DNMR spectra for this system it would be sufficient to take into account only those transitions which are allowed in the stick spectra of the individual rotamers *S* and *A*. What are the implications of the fact that at a microscopic level (that is, for single molecules) no symmetry is conserved in the course of exchange? The answer is simple: under such cicumstances it is not possible to separate out any independent symmetry subspectra from the total DNMR spectrum. The four symmetry subspectra of the static systems AA'BB' and CC'DD' will be

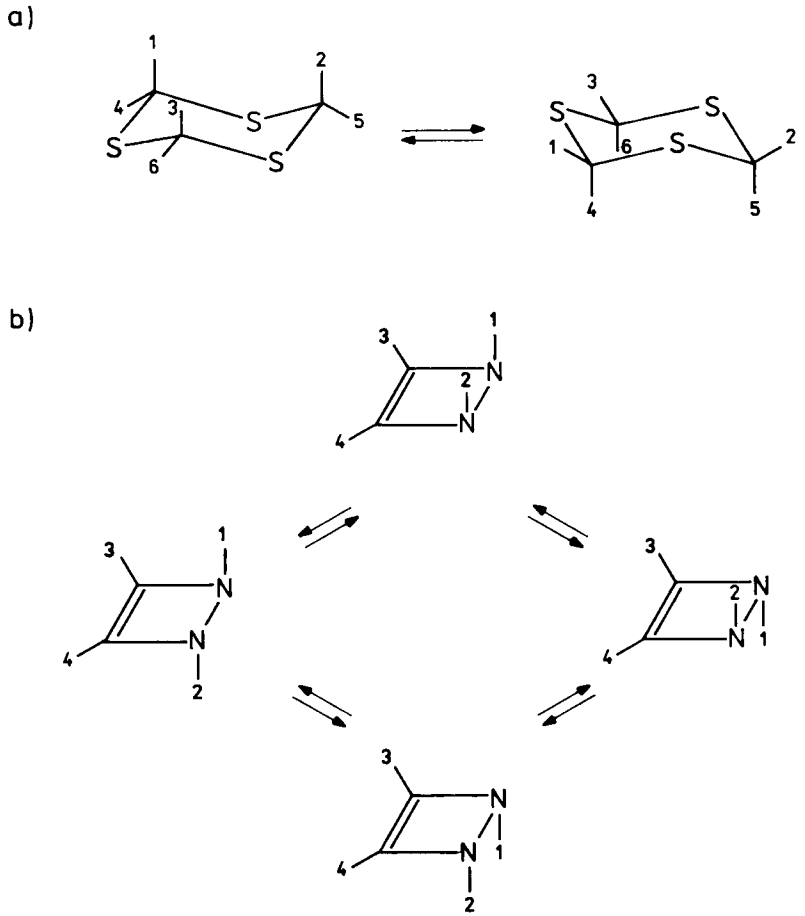

Fig. 2. Ring inversion in *s*-trithiane and nitrogen inversions in 3,4-diazacyclobutene as examples of total microscopic symmetry invariances in (a) degenerate and (b) nondegenerate intramolecularly exchanging systems. The microscopic symmetry groups in (a) and (b) are isomorphic with C_{3v} and C_2 point groups, respectively.

completely mixed by exchange. Decomposition into independent DNMR symmetry subspectra is possible only in the instance where certain symmetries of the nuclear systems in individual rearranging molecules are preserved in any sequence of exchange events. This is the instance of "microscopic symmetry invariance".[21]

The microscopic symmetry group, hereafter denoted $\mathscr{K}$, is defined as the intersection of the permutation groups of individual permutamers spanning the exchange network. For practical purposes, it is convenient to distinguish two kinds of microscopic symmetry invariance: partial and total. The latter occurs in the situation where the permutation groups of all the permutamers in the exchange network are identical. By definition, $\mathscr{K}$ is then identical to the common permutation group of these permutamers. Some examples of total microscopic invariance are depicted in Fig. 2. If $\mathscr{K}$ is nontrivial and is a *proper* subgroup of the permutation group of at least one permutamer in the network,

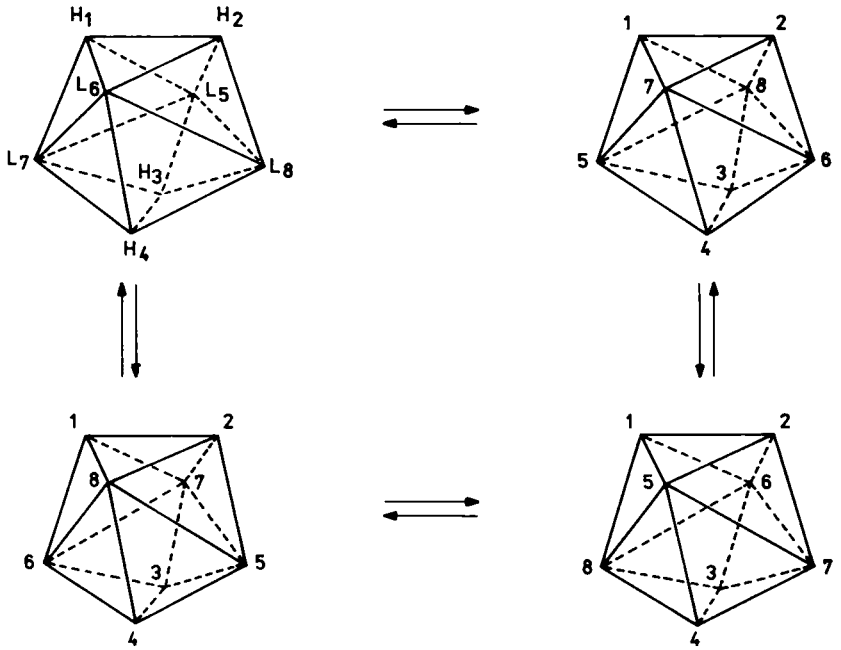

Fig. 3. Partial microscopic symmetry invariance for a probable ligand permutation mechanism in stereochemically nonrigid dodecahedric (D_{2d} symmetry) phosphine complexes of tetrahydrides of tungsten and molybdenum.[31] The microscopic symmetry group, isomorphic with the S_4 subgroup of D_{2d}, is $\{e, (1324)(5867), (12)(34)(56)(78), (1423)(5768)\}$, where e denotes the identity permutation.

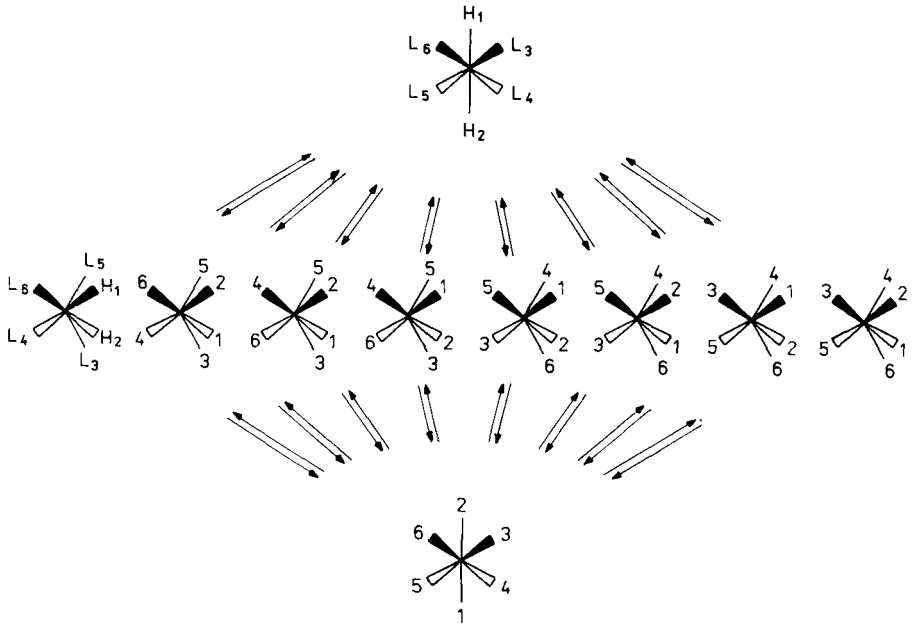

Fig. 4. Partial microscopic symmetry invariance for a probable interconversion mechanism in the system of *trans* (D_{4h} symmetry) and *cis* (C_{2v} symmetry) isomers of dihydrotetrakis(diethoxyphenylphosphine)ruthenium(II).[32] The microscopic group, isomorphic to C_2, is $\{e, (12)(35)(46)\}$.

then one speaks of partial microscopic invariance. This is illustrated in Figs. 3 and 4. Experimental DNMR spectra of the systems depicted in Figs. 3 and 4 have been published by Meakin *et al.*[31,32]

The microscopic symmetry invariance, as defined above, was once believed to be the only symmetry invariance that is relevant in DNMR spectroscopy. The corresponding invariance properties of the spectral matrices were first derived for the formulation of DNMR theory in terms of individual permutamers.[5] The invariance properties resulting from a two-element microscopic symmetry can be exploited in DNMR lineshape computations using the programs already quoted.[6–9] The theory of microscopic symmetry developed recently involves the more convenient, compact form of DNMR equation. It was shown[21] that, when combined with the basic, macroscopic invariance, the microscopic invariance affords a decomposition of the relevant block of the spectral matrix involved, one including symmetry-allowed coherences, into independent sub-blocks. Each such sub-block comprises a

number of static symmetry subspectra (or sometimes a single subspectrum) which coalesce into the same DNMR symmetry subspectrum. The latter are in a one-to-one correspondence with certain disjoint subsets of the irreducible representations of $\mathscr{K}$. These subsets can be determined once the permutation group, $\mathscr{P}^{av}$, which describes the average symmetry of the system in the limit of rapid exchange, is known. In the group-theoretical literature, these subsets are called "orbits"[33] of $\mathscr{K}$ relative to $\mathscr{P}^{av}$. The procedure of finding the coalescence scheme for the static subspectra using the orbits of $\mathscr{K}$ relative to $\mathscr{P}^{av}$ exploits group-correlation diagrams the use of which in the context of DNMR theory was initiated by Luz and Naor.[13] Formal description of this procedure is given in Section 6.3.

The present definition of $\mathscr{K}$ as a purely permutational group is found to be more appropriate than the previous one[21] which was formulated in terms of permutation inversions. In both formulations the underlying idea is the same, but the permutation-inversion formalism, which is suitable for describing the macroscopic invariance, proves too restrictive for a proper account of microscopic symmetry for the purposes of NMR spectroscopy. This can be clarified using an example. According to the present definition, the system depicted in Fig. 2(b) is one with total microscopic invariance. In the previous approach,[21] it would be classified as a system with a complete symmetry breaking since the permutation-inversion formalism would distinguish between the permutation (12)(34) describing an improper operation (for the permutamers of the isomer *cis*) and the same permutation representing a proper operation (for the permutamers of the isomer *trans*). However, for the systems shown in Figs. 2(a) and 3, the two definitions are equivalent. It should be stressed that the theory of microscopic symmetry developed previously remains entirely valid also for the present definition of $\mathscr{K}$.

As follows from its definition, the microscopic symmetry is a long-term feature of the spin system in a rearranging molecule and, as such, can be attributed only to those systems where the integrities of the spin systems in individual molecules are preserved in the course of exchange. In systems undergoing intermolecular exchange the above prerequisite is obviously not fulfilled and, accordingly, the concept of microscopic invariance of symmetry does not apply to such systems.[23]

However, the notion of macroscopic symmetry invariance is associated with a short-memory description of the exchange process. In the short-memory approach, which is implied in the DNMR theory, both intra- and intermolecular exchange processes look essentially identical. It is thus not surprising that, as demonstrated previously,[23] the macroscopic selection rules are also identical for both types of exchange: neither intra- nor inter-molecular exchange can activate the transitions which are forbidden by molecular (feasible) symmetries in the static stick spectra.

2.2. Macroscopic and microscopic symmetry in NMR relaxation

Molecular processes that are responsible for nuclear spin relaxation in liquids are usually different in nature from and proceed on a different time-scale from the exchange processes considered in DNMR spectrocopy. Nevertheless, the essential aspects of the problem of permutation symmetry prove to be the same as for the exchange processes. Here, too, the problem must be considered at two levels or, in fact, on two time-scales (macroscopic and microscopic) which can be distinguished in relaxation phenomena. This was noticed by Pyper long ago,[18–20] but a proper interpretation and the theoretical consequences of this observation were reported only recently.[22,25]

In NMR relaxation, as long as it can be described in terms of the semiclassical WBR theory,[14–17] the microscopic description involves individual molecules and is concerned with time increments of the order of typical molecular orientational correlation time, τ_c. The macroscopic level involves a macroscopic ensemble of tumbling molecules and is concerned with a more coarse time-scale which, like that in DNMR theory, determines the physical sense of the "infinitesimal" time increment dt in the WBR equation of motion. This increment is much longer than τ_c but simultaneously much shorter than the inverse of the amplitude of the random spin interactions that are responsible for relaxation; the existence of such a scale is an indispensible condition for the applicability of the WBR approach.[22]

The microscopic symmetry group, $\mathscr{K}$, of a relaxing spin system is defined[22] as the common part of the instantaneous permutation groups of the total semiclassical time-dependent spin Hamiltonian, $H(t)$, of a single molecule. It is clear that the microscopic symmetry cannot be higher than the lowest instantaneous symmetry of $H(t)$. Therefore, if $H(t)$ also includes random intermolecular interactions, i.e. those dependent on the instantaneous configurations of the local fields originating from the neighbouring molecules, the microscopic symmetry cannot be other than trivial. Nontrivial microscopic symmetry can occur only for systems where the intermolecular contributions to relaxation can be neglected.

There are five basic types of intramolecular interactions that can lead to relaxation: spin–rotation (SR) interactions; dipole–dipole (DD) interactions; quadrupole (Q) interactions; and interactions concerned with indirect spin–spin coupling (ICA) and chemical-shielding anisotropies (CSA). For any such interaction, the corresponding term in $H(t)$, involving either a single nucleus (for SR, Q, and CSA) or a pair of nuclei (for ICA and DD), is invariant under inversion of the laboratory space in any instant of time. Therefore, if the molecule possesses a centre of symmetry, then at any time instant $H(t)$ is invariant under the permutation of nuclei that represents the inversion of the molecule. A general conclusion is that, in the absence of intermolecular

interactions, $\mathscr{K}$ is always nontrivial and is isomorphic with the C_i subgroup of the molecular point group. For certain molecular symmetries not including a symmetry centre, e.g. C_{2nv}, the DD interactions are invariant under the rotation about the C_2 axis. Any higher microscopic symmetry can only occur in systems where the DD and ICA interactions can be neglected. Apart from inversion, the microscopic group may then also include those point symmetry operations that leave the *directions* (the signs do not matter) of the principal axes of the Q and CSA tensors unchanged. For example, for a molecule of point symmetry D_{4h} composed of five nuclei of which four are quadrupolar, the group $\mathscr{K}$ is isomorphic with the subgroup of D_{4h} composed of e, C_4^2, σ_v, and σ_v', where each of the symmetry planes intersects the sites of two quadrupolar nuclei.

The definition of macroscopic symmetry in NMR relaxation is very simple: it is the symmetry of $H(t)$, the total semiclassical spin Hamiltonian, averaged over a macroscopic molecular ensemble. The average Hamiltonian does not contain the fluctuating terms and thus the macroscopic symmetry can be identified with the molecular point group or, for non-rigid molecules, with the feasible group of Longuett-Higgins[30] comprising the operations which are feasible on the macroscopic WBR time-scale defined above (see also Section 2.3).

The spectroscopic manifestations of the macroscopic and microscopic symmetry invariances are essentially identical with those in exchange. The macroscopic invariance leads to the macroscopic selection rule: the coherences forbidden by molecular (feasible) symmetry in the static stick spectrum remain forbidden when relaxation is included.[22] This contradicts an earlier claim,[18] probably due to a misinterpretation of the concept of microscopic symmetry, that for non-Abelian symmetries relaxation can couple symmetry-allowed with symmetry-forbidden transitions.

The microscopic symmetry, if present, manifests itself in the form of appropriate microscopic selection rules.[22] The latter enables one to decompose the entire set of coherences allowed by macroscopic symmetry onto disjoint subsets in such a way that there is no cross-relaxation between different subsets. A formal description of macro- and micro-scopic symmetry in NMR relaxation is given in Sections 5 and 6.

2.3. Macroscopic symmetry vs. permutation symmetry of the effective Hamiltonian

The symmetry selection rules for a static stick spectrum are governed by the permutation symmetry of the effective spin Hamiltonian, H^{eff}, which is derived from the complete static Hamiltonian by neglecting scalar spin–spin coup-

lings between magnetically equivalent nuclei. The permutation symmetry of H^{eff} can be higher than the point (or feasible) symmetry of the molecule involved. Accordingly, the selection rules based on the symmetry of H^{eff} can be more restrictive than those derived from the molecular symmetry.

In considering the issue of permutation symmetry and, in particular, that of macroscopic symmetry, in the context of exchange and relaxation, we are allowed to take into account only those symmetries of the spin Hamiltonians which originate directly from the symmetries of the molecules involved. This is understandable if one realizes that the corresponding selection rules are concerned with the symmetries of the exchange and/or relaxation terms in the pertinent equation of motion. These terms, as featured by the molecular motions, reflect the molecular symmetries rather than the symmetries of the effective Hamiltonians. The symmetries of the latter need not be conserved in exchange and relaxation. Furthermore, there is no theoretical justification for a general neglect of the couplings between magnetically equivalent nuclei. Conversely, the reasoning presented recently[24] demonstrates that, for certain specific exchanging systems, such couplings do influence the calculated DNMR lineshapes. Similar effects are expected to occur in relaxing systems. The theoretical findings[24] clearly point to the incorrectness of the commonly adopted assumption[11,34,35] that, as in static NMR, in DNMR spectroscopy the complete spin Hamiltonian can always be replaced by the effective Hamiltonian. This problem has implications for the question of a possible differentiability of rearrangement mechanisms in DNMR spectroscopy which is considered in Section 4.

3. USE OF PERMUTATION-INVERSION GROUPS IN A DESCRIPTION OF EXCHANGE

The main purpose of this section is to describe in terms of group theory the fundamental concept of DNMR theory for symmetric systems, i.e. the concept of macroscopic symmetry invariance. In doing this one can essentially follow the common practice of using ordinary permutation groups in a description of stereodynamic problems.[26] However, except for the simplest exchanging systems such as the one shown in Fig. 1, a pure permutation formalism becomes highly cumbersome when applied to the most typical situation, i.e. exchange in achiral systems. This involves in particular intermolecular exchange. The notation simplifies considerably if, following the papers already quoted,[21,23] permutation-inversion groups[28–30] are employed instead of ordinary permutation groups. In the present section, we continue the previous policy[21,23] which implies that our considerations essentially involve achiral systems. This does not cause any serious loss of generality since upon a trivial

reinterpretation of the meaning of the symbols introduced the formalism becomes entirely valid for chiral systems also.

3.1. Intramolecular exchange

A basic structure in the description of intramolecular rearrangements is the full permutation-inversion group

$$\mathscr{S} = \mathscr{P} \cup \bar{e}\mathscr{P} \tag{1}$$

where $\mathscr{P}$ is the full permutation group of like nuclei and $\bar{e}$ denotes inversion of the skeletons of the molecules involved. In some places in the text we also use a subgroup of $\mathscr{S}$ which is further referred to as the group of allowed transformations, $\mathscr{S}^{\text{all}}$, and which, by definition, includes only those operations from $\mathscr{S}$ that can be performed on the molecules involved without crossing excessively high energy barriers. $\mathscr{S}^{\text{all}}$ is closely related to (but not identical with) the group $\mathscr{P}^{\text{av}}$ introduced in Section 2.1. The relationship between the latter groups is explained in Section 6.3.

The permutamers of a given species K can be represented by the right cosets is $\mathscr{S}$ of the permutation-inversion group $\mathscr{Q}_K$ that comprises feasible operations on a labelled molecule taken as the reference molecule for species K. A corresponding reference molecule must be defined for each chemically distinct species participating in the dynamic equilibrium. The reference permutamer for species K is represented by the coset $\mathscr{Q}_K e$, where e is the identity permutation. The number of permutamers of a given species, n_K, is given by

$$n_K = |\mathscr{S}|/|\mathscr{Q}_K| \tag{2}$$

where, and in the remainder of the present chapter, the symbol $|\mathscr{A}|$ denotes the number of elements in set $\mathscr{A}$. The group $\mathscr{Q}_K$ can be expressed as

$$\mathscr{Q}_K = \mathscr{R}_K \cup \bar{e}\sigma_K\mathscr{R}_K \tag{3}$$

where $\mathscr{R}_K$ is the (purely permutational) group comprising proper symmetry operations on the reference molecule (overall rotations and/or feasible internal rotations) and σ_K is the permutation describing an improper symmetry operation on the molecule concerned. (The combination of two, in general "unfeasible" operations, σ_K and $\bar{e}$, gives a feasible operation and this is why the use of permutation-inversions enables one to also represent improper molecular symmetries in terms of physically feasible operations.) For brevity, we hereafter speak of operations performed on a permutamer, bearing in mind that they are performed on a labelled molecule belonging to the permutamer.

A permutamer $\mathscr{Q}_K S_k$ of species K is obtained from the corresponding

reference permutamer by performing on it the operation $s_k^{-1} \in \mathscr{S}$. Accordingly, performing an operation $s^{-1} \in \mathscr{S}$ on $\mathscr{Q}_K s_k$ gives another permutamer of the same species

$$\mathscr{Q}_K s_{k'} \equiv \mathscr{Q}_k s_k s \tag{4}$$

unless s belongs to the group

$$\mathscr{Q}_k = s_k^{-1} \mathscr{Q}_K s_k \tag{5}$$

In the latter case, s^{-1} leaves the permutamer $\mathscr{Q}_K s_k$ unchanged. The group $\mathscr{Q}_k$ (isomorphic with $\mathscr{Q}_K$) is the feasible group of the permutamer $\mathscr{Q}_K s_k$. The concepts invoked above enable us to explain the kinematic background of the property of macroscopic symmetry invariance in a more rigorous way than was done in Section 2.1. For this purpose it is necessary to use an auxiliary concept, i.e. that of the "basic mode of rearrangement".[21]

Any conceivable rearrangement of a species K into an isomeric species L can be described in terms of an appropriate family of elementary reactions. An elementary reaction transforming permutamer $\mathscr{Q}_K s_k$ into permutamer $\mathscr{Q}_L s_l$ can be represented by the ordered pair

$$(\mathscr{Q}_K s_k, \mathscr{Q}_L s_l) \tag{6}$$

with the substrate written first. The set of all conceivable elementary reactions transforming K into L, containing $n_K n_L$ ordered pairs (6), can be decomposed into (disjoint) equivalency classes, i.e. the basic modes of rearrangement. Each such mode groups elementary reactions of the same rate constant. The significance of the concept of basic modes for our considerations stems from two facts. Firstly, as is shown later, the basic modes are the smallest subsets of elementary reactions that exhibit the property of macroscopic symmetry conservation. Secondly, any rearrangement mechanism comprises some total number of basic modes and often only a single mode. In order to show the general validity of the property of macroscopic symmetry conservation, it is thus sufficient to demonstrate it for a single basic mode.

The equivalence relationship between elementary reactions that defines the basic modes can be formulated as follows: two reactions, $(\mathscr{Q}_K s_k, \mathscr{Q}_L s_l)$ and $(\mathscr{Q}_K s_{k'}, \mathscr{Q}_L s_{l'})$, are equivalent, that is belong to the same basic mode α if and only if, there exists an operation $s \in \mathscr{S}$ such that simultaneous transformation of the substrate and product in one of them with s^{-1} gives the substrate and product, respectively, of the other (see (4)),

$$(\mathscr{Q}_K s_k s, \mathscr{Q}_L s_l s) \equiv (\mathscr{Q}_K s_{k'}, \mathscr{Q}_L s_{l'}) \tag{7}$$

In order to generate an entire basic mode from a single representative reaction $(\mathscr{Q}_K s_k, \mathscr{Q}_L s_l)$ it is sufficient to repeat the transformation on the left-hand side of (7) for all elements of $\mathscr{S}$. The generating reaction remains unchanged under

such operations from $\mathscr{S}$ that belong to the group

$$\mathscr{Q}^{(kl)} = \mathscr{Q}_k \cap \mathscr{Q}_l \tag{8}$$

$\mathscr{Q}^{(kl)}$ comprises the feasible symmetry elements that are common for the substrate and the product of the generating reaction. The groups of common feasible elements for the remaining reactions from the same mode are isomorphic with $\mathscr{Q}^{(kl)}$. For brevity, the group of common elements for the generating reaction is hereafter denoted as $\mathscr{Q}^{\alpha}$, that is

$$\mathscr{Q}^{(kl)} \equiv \mathscr{Q}^{\alpha} \tag{9}$$

By taking one representative element s_v from each right coset of $\mathscr{Q}^{\alpha}$ in $\mathscr{S}$, the basic mode in question can be described as

$$\{(\mathscr{Q}_k s_k s_v, \mathscr{Q}_L s_l s_v)\} \tag{10}$$

where $v = 1, 2, \ldots, n_{\alpha}$, with n_{α} denoting the number of reactions in the mode α,

$$n_{\alpha} = |\mathscr{S}|/|\mathscr{Q}^{\alpha}| \tag{11}$$

Some of the generating elements s_v in (10) leave the substrate $\mathscr{Q}_k s_k$ unchanged; these are precisely those elements which belong to the feasible group $\mathscr{Q}_k$ (5). The number of such elements, w_{α}, is equal to the number of right cosets of $\mathscr{Q}^{\alpha}$ in $\mathscr{Q}_k$,

$$w_{\alpha} = |\mathscr{Q}_k|/|\mathscr{Q}^{\alpha}| \tag{12}$$

Similarly, the elements s_v that belong to the feasible group of $\mathscr{Q}_L s_l$ leave the product unchanged. The number of such elements, z_{α}, is given by

$$z_{\alpha} = |\mathscr{Q}_l|/|\mathscr{Q}^{\alpha}| \tag{13}$$

We denote these elements $q_l^{(i)}$, where $i = 1, 2, \ldots, z_{\alpha}$. The subset of elementary reactions from the set (10) that have the same product $\mathscr{Q}_L s_l$ in common can now be described as

$$\{(\mathscr{Q}_k s_k q_l^{(i)}, \mathscr{Q}_L s_l)\} \tag{14}$$

where $i = 1, 2, \ldots, z_{\alpha}$. Obviously, the substrates in the set (14) are all different. Calculating a set-thoretical union of the right cosets that represent the substrates in (14) gives[21]

$$\bigcup_{i=1}^{z_{\alpha}} \mathscr{Q}_K s_k q_l^{(i)} = \mathscr{Q}_K s_k \mathscr{Q}_l \tag{15}$$

Equation (15) clearly demonstrates that the set of substrates which is transformable into the same product $\mathscr{Q}_L s_l$ is closed under the feasible group of this product. Indeed, the performance of any operation $q_l \in \mathscr{Q}_l$ on these substrates amounts to postmultiplying the double coset on the right-hand side

of (15) by q_l^{-1} (see the comment preceding (4)). Obviously, the latter operation leaves the double coset unchanged, which proves the general validity of the property of macroscopic symmetry conservation backwards. The corresponding forward property can be proven in a similar way. The above formal reasoning is illustrated in Fig. 5.

The groups $\mathcal{Q}^\alpha$ defined by (8) and (9) have an interesting physical interpretation. This follows from the considerations described by Pechukas,[36] whose inferences formulated in terms of pure permutation groups are also valid for the permutation-inversion approach employed here: namely, in the instance where the saddle points on the energy surface in the nuclear configuration space are "simple saddle points"[36] with only a two-fold branching, the groups $\mathcal{Q}^\alpha$ describe the symmetries of the transition states for the elementary reactions involved. In the latter instance, which seems to be frequent in practice, the kinetic rate constants of the individual elementary reactions have a clear physical interpretation[37] in terms of absolute reaction-rate theory. The above comment also involves bimolecular reactions which are considered in Section 3.2.

The quantities w_α and z_α defined in (12) and (13), respectively, using the appropriate group $\mathcal{Q}^\alpha$ are nothing other than the connectivities[38] of the substrate and product permutamers, respectively, for the basic mode involved. Equations (12) and (13) show how simply these two fundamental characteristics of an exchange network can be expressed in terms of permutation-inversion groups (see also the legend to Fig. 5).

3.2. Intermolecular exchange

As the prototype of an intermolecular exchange we take a system of four species I, J, M and N which rearrange according to the general scheme

$$I + J = M + N \tag{16}$$

Here the basic chemical entities that participate in elementary reactions are the permutamer pairs[23] which, as in intramolecular exchange, are represented by appropriate right cosets. Now the latter assume the form

$$\mathcal{Q}_{KL} s_{kl} \tag{17}$$

where s_{kl} is an element of the pertinent group $\mathcal{S}$ (see below), and the feasible groups $\mathcal{Q}_{IJ}$ and $\mathcal{Q}_{MN}$ are defined for the pairs of species on each side of (16). Precisely, the group $\mathcal{Q}_{KL}$ describes the feasible operations on a pair of reference molecules for the species K and L. The nuclei in the reference molecules are labelled with natural numbers from two disjoint sets, $\{K\}$ and $\{L\}$, respectively. If the exchanging system includes several different fragmentary

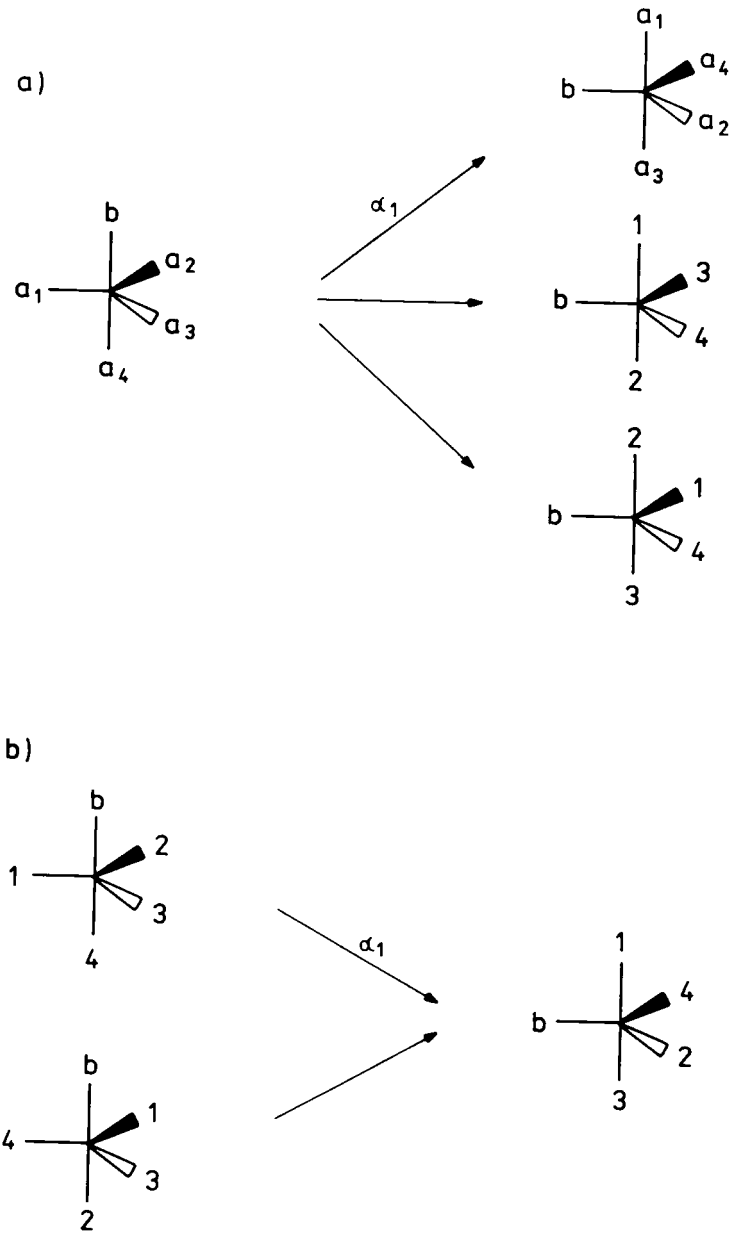

Fig. 5. Use of permutation-inversion groups in the description of macroscopic symmetry invariance in intramolecular exchange. The depicted fragments of the exchange network that represents a Berry pseudo-rotation illustrate the forward (a)

equilibria A, B, etc., involving various combinations of the species $I, J, \ldots, N$, then the corresponding sets of nuclear labels should be defined separately for each equilibrium. Obviously, the nuclei in the substrates and products from a given fragmentary equilibrium A take their labels from the same total label set, $\mathscr{Z}^A$. For example, for the scheme in (16) we have

$$\mathscr{Z}^A = \{I\}^A \cup \{J\}^A = \{M\}^A \cup \{N\}^A \tag{18}$$

The corresponding full group of permutation-inversions of like nuclei, $\mathscr{S}$, comprises operations on the given nuclear set $\mathscr{Z}^A$ and hence it should be defined separately for each fragmentary equilibrium. In the sequel, the superscripts A, B, etc., referring the quantities involved to the corresponding fragmentary equilibria, will be omitted wherever such an omission will not lead to confusion. These introductory remarks must be augmented by a closer characterization of the feasible group for a permutamer pair.

For two different species K and L the feasible group $\mathscr{Q}_{KL}$ of the reference permutamer pair can be expressed as[23]

$$\mathscr{Q}_{KL} = \mathscr{R}_K \otimes \mathscr{R}_L \cup \bar{e}(\sigma_K \mathscr{R}_K \otimes \sigma_L \mathscr{R}_L) \tag{19}$$

where $\bar{e}$ denotes a simultaneous inversion of the skeletons of both molecules and the meaning of the remaining symbols is the same as in (3). (For planar molecules σ_M is an element of $\mathscr{R}_M$ and thus one puts $\mathscr{R}_M$ in place of $\sigma_M \mathscr{R}_M$.) If the species K and L are identical, in which instance we use the labels K and K', then an interchange of the two molecules is also a feasible operation. This interchange can be described by a permutation $\rho_{KK'}$, such that $\rho_{KK'}^2 = e$, which interchanges the respective nuclei between the molecules. The feasible group for such a degenerate pair of species, $\mathscr{Q}_{KK'}$, assumes the form

$$\mathscr{Q}_{KK'} = [\mathscr{R}_K \otimes \mathscr{R}_{K'} \cup \bar{e}(\sigma_K \mathscr{R}_K \otimes \sigma_{K'} \mathscr{R}_{K'})] \wedge \{e, \sigma_{KK'}\} \tag{20}$$

where the symbol $\wedge$ denotes a semidirect product.

For a permutamer pair $\mathscr{Q}_{KL} s_{kl}$, which is obtained from the reference pair by performing on it the operation s_{kl}^{-1}, the corresponding feasible group is (cf. (5))

$$\mathscr{Q}_{kl} = s_{kl}^{-1} \mathscr{Q}_{KL} s_{kl} \tag{21}$$

---

and backward (b) symmetry invariances. The substrate and product of the elementary reaction α_1 are taken as the reference permutamers. The corresponding feasible groups are: $\mathscr{Q}_K = \{e, (123), (132), \bar{e}(12), \bar{e}(13), \bar{e}(23)\} \simeq C_{3v}$ and $\mathscr{Q}_L = \{e, (13)(24), \bar{e}(13), \bar{e}(24)\} \simeq C_{2v}$. The group of common feasible elements for reaction α_1 is $\mathscr{Q}^\alpha = \mathscr{Q}_K \cap \mathscr{Q}_L = \{e, \bar{e}(13)\}$. The substrate and product connectivities for the depicted interconversion mechanism are: $w_\alpha = |\mathscr{Q}_K|/|\mathscr{Q}^\alpha| = 3$ and $z_\alpha = |\mathscr{Q}_L|/|\mathscr{Q}^\alpha| = 2$. It can easily be verified that the set of products in fragment (a) is closed under operations from $\mathscr{Q}_K$, the feasible group of the common substrate. Similarly, the set of substrates in fragment (b) is closed under operations from $\mathscr{Q}_L$, the feasible group of the common product.

Equation (21) is also valid for degenerate pairs $KL=KK'$ and $kl=kk'$.

All the concepts invoked in the preceding subsection and in the formalism developed there are also valid for intermolecular rearrangements. In particular, a basic mode of rearrangement represented by the elementary reaction $(\mathcal{Q}_{IJ}s_{ij}, \mathcal{Q}_{MN}s_{mn})$ can be described by analogy with (10) as

$$\{(\mathcal{Q}_{IJ}s_{ij}s_v, \mathcal{Q}_{MN}s_{mn}s_v)\} \tag{22}$$

where $v=1,2,\ldots,n_\alpha$. The number of elementary reactions in the mode (22), n_α, is defined in (11) where the group of common feasible elements for the generating reaction now assumes the form

$$\mathcal{Q}^\alpha = \mathcal{Q}_{ij} \cap \mathcal{Q}_{mn} \tag{23}$$

The generating elements s_v in (22) are the representatives of the right cosets of $\mathcal{Q}^\alpha$ in $\mathcal{S}$. The substrate and product connectivities for the mode (22) are given by (see (12) and (13))

$$w_\alpha = |\mathcal{Q}_{IJ}|/|\mathcal{Q}^\alpha| \tag{24}$$

$$z_\alpha = |\mathcal{Q}_{NM}|/|\mathcal{Q}^\alpha| \tag{25}$$

As in intramolecular exchange, the property of macroscopic symmetry conservation is valid for individual basic modes. A formal proof of this property is strictly analogous to that for intramolecular exchange and will not be repeated here. In Fig. 6 it is shown how this property manifests itself in an exchanging system involving degenerate permutamer pairs. Without invoking the concept of the feasible group (20), a correct description of exchange in systems of a similar degree of complexity as that shown in Fig. 5 may sometimes pose serious problems. In particular this involves the determination of the connectivities w and z. Even for the exchange scheme depicted in Fig. 6 (which may illustrate one of the triton–proton exchange processes in a mixture of tritium labelled ammonium cations), the determination of the corresponding connectivities by inspection of molecular models is a formidable task. The main difficulty lies in the fact that there is no simple way to verify the correctness of the outcome of such a procedure. However, in the formal approach described above, the problem reduces to determining the appropriate group $\mathcal{Q}^\alpha$, which is a relatively easy task. Once this group has been determined, the connectivities in question can immediately be calculated from (24) and (25) to give $w_\alpha=16/2=8$ and $z_\alpha=18/2=9$.

3.3. Enumeration of basic modes of rearrangement

In a complex dynamic equilibrium, enumeration of the basic modes of rearrangement must be carried out separately for each fragmentary equilib-

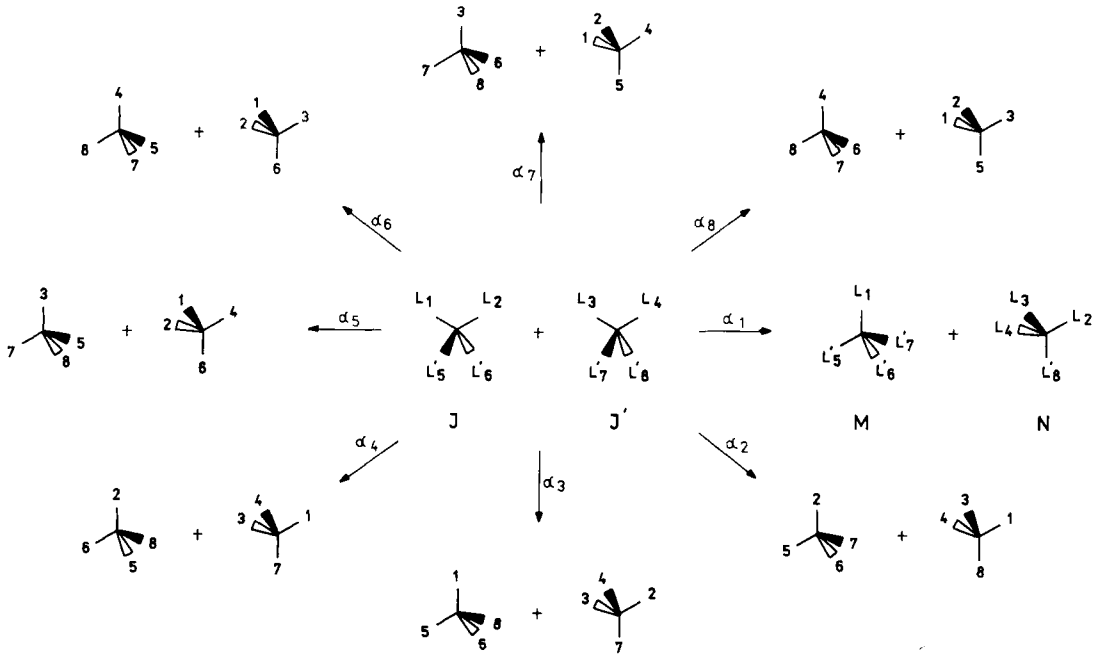

Fig. 6. Use of permutation-inversion groups in the description of macroscopic symmetry invariance in intermolecular exchange. The depicted fragment of the exchange network representing an intermolecular ligand exchange mechanism illustrates the forward symmetry invariance. The substrates and products of the elementary reaction α_1 are taken as the reference permutamer pairs. Their corresponding feasible groups are: $\mathcal{Z}_{JJ'} = \{e, (12)(56), (34)(78), (12)(34)(56)(78), (1324)(5768), (14)(23)(58)(67), (1423)(5867), (13)(24)(57)(68), \bar{e}(12)(34), \bar{e}(56)(78), \bar{e}(12)(78), \bar{e}(34)(56), \bar{e}(14)(23)(57)(68), \bar{e}(13)(24)(58)(67), \bar{e}(1324)(5867), \bar{e}(1423)(5768)\}$, where the underlined element describes an interchange of the molecules involved (see (20)), and $\mathcal{Z}_{MN} = \{e, (234), (243), (567), (576), (234)(567), (234)(576), (243)(567), (243)(576), \bar{e}(24)(56), \bar{e}(24)(57), \bar{e}(24)(67), \bar{e}(23)(56), \bar{e}(23)(57), \bar{e}(23)(67), \bar{e}(34)(56), \bar{e}(34)(57), \bar{e}(34)(67)\}$. The group of common feasible elements for the reaction α_1 is $\mathcal{Z}^{\alpha} = \mathcal{Z}_{JJ'} \cap \mathcal{Z}_{MN} = \{e, \bar{e}(34)(56)\}$. The substrate and product connectivities for the depicted ligand-exchange mechanism are: $w_{\alpha} = |\mathcal{Z}_{JJ'}|/|\mathcal{Z}^{\alpha}| = 16/2 = 8$ and $z_{\alpha} = |\mathcal{Z}_{MN}|/|\mathcal{Z}^{\alpha}| = 18/2 = 9$. It may be verified that the set of permutamer pairs produced in reactions α_1 to α_8 is closed under operations from $\mathcal{Z}_{JJ'}$, the feasible group of the common substrate permutamer pair.

rium. Formulation of the equivalence relationship between elementary reactions according to (7) is not the most convenient for this purpose. A more suitable formulation invokes double cosets formed from the feasible groups of the corresponding substrates and products. Namely, two elementary reactions $(\mathcal{2}_\Lambda s_\lambda, \mathcal{2}_\Gamma s_\gamma)$ and $(\mathcal{2}_\Lambda s_{\lambda'}, \mathcal{2}_\Gamma s_{\gamma'})$ are equivalent in the sense of (7) (and, as such, both belong to the same basic mode α) if, and only if,[21,23]

$$s_{\gamma'} s_{\lambda'}^{-1} \in \mathcal{2}_\Gamma s_\alpha \mathcal{2}_\Lambda, \tag{26}$$

where

$$s_\alpha = s_\gamma s_\lambda^{-1} \tag{27}$$

Equations (26) and (27) are valid for both intra- and inter-molecular exchange processes. This is emphasized by the use of Greek indices which can designate both single permutamers and permutamer pairs, depending on the kind of equilibrium being dealt with.

The basic modes defined by (10) or (22) and the double cosets (26) are in one-to-one correspondence. Two basic modes that have an elementary reaction in common are identical. Similarly, two double cosets (26) that have a common element are also identical. In the sequel, we sometimes refer to such double cosets as the basic modes themselves. This should not lead to any confusion. For a given fragmentary nondegenerate equilibrium, the number of basic modes of one-way rearrangements is equal to the number of the corresponding double cosets $\mathcal{2}_\Gamma s_\alpha \mathcal{2}_\Lambda, \mathcal{2}_\Gamma s_{\alpha'} \mathcal{2}_\Lambda, \ldots$, etc., contained in the group $\mathcal{S}$. The corresponding reverse rearrangements are enumerated with the double cosets $\mathcal{2}_\Gamma s_{\bar{\alpha}} \mathcal{2}_\Lambda, \mathcal{2}_\Gamma s_{\bar{\alpha}'}, \mathcal{2}_\Lambda, \ldots$, etc., where

$$s_{\bar{\alpha}} = s_\alpha^{-1}, s_{\bar{\alpha}'} = s_\alpha^{-1}, \ldots, \text{etc.} \tag{28}$$

In a degenerate equilibrium ($\Lambda = \Gamma$) it can happen that for some basic modes

$$\mathcal{2}_\Lambda s_\beta \mathcal{2}_\Lambda = \mathcal{2}_\Lambda s_{\bar{\beta}} \mathcal{2}_\Lambda \tag{29}$$

The basic modes of (degenerate) rearrangement that obey (29) are called *self-inverse* modes.

The use of permutation-inversion double cosets in the description of exchange, recommended in the papers already quoted,[21,23] is an adaptation of the approach of Brocas and Fastenakel[39] who employed this formalism in order to enumerate, for the purposes of microwave spectroscopy, quantum-mechanical tunnelling processes in non-rigid molecules. In the present context, the advantages of the permutation-inversion approach become apparent in view of the single fact that in the conventional approach[40] a union of two (purely permutation) double cosets should be used to describe a basic mode. Precisely, when s_α is a permutation-inversion, $s_\alpha = \bar{e}p_\alpha$, the basic

mode (of an intramolecular rearrangement) $\mathscr{Q}_K s_\alpha \mathscr{Q}_L$ is described by the union

$$\mathscr{R}_K p_\alpha \mathscr{R}_L \cup \mathscr{R}_K \sigma_K p_\alpha \sigma_L \mathscr{R}_L \tag{30}$$

and when s_α is a pure permutation, $s_\alpha = p_\alpha$, the corresponding double coset union is[21]

$$\mathscr{R}_K p_\alpha \sigma_L \mathscr{R}_L \cup \mathscr{R}_K \sigma_K p_\alpha \mathscr{R}_L \tag{31}$$

3.4. Exchange in chiral systems

In chiral systems, the inversion operation $\bar{e}$ ceases to be a valid symmetry operation and, moreover, the only molecular symmetries that can be taken into account are the proper symmetries. Exchange processes in chiral systems are described in terms of pure permutations. However, the forms of the relevant group-theoretical expressions remain exactly the same as for achiral systems, except that the symbols $\mathscr{S}, s, \mathscr{Q}$, and q are replaced by $\mathscr{P}, p, \mathscr{R}$, and r, respectively.

4. DNMR EQUATION OF MOTION FOR SYMMETRIC SYSTEMS

As mentioned in Section 2, the DNMR equation of motion for symmetric systems assumes a convenient, compact forms when the rate processes are described in terms of nuclear exchange between skeleton sites. In such "skeleton-site representation" the spin system of each chemically distinct species I is described by only one spin-density matrix ρ_I. The alternative approach in which individual permutamers are treated as distinct species may be effective only for some intramolecularly exchanging systems where the exchange network includes a small number of permutamers. However, the approach invoking skeleton sites is capable of handling multicomponent equilibria of any complexity, with intra- and inter-molecular processes operating simultaneously. The practical applicability of this approach is limited only by the efficiency of the computing system employed. In a previous rigorous derivation of such a general version of the DNMR equation,[41-43] the issue of permutation symmetry was not addressed explicitly; this gap was filled only recently.[21,23] Below we reproduce the essential steps of the recent approach which succeeded in providing a general equation of motion for symmetric systems. We start by presenting some auxiliary notions involving the description of exchange in terms of skeleton sites.

4.1. Skeleton-site description of exchange

Based on a system of nuclear labels, the description of exchange in terms of permutamer or permutamer pair switches, when combined with the use of permutation-inversion groups, affords a simple, pictorial explanation of the concepts of macroscopic and microscopic symmetry invariance (see Figs 5 and 6). More importantly it provides convenient tools for the enumeration of basic modes of rearrangement and of individual elementary reactions within these modes. This information is necessary for deriving the DNMR equation of motion for symmetric systems. The description in terms of nuclear labels is, however, insufficient when a complex multicomponent equilibrium is dealt with where one or more of the exchanging species participate in several different fragmentary equilibria involving intermolecular processes. Each such fragmentary equilibrium A requires its own set of nuclear labels $\mathscr{L}^A$ (see (18)) and, accordingly, its own group $\mathscr{S}^A$, not to mention the reference molecules which must bear different nuclear labels for different fragmentary equilibria. Therefore, using only the nuclear labels there is no way to define a unique density matrix for a species participating in different fragmentary equilibria of this kind. Purely intramolecular equilibria and those rare intermolecular equilibria where all the exchange processes conform to the same general scheme are exceptional in this respect.

In developing a completely general DNMR theory it is necessary to introduce an additional system of labels, the skeleton-site labels which are unique for each species participating in the exchange. The set of skeleton-site labels for species K is denoted $\{\bar{K}\}$. Obviously, the skeleton-site labels for any two molecules of the same species are, by definition, superimposable. Using the site labels, one can gather together the effects exerted on the spin states of a given species by exchange events occurring in various fragmentary equilibria in which the species participates. A connection between the "global" reference system employing the site labels and the "local" systems based on the nuclear labels is established via the reference molecules, the skeleton sites of which obviously bear the same labels in different fragmentary equilibria.

The mutual assignment of the nuclear and skeleton labels in the reference molecule for a species K in a fragmentary equilibrium A is described in terms of the one-to-one mapping

$$f_K^A(a_K) = a \tag{32}$$

where $a \in \{K\}^A$ denotes the nucleus at the site $a_K \in \{\bar{K}\}$. Accordingly, the label assignment in a reference molecular pair is described by the function

$$f_{KL}^A(a_M) = \begin{cases} f_K^A(a_M) & \text{if } M = K \\ f_L^A(a_M) & \text{if } M = L \end{cases} \tag{33}$$

Now, using the appropriate functions ((32) or (33)), an elementary reaction $(\mathcal{Q}_\Lambda s_{\lambda'}, \mathcal{Q}_\Gamma s_{\gamma'})^A$ from mode α in fragmentary equilibrium A can be described by the following one-to-one mapping of the skeleton sites in the substrate(s) onto those in the product(s):

$$f_{\alpha_v} = f_\Gamma^{A-1} \tilde{s}_{\gamma'}^A \tilde{s}_{\lambda'}^{A-1} f_\Lambda^A \tag{34}$$

where v is an element from the set $\{1, 2, \ldots, n_\alpha\}$, with n_α being defined by (11), and the Greek indices have the same meaning as in (26) and (27); in (34) and in the remaining part of this chapter, the tilde denotes the purely permutational part of the permutation-inversion involved. From here on, the basic modes in the fragmentary equilibria $A, B, \ldots$, etc., are denoted by the corresponding labels $\alpha, \bar{\alpha}, \alpha', \bar{\alpha}', \ldots$, etc. and $\beta, \bar{\beta}, \beta', \bar{\beta}', \ldots$, etc. (see (28)). For the skeleton-site mappings defined by (34), the superscripts $A, B, \ldots$, etc. are thus redundant and are omitted.

The corresponding skeleton-site mappings can be written for the remaining $n_\alpha - 1$ elementary reactions from the mode concerned. It must be remembered that in defining these mappings the coset representatives $s_\lambda, s_{\lambda'}, \ldots$, $s_\gamma, s_{\gamma'}, \ldots$, etc., for the substrate and product permutamers (or permutamer pairs) spanning the exchange network are to be fixed once and for all. This proviso is important for the reason which will be explained by the use of an example of a basic mode of intramolecular rearrangement. As shown by (10), all elementary reactions from the same mode can be represented by the ordered pairs $(\mathcal{Q}_K s_k s_v, \mathcal{Q}_L s_l s_v)$ with varying s_v. This might suggest that in determining the site mapping (34) for the vth reaction one can take the elements $s_k s_v$ and $s_l s_v$ as the coset representatives to be inserted in (34) in place of $s_{\lambda'}$, and $s_{\gamma'}$, respectively. However, by proceeding in this way for each of the remaining reactions from the mode in question one would obtain the same skeleton-site mapping each time. The incorrectness of such a procedure lies in the fact that one and the same permutamer, say a substrate $\mathcal{Q}_K s_{k'}$, which participates in two or more elementary reactions, would each time be represented by another element $s_k s_v = q_K s_{k'}$, $s_k s_{v'} = q'_K s_{k'}$, etc., of the coset $\mathcal{Q}_K s_{k'}$. The above does not imply, however, that all the skeleton-site mappings, f_{α_v}, with $v = 1, 2, \ldots, n_\alpha$, derived according to the correct procedure, that is, for fixed coset representatives, must always be different. All the mappings belong to the same double coset $\mathcal{G}_\Gamma f_\alpha \mathcal{G}_\Lambda$ which constitutes a subset in the set of all one-to-one mappings of the skeleton sites in the substrate(s), Λ, onto the sites in the product(s), Γ (see below). It must be emphasized that the elements f_{α_v}, with $v = 1, 2, \ldots, n_\alpha$, need not exhaust the double coset concerned; as we show later, it is this point which renders the derivation of the DNMR equation of motion for symmetric systems highly nontrivial.

The double coset $\mathcal{G}_\Gamma f_\alpha \mathcal{G}_\Lambda$ is the image of the double coset in (26) (and, in

fact, of its purely permutational counterpart),

$$\mathscr{G}_\Gamma f_\alpha \mathscr{G}_\Lambda = f_\Gamma^{A-1} \tilde{\mathscr{D}}_\Gamma^A \tilde{s}_\alpha \tilde{\mathscr{D}}_\Lambda^A f_\Lambda^A \tag{35}$$

where, and in the remainder of this chapter, the tilde over the symbol designating a permutation-inversion group denoting the purely permutational representation (not necessarily faithful) of that group, one obtained by dropping the inversion $\bar{e}$. Equation (35) stems from (26), (27) and (32)–(34). The site mapping f_α in (35) is an arbitrarily chosen element from the set $\{f_{\alpha v}; v = 1, 2, \ldots, n_\alpha\}$ and can be expressed as (see (27) and (34))

$$f_\alpha = f_\Gamma^{A-1} \tilde{s}_\alpha f_\Lambda^A \tag{36}$$

The groups $\mathscr{G}_\Gamma$ and $\mathscr{G}_\Lambda$ in (35) describe symmetries of the corresponding molecules or molecular pairs in terms of skeleton sites. Namely, for Δ denoting a single species K

$$\mathscr{G}_\Delta \equiv \mathscr{G}_K = f_K^{A-1} \tilde{\mathscr{D}}_K^A f_K^A \tag{37}$$

and for Δ denoting a pair of species KL

$$\mathscr{G}_\Delta \equiv \mathscr{G}_{KL} = f_{KL}^{A-1} \tilde{\mathscr{D}}_{KL}^A f_{KL}^A \tag{38}$$

The group $\mathscr{G}_K$ in (37) is the well-known molecular symmetry group expressed in terms of the permutations of nuclear sites (the improper operations in $\mathscr{G}_K$ are no longer feasible operations). The group $\mathscr{G}_{KL}$ in (38) is a halving subgroup of the direct product group $\mathscr{G}_K \otimes \mathscr{G}_L$ since, as is seen from (19), (32), (33) and (37), the latter can be written as

$$\mathscr{G}_K \otimes \mathscr{G}_L = \mathscr{G}_{KL} \cup \sigma_K^s \mathscr{G}_{KL} = \mathscr{G}_{KL} \cup \sigma_L^s \mathscr{G}_{KL} \tag{39}$$

where σ_K^s and σ_K^s are skeleton-site permutations describing improper operations on the molecules involved. The description of the exchange in terms of the mappings (34), which will henceforth be referred to as "site-exchange schemes", is usually concerned with the loss of a piece of information about the exchange mechanism. For example, two physically distinct basic modes concerned with the permutation-inversion double cosets (26) differing by inversion, $\mathscr{D}_\Gamma s_\alpha \mathscr{D}_\Lambda$ and $\mathscr{D}_\Gamma \bar{e} s_\alpha \mathscr{D}_\Lambda$, are described by the same set of site-exchange schemes. It should be emphasized that in the derivation of the DNMR equation of motion (Section 4.3) the site-exchange schemes are exploited in such a way that there is no need to keep track of this difference. However, the remaining information about the exchange, which is contained in the description in terms of nuclear labels and permutation-inversions, is still relevant and is used in the following sections.

The use of site-exchange schemes in the description of the exchange in complex intermolecular equilibria is illustrated in Fig. 7.

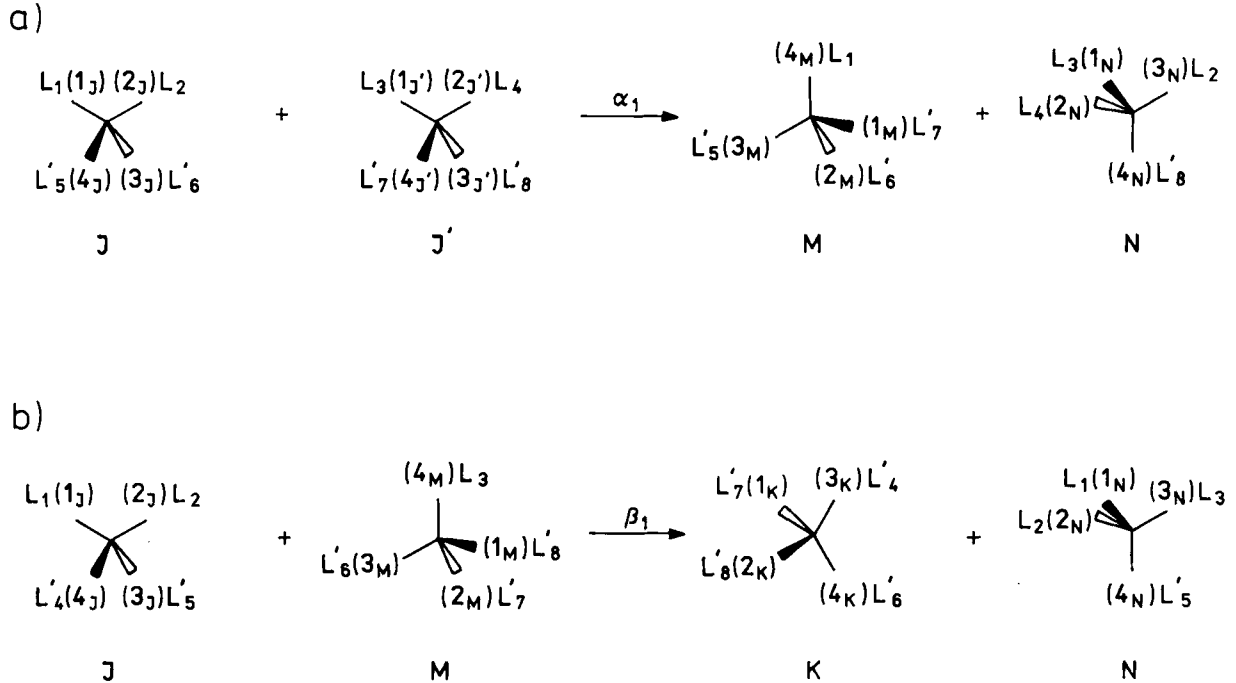

Fig. 7. Use of skeleton-site labels (subscript numbers in parentheses) in a description of exchange in complex equilibria. The elementary reactions (a) and (b) belong to two different fragmentary equilibria, *A* and *B*, engaging the same species *J*, *M* and *N*. Each of the species bears the same site labelling in different fragmentary equilibria. The site-exchange schemes are determined using the auxiliary nuclear labels (non-subscript numbers); which are valid only within a given fragmentary equilibrium. The site-exchange schemes for reactions (a) and (b) are: $f_{\alpha_1} = (1_J \rightarrow 4_M, 2_J \rightarrow 3_N, 3_J \rightarrow 2_M, 4_J \rightarrow 3_M, 1_{J'} \rightarrow 1_N, 2_{J'} \rightarrow 2_N, 3_{J'} \rightarrow 4_N, 4_{J'} \rightarrow 1_M)$ and $f_{\beta_1} = (1_J \rightarrow 1_N, 2_J \rightarrow 2_N, 3_J \rightarrow 4_N, 4_J \rightarrow 3_K, 1_M \rightarrow 2_K, 2_M \rightarrow 2_K, 3_M \rightarrow 4_K, 4_M \rightarrow 3_N)$.

4.2. Macroscopic symmetry conservation in skeleton-site representation

Equation (15), which describes the property of backwards macroscopic symmetry conservation, can be generalized to the description of intermolecular processes, namely

$$\bigcup_{i=1}^{z_\alpha} \mathcal{Q}_\Lambda s_\lambda q_\gamma^{(i)} = \mathcal{Q}_\Lambda s_\lambda \mathcal{Q}_\gamma \tag{40}$$

where $\mathcal{Q}_\gamma$ is the feasible group of the permutamer (or permutamer pair) $\mathcal{Q}_\Gamma s_\gamma$ and $q_\gamma^{(i)}$, with $i = 1, 2, \ldots, z_\alpha$, are the representatives of the right cosets of the appropriate group $\mathcal{Q}^\alpha$ (see (8), (9) and (23)) in $\mathcal{Q}_\gamma$. Equation (40) remains valid when all the permutation inversions contained in it are transformed into ordinary permutations by dropping $\bar{e}$. Replacing individual permutations in the modified equation by their inverses and pre- and post-multiplying both sides of the resulting equation by $f_\Gamma^{-1}\tilde{s}_\gamma$ and f_Λ, respectively, one gets (see (32) and (38))

$$\bigcup_{\{v\}_\gamma} f_{\alpha_v} \mathcal{G}_\Lambda = \mathcal{G}_\Gamma f_\alpha \mathcal{G}_\Lambda \tag{41}$$

where the set-theoretical summation is over the subset of the equivalent elementary reactions that yield the same product $\mathcal{Q}_\Gamma s_\gamma$. Equation (41) and, in fact, its group-algebraic counterpart in Liouville space, plays a crucial role in the derivation of the DNMR equation of motion. It describes the property of backwards macroscopic symmetry conservation as the latter is reflected in the skeleton-site representation of exchange. Obviously, (41) remains valid when the set-theoretical summation on the left-hand side is extended over the whole set of elementary reactions from the basic mode involved, thus

$$\bigcup_{v=1}^{n_\alpha} f_{\alpha_v} \mathcal{G}_\Lambda = \mathcal{G}_\Gamma f_\alpha \mathcal{G}_\Lambda \tag{42}$$

The results presented in (41) and (42) might at first glance seem trivial since, as mentioned in the discussion preceding (35), the site-exchange schemes from the same basic mode all belong to the appropriate double coset $\mathcal{G}_\Gamma f_\alpha \mathcal{G}_\Lambda$. However, this is not so if one takes into account the fact already commented upon that the set $\{f_{\alpha_v}; v = 1, 2, \ldots, n_\alpha\}$ is usually a subset only of the double coset concerned and the number of distinct elements in it can be much smaller than $|\mathcal{G}_\Gamma f_\alpha \mathcal{G}_\Lambda|$.

4.3. DNMR equation of motion in skeleton-site representation

The general DNMR equation of motion for symmetric systems was derived[23] by incorporating symmetry at some intermediate stage of the theory developed previously.[41-43] At that stage, the equation of motion for the spin-density matrix, ρ_M, of a species M, written in the skeleton-site representation, assumes the form

$$\mathrm{d}|\rho_M\rangle/\mathrm{d}t = -i\mathbf{L}_M|\rho_M\rangle + \mathbf{R}_M|\rho_M - \rho_{oM}\rangle + \tau_m^{-1}(|\rho_M^f\rangle - |\rho_M\rangle) \quad (43)$$

where the spin-density matrices ρ_M, ρ_{oM} (the equilibrium matrix) and ρ_M^f (see below) are treated as vectors (superkets[4]) in the spin Liouville space of the species M; $\mathbf{L}_M$ and $\mathbf{R}_M$ are the super-Hamiltonian and the WBR relaxation matrices, respectively. Unless stated otherwise, the spin-density superkets used in this chapter are normalized to unit trace,

$$\langle E_M|\rho_M\rangle \equiv \mathrm{Tr}\,\rho_M = 1 \quad (44)$$

where $\langle E_M|$ is the superbra[4] representing unit operator E_M. In (43), τ_M is the pre-exchange life time for species M and $|\rho_M^f\rangle$ is the spin-density superket of the (macroscopic) ensemble of molecules of species M formed in the interval $(t - \mathrm{d}t, t)$ (see Section 2.1),

$$|\rho_M^f\rangle = \sum_{A(M)} \sum_{\alpha} \pi_{M\alpha} \sum_{v=1}^{n_\alpha} |\rho_{M\alpha}^v\rangle \quad (45)$$

where the first summation is taken over all fragmentary equilibria which involve species M, the second one is over all basic modes within a given fragmentary equilibrium, and the third is over all elementary reactions within a given mode. In (45), $|\rho_{M\alpha}^v\rangle$ designates the spin-density superket of the subensemble of molecules of species M created in the vth elementary reaction from the mode α which contributes to the fragmentary equilibrium $A(M)$; $\pi_{M\alpha}$ is the fraction of such molecules related to the entire ensemble of molecules of species M formed in the time interval mentioned above. Obviously, as implied by the notation, the fractions of molecules created in individual elementary reactions from the same mode are identical. Therefore, the corresponding normalization condition is

$$\sum_{A(M)} \sum_{\alpha} \pi_{M\alpha} n_\alpha = 1 \quad (46)$$

where n_α is the number of elementary reactions in mode α. Hence, $|\rho_M^f\rangle$ in (45) is normalized according to (44) if the superkets $|\rho_{M\alpha}^v\rangle$ are normalized in the same way.

The superkets $|\rho_{M\alpha}^v\rangle$ can be expressed in terms of the spin-density superkets

of the corresponding substrates using the site-exchange schemes concerned. The (unnormalized) density superket $|\rho_{M\alpha}\rangle^u$ describing the ensemble of molecules of species M formed in all reactions of a given mode α can be written as

$$|\rho_{M\alpha}\rangle^u = \sum_{v=1}^{n_\alpha} |\rho_{M\alpha}^v\rangle = \mathbf{T}_\Gamma^M \left(\sum_{v=1}^{n_\alpha} \mathbf{P}(f_{\alpha_v}) \right) |\rho_\Lambda\rangle \tag{47}$$

where, as before, Λ and Γ denote the substrate(s) and product(s), respectively, of the reactions involved (that is, Δ stands for K or KL, where $\Delta = \Lambda, \Gamma$). In (47), $\mathbf{P}(f_{\alpha_v})$ is the superoperator that maps the Liouville space of the substrate(s) onto that of the product(s) according to the site exchange scheme f_{α_v}, where the space of a pair of species KL is a direct product of the "primitive spaces"[44] of K and L; the spin-density superket of a pair of species is a direct product of the density superkets of these species. Thus, when $\Lambda = IJ$, then

$$|\rho_\Lambda\rangle = |\rho_I\rangle \otimes |\rho_J\rangle \tag{48}$$

The superoperator $\mathbf{T}_\Gamma^M$ in (47) is the unit superoperator $\mathbf{E}_M$ when species M is the only product of the reactions involved; when there are two products, M and N, then $\mathbf{T}_\Gamma^M$ assumes one of the two following forms[22,23,42,43]

$$\mathbf{E}_M \otimes \langle E_N| \text{ or } \langle E_N| \otimes \mathbf{E}_M \tag{49}$$

depending on the adopted ordering of the primitive spaces forming the direct product space concerned. The superoperators (49) project the spin-density superket describing the ensemble of newly formed pairs of product molecules onto the appropriate primitive space.

Now follows the essential point of our reasoning. We want to show that (43) exhibits the property of macroscopic symmetry conservation. Let us denote by $\mathbf{G}_K$ the totally symmetric superprojector of the skeleton symmetry group of species K, $\mathscr{G}_K$,

$$\mathbf{G}_K = |\mathscr{G}_K|^{-1} \sum_{g_K \in \mathscr{G}_K} \mathbf{P}(g_K) \tag{50}$$

In (50), $\mathbf{P}(g_K)$ denotes the permutation superoperator representing the permutation g_K in Liouville space of species K. Our goal is to demonstrate that all the spin-density superkets $|\rho_I\rangle, |\rho_J\rangle, \ldots, |\rho_M\rangle$ entering a closed system of the equations of motion (43) can be replaced by the corresponding totally symmetric superprojections $\mathbf{G}_I|\rho_I\rangle, \mathbf{G}_J|\rho_J\rangle, \ldots, \mathbf{G}_M|\rho_M\rangle$. In other words, we want to demonstrate that in an exchanging system the two orthogonal projections of the spin-density superket of each species K, $\mathbf{G}_K|\rho_K\rangle$ and $(\mathbf{E}_K - \mathbf{G}_K)|\rho_K\rangle$, evolve independently.

The first two terms in (43) do not violate such a symmetry partitioning,

because $\mathbf{G}_K$ commutes with both $\mathbf{L}_K$ and $\mathbf{R}_K$,

$$[\mathbf{L}_K, \mathbf{G}_K] = 0 \tag{51}$$

and

$$[\mathbf{R}_K, \mathbf{G}_K] = 0 \tag{52}$$

Equation (52), which appears in the present context as merely a postulate, is commented on in Section 4.4. Equation (51), however, is a straightforward consequence of the fact that the corresponding static Hamiltonian is invariant under $\mathscr{G}_K$. In order to prove that the third term in (43) also exhibits the required property, it is sufficient to show that the latter is valid for a single mode of rearrangement. Precisely, one must demonstrate that, when the spin-density superket of the substrate(s), $|\rho_\Lambda\rangle$, in (47) is replaced by the corresponding totally symmetric superprojection

$$\mathbf{G}_J|\rho_J\rangle \text{ or } (\mathbf{G}_I \otimes \mathbf{G}_J)(|\rho_I| \otimes |\rho_J\rangle) \tag{53}$$

then the superket $|\rho_{M\alpha}\rangle^{\mathrm{u}}$ describing the newly formed product molecules will automatically be replaced by its projection $\mathbf{G}_M|\rho_{M\alpha}\rangle^{\mathrm{u}}$. The detailed proof is carried out here for a basic mode conforming to the general scheme $I + J \rightarrow M + N$.

For the following argument, we exploit the identity

$$\mathbf{G}_I \otimes \mathbf{G}_J = \mathbf{G}_{IJ}(\mathbf{G}_I \otimes \mathbf{G}_J) \tag{54}$$

where $\mathbf{G}_{IJ}$ is the totally symmetric superprojector of $\mathscr{G}_{IJ}$ (see (38)) and is defined in the product space of I and J using the appropriate generalized version of (50). Equation (54) stems from the fact that $\mathscr{G}_{IJ}$ is a subgroup of $\mathscr{G}_I \otimes \mathscr{G}_J$ (see (39)). Substituting $|\rho_\Lambda\rangle$ in (47) by the totally symmetric projection of $|\rho_I\rangle \otimes |\rho_J\rangle$, and using (54) gives

$$|\rho_{M\alpha}\rangle^{\mathrm{u}}_{+} = \mathbf{T}^M_\Gamma \left(\sum_{v=1}^{n_\alpha} \mathbf{P}(f_{\alpha_v})\mathbf{G}_{IJ} \right)(\mathbf{G}_I \otimes \mathbf{G}_J)(|\rho_I\rangle \otimes |\rho_J\rangle) \tag{55}$$

The sum in parentheses in (55) is merely a group-algebraic version of the set-theoretical expression on the left-hand side of (42) which describes the property of macroscopic symmetry invariance in the skeleton-site representation. This sum can thus be calculated immediately:

$$\sum_{v=1}^{n_\alpha} \mathbf{P}(f_{\alpha_v})\mathbf{G}_{IJ} = n_\alpha \mathbf{G}_{MN}\mathbf{P}(f_\alpha)\mathbf{G}_{IJ} \tag{56}$$

where f_α has the same meaning as in (36), that is, we may put

$$\mathbf{P}(f_\alpha) = \mathbf{P}(f_{\alpha_v}) \tag{57}$$

and $\mathbf{G}_{MN}$ is the totally symmetric superprojector of $\mathscr{G}_{MN}$. The multiplier n_α appears in (56) as a result of passing from set-theoretical to group-algebraic

calculus. Substituting (56) in (55), performing the projection $\mathbf{T}_\Gamma^M$ on $\mathbf{G}_{MN}$ which gives (see (50), (49), (38) and (19))

$$\mathbf{T}_\Gamma^M \mathbf{G}_{MN} = \mathbf{G}_M \mathbf{T}_\Gamma^M \tag{58}$$

and invoking again (54), one gets

$$|\rho_{M\alpha}\rangle_+^{\mathrm{u}} = n_\alpha \mathbf{G}_M \mathbf{T}_\Gamma^M \mathbf{P}(f_\alpha) \mathbf{G}_{IJ} (\mathbf{G}_I \otimes \mathbf{G}_J)(|\rho_I\rangle \otimes |\rho_J\rangle) \tag{59}$$

Premultiplying the right-hand side of (59) by $\mathbf{G}_M$ leaves it unchanged, which means that $|\rho_{M\alpha}\rangle_+^{\mathrm{u}}$ is indeed the totally symmetric part of $|\rho_{M\alpha}\rangle^{\mathrm{u}}$ from (47),

$$|\rho_{M\alpha}\rangle_+^{\mathrm{u}} = \mathbf{G}_M |\rho_{M\alpha}\rangle^{\mathrm{u}} \tag{60}$$

The above result can be derived for any other type of exchange scheme, representing intra- or inter-molecular processes. We have thus proven that, indeed, in an exchanging system the totally symmetric parts of the spin-density superkets of individual species evolve independently, which is a consequence of the property of macroscopic symmetry conservation. These are the only relevant parts in calculating observables; the remaining parts are never needed and can be discarded. In the following we use the same symbol to designate a spin-density superket and its totally symmetric projection. This is justified because, as pointed out elsewhere,[21] in the state of dynamic equilibrium the complementary projections of the spin-density superkets of individual species must vanish.

As a by-product of the reasoning leading to (59), one obtains the exchange term expressed in a convenient form in which an explicit knowledge of only one site-exchange scheme is required for each basic mode of rearrangement. We exploit this in the sequel where the general DNMR equation of motion (43) is presented in its linearized, approximate version[45,46] which applies as long as the standard high-temperature condition $\hbar\omega_0/kT \ll 1$ is fulfilled.

In the high-temperature regime, which is valid for most if not all NMR experiments on liquids, the density superket products can be approximated according to

$$|\rho_I\rangle \otimes |\rho_J\rangle \cong |\rho_I\rangle \otimes |\bar{E}_J\rangle + |\bar{E}_I\rangle \otimes |\rho_J\rangle - |\bar{E}_I\rangle \otimes |\bar{E}_J\rangle \tag{61}$$

where

$$|\bar{E}_K\rangle = \langle E_K | E_K\rangle^{-1} |E_K\rangle \tag{62}$$

with $K = I, J$. Substituting (61) in place of the superket products wherever such products appear in the equation of motion and performing straightforward algebraic manipulations, one obtains the required linear version of (43):

$$\mathrm{d}|\rho_M\rangle/\mathrm{d}t = -i\mathbf{L}_M|\rho_M\rangle + \mathbf{R}_M|\rho_M - \rho_{0M}\rangle - \tau_M^{-1}(|\rho_M - \bar{E}_M\rangle$$

$$+\sum_L\left(\sum_\beta k_{m\beta}\mathbf{Y}^\beta_{ML}\right)|\rho_L\rangle \tag{63}$$

where the first summation is over all the species which rearrange into M in uni- and bi-molecular reactions (including degenerate reactions where $L = M$) and the second summation is over all such basic modes in which L is a substrate and M is a product; $k_{M\beta}$ is the corresponding rate parameter. In (63), the mode superoperators $\mathbf{Y}^\beta_{ML}$ are

$$\mathbf{Y}^\beta_{ML} = \langle E_\Lambda|E_\Lambda\rangle^{-1}\langle E_L|E_L\rangle\mathbf{G}_M\mathbf{T}^M_\Gamma\mathbf{P}(f_\beta)(\mathbf{T}^L_\Lambda)^\dagger\mathbf{G}_L \tag{64}$$

where Λ and Γ denote the substrate(s) and product(s) for reactions of mode β and $|E_\Lambda\rangle$ designates the unit superket in the space of product(s) (a direct product space or a primitive space); the superoperators $\mathbf{T}^K_\Delta$ are either unit superoperators or the appropriate projection superoperators (49). The structure of the mode superoperators and the meaning of the rate parameters for various types of exchange processes (in (22) of Ref. 23 defining $k_{M\alpha}$ the symbol k_α should be replaced by $k_{\bar{\alpha}}$) are displayed in Table 1.

The system of equations of motion (63) for all the exchanging species can conveniently be formulated in composite Liouville space[44] which is spanned by the primitive spaces involved. In composite space, the spin-density

Table 1. Mode superoperators and rate parameters for various types of exchange processes in symmetric systems (see text).

Process	Mode superoperator,[a] $\mathbf{Y}^\beta_{ML}$	Rate parameter,[b] $k_{M\beta}$
$L \rightarrow M$	$\mathbf{G}_M\mathbf{P}(f_\beta)\mathbf{G}_L$	$z_\beta k_{\bar{\beta}}$ $(= w_\beta k_\beta c_L/c_M)$
$K + L \rightarrow M$	$\mathbf{G}_M\mathbf{P}(f_\beta)(\|\bar{E}_K\rangle \otimes \mathbf{G}_L)$	$z_\beta k_{\bar{\beta}}$ $(= w_\beta k_\beta c_K c_L/c_M)$
$L + K \rightarrow M$	$\mathbf{G}_M\mathbf{P}(f_\beta)(\mathbf{G}_L \otimes \|\bar{E}_K\rangle)$	$z_\beta k_{\bar{\beta}}$ $(= w_\beta k_\beta c_K c_L/c_M)$
$L + L' \rightarrow M$	$\mathbf{G}_M\mathbf{P}(f_\beta)(\mathbf{G}_L \otimes \|\bar{E}_L\rangle)$	$z_\beta k_{\bar{\beta}}$ $(= w_\beta k_\beta c_L^2/c_M)$
$L \rightarrow M + N$	$(\mathbf{G}_M \otimes \langle E_N\|)\mathbf{P}(f_\beta)\mathbf{G}_L$	$z_\beta k_{\bar{\beta}} c_N$ $(= w_\beta k_\beta c_L/c_M)$
$L \rightarrow N + M$	$(\langle E_N\| \otimes \mathbf{G}_M)\mathbf{P}(f_\beta)\mathbf{G}_L$	$z_\beta k_{\bar{\beta}} c_N$ $(= w_\beta k_\beta c_L/c_M)$
$L \rightarrow M + M'$	$(\mathbf{G}_M \otimes \langle E_M\|)\mathbf{P}(f_\beta)\mathbf{G}_L$	$z_\beta k_{\bar{\beta}} c_M$ $(= w_\beta k_\beta c_L/c_M)$
$K + L \rightarrow M + N$	$(\mathbf{G}_M \otimes \langle E_N\|)\mathbf{P}(f_\beta)(\|\bar{E}_K\rangle \otimes \mathbf{G}_L)$	$z_\beta k_{\bar{\beta}} c_N$ $(= w_\beta k_\beta c_K c_L/c_M)$
$L + K \rightarrow M + N$	$(\mathbf{G}_M \otimes \langle E_N\|)\mathbf{P}(f_\beta)(\mathbf{G}_L \otimes \|\bar{E}_K\rangle)$	$z_\beta k_{\bar{\beta}} c_N$ $(= w_\beta k_\beta c_K c_L/c_M)$
$L + L' \rightarrow M + N$	$(\mathbf{G}_M \otimes \langle E_N\|)\mathbf{P}(f_\beta)(\mathbf{G}_L \otimes \|\bar{E}_L\rangle)$	$z_\beta k_{\bar{\beta}} c_N$ $(= w_\beta k_\beta c_L^2/c_M)$
$M + M' \rightarrow M + M'$	$(\mathbf{G}_M \otimes \langle E_M\|)\mathbf{P}(f_\beta)(\mathbf{G}_M \otimes \|\bar{E}_M\rangle)$	$z_\beta k_{\bar{\beta}} c_M$ $(= w_\beta k_\beta c_M)$

[a] The assumed order of primitive spaces forming the direct product space for substrates and/or products is the same as in the exchange scheme given in column 1.

[b] k_β and $k_{\bar{\beta}}$ are the kinetic rate constants for single elementary reactions of mutually reverse basic modes of rearrangement, β and $\bar{\beta}$, respectively; c_K is the molar concentration of species K; w_β and z_β are the substrate and product connectivities, respectively, for mode β.

superket, the super-Hamiltonian, and the relaxation matrix are direct sums of the corresponding primitive quantities $|\rho_K\rangle$, $\mathbf{L}_K$, and $\mathbf{R}_K$, and are denoted by $|\rho\rangle_c$, $\mathbf{L}_c$ and $\mathbf{R}_c$, respectively; exchange is described by the superoperator $\mathbf{X}$ which is composed of blocks $\mathbf{X}_{ML}$, where $M, L \in \{I, J, \ldots, N\}$, connecting the primitive spaces concerned (see (63)),

$$\mathbf{X}_{ML} = \delta_{ML}\tau_M^{-1}(|E_M\rangle\langle E_M| - \mathbf{E}_M) + \sum_\beta k_{M\beta}\mathbf{Y}^\beta_{ML} \tag{65}$$

where δ_{ML} is the Kronecker delta. If the primitive superkets are renormalized according to

$$|\rho_K\rangle^r = (\Pi_K\langle E_K|E_K\rangle)^{1/2}|\rho_K\rangle \tag{66}$$

where Π_K is the molar fraction of species K, and if $|\rho\rangle_c$ is replaced by the corresponding renormalized density superket $|\rho\rangle_c^r$, then the composite superoperators $\mathbf{L}_c$ and $\mathbf{R}_c$ will remain unchanged while $\mathbf{X}$, which is in general non-Hermitian, will be replaced by its Hermitian counterpart,[43,47] $\mathbf{X}^r$, such that

$$\mathbf{X}^r_{ML} = (\mathbf{X}^r_{LM})^\dagger = [(\Pi_M\langle E_M|E_M\rangle)/(\Pi_L\langle E_L|E_L\rangle)]^{1/2}\mathbf{X}_{ML} \tag{67}$$

The renormalized composite space DNMR equation of motion assumes the form

$$\mathrm{d}|\rho\rangle_c^r/\mathrm{d}t = -i\mathbf{L}_c|\rho\rangle_c^r + \mathbf{R}_c|\rho - \rho_0\rangle_c^r + \mathbf{X}^r|\rho\rangle_c^r \tag{68}$$

For computational purposes, (68) is much more suitable than the version involving $|\rho\rangle_c$.

It must be remembered that any observable $\langle 0\rangle$ for an exchanging system is expressed as a sum of contributions from individual species weighted by the corresponding molar fractions,

$$\langle 0\rangle \simeq \sum_K \Pi_K\langle 0_K|\rho_K\rangle \tag{69}$$

Therefore, in forming the pertinent composite vector $|0\rangle_c^r$ which represents the observable in the renormalized composite space, the primitive superkets $|0_K\rangle^r$ entering $|0\rangle_c^r$ should be normalized accordingly, thus,

$$|0_K\rangle^r = (\Pi_K/\langle E_K|E_K\rangle)^{1/2}|0_K\rangle \tag{70}$$

4.4. A comparison with previous approaches

The former formulation of the DNMR equation of motion incorporating symmetry proposed by Meakin *et al.*,[10-12] which is still in use,[46] encompasses

intramolecular degenerate rearrangements and intermolecular rearrangements of the type $M + N \rightarrow M + N$, where N denotes a species containing a single magnetic nucleus. It is instructive to compare this with the formulation presented above. The following discussion is confined essentially to intramolecular degenerate rearrangements and thus the species index is dropped for simplicity since one-component systems are dealt with. For such systems, the skeleton-site mappings can be treated as permutations, because they map a set of skeleton-site labels onto itself.

In the approach reported here, the relevant terms in the exchange superoperator which describe individual basic modes of (degenerate) rearrangement are of the form (see (63) and Table 1)

$$z_\alpha k_{\bar{\alpha}} \mathbf{G}\mathbf{P}(f_\alpha)\mathbf{G} \tag{71}$$

where $k_{\bar{\alpha}} (= k_\alpha)$ is the first-order rate constant of *any elementary reaction* of the mode $\bar{\alpha}$ which is the inverse of α (see (28)), and f_α is the site-exchange scheme of an arbitrary elementary reaction of mode α; z_α is the product connectivity (13) for mode α. We limit ourselves to self-inverse modes (29) which are often encountered in practice.

In the present notation, the corresponding term in the approach[10,11] is

$$1/2 \sum_{p_i \in \mathscr{P}_\alpha} \tau_i^{-1} \mathbf{P}(p_i), \tag{72}$$

where, in the nomenclature of the papers quoted,[10-12] $\mathscr{P}_\alpha$ is the appropriate "basic permutational set". In the present notation, the latter can be defined as a set of all such distinct skeleton-site permutations, p_i, which can be derived from f_α according to

$$p_i = g^{(i)} f_\alpha (g^{(i)})^{-1} \tag{73}$$

where $g^{(i)}$ are the elements of the skeleton-site symmetry group $\mathscr{G}$ (see below). In (72), $\mathbf{P}(p_i)$ is the permutation superoperator representing p_i in Liouville space involved, and τ_i is defined, somewhat loosely, as "the average time between exchanges of the ith type".[11] The number of elements in a basic permutational set $\mathscr{P}_\alpha$ is given by

$$|\mathscr{P}_\alpha| = |\mathscr{G}|/|\mathscr{G}_\alpha| \tag{74}$$

where the group $\mathscr{G}_\alpha \subset \mathscr{G}$ is composed of all the elements in $\mathscr{G}$ that commute with f_α. The generating elements $g^{(i)}$ in (73) are representatives of right cosets of $\mathscr{G}_\alpha$ in $\mathscr{G}$.

Taking into account the fact that each superoperator $\mathbf{P}(p_i)$ in (72) can be expressed as

$$\mathbf{P}(p_i) = \mathbf{P}(g^{(i)})\mathbf{P}(f_\alpha)\mathbf{P}(g^{(i)})^{-1} \tag{75}$$

where $\mathbf{P}(f_\alpha)$ has the same meaning as in (72), then by virtue of the definition of $\mathscr{P}_\alpha$

$$\left[\sum_{p_i \in \mathscr{P}_\alpha} \mathbf{P}(p_i), \mathbf{G}\right] = 0 \tag{76}$$

where $\mathbf{G}$ is the totally symmetric superprojector of $\mathscr{G}$ (50). If, following the papers quoted,[10,11] one assumes that the lifetimes, τ_i, for individual permutations from the same basic permutational set are identical, regardless of how they are to be interpreted physically,

$$\tau_1 = \tau_2 = \cdots \equiv \tau_\alpha \tag{77}$$

then it is seen from (76) that the exchange term (72) also commutes with $\mathbf{G}$. This implies that the corresponding equation of motion[10,11] can be projected onto the eigenspace of $\mathbf{G}$ without introducing any approximations. On the projection, the relevant part of the exchange term (72) assumes the form

$$(2\tau_\alpha)^{-1} |\mathscr{P}_\alpha| \mathbf{G}\mathbf{P}(f_\alpha)\mathbf{G} \tag{78}$$

Thus, by comparing (78) with (71) it can be concluded that, for intramolecular degenerate rearrangements, the previous approach[10,11] and that reported presently can give identical results provided that the pre-exchange lifetime, τ_α, is redefined such that

$$\tau'_\alpha = |\mathscr{P}_\alpha|(2z_\alpha k_{\tilde{\alpha}})^{-1} \tag{79}$$

However, it does not seem possible to propose a consistent interpretation of τ'_α that obeys (79). Namely, for the same molecule the physical meaning of τ'_α can be different for different exchange mechanisms. Consider, for example, a system of five identical ligands placed at the vertices of a trigonal bipyramid (D_{3h} symmetry). For a Berry pseudo-rotation in such a system, the product connectivity, z_α, is equal to 3 while the corresponding set $\mathscr{P}_\alpha$ contains six elements. As is seen from (79), in this instance τ'_α is equal to the inverse of the rate constant for a single elementary pseudo-rotation reaction, $\tau'_\alpha = (k_{\tilde{\alpha}})^{-1}$. However, for a mechanism α' where a single exchange event involves an interchange of an apical and an equatorial ligand one has $|\mathscr{P}_{\alpha'}| = z_{\alpha'} = 6$ and thus $\tau'_\alpha = (2k_{\tilde{\alpha}})^{-1}$. This is a real inconsistency if one takes into account that in both cases the rate constants $k_{\tilde{\alpha}}$ and $k_{\tilde{\alpha}'}$ should have a well-defined physical interpretation (see the concluding remarks at the end of Section 3.1). We believe that our definition of the kinetic parameters entering the DNMR equation of motion is correct since it emerges, in a natural way, from a rigorous derivation of the equation from "first principles". However, the former formulation of the DNMR equation[10,11] is based on an intuitive reasoning which is insufficient for a proper description of all the subtleties of the problem. This does not imply that the previous equation[10,11] did not serve well the main

purpose for which it was employed, namely mechanistic studies using DNMR spectra. In the latter context, it is not of crucial importance what physical sense one ascribes to the rate parameters involved.

The above remarks on the interpretation of the lifetimes, τ_α, pertain equally to the version[12] of the DNMR equation[10,11] extending over the specific class of intermolecular rearrangements mentioned at the beginning of this section. Other aspects of the approach of Meakin *et al.*[10-12] reviewed above are discussed in Section 6.4.

4.5. NMR modes of rearrangement

In the derivation presented of the general DNMR equation of motion for symmetric systems (Section 4.3), the basic modes of rearrangement were referred to as the most fundamental classification units for elementary reactions. This is quite natural if one takes into account that the possibility of a proper grouping of reactions with the same kinetics is of crucial importance to the whole reasoning. However, it can be seen from the final form of the equation that, as far as its practical applications are concerned, such a classification is too detailed since different basic modes can be represented in it by the same mode superoperator (see (64) and Table 1). There thus arises a need for an additional classification which does not involve individual elementary reactions but the basic modes. It should be designed in such a way that the corresponding classification units grouped the basic modes which are represented by the same mode superoperator. This is especially important in mechanistic studies using DNMR spectra. Once the basic modes have been classified in this way, the strategy of the corresponding trial DNMR lineshape calculations can be simplified considerably: all conceivable experimental lineshape patterns can, in principle, be reproduced by taking only one basic mode from each such classification unit and, when necessary, allowing also for linear combinations of the representative modes. Following Willem *et al.*,[35] the classification units are called "NMR-modes of rearrangement"; the classification principle specified above is, however, different from that adopted in the paper quoted[35] (see below).

Even without referring to the structure of the mode superoperators, it is clear that any two basic modes differing only by inversion, $\mathscr{Q}_\Gamma s_\alpha \mathscr{Q}_\Lambda$ and $\mathscr{Q}_\Gamma \bar{e} s_\alpha \mathscr{Q}_\Lambda$, must belong to the same NMR mode. This fact, stemming from the sole properties of spin spaces, was commented on in Section 4.1. Hence the classification of basic modes to NMR modes in fact involves the pairs of the former possessing the same representation in terms of ordinary permutations, $\tilde{\mathscr{Q}}_\Gamma \tilde{s}_\alpha \tilde{\mathscr{Q}}_\Lambda$, and, accordingly, the same representation in terms of skeleton-site mappings, $\mathscr{G}_\Gamma f_\alpha \mathscr{G}_\Lambda$ (see (35)). (It can happen that the permutation-inversion

double cosets $\mathscr{Q}_\Gamma s_\alpha \mathscr{Q}_\Lambda$ and $\mathscr{Q}_\Gamma \bar{e} s_\alpha \mathscr{Q}_\Lambda$ are identical; the basic mode depicted in Fig. 4 serves as an example of such a "self-reflective"[26] mode of rearrangement. However, referring generally to a double coset $\tilde{\mathscr{Q}}_\Gamma \tilde{s}_\alpha \tilde{\mathscr{Q}}_\Lambda$ or $\mathscr{G}_\Gamma f_\alpha \mathscr{G}_\Lambda$ as a pair of basic modes should not lead to any confusion.)

For intramolecular exchange, the consideration of the structure of the corresponding mode superoperators from Table 1 adds no new elements to the argument presented above and the NMR modes of intramolecular rearrangements can simply be identified by using the double cosets

$$\mathscr{G}_L f_\alpha \mathscr{G}_K \tag{80}$$

Each such NMR mode thus comprises at most a pair of basic modes.

For intermolecular exchange, the situation is different. Here, the NMR modes are also described in terms of appropriate double cosets, but the form of the latter depends on the type of exchange scheme and can be determined by examining the structure of the pertinent mode superoperators from Table 1. For example, for rearrangements of the type $I + J \rightarrow M + N$, the NMR modes are of the form

$$(\mathscr{G}_M \otimes \mathscr{G}_N) f_\alpha (\mathscr{G}_I \otimes \mathscr{G}_J) \tag{81}$$

since, as can be seen from (39) and (64), each pair of basic modes, $\mathscr{G}_{MN} f_{\alpha'} \mathscr{G}_{IJ}$, belonging to the double coset (81) will be represented by the same set of mode superoperators, $\mathbf{Y}^\alpha_{IM}$, $\mathbf{Y}^\alpha_{IN}$, $\mathbf{Y}^\alpha_{JM}$ and $\mathbf{Y}^\alpha_{JN}$ (see Table 1). In general, there can be as many as four such pairs (that is, eight basic modes) that belong to the same NMR mode (81) and, as such, they are nondifferentiable on the basis of DNMR spectra. For other types of intermolecular rearrangement, the NMR modes can be defined in an analogous way.

The previous definitions of NMR modes[11,34,35] (also called "sets of indistinguishable permutationsl sets"[11] or "sets of NMR nondifferentiable reactions"[34]) differ from that presented above in that they are based on symmetries of the effective Hamiltonians (see Section 2.3) rather than on the molecular symmetries. In practice, the two approaches give the same classification of rearrangements for all such systems where the molecular, $\mathscr{G}_K$, and effective Hamiltonian symmetry groups, $\mathscr{G}^{\text{eff}}$, are identical for each species $K = I, J, \ldots, N$. However, for certain systems containing magnetically equivalent nuclei, for which the symmetry $\mathscr{G}^{\text{eff}}$ is higher than $\mathscr{G}_K$, the predictions of both approaches differ. This involves such molecules in which the integrity of a set of magnetically equivalent nuclei is not conserved in the course of exchange. As was demonstrated elsewhere,[24] in a system of this kind two basic modes, which according to the previous definition[11,34,35] are classified as NMR nondifferentiable, are in fact differentiable since the corresponding theoretical DNMR lineshape patterns are not identical. In view of this finding, which is commented upon further below, the reasoning

underlying the previous approach[11,34,35] must be rejected. It is instructive to point out two false premises implied in this reasoning. Firstly, in systems not conserving magnetic equivalence the scalar couplings between magnetically equivalent nuclei, and, precisely, between magnetically equivalent skeleton sites, can be relevant[24] and hence in calculating DNMR spectra the complete Hamiltonian cannot in general be replaced by the effective Hamiltonian. Secondly, even when all such couplings vanish by accident, the theoretical DNMR spectra calculated for two different basic modes belonging to the same double coset $\mathcal{G}_L^{\text{eff}} f_\alpha \mathcal{G}_K^{\text{eff}}$ but to two different double cosets $\mathcal{G}_L f_{\alpha'} \mathcal{G}_K$ and $\mathcal{G}_L f_{\alpha''} \mathcal{G}_K$ need not be identical.[24] This is understandable in the light of the discussion in Section 2.3. However, one should be aware that the above argument does not exhaust the problem of differentiability of rearrangements in DNMR spectroscopy. Some important aspects of this argument are discussed in the remainder of this section.

In the rearrangement classification presented above it is warranted that any two basic modes whose respective DNMR lineshape patterns are not identical will be ascribed to different NMR modes. However, the reverse implication need not hold, which is concerned with the sole logical structure of the classification problems of this kind. The lineshape patterns of basic modes belonging to different NMR modes may be identical simply by accident. The study already quoted[24] has revealed that for spin-$\frac{1}{2}$ systems, which are the most interesting ones in the context of DNMR spectroscopy, there can also occur instances where such a coincidence of lineshape patterns is not accidental and can be predicted theoretically. This again involves the specific systems in which the molecular symmetries are lower than the symmetries of the corresponding effective Hamiltonians. Limiting ourselves to degenerate intramolecular rearrangements for the sake of simplicity, we characterize these instances in more detail. Namely, two different NMR modes $\mathcal{G} f_\alpha \mathcal{G}$ and $\mathcal{G} f_{\alpha'} \mathcal{G}$ (i.e. the corresponding representative basic modes) give identical lineshape patterns if a premultiplication (or, equivalently, a postmultiplication) of each of them by $\mathcal{G}^{\text{eff}}$ gives the same double coset of $\mathcal{G}^{\text{eff}}$. Formally,

$$\mathcal{G}^{\text{eff}} \mathcal{G} f_\alpha \mathcal{G} \equiv \mathcal{G}^{\text{eff}} f_\alpha \mathcal{G} = \mathcal{G}^{\text{eff}} f_\alpha \mathcal{G}^{\text{eff}} \tag{82a}$$

$$\mathcal{G}^{\text{eff}} \mathcal{G} f_{\alpha'} \mathcal{G} \equiv \mathcal{G}^{\text{eff}} f_{\alpha'} \mathcal{G} = \mathcal{G}^{\text{eff}} f_{\alpha'} \mathcal{G}^{\text{eff}} \tag{82b}$$

The commutativity of $\mathcal{G}^{\text{eff}}$, in the sense of (82), with an NMR mode $\mathcal{G} f_{\alpha''} \mathcal{G}$ holds in a trivial way if the rearrangements in question conserve magnetic equivalence, because in such a case each representative element $g f_{\alpha''} g'$ from $\mathcal{G} f_{\alpha''} \mathcal{G}$ separately commutes with $\mathcal{G}^{\text{eff}}$. For equivalence-breaking processes, the latter property does not occur. In spite of this, in certain specific systems (82) can be fulfilled for some or even all of the equivalence-breaking NMR modes possible in a given system.[24] The latter situation occurs, e.g. for a system

of five nuclei placed at the vertices of a square pyramid ($\mathscr{G} \sim C_{4v}$, $\mathscr{G}^{eff} \sim \mathscr{P}(4)$, the symmetric group of degree 4 and order 4!). However, in a system of six nuclei forming a distorted octahedron ($\mathscr{G} \sim D_{4h}$, $\mathscr{G}^{eff} \sim \mathscr{P}(2) \otimes \mathscr{P}(4)$) (82) is fulfilled for only two of the six equivalence-breaking NMR modes possible in the system.[24] (Actually, the argument reported above invalidating the previous rearrangement classification[11,34,35] was supported by the results of DNMR lineshape computations for the four NMR modes for which (82) is not fulfilled.)

The mechanism which warrants that the NMR modes obeying (82a) and (82b) will give identical lineshape patterns is based on certain specific properties of scalar interactions between spin-$\frac{1}{2}$ particles. It has been proven[24] that:

(i) the super-Hamiltonian of scalar interactions between a pair (k,l) of spin-$\frac{1}{2}$ nuclei, $\mathbf{L}_{kl}^{sc}$, always commutes with the totally symmetric superprojector of any such permutation group which contains the permutation (kl) as an element;

(ii) the block of $\mathbf{L}_{kl}^{sc}$ belonging to the eigenspace of this superprojector vanish.

By virtue of the above properties, for any set of NMR modes obeying (82) the pertinent DNMR equation of motion can be projected on the eigenspace of $\mathbf{G}^{eff}$, the totally symmetric superprojector of $\mathscr{G}^{eff}$, without introducing any approximations. This is because $\mathscr{G}^{eff}$ includes all permutations (kl) which interchange only the nuclei k and l within a given pair (k,l) of magnetically equivalent nuclei leaving the remaining (equivalent and/or nonequivalent) nuclei unmoved. In the eigenspace of $\mathbf{G}^{eff}$, the relevant parts of the mode superoperators involved become identical, assuming the form $\mathbf{G}^{eff}\,\mathbf{P}(f_\alpha)\,\mathbf{G}^{eff}$. It is thus clear that the corresponding lineshape patterns will also be identical. Moreover, as follows from the property (ii) above, none of the scalar spin–spin couplings between equivalent nuclei will affect the spectral lineshapes, despite the fact that the exchange processes in question do not conserve magnetic equivalence. Similar effects may also occur in nondegenerate systems.

In view of the fact that the DNMR theory for symmetric systems stems from the property of macroscopic conservation of *molecular* symmetry, both the coincidence of lineshape patterns for different NMR modes and the lack of dependence of the lineshapes on the couplings between equivalent nuclei appear as pathological effects that are due to the specific properties of spin-$\frac{1}{2}$ systems. In systems composed of nuclei of spin $> \frac{1}{2}$, which in the context of DNMR spectroscopy are merely of theoretical interest, the whole picture is more consistent. Here, for any equivalence-breaking rearrangement all the couplings involved will affect the DNMR lineshapes and, accordingly, the

lineshape patterns corresponding to different NMR modes will not, in general, be the same.

Turning back to spin-$\frac{1}{2}$ systems, we emphasize that even in the instance where (82) is not fulfilled, the analogy with spin $> \frac{1}{2}$ systems is incomplete. Owing to the mentioned properties of scalar interactions, not all the couplings between equivalent nuclei will influence the DNMR lineshapes. Namely, coupling between any two equivalent nuclei the interchange of which is a valid symmetry operation for the molecule involved is totally irrelevant. For example, in the system of D_{4h} symmetry mentioned above only the couplings between the nuclei in the σ_h plane situated *cis* to each other are of relevance to the DNMR lineshapes (not to mention the couplings between nonequivalent nuclei). The couplings between the nuclei situated *trans* to each other and the coupling between the nuclei lying on the C_4 axis are irrelevant since they all involve pairs of nuclei which are interchangeable by appropriate operations from D_{4h}.

It should be added that the vast majority of DNMR spectra published so far involve relatively simple (spin-$\frac{1}{2}$) systems which are free of lineshape effects due to couplings between magnetically equivalent nuclei. However, in future DNMR studies extended to more complicated systems, effects of this kind may pose serious problems. Preliminary lineshape calculations[24] have revealed that the effects in question are not large and, therefore, one cannot expect that the use of quantitative procedures of DNMR lineshape analysis will provide reliable estimates of the coupling constants between equivalent nuclei. However, in an iterative analysis of DNMR spectra, a complete neglect of such effects by ascribing arbitrary values to the coupling constants concerned would seriously bias the estimates of the remaining lineshape parameters in a systematic way. For kinetic parameters, the corresponding relative errors can exceed 6%,[24] which is quite a lot if one takes into account that these are systematic errors. It seems that the only reasonable approach to the problem in question is to use as good as possible estimates of the coupling constants concerned and to keep them constant in the course of the iterative process of spectral analysis.

5. WANGSNESS–BLOCH–REDFIELD EQUATION OF MOTION FOR SYMMETRIC SYSTEMS

Outstripping the course of the reasoning, we have already mentioned that the relaxation matrix in the WBR equation of motion

$$\mathrm{d}|\rho\rangle/\mathrm{d}t = -i\mathbf{L}|\rho\rangle + \mathbf{R}|\rho - \rho_0\rangle \tag{83}$$

commutes with the totally symmetric superprojector, $\mathbf{G}$, of the molecular

symmetry group $\mathcal{G}$ (see (52)). This implies that relaxation processes do not couple the two projections of $|\rho\rangle$, $\mathbf{G}|\rho\rangle$ and $(\mathbf{E}-\mathbf{G})|\rho\rangle$, which is a manifestation of the property of macroscopic symmetry conservation. It remains to explain how this property is reflected in the structure of the WBR relaxation matrix.

The semiclassical Hamiltonian of the random-spin interactions leading to relaxation, $H_1(t) = H(t) - \bar{H}(t)$, can be expressed in irreducible spherical tensor form,

$$H_1(t) = \sum_m \sum_{\mu=\lambda_m}^{-\lambda_m} (-1)^\mu S_{m\mu} B_{m-\mu}(t) \tag{84}$$

where m indicates the individual interaction tensor, λ_m is the rank of tensor m, and $S_{m\mu}$ and $B_{m-\mu}$ are components of the spin operators and bath functions, respectively, both written in irreducible spherical tensor forms. H_1 encompasses both intra- and inter-molecular interactions, as long as the latter can be described within the so-called random field (RF) model.[17] For RF, SR, CSA and Q interactions (see Section 2.2) the label m collectively denotes the skeleton site involved, a, and the interaction type, δ, that is

$$m \equiv (a;\delta) \tag{85}$$

For DD and ICA interactions, m denotes the corresponding pair of sites and the interaction type

$$m \equiv (a,b;\delta) \tag{86}$$

The use of the skeleton sites instead of the nuclei themselves is made for the sake of conformity with the convention adopted for exchange.

With the interaction Hamiltonian written in the form of (84), the relaxation matrix in its most general form can conveniently be expressed as a sum of relaxation superoperators $\mathbf{R}_{mm'}$ for individual auto- ($m = m'$) and cross-relaxation ($m \neq m'$) mechanisms, each of which is defined by a pair of interactions,[22]

$$\mathbf{R} = -\sum \mathbf{R}_{mm'} \tag{87}$$

where

$$\mathbf{R}_{mm} = \sum_{\mu=\lambda_m}^{-\lambda_m} \mathbf{S}^{\mathrm{D}}_{m\mu} \mathbf{S}^{\mathrm{D}}_{m-\mu} J_{mm-\mu}(-\mu\omega_0) \tag{88}$$

and

$$\mathbf{R}_{mm'} = \sum_{\mu=\lambda_m}^{-\lambda_m} \sum_{\mu'=\lambda_{m'}}^{-\lambda_{m'}} \delta_{\mu\mu'} [\mathbf{S}^{\mathrm{D}}_{m\mu} \mathbf{S}^{\mathrm{D}}_{m'-\mu'} + \mathbf{S}^{\mathrm{D}}_{m\mu} \mathbf{S}^{\mathrm{D}}_{m'-\mu'}] J_{mm'-\mu}(-\mu\omega_0) \tag{89}$$

In (88) and (89), $\mathbf{S}^{\mathrm{D}}_{nv}$ denotes a derivation superoperator generated by S_{nv}, and

$J_{nn'\nu}(\omega)$ are the spectral densities of the corresponding ensemble-averaged angular correlation functions $C_{nn'\nu}(\tau)$

$$J_{nn'}(\omega) = 1/2 \int_{-\alpha}^{\alpha} C_{nn'\nu}(\tau) \exp(-i\omega\tau)\, d\tau \tag{90}$$

with

$$C_{nn'\nu}(\tau) = \overline{B_{n\nu}(0) B_{n'-\nu}(\tau)^*} \tag{91}$$

The commutativity of $\mathbf{R}$ with $\mathbf{G}$ stems from the invariance of $\mathbf{R}$ under individual permutations, g, from $\mathcal{G}$,

$$\mathbf{P}(g)^{-1} \mathbf{R} \mathbf{P}(g) = \mathbf{R} \tag{92}$$

The property described in (92) results in turn from the appropriate equalities among the spectral densities or, in fact, among the correlation functions,

$$C_{nn'\nu}(\tau) = C_{g(n)g(n')\nu}(\tau) \tag{93}$$

where $g(m)$ denotes an interaction of the same type as that of m but involving the site $g(a)$ (or, for DD and ICA interactions, the sites $g(a)$ and $g(b)$) when m involves the site a (or the sites a and b).

In addition to the macroscopic invariance properties described in (92), which are of a general validity, under the specific conditions described in Section 2.2 $\mathbf{R}$ can also exhibit microscopic invariance properties. The corresponding microscopic symmetry group $\mathcal{K}$ is always an invariant subgroup of $\mathcal{G}$,[21,22,25]

$$g \mathcal{K} g^{-1} = \mathcal{K} \tag{94}$$

for each $g \in \mathcal{G}$. The microscopic symmetry properties of $\mathbf{R}$ can be expressed in terms of the appropriate invariance properties under the direct product group $\mathcal{K} \otimes \mathcal{K}$ but this would be unproductive.[22] Practically useful results can be obtained when microscopic symmetry is considered in the context of macroscopic symmetry partitioning of the WBR equation of motion. This is discussed in Section 6.

Strictly speaking, the WBR equation of motion written in the form of (83) is incomplete as it does not contain the so-called dynamic shift term,[49] $-i\Delta|\rho\rangle$, the appearance of which is predicted theoretically outside the extreme narrowing limit. A detailed presentation of Δ is given elsewhere.[22] We do not reproduce it here because this term can usually be neglected in practical relaxation studies. For the sake of completeness, we only mention that Δ exhibits the same macroscopic and microscopic symmetry properties as does $\mathbf{R}$.

We also add that for isotropic liquids in the extreme narrowing regime the structure of $\mathbf{R}$ undergoes a considerable simplification. Under such conditions

R exhibits invariance under the full rotation group in three dimensions, R(3), provided that relaxation mechanisms involving CSA interactions can be neglected. In the context of permutation symmetry, this specific instance of relaxation requires a more specialized approach than the general one presented in the following section. Some problems concerned with an invariance of **R** under R(3) are considered in Section 7.3.

6. SYMMETRY-ADAPTED BASES IN LIOUVILLE SPACE

As already mentioned in the discussions in the two preceding sections, owing to the macroscopic symmetry conservation the equation of motion for an exchanging and/or relaxing system can be projected, without any loss of information, onto the eigenspace of the corresponding totally symmetric superprojector. The latter may be a primitive superprojector **G** or, for multicomponent equilibria, the appropriate composite superprojector

$$\mathbf{G}_c = \mathbf{G}_I \oplus \mathbf{G}_J \oplus \cdots \oplus \mathbf{G}_N \tag{95}$$

(As in the preceding sections, the species index is dropped wherever it does not lead to ambiguities.) In any case, in order to perform such a projection in practice one has to know how to determine a complete set of the eigensuperkets, concerned with eigenvalue 1, of the totally symmetric superprojector **G** of any permutation group $\mathscr{G}$. The remaining superkets, i.e. those spanning the eigenspace of the complementary superprojector $\mathbf{E} - \mathbf{G}$, are totally irrelevant and need not concern us any further. The properties of the eigenspace of **G**, which is the only relevant one in NMR spectroscopy, were examined in the paper already quoted.[21] Below we reproduce the main results of that paper, placing them in a wider context.

6.1. Liouville bases adapted to macroscopic symmetry

The primitive superket bases which are used to describe exchange and relaxation phenomena are usually adapted to the existing rotational symmetries of the system under consideration. Thus, the basic superkets are usually simultaneous eigensuperkets of an appropriate subset Φ of the following superoperator set:

$$\mathscr{F} = \{\mathbf{F}_z^{\mathrm{U}}(\mathrm{U} = \mathrm{L}, \mathrm{R}, \mathrm{D}), \mathbf{F}_z^{\mathrm{U}}(\mathrm{M})\ (\mathrm{U} = \mathrm{L}, \mathrm{R}, \mathrm{D};\ \mathrm{M} = \mathrm{A}, \ldots, \mathrm{X}),$$
$$\mathbf{F}^{\mathrm{D2}} = \mathbf{F}_x^{\mathrm{D2}} + \mathbf{F}_y^{\mathrm{D2}} + \mathbf{F}_z^{\mathrm{D2}}\} \tag{96}$$

where the superscripts L, R, and D designate the left-translation, right-

translation and derivation superoperators,[3] respectively, of a corresponding component of the total spin operator of the spin system concerned, and A,..., M,..., X denote individual homonuclear subsystems of a heteronuclear system. Note that any subset $\Phi \subset \mathscr{F}$ that can be taken into account in defining the basis will not include simultaneously $\mathbf{F}^{D2}$ and any of the left- and right-translation superoperators from $\mathscr{F}$ since the latter do not commute with $\mathbf{F}^{D2}$. The left- and right-translation superoperators of F_z or F_z (M) are of use in describing intramolecular exchange.[5] The superoperator $\mathbf{F}^{D2}$ can be exploited in the instances where $\mathbf{R}$ is invariant under R(3).

The basis superkets adjusted to a subset $\Phi \subset \mathscr{F}$ of mutually commuting superoperators is denoted by $|\phi i\rangle$; symbolically, we can write

$$\Phi|\phi i\rangle = \phi|\phi i\rangle \tag{97}$$

where ϕ designates a set of simultaneous eigenvalues (good quantum numbers) of the superoperators from Φ, and $i = 1, 2, \ldots, m_\phi$ enumerates the superkets concerned with the same set ϕ of degeneracy m_ϕ. When a multicomponent system is to be dealt with, the appropriate rotational-symmetry-adapted bases are defined in each of the primitive spaces involved. Since the latter may differ in both the number and type of nuclei (for intermolecular exchange), the corresponding primitive basis subsets

$$\{|I\phi i\rangle, i = 1, 2, \ldots, m_\phi^I\}, \ldots, \{|N\phi k\rangle, k = 1, 2, \ldots, m_\phi^N\} \tag{98}$$

concerned with the same set ϕ of good quantum numbers will, in general, include different numbers of vectors. In particular, it can happen that for some species K the corresponding set in (98) will be empty, that is, m_ϕ^K wil be equal to zero.

Using the bases (98), the DNMR equation of motion can be decomposed into appropriate constituent equations concerned with individual sets ϕ, ϕ', etc. A constituent ϕ of the equation of motion is written in the composite subspace whose dimension is

$$m_\phi^c = m_\phi^I + \cdots + m_\phi^N \tag{99}$$

For one-component systems, the dimensions of the constituent subspaces of ϕ, ϕ', etc., are obviously identical to the corresponding degeneracy factors m_ϕ, $m_{\phi'}$, etc.

All the superoperators in the set $\mathscr{F}$ commute with the totally symmetric superprojector $\mathbf{G}$ of any permutation group $\mathscr{G}$. Therefore, the macroscopic symmetry factoring can be performed separately for each of the constituent equations defined above. This is achieved by eliminating redundant dimensions from each primitive constituent subspace and retaining only the part of the latter which belongs to the eigenspace of $\mathbf{G}$. A complete orthonormal basis set spanning the relevant, totally symmetric primitive subspace of dimension

$\bar{m}_\phi < m_\phi$ is written as

$$\{|\mathscr{G}\phi j\rangle, j = 1, 2, \ldots, \bar{m}_\phi\} \tag{100}$$

where

$$\bar{m}_\phi = \mathrm{Tr}_\phi \mathbf{G} = \sum_{i=1}^{m_\phi} \langle \phi i|\mathbf{G}|\phi i\rangle \tag{101}$$

and the superkets $|\mathscr{G}\phi j\rangle$ obey

$$\mathbf{G}|\mathscr{G}\phi j\rangle = |\mathscr{G}\phi j\rangle. \tag{102}$$

The set (100) can be derived by letting $\mathbf{G}$ operate successively on the basic superkets $|\phi 1\rangle, |\phi 2\rangle, \ldots, |\phi m_\phi\rangle$ and by orthogonalizing the superket set thus obtained.

For multicomponent systems, the dimension $\bar{m}^c_\phi$ $(< m^c_\phi)$ of the totally symmetric composite constituent subspace concerned with ϕ is given by

$$\bar{m}^c_\phi = \bar{m}^I_\phi + \cdots + \bar{m}^N_\phi \tag{103}$$

where $\bar{m}^K_\phi$ denotes the trace of $\mathbf{G}_K$ calculated over the corresponding primitive basis subset (98). Note that even for intramolecular equilibria for which $m^I_\phi = \cdots = m^N_\phi$ (the species $I, \ldots, N$ are necessarily isomeric) the corresponding reduced dimensions $\bar{m}^I_\phi, \ldots, \bar{m}^N_\phi$ are, in general, different as are the macroscopic symmetries $\mathscr{G}_I, \ldots, \mathscr{G}_N$.

The procedure described above of forming an eigenbasis of $\mathbf{G}$, though the most natural, need not be the most convenient. In particular, it does not provide any direct insight into the physical interpretation of the eigenspace of $\mathbf{G}$ which, as has already been mentioned, can be identified with the space of coherences allowed by symmetry $\mathscr{G}$. To see this, we derive an equivalent eigenbasis of $\mathbf{G}$ starting from the familiar symmetry adapted basic vectors from Hilbert space and using the standard symmetry operators[2]

$$P^{uv}_\mu = d_\mu |\mathscr{G}|^{-1} \sum_{g \in \mathscr{G}} [\mu(g)]^*_{uv} P(g) \tag{104}$$

of which those concerned with $w = v$ are projection operators. In (104), μ is an irreducible representation of $\mathscr{G}$, d_μ is the dimension of μ, and $P(g)$ is the (in general, reducible) representation of g in Hilbert space; u and v take on values from the set $\{1, 2, \ldots, d_\mu\}$. By definition, a symmetry adapted basis ket $|\mu 1 r)$ transforming as the first row of the irreducible representation μ obeys

$$P^{11}_\mu |\mu 1 r) = |\mu 1 r) \tag{105}$$

where r enumerates different kets of the same transformation property. The partner vectors, that is, ones transforming as the successive rows $2, \ldots, d_\mu$ of μ

are given by

$$|\mu v r) = P_{\mu}^{v1} |\mu 1 r) \tag{106}$$

where $v = 2, \ldots, d_{\mu}$. Obviously, the concept of partner vectors and, accordingly, (106), do not apply to one-dimensional irreducible representations.

According to the standard theory,[2] symmetry allowed coherences can be identified with shift operators constructed from the vectors that transform as the same row of μ, $|\mu v r)(\mu v r'|$. In Liouville space, such coherences will be denoted by $|\mu v r r'\rangle$, thus

$$|\mu v r r'\rangle \equiv |\mu v r)(\mu v r'| \tag{107}$$

Coherence between different μ terms and between different partners of the same μ are forbidden.[2]

Before comparing the eigenspace of **G** with the space of allowed coherences, the latter should be defined rigorously. For an Abelian $\mathcal{G}$, this resolves itself to a tautology: the space of allowed coherences is simply the space spanned by all superkets of the form given by (107) where the label v can be dropped as redundant (all d_{μ} terms are equal to 1 for Abelian $\mathcal{G}$). However, for non-Abelian groups the problem is more ambiguous, which was recognized only recently.[21] This is concerned with the presence of symmetry-degenerate (i.e. partner) coherences. Partner coherences can never be distinguished experimentally and, therefore, including them all in the space in question would be unreasonable. There remain two options:

(i) to represent each degenerate set $\{|\mu v r r'\rangle, v = 1, \ldots, d_{\mu}\}$ by only one coherence, say $|\mu 1 r r'\rangle$; or

(ii) to replace each set by a single coherence $|\mu r r'\rangle$ defined according to

$$|\mu r r'\rangle = d_{\mu}^{-1/2} \sum_{v=1}^{d_{\mu}} |\mu v r r'\rangle \tag{108}$$

The spaces defined according to (i) and (ii) have the same dimension, equal to the number of (in principle) distinguishable symmetry-allowed coherences, and both can be used exchangeably in the description of the stick structure of the NMR spectra. (Using variant (i), one must remember that the theoretical symmetry subspectra concerned with particular irreducible representations μ, μ', etc., are subject to intensity rescaling by the corresponding degeneracy factors d_{μ}, $d_{\mu'}$, etc.; in variant (ii) a proper scaling of the intensities is effected automatically.[21])

As shown in the paper already quoted,[21] the eigenspace of **G** is identical to the space of the allowed coherences defined according to (ii), (108). The proof of this is based on the observation that the totally symmetric superprojector of any permutation group $\mathcal{G}$ can be expressed as a sum of mutually orthogonal

"parentage superprojectors", $\mathbf{G}_\mu$, concerned with individual irreducible representations of $\mathcal{G}$,

$$\mathbf{G} = \sum_\mu \mathbf{G}_\mu \tag{109}$$

where

$$\mathbf{G}_\mu = d_\mu^{-1} \sum_{u,v=1}^{d_\mu} P_\mu^{uv} \otimes P_\mu^{uv*} \tag{110}$$

The set of all superkets $|\mu r r'\rangle$, (108), with fixed μ and variable r and r' constitutes a complete orthonormal basis in the eigenspace of $\mathbf{G}_\mu$,[21]

$$\mathbf{G}_\mu |\mu' r r'\rangle = \delta_{\mu\mu'} |\mu' r r'\rangle \tag{111}$$

Therefore, the union of such sets of all μ terms forms a complete orthonormal basis in the eigenspace of $\mathbf{G}$. Such bases are here referred to as "parentage bases". Parentage bases can also be derived directly in Liouville space. In such a direct procedure one exploits only the characters of the irreducible matrices involved and not the individual elements of the latter.[23] The use of parentage bases in individual primitive spaces is necessary if one wants to exploit the existing microscopic symmetry. This is described in the following two sections.

We now return to the problem of the simultaneous exploitation of rotational and permutation symmetry invariances of the equation of motion. It can be seen from (104) and (110) that not only $\mathbf{G}$ but also the individual parentage superprojectors of which it is composed commute with all the superoperators from the set $\mathcal{F}$ (96). It follows that a primitive parentage basis can be adapted to any set $\Phi \subset \mathcal{F}$ of rotational constants of motion and, vice versa, an eigenbasis of Φ can be a simultaneous eigenbasis of the parentage superprojectors involved. The corresponding basis subset in the eigenspace of $\mathbf{G}_\mu$ concerned with the set ϕ of rotational quantum numbers is written as

$$\{|\mu \phi j\rangle, j = 1, 2, \ldots, \bar{m}_{\phi\mu}\} \tag{112}$$

where

$$\bar{m}_{\phi\mu} = \mathrm{Tr}_\phi \mathbf{G}_\mu = \sum_{i=1}^{m_\phi} \langle \phi i | \mathbf{G}_\mu | \phi i \rangle. \tag{113}$$

When the Hilbert space vectors $|\mu 1 r)$ (105) are chosen as eigenvectors of F_z and, for heteronuclear systems, also of $F_z(\mathrm{A}), \ldots, F_z(\mathrm{X})$, then the parentage superkets $|\mu r r'\rangle$ defined according to (108) are automatically eigensuperkets of each such set $\Phi \subset \mathcal{F}$ which does not contain $\mathbf{F}^{\mathrm{D}2}$. In such an instance we have (cf. (97))

$$\Phi |\mu r r'\rangle = \phi(r, r') |\mu r r'\rangle \tag{114}$$

where the notation employed emphasizes the fact that the quantum numbers in the set ϕ are derived from the corresponding quantum numbers that characterize the kets $|\mu 1 r)$ and $|m 1 r')$. Hence we may write

$$|\mu r r'\rangle = |\mu\phi(r, r')j\rangle \tag{115}$$

where the label j is superfluous and is inserted only in order to maintain conformity with the notation in (112). The construction of such a parentage basis is straightforward and can easily be implemented on a computer.

We now discuss briefly the situation where the relevant set of rotational constants of motion includes $\mathbf{F}^{D2}$. The natural eigenbasis of the latter is composed of irreducible spherical tensor superkets $|kqi\rangle$ which obey

$$\mathbf{F}^{D2}|kqi\rangle = k(k+1)|kqi\rangle \tag{116a}$$

$$\mathbf{F}_z^{D}|kqi\rangle = q|kqi\rangle \tag{116b}$$

and the ranks, k, of which take on values $0, 1, \ldots, q_{max}$, where q_{max} is the largest eigenvalue of $\mathbf{F}_z^{D}$; the label i enumerates different (orthogonal) tensors of the same rank,

$$i = 1, 2, \ldots, n_k \tag{117}$$

The use of irreducible spherical-tensor bases can be advantageous in describing relaxation processes in the instances where $\mathbf{R}$ is invariant under R(3).[20,50,51] Unfortunately, for systems comprising more than 3–4 nuclei the derivation of a complete orthonormal set of irreducible spherical-tensor operators is a tedious (though routine) task. The problem becomes even more involved when these operators are to be adapted to the existing permutation symmetry. A series of papers has recently been published[52-54] where, using standard methods of angular momentum algebra, such bases were derived for several specific systems of (Abelian) permutation symmetries isomorphic with C_2 and D_2. However, the general considerations of the papers quoted[52-54] on permutation symmetry in Liouville space contain substantial errors.† In the present authors' opinion, in instances of relatively high permutation symmetry, an explicit knowledge of an analytical form of the corresponding

† In Refs. 52 and 53, the standard concept of symmetry species in Liouville space is confused with the notion which, following Refs. 21 and 22, is here termed "symmetry parentage". The expression for the trace of a permutation superoperator, (9) of Ref. 53, is incorrect. Equation (11) of Ref. 53 and (7) and (8) of Ref. 54 define the trace of a symmetry superprojector rather than the projector itself. The symmetry superprojectors for individual irreducible representation of a non-Abelian group should include all permutation superoperators representing the group rather than, as is done in (30)–(33) of Ref. 54, only a single representative permutation superoperator from each symmetry class.

symmetry-adapted irreducible spherical-tensor basis is essentially useless. This is because the pertinent expressions for the basis superkets would be too complicated to be employed effectively in the evaluation of analytical formulae for the supermatrix elements concerned. However, it would be desirable to write a computer procedure that is capable of deriving such a basis for any number of spins and any group $\mathcal{G}$. This would offer a means for the numerical evaluation of the required supermatrix elements. To our knowledge, such a procedure has not so far been published. Some rudiments of the pertinent algorithm are presented in Section 7.3. In particular, a way is described of counting the irreducible spherical-tensor superkets of a given parentage. Precisely, it is shown how to determine, for each $0 \leqslant k \leqslant q_{\max}$, the number of orthogonal tensor superkets $|\mu k q j\rangle$ which obey

$$\mathbf{G}_{\mu}|\mu k q j\rangle = |\mu k q j\rangle \tag{118}$$

where $j = 1, 2, \ldots, \bar{n}_{k\mu}$. The sum of the $\bar{n}_{k\mu}$ terms over all irreducible representations of $\mathcal{G}$ gives $\bar{n}_k$, the number of orthogonal irreducible spherical tensors of rank k that transform as the totally symmetric irreducible representation of $\mathcal{G}$. Even without an explicit knowledge of the symmetrized-tensor operators themselves, the knowledge of the numbers $\bar{n}_{k\mu}$ may often give some insight into the relaxation behaviour of the system under study. The calculation of $\bar{n}_k$ and $\bar{n}_{k\mu}$ (Section 7.3) exploits the quantities $\bar{m}_{\phi}$ and $\bar{m}_{\phi\mu}$ ((101) and (113)) which characterize an arbitrary parentage basis in Liouville space. The latter quantities can be determined according to a straightforward procedure which was employed elsewere[21-23] without a sufficient explanation. It seems instructive to describe the procedure here in some detail.

It is a fortunate circumstance that all the data which are necessary to determine the numbers $\bar{m}_{\phi}$ and $\bar{m}_{\phi\mu}$ can be derived from the (reducible) representation of $\mathcal{G}$ in Hilbert space and from the character table of $\mathcal{G}$. This is not immediately visible from the definitions of $\bar{m}_{\phi}$ and $\bar{m}_{\phi\mu}$ in (101) and (113). We exploit the fact that individual permutation superoperators $\mathbf{P}(g)$ entering $\mathbf{G}$, (50), can be expressed in terms of the corresponding permutation operators $P(g)$ that represent the elements $g \in \mathcal{G}$ in Hilbert space,

$$\mathbf{P}(g) = P(g) \otimes P(g)^{*} \tag{119}$$

Hence the trace of $\mathbf{G}$ can be written as a sum of products $\mathrm{Tr}\, P(g) \cdot \mathrm{Tr}\, P(g)^{*}$. When one is interested in the trace of $\mathbf{G}$ over a Liouville subspace concerned with a set ϕ of rotational quantum numbers, the traces of $P(g)$ are to be calculated over the corresponding Hilbert subspaces ψ, ψ', etc., the products of which fall into the required Liouville subspace. The trace of $\mathbf{G}$ over a subspace ϕ can finally be expressed as

$$\mathrm{Tr}_{\phi}\, \mathbf{G} = |\mathcal{G}|^{-1} \sum_{g \in \mathcal{G}} \left(\sum_{\psi\psi'} [\mathrm{Tr}_{\psi} P(g)]\, [\mathrm{Tr}_{\psi'} P(g)]^{*} \right) \tag{120}$$

The knowledge of the character table of $\mathscr{G}$ is required only when one wants to count the basis superkets of definite parentage μ (see (113)). The trace of the corresponding parentage superprojector, (110), is given by

$$\operatorname{Tr} \mathbf{G}_\mu = d_\mu^{-1} \sum_{v=1}^{d_\mu} (\operatorname{Tr} P_\mu^{vv}) (\operatorname{Tr} P_\mu^{vv})^* \tag{121}$$

which stems from the fact that the traces of P_μ^{uv} vanish for $u \neq v$. An indirect reference to individual elements $\mu(g)_{vv}$ (see (104)) of the irreducible matrices involved can be eliminated from (121) by noting that[2]

$$\operatorname{Tr} P_\mu^{vv} = d_\mu^{-1} \operatorname{Tr} \bar{P}_\mu \tag{122}$$

where

$$\bar{P}_\mu = d_\mu |\mathscr{G}|^{-1} \sum \chi(g)^* P(g) \tag{123}$$

is the projection operator based on the characters, $\chi(g)$, of the irreducible matrices concerned.[2] Equation (121) now becomes

$$\operatorname{Tr} \mathbf{G}_\mu = d_\mu^{-2} (\operatorname{Tr} \bar{P}_\mu) (\operatorname{Tr} \bar{P}_\mu^*) \tag{124}$$

By analogy with (120), the trace of $\mathbf{G}_\mu$ over a subspace ϕ, that is the quantity $\bar{m}_{\phi\mu}$, can be expressed as a sum of the products of the traces of $\bar{P}_\mu$ and $\bar{P}_\mu^*$ over the corresponding Hilbert subspaces ψ, ψ', etc.

The projection operator defined by (123) is merely a sum of the corresponding partner projectors, P_μ^{vv} (see (104)); this operator is frequently referred to in our further discussion.

6.2. Microscopic symmetry factoring—NMR relaxation

The property of the microscopic group $\mathscr{K}$ of being an invariant subgroup of the macroscopic group (see (94)) warrants that the correlation diagram of the irreducible representations of $\mathscr{K}$ and those of $\mathscr{G}$ decompose into a number of disconnected subdiagrams. The subsets of irreducible representations of $\mathscr{K}$ and $\mathscr{G}$ forming each such subdiagram are called "orbits" relative to $\mathscr{G}$ and "associate sets" relative to $\mathscr{K}$, respectively.[33] The orbits of $\mathscr{K}$ and the corresponding associate sets of $\mathscr{G}$ are here denoted by $\mathscr{O}_q$, $\mathscr{O}_{q'}, \ldots$ and $\mathscr{A}_q$, $\mathscr{A}_{q'}, \ldots$, respectively. The theory developed elsewhere[21,22] states that the relaxation superoperator can only connect those totally symmetric basis superkets whose parentages belong to the same associate set. Formally, for each constituent ϕ of the WBR equation we can write

$$\langle \mu \phi i | \mathbf{R} | \mu' \phi i' \rangle = 0 \tag{125}$$

unless μ and μ' belong to the same set $\mathscr{A}_q$. Although this does not lead to any further dimensionality reduction for the relevant Liouville subspace beyond

that already achieved by macroscopic symmetry factoring, it results in a further factorization of **R** into subblocks. The dynamic-shift superoperator, Δ (see Section 5), exhibits the same and the super-Hamiltonian, **L**, at least the same factorization, for

$$\langle \mu\phi i|\mathbf{L}|\mu'\phi i'\rangle = \delta_{\mu\mu'}\langle \mu\phi i|\mathbf{L}|\mu\phi i'\rangle \tag{126}$$

Therefore, for any constituent ϕ of the WBR equation, each of its "microscopic" subblocks defined by (125) develops in time independently of the others and can be treated separately.

It was once believed that a correct relaxation matrix would have only a single zero eigenvalue, one concerned with a unit superket $|E\rangle$, which would lead to the existence of only a single relaxation invariant, the trace of ρ which can be expressed as $\langle E|\rho\rangle$. In 1971, Pyper[19] predicted that strong correlations between the random interactions that are responsible for relaxation would cause a degeneracy of the eigenvalue zero thereby making the system "non-fully dissipative". Recent analyses[25,55] provide an interpretation of this observation in terms of microscopic symmetry invariance. Namely, when $\mathscr{K}$ is nontrivial then each of the symmetry projectors $\bar{P}_\kappa$ defined according to (123) for individual irreducible representations κ of $\mathscr{K}$ obeys[25]

$$\mathbf{R}|\bar{P}_\kappa\rangle = 0 \tag{127}$$

where

$$\sum_\kappa |\bar{P}_\kappa\rangle = |E\rangle \tag{128}$$

and

$$\langle \bar{P}_\kappa|\bar{P}_{\kappa'}\rangle = \delta_{\kappa\kappa'}\langle \bar{P}_\kappa|\bar{P}_\kappa\rangle \tag{129}$$

Under favourable circumstances, the existence of such a degeneracy could probably be detected experimentally. We discuss this problem further in Section 7.3.

For the relevant, totally symmetric part of **R**, **GR**, the set of orthogonal eigensuperkets concerned with eigenvalue zero of **GR** comprises as many elements as there are different orbits of $\mathscr{K}$ relative to $\mathscr{G}$. This stems from the fact that, as can easily be verified using (109), (110) and (123), for which κ belonging to a given orbit $\mathscr{O}_q$,

$$\mathbf{GR}|\bar{P}_\kappa\rangle = \mathbf{RG}|\bar{P}_\kappa\rangle = \mathbf{R}|E_q\rangle = 0 \tag{130}$$

where

$$|E_q\rangle = \sum_{\mu\in\mathscr{O}_q} |\bar{P}_\mu\rangle \tag{131}$$

where $\bar{P}_\mu$ denotes a symmetry projector of $\mathscr{G}$ defined according to (123). The superkets $|E_q\rangle$, which add up to $|E\rangle$, are also eigensuperkets of $\mathbf{L}$ and Δ concerned with the eigenvalue zero. It follows, therefore, from the above and from (130) that in systems exhibiting microscopic symmetry invariance the single relaxation invariant $\langle E|\rho\rangle$ partitions into as many independent invariants $\langle E_q|\rho\rangle$ as there are different orbits of $\mathscr{K}$ relative to $\mathscr{G}$. Each of these invariants is associated with the corresponding microscopic subblock of the constituent ϕ of the WBR equation which is concerned with the eigenvalue zero of $\mathbf{F}_z^{\mathrm{D}}$.

6.3. Microscopic symmetry factoring—spin exchange

The discussion presented below concerns the microscopic symmetry properties of the exchange superoperator which are different from those of the relaxation matrices entering the DNMR equation of motion. Therefore, the microscopic factoring of the DNMR equation is determined by the properties of the exchange superoperator only in those instances where the relaxation effects, independent of exchange, are unimportant. In practice, such situations occur frequently for systems of spin-$\frac{1}{2}$ nuclei where, except for the limiting cases of very fast and very slow exchange, the relaxation effects can sufficiently be accounted for by introducing the appropriate effective relaxation matrices. We do not formulate any specific requirements as to the form of the latter beyond the assumption that they do not violate the microscopic symmetry factoring resulting from the symmetry properties of the exchange superoperator. This does not seem to be a serious limitation for the practical validity of the theory exposed below.

The previous formulation[21] of microscopic factoring of the DNMR equation only indirectly invokes the skeleton-site description of exchange which, for reasons explained in Section 4.1, is used here in an explicit form. Moreover, it exploits the definition of microscopic symmetry which, as pointed out in Section 2.1, may in some instances be too narrow for the purposes of DNMR spectroscopy. This need not trouble us, however, since the previous theory also remains entirely valid in the present context provided that only fundamental concepts defined in the paper quoted[21] are recast appropriately. The necessary modifications presented below are reduced to a minimum by the use of a specific labelling of skeleton sites which is possible only for systems of isomeric species undergoing purely intramolecular exchange. Since it is only this type of system that concerns us in the context of microscopic symmetry invariance, such a policy does not imply any loss of generality.

Thus, the labelling of nuclei in the reference permutamers of individual

(isomeric) species $I,\ldots,N$ will in the remaining part of this section bear a double meaning and will also serve for the description of the skeleton sites for the species involved. Accordingly, for each species L the molecular group $\mathscr{G}_L$ defined by (37) can be identified with the purely permutational representation, $\tilde{\mathscr{D}}_L$, of the feasible group of the reference permutamer concerned,

$$\mathscr{G}_L \equiv \tilde{\mathscr{D}}_L \tag{132}$$

where $L = I,\ldots,N$. Similarly, the site-exchange schemes, (36), for all rearrangements operating in the system can be interpreted as the corresponding elements of $\tilde{\mathscr{S}}$, the purely permutational representation of the group $\mathscr{S}$, (1).

$$f_\alpha \equiv \tilde{s}_\alpha \tag{133}$$

where $\tilde{s}_\alpha \in \tilde{\mathscr{S}}$. Equation (133) is applicable to degenerate as well as non-degenerate rearrangements.

In the present work, the microscopic group $\mathscr{K}$ is defined as the common part of the purely permutational representations of the feasible groups of all permutamers spanning the exchange network,

$$\mathscr{K} = \bigcap_{L=I,\ldots,N} \bigcap_{l=1}^{n_L} \tilde{\mathscr{D}}_l \tag{134}$$

where $\tilde{\mathscr{D}}_l$ is the purely permutation counterpart of $\mathscr{D}_l$, the feasible group of the permutamer $\mathscr{D}_L s_l$ of species L (see (5)), and n_L is the number of permutamers of species L involved in the network. The latter quantity is defined by (2) where the group $\mathscr{S}$ is to be replaced by its subgroup $\mathscr{S}^{\text{all}}$ which is characterized in the comment following (1) as the group of allowed transformations. It is worthwhile mentioning that, in the considerations in the present chapter, the definition of microscopic symmetry group constitutes the only context where the permutamer count must be restricted to the group of allowed transformations. In the discussions in Sections 3 and 4, the groups $\mathscr{S}$ and $\mathscr{S}^{\text{all}}$ can be used interchangeably.

Augmenting the definition of $\mathscr{S}^{\text{all}}$ given in Section 3.1, we characterize more closely the relationship between $\mathscr{S}^{\text{all}}$ and the group $\mathscr{P}^{\text{av}}$ introduced in Section 2.1. Although $\mathscr{P}^{\text{av}}$ is always identical to $\tilde{\mathscr{S}}^{\text{all}}$ (the purely permutational representation of $\mathscr{S}^{\text{all}}$), it must be remembered that the parent group $\mathscr{S}^{\text{all}}$ can be related to $\mathscr{P}^{\text{av}}$ in two different ways, depending on the type of exchange mechanism operating. If for at least one of the species participating in the exchange there exists an energetically allowed path (which may consist of a sequence of several allowed elementary reactions) connecting a permutamer $\mathscr{D}_K s_k$ with its mirror image, $\mathscr{D}_K \bar{e} s_k$, then $\mathscr{S}^{\text{all}}$ is homomorphic (but not isomorphic) with $\mathscr{P}^{\text{av}}$ and can be expressed as $\mathscr{P}^{\text{av}} \cup \bar{e}\mathscr{P}^{\text{av}}$. Otherwise, $\mathscr{S}^{\text{all}}$ is isomorphic with $\mathscr{P}^{\text{av}}$. The two types of relationship between $\mathscr{S}^{\text{all}}$ and $\mathscr{P}^{\text{av}}$ are

illustrated in Figs 4 and 3, respectively. The above properties should be remembered when applying the theory of microscopic symmetry in practice.

The microscopic group defined by the version of (134) in which $\tilde{\mathscr{Q}}_l$ is replaced by $\mathscr{Q}_l$ was shown to be an invariant subgroup of $\mathscr{S}^{\text{all}}$.[21] It is easy to see that the microscopic group defined presently exhibits the same property with respect to $\tilde{\mathscr{S}}^{\text{all}} = \mathscr{P}^{\text{av}}$,

$$\tilde{s}\mathscr{K}\tilde{s}^{-1} = \mathscr{K} \tag{135}$$

for each $\tilde{s} \in \tilde{\mathscr{S}}^{\text{all}}$.

By virtue of the convention adopted above regarding the labelling of skeleton sites, we may consider the elements of $\mathscr{K}$ as operating also on the skeleton sites of individual species. Formally.

$$\mathscr{K} \equiv \mathscr{K}_I \equiv \cdots \equiv \mathscr{K}_N \tag{136}$$

and, therefore, $\mathscr{K}$ can be considered as a subgroup of the macroscopic group of each species L defined in terms of skeleton sites,

$$\mathscr{K} \equiv \mathscr{K}_L \subseteq \mathscr{G}_L \tag{137}$$

where $L = I, \ldots, N$. Thus, taking into account the fact that the groups $\tilde{\mathscr{Q}}_I, \ldots, \tilde{\mathscr{Q}}_N$ are subgroups of $\tilde{\mathscr{S}}^{\text{all}}$, then by means of (135) and (132) we can state that $\mathscr{K}$ is an invariant subgroup in each of the groups $\mathscr{G}_I, \ldots, \mathscr{G}_N$,

$$g_L^{-1}\mathscr{K}_L g_L = \mathscr{K}_L \equiv \mathscr{K} \tag{138}$$

where g_L denotes any element of $\mathscr{G}_L$ and $L = I, \ldots, N$. Similarly, by virtue of (135) and (133), for each (allowed) site-exchange scheme f_α that maps the skeleton sites in L onto those in M we have

$$f_\alpha^{-1}\mathscr{K}_L f_\alpha = \mathscr{K}_M \equiv \mathscr{K} \tag{139}$$

where $L, M \in \{I, \ldots, N\}$.

The properties described by (135), (138) and (139) warrant that the theory of microscopic symmetry developed previously[21] is entirely valid also for the present, modified definition of the microscopic symmetry group, (134). The essential results of that theory are presented below.

Because $\mathscr{K}$ is an invariant subgroup of $\tilde{\mathscr{S}}^{\text{all}}$, the irreducible representations of $\mathscr{K}$ can be classified into orbits relative to $\tilde{\mathscr{S}}^{\text{all}}$. These orbits are denoted by

$$\mathscr{O}_1, \mathscr{O}_2, \ldots, \mathscr{O}_Q, \tag{140}$$

where Q is the number of orbits. The use of the same symbols as in the case of relaxation should not lead to confusion. By virtue of (137), for each species $L = I, \ldots, N$ one can speak of correlations between irreducible representations

of $\mathscr{K}$ and those of $\mathscr{G}_L$. The set of irreducible representations of $\mathscr{G}_L$ that are correlated with those in orbit $\mathscr{O}_q$ are denoted by $\mathscr{A}_q^L$. By virtue of (138), for each species $L = I, \ldots, N$ the sets

$$\mathscr{A}_1^L, \mathscr{A}_2^L, \ldots, \mathscr{A}_Q^L \tag{141}$$

concerned with the corresponding orbits (140) are disjoint. (Since the group $\mathscr{G}_L$ can be regarded as a subgroup of $\tilde{\mathscr{P}}^{\text{all}}$, see (132), any orbit $\mathscr{O}_q$ comprises an entire number of orbits $\mathscr{O}_{k(q)}$ of $\mathscr{K}$ relative to $\mathscr{G}_L$; hence, the set $\mathscr{A}_q^L$ comprises the associate sets[31] of the orbits $\mathscr{O}_{k(q)}$.) The theory quoted[21] states that each constituent ϕ (that is, its totally symmetric part) of the DNMR equation can be factorized into independent microscopic subblocks which are in one-to-one correspondence with the orbits given by (140). The composite subspace carrying subblock q, one associated with $\mathscr{O}_q$, includes the primitive subspaces which are concerned, in the sense specified below, with the sets $\mathscr{A}_q^I, \ldots, \mathscr{A}_q^N$. For a given species L, the primitive subspace concerned with $\mathscr{A}_q^L$ is spanned by the basic subset of the form (see (112) and (113))

$$\{|\mu(L)\phi i\rangle, \quad i = 1, 2, \ldots, \bar{m}_{\phi\mu(L)}\}, \quad \mu(L) \in \mathscr{A}_q^L \tag{142}$$

where $\mu(L)$ enumerates the corresponding irreducible representations of $\mathscr{G}_L$ and $\bar{m}_{\phi\mu(L)}$ has the same meaning as in (113) but is specifically referred to the symmetry group of species L. The dimension of this primitive subspace is

$$\bar{m}_{\phi q}^L = \sum_{\mu(L) \in \mathscr{A}_q^L} \bar{m}_{\phi\mu(L)} \tag{143}$$

and hence the dimension of the composite subspace involved, $\bar{m}_{\phi q}^{\text{c}}$, can be expressed as

$$\bar{m}_{\phi q}^{\text{c}} = \bar{m}_{\phi q}^I + \cdots + \bar{m}_{\phi q}^N \tag{144}$$

In compact form, the microscopic factoring described above can be expressed in terms of the corresponding microscopic selection rule for supermatrix elements of the exchange superoperator, thus

$$\langle \mu(L)\phi i|_{\text{c}} \mathbf{X} |\mu(M)\phi i'\rangle_{\text{c}} = 0 \tag{145}$$

unless $\mu(L) \in \mathscr{A}_q^L$ and $\mu(M) \in \mathscr{A}_q^M$. In (145), the subscript c denotes that the primitive superkets are embedded in the composite space involved. Obviously the two remaining superoperators in the DNMR equation, the super-Hamiltonian $\mathbf{L}_{\text{c}}$ and the effective relaxation matrix $\mathbf{R}_{\text{c}}^{\text{eff}}$, undergo at least the same factorization.

In Section 7.2 we demonstrate with examples to what extent the approach presented in this section can simplify certain DNMR lineshape problems which at first glance appear intractable.

6.4. A survey of other methods of symmetry factoring

The previously used methods of tackling the problem of permutation symmetry factoring in DNMR spectroscopy, briefly commented upon in Section 1, will now be reviewed against the background of the theory exposed in Sections 6.1 and 6.3.

The earliest method, that proposed by Kleier and Binsch,[5] pertains to the formulation of the DNMR theory where individual permutamers are treated as distinct components. In the nomenclature of the present work, it can best be characterized as a method of full exploitation of any Abelian microscopic symmetry in the composite space of individual permutamers. In this space, the DNMR equation factorizes into independent blocks which are in one-to-one correspondence with individual irreducible representations of the pertinent (Abelian) microscopic group. For nondegenerate rearrangements with total microscopic invariance of (Abelian) symmetry, the method of Kleier and Binsch[5] provides a complete solution to the problem. Among the numerous examples of its practical realizations it is worth mentioning that this method is incorporated, as an option, in the DNMR5 program.[8,9] An exploitation of this option was crucial for a successful performance of the iterative least-squares analysis of the DNMR spectrum of *N,N'*-dinitroso-1,4-diazacyclohexane,[56] which is one of the cumbersome DNMR problems to have been tackled quantitatively so far.

The method of Meakin *et al.*,[10-12] some aspects of which were discussed in Section 5.4, is confined to degenerate systems, but involves the more suitable, compact version of the DNMR equation, which is formulated in terms of basic permutational sets, (72). Since this version is based in part on some *ad hoc* assumptions (see below), the authors considered it to be an approximate method when applied to systems of non-Abelian symmetry. However, in view of the theory described here, their objections prove unjustified: within the intended scope of its applicability, the method considered gives *exact* theoretical DNMR lineshapes. (In the present context, the problem discussed in Section 4.4 of a proper interpretation of the lifetimes τ_α is totally irrelevant.) It is instructive to consider this in some detail.

The approach discussed[10-12] relies upon a brute-force factoring of the DNMR equation of motion into two blocks of which only one is retained. The relevant block is spanned by superkets of the form

$$|\mu qq'\rangle' = |\mu q)(\mu q'| \tag{146}$$

where μ goes over the set of irreducible representations of $\mathscr{G}$ and the kets $|\mu p)$ are eigenkets, concerned with eigenvalue 1, of the symmetry projector $\bar{P}_\mu$, (123); the prime on the superket symbol is used to distinguish it from the quantity defined by (108). For individual μ terms, the superkets of (146) span

the eigenspaces of the mutually orthogonal superprojectors

$$\bar{\mathbf{G}}_\mu = \bar{P}_\mu \otimes \bar{P}_\mu^* \tag{147}$$

of which those concerned with the one-dimensional irreducible representations, ν, are merely the parentage superprojectors, (110),

$$\bar{\mathbf{G}}_\nu = \mathbf{G}_\nu \tag{148}$$

and those corresponding to multidimensional irreducible representations γ obey

$$\bar{\mathbf{G}}_\gamma \mathbf{G}_\gamma = \mathbf{G}_\gamma \bar{\mathbf{G}}_\gamma \tag{149}$$

where

$$\mathrm{Tr}\, \bar{\mathbf{G}}_\gamma > \mathrm{Tr}\, \mathbf{G}_\gamma \tag{150}$$

with $\mathbf{G}_\gamma$ denoting the appropriate parentage superprojector, (110), for a multidimensional irreducible representation. It can be seen from (148)–(150) that for any $\mathscr{G}$ the Liouville subspace spanned by the superkets $|\mu q q'>'$, (146), with μ spanning all irreducible representations of $\mathscr{G}$, is either identical with the eigenspace of the totally symmetric superprojector $\mathbf{G}$ (for Abelian $\mathscr{G}$) or contains the latter as a proper subspace (for non-Abelian $\mathscr{G}$).

As pointed out in Section 4.4, the version of the DNMR equation used in the papers quoted[10–12] reproduces correctly the property of macroscopic symmetry invariance. Therefore, the equation in question remains correct on projection onto any Liouville subspace that includes the entire eigenspace of $\mathbf{G}$. In particular, it remains correct on projection onto the subspace of concern to Meakin *et al.*[10–12] which is spanned by the eigenspaces of the superprojectors $\bar{\mathbf{G}}_\mu$. Therefore, the *ad hoc* approach of the latter authors is in fact fully justified theoretically. As far as the sole macroscopic factoring is concerned, this approach is exhaustive in the case of Abelian symmetry; for non-Abelian symmetries it still retains many redundant dimensions (this is clearly seen from (150), (147) and (124)). The latter are concerned with the symmetry-forbidden transitions that involve different partner kets of the same symmetry species.

The elements of the exchange superoperator that connect these with the remaining forbidden transitions are, in general, non-vanishing. These are the offending elements that are discarded when, according to the procedure discussed,[10,12] performing the brute-force factoring of the DNMR equation. The authors cited[10,12] worried needlessly about this as a possible source of error biasing the calculated DNMR lineshapes since, as we have shown above, the elements in question are totally irrelevant and can be neglected.

The method of Meakin *et al.*[10–12] was employed in a number of excellent studies on rearrangement mechanisms in various transition-metal complexes.

A comprehensive survey of the relevant papers has been published by Jesson and Muetterties.[57]

At the end of this brief review we present the method of Luz and Naor[13] who were the first to tackle the problem of non-Abelian symmetry for a specific class of intramolecular degenerate rearrangements. In our nomenclature, these rearrangements are referred to as ones having total microscopic symmetry conservation (see Fig. 2(a)), that is the degenerate rearrangements for which

$$\mathscr{K} = \mathscr{G} \tag{151}$$

and

$$\tilde{\mathscr{G}}^{\text{all}} = \mathscr{G} \cup f\mathscr{G} \tag{152}$$

where f is the site-exchange scheme which represents the (only) rearrangement operating in the system (as in Section 4.4, f can be treated as a permutation on the skeleton sites). The authors cited[13] were also the first to employ group correlation diagrams for the purposes of DNMR spectroscopy. For the specific class of rearrangements addressed in the paper quoted,[13] the coalescence scheme for the static symmetry subspectra stems directly from the correlation diagram between the irreducible representations of $\mathscr{G}$ and those of $\tilde{\mathscr{G}}^{\text{all}}$.

It was noticed that in most systems with total microscopic invariance that can be of interest from the point of view of DNMR spectroscopy each static subspectrum concerned with a multidimensional representation γ of $\mathscr{G}$ coalesces only with itself and, as such, it constitutes a separate DNMR subspectrum.[13] The method reviewed[13] relies upon a decomposition of the static (d_γ-fold degenerate) subspectrum into its partner sub-subspectra in such a way that each of the latter forms a separate DNMR partner sub-subspectrum and can be calculated independently. This is effected by an appropriate choice of the irreducible (unitary) matrices of γ. The latter problem is solved in three steps:

(i) starting from an arbitrary set of γ, one determines the representation of f in the carrier space adopted for γ (this is certainly possible if both $\mathscr{G}$ and $\tilde{\mathscr{G}}^{\text{all}}$ are isomorphic to point groups);
(ii) one finds the appropriate $d_\gamma \times d_\gamma$ unitary matrix w that brings the representation of f into diagonal form; and
(iii) the starting irreducible matrices of γ are similarly transformed with w and are then used as the new set of γ—this new set is here denoted by $\bar{\gamma}$.

The required partner subspectra are defined by means of the projection operators $P^{vv}_{\bar{\gamma}}$, (104), based on the transformed irreducible matrices $\bar{\gamma}(g)$, $\bar{\gamma}(g')$, etc., in the sense that the Hilbert-space basis used to describe the static

spectrum is composed of eigenkets of these projectors. The partner (static) sub-subspectra defined in this way are not mixed by exchange, which stems from the fact that[13]

$$[P^{vv}_{\tilde{\gamma}}, P(f)] = 0 \tag{153}$$

where $v = 1, 2, \ldots, d_\gamma (= d_{\tilde{\gamma}})$ and $P(f)$ is the Hilbert-space representation of f. It is sufficient to calculate only one of the corresponding DNMR partner sub-subspectra and then recalibrate it by multiplying its amplitude by d_γ.[13] The calculations are performed using the DNMR equation in which the exchange superoperator has the form

$$(2\tau)^{-1}[\mathbf{P}(f) + \mathbf{P}(f^{-1}) - 2\mathbf{E}] \tag{154}$$

For the systems of interest to Luz and Naor,[13] the approach of Jesson *et al.*[10,11] would yield the same form of exchange superoperator (cf. (72)). Therefore, our comment in Section 4.4 about the interpretation of the kinetic parameters in the latter approach pertains equally to the lifetime τ in (154).

For the specific class of systems for which it was designed, the method of Luz and Naor[13] provides an ultimate symmetry factoring of the DNMR problem and enables one to eliminate from calculations all redundant dimensions even for non-Abelian symmetries. Obviously, the general method,[21] when applied to such system, gives the same degree of symmetry factoring. Use of the latter method may be advantageous in instances where the transformed irreducible matrices defined under point (iii) above are complex while the starting matrices of γ can be chosen to be real. Then, in the approach of Luz and Naor,[13] one must use complex symmetry-adapted bases in Hilbert and Liouville space, while the corresponding bases in the general method[21] are real, which simplifies the computations.

The difference between these two approaches is best understood in terms of the two definitions of the space of allowed coherences presented under points (i) and (ii) in the discussion preceding (108). The method of Luz and Naor[13] makes use of the space defined under (i) while the general approach[21] exploits the isomorphic space described under (ii). It is worthwhile emphasizing that the two spaces, despite being isomorphic, have a completely different nature insofar as their connections to the underlying Hilbert space are concerned: the former is a direct product of certain Hilbert subspace and the dual space of the same or some other Hilbert subspace; and the latter has no such direct product structure since none of its conceivable basis sets is composed exclusively of shift operators.

The method of Luz and Naor was exploited in the calculation of the DNMR spectra for systems dissolved in oriented nematic solvents. One of the most spectacular examples of its application is the calculation of the DNMR spectrum of cyclooctatetraene undergoing valence tautomerism (or ring

inversion) in a nematic medium (eight tightly coupled protons, $\mathscr{K} = \mathscr{G} = D_{2d}$).[13,58] In a slightly modified version, it was also used in the derivation of an approximate DNMR equation of motion that is valid in the limit of fast exchange.[59] Using the approximate equation, the authors of the latter paper were able to calculate DNMR spectra for the process of ring inversion in the cyclohexane molecule (12 tightly coupled protons, $\mathscr{K} = \mathscr{G} = C_{3v}$)! This is probably the largest dynamic system that has been handled so far.

Recently, Gamliel *et al.*[60] presented a lineshape theory that describes multiquantum DNMR spectra measured in the time-proportional-phase-increment (TPPI) experiment. The theory applies to both isotropic and oriented liquid crystalline media. The method of symmetry factoring[13] described above exploited in the context of this theory enabled the latter authors to calculate theoretical multiquantum DNMR spectra for a variety of tightly coupled symmetric-spin consisting of up to eight spin-$\frac{1}{2}$ nuclei. These calculations reveal that the use of TPPI DNMR spectra may open new perspectives for studies on the dynamics and mechanisms of molecular rearrangements.

7. EXAMPLES

From selected examples of exchanging and relaxing systems, we demonstrate in this section to what extent the sizes of the spectral matrices involved can be reduced by a proper exploitation of the macroscopic and microscopic symmetry selection rules. In the context of spin relaxation, we also illustrate novel aspects, brought about by the notion of microscopic symmetry, in the description of the relaxation behaviour of a spin-$\frac{1}{2}$ nucleus scalar coupled to a group of rapidly relaxing quadrupolar nuclei. In the same context, a brief presentation is given of some problems concerning the symmetry adaptation of irreducible spherical-tensor bases in Liouville space.

7.1. Intermolecular exchange (macroscopic invariance only)

As has already been mentioned, in intermolecularly exchanging systems the only relevant feature is the macroscopic symmetry invariance. In this section, we present the macroscopic factoring of the spectral matrix for the system which was referred to in Sections 3.2 and 4.1 and whose two subsystems are depicted in Figs 6 and 7. The complete system includes the following five species:

$$L_4M,\ L_3L'M,\ L_2L'_2M,\ LL'_3M \quad \text{and} \quad L'_4M \tag{155}$$

the symmetries of which are isomorphic with $T_d, C_{3v}, C_{2v}, C_{3v}$ and T_d, respectively. In the following we assume that M is a non-magnetic nucleus and that each of the ligands L and L' contain only one magnetic nucleus of spin-$\frac{1}{2}$. In addition, the symbol M is omitted. We consider two cases: homonuclear and heteronuclear. The homonuclear case may depict the situation where two different tertiary phosphine ligands exchange intermolecularly around a tetrahedral, four-coordinate centre. The heteronuclear case represents, for example, intermolecular proton–triton exchanges in the ammonium cation which are monitored by ^{14}N decoupled DNMR spectra. In contrast to the standard studies on the isotopically pure system, the use of isotopically labelled compounds might give some insight into the exchange mechanism.

In the homonuclear case, for each of the exchanging species the relevant set of rotational constants of motion, (96), includes only the superoperator $\mathbf{F}_z^D$, while in the heteronuclear case for the species $L_3, L', L_2L'_2$ and LL'_3 the corresponding sets comprise two superoperators, $\mathbf{F}_z^D(L_n)$ and $\mathbf{F}_z^D(L'_{4-n})$, concerned with the homonuclear subsystems involved. In the latter case, experiments involving simultaneous radiofrequency stimulations of both homonuclear subsystems are excluded. With this proviso, the degeneracies of the eigenvalues of $\mathbf{F}_z^D(L_n)$ and $\mathbf{F}_z^D(L'_{4-n})$ measure the dimensions of the corresponding (primitive) quantum domains as do the degeneracies of the eigenvalues of $\mathbf{F}_z^D$ in a homonuclear system.

In order to calculate the dimensions of the relevant blocks of the DNMR equation, it is sufficient to know only the traces of individual symmetry operators from the groups T_d, C_{3v} and C_{2v} over the appropriate Hilbert subspaces. The required data are displayed in Tables 2 and 3.

For the homonuclear case, the dimensions of the primitive Liouville subspaces concerned with individual eigenvalues of the pertinent superoperator $\mathbf{F}_z^D$ (that is, the dimensions of the corresponding quantum domains) and the respective numbers of symmetry-allowed coherences are given in Table 4. The data listed in Table 4 were calculated from the corresponding data in Table 2 using (120). For example, the number of allowed coherences in the two-quantum domain for the species L_3L' (and LL'_3) is calculated as follows. The two-quantum domain involves three pairs of eigenvalues of F_z (three pairs of Hilbert subspaces): $(2, 0), (1, -1)$ and $(0, -2)$. For the pair $(1, -1)$, the traces of the representative symmetry operators from individual symmetry classes of the pertinent group, C_{3v}, are displayed in row 2 of Table 2. The contribution from this pair is given by

$$\tfrac{1}{6}[1\cdot(4\cdot4) + 2\cdot(1\cdot1) + 3\cdot(2\cdot2)] = 5$$

where the multipiliers weighting the trace products in parentheses are the numbers of operations in the symmetry classes involved. The two remaining pairs, $(2, 0)$ and $(0, -2)$, give identical contributions which are calculated in the

Table 2. Traces of symmetry operators in Hilbert subspaces for homonuclear spin-$\frac{1}{2}$ systems $L_nL'_{4-n}$.

	$T_d(L_4, L'_4)$					$C_{3v}(L_3L', LL'_3)$			$C_{2v}(L_2L'_2)$			
F_z	e	$8C_3$	$3C_2$	$6S_4$	$6\sigma_d$	e	$2C_3$	$3\sigma_v$	e	C_2	σ_v	σ'_v
± 2	1	1	1	1	1	1	1	1	1	1	1	1
± 1	4	1	0	0	2	4	1	2	4	0	2	2
0	6	0	2	0	2	6	0	2	6	2	2	2

Table 3. Traces of symmetry operators in Hilbert subspaces for heteronuclear spin-$\frac{1}{2}$ systems $L_nL'_{4-n}$.

			$C_{3v}(L_3L', LL'_3)$			$C_{2v}(L_2L'_2)$			
n	$F_z(L_n)$	$F_z(L'_{4-n})$	e	$2C_3$	$3\sigma_v$	e	C_2	σ_v	σ'_v
3	$\pm 3/2$	$\pm 1/2$	1	1	1	—	—	—	—
	$\pm 1/2$	$\pm 1/2$	3	0	1	—	—	—	—
2	± 1	± 1	—	—	—	1	1	1	1
	0	± 1	—	—	—	2	0	0	2
	± 1	0	—	—	—	2	0	2	0
	0	0	—	—	—	4	0	0	0
1	$\pm 1/2$	$\pm 3/2$	1	1	1	—	—	—	—
	$\pm 1/2$	$\pm 1/2$	3	0	1	—	—	—	—

Table 4. Macroscopic symmetry factoring of the DNMR equation for the homonuclear system described in the text.

Quantum domain	No. of coherences	No. of allowed coherences			Total No. of coherences	Total No. of allowed coherences
		(L_3L', LL'_3)	$L_2L'_2$	(L_4, L'_4)		
± 4	1	1	1	1	5	5
± 3	8	4	4	2	40	16
± 2	28	9	12	4	140	38
± 1	56	16	20	6	280	64
0	70	20	26	9	350	84

Table 5. Macroscopic symmetry factoring of the DNMR equation for the heteronuclear system described in the text (stimulated homonuclear subsystem of L nuclei).

Quantum domain	No. of coherences (No. of allowed coherences)				Total no. of coherences	Total no. of allowed coherences
	L_4	L_3L'	$L_2L'_2$	LL'_3		
± 4	1(1)	—	—	—	1	1
± 3	8(2)	2(2)	—	—	10	4
± 2	28(4)	12(4)	6(4)	—	46	12
± 1	56(6)	30(8)	24(8)	20(6)	130	28
0	70(9)	40(12)	36(16)	40(12)	186	49

same way, but using the data from rows 1 and 3 of Table 2, thus

$$\tfrac{1}{6}[1\cdot(1\cdot 6)+2\cdot(1\cdot 0)+3\cdot(1\cdot 2)]=2$$

Therefore, the required number is $5+2+2=9$. The dimensions of the composite constituent blocks of the DNMR equation, without and with the macroscopic factoring, are given in the two last columns of Table 4. By comparing the figures in these columns it becomes apparent to what extent a proper exploitation of permutation symmetry can bring the block size down and, thereby, to what extent it can facilitate lineshape computations.

For the heteronuclear system, the corresponding characteristics of the DNMR equation are listed in Table 5. The data involve experiments in which only one of the two homonuclear subsystems is stimulated, i.e. that composed of nuclei of type L. Owing to a mutual structural correspondence between both subsystems, on a trivial reinterpretation of the column headings, the data of Table 5 become valid for the analogous experiments involving the subsystem of L' nuclei. As for Table 4, the data in Table 5 were calculated using (120), but with the appropriate data from Table 3. For instance, the size of the primitive block of the allowed two-quantum coherences for L_3L', 4, is given as a sum of four terms (a, b, c, and d), each of which is concerned with an appropriate pair (m, m') of eigenvalues of $F_z(L_3)$ such that $m'-m=2$ and with a pair (m'', m'') of identical eigenvalues of $F_z(L')$, where $m'\in\{\frac{3}{2},\frac{1}{2}\}$, and $m''\in\{\frac{1}{2},-\frac{1}{2}\}$. For this particular item it happens that

$$a=b=c=d=\tfrac{1}{6}[1\cdot(1\cdot 3)+2\cdot(1\cdot 0)+3\cdot(1\cdot 1)]=1$$

It should be emphasized that in the above-described procedure for counting the symmetry-allowed coherences the irreducible matrices of the symmetry groups involved are never invoked. Neither these matrices themselves nor their elements are required to construct the appropriate macroscopic-

symmetry-adapted Liouville bases; the pertinent algorithm that can easily be implemented on a computer has been described elsewhere.[23]

Finally, we should mention that the systems considered above are systems with magnetic equivalence broken by exchange. Therefore, it is not unjustified to ask about a possible spectroscopic manifestation of the scalar spin–spin couplings between the equivalent nuclei. Such couplings could be relevant if the nuclear spins in the exchanging ligands are greater than $\frac{1}{2}$. For the spin-$\frac{1}{2}$ nuclei considered here, the symmetry argument presented elsewhere[24] and reproduced briefly in Section 4.5 applies to each of the exchanging species. For each exchanging species, an interchange of any two equivalent skeleton sites is a valid symmetry operation on the molecule concerned and, accordingly, the corresponding coupling term does not enter the DNMR equation.

7.2. Intramolecular exchange (macroscopic plus microscopic invariance)

We consider two exchanging systems which can be of immediate practical interest:

(i) the intramolecular exchange of tertiary phosphine ligands, L, in the dodecahedral complexes (D_{2d} symmetry) of tetrahydrides of molybdenum and tungsten, H_4ML_4; and
(ii) the interconversion between the *cis* (C_{2v}) and *trans* (D_{4h}) forms of dihydrotetrakis(diethoxyphenylphosphine)ruthenium(II), *cis*-H_2RhL_4 and *trans*-H_2RhL_4.

The experimental DNMR spectra for the systems (i) and (ii) were reported by Meakin *et al.*[31,32] in 1973. The corresponding DNMR lineshape calculations were not undertaken at that time because of an insufficient advance in the symmetry theory of DNMR. The hypothetical exchange mechanisms postulated[31,32] by analogy with related systems are shown in Figs 3 and 4. Below we demonstrate that the use of the theoretical apparatus presently available can bring the computational aspects of these lineshape problems to a routine level. First we consider system (ii).

7.2.1. *Dihydrotetrakis(diethoxyphenylphosphine)ruthenium(II)*

As mentioned in the legend to Fig. 3, this is a system with partial microscopic invariance where the microscopic group, $\mathscr{K} \sim C_2$, is a degree-8 (invariant) subgroup of the molecular symmetry group of the *trans* isomer, $\mathscr{G}_T \sim D_{4h}$, and a halving subgroup of the molecular group of the *cis* isomer, $\mathscr{G}_c \sim C_{2v}$. The purely permutational representation, $\tilde{\mathscr{P}}^{all}$, of the group of allowed transform-

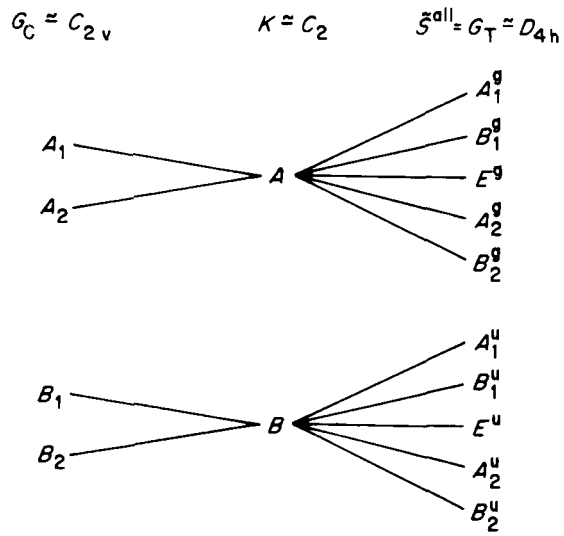

Fig. 8.

ations is identical to the molecular group of the *trans* isomer, which can be seen immediately from inspection of Fig. 4. (The group $\mathcal{S}^{all}$ is here homomorphic with $\tilde{\mathcal{S}}^{all}$; that is, $\mathcal{S}^{all} = \tilde{\mathcal{S}}^{all} \cup \bar{e}\tilde{\mathcal{S}}^{all}$; see Section 6.3.) The relevant correlation diagrams (see Section 6.3) are displayed in Fig. 8.

As in any system with a two-element microscopic group, in the case considered each of the two irreducible representations of $\mathcal{K}$ itself constitutes an orbit relative to $\tilde{\mathcal{S}}^{all}$,

$$\mathcal{O}_1 = \{A\} \text{ and } \mathcal{O}_2 = \{B\} \tag{156}$$

Accordingly, each constituent block of the DNMR equation can be decomposed into two independent subblocks. The sets of parentage labels, (141), which correspond to the orbits in (156) and describe the coalescence scheme for the static symmetry subspectra can be determined directly from the correlation diagram (Fig. 8), namely

$$\begin{aligned} \mathcal{A}_1^C &= \{A_1, A_2\}, \quad \mathcal{A}_1^T = \{A_1^g, B_1^g, E^g, A_2^g, B_2^g\} \\ \mathcal{A}_2^C &= \{B_1, B_2\}, \quad \mathcal{A}_2^T = \{A_1^u, B_1^u, E^u, A_2^u, B_2^u\} \end{aligned} \tag{157}$$

where the superscripts C and T denote the *cis* and *trans* isomers, respectively.

Unlike in intermolecular exchange, in intramolecular exchange the set of good quantum numbers concerned with exchange-invariant rotational symmetry includes not only the eigenvalues of $\mathbf{F}_z^D$ but also those of its two mutually commuting components, $\mathbf{F}_z^L$ and $\mathbf{F}_z^R$.[5] (Note in passing that, by analogy with permutation symmetry, the invariance of the DNMR equation

under $\mathbf{F}_z^{\mathrm{D}}$ can be regarded as a macroscopic rotational invariance while the invariances under $\mathbf{F}_z^{\mathrm{L}}$ and $\mathbf{F}_z^{\mathrm{R}}$ are in fact microscopic invariances since they can be traced back to the corresponding conservative properties that pertain to each individual spin system subject to any sequence of intramolecular exchange events.) In heteronuclear systems, the corresponding left- and right-translation superoperators for individual homonuclear subsystems provide an additional set of good quantum numbers. (As in the preceding subsection, we do not consider Hartmann–Hahn-type experiments on heteronuclear systems). Therefore, in the case considered individual constituents of the DNMR equation of motion can be enumerated with sets of simultaneous eigenvalues, ϕ, of the following set of mutually commuting superoperators

$$\Phi = \{\mathbf{F}_z^{\mathrm{L}}(\mathrm{H}_2), \mathbf{F}_z^{\mathrm{L}}(L_4), \mathbf{F}_z^{\mathrm{R}}(\mathrm{H}_2), \mathbf{F}_z^{\mathrm{R}}(L_4)\} \tag{158}$$

In order to count the parentage superkets that span the relevant subspaces of allowed coherences for each such constituent, one has first to classify the simultaneous eigenbases of $F_z(\mathrm{H}_2)$ and $F(L_4)$ in the Hilbert spaces of *cis*-$\mathrm{H}_2\mathrm{Ru}L_4$ and *trans*-$\mathrm{H}_2\mathrm{Ru}L_4$ into the symmetry species of the corresponding molecular groups. This is displayed in Table 6. The required characteristics of the parentage bases involved are presented in Table 7. For the sake of compactness, only the constituents comprising single-quantum coherences are accounted for. Heteronuclear combination coherences are excluded. The items in Table 7 were calculated from the data of Table 6 using (124) where the traces of $\bar{P}_\mu$, (123), were calculated over the appropriate Hilbert subspaces. For instance, the number of basic superkets of parentage E^{g} in the primitive subspace $\phi = \{0, -1, 0, 0\}$ (see (158)) of the *trans* isomer is given as a product of the corresponding items from rows 5 and 6 of Table 6 divided by the square of the dimension of E^{g} (see footnote to Table 6),

$$1 = 2 - 2/2^2$$

Without permutation symmetry factoring, in calculating single-quantum DNMR spectra for the system considered, the largest spectral matrix to be handled would have a dimension of 192×192. The macroscopic factoring alone, independent of the type of exchange mechanisms operating, would bring the matrix size down to 36×36. For the specific mechanism considered here, the microscopic invariance affords further factorization of this matrix into two blocks, each with dimensions of 18×18.

Since the irreducible matrices of the molecular groups in question are readily available, the parentage bases involved can be derived according to the procedure described in (105), (106), and (108).

It should be added that the system discussed above constitutes another example of a system with magnetic-equivalence breaking. In the *trans* isomer, the spin–spin couplings between the (magnetically equivalent!) phosphorous nuclei situated *cis* to each other cannot, in principle, be ignored in DNMR

Table 6. Classification of simultaneous eigenkets of $F_z(H_2)$ and $F_z(L_4)$ into symmetry species of C_{2v} and D_{4d} groups.

$F_z(H_2)$	$F_z(L_4)$	Degeneracy	C_{2v} (*cis*-H_2RuL_4)	D_{4h} (*trans*-H_2RuL_4)[a]
± 1	± 2	1	$1A_1$	$1A_1^g$
± 1	± 1	4	$2A_1 + 1B_1 + 1B_2$	$1A_1^g + 1B_1^g + 2E^u$
± 1	0	6	$3A_1 + 1A_2 + 1B_1 + 1B_2$	$2A_1^g + 1B_1^g + 1B_2^g + 2E^u$
0	± 2	2	$1A_1 + 1B_2$	$1A_1^g + 1A_2^u$
0	± 1	8	$3A_1 + 1A_2 + 1B_1 + 3B_2$	$1A_1^g + 1B_1^g + 2E^g + 1B_2^u + 2E^u$
0	0	12	$4A_1 + 2A_2 + 2B_1 + 4B_2$	$2A_1^g + 1B_1^g + 1B_2^g + 2E^g + 2A_1^u + 1B_1^u + 1B_2^u + 2E^u$

[a] For a degenerate irreducible representation γ, the symbol n_γ denotes all vectors of species γ, that is, n is equal to the trace of $\bar{P}_\gamma$ (123), over the corresponding Hilbert subspace.

Table 7. Macroscopic and microscopic symmetry factoring for single-quantum constituents of the DNMR equation for the system shown in Fig. 4.

ϕ^a	No. of coherences *cis* + *trans*	No. of allowed coherences *cis* + *trans*	Microscopic factoring[b]					
			$\mathscr{A}_1^C$	$\mathscr{A}_1^T$	Total	$\mathscr{A}_2^C$	$\mathscr{A}_2^T$	Total
$\pm1\ -2\ \pm1\ -1$ $\pm1\ \ 1\ \pm1\ \ 2$	4 + 4	2 + 1	$2A_1$	$1A_1^g$	3	—	—	0
$\pm1\ -1\ \pm1\ \ 0$ $\pm1\ \ 0\ \pm1\ \ 1$	24 + 24	8 + 4	$6A_1$	$2A_1^g + 1B_1^g$	9	$1B_1 + 1B_2$	$1E^u$	3
$0\ -2\ \ 0\ -1$ $0\ \ 1\ \ 0\ \ 2$	16 + 16	6 + 2	$3A_1$	$1A_1^g$	4	$3B_2$	$1A_2^u$	4
$0\ -1\ \ 0\ \ 0$ $0\ \ 0\ \ 0\ \ 1$	96 + 96	28 + 8	$12A_1 + 2A_2$	$2A_1^g + 1B_1^g + 1E^g$	18	$2B_1 + 12B_2$	$2A_2^u + 1B_2^u + 1E^u$	18
$-1\ \pm2\ \ 0\ \pm2$ $0\ \pm2\ \ 1\ \pm2$	2 + 2	1 + 1	$1A_1$	$1A_1^g$	2	—	—	0
$-1\ \pm1\ \ 0\ \pm1$ $0\ \pm1\ \ 1\ \pm1$	32 + 32	10 + 3	$6A_1$	$1A_1^g + 1B_1^g$	8	$1B_1 + 3B_2$	$1E^u$	5
$-1\ \ 0\ \ 0\ \ 0$ $0\ \ 0\ \ 1\ \ 0$	72 + 72	20 + 7	$12A_1 + 2A_2$	$4A_1^g + 1B_1^g + 1B_2^g$	20	$2B_1 + 4B_2$	$1E^u$	7

[a]See (158); [b]See (157).

lineshape calculations (cf. discussion in Section 4.5). However, the remaining couplings between equivalent nuclei are irrelevant, which stems from the theorem already quoted.[24]

7.2.2. *Complexes of tetrahydrides of tungsten and molybdenum*

For the degenerate rearrangement depicted in Fig. 3, the microscopic group $\mathscr{K}$ is identical to the S_4 subgroup of the molecular group $\mathscr{G} \sim D_{2d}$. The pertinent groups $\mathscr{S}^{all}$ and $\tilde{\mathscr{S}}^{all}$, which are mutually isomorphic in this case both being of order 32, are not isomorphic with any point group. Therefore, the determination of the required orbits of $\mathscr{K}$ is not immediate since the irreducible representations of $\tilde{\mathscr{S}}^{all}$ are not known. Fortunately, this problem can be circumvented.[21] The group $\mathscr{S}^{all}$ can be expressed as a set-theoretical union of four right cosets which represent the four permutamers spanning the exchange network,

$$\mathscr{S}^{all} = \mathscr{Q}e \cup \mathscr{Q}p \cup \mathscr{Q}p^2 \cup \mathscr{Q}p^3 \tag{159}$$

where $p = (5768)$ and $\mathscr{Q} \sim D_{4h}$ is the permutation-inversion group of the reference molecule which is distinguished in Fig. 3 by the use of the complete ligand symbols. The orbits of $\mathscr{K}$ relative to $\tilde{\mathscr{S}}^{all} \sim \mathscr{S}^{all}$ can be derived from correlation diagrams of $\mathscr{K}$ and $\tilde{\mathscr{Q}} \equiv \mathscr{G}$, and of $\mathscr{K}$ and the semidirect product group $\mathscr{K} \wedge \{e, p, p^2, p^3\}$.[21] The determination of the latter is an easy task. The required orbits of $\mathscr{K}$ and the corresponding associate sets of $\mathscr{G}$ are listed below.

$$\begin{aligned} &\mathscr{O}_1 = \{A\}, \qquad \mathscr{O}_2 = \{B\}, \qquad \mathscr{O}_3 = \{E^a, E^b\} \\ &\mathscr{A}_1 = \{A_1, B_1\}, \quad \mathscr{A}_2 = \{B_1, B_2\}, \quad \mathscr{A}_3 = \{E\} \end{aligned} \tag{160}$$

The characteristics of the symmetry-adapted parentage bases for the constituents concerned with the set of mutually commuting superoperators

$$\Phi = \{\mathbf{F}_z^L(H_4), \mathbf{F}_z^L(L_4), \mathbf{F}_z^R(H_4), \mathbf{F}_z^R(L_4)\} \tag{161}$$

are presented in Table 8. Only single-quantum coherences are accounted for. The data displayed in Table 8 were derived in an analogous way to those of Table 7. Inspection of these data reveals that, as far as computational aspects are concerned, by a proper exploitation of the existing symmetry invariances this forbidding-looking DNMR problem can be resolved into a routine task: the largest block to be handled is only of dimension 48×48.

7.3. Selected symmetry problems in NMR relaxation

Except for some specific classes of relaxing systems and specific types of experiments which require a separate discussion, in the general context of

Table 8. Macroscopic and microscopic symmetry factoring for single-quantum constituents of the DNMR equation for the system shown in Fig. 3.

ϕ^a	No. of coherences	No. of allowed coherences	Microscopic factoring[b]					
			$\mathscr{A}_1$	Total	$\mathscr{A}_2$	Total	$\mathscr{A}_3$	Total
$2\pm2 \quad 1\pm2$ $-1\pm2 \quad -2\pm2$	4	1	$1A_1$	1	—	0	—	0
$1\pm2 \quad 0\pm2$ $0\pm2 \quad -1\pm2$	24	4	$2A_1$	2	$1B_2$	1	1E	1
$2\pm1 \quad 1\pm1$ $-1\pm1 \quad -2\pm1$	64	10	$3A_1$	3	$3B_2$	3	4E	4
$1\pm1 \quad 0\pm1$ $0\pm1 \quad -1\pm1$	384	52	$12A_1 + 2A_2$	14	$2B_1 + 12B_2$	14	24E	24
$2 \quad 0 \quad 1 \quad 0$ $-1 \quad 0 \quad -2 \quad 0$	144	20	$8A_1$	8	$2B_1 + 4B_2$	6	6E	6
$1 \quad 0 \quad 0 \quad 0$ $0 \quad 0 \quad -1 \quad 0$	864	112	$28A_1 + 6A_2$	34	$10B_1 + 20B_2$	30	48E	48

[a]See (161).
[b]See (160).

NMR relaxation, the issue of permutation symmetry does not create any new problems beyond those which have already been illustrated in the previous sections in the context of exchange. As in intermolecular exchange, in relaxation the basic rotational invariants of the WBR equation that can be combined with permutation symmetry are $\mathbf{F}_z^{\mathrm{D}}$ and, for heteronuclear systems, the appropriate homonuclear superoperators $\mathbf{F}_z^{\mathrm{D}}(\mathrm{A}), \ldots, \mathbf{F}_z^{\mathrm{D}}(\mathrm{X})$. The situation is even simpler here since one is dealing only with a primitive Liouville space. The general aspects of permutation symmetry in NMR relaxation do not therefore require any further comment and we can focus on the specific problems stated at the beginning of the present section.

7.3.1. Microscopic symmetry and scalar relaxation of the second kind

As we have already mentioned, in the context of this specific kind of relaxation the concept of microscopic symmetry enables one to systematize the ideas once exposed by Pyper[19,20] and to derive, for certain systems of practical interest, simple analytical expressions for the scalar relaxation rates. A detailed discussion of this issue has been presented elsewhere.[25,55] Here we only illustrate the essential points using an example.

We consider two strictly related systems, each composed of four equivalent, rapidly relaxing quadrupolar nuclei that are scalar coupled to a single spin-$\frac{1}{2}$ nucleus, and differing only in the symmetries of the molecules involved which we assume to be $\mathrm{T_d}$ and $\mathrm{D_{4h}}$. In the system of $\mathrm{T_d}$ symmetry, no permutation symmetry other than trivial is microscopically conserved. It follows that[55] the scalar relaxation rate for the spin-$\frac{1}{2}$ nucleus can be expressed as a sum of the contributions from the individual quadrupolar nuclei,

$$(T_2^{\mathrm{sc}})^{-1} = 4[\tfrac{4}{3}\pi^2 \bar{J}^2 I(I+1)T_1] \tag{162}$$

where T_1 is the longitudinal relaxation time of each of the quadrupolar nuclei (extreme narrowing regime assumed) and $\bar{J}$ (in Hz) is the coupling constant between the latter and the spin-$\frac{1}{2}$ nucleus; the expression in square brackets describes the contribution from a single quadrupolar nucleus.

For the system of $\mathrm{D_{4h}}$ symmetry, the additivity rule is no longer valid and, moreover, the predicted scalar relaxation behaviour is multiexponential in character.[25] This is a consequence of the fact that for the latter system the microscopic symmetry is nontrivial; the corresponding microscopic group $\mathscr{K} \sim \mathrm{C_{1v}}$ is given on p. 220. The above implication is not totally obvious and is considered below in some detail.

The macroscopic group of the nuclear system involved is the $\mathrm{C_{4v}}$ subgroup of $\mathrm{D_{4h}}$, the molecular point group. The orbits of $\mathscr{K} \sim \mathrm{C_{2v}}$ relative to $\mathrm{C_{4v}}$ and the associate sets of $\mathrm{C_{4v}}$ are listed below (see Section 6.2).

$$\begin{aligned} \mathscr{O}_1 &= \{A_1\}, & \mathscr{O}_2 &= \{A_2\}, & \mathscr{O}_3 &= \{B_1, B_2\} \\ \mathscr{A}_1 &= \{A_1', B_1'\}, & \mathscr{A}_2 &= \{A_2', B_2'\}, & \mathscr{A}_3 &= \{E\}, \end{aligned} \tag{163}$$

where the primes are used to distinguish between the irreducible representations of C_{4v} and those of C_{2v}. Accordingly, the totally symmetric block of the WBR equation undergoes factorization into three independent microscopic subblocks. In the regime of rapid quadrupolar relaxation, which is of interest to us here, the standard scalar relaxation theory[19,25] can be applied to each of those blocks which succeeds in the derivation of three independent Bloch-type equations describing three (uncoupled) scalar relaxation modes for the spin-$\frac{1}{2}$ nucleus involved.[25] The corresponding scalar relaxation rates are

$$(T_{2(k)}^{sc})^{-1} = (T_2^{sc})^{-1} c_k w_k^{-1} \tag{164}$$

where $(T_2^{sc})^{-1}$ is given by (162), and $k = 1, 2$ and 3 enumerates the orbits (163); the quantities c_k and p_k are given by

$$c_k = \langle F_z(X) | F_z(X) \rangle^{-1} \sum_{\mu \in \mathscr{A}_k} \langle F_z(X) | \mathbf{G}_\mu | F_z(X) \rangle \tag{165}$$

$$w_k = \langle E(X) | E(X) \rangle^{-1} \sum_{\mu \in \mathscr{A}_k} \langle \bar{P}_\mu | \bar{P}_\mu \rangle \tag{166}$$

In (165) and (166), X denotes the set of quadrupolar nuclei, $E(X)$ is the unit operator in the space X, $\mathbf{G}_\mu$ is the parentage superoperator (110), and $\bar{P}_\mu$ is defined by (123). In the standard spin-echo or rotating-frame scalar relaxation measurements performed on a sample which is initially in a state of thermal equilibrium, each of the three above-defined relaxation modes is weighted by the corresponding coefficient w_k, (166).[25] The relative magnitudes of the relaxation rates (164) and of the respective weighting factors are dependent on the spin number of the quadrupolar nuclei. For $I = 1$, the corresponding ratios of these quantities are

$$(T_{2(1)}^{sc})^{-1} : (T_{2(2)}^{sc})^{-1} : (T_{2(3)}^{sc})^{-1} = 10:4:7 \tag{167}$$

$$w_1 : w_2 : w_3 = 4:1:4 \tag{168}$$

For an appropriately chosen model compound, the occurrence of such widely diverse relaxation modes could probably be detected experimentally.

Equation (164)–(166) and, in fact, their appropriate analogues, can be used to describe the modes of scalar relaxation in any system AX_n exhibiting nontrivial microscopic symmetry. In particular, they are valid for the systems AX_2 of C_i symmetry ($\mathscr{K} \sim C_i$, two modes of scalar relaxation) and for the ones AX_6 of O_h symmetry ($\mathscr{K} \sim D_{2h}$, four modes of scalar relaxation). The power of the method presented above becomes apparent when one takes into account

that the relevant expressions for the scalar relaxation rates as well as for the weighting factors can be derived in an analytical form even for spin systems that are as highly complicated as AX_6.

7.3.2. *Dipolar relaxation in isochronous systems: use of symmetrized irreducible spherical bases*

This class of relaxing systems is especially interesting in the context of longitudinal relaxation measurements using the inversion-recovery or saturation-recovery techniques. As far as permutation symmetry is concerned, systems of this type can be treated using the general method, as was mentioned at the beginning of the present Section 7.3. However, the general approach is insufficient when the relaxation matrix exhibits full rotational invariance under R(3). The latter property is manifested in any molecular system, not necessarily isochronous, reorienting so rapidly that the extreme narrowing condition, $1/\tau_c \gg \omega_0$, is fulfilled and where, moreover, the relaxation mechanisms involving CSA interactions can be neglected.

As far as an isochronous system is concerned, even under these specific conditions its relaxation behaviour remains nontrivial when the principal relaxation mechanisms include DD and/or ICA interactions.[18] (Since the ICA interactions are merely of theoretical interest, such nontrivial relaxation behaviour can be expected to occur only in spin-$\frac{1}{2}$ systems in which the DD interactions usually dominate.) This is just the context where the use of irreducible spherical bases reveals the full power of the approach: for an isochronous system, not only the relaxation matrix but also the spin super-Hamiltonian can be factorized into independent constituents that are irreducible under R(3). The latter are concerned with pairs of eigenvalues of the mutually commuting superoperators $\mathbf{F}^{D2}$ and $\mathbf{F}_z^D$ whose simultaneous eigenvectors, the irreducible spherical-tensor superkets $|kqi\rangle$, obey (116a) and (116b). In the relaxation experiments, only the constituents concerned with $k=1$ and $q=0, \pm 1$ are of relevance, and in longitudinal relaxation measurements, to which our further discussion is confined, only the constituents associated with $k=1$ and $q=0$.

In considering the evolution of the spin density superket in the context of the existing symmetry $\mathscr{G}$ we can therefore limit ourselves to the totally symmetric part of the manifold spanned by superkets $|10i\rangle$. Below we describe the method for determining the dimension of this totally symmetric subspace, $\bar{n}_1$, that is; the number of relaxation modes participating in the evolution and, for systems with nontrivial microscopic symmetry, also the dimensions $\bar{n}_{1\mu}$ (see comment to (118)) of the corresponding sub-subspaces that are concerned with the individual parentages, μ, of $\mathscr{G}$. Knowledge of the latter quantities may give further insight into the relaxation behaviour of the system since it enables one

to calculate the numbers of relaxation modes that belong to the pertinent microscopic, independently evolving subblocks (there can only be two such subblocks since in the presence of DD and/or ICA interactions the microscopic symmetry is never higher than C_i). For a more complete characterization of the relaxation process it may prove necessary to sort out the symmetrized irreducible spherical-tensor superkets that correspond to "pure T_1 modes", that is, the modes involving only combinations of energy-level populations. This question is considered later. We start from calculations of the quantities $\bar{n}_1$ and $\bar{n}_{1\mu}$. The expressions presented below involve an arbitrary rank k.

For any multispin system, the number of (orthogonal) basic irreducible spherical-tensor superkets of rank k, n_k, is given as a difference between the degeneracy factors, m_k and m_{k+1}, of two subsequent eigenvalues of $\mathbf{F}_z^{\mathrm{D}}$, $q = k$ and $q = k + 1$,[18]

$$n_k = m_k - m_{k+1} \tag{169}$$

For any permutation group $\mathscr{G}$, (169) remains valid also when the irreducible spherical basis is projected onto the eigenspace of $\mathbf{G}$, since $\mathbf{G}$ commutes with both $\mathbf{F}_z^{\mathrm{D}}$ and $\mathbf{F}^{\mathrm{D}2}$. Thus,

$$\bar{n}_k = \bar{m}_k - \bar{m}_{k+1} \tag{170}$$

where $\bar{m}_q$ is the degeneracy of the eigenvalue q of $\mathbf{F}_z^{\mathrm{D}}$ in the eigenspace of $\mathbf{G}$ (see (101)). The same pertains to the eigenspaces of individual parentage superprojectors $\mathbf{G}_\mu$ that make up $\mathbf{G}$, since each $\mathbf{G}_\mu$ also commutes with $\mathbf{F}_z^{\mathrm{D}}$ and $\mathbf{F}^{\mathrm{D}2}$,

$$\bar{n}_{k\mu} = \bar{m}_{k\mu} - \bar{m}_{k+1\mu} \tag{171}$$

where $\bar{m}_{q\mu}$ is the degeneracy of q in the eigenspace of $\mathbf{G}_\mu$ (see (113)). The methods of calculating the quantities $\bar{m}_q$ and $\bar{m}_{q\mu}$ are explained in Sections 7.1 and 7.2, respectively. The procedure for evaluating $\bar{n}_k$ and $\bar{n}_{k\mu}$ is a necessary constituent element of any computer routine which is to produce permutation-symmetry-adapted irreducible spherical bases.

Departing from the main course of our discussion, we present a general formalism which can serve as a foundation for the design of such a routine. It exploits a formula reported by Blum[61] which enables one to produce irreducible spherical-tensor superkets from appropriate shift operators. The latter are constructed from simultaneous eigenkets, $|Jmr)$, of $F^2 = F_x^2 + F_y^2 + F_z^2$ and F_z, concerned with eigenvalues $J(J+1)$ and m, respectively, where r enumerates different kets of the same J and m. The general expression for an unnormalized superket $|kqi\rangle^{\mathrm{u}}$ reads

$$|kqi\rangle^{\mathrm{u}} \equiv \sum_{m=J}^{-J} \sum_{m'=J'}^{-J'} (-1)^{J'-m'} (JJ'mm'|kq)|Jmr)(J'm'r'| \tag{172}$$

where $|J-J'| \leqslant k \leqslant J+J'$ and the symbol $(JJ'mm'|kq)$ denotes a Clebsch–Gordan coefficient.[62] The essential point of the approach proposed here involves the use as a basis in Hilbert space of the simultaneous eigenkets of F^2 and F_z which are adapted to the existing permutation symmetry $\mathscr{G}$, in the sense that they are eigenkets of the pertinent symmetry projectors, (104), and obey (106). The symmetry-adapted simultaneous eigenkets of F^2 and F_z are denoted by $|Jm\mu vr)$, where the symbols μ, v, and r have the same meaning as in (105) and (106). The construction of such a basis is always feasible since both F^2 and F_z commute with individual symmetry operators from $\mathscr{G}$. Now, the required symmetry-adapted irreducible spherical-tensor superkets can be produced by the combined use of (172) and (108), namely

$$|kq\mu i\rangle^{\mathrm{u}} = \sum_{v=1}^{d_\mu} |kq\mu vi\rangle^{\mathrm{u}} \tag{173}$$

where d_μ is the dimension of μ and

$$|kq\mu vi\rangle^{\mathrm{u}} \equiv \sum_{m=J}^{-J} \sum_{m'=J'}^{-J'} (-1)^{J'-m}(JJ'mm'|kq)|Jm\mu vr)(J'm'\mu vr'| \tag{174}$$

It can be demonstrated that the set of superkets $|kq\mu i\rangle^{\mathrm{u}}$ (k, q and μ fixed) derived from a complete orthonormal basis of the kets $|Jm\mu vr)$ according to (173) is orthogonal and complete in the manifold of all such irreducible spherical-tensor superkets $|kqj\rangle$ (k and q fixed) that belong to the eigenspace of $\mathbf{G}_\mu$. The proof is straightforward but lengthy and is, therefore, not given here. The formalism presented above can easily be implemented on a computer.

Turning back to our main subject, we now show how one enumerates pure T_1 modes of relaxation in an isochronous system. The number of such modes is equal to the dimension of the manifold spanned by those of the symmetry-adapted rank-1 superkets $|10\mu i\rangle$ which are constructed from shift operators of the form $|Jm\mu vr)(Jm\mu vr|$, where $J \geqslant \frac{1}{2}$. If we denote by $\bar{N}_{J\mu}$ the number of basis kets which are concerned with the eigenvalues $J(J+1)$ of F^2 and $m = J$ of F_z, and belong to the symmetry species μ, then the number of pure T_1 modes of parentage μ, N_μ, can be expressed as

$$N_\mu = d_\mu^{-1} \sum_{J \geqslant 1/2}^{J_{\max}} \bar{N}_{J\mu} \tag{175}$$

where $J_{\max} = m_{\max}$, the maximum eigenvalue of F_z. The quantities $\bar{N}_{J\mu}$ can be determined by a recursive subtraction which is strictly analogous to the Liouville space proceeding in (171), namely

$$\bar{N}_{J\mu} = \bar{M}_{J\mu} - \bar{M}_{J+1\mu} \tag{176}$$

where $\bar{M}_{J\mu}$ and $\bar{M}_{J+1\mu}$ denote the degeneracies of two subsequent eigenvalues, $m = J$ and $m' = J+1$, respectively, of F_z in the eigenspace of the symmetry

projector $\bar{P}_{\mu}$, (123). In other words, $\bar{M}_{m\mu}$ denotes the trace of $\bar{P}_{\mu}$ over the Hilbert subspace concerned with the eigenvalue m of F_z. For any symmetry $\mathcal{G}$, the determination of the number of pure T_1 modes is, therefore, a simple task, since it resolves itself to the standard calculations of traces of the symmetry projectors involved.

A collection of the relevant data calculated using (170), (171) and (175) is presented in Table 9 for some selected isochronous spin-$\frac{1}{2}$ systems. In the cases where the microscopic symmetry can be nontrivial, the relaxation modes are classified into two subsets associated with the respective orbits of the (two-element) microscopic group.

It can be seen from the data in the first four rows of Table 9 that the relaxation behaviour of the corresponding systems involves only pure T_1 modes. For the remaining three systems, the pure T_1 modes are coupled with zero-quantum coherences. If the eigenfrequencies of the latter are large in comparison with the magnitudes of the relaxation matrix elements, the coupling terms can be neglected as nonsecular and the relaxation process can still be described in the manifold of pure T_1 modes. However, if the eigenfrequencies of some or all of the zero-quantum coherences and the elements of **R** are of comparable magnitude, then for a proper description of relaxation one must also include the pertinent zero-quantum coherences.

In the latter instance it is again necessary to include the indirect influence on the NMR spectra of spin–spin couplings between magnetically equivalent nuclei, since it is these couplings which determine the magnitudes of eigenfrequencies of zero-quantum coherences. To make this more clear, we consider a hypothetical situation where relaxation experiments are performed on two strictly related isochronous spin-$\frac{1}{2}$ systems, each composed of six nuclei situated at the vertices of a regular octahedron (O_d symmetry, see row 7 of Table 9). We assume that both systems are characterized by exactly the same relaxation parameters and that they differ only in the magnitude of the coupling constant, J_c, between the nuclei situated *cis* to each other (by virtue of the theorem[24] repeatedly referred to in the context of exchange, the coupling between the nuclei arranged *trans* is totally irrelevant). If in one of the systems J_c is equal to zero and in the other it is much larger than a typical element of **R** then the course of relaxation observed for each of these systems will, in general, be different: in the former case the relaxation process will involve all nine modes possible in the system and a nine-exponential recovery is expected, while in the latter only pure T_1 modes will be observed, with the recovery curve including only seven exponentials (see row 7 of Table 9). Effects of this type may be non-negligible and should be taken into account in accurate relaxation measurements.

The discussion given in the present section clearly demonstrates that the use of the existing theoretical tools can provide a lot of information about

Table 9. Symmetry classification of longitudinal relaxation modes for selected isochronous spin-$\frac{1}{2}$ systems A_N^a.

			Number and parentage of relaxation modes (pure T_1 modes)		
N	$\mathcal{G}$	$\mathcal{K}$	$\mathcal{O}_1^b$	$\mathcal{O}_2$	Total
3	D_3	$\{e\}$	$1A_1 + 1E(1A_1 + 1E)$	—	2(2)
4	T_d	$\{e\}$	$1A_1 + 1T_2(1A_1 + 1T_2)$	—	2(2)
4	D_4	$\{e, C_4^2\}^c$	$1A_1 + 1B_2(1A_1 + 1B_2)$	$1E(1E)$	3(3)
4	D_2	$\{e, C_2\}^c$	$1A + 1B_1(1A + 1B_1)$	$1B_2 + 1B_3(1B_2 + 1B_3)$	4(4)
5	D_5	$\{e\}$	$2A_1 + 4E_1 + 4E_2(2A_1 + 2E_1 + 2E_2)$	—	10(6)
6	D_6	$\{e, C_6^3\}^c$	$5A_1 + 9E_2(3A_1 + 3E_2)$	$1B_1 + 1B_2 + 6E(1B_1 + 1B_2 + 2E_1)$	22(10)
6	O_d	$\{e, i\}^c$	$2A_1^g + 4E^g + 1T_2^g(2A_1^g + 2E^g + 1T_2^g)$	$1T_1^u + 1T_2^u(1T_1^u + 1T_2^u)$	9(7)

[a] In the extreme narrowing regime, in the absence of CSA interactions.

[b] The orbit including the totally symmetric irreducible representation of the group given in column 3.

[c] In the absence of intermolecular interactions.

relaxation processes in symmetric molecules without resorting to any computer calculations. Performing such analyses such as presented above is in fact a prerequisite to the efficient use of a computer to handle experimental relaxation data for symmetric systems. Generalized with respect to exchange phenomena in symmetric molecules, the latter statement can also serve as a succinct conclusion for the entire contents of the present chapter.

ACKNOWLEDGEMENTS

The present work was sponsored by the CPBP 01.12.10.19 Project of the Polish Academy of Sciences.

REFERENCES

1. H.M. McConnel, A.D. McLean and C.A. Reilly, *J. Chem. Phys.*, 1955, **23**, 1152.
2. P.L. Corio, *Structure of High-Resolution NMR Spectra*, Chap. 8. Academic Press, New York, 1966.
3. U. Fano, in *Lectures on the Many-Body Problem*, Vol. 2, p. 217 (ed. E.R. Caianiello). Academic Press, New York, 1964.
4. J. Jeener, in *Advances in Magnetic Resonance*, Vol. 10, p. 2 (ed. J.S. Waugh). Academic Press, London, 1982.
5. D.A. Kleier and G. Binsch, *J. Magn. Reson.*, 1970, **3**, 146.
6. D.A. Kleier and G. Binsch, *Quantum Chemistry Program Exchange, Program 165*. Indiana University, Bloomington, IN, 1970.
7. S. Szymanski and A. Gryff-Keller, *J. Magn. Reson.*, 1976, **22**, 1.
8. D.S. Stephenson and G. Binsch, *J. Magn. Reson.*, 1978, **32**, 145.
9. D.S. Stephenson and G. Binsch, *Quantum Chemistry Program Exchange, Program 365*. Indiana University, Bloomington, IN, 1978.
10. P. Meakin, E.L. Muetterties and J.P. Jesson, *J. Am. Chem. Soc.*, 1971, **93**, 4701.
11. J.P. Jesson and P. Meakin, *Acc. Chem. Res.*, 1973, **6**, 269.
12. P. Meakin, A.D. English and J.P. Jesson, *J. Am. Chem. Soc.*, 1976, **98**, 414.
13. Z. Luz and R. Naor, *Mol. Phys.*, 1982, **46**, 891.
14. R.K. Wangsness and F. Bloch, *Phys. Rev.*, 1953, **89**, 728.
15. F. Bloch, *Phys. Rev.*, 1956, **102**, 104.
16. A.G. Redfield, *IBM J. Res. Dev.*, 1957, **1**, 19.
17. A.G. Redfield, in *Advances in Magnetic Resonance*, Vol. 1, p. 1 (ed. J.S. Waugh). Academic Press, New York, 1965.
18. N.C. Pyper, *Mol. Phys.*, 1971, **20**, 1.
19. N.C. Pyper, *Mol. Phys.*, 1971, **21**, 961.
20. N.C. Pyper, *Mol. Phys.*, 1971, **21**, 977.
21. S. Szymanski, *Mol. Phys.*, 1985, **55**, 763; 1986, **58**, 439.
22. S. Szymanski, A.M. Gryff-Keller and G. Binsch, *J. Magn. Reson.*, 1986, **68**, 399.
23. S. Szymanski, *Mol. Phys.*, 1987, **60**, 897.
24. S. Szymanski, *J. Magn. Reson.*, 1988, **77**, 320.
25. S. Szymanski and G. Binsch, *J. Magn. Reson.*, 1989, **81**, 104.

26. R. Willem, in *Progress in NMR Spectroscopy*, Vol. 20 (ed. J.W. Emsley, J. Feeney and L.H. Sutcliffe). Pergamon Press, Oxford, 1987.
27. G. Binsch, E.L. Eliel and H. Kessler, *Angew. Chem. Int. Ed. Engl.*, 1971, **10**, 570.
28. J.T. Hougen, *J. Chem. Phys.*, 1962, **37**, 1433.
29. J.T. Hougen, *J. Chem. Phys.*, 1963, **39**, 358.
30. H.C. Longuett-Higgins, *Mol. Phys.*, 1963, **6**, 445.
31. P. Meakin, L.J. Guggenberger, W.S. Peet, E.L. Muetterties and J.P. Jesson, *J. Am. Chem. Soc.*, 1973, **95**, 1467.
32. P. Meakin, E.L. Muetterties and J.P. Jesson, *J. Am. Chem. Soc.*, 1973, **95**, 75.
33. L. Jansen and M. Boon, *Theory of Finite Groups. Applications in Physics*, Chap. 6. North-Holland, Amsterdam, 1967.
34. W.G. Klemperer, in *Dynamic Nuclear Magnetic Resonance Spectroscopy* (ed. L.M. Jackmann and F.L. Cotton), Chap. 2. Academic Press, New York, 1975.
35. R. Willem, J. Brocas and D. Fastenakel, *Theor. Chim. Acta*, 1975, **40**, 25.
36. P. Pechukas, *J. Chem. Phys.*, 1976, **64**, 1516.
37. E. Pollak and P. Pechukas, *J. Am. Chem. Soc.*, 1978, **100**, 2984.
38. E.L. Muetterties, *J. Am. Chem. Soc.*, 1969, **91**, 1636.
39. J. Brocas and D. Fastenakel, *Mol. Phys.*, 1975, **30**, 193.
40. W. Haesselbarth and E. Ruch, *Theor. Chim. Acta*, 1973, **29**, 259.
41. S. Szymanski, *Bull. Acad. Polon. Sci., Ser. Sci. Chim.*, 1978, **26**, 317.
42. A. Gryff-Keller and S. Szymanski, *Bull. Acad. Polon. Sci., Ser. Sci. Chim.*, 1979, **27**, 351.
43. S. Szymanski, M. Witanowski and A. Gryff-Keller, in *Annual Reports on NMR Spectroscopy*, Vol. 8 (ed. G.A. Webb) p. 227. Academic Press, London, 1978.
44. G. Binsch, *J. Am. Chem. Soc.*, 1969, **91**, 1304.
45. S. Alexander, *J. Chem. Phys.*, 1962, **37**, 974.
46. G. Fraenkel and J.I. Kaplan, *J. Am. Chem. Soc.*, 1972, **94**, 2907.
47. S. Szymanski and A. Gryff-Keller, *J. Magn. Reson.*, 1974, **16**, 182.
48. F.A. Van-Catledge, S.D. Ittel and J.P. Jesson, *Organometallics*, 1985, **4**, 18.
49. R.L. Vold and R.R. Vold, in *Progress in NMR Spectroscopy*, Vol. 12 (ed. J.W. Emsley, J. Feeney and L.H. Sutcliffe) p. 79. Pergamon Press, Oxford, 1978.
50. A.D. Bain and R.M. Lynden-Bell, *Mol. Phys.*, 1975, **30**, 325.
51. B.C. Sanctuary and L. Selwyn, *J. Chem. Phys.*, 1981, **74**, 906.
52. B.C. Sanctuary and F.P. Temme, *Mol. Phys.*, 1985, **55**, 1049.
53. F.P. Temme and B.C. Sanctuary, *J. Magn. Reson.*, 1986, **69**, 1.
54. F.P. Temme, *Chem. Phys.*, 1989, **132**, 9.
55. S. Szymanski and G. Binsch, *J. Magn. Reson.*, 1990, **87**, 166.
56. D. Hoefner, D.S. Stephenson and G. Binsch, *J. Magn. Reson.*, 1978, **32**, 131.
57. J.P. Jesson and E.L. Muetterties, in *Dynamic Nuclear Magnetic Resonance Spectroscopy* (ed. L.M. Jackmann and F.L. Cotton), Chap. 8. Academic Press, New York, 1975.
58. Z. Luz and R. Naor, *J. Chem. Phys.*, 1982, **76**, 891.
59. D. Gamliel, Z. Luz and S. Vega, *J. Chem. Phys.*, 1986, **85**, 2516.
60. D. Gamliel, Z. Luz and S. Vega, *J. Chem. Phys.*, 1988, **88**, 25.
61. K. Blum, *Density Matrix Theory and Applications*, p. 87. Plenum Press, New York and London, 1981.
62. D.M. Brink and G.R. Satchler, *Angular Momentum*, p. 136. Clarendon Press, Oxford, 1968.

Nuclear Spin Relaxation in Diamagnetic Fluids

Part 2. Organic Systems and Solutions of Macromolecules and Aggregates

JOZEF KOWALEWSKI

Division of Physical Chemistry, Arrhenius Laboratory, University of Stockholm, S-106 91 Stockholm, Sweden

1. INTRODUCTION

This review is a continuation and conclusion of the review of the nuclear relaxation in diamagnetic fluids commenced in Volume 22 of this series, referred to below as Part 1.[1] It will be assumed throughout the present text that the reader has access to Part 1 and the repetition of references and equations is avoided as far as possible.

This review is organized as follows. This introductory section contains an update of Part 1, i.e. it covers a selection of important papers that deal with the

ANNUAL REPORTS ON NMR SPECTROSCOPY
VOLUME 23 ISBN 0-12-505323-1

Copyright © 1991 Academic Press Limited
All rights of reproduction in any form reserved

general aspects or inorganic applications, which were either overlooked during the writing of Part 1 or appeared too late to be included there. Section 2 is concerned with the applications of relaxation measurements to studies of organic systems. According to the working definition, the "organic" systems are systems containing carbon compounds of low molecular weight. Section 2 is further divided according to the chemical nature of the systems studied and, in the case of the relaxation in organic solutes dissolved in isotropic solvents, to the nature of the nucleus under consideration. Section 3 is devoted to selected aspects of nuclear spin relaxation in solutions of aggregates and macromolecules. Finally, Section 4 contains the concluding remarks pertinent to both parts of the review. This work was completed during the autumn of 1989 and covers the literature that appeared in *Chemical Abstracts* (and some major journals) up to June 1989.

The first paper I wish to mention in this update is the latest yearly review of nuclear spin relaxation by Weingärtner.[2] I then follow the original organization of Part 1. Thus, I begin with relaxation theory and, in particular, its general aspects and relaxation mechanisms. Two papers dealing with the general aspects of nuclear relaxation appeared during early 1989. Szymanski and Binsch[3] followed up their work on the Liouville space formulation of the Wangness–Bloch–Redfield relaxation theory, discussed in Part 1. Their new paper concentrates on scalar relaxation, where attention is focused on only a part of the spin system, while the remainder is treated as a pseudobath. It should be observed that in the discussion of the "scalar relaxation of the second kind" (scalar interaction modulated by relaxation of one of the spins), the authors assume the relaxation of the spins belonging to the pseudobath to be in the "extreme narrowing" limit.

The nuclear spin relaxation rate induced by two-site jumps with arbitrary correlation times and Zeeman fields, i.e. not limiting the calculations to the strong narrowing regime (see Part 1) has been studied.[4] Henry and Szabo[5] reformulated the theory of dipolar and quadrupolar relaxation in a particularly convenient way for carrying out vibrational averaging, and investigated its effects. A comprehensive review of the theory of longitudinal relaxation in coupled spin systems with magnetic equivalence, and of the experimental methods available for studying coupled systems has appeared.[6] Several papers dealing with the dynamic aspects of relaxation theory, related to Sections 2.2–2.7. of Part 1, should be given due attention. The correlation functions and spectral densities of relevance for the spin–rotation relaxation in a symmetric-top molecule undergoing small-step diffusion were derived in an early important paper.[7]

Two reports[8,9] have appeared on the influence of the director fluctuations on molecular reorientation of a solute molecule in a liquid-crystalline solvent and on the nuclear spin relaxation. Bull[10] has presented a study of internal

motion using the extended J diffusion (EDJ) and the Fokker–Planck–Langevin (FPL) models of collision dynamics. He has investigated, among other problems, the effect of the height of the barrier on relaxation rates. Uusvuori and Luonasmaa[11] have discussed different motional models based on the small-step diffusional description of the overall reorientation and allowing for internal motion. Baldo and Grassi[12] have developed a model for the relaxation rates of flexible molecules in solution. The model involves conformational changes, modelled as a Brownian motion between different conformational states, and rotational tumbling.

The frequency dependence of the spectral densities occurring in the theory of dipolar relaxation caused by translational diffusion have been discussed.[13] Three papers have dealt with the interrelation of relaxation and exchange. Vasavada and Kaplan[14] have considered the relaxation and lineshapes in an exchanging system where the exchange lifetime approaches the correlation time. Westlund and Wennerström[15] have treated the case of quadrupolar relaxation and lineshapes for a spin-$\frac{3}{2}$ nucleus involved in a two-site chemical exchange between an isotropic and an anisotropic site. Finally, Ichikawa[16] studied the effect of chemical exchange on the shape of the longitudinal magnetization recovery curves under various conditions.

Several papers concerned with experimental methods (Section 3 of Part 1) should be mentioned here. A superfast version of the inversion-recovery method has been proposed.[17] The technique is based on the inference that a reference spectrum and a single partially relaxed spectrum should be sufficient for determining the time constant for a single monoexponential recovery. Another technique for the rapid determination of T_1 was examined by Homer and Roberts.[18] A method for measuring ^{13}C spin–spin relaxation times using a two-dimensional heteronuclear correlation technique has been proposed.[19] The nuclear Overhauser enhancement (NOE) measurements continue to attract considerable attention. A comprehensive treatment of the phenomenon has appeared in the form of a book.[20] Keeler and coworkers have discussed the NOE effect in strongly coupled spin system[21] and the influence of cross-correlation on multiplet patterns in NOE spectra.[22] Landy and Rao[23] analysed the dynamic NOE of a multiple-spin system undergoing chemical exchange. Oschkinat *et al.*[24] have discussed modifications of a NOESY experiment (small flip angle NOESY, soft NOESY) for elucidating longitudinal relaxation pathways in scalar-coupled systems and for measuring individual transition probabilities, while Emsley and Bodenhausen[25] have proposed using 270° Gaussian-shaped pulses in the selective NOESY experiment. A practical guide to two-dimensional NOE studies on small molecules has appeared.[26] Zhao Dezheng *et al.*[27] have reported a scheme for suppressing off-resonance effects in one- and two-dimensional rotating frame Overhauser enhancement (ROESY) spectra. The role of mixing time in the

two-dimensional heteronuclear NOE experiments has been discussed.[28] Relaxation-allowed coherence transfer and multiple-quantum phenomena were recently discussed.[29,30] Finally, Böhlen and coworkers[31] have proposed methods for measuring dipole–dipole (DD) cross-correlations based on the observation of the longitudinal three-spin order and on the triple-quantum filtering of NOESY spectra.

Turning to the analysis of relaxation data, I wish first to quote a paper[32] relating to the analysis of information available (and unavailable) from multiexponential relaxation data. A large number of papers related to the analysis of the NOE data should be mentioned. As the first step in the analysis, the quantitative interpretation of one- and two-dimensional NOE experiments requires an accurate quantification of the signal intensities. Several important papers concerned with this problem have appeared during the last few years [33–37] and were overlooked in Part 1. The subsequent analysis step, involving the interpretation of the NOE data in terms of molecular structure and dynamics also continues to attract wide interest.[38–42]

With regard to the nuclear relaxation in gases (Section 4 of Part 1), I wish to mention here the paper[43] on the ^{19}F relaxation in gaseous hexafluorides, XF_6, with X = S, Mo, W or U. The data were analysed to provide information on the anisotropic part of the intermolecular potential. Several recent papers on the applications of relaxation studies to inorganic systems (corresponding to Section 5 of Part 1) were found to be of sufficient interest to be included in this update. Brunet and coworkers[44] have studied the nuclear relaxation of metal nuclei in pure liquid metal hexafluorides, MF_6, with M = ^{235}U, ^{95}Mo, or ^{97}Mo. The relaxation was found to be caused by fluctuations in the quadrupolar interaction, and the mechanism of these fluctuations was analysed. Van der Maarel[45] has investigated the water nuclei (^1H, ^2H and ^{17}O) relaxation in concentrated aqueous solutions of zinc chloride and obtained information on the interaction strengths and dynamic parameters. Ichikawa and Jin[46] have studied the ^{27}Al relaxation in aqueous $Al_2(SO_4)_3$, while Pronin and Vashman[47] have studied ^1H and ^{14}N relaxation in zirconium nitrate solutions.

Turning to the subject of Section 5.3 of Part 1, I should mention the work of Holz and Sacco,[48] who studied ^2H, ^{14}N and ^{23}Na relaxation in sodium iodide solutions in binary solvent mixtures. Buchanan *et al.*[49] have studied ^{13}C relaxation in 14-crown-4 ethers and their lithium complexes, while Delville *et al.*[50] have studied ^{23}Na relaxation in dibenzocrown ether complexes of the sodium cation. The germanium relaxation mechanisms in tetraalkylgermanes have been studied by Harazono *et al.*,[51] while Liepins and coworkers[52] have reviewed critically the available data on the ^{73}Ge relaxation. Two papers on relaxation studies of organotin compounds should be mentioned. Sakai

et al.[53] studied ^{1}H relaxation in dimethyltin dichloride and its complexes in solution, while Chapelle and Granger[54] investigated the ^{13}C and ^{119}Sn relaxation in some axially-symmetric compounds.

I turn now to transition-metal compounds (Section 5.4 of Part 1). Helm *et al.*[55] have reported an investigation of ^{45}Sc linewidths in Sc(II) complexes with trimethylphosphate. Brownlee and coworkers,[56,57] have reported investigations of ^{95}Mo relaxation times and quadrupole coupling constants in molybdenum carbonyl and cyanide complexes. Findeisen *et al.*[58] have studied ^{99}Tc relaxation in technetium carbonyl compounds, while Cotton and Luck[59] measured the proton T_1 of several hydride complexes of rhenium as a function of temperature and used the data to distinguish between classical and non-classical hydride structures. ^{59}Co spin–lattice relaxation was studied in aqueous solutions of tris(ethylendiamine)cobalt(III) salts[60] and in hexakis(phosphite)cobalt(III) complexes[61]. Bodner and Bauer[62] have reported ^{13}C T_1 measurements for trialkylphosphines and their tris(carbonyl)nickel complexes.

Finally, I wish to mention two papers on other inorganic systems (Section 5.5. of Part 1). McIntyre *et al.*[63] have published a paper on ^{14}N relaxation in N_2 dissolved in acetone (at different temperatures) and in a variety of other solvents. Miura *et al.*[64] have studied the interaction between the chloride ion and trihalomethanes by means of ^{35}Cl linewidth measurements.

2. ORGANIC LIQUIDS AND SOLUTIONS OF SMALL MOLECULES

In this section, I review nuclear spin relaxation studied in organic systems. The section is organized as follows. Section 2.1 deals with pure liquids of carbon containing molecules. Section 2.2 deals with binary liquid mixtures; an important group of such mixtures contains water as one of the components and an important problem addressed in many papers is the effect of the second component on the molecular dynamics of water. Therefore, it is practical to include in the same section papers dealing with water nuclei relaxation in binary systems composed of water and nonelectrolytes of more general nature. Relaxation of nuclei residing in organic solutes in aqueous or other isotropic solution are covered in Sections 2.3–2.5. The division between these three sections is based on the nature of nuclei under consideration: the work on ^{13}C and ^{2}H is included in Section 2.3, that proton relaxation is covered in Section 2.4, while the papers dealing with other nuclei are reviewed in Section 2.5. Finally, the work on organic solutes in anisotropic solvents is collected in Section 2.6.

2.1. Pure organic liquids

The work on pure liquids published during the last decade or so is concentrated on investigations of molecular dynamics and, to a lesser extent, of relaxation mechanisms. Many papers also report measurements of translational diffusion coefficients. The state of the liquid is usually varied by varying the temperature and, sometimes, the pressure. In certain cases, the isotope composition is also a variable—here all mixtures of isotopic species are considered as pure liquids. Among numerous review articles of relevance to this section, I wish to mention in particular the paper by Wright and coworkers[65] on the physico-chemical applications of ^{13}C relaxation studies, that by Boeré and Kidd[66] on rotational correlation times, and that by Jonas[67] on variable-pressure work. These three papers together provide a good coverage of earlier work and allow me to be highly selective in referring to papers published prior to 1980—I include in the first place the older work that provides the necessary background for the more recent contributions.

First, some papers on the liquids of diatomic and triatomic molecules are mentioned. Fukushima *et al.*[68] studied the ^{13}C T_1 and T_2 relaxation times in liquid carbon monoxide at two fairly low magnetic fields as a function of temperature and pressure. The relaxation processes were dominated by the spin–rotation (SR) mechanism, in analogy with the ^{15}N relaxation in liquid nitrogen, and the authors compared the relaxation data on the two diatomic liquids, employing the known SR constants. Li *et al.*[69] reported an ^{17}O relaxation study on liquid (and solid) carbon monoxide, and discussed the temperature dependence of the rotational correlation time. A linear triatomic, deuterium cyanide, was studied in the liquid form[70] by measuring the relaxation rates for ^{2}H, ^{13}C, ^{14}N and ^{15}N as a function of temperature. The quadrupolar nuclei (^{2}H and ^{14}N) relax by the quadrupolar mechanism and yield the rotational correlation times. For the spin-$\frac{1}{2}$ nuclei, the SR mechanism dominated and the authors were able to estimate the angular momentum correlation time. The two sets of correlation times were discussed within the framework of the small-step diffusion and the extended J diffusion models.

Next in size come five-atomic halomethanes, which have attracted considerable attention over the years. Depending on the number and type of halogens, the molecules can be spherical, symmetric or asymmetric tops, and they are considered here in the order of decreasing symmetry. Garg *et al.*[71] have discussed the molecular reorientation of liquid CF_4 under a variety of conditions combining the ^{19}F relaxation data and Raman studies. The applicability of the J diffusion model was confirmed. ^{13}C and ^{35}Cl relaxation in carbon tetrachloride have been studied.[72] It was found that the carbon relaxation is dominated by the SR mechanism and the results are consistent

with the J diffusion model. On the other hand O'Reilly *et al.*[73] have reported ^{35}Cl relaxation data on the same molecule over a much wider temperature range, and argued against the J diffusion model. Ohuchi *et al.*[74] have studied the ^{13}C, $T_{1\rho}$ in carbon tetrachloride (and some other chlorine compounds as well as decaline), which was found to be dominated by the scalar interaction with chlorines, and estimated the carbon–chlorine coupling constants. Pettitt and Wasylishen[75] have studied ^{13}C relaxation in liquid (and solid) CBr_4 as a function of temperature. The complexity of the carbon relaxation in this system, due to the properties of bromine nuclei (strong quadrupolar interaction and Larmor frequency close to that of ^{13}C), was discussed.

Mono- or tri-halogenated methanes reorient as symmetric tops, i.e. are characterized by two distinct rotational correlation times. Radkowitsch and coworkers[76–78] have reported proton, deuteron and ^{19}F relaxation data on fluoromethane, fluroform and their deuteriated analogues over wide temperature and pressure ranges. The relaxation rates were decomposed into contributions from individual mechanisms, and the reorientational and angular momentum correlation times were derived. For both liquids, it was found that the inertial effects were important. In the case of fluoromethane, the data could successfully be interpreted in terms of the extended M diffusion[77] model, while the Fokker–Planck–Langevin model was found to be successful for the fluoroform case.[78] Lassigne and Wells[79] have reported proton, deuteron and ^{13}C spin–lattice relaxation rates in liquid bromomethane (and its isotopic modifications) over a wide temperature range. The proton relaxation contains contributions from the intra- and inter-molecular dipole–dipole (DD) mechanisms; the carbon relaxation is free from the intermolecular contributions, but contains a term caused by the scalar interaction with ^{79}Br. The molecular dynamics was also discussed and it was concluded that the reorientation about the symmetry axis is not well described by the extended J diffusion model. The scalar and SR contributions to the ^{13}C relaxation in this molecule was also discussed.[80] Schwartz[81] has studied the ^{13}C spin–lattice relaxation in iodomethane. By combining the T_1 and NOE results, he was able to obtain estimates of both the DD and SR contributions and reached similar conclusions regarding the molecular dynamics in this liquid. Chloroform has been the subject of a score of investigations. Here, I wish to mention three of the older papers. As long as 20 years ago, Huntress[82] studied the deuteron and ^{35}Cl relaxation in deuterochloroform as a function of temperature, and characterized the rotational motion in terms of the small-step diffusion model. The deuteron relaxation was later studied as a function of pressure,[83] while Bender and Zeidler[7] studied proton relaxation in mixtures of the proton and deuteron bearing species. This isotopic dilution method allowed the inter- and intra-molecular contributions to the relaxation rate to be separated. The intramolecular relaxation data were interpreted successfully

in terms of anisotropic small-step diffusion. The intermolecular relaxation rates of Bender and Zeidler[7] were recently interpreted[84] in terms of proton–proton pair correlation functions obtained from the reference interaction site model. In another recent paper[85] a report is given of the proton coupled and decoupled ^{13}C relaxation (caused predominantly by the DD mechanism) in liquid chloroform. Still another symmetric-top halomethane, $CFCl_3$, has been studied by De Zwaan and Jonas.[86] They measured the ^{19}F relaxation rates as a function of temperature and pressure and reported the density dependence of the angular momentum correlation time.

Some authors have been concerned with nuclear relaxation in neat liquid halomethanes with symmetry lower than symmetric top. Sandhu[87] has studied the proton relaxation in mixtures of CH_2Cl_2 with its deuterated analogue and the deuteron relaxation in liquid CD_2Cl_2 as a function of temperature. The proton relaxation was assumed to contain contributions from intra- and inter-molecular DD interactions only. The molecular dynamics were also discussed. It was argued that the molecule reoriented as a quasi-symmetric top with the unique axis coincident with the dipole axis. More recently,[88] ^{13}C relaxation in dichloromethane has been studied as a function of temperature. By combining the T_1 and NOE measurements, it was possible to separate the DD and SR contributions to the relaxation rate (cf. Fig. 1). Comparing their results with the data of Sandhu,[87] Rodriguez *et al.*[88] found his assumption of negligible SR contribution to proton T_1 to be unjustified. In the discussion of the molecular dynamics, they also argued for a quasi-symmetric-top treatment but placed the unique axis along the Cl–Cl axis. The results were found to be consistent with the extended J diffusion model. Vardag and Lüdemann[89] have studied a similar molecule, difluorochloromethane, in the liquid state over a wide range of temperature and pressure. The deuteron relaxation rates provided the rotational correlation times; a comparison with some ^{35}Cl results showed no strong motional anisotropy. The ^{19}F spin–lattice relaxation mechanism was shown to contain the DD and SR contribution, with the relative importance varying with density. However, the ^1H relaxation was found to be dominated by the DD mechanism over the whole range of conditions. The molecular dynamics was discussed in terms of the small-step diffusion and the FPL models.

I now turn to pure liquids composed of larger molecules. I proceed in the first place with molecules which, by analogy with the halomethanes discussed above, are rigid from the point of view of nuclear relaxation, i.e. they do not possess internal degrees of freedom which efficiently modulate the interactions involving nuclear spin and thus contribute to the relevant spectral densities. The work on three rigid, symmetric top hydrocarbon molecules is discussed first. Besnard *et al.*[90] have studied liquid cyclopropane over wide temperature and pressure ranges, combining the ^{13}C and deuteron relaxation

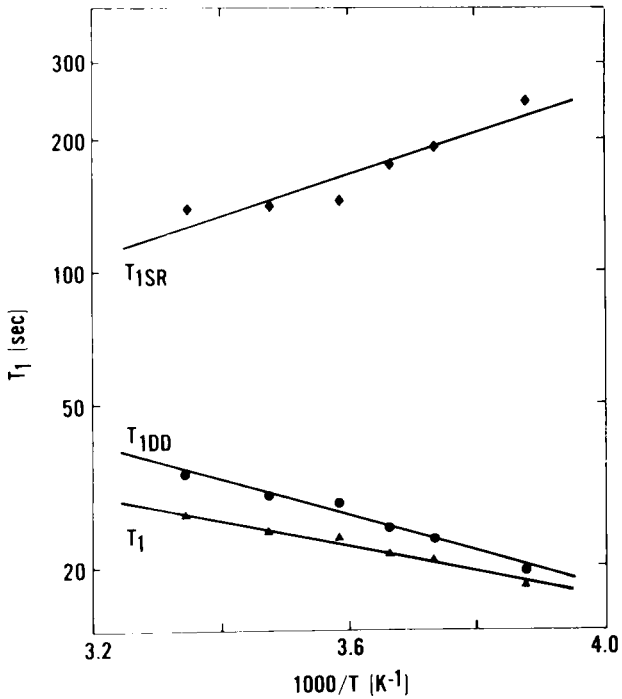

Fig. 1. Temperature dependence of ^{13}C relaxation times in dichloromethane. (Reproduced with permission from Rodrigues *et al.*[88])

measurements with Raman experiments. The results were interpreted in terms of the small-step rotational diffusion model; however, it was pointed out that this description was suitable only for tumbling of the axis at low temperature. The reorientational dynamics of liquid benzene has caused much controversy over the years, which has not really been settled until now. The difficulties are related to the fact that the quadrupolar relaxation of deuterons in C_6D_6 (or the DD relaxation of carbon in C_6H_6) can only provide linear combinations of $\tau^{(2,0)}$ and $\tau^{(2,2)}$. Gillen and Griffiths[91] combined variable-temperature measurements of deuteron relaxation and Raman lineshape studies and found the reorientational motion to be highly anisotropic. A similar conclusion was reached by Tanabe,[92] who performed similar measurements using pressure as an additional variable (Tanabe's paper provides a compilation of deuteron relaxation data originally reported by J.H. Campbell, Ph.D. thesis, University of Illinois, 1975). Yamamoto and Yanagisawa[93] combined deuteron relaxation studies with ^{13}C relaxation measurements on C_6D_6. The latter nucleus relaxes predominantly by the SR mechanism and can provide the

angular momentum correlation time. Using these τ_J values and the extended J diffusion model, the authors were able to reproduce the rotational correlation times from deuteron experiments. The estimated rotational diffusion constants differed at low temperatures by a factor of less than 2. In this context it is worth mentioning a molecular dynamics simulation of liquid benzene,[94] where the angular velocity correlation functions were found to be highly anisotropic (which invalidates the extended J diffusion model); however, it was found that the estimated rotational diffusion constants differed by a factor of not more than roughly 2. The old NMR relaxation data on benzene were used in recent work.[95,96] In addition, I wish to mention the work by Gaisin and Khusainov,[97] who studied intermolecular proton relaxation in liquid benzene. Similar measurements on liquid benzene (as well as liquid dioxane and 1,3,5-trimethylbenzene in CCl_4 solution) were also reported by Homer and Cedeno.[98] The third rigid hydrocarbon to be mentioned is cyclohexane. It was studied by means of proton and deuteron relaxation time measurements.[99] More recently, Tanabe[100] combined these results with Raman lineshape measurements and found that the reorientational motion of the molecule was somewhat anisotropic.

Another liquid of rigid symmetric-top molecules that has received a lot of attention is acetonitrile. Comprehensive sets of deuteron and ^{14}N relaxation data were reported previously in classic papers;[101,102] in these works pressure was included as a variable. Bull[103] interpreted the data successfully using the extended J diffusion model. More recently, Braun and Holz[104] have reported new ^{14}N relaxation data, obtained using a high-field instrument with greatly improved sensitivity. Besides deuteron and nitrogen, Woessner *et al.*[105] also studied proton relaxation as a function of isotopic dilution, which enabled them to separate the intra- and intermolecular relaxation rates. The intermolecular relaxation data from this work were recently used in theoretical studies.[84,106] The ^{13}C relaxation in acetonitrile has also been reported.[107,108] More recently, Schwartz[81] used the data of Leipert *et al.*[107] and pointed out that they were not consistent with the J diffusion model. The deficiency of the J diffusion model was also pointed out by Bien *et al.*[109] who reported Raman measurements, and by Böhm *et al.*[110] who performed molecular dynamics simulations. Plantenga and coworkers[111] reported deuteron and proton relaxation measurements on liquid acetonitrile aligned by an electric field. They were not able to find any systematic effects, contrary to the results of earlier work on other polar molecules.[112] A similar system, liquid trifluoroacetonitrile, was recently studied[113] by means of nitrogen, fluorine and ^{13}C relaxation rates as a function of temperature. The data obtained were found to be consistent with the J diffusion model.

Numerous other rigid, organic molecules of symmetry lower than symmetric top have been studied in the form of pure liquids. Kawanishi and

coworkers[114-117] studied proton spin–lattice relaxation in several vinyl compounds as a function of temperature and pressure. In several cases, they detected discontinuities in the relaxation rate vs. pressure curves. The findings were interpreted in terms of liquid–liquid phase transitions. Pyridine is a planar heterocycle whose dynamics in the liquid form have been studied for many years using NMR relaxation. In the early 1970s Kintzinger and Lehn[118] reported the ^{14}N and deuteron relaxation rates in neat pyridine as a function of temperature. Employing the fact that the quadrupolar interaction of nitrogen is not cylindrically symmetric, they were able to determine three principal rotational diffusion constants. Schweizer and Spiess[119] reported the ^{15}N and ^{13}C spin–lattice relaxation rates in pyridine and analysed the relaxation mechanisms and molecular dynamics. More recently, Stryczek[120] reinterpreted the earlier experimental results in terms of a model involving the microscopic friction tensor. Pedersen *et al.*[121] have studied ^{13}C and ^{14}N relaxation in liquid diazabenzenes and characterized the anisotropy of the molecular reorientation. Eriksen and Pedersen[122] have studied nuclear relaxation rates of ^{13}C and ^{14}N in other neat liquid heterocycles, thiazole and isothiazole, as a function of temperature. The angle between the diffusional and inertial axes in the molecular plane was determined and the accuracy of the results discussed. Rzanny *et al.*[123] studied deuteron relaxation rates and Raman lineshapes for liquid furan and found the reorientation of the molecule to be very close to isotropic. In another paper from the same group, Carius *et al.*[124] employed deuteron relaxation measurements, along with Raman spectroscopy and dielectric relaxation, to investigate the reorientational dynamics of chloro-, bromo-, and iodo-benzene over a wide range of temperatures.

The remainder of this section deals with molecules characterized by the presence of internal degrees of freedom which do influence the nuclear spin relaxation. I begin with hydrocarbons and their fluorinated analogues. Besnard and coworkers[125] studied ^{13}C dipolar relaxation in liquid cyclopentene. The analysis of the data in terms of the anisotropic rotational diffusion of a rigid body was found to have little physical meaning. However, the authors found that a superposition of an isotropic reorientation and a ring-puckering motion provided a satisfactory description of the results. A classical case of a liquid of molecule with one internal degree of freedom is toluene, the methyl group of which is only slightly hindered. Some of the earlier papers should be mentioned. Woessner and Snowden[126] reported a variable-temperature deuteron relaxation study and discussed the influence of the weakly hindered internal rotation on the relaxation rates. Spiess and coworkers[127] studied the molecular motions in liquid toluene by means of ^{13}C, ^{2}H and ^{1}H relaxation measurements. The ^{13}C relaxation mechanism was analysed and the SR contribution used to characterize the internal

rotation. Wilbur and Jonas[128] studied the deuteron relaxation as a function of temperature and pressure and considered various theoretical models for the motional dynamics. More recently, the data of Woessner and Snowden[126] were reinterpreted[129] by modelling the internal rotation as an extended diffusion process. A similar approach was taken by Bull,[130] who studied the internal motion in deuterated mesitylene, methyltrifluorosilane and t-butylchloride (representing low-, medium- and high-barrier internal rotation cases, respectively). Tancredo and co-workers,[131,132] have studied toluene and several other compounds containing methyl groups and related the SR relaxation rate for the methyl carbon to the barrier to internal rotation. The ^{13}C SR relaxation of methyl carbons in toluene and xylenes was also studied by Dilin Xie *et al.*[133]. Hamza and coworkers[134] compared the ^{13}C relaxation in neat toluene and perfluoro-toluene and analysed the data in terms of the superposition of symmetric top overall reorientation and the random internal 60° jumps. Bluhm[135,136] has reported ^{13}C spin–lattice relaxation measurements on toluene and other methylbenzenes. His analysis clearly shows the problems that occur in interpreting relaxation data, taking into account the complete anisotropy of the motions involved. Two papers have been published that are concerned with the properties of liquid toluene under extreme conditions. Shimokawa[137] studied proton relaxation in the high-temperature, high-pressure range up to (and above) the critical point. Conversely, Rössler and Sillescu[138] studied deuteron relaxation in partially deuteriated toluenes at low temperatures, down to the supercooled region. Beguin and Dupeyre[139] have investigated the proton, fluorine and deuteron relaxation in pure benzyl-fluoride. Inter- and intramolecular processes were separated by isotopic dilution and the molecular dynamics was characterized. Kowalewski and Ericsson[140] have studied the overall and internal reorientation in perfluoro-toluene using ^{13}C relaxation measurements.

In addition, other hydrocarbons have been studied in the supercooled liquid state. Dries *et al.*[141] have studied ^{2}H relaxation in *o*-terphenyl as a function of temperature down to the supercooled, glassy region. Arndt and Jonas[142] have studied proton and deuteron spin–lattice relaxation in isopropylbenzenes of different isotopic compositions. The data were consistent with the Cole–Davidson distribution of correlation times. Selectively deuterated isopropyl-benzene was studied more recently by Artaki and Jonas[143] who also employed ^{13}C T_1 and proton $T_{1\rho}$ experiments and used pressure as a variable. In another paper by the same authors[144] a series of different hydrocarbons was studied in the form of supercooled viscous fluids under high pressure. The role of rotational–translational coupling for systems of different symmetries was discussed. The ^{13}C relaxation in neat liquid n-heptane has been studied[145] as a function of temperature and the results discussed in terms of segmental

motion. Finally, I wish to mention a paper by Sazonov,[146] who found linear correlations between the translational diffusion coefficient and the proton spin–lattice relaxation rates in linear hydrocarbons ranging from hexane to tetradecane.

Several authors have studied nuclear relaxation in neat alcohols. Versmold[147] reported deuteron spin–lattice relaxation rates for selectively deuterated methanols over a wide temperature range, down to supercooled region. Ansari and Hertz[148] have studied proton relaxation in selectively deuterated ethanols and in mixtures of different isotopic species over a wide range of temperature down to 120 K, which was sufficient for the molecular motions to depart from the extreme narrowing regime. It was attempted, unsuccessfully, to interpret the intramolecular relaxation using the Woessner theory for internal group rotations. General aspects of this problem have also been discussed in a review.[149] Eguchi *ett al.*[150] have studied proton relaxation in the supercooled and glassy liquid state of ethanol. Frech and Hertz[151] have investigated deuteron and proton spin–lattice relaxation in isotopically substituted isopropanols as a function of temperature and magnetic field, extending the measurements to temperatures low enough to leave the extreme narrowing regime and enter the dispersion range (where the relaxation rate depends on the field strength). Attempts to use Woessner's approach did not give satisfactory results in this case either. Dugue and coworkers[152] have compared the results of ^{13}C relaxation studies with ultrasonic relaxation data on isomeric octanols. In a similar vein, Whittenburg and coworkers[153] have compared the correlation times from ^{13}C relaxation measurements on cresols with the depolarized Rayleigh light-scattering experiments. Sazonov[146] has found linear correlation between the translational diffusion coefficient and the proton spin–lattice relaxation rates in a series of linear alcohols ranging from methanol to pentanol.

An alcohol which has received much attention because of its high viscosity at room temperature is glycerol. More than 20 years ago, Noack and Preissing[154] studied proton relaxation in glycerol at various temperatures, using the field-cycling technique and thus covering a very broad range of resonance frequencies. They were not able to interpret the data using the Cole–Davidson distribution of correlation times. In another early study, Kintzinger and Zeidler[155] separated the intra- and intermolecular contributions to the proton relaxation rate by using the isotopic dilution technique. They also performed their experiments at variable temperature and over a range of resonance frequencies. The Cole–Davidson distribution was found to rationalize the intramolecular relaxation data in a satisfactory manner, while attempts to interpret the intermolecular relaxation rates using the Torrey theory were unsuccessful. Their results were later successfully rationalized.[156] Wolfe and Jonas[157] studied deuteron spin–lattice relaxation rates of selectively

deuterated glycerols. These results could also be successfully interpreted using the Cole–Davidson distribution of correlation times, while the models allowing for internal and overall reorientation failed. James and coworkers[158] have proposed a rotating frame spin–lattice experiment in the presence of an off-resonance irradiation field as a method for studying moderately slow motions, such as those characterizing pure glycerol at $-20°C$. Their results were reinterpreted more recently by Bendel,[159] who included the translational motion in the analysis. Finally, Aparkin and Daragan[160] have investigated the ^{13}C relaxation in phenol as a function of temperature.

I now turn to other pure liquid studies, roughly in the order of increasing molecular size. Suchanski and Canepa[161] have reported deuteron and proton relaxation rates in liquid nitromethane. The inter- and intramolecular contributions were separated and the SR mechanism was identified as an important part of the proton spin–lattice relaxation. Halliday and coworkers[162] have derived the ^{14}N relaxation rates in ammonia, aminomethane and dimethylamine over a wide temperature range from the proton lineshapes. Rotational correlation times and activation energies were determined. The ^{13}C relaxation in liquid bromoethane has been investigated.[163] Ancian *et al.*[164] have studied the ^{17}O linewidth in acetone over a wide temperature range and found the molecular reorientation consistent with a hydrodynamic description using the slipping boundary condition; the ^{13}C relaxation in this compound was reported in an earlier study.[108] Daragan and coworkers[165] have reported ^{13}C measurements on 2-methylfuran and analysed the data in terms of anisotropic rotational diffusion and internal motion. Variable-temperature proton and ^{13}C T_1 data for liquid (and solid) 2,2-dichloropropane and 2,2-dibromopropane have been reported[166] and analysed in terms of effective rotational correlation times and the corresponding activation energies (see Section 2.3). Several groups have reported variable-temperature studies of tertiary butyl compounds, covering the liquid and solid range and concentrating mainly on liquid–solid and solid–solid phase transitions. Pettitt and coworkers[167] have investigated deuteron relaxation in t-butylbromide while Hasebe and Ohtani[168] have studied proton relaxation in the corresponding chloride. ^{13}C T_1 and linewidth data in t-butylbromide and cyanide have been reported,[169] as well as carbon and deuteron relaxation in both the chloride and the nitrate.[170] Aksnes and Ramstad[171] have reported proton and ^{13}C relaxation results for t-butylthiol. Moreover, carbon and deuteron relaxation in the same compound was investigated by Mooibroek and Wasylishen.[172] In a similar study, Mooibroek *et al.*[173] further reported measurements for t-butyliodide and aldehyde. The authors also reported ^{17}O T_1 measurements on the latter molecule.

Several authors have reported studies of similar compounds, with the central carbon atom replaced by a silicon. Geller *et al.*[174] have studied proton T_1 and the proton-coupled ^{13}C relaxation, as well as ^{13}C NOE, in tetramethylsilane at different temperatures. Storek[175] has reported variable temperature ^{13}C, ^{29}Si and ^{35}Cl relaxation measurements for trimethylchlorosilane. The silicon relaxation was found to be dominated by the SR mechanism and the overall and internal reorientation dynamics was discussed. Larsson *et al.*[176] have studied chlorodimethylsilane and dichloromethylsilane (as well as trichloromethylsilane which was mentioned in the inorganic section, Part 1). For the proton-bearing silicon nucleus, it was found that the DD and SR mechanisms contribute roughly equally to the spin–lattice relaxation rate. Some larger silicon organic systems have also been studied. Proton spin–lattice relaxation rates for solid and liquid hexamethyldisiloxane and decamethylcyclopentasiloxane have been reported.[177] Kowalewski and Berggren[178] measured ^{17}O, ^{29}Si and ^{13}C relaxation rates in another cyclic siloxane, octamethylcyclotetrasiloxane. The oxygen data (and quantum-chemical calculations) were used to obtain the overall rotational correlation times at different temperatures; the ^{13}C data were then used to provide information on the internal rotation of the methyl group. Moore *et al.*[179] have studied proton T_1 and $T_{1\rho}$ in liquid and solid octaphenylcyclotetrasiloxane. Another group of organic compounds containing the second-row atoms—the phosphonates, $R_1PO(OR_2)_2$—was studied by Ejchart *et al.*[180] They measured ^{31}P spin–lattice relaxation rates at a single temperature and analysed the intra- and intermolecular contributions to the DD relaxation rate by means of the isotopic dilution technique. Petr *et al.*[181] have combined ^{2}H, ^{13}C and ^{31}P spin–lattice relaxation measurements on n-hexane phosphonic acid diethyl ester over an extended temperature interval. The relaxation mechanisms for ^{31}P and the molecular dynamics were characterized.

Pajak and Szczesniak[182] studied the spin–lattice relaxation of different protons in liquid propionic acid and discussed the overall and internal rotational motion. The ^{13}C relaxation in solid and liquid 2,2-dimethylpropanoic acid has also been studied.[183] In the liquid state, it was found that the relaxation data were consistent with isotropic rotational motion. Richter and Zeidler[184] have studied pure liquid 18-crown-6 ether. They measured proton relaxation as a function of the content of deuterated material, temperature, and the magnetic field. Some deuteron relaxation rates were also reported. The intramolecular relaxation was interpreted in terms of extremely anisotropic rotational diffusion; the intermolecular proton relaxation rate was rationalized using several models. Ahlnäs *et al.*[185] have reported ^{13}C measurements for nonionic surfactants, the oligo(oxyethylene)dodecyl ethers, as neat liquids (and in water solutions). The neat liquids displayed field-

dependent T_1 values, which could be interpreted using the so-called two-step model (see Section 3.2). Martin and coworkers[186] have studied nematogen *p*-methoxybenzylidene-*p*-n-butylaniline at temperatures just above the isotropic–nematic phase transition using deuteron relaxation time measurements. It was found that T_2 displayed an unusual pretransitional behaviour, which was not observed for T_1. Finally, Quinn[187] and Ginsburg, Croll and coworkers[188] have reported variable-temperature ^{13}C T_1, linewidth and NOE measurements on neat liquid cholesterol esters. The results were interpreted in terms of anisotropic reorientational motion outside of the extreme narrowing region.

Additional data on pure liquids may also be found in the following section. It deals with relaxation studies on binary mixtures, but many of the papers mentioned also contain data on pure compounds.

2.2. Binary liquid mixtures and molecular dynamics of water in aqueous solutions of non-electrolytes

The description of a liquid mixture is more complicated than that of a one-component fluid. Thus, the work on mixtures usually aims at a more qualitative understanding. The discussion of the intramolecular relaxation and rotational motion is usually carried out in terms of effective correlation times and their variation with composition. The motional anisotropy or other fundamental aspects of molecular dynamics are usually treated, in the best case, in a semiquantitative way.

I begin this section by reviewing the work on mixtures containing water as one component. Early work in the field was reviewed by Zeidler.[189] An important early original work, concerned with several binary mixtures, that should be mentioned is the paper by von Goldammer and Hertz.[190] The conclusion arising from these studies was that the addition of nonelectrolytes at low concentration usually slowed down the water reorientation and enhanced the water structure. The dynamic behaviour of the nonaqueous component varied, depending on the strength of intermolecular interactions. More recently, some workers have considered aqueous mixtures of alcohols and carboxylic acids. The paper by Versmold[147] on methanol–water mixtures has already been mentioned above. Woznyi *et al.*[191] have studied the water nuclei relaxation and the proton relaxation in t-butanol in its mixtures with water. The mixture composition, temperature and pressure were varied. The association of t-butanol molecules was only observed in a certain temperature interval. Podenko *et al.*[192] have studied water proton relaxation in the mixture of ethylene glycol with water in the vicinity of the liquid–liquid phase separation. Hallenga and coworkers[193] presented dielectric relaxation data on aqueous solutions of alcohols and carboxylic acids, complemented

by some NMR relaxation work. Bjorholm and Jacobsen[194] have reported ^{13}C and deuteron relaxation measurements for mixtures of water with formic and acetic acids. The isotope effects on the relaxation rates were investigated (see below). Lankhorst *et al.*[195] have studied hydrogen exchange in aqueous solutions of carboxylic acids by means of T_1 and T_2 measurements for protons and deuterons.

A mixture that has attracted a great deal of attention throughout the years is that of water with dimethylsulphoxide (DMSO). I mention here only the work published during the 1980s. Baker and Jonas[196] have studied the pressure dependence of deuteron and proton T_1 in mixtures of DMSO with D_2O and of DMSO-d_6 with H_2O. They found that at low DMSO content the effect of the organic component was to enhance the water structure. In the same composition range, the initial application of pressure increased the motional freedom of the water. Another paper presented proton and deuteron relaxation investigations of the water–DMSO mixture at a single composition and pressure, but with varying magnetic field and temperature.[197] The relaxation dispersion (relaxation rate as a function of the magnetic field) data could not be explained in terms of the Woessner theory. Kowalewski and Kovacs[198] have studied ^{17}O and deuteron relaxation in a series of mixtures of deuterated compounds. The effective correlation times for both components were derived assuming the composition-independent quadrupole coupling constants (QCCs). The water reorientation was found to be isotropic for most compositions and temperatures, while the methyl groups in DMSO were found to display moderately fast internal motion. In another paper, Kovacs *et al.* [199] have studied the ^{33}S relaxation in the same mixture. Gordalla and Zeidler[200] have reported on ^{1}H relaxation in normal and ^{17}O enriched water and on deuteron relaxation of heavy water in mixtures with DMSO. Using the ^{17}O induced proton relaxation rates as the information source for the correlation time, they found the deuteron QCC to vary with composition, contrary to the assumptions of Kowalewski and Kovacs.[198]

Braun and Holz[201] have studied the ^{14}N spin–lattice relaxation in the acetonitrile–water system as a function of the mixture composition and have determined the correlation time for the tumbling motion. ^{17}O and ^{14}N studies of several simple amides have been reported[202] as a function of the composition in aqueous mixtures and effective correlation times were estimated. The mixtures of water with hexamethylphosphoric triamide (HMPT) were studied.[203] Intramolecular proton relaxation in aqueous solutions of deuterated dimethylformamide (DMF), HMPT and pyridine was studied as a function of temperature and magnetic field.[204] The mixture of pyridine (and of 2,4-dimethylpyridine) with water was also studied[205] and the ^{13}C relaxation data were compared with the results of depolarized Rayleigh scattering experiments. In another study[206] the molecular dynamics in the system were considered in the light of ^{13}C T_1 experiments and other physico-

chemical properties. Richardson *et al.*[207] have studied the water mobility in sucrose solutions using deuteron and ^{17}O measurements. Carlström and Halle[208] have reported ^{17}O longitudinal and transverse relaxation study of the dynamic state of water in aqueous solutions (and mesophases) of alkyl oligo(ethylene oxide) surfactants as a function of concentration and temperature. Yoshino *et al.*[209] have investigated the effect of a small amount of a volatile halogenated ether on the deuteron relaxation and molecular dynamics of heavy water.

The work mentioned above is centered around intramolecular dipolar or quadrupolar relaxation. Hertz and his group have developed a complementary approach, based on the studies of intermolecular dipolar relaxation rates in mixtures and the variation of these rates with composition. The details of the method are given in a review.[210] Briefly, one defines an association parameter A_{ij} for spins i and j:

$$A_{ij} = \left(\frac{1}{T_1}\right)_{i,\text{inter}(j)} \frac{D}{c'_j} \tag{1}$$

where $(1/T_1)_{i,\text{inter}(j)}$ is the intermolecular relaxation rate of nucleus i caused by the DD interaction with nucleus j, D is the mean self-diffusion coefficient of the molecules carrying spins i and j, and c'_j is the number density of spins j. In an ideal solution, A remains constant over the whole composition range. An increase in A with decreasing c'_j indicates association phenomena. The approach based on measurements of the association parameter was applied to a study of water mixtures with amides[211] and to aqueous mixtures of several small organic molecules.[212] Usually, the intermolecular relaxation rates were determined using the isotopic dilution technique. An alternative method was proposed by Smith and Ternai[213] who combined the conventional relaxation rate measurements with intermolecular proton–proton NOE experiments and applied the method to study water–pyridine mixtures.

I now turn to nonaqueous binary mixtures. The division of the material between this section and Sections 2.3–2.5 is somewhat arbitrary. The leading principle is that the work reviewed here should either use the mixture composition as a variable of primary importance or characterize the dynamic behaviour of both components in a roughly equimolar mixture. I begin the discussion with mixtures of nonpolar molecules, then proceed with the mixtures where one component is polar and finish with binary systems of polar molecules. Mikhailenko and Yakuba[214] have studied relaxation in liquid mixtures of methane and carbon tetrafluoride as a function of temperature and composition. Suhm *et al.*[215] have reported ^1H, ^2H, ^{13}C and ^{19}F relaxation measurements for binary mixtures of hexafluorobenzene with benzene and cyclohexane. The association phenomena were discussed. Mixtures of carbon tetrachloride with benzene, cyclohexane and dimethylsulphoxide

have been studied, determining the association parameters and the rotational correlation times.[216] Pajak *et al.*[217] have studied the proton relaxation and rotational diffusion of cyclohexene and cyclohexadiene in mixtures with carbon tetrachloride. The association parameter method was applied to the self-association of methanol in mixtures with CCl_4.[218] The same binary system was also studied by Hertz and Holz,[219] who used deuteron relaxation experiments. They found that the reorientation rate of the OD and the CD_3 groups became equal at high methanol dilution, while the reorientation of the hydroxyl was about ten times slower in pure alcohol. Similar studies were also reported on the methanol–cyclohexane systems, where Kratochwill[220] measured the deuteron relaxation rates and Cebe *et al.*[221] studied the intermolecular relaxation, and for methanol–benzene mixtures.[222] Koch and coworkers applied the association parameter method to study the association of acetic acid in CCl_4 and in cyclohexane[223] as well as to hydrogen bonding in the phenol–CCl_4 system.[224] Huntress' paper[82] on the benzene–chloroform mixture has already been mentioned above. Nikolaev[225] reported on proton and ^{13}C relaxation measurements on several polar compounds mixed with carbon tetrachloride and tin tetrachloride. Ratajczak and Ladd[226] have studied ^{14}N relaxation and interactions in mixtures of pyrrole with different solvents.

Jacobsen[227] has studied 1:1 binary mixtures of all possible pairs among methanol, acetone, DMSO, acetonitrile, benzene and water using ^{13}C and deuteron measurements. The goal of the study was to determine the isotope effects on correlation times, which were found to be sizeable in methyl groups. Kovacs *et al.*[228] have reported a multinuclear (^2H, ^{13}C, ^{14}N and ^{35}Cl) relaxation study of mixtures of two symmetric tops, perdeuterated acetonitrile and chloroform. The variation in the tumbling motion of both species with the composition was explained in terms of intermolecular forces. The relaxation rates of the nuclei residing off the symmetry axis were used to test dynamic models for rotational motion. The J diffusion model was found to be unsatisfactory. The same binary system was also studied by Tokuhiro,[229] who used the deuteron and ^{14}N relaxation data. The trends in the data were similar, but their interpretation differed from the work of Kovacs *et al.*[228] Leiter *et al.*[230] reported proton and deuteron relaxation rates in mixtures of acetonitrile with formamide and *N*-methylformamide. By preparing selectively deuterated species, the authors were able to measure and interpret the association parameters for different protons in formamide. Hertz *et al.*[231] have studied proton relaxation in mixtures of ethanol (of different isotopic composition) with glycerol at low temperatures. As opposed to the case of pure ethanol, the double minima due to internal motion were observed in the relaxation vs. inverse temperature curves (see Fig. 2). For comparison, mixtures of methanol and isopropanol with glycerol were also studied. Finally,

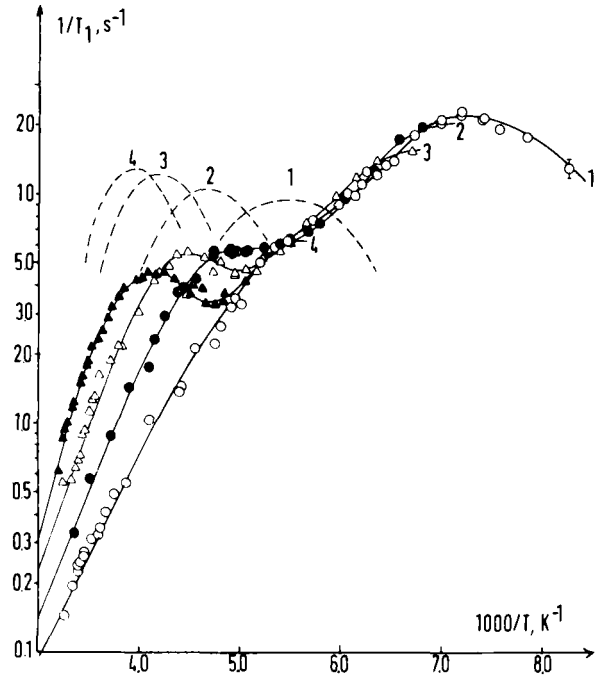

Fig. 2. Proton relaxation rates of CH_3CD_2OD in mixtures with deuterated glycerol (mole fractions ethanol:0.81 (○, curve 1), 0.60 (●, curve 2), 0.40 (△, curve 3), 0.21 (▲, curve 4)) as a function of reciprocal temperature. (– – – –) The relaxation rates of hydroxyl protons in mixtures of similar compositions, but containing the isotopic species CD_3CD_2OH. (Reproduced with permission from Hertz *et al.*[231])

field- and temperature-dependent proton relaxation data on DMSO have been presented in mixtures with acetic acid and methanol as well as on protons and deuterons in the other component.[232] The form of the rotational time correlation functions was discussed.

2.3. ^{13}C and ^{2}H relaxation in organic solutes

The reason for collecting the ^{13}C and deuteron relaxation measurements in a common section is that the two nuclei provide essentially identical information when applied to low-molecular-weight molecules in low-viscosity solutions. The ^{13}C spin–lattice relaxation of proton-bearing carbons is usually dominated by the DD mechanism. Assume the following:

(i) extreme narrowing conditions;

(ii) broadband proton decoupling;
(iii) negligible cross-correlation effects;
(iv) negligible contributions from distant (not directly bonded) protons and from all other nuclei.

The spin–lattice relaxation under these conditions is a simple exponential process with the rate given by the relation:

$$1/T_{1DD} = n_H(DCC)^2\tau_{eff} \tag{2}$$

where n_H is the number of directly bonded protons, τ_{eff} is the effective correlation time, and DCC denotes the dipolar coupling constant:

$$DCC = (\mu_0/4\pi)\gamma_C\gamma_H\hbar/r_{CH}^3 \tag{3}$$

where μ_0 is the permeability of vacuum, γ_C and γ_H are the magnetogyric ratios of ^{13}C and ^{1}H, respectively, and r_{CH} is the carbon–proton distance. The carbon–proton distances do not vary much and the DCC can usually be assumed to be known. Thus, the measurement of $1/T_{1DD}$ (which may require two experiments, a T_1 determination and a NOE measurement, see Sections 3.1 and 3.3 of Part 1) yields immediately the effective correlation time. Similarly, the quadrupolar deuteron ($I = 1$) spin–lattice relaxation rate, under extreme narrowing conditions and neglecting the asymmetry of the field gradient, is given by

$$1/T_{1Q} = \tfrac{3}{8}(QCC)^2\tau_{eff} \tag{4}$$

The quadrupole coupling constant (QCC) can also usually be assumed known (an extensive list of the deuteron QCCs was given by Loewenstein[233]) and the relaxation rate provides the correlation time. Moreover, the principal axes of the quadrupolar interaction (of a deuteron bonded to carbon) and of the carbon–proton DD interaction coincide, which makes the τ_{eff} in (2) and (4) very similar to each other even under anisotropic motion. The close analogy of the ^{13}C and deuteron relaxation was first discussed by Saito *et al.*[234] as early as 1973. The same year, Spiess *et al.*[127] found in their study of toluene that the correlation times obtained from ^{13}C (in the compounds of natural isotopic composition among hydrogen isotopes) and from deuterons in the deuterium enriched material differed, particularly in the methyl group. The deuterium isotope effects on the rotational correlation times were subsequently studied by Jacobsen and coworkers.[194,227,235] Even more recently, Söderman[236] has discussed the ratio of the ^{13}C and deuteron interaction constants based on the data on specifically deuterated and protonated sodium hexanoate.

Whichever of the two nuclei is selected as the source of the effective correlation time, it is common that temperature is used as a variable in a series of experiments. As mentioned in Section 5.1 of Part 1, it is also common to

interpret the temperature dependence of the correlation time in terms of an "Arrhenius equation". $\tau_{eff} = \tau^0_{eff} \exp(E_a/RT)$. In some other cases, the τ_{eff} is interpreted in terms of the rotational diffusion constants and the Arrhenius-type equation is applied to those physically more fundamental quantities.

Several review articles of relevance to this section should be mentioned. The earlier ^{13}C work was reviewed by Wehrli[237] and Wright *et al.*[65] Lambert *et al.*[238] have reviewed the measurement of spin–lattice relaxation as a tool for studying the kinetics of intramolecular reactions. The general problems related to the internal motion were discussed in a review by Hertz.[149] Kövér and Batta[239] have covered the heteronuclear Overhauser experiments and selective ^{13}C T_1 measurements as a tool for determining interatomic distances. Dölle and Bloom[240] have reviewed studies of anisotropic motion, focusing on the orientation of the rotational diffusion tensor. Finally, Smith has reviewed the applications of deuteron NMR, including relaxation studies.[241]

The organization of this section, covering a large number of references, is as follows. The chemical nature of the studied solutes is used as the criterion for dividing the work into four subsections covering the aliphatic, alicyclic, aromatic and heterocyclic systems, respectively. Within each subsection I begin with the work on small, rigid molecules, where the goals of the investigations are not very different from those in pure liquids, and proceed to larger systems which are studied in a more qualitative fashion. Work on certain important classes of compounds (amino acids, peptides and carbohydrates) is grouped together.

2.3.1. Aliphatic solutes

Some papers have dealt with the relaxation in small, highly symmetric molecules in solution. Ancian *et al.*[242] have studied ^{13}C (and the quadrupolar nuclei) relaxation in the spherical-top carbon tetrachloride and linear carbon disulphide molecules, dissolved in alkanes. The viscosity dependence of the unique (by symmetry) correlation time and the models for the reorientational dynamics were discussed. In another paper on the same systems and by the same group,[243] the authors studied the intermolecular $^{13}C-\{^1H\}$ NOE, proving the occurrence of the intermolecular DD relaxation. Vold and coworkers[244] have studied ^{13}C (and ^{114}N) relaxation in the linear dicyanoacetylene molecule in hydrocarbon solvents. The relaxation mechanisms for both types of carbon were analysed. Deuteron (and ^{14}N) relaxation in symmetric tops acetonitrile-d_3 and deuterochloroform dissolved in viscous liquids has been studied as a function of temperature and the magnetic field.[245] The viscosity dependence and the local ordering effects were discussed. Gregory *et al.*[246] have determined the deuteron QCC for deuterochloroform in various solvents by combining the deuteron relaxation rates with Raman lineshape analysis. A

substantial lowering of the QCC was observed in the polar solvents. The same group also reported a similar study for 3,3-dimethyl-1-butyne with acetylenic proton replaced by a deuteron.[247]

Two groups have studied dichloromethane in solution. Chenon and coworkers[248] have investigated the proton-coupled ^{13}C relaxation in ^{13}C enriched material dissolved in carbon disulphide at different temperatures. The results were analysed in terms of the small-step rotational diffusion and discussed in the light of current theories of liquid diffusion. Chenon *et al.*[249] have also performed similar measurements in acetone and acetone-d_6 solutions, and discussed the differences caused by the isotopic composition of the solvent. Rodriguez *et al.*[250] have reported conventional proton-decoupled ^{13}C T_1 and NOE experiments on dichloromethane in various solvents and discussed the results in terms of hydrodynamic models. A similar compound, diiodomethane (and some other iodoorganic compounds) was studied by Mlynarik[251] who measured ^{13}C T_1 at different fields as well as the NOE and $T_{1\rho}$. In this way, he was able to separate the scalar and dipolar contributions to the relaxation rates and to determine the relaxation rates for ^{127}I and the carbon–iodine coupling constants. Two other rigid, asymmetric tops have been studied. Levy and Bailey[252] have studied the ^{13}C relaxation and effective correlation time for the formate ion in different solvents. Nery *et al.*[253] have studied the ^{13}C spin–lattice relaxation in acrylonitrile in solution. The proton and ^{14}N relaxation rates were also reported and the information available discussed.

We turn now to molecules with internal degrees of freedom and begin by discussing hydrocarbons. Seidman and coworkers[254] have studied deuteron relaxation in perdeuterated tetracosane, $CD_3(CD_2)_{22}CD_3$, in carbon tetrachloride solution. The deuteron nuclei at different positions along the chain had nearly the same chemical shift but different relaxation rates because of a varying number of internal rotations. This resulted in an unresolved band, characterized by a strong multiexponential decay, which the authors were able to analyse. Brown *et al.*[255] have reported a proton-coupled ^{13}C relaxation study of selectively labelled nonane, $C_4D_9{}^{13}CH_2C_4D_9$, and heneicosane, $C_{10}D_{21}{}^{13}CH_2C_{10}D_{21}$ in solution. Various spectral densities were derived, from selective and nonselective experiments, and compared with the Brownian dynamics simulations.

Several papers have dealt with alcohols in solution. Dais and coworkers[256] have reported ^{13}C relaxation of n-butanol and t-butanol in very dilute cyclohexane solutions. Molecular clustering was discussed. Sweeting and Becker[257] have presented a similar study of t-butanol, but were able to decrease the alcohol concentration even further. Daragan and Ilina[258,259] have studied ^{13}C relaxation in ethanol, ethylene glycol and glycerol (as well as dioxane and several sugars) in DMSO and in aqueous solution. Levy *et al.*[260]

have studied ^{13}C relaxation in long-chain diols and triols (as well as some polymers) and interpreted the data using a model involving the combination of internal librations and the distribution of correlation times. Finally, Williamson *et al.*[261] have studied ^{13}C relaxation in several isomeric alcohols. An empirical additivity relationship for T_1 was derived.

Turning to other aliphatic compounds, I begin with the work aimed at quantitative or semiquantitative understanding of the internal rotation of methyl groups. Lambert and Nienhuis[262] have measured ^{13}C dipolar spin–lattice relaxation rates and applied the Woessner model (see Section 2.4 of Part 1) to derive the internal rotation rates for methyl groups in substituted propenes and toluenes. The methyl jump rate, R_i, at a single temperature was then related to the barrier height, V_0, following the relation[263]

$$R_i = \frac{3}{2}\left(\frac{kI}{I}\right)^{1/2} \exp(-V_0/kT) \tag{5}$$

where I is the moment of inertia of a methyl group. This approach, or a similar one using the internal diffusion coefficient, D_i, instead of R_i, was common in earlier relaxation work on methyl rotation. Kakihana *et al.*[264] have studied ^{13}C relaxation and methyl reorientation in the acetate ion. The Woessner model was also used here, but the measurements were performed at variable temperature and an Arrhenius relation for the internal diffusion constant D_i was used in the manner proposed earlier for the case of deuteron and ^{13}C relaxation,[265]

$$D_i = A \exp(-E_a/kT) \tag{6}$$

This approach uses both A and E_a as parameters to be fitted to a variable-temperature series of experiments. Gryff-Keller and Poppe[266] have reported multinuclear measurements for (*E*)- and (*Z*)-methyl groups in *N,N*-dimethylamides. In particular, the classical case of *N,N*-dimethylformamide (studied earlier by, among others, Wallach and Huntress[267] and Daragan *et al.*[268]) was analysed carefully and the effects of different approximations discussed. The main conclusion was that, as long as the D_i values are treated as semiquantitative estimates, it is acceptable to assume the overall reorientation to be isotropic.

I now turn to other work on aliphatic systems and begin with papers reporting relaxation mechanisms and relaxation experiments other than the usual T_1 measurements. Fuson and Prestegard[269] have studied proton-coupled ^{13}C relaxation in malonic acid in DMSO solution. The analysis of the recovery curves included the dipolar autocorrelation and cross-correlation spectral densities, as well as the random field terms. The description of the motion of the molecule in terms of an axially symmetric diffusion tensor was consistent with the data. Jaccard *et al.*[270] have studied a solution of

methyl formate, using a novel technique involving the creation of the two-spin order. The method permitted the estimation of the cross-correlation spectral density arising from the interference of the chemical shift anisotropy (CSA) and the DD interactions. Sterk and Mittelbach[271] have studied the relaxation behaviour of the nitrile groups. They found the CSA contributions to be dominant even at the rather low magnetic field of 4.7 T, T_{1DD} and T_{1SR} were also estimated. Moreover, the same group[272] have studied the relaxation mechanisms of the carbonyl carbon in a series of aliphatic, alicyclic and aromatic ketones. In small aliphatic molecules, the SR mechanism was predominant, while DD and CSA competed for the aromatic systems. Kelly *et al.*[273] have studied the relaxation mechanisms in the t-butyl cation in a superacid solution and found, for the case of the cationic carbon, an important contribution from the CSA mechanism even at low field. Mlynarik has reported $T_{1\rho}$ measurements on amines[274] and chlorine containing molecules.[275] The difference between the relaxation in the rotating frame and the conventional T_1^{-1} gave the scalar relaxation rate and allowed the determination of the scalar coupling constants and the relaxation rates of the quadrupolar nuclei. Hayashi *et al.*[276] have studied ^{13}C spin–lattice relaxation in several bromine containing organic compounds. The revovery curves in an inversion-recovery experiment on carbons bonded to bromine were found to be biexponential, because of the difference in the efficiency of ^{79}Br and ^{81}Br in providing the scalar T_1 relaxation pathway (the same problem was discussed in some of the papers on bromine containing pure liquids[75,79,167,169]). Moreover, the DD contributions to T_1^{-1} were separated by NOE measurements.

Turning now to the measurements of the DD dominated ^{13}C spin–lattice relaxation, we begin with the paper by Brunn *et al.*[277] who studied the solvent effects on the relaxation rates in vinylacetate and ethylacetate. Vuik *et al.*[278] have studied ^{13}C relaxation in aldehydes and aldehyde oximes. The data were interpreted in terms of self-association and segmental motion. Chin Yu and Levy[279] have studied ^{13}C (and ^{15}N) relaxation in pentane-2,4-diamine. Levy *et al.*[280] also studied ^{13}C relaxation in aliphatic diastereoisomers with asymmetric centres, 2,3-disubstituted butanes and 5,6-disubstituted n-decanes, in different solvents. The results were related to conformational properties. The ^{13}C T_1 and effective correlation times have been reported[281,282] for several chlorinated alkanes. Ng[283] has studied a large number of small aliphatic compounds and found that the terminal methyl carbon of the n-propyl fragment bonded to an electronegative atom displayed reduced T_1 values. Okubo *et al.*[284] have used ^{13}C T_1 as an indicator for the assignment of terminal *cis* and *trans* methyl groups in the 2-methyl-1-propenyl moiety. In a similar vein, Bernassau and Fetizon[285] reported ^{13}C T_1 data for several fatty acids and esters and used the results to assign resonances and locate double

bonds along the chain. Ranadive and coworkers[286] have studied the ^{13}C relaxation in a long-chain unsaturated molecule, squalene oxide, and discussed its mobility. Hosur and Govil[287] have measured $^{13}C\,T_1$ in glyceryl trivalerate as a function of concentration in chloroform solution.

Two groups have studied ^{13}C relaxation in tetraalkylammonium salts. Dando *et al.* studied various symmetric salts in acetonitrile solutions and used the concentration dependence of the T_1 values for assignment purposes[288] and to elucidate the solute–solvent interactions.[289] Coletta and coworkers[290,291] have reported ^{13}C relaxation studies of several symmetric tetraalkylammonium salts in different solvents. The results were interpreted using recently developed theoretical models, considering the overall reorientation and internal conformational transitions. Some ^{13}C relaxation data were also reported for aliphatic compounds containing second-row atoms. This work is reviewed in Section 2.5 in connection with the relaxation of heteronuclei.

In the final part of this subsection I review the ^{13}C and ^{2}H relaxation studies on amino acids and peptides. For consistency, the work on the common peptide-building aromatic and heterocyclic amino acids is also included here. Nery and Canet[292] have studied longitudinal ^{13}C relaxation in doubly enriched (in ^{13}C and ^{2}H) glycine. By combining the results obtained from this isotopic species with the more common ones, the authors were able to derive the spectral densities for the dipolar CC and CH interactions as well as the random field contributions and the interference terms involving the CSA interactions. The carbon relaxation in the uniformly ^{13}C enriched glycine and aspartic acid was studied and reported in another paper by the same group.[293] It was observed that the inversion-recovery experiments could be interpreted on the basis of Solomon equations (see Section 2.2 of Part 1), but that the explanation of the NOE results required including the DD–CSA interference terms. In the paper already mentioned above, Nirmala and Wagner[19] have measured the ^{13}C spin–spin relaxation rates in alanine, ^{13}C enriched in either the α or β positions.

Turning now to more conventional $^{13}C\,T_1$ experiments, I begin with ^{13}C (and ^{1}H) relaxation study in glycine.[294] Van Havebeke *et al.*[295] have reported deuteron relaxation measurements in deuterated glycine and alanine as a function of pH and related the results to the intra- and intermolecular interactions. Pogliani *et al.*[296] have studied ^{13}C relaxation in serine, threonine, their phospho derivatives and some small peptides. The empirical relations between the relaxation rate and the molecular weight were tested. Gaggelli *et al.*[297] have reported $^{13}C\,T_1$ (and proton relaxation rates) for mandelylaspargine and related compounds. The molecular dynamics were discussed. Inoue and coworkers have studied the inclusion complexes between phenylalanine and cycloamylose[298] and methylated cyclodextrin.[299] Bleich *et al.*[300] have studied the rotational diffusion properties of peptides. They

concluded that the near equality of observed relaxation rates for different α carbons might hide marked rotational anisotropy. The ^{13}C T_1 data for the α carbons in cyclic octapeptides have been reported.[301] Howarth and Yun Lian[302] have studied gramicidin-S and the glutathione dimer and interpreted the data in terms of a model involving molecular motions at three levels. Gramicidin-S was also studied[303] by combining ^{13}C T_1 measurements with selective ^{13}C–$\{^1H\}$ NOE experiments to estimate the conformation of the molecule in the DMSO solution. In another paper from the same group[304] the ^{13}C relaxation data on another peptide were combined with proton relaxation and NOE measurements to provide structural information. The work on larger peptides and proteins is discussed in Section 3.3.

2.3.2. Alicyclic solutes

Alicyclic compounds deserve a section of their own, not so much because of the large number of papers, but rather due to the large percentage of advanced and highly interesting work. Cyclic hydrocarbons and their derivatives are attractive model systems for studies of anisotropic motion, because of their rigid structures and their large number of independent CH axes. Indeed, the first applications of the fully anisotropic rotational diffusion model (but assuming the coincidence of the inertial and diffusion principal axis systems) to the analysis of ^{13}C relaxation rates, presented by Berger[305] in the mid-1970s dealt with molecules of this type.

I begin this section by reviewing the work on monocyclic compounds and proceed with polycyclic systems. Brown *et al.*[306] have reported a variable-temperature study of a selectively labelled cyclopropane, enriched in ^{13}C at one position and deuterated at the other two carbon atoms. The resulting AX_2 spin system was subjected to selective and nonselective carbon and proton 180° pulses and the recovery curves were analysed in terms of the small-step rotational diffusion of a symmetric top. Other three-membered ring systems, derivates of chrysantemic acids, were studied by means of conventional ^{13}C T_1 measurements.[307] Costas *et al.*[308] have reported a variable-temperature deuteron T_1 study of cyclopentane-d_{10} (and some measurements for cyclohexane-d_{12}) in different alkane solutions and related their results to thermodynamic properties of mixtures. Chin Yu *et al.*[309] have reported ^{13}C and ^{15}N T_1 data on isomers of 1,3,5-triaminocyclohexane. The pH was varied and the results were found to be consistent with the isotropic overall reorientation of the carbon skeleton. Jost and Sommer[310] have reported ^{13}C T_1 values for 2-bromocyclohexanone, protonated in superacid media, as a function of temperature and acidity. Finally, Pattaroni and Lauterwein[311] have studied ^{13}C relaxation in all-*trans* retinal at two magnetic fields and discussed the role of the CSA mechanism. The CSA was found to be important

for quaternary carbons, while the dipolar mechanism dominated for the proton-bearing carbon nuclei.

Bicyclic compounds have attracted considerable attention which resulted in several interesting papers. Axelson and Holloway[312] have analysed $^{13}CT_1$ data in several bicyclic hydrocarbons using the anisotropic diffusion model (with coinciding inertial and diffusion principal-axis systems) and discussed the magnitude of errors in the three diffusion constants. Moseley[313] has reported $^{13}CT_1$ data for *trans*-decalin in several solvents. The fully anisotropic rotational diffusion results were discussed in view of hydrodynamic models. Stilbs and Moseley[314] have noted that the assumption about the coincident axis systems may be incorrect in the presence of strong intermolecular forces, using the data on borneol in different solvents as an example. Beierbeck *et al.*[315] have studied ^{13}C relaxation in norbornane and adamantane derivatives. They treated the data in terms of a symmetric-top diffusion model, but tested different possible locations of the main diffusion axis in the molecular frame. Moreover, they studied internal rotation barriers for methyl groups in some of the compounds by determining the methyl jump rates at a single temperature and employing (5). Ericsson *et al.*[265] measured $^{13}CT_1$ values in four terpenes as a function of temperature. The overall motion was treated as isotropic rotational diffusion and the D_i values for methyl groups were derived. They argued that a more accurate estimate of the methyl barriers could be obtained by employing (6), i.e. by actually fitting the variable-temperature D_i (or R_i) data to an Arrhenius equation with both the activation energy and the preexponential factor as parameters, and by identifying the E_a with the barrier height.[316] The experimental data of Ericsson *et al.*[265] were used by Newman[317] who investigated the effect of explicitly including the torsional vibrations on the apparent values of the activation energy. Bernassau and coworkers[318] have studied a series of methyl containing terpenes and steroids. They treated the overall reorientation as fully anisotropic rotational diffusion without any assumptions being made about the principal-axis system. The methyl group rotation was characterized by an internal rotational diffusion constant, the logarithm of which was found (in agreement with (5)) to correlate with the barrier height calculated using molecular mechanics (MM2) (cf. Fig. 3). In a more qualitative application of $^{13}CT_1$ relaxation data in bicyclooctanols, Zahra *et al.*[319] have studied solute–solvent interactions in different solvents.

Among tricyclic compounds, adamantane and its derivatives attracted considerable attention. The parent compound itself is a spherical top and, therefore, an interesting model for the discussion of various aspects of molecular dynamics in solution. The first $^{13}CT_1$ measurement for adamantane solutions were reported almost 20 years ago.[320] Wasylishen and Pettitt[321] have reported a variable temperature deuteron relaxation study of

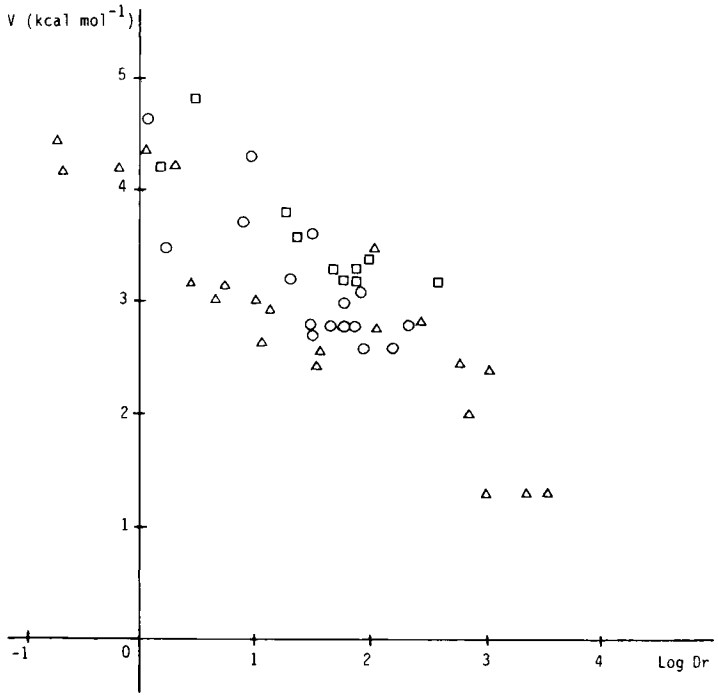

Fig. 3. Plot of methyl rotation barrier vs. internal rotation diffusion constant for steroids (□), monoterpenes (△) and diterpenes (○). (Reproduced with permisssion from Bernassau *et al.*[318])

adamantane dissolved in halomethanes. The rotational correlation times were discussed in terms of small-step vs. large-step (extended) diffusion, slipping vs. sticking boundary in the hydrodynamic description, etc. A similar study of adamantane motion in hydrocarbon solutions has also been presented.[322] Ancian and Tiffon[323] have studied ^{13}C, ^{1}H and ^{2}H relaxation in adamantane in carbon tetrachloride and chloroform solutions, and derived the deuteron QCCs. A combined ^{13}C and proton relaxation study was also reported.[294] Brondeau and coworkers[324] have used the adamantane solution as a model system in their study of the time evolution of methylene carbon multiplet asymmetry after a perturbation, which was shown to provide cross-correlation spectral densities. Adamantanes substituted in position 1 become symmetric tops and their anisotropic diffusion has been studied.[325–327] Gerhards and coworkers[328] have studied $^{13}C\,T_1$ in 2-substituted adamantanes and used the data for assignment purposes. Disubstituted adamantanes were also studied.[315]

The molecular dynamics of less symmetric tricyclic systems, e.g. tricyclo-[3.1.0.0]hexanes, have been studied by Mellink and Kaptein,[329] who treated, the overall reorientation as isotropic and studied internal methyl rotation at a single temperature. More sophisticated studies have also been reported in which the overall rotational diffusion of podacarpane derivatives and steroids is analysed in terms of the fully asymmetric model; this includes the internal rotation of methyl groups.[330-333] The linear relation between the logarithm of the internal rotation diffusion constant and the MM2 barrier height, illustrated in Fig. 3, was also applied.[332,333] Finally, Murari and coworkers[334] have reported deuteron spin–lattice relaxation rates in selectively deuterated cholesterol derivatives in various solvents. The dependence of the correlation times on viscosity was studied and the motional anisotropy discussed.

At the end of this section on alicyclic compounds, and just before turning to the aromatic systems, I wish to mention some papers dealing with molecules containing both an alicyclic and an aromatic part. Harris and Newman[335] have investigated ^{13}C relaxation in 1-phenyladamantane in various solvents and treated the data using the rotational diffusion model for rigid, symmetric tops, but allowed each moiety to have its own diffusion constant parallel to the symmetry axis. The differences between $D_{\|}$ for the two parts of the molecule were found to be solvent dependent. Kolodziejski and Laszlo[336] have studied the $^{13}CT_1$ data for the same compound as well as for 1,3-diphenyl-adamantane. Craik and coworkers[337] have reported $^{13}CT_1$ measurements for similar compounds, substituted phenylbicyclo[2.2.2]octanes. They interpreted the data in terms of a model including the symmetric top overall rotation and internal motion.

Compounds in which the phenyl ring is fused with a saturated, bicyclic fragment have also attracted some attention. Two groups studied almost identical benzonorbornyl derivatives. Levy and coworkers[338] have studied the $^{13}CT_1$ data as a function of temperature and analysed the results in terms of anisotropic rotational diffusion, assuming the principal-axis systems of the inertial and diffusion tensors to coincide. Dölle and Bluhm[339,340] have studied a derivative with two methyl groups and analysed the results allowing for the two principal axis systems to be displaced relative to each other. In addition, the internal motion of the methyl group was considered. Finally, Rabideau and coworkers[341] have reported some $^{13}CT_1$ results for isopropyl substituted 9,10-dihydroanthracenes.

2.3.3. Aromatic solutes

Among the early ^{13}C work on aromatic systems, I wish to single out the seminal paper by Levy *et al.*[342] which covers the essential aspects of relaxation

mechanisms and of molecular dynamics of substituted benzenes in solution. In this section I begin with benzene and substituted benzenes, continue with systems containing several nonfused rings (molecules such as biphenyl) and finish with fused ring systems (e.g. naphthalene).

Substituted benzenes have attracted the attention of numerous authors. I begin here with work done on benzene itself, halobenzenes and other rigid benzene derivatives. Daragan and coworkers[343] have reported rotational correlation obtained from ^{13}C T_1 measurements and from theoretical calculations on benzene, some halobenzenes, and other singly and doubly substituted benzenes. Variable-temperature deuteron T_1 values for benzene in toluene and DMF solutions have been reported[344] and the influence of weak intermolecular interactions on rotational motion discussed in terms of hydrodynamics. Maitra[345] has studied the dynamic behaviour of benzene solubilized in inverse micelles (in the water–aerosol OT–isooctane system) using deuteron relaxation and discussed intermolecular interactions. Rudakoff and Oehme[346] have studied deuteron and ^{19}F relaxation in fluorobenzene in DMF and toluene as solvents. Reorientational and angular momentum correlation times were determined. The ^{13}C relaxation data in several polyfluorobenzenes (and toluenes) was studied[347] and analysed to give relaxation mechanisms and effective correlation times. Lee and McClung[348] have reported ^{19}F and deuteron spin–lattice relaxation times for 1,3,5-trifluorobenzene-d_3 in various solvents and as a function of temperature. They have derived the reorientational and angular momentum correlation times and compared the results with the extended J diffusion and the Fokker–Planck–Langevin (FPL) models. It was found that the rotational motion was better described by the FPL model allowing for different correlation times of angular velocity components along and perpendicular to the symmetric-top axis. Königsberger and Sterk[349] have studied proton-coupled ^{13}C relaxation of the CH carbon in pentachlorobenzene and analysed the motional anisotropy taking into consideration the DD–CSA interference terms. Chen and coworkers[350] have studied the ^{13}C relaxation of proton-bearing carbons in 1,3,5-tribromobenzene in a number of solvents of widely varying viscosity. The derived correlation times were discussed in view of different hydrodynamic theories. The same authors[351] also reported infra-red (IR) and Raman studies on some of the solutions and found the dynamic information from these methods to agree with the NMR data.

Two groups have studied phenylacetylene. Farrar and coworkers[352] have studied the differential line broadening (DLB) for various carbon doublets as a function of temperature and magnetic field. The DLB is caused by the interference of the DD and CSA interactions. Benn[353] has studied the relaxation of the ^{13}C satellites in the compound and found them to relax significantly faster than the corresponding central signals. Proton-coupled

and proton-decoupled ^{13}C relaxation in cinnamic acid and methyl cinnamate has been investigated and the anisotropic rotational diffusion coefficients determined.[354] Mlynarik[355] has measured $T_{1\rho}$ of carbons and protons in nitroanilines and thus determined the quadrupolar relaxation rates of ^{14}N and the coupling constants to the amine nitrogen. Tao Ji *et al.*[356] have studied ^{13}C T_1 data in butylaniline. Jackman *et al.*[357] have reported ^{13}C T_1 for several intramolecularly hydrogen-bonded aromatic systems and analysed the motional anisotropy. In addition, they have measured relaxation rates of deuterons involved in hydrogen bonds and, by coupling these data with the dynamic information from ^{13}C, determined the QCCs. Ford *et al.*[358] have proposed a method, based on the selective ^{13}C–$\{^1H\}$ NOEs for quaternary carbons, for studying the carbon–proton distances in several hydrogen-bonded aromatic systems. In a subsequent paper, Niccolai and coworkers[359] have developed the approach further by combining the selective NOEs with ^{13}C T_1 measurements and tested their approach on salicylaldehyde. A two-dimensional version of the experiment was more recently applied to a larger aromatic molecule, procaine.[360] The relaxation properties of quaternary carbons were studied earlier by Shapiro and Kahle[361] who investigated the effect of deuterium substitution on the relaxation rates; it was shown how this could provide structural information using benzamide as an example. Norton[362] has reported a similar, but somewhat more quantitative, study of the same compound using the same method. Malterud and Anthonsen[363] have measured ^{13}C T_1 values for the quaternary carbons in 15 partially *O*-methylated phenols and found the results to be a useful tool for signal assignment. ^{13}C T_1 measurements as an assignment tool were also used in work on phenyl acetates.[364]

I now turn to work addressing the problem of the internal motion of substituents. Lambert *et al.*[365] have studied the methyl rotation barrier in toluene and its *para* substituted derivatives. The overall motion was described as isotropic or symmetric top rotational diffusion and the methyl diffusion rate, D_i, at a single temperature was evaluated and related to the barrier height using (5). Dupeyre and Beguin[366] have studied variable-temperature deuteron relaxation in deuterated benzylfluoride in several solvents and evaluated the internal rotation barrier using (6). Ribeiro–Claro and coworkers[367] have studied $C_6H_5CHCl_2$ in solution and reported a variable-temperature ^{13}C T_1 study of the overall reorientation (assumed to follow the equations for a symmetric top) and the internal rotation barrier (evaluated using (6)). In another paper,[368] the same authors reported ^{13}C T_1 data on C_6H_5X molecules, with $X = CH_3$, CH_2Cl, CCl_3 or CCH_3, and compared the results with Raman bandshape analysis. Jo Woong Lee *et al.*[369] have studied the temperature dependence of ^{13}C T_1 data in *p*-xylene derivatives with an additional ring substituent, with particular reference to the internal motion and SR relaxation

of the methyl carbons. Azancheev *et al.*[370] have studied molecular motions, including the internal methyl rotation, in some phthalic acid esters. Andersson and coworkers[371] have used $^{13}C\,T_1$ measurements to determine the barrier to internal rotation of neopentyl groups in 1,3,5-trineopentylbenzene. The Woessner model was used to obtain the internal motion rate constant and the Eyring equation to yield the free energy of activation for the process. Moreover, the deuteron relaxation measurements on the deuterated compound were reported and used to provide the deuteron QCCs. More recently, the same authors have studied ^{13}C relaxation in 2,4,6-trialkyl substituted styrenes and related systems.[372] The internal motions were treated using a model based on multiple rotations of restricted amplitude (see Section 2.4 of Part 1). Huet and Zimmermann[373] have studied the molecular dynamics of unsaturated enol ethers using $^{13}C\,T_1$ measurements and including in the analysis the overall reorientation (of a symmetric top) and internal methyl rotation. In some cases, the methyl barriers were derived using (5). Makriyannis and Knittel[374] have measured $^{13}C\,T_1$ data for the methyl carbons in some methoxybenzenes. They found large differences in the relaxation rates of different methoxy groups within the same compound and explained the observation by a more hindered internal rotation of the groups with the OC bond (in the OCH_3 group) in the ring plane compared to the OC bond perpendicular to the plane. Makriyannis and coworkers[375] subsequently used the methoxy carbon $^{13}C\,T_1$ measurements as a tool in conformational studies.

Next, I turn to molecules containing several phenyl groups and begin with the simplest of such systems, biphenyl. Akiyama *et al.*[376] have studied deuteron spin–lattice relaxation in fully deuterated biphenyl in DMSO solution. The dynamics were modelled using the Woessner theory for symmetric tops with internal motion (the number of independent observations was not really sufficient for that and simplifying assumptions concerning the two overall rotational diffusion constants had to be introduced) and (6) was used to estimate the barrier for internal rotation. The NMR results were combined with IR measurements to provide the potential function for the internal motion. The ^{13}C relaxation in biphenyl has also been studied,[342,377] while Rudakoff and Oehme[378] have investigated the overall and internal motion in 3-chlorobiphenyl. London and Phillippi[379] have studied $^{13}C\,T_1$ data for 1,3,5-triphenylbenzene in chloroform solution at variable temperature and tested different dynamic models. The differences between various carbons could not be readily explained by anisotropic tumbling of a rigid molecule, while models including internal jumps were more satisfactory.

Several groups have presented studies of systems of the type Ph–X–Ph in which the two phenyl moieties are separated by an atom or group of atoms. The ^{13}C relaxation in several such systems with different X has been

studied by Dais.[380] The analysis employed models including the internal phenyl rotation superimposed on the isotropic and anisotropic overall rotational diffusion. The barrier heights for the phenyl rotation were estimated using single temperature results and a modification of (5). Harris and Newman[381] have studied ^{13}C (and ^{29}Si) T_1 data in a series of compounds of general formula Ph_nXH_{4-n} ($n = 1$–4, X = C or Si). The molecular dynamics were discussed. It was found that the internal motion was more hindered in carbon compounds than in the silicon analogues. Results for diphenylmethane and diphenylsilane were consistent with strong coupling between internal and overal motion. Korp *et al.*[382] have studied ^{13}C relaxation in a compound containing two phenyl groups (one of them with additional substituents) linked together by a sulphur atom. Dais[383] has used $^{13}CT_1$ measurements to study rotational dynamics of flexible-chain alkanes attached to the benzophenon moiety. Some authors have used $^{13}CT_1$ measurements in polyphenyls for structural studies. Norton and coworkers[384,385] have studied quaternary carbon relaxation in several substituted diphenyl ethers with this goal in mind. The $^{13}CT_1$ measurements were employed in combination with non-selective and selective ^{13}C–$\{^1H\}$ NOE experiments in the structure determination of the product of self-condensation of 1-phenylpentane-2,4-dione.[386]

Finally, I turn to aromatic systems with fused rings. The ^{13}C relaxation in the simplest such molecule—naphthalene—was studied in solution by Berezhnoi and Niyazov[387] and by Alger *et al.*[388] who also considered a series of other condensed aromatic compounds. The DD mechanism was found to dominate the relaxation of the proton-bearing carbons, while the CSA mechanism was important for the quaternary carbons. More recently, Lamb *et al.*[389] have studied the deuteron relaxation in naphthalene-d_8 dissolved in supercritical fluids at different temperatures and pressures. Berezhnoi and Niyazov[390] have also studied carbon relaxation in substituted naphthalenes and discussed the internal motion of methyl substituents. Ericsson and Kowalewski[391] have compared variable-temperature $^{13}CT_1$ data for 1-methylnaphthalene with deuteron T_1 results in the perdeuterated species. The Woessner model (with isotropic overall tumbling and internal rotation) was employed, the methyl barriers were evaluated using (6), and the difference between the barriers in the two isotopic species was discussed. Harris and Newman[392] have studied $^{13}CT_1$ data for larger systems, 9*H*-fluorene and triptycene. The results were interpreted in terms of anisotropic reorientation and hydrodynamic models. Moreover, the effects of assumed bond distances were discussed. Wilson[393] has studied ^{13}C relaxation in the related compound 9-fluorenone and its methyl derivatives. The data were collected at variable temperature and the barriers to the internal methyl rotation were estimated using (6). Wasylishen *et al.*[394] have studied proton, deuteron and ^{13}C relaxation in triphenylene in various solvents as a function of temperature. The

results were discussed with particular reference to hydrodynamic models. Delpuech *et al.*[395] have developed a methodology for deriving the three rotational diffusion constants for planar asymmetric rotors and applied it to the case of chrysene (a compound with four condensed rings) in solution. Gryff-Keller and Poppe[396] have reported ^{13}C (as well as ^{1}H and ^{14}N) relaxation data on a condensed four-ring system substituted with a *N,N*-dimethylcarboxamide moiety and discussed the overall and internal motions. Finally, Alger *et al.*[397] have studied several compounds containing fused aromatic and saturated rings, and discussed the relaxation mechanisms.

2.3.4. Heterocyclic solutes

Several heteroatoms capable of forming heterocyclic compounds have magnetic isotopes, e.g. ^{14}N, ^{15}N, ^{17}O and ^{33}S, whose relaxation can be studied as a complement to ^{13}C work. The papers in which the measurements for heteronuclei constitute an important part are reviewed in Section 2.5. Here, I concentrate on the work in which ^{13}C or ^{2}H relaxation constitutes the main part. I begin with work done on monocyclic compounds and proceed roughly according to the molecular size. An exception to this rule are carbohydrates and their derivatives; papers dealing with these compounds are collected in the last part of this section.

A compound that has attracted considerable attention is pyridine. Campbell *et al.*[398] have studied ^{13}C relaxation in pyridine dissolved in several alcohols and in water. They demonstrated that pyridine could function as a motional anisotropy probe, i.e. that its participation in transient hydrogen-bonded complexes led to the motional anisotropy, evident in the ratios of relaxation times for different nuclei. Similarly, Smith[399] has studied ^{13}C relaxation of pyridine in the presence of iodine and found the evidence of formation of a complex characterized by a preferential tumbling about the C–N–I axis. Van Havebeke *et al.*[400] have studied deuteron relaxation in pyridine-d_5 in the presence of alcohols and acids in various (non-hydrogen-bonding) solvents. Rather than employing the ratios of relaxation rates of various nuclei within the molecule, they found the evidence of intermolecular interactions in the changes of the pyridine deuteron relaxation rates relative to cyclohexane-d_{12}, added in small amount as a relaxation rate reference. Hall and Yalpani[401] have studied the relaxation of pyridine carbons in more complicated systems, aqueous solutions containing carbohydrates, and found some of the results difficult to interpret. Derivatives of pyridine have also attracted some attention. Hopkins and Ali[402] have studied ^{13}C spin–lattice relaxation in methyl substituted pyridines as neat liquids, and in neutral and acidified water–methanol solution. For all proton-bearing carbons, the T_1 values decrease strongly in going from neat liquid to solution. Protonation of

the nitrogen played only a minor role. The barriers to the methyl rotation (estimated using T_{1SR} for the methyl carbons) were found to be close to zero. The same authors also reported a similar study on t-butylpyridines.[403] Blonski *et al.*[404] have investigated relaxation in 2-methoxypyridine and employed the data to study conformational preferences, in the manner proposed by Makriyannis and Knittel.[374] The ^{13}C relaxation in 2-pyridone and *N*-methyl-2-pyridone in methanol and toluene as solvents has been reported and it was found to provide evidence of complex formation in the alcohol solution. In a later paper by the same group, Tiffon *et al.*[406] extended the study to additional solvents and reported in addition ^{2}H and ^{14}N relaxation data. Pedersen *et al.*[407] have studied deuteron (as well as proton and ^{14}N) relaxation in partially deuterated pyridine-*N*-oxide and were able to determine the three rotational diffusion constants as a function of temperature. Pyridazine-*N*-oxide was studied by means of ^{13}C T_1 measurements which found them to be consistent with isotropic reorientation.[408]

I now turn to the saturated, bicyclic heterocyclic compounds with rather high symmetry. Maliniak and coworkers[409,410] have studied ^{13}C (and ^{14}N) relaxation in a symmetric-top molecule, quinuclidine (1-azabicyclo[2.2.2]octane) as a function of temperature in different solvents and determined the anisotropy of the rotational diffusion tensor. It was found that the molecule reoriented almost isotropically in cyclohexane, and that the motional anisotropy increased dramatically in the hydrogen-bonding solvents. The benzene solution held an intermediate position, which motivated the authors to perform MD simulations.[411] Craik *et al.*[412] have reported ^{13}C and ^{15}N relaxation data on a similar compound, diazabicyclo[2.2.2]octane (DABCO), and for hexamethylenetetramine (HMTA) in aqueous (H_2O and D_2O) solution as a function of pH. HMTA is a spherical top and the ^{13}C relaxation in its solutions was also reported in two of the papers dealing with the similarly shaped adamantane.[321,323] The less symmetrical saturated bicyclic heterocycles, tropine and pseudotropine, were studied by Uusvuori and Lounasmaa.[11,413] These authors reported ^{13}C T_1 data as a function of concentration in chloroform and analysed the results using an anisotropic diffusion model, including determination of the angle by which the principal diffusion axis was shifted relative to the principal inertial axis. Dais and Fainos[414] have reported a similar work on another low-symmetry heterocycle consisting of a pyrone and an epoxypropyl moiety; the rotational dynamics of the molecule was approximated as a superposition of a symmetric top overall diffusion and internal motion. Samitov and Sadykov[415] have reported a ^{13}C T_1 study of methyl substituted oxygen and sulphur heterocycles and estimated the methyl rotation barriers.

I turn next to planar, unsaturated bicyclic compounds. Platzer[416] has reported $^{13}CT_1$ results for benzofuran and its methyl derivatives in chloroform

solution, and analysed the motional anisotropy and internal methyl rotation using the Woessner models. The results have subsequently been reinterpreted by Fujiwara *et al.*:[417] by considering the rotational dynamics of the molecule to be those of a symmetric top, the direction of its principal diffusion axis was determined. A similar series of compounds was also studied by Edneral.[418] Friesen and Blackburn[419] have studied ^{13}C relaxation in 2-methylindole as a function of temperature and solvent. The data were analysed using hydrodynamic concepts. The complex formation with 1,3,5-trinitrobenzene was also investigated. Al-Najjar and Amin[420] have measured ^{13}C T_1 data and NOE values for quinoline derivatives and used the results as an assignment tool. The ^{13}C T_1 data are reported for some isocarbostyril derivatives and discussed in terms of motional anisotropy. Vander Elst *et al.*[422] have employed the DD relaxation of quaternary carbons in 2-acetylbenzimidazole and 4-azabenzimidazole in order to study the prototropic equilibria. Finally, two groups have studied purine derivatives: Rossi and Niccolai[423] have obtained the dipolar ^{13}C relaxation rates for purine in D_2O solution by comparing the relaxation rates of protons bound to ^{12}C and ^{13}C nuclei; Sterk and Gruber[424] have combined proton and ^{13}C relaxation measurements (at different magnetic fields) in order to obtain information on the self-association of 6-methylpurine in D_2O solution.

Several groups have studied similar, but partly saturated, or somewhat larger systems. Sugiura *et al.*[425] have studied ^{13}C T_1 values in tetrahydroisoquinoline derivatives and reported data on anisotropic rotational diffusion, including estimating the direction of the principal diffusion axis. Baldo *et al.*[426] have reported similar work on 2-chlorodibenzo-*p*-dioxine and have also discussed the conformation of the molecule. Kövér *et al.*[427] have reported a quantitative application of two-dimensional heteronuclear NOE measurements on a rigid, nonplanar, tricyclic compound. The same group have also proposed a method for determining carbon–proton distances using selective and biselective ^{13}C spin–lattice relaxation experiments, and applied it to the same compound.[428] Womack *et al.*[429] have utilized the ^{13}C relaxation data to discriminate between isomeric indenoisoxazoles. Pitner *et al.*[430] have obtained ^{13}C T_1 data for nicotine and determined the three rotational diffusion constants. Rozhnov[431] has studied ^{13}C T_1 results in compounds with a phenyl group connected to nitrogen or phosphorus heterocycles, while Aksnes and coworkers[432] have studied ^{13}C T_1 measurements in compounds where the phenyl group was bound to dioxa- and dithia-arsolanes. Variable-temperature data were reported and the correlations between dynamic and structural properties discussed. Arsenic heterocycles were also studied by employing ^{13}C relaxation measurements in order to characterize anisotropic reorientation.[433] Stoddart and Hooper[434] have studied still another molecule consisting of two ring systems connected

by a single bond and discussed the temperature dependence of various rotational diffusion constants. Takeuchi[435] has reported ^{13}C T_1 data for another similar molecule and used the data to confirm the assignments. The ^{13}C T_1 data for bilirubin, a natural degradation product of the porphyrin moiety, and some of its derivatives have also been reported.[436] The overall and segmental mobility was discussed. Martin *et al.*[437] have reported a ^{13}C T_1 investigation of a steroid derivative containing oxygen-heterocyclic fragments.

Some authors have studied macrocyclic ethers (crown ethers) and similar compounds. Some work on these systems was mentioned in Section 5.3 of Part 1 and these references will not be repeated here. Erk[438] has studied ^{13}C T_1 data of several macrocyclic ethers and polyoxalactones. Grootenhuis *et al.*[439] have reported ^{13}C T_1 values for 2,6-pyridocrown ethers and their complexes with guanidimium perchlorate. In another paper the authors reported[440] ^{13}C T data on pyrido- and benzo-crown ethers with varying size of the macrocycle. They found that sufficiently large rings could adopt a conformation in which the aromatic moiety was encapsulated by the macrocycle. Finally, Kleinpeter *et al.*[441] have studied a series of benzocrown ethers with additional multiple bonds in the macrocyclic structure and found evidence of segmental motion.

Several papers have been published that are concerned with ^{13}C relaxation in heterocyclic natural products and synthetic drugs. Baldo *et al.*[442] have studied ^{13}C relaxation and anisotropic reorientation for a pyrrolidine derivative. Niccolai and coworkers[443,444] have reported selective $^{13}C-\{^1H\}$ heteronuclear NOE studies of hydrogen bonding patterns. Rossi *et al.*[445] have combined the dynamic information from ^{13}C T_1 measurements with the structural data offered by selective heteronuclear NOEs. More recently, Gaggelli *et al.* have published two papers[446,447] on synthetic drugs in which the conventional ^{13}C T_1 data were combined with proton relaxation and one- and two-dimensional homo- and hetero-nuclear NOE measurements, in order to characterize molecular dynamics and conformation. Kovar and Linden[448] have reported ^{13}C spin–lattice relaxation times for still another synthetic drug, while Grassi and coworkers[449,450] have presented a ^{13}C T_1 investigation of overall motional anisotropy and internal motions in morphine and related compounds.

In the final part of this section, I review ^{13}C relaxation work on carbohydrates. Two papers[451,452] deal with ^{13}C T_1 measurements on a series of sugars and their derivatives. Dais and Perlin[453] have studied ^{13}C T_1 data for D-fructose in DMSO and D_2O solutions and characterized qualitatively the rotational dynamics of each of the tautomers present. Several authors have expressed interest in sucrose solutions. The first ^{13}C T_1 data on sucrose in aqueous solution were presented in the early days of ^{13}C relaxation studies.[454] Bock and Lemieux[455] have reported ^{13}C (and ^1H) relaxation rates, and found

the data to be consistent with isotropic tumbling of the molecule in D_2O solution. ^{13}C T_1 and T_2 data obtained under similar conditions have also been reported.[456] Extensive variable-concentration, variable-temperature, multiple-field studies of $^{13}CT_1$ and NOE in aqueous solution have been presented by McCain and Markley.[457-459] In the first of the papers,[457] the authors investigated the motional anisotropy by introducing normalized relaxation rates for each carbon (the relaxation rates divided by an average of the ring CH carbon relaxation rate). The normalized rates were found to be essentially independent of concentration, temperature and magnetic field. A certain anisotropy of the overall rotation and some internal mobility of the CH_2OH groups was found. The second paper[458] concentrated on the ring carbons; the weak field-dependence of the relaxation rates, indicative of coming out of the extreme narrowing region, was employed to estimate the amplitudes of the spectral densities for the individual ring carbons. In the third paper,[459] the authors concentrated their interest on the hydroxymethyl groups. Kovacs *et al.*[460] extended this work to the region of much longer correlation times, by using the mixed D_2O–DMSO cryosolvent and extending the measurements to lower temperatures. They found the average $^{13}CT_1$ and NOE data on the ring carbons to follow a very simple model of isotropic motion with the Arrheniustype temperature dependence of the correlation time (see Fig. 4).

Other disaccharides have also received some attention. Kovacs *et al.*[460] compared their sucrose data with similar results for another disaccharide. Dais and Perlin[461] have studied carbon relaxation in another disaccharide and discussed the internal oscillations and puckering motions. The same authors also reported a combined ^{13}C and ^{1}H relaxation study of another sugar.[462] Similar work on still other disaccharides has also been reported.[463]

Some T_1 and T_2 measurements on a tetrasaccharide, stachyose, in aqueous solution have been reported.[456] Larger oligo- and poly-saccharides have also been studied by means of ^{13}C relaxation measurements;[464-466] in the last paper a $^{13}CT_1$ determination of correlation time was combined with ^{1}H ROESY studies of molecular conformation.

^{13}C relaxation studies of model compounds of interest to nucleoside and nucleotide chemistry have attracted the attention of various authors, beginning with Allerhand *et al.*[454] More recently, two groups have reported work of this type. Rossi and coworkers[467,468] have compared the ^{13}C relaxation behaviour in thymidine under different perturbation conditions (broad-band or selective irradiation) of protons, and were able to obtain both dynamic and structural information. Rossi *et al.*[469] also reported a ^{13}C and ^{1}H relaxation study of thymidine–thymidine interactions in solution. Two ^{13}C relaxation studies have been aimed at determining major tautomers and protonation sites of 1-methylisoguanosine.[470,471] The ^{13}C relaxation of still other sugar derivatives have also been reported.[435,472]

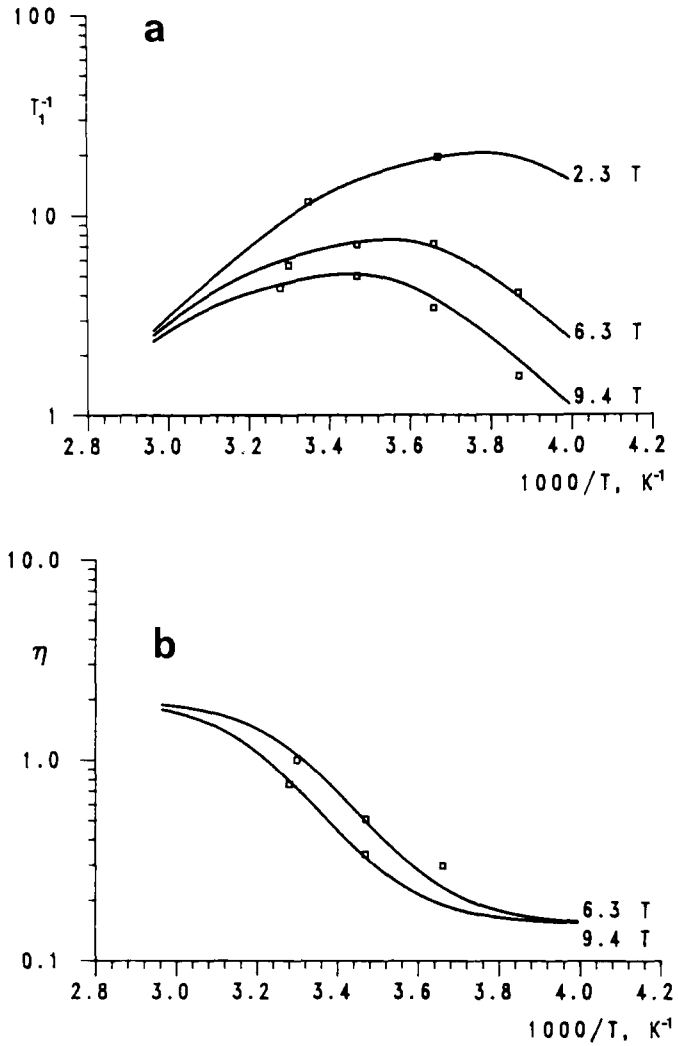

Fig. 4. Average spin–lattice relaxation rates (a) and NOEs (b) of the eight protonated ring carbons in sucrose plotted as a function of the magnetic field and inverse temperature. (Reproduced with permission from Kovacs *et al.*[460])

2.4. Proton relaxation in organic solutes

Proton relaxation studies of organic solutes differ typically from the ^2H or ^{13}C work in several ways. The work with protons has the obvious advantage of greater sensitivity. However, the proton relaxation behaviour is usually more

complicated, for several reasons. First, the nature of the homonuclear DD relaxation processes is inherently nonexponential (unless one is dealing with pairs of equivalent protons or saturates all the protons except the observed one). Furthermore, the multispin effects and the homonuclear spin–spin coupling complicate the situation even more. These complications are well known (see Sections 2.2 and 3.3 of Part 1) and have been discussed in detail in numerous reviews and monographs.[20,473,474] These complicating phenomena make the ^1H relaxation a less frequent choice as a tool for studies of molecular dynamics in liquids. However, the delineation of cross-relaxation networks offers the possibility of obtaining structural information on molecules in solution, in the first place the proton–proton distances or their ratios.

A wide variety of experimental methods has been applied in proton relaxation (or cross-relaxation) work (cf. Section 3.3. of Part 1). I include in this section the work employing nonselective and selective inversion-recovery and related experiments. The notation of various relaxation rates in the literature is somewhat confusing and the concept of "proton T_1" is occasionally used in the sense of a time constant obtained by fitting the experimental data, whatever their nature, to a single exponential.[20] I do not intend to clarify all the confusing nomenclature here, but do not wish to perpetuate the obscurities. Therefore, I avoid the concept of T_1 unless its use is truly motivated.

Because of the availability of a recent monograph,[20] I do not cover here the work dealing in the first place with steady-state NOE experiments. In addition, the account given here of the work using two-dimensional NOE spectroscopy (NOESY and ROESY) is restricted. As a rule, I include only the studies that can be denoted as time resolved in the sense of following the dynamics of the time development of the cross-peak intensities as a function of the mixing time. The organization of this section is similar to the previous one in the sense that it follows the chemical nature of the compounds investigated. Thus, I begin with aliphatic compounds (including amino acids and peptides), continue with alicyclic and aromatic systems and conclude with heterocycles (including carbohydrates). Within each category, papers are reviewed roughly in the order of increasing molecular size of the compound studied.

Some authors have reported ^1H relaxation studies of small aliphatic solutes. Raj *et al.*[475] have reported the spin–lattice relaxation rates for methane and trideuteromethane in D_2O solution. The relaxation in the latter species is dominated by the SR mechanism; the comparison of the relaxation rates of the two species allows the DD relaxation rate for CH_4 and the rotational correlation time to be estimated. Another very simple proton system, that of dichloromethane, has also been studied.[248,249] Two groups have reported intermolecular proton relaxation work, which I feel it is appropriate to mention

here rather than in Section 2.2. on binary mixtures. Smith and Ternai[476] have studied interactions between the small, polar solutes and benzene as solvent. A similar work, including a more elaborate theoretical discussion, and presenting data on several solute–solvent pairs, has been presented by Homer and Cedeno.[477] Blicharska[478] has studied the nonexponential proton spin–lattice relaxation in the methyl group of methanol in aqueous solution. As was discussed some time ago,[479] and more recently,[480,481] the signal of a system of three identical protons consists of a doublet and a quartet component characterized by identical resonance frequencies, but different relaxation properties. Finally, Dimitrov and Ladd[482] have reported the Carr–Purcell–Meiboom–Gill spin–echo experiments on methyl groups in *N*,*N*-dimethyltrichloroacetamide.

I now turn to amino acid and peptide studies. Parbhoo and Nagy[294] have studied proton T_1 values in the CH_2 group of deuterated glycine and compared the results with ^{13}C work. Niccolai and Tiezzi[483] have studied the motional behaviour of a model compound, a phenylalanine derivative, using selective excitation spin–lattice relaxation experiments. More recently a similar methodology has been employed to study larger peptides.[484,485] Gaggelli *et al.*[297] have studied the conformation of mandelylaspargine and related compounds by combined ^{13}C T_1 and selective and nonselective proton relaxation experiments. Mizuno and coworkers[486] have employed ^1H (and ^{13}C) relaxation measurements in a study of interactions between 2-chloroethanol and amino acid derivatives. Selective and nonselective proton relaxation experiments on a dipeptide in the presence of an enzyme have also been reported.[487] The initial relaxation rate in the selective experiments was found to be particularly sensitive to the presence of the enzyme. Valensin and coworkers[488] have also studied conformational dynamics for a tripeptide in solution using selective and nonselective relaxation experiments on protons and on tritium nuclei (^3H) in partially tritiated analogues.

Several groups have employed ^1H relaxation experiments in studies of cyclic peptides. Kessler *et al.*[489] used the NOESY and ROESY methods, combined with ^{13}C T_1 studies, to determine the conformation of cyclic peptides. Bruch *et al.*[490] have studied ^1H spin–lattice relaxation as well as transient and steady-state NOE for a cyclic pentapeptide and derived the conformation in solution. Kopple *et al.*[301] have reported measurements of the laboratory and rotating-frame relaxation for protons in cyclic octapeptides. Finally, Gibbons and corworkers[491,492] have reported nonselective, mono- and bi-selective proton relaxation measurements on two cyclic decapeptides and used the data to derive stereochemical information. Work on even larger polypeptides is discussed in Section 3.3.

I now turn to alicyclic compounds in solution. An early application of nonselective as well as mono-, bi-, and tri-selective proton relaxation experiments on a small, bicyclic compound was to determine the interproton

distances.[493] Bovée *et al.*[494] have studied the dipolar interactions between the protons of a rotating methyl group and protons in the rigid framework of another small, bicyclic molecule. The proton relaxation measurements on steroids have been surveyed.[495] Morris[496] has used cholesteryl acetate as a model compound for presenting indirect measurements of proton relaxation by polarization transfer to the ^{13}C nuclei, featuring a better-resolved spectrum. Finally, before turning to aromatic compounds, I wish to mention a paper on proton longitudinal relaxation studies in conformational work on compounds consisting of aromatic fragments linked together into a macrocycle by (substituted) methylene groups.[497]

Turning to aromatic systems, I begin by mentioning some papers on simple benzene derivatives. Stark *et al.*[498] have studied *o*-dichlorobenzene in dilute solution in carbon disulphide. They combined the nonselective proton inversion-recovery experiments with ^{13}C T_1 studies. Employing the exact density matrix analysis of the relaxation in a strongly coupled system, they were able to characterize quantitatively the motional anisotropy of the molecule. Kratochwill *et al.*[499] have employed the same procedure to study dichlorophenol dissolved in the mixture of pyridine and carbon tetrachloride. Balonga *et al.*[500] have reported NOE measurements on 2,4-dinitrophenol; under certain conditions, evidence was obtained of scalar relaxation of the first kind being operative for ring protons. Solute and solvent proton relaxation in methanol solutions of hydroquinone and 1,4-naphthaquinone have also been reported.[501]

Several authors have reported proton relaxation studies of toluene and related systems. Chazin and Colebrook[502] have studied proton relaxation in nonselective experiments on a large number of toluenes (substituted in either the 2- or 3-position) and related compounds. For some of the compounds ^{13}C relaxation data were also reported. The results were discussed qualitatively in terms of barriers to methyl rotation. Homer and Cedeno[503] have studied proton and ^{13}C relaxation in 1,3,5-trimethylbenzene. They used the ^{13}C T_1 and NOE data in order to separate the intra- and inter-molecular contributions to proton relaxation. The analysis of the proton relaxation in terms of intra- and inter-molecular contributions has been presented for benzylfluoride dissolved in deuteromethanol and deuteroacetone.[504] Rowan *et al.*[505] have studied proton relaxation in the methyl and partially deuterated methyl groups in 3,5-dichlorotoluene. The relaxation mechanisms were discussed. A similar work, also including ^{13}C and ^{2}H relaxation measurements on other chlorotoluenes has also been reported.[506]

Other benzene derivatives have also attracted some attention, mainly in the context of conformational studies. Bruce *et al.*[507] have studied ^{1}H and ^{13}C relaxation in acylbezoquinones in solution. A similar approach was taken for the case of phenylmethyl ethers, phenylmethyl ketones and related compounds,[508] for tolyl-di-t-butylcarbinols[509] and for a synthetic drug.[510]

Another pharmacological agent was studied by employing selective and nonselective relaxation measurements in order to determine the conformation of the molecule.[511] In a somewhat different study, a relaxation technique involving the proton–carbon polarization transfer was proposed and compared with selective and nonselective direct proton measurements on a compound called eugenol (a phenol derivative).[512]

Yonemitsu *et al.*[513] have studied proton relaxation in partially deuterated nahthalenes. Other larger aromatic compounds were studied by Haslinger and Robien[481] who measured the nonexponential proton relaxation in pyrene derivatives, and by Ashley *et al.*[514] who used proton relaxation measurements for structure elucidation in chlorinated polyaromatic compounds.

In the field of heterocyclic solutes, Kratochwill and Vold[515] have studied proton (and carbon) relaxation in 2-bromothiophene. The density-matrix analysis of the full recovery curves obtained in nonselective and semiselective inversion-recovery experiments allowed a partial characterization of the motional anisotropy. A similar study has been reported for pyridine-*N*-oxide in solution.[407] Combining the proton data with the results of ^{14}N and ^{2}H relaxation studies, the authors were able to determine the three rotational diffusion constants of the molecule. Rossi *et al.*[516] have measured transverse and longitudinal (selective and nonselective) proton relaxation in histidine in aqueous solution and used the data to discuss the molecular dynamics. Sugiura and coworkers[517] have studied methyl proton relaxation in quaternary piperidinium salts. More recently, the same group employed biselective proton relaxation measurements to characterize the conformation of vinylpyridine.[518] The ^{1}H (and ^{14}N) relaxation in pyrrole (and its derivative) in pyridine and cyclohexane solutions have been studied under variable-temperature conditions.[519] The correlation times obtained from the measurements on the two nuclei were compared.

Several authors have been interested in larger heterocyclic molecules. Haslinger *et al.*[520] have studied the nonexponential methyl proton relaxation in 3-methyl-2,4,10-trioxaadamantane, and discussed the molecular dynamics in solution. Haruyama *et al.*[521] have used proton relaxation measurements to characterize the conformation of a bicyclic compound containing a benzene ring fused with a saturated nitrogen and a sulphur heterocycle. Sadykov *et al.*[522] have studied similar compounds, but containing two oxygen atoms in the saturated ring. In two earlier-mentioned works,[423,424] proton relaxation was used in studied of purine and its derivative. The NOESY spectra have been reported of a tricyclic, rigid compound as a function of the mixing time and the data used as a test for the full relaxation matrix treatment of the two-dimensional NOE measurements.[523] Proton relaxation in compounds containing a heterocycle and a phenyl group connected by a single bond have been reported and the data were used to discuss the stereochemistry.[524,525] Hennig

and Limbach[526] have reported a variable-temperature, combined proton and ^{15}N relaxation study of a porphyrine derivative. Minima in the relaxation rate vs. inverse-temperature curves were observed and the nitrogen–proton distances estimated. Porphyrin derivatives have also been studied.[480,481]

Related, but not macrocyclic, compounds have been studied using a combination of selective and nonselective proton relaxation data to characterize the conformational behaviour.[527] A similar approach was taken in several studies of synthetic drugs and natural products.[446,447,528,529] The molecular dynamics and conformation of another heterocyclic natural product have been studied by means of time-dependent NOE measurements.[530] Chazin *et al.*[531] and Haruyama and Kondo[532] have combined nonselective inversion-recovery experiments with steady-state NOE measurements. Finally, conformational studies based on nonselective proton relaxation measurements have been reported.[533,534]

Proton relaxation work on carbohydrates has been reviewed recently.[535] The sugars became early on the subject of careful proton relaxation studies, combining selective and nonselective inversion-recovery experiments.[536] More recently, monosaccharides were studied using ^1H relaxation where nonselective proton relaxation measurements were compared with a ^{13}C T_1 result.[537,538] Dais *et al.*[539] have reported proton relaxation and NOE data, together with ^{13}C T_1 results, for mannose derivatives. The same group also reported combined ^1H and ^{13}C relaxation experiments[462] and nonselective and selective proton experiments on disacchrides.[540] Avent and Freeman[541] have studied ^1H relaxation in sucrose using a heteronuclear magnetization transfer technique. The ^{13}C and ^1H relaxation and a NOE study has also been reported on antibiotics containing sugar moieties.[542]

Some groups studied ^1H relaxation in nucleosides and nucleotides. Rossi *et al.*[469] have employed ^1H relaxation to study the thymidine–thymidine interaction. Another nucleoside was studied in ^{15}N enriched form where relaxation data for the imino protons were considered including the relaxation differential between the components of the doublet (due to ^1H–^{15}N spin–spin coupling).[543] The relaxation-rate differentials were assigned to the DD–CSA interference. Finally, Andrew and Gaspar[544] have studied proton relaxation in adenosine monophosphate, as well as adenosine di- and triphosphate[545] in solution and discussed the results in terms of molecular motions.

2.5. Other nuclei relaxation in organic solutes

In this section, I describe the work dealing with the relaxation of less common nonmetal nuclei. The organization of the section is as follows. I deal with one nucleus at a time and begin with the work on spin-$\frac{1}{2}$ nuclei. Within this

category, the nuclei are considered in the order of increasing atomic number. I then continue with quadrupolar nuclei, following an analoguous order. Following the procedure adopted in the sections on inorganic applications (Sections 5.2 and 5.3 of Part 1), the work merely listing isolated linewidth data on quadrupolar nuclei is not covered here.

Nitrogen NMR spectroscopy has recently been reviewed by Witanowski *et al.*[546] The earlier work on ^{15}N relaxation has also been discussed at length in the book by Levy and Lichter.[547] Here, I concentrate strictly on the work published during the last decade. The ^{15}N relaxation in amines and ammonium ions has been studied in connection with ^{13}C work by Levy *et al.*[279,309,412] The DD contributions to the relaxation rates were determined and used as a complement to the ^{13}C T_1 data. For the case of tertiary cyclic amines,[412] the role of intermolecular relaxation caused by solvent protons was also discussed. Lambert and Stec[548] have reported similar work on anilines and anilinium ions, while Marchal *et al.*[549] performed related measurements on lactams. Sterk and Mittelbach[271] studied the ^{15}N relaxation mechanism in the nitrile group and found the CSA mechanism to be important. The ^{15}N relaxation rate in tetramethyldisilazane was measured using INEPT signal enhancement.[550] Marion *et al.*[551] have proposed another INEPT-based technique and applied it to measurements of the recovery of ^{15}N magnetization difference within one multiplet. The same authors have also studied linear peptides, combining the conventional ^{13}C and ^{15}N T_1 data (which were used to discuss molecular dynamics) with such "antisymmetric" T_1 measurements, employed to study conformational preferences.[552]

The ^{19}F relaxation in fluorine-containing organic solutes is the subject of only one paper: Beguin and Dupeyre[553] studied benzylfluoride in acetone and methanol solutions and discussed the relaxation mechanisms. The ^{29}Si relaxation in organosilicon compounds was studied for quite some time, in spite of technical difficulties,[554] but has received limited attention during the last decade. ^{29}Si T_1 measurements on tetramethyldisilazane using the INEPT-type technique have been reported.[550] Knight[555] has reported ^{29}Si T_1 data for tetramethoxysilane and its hydrolysis products. Moreover, ^{29}Si relaxation studies in linear[556] and cyclic[557] siloxanes have been reported. In the latter work, the relaxation mechanism and rotational correlation times were discussed.

The ^{31}P nucleus is highly sensitive but its relaxation in organophosphorus systems has not attracted much interest. Some exploratory work was presented in the second half of the 1970s.[558,559] Robert *et al.*[560] studied ^{31}P spin–lattice relaxation in trimethylphosphine in toluene solution over a wide temperature range. The DD mechanism, inefficient at high temperature, dominated in the low temperature range. T_1 and NOE were also studied as a function of concentration, in order to separate the intra- and inter-molecular

DD contributions. Phosphorus relaxation in certain classes of organophosphorus compounds has also been discussed by Ramarajan *et al.*[561] Nanda *et al.*[562] have studied T_1, T_2 and NOE data for ^{31}P in trimethylphosphite and adenosine monophosphate (AMP) as a function of temperature, and discussed the relaxation mechanisms. Transverse ^{31}P relaxation and the off-resonance $T_{1\rho}$ in another AMP has also been studied.[563] Finally, ^{31}P data in low-molecular-weight compounds in systems of biochemical interest were recently reported.[564,565]

I now turn to quadrupolar nuclei and begin with the other magnetic isotope of nitrogen, ^{14}N.[546] The ^{14}N is a quadrupolar nucleus whose relaxation has been studied diligently. As for many other quadrupolar nuclei, the goal of the relaxation measurements has been either to provide the dynamic information (if the QCC is known) or to provide the QCC, if the correlation time can be obtained from, for example, ^{13}C T_1 data (the approach sometimes referred to as the "dual spin probe method"). I begin the survey of ^{14}N relaxation with small molecules in solutions. Tiffon *et al.*[566] have studied ^{14}N relaxation in acetonitrile in dilute solutions in carbon tetrachloride. The rotational correlation time for the tumbling motion of the symmetric top was found not to follow the hydrodynamically derived, linear relation to η/T (where η is the viscosity, see (30), Section 2.3 of Part 1). Tiffon and Ancian[567] have also studied acetonitrile dissolved in alkanes and found the linear relation between $\tau_\perp$ and η/T to be fulfilled, even though the slopes were lower than expected from hydrodynamics with the "slipping" boundary condition. Similar observations were also reported for acetonitrile solutions in other solvents, under the conditions of high temperature and low viscosity.[245] In contrast, at low temperatures and high viscosities the ^{14}N relaxation was found to be almost independent of η/T.[245] Kovacs *et al.*[568] have studied ^{14}N relaxation in acetonitrile in dilute solutions in mixtures of water and propanol and proposed to explain the deviations from hydrodynamics by using the concept of dielectric friction. Deviations from hydrodynamic behaviour were also reported for dicyanoacetylene in a hydrocarbon solution.[244]

Halliday *et al.*[569] have reported indirect measurements of ^{14}N relaxation in methyl substituted ammonium ions through the lineshape analysis of nitrogen bonded protons. Similar work has been reported on thioacetamide,[570] while Galat and Titov[571] presented a somewhat more complicated study involving strongly coupled proton spin systems and chemical exchange. Mlynarik[274,355] has reported ^{14}N relaxation data obtained from carbon T_2 or $T_{1\rho}$ measurements in amines. Robert and Evilia[572] have reported ^{14}N linewidth studies on several organic compounds dissolved in supercritical fluids.

I turn next to ^{14}N relaxation studies in heterocyclic compounds. The ^{14}N relaxation in pyridine-*N*-oxide has been reported.[407] Combining these results with ^{13}C derived dynamic information, the authors obtained the nitrogen

QCC. Similar work on lactams has been presented.[573] In the same study, the authors used the ^{14}N (and ^{17}O) relaxation data together with ^{13}C results in order to characterize the motional anisotropy of another compound, 2-pyrrolidone. Ogino *et al.*[574] have studied pyridinium salts using ^{14}N and halide counterion linewidth measurements. Finally, ^{14}N relaxation in symmetric bicyclic compounds was reported in several papers mentioned above in connection with ^{13}C work.[321,323,409,410]

With regard to sensitivity, ^{17}O measurements are significantly less favourable than ^{14}N ones, but nevertheless have attracted considerable attention. Tiffon *et al.*[575] have studied ^{17}O linewidths in acetone dissolved in alkanes. The correlation times were determined and discussed using various models. The ^{17}O (as well as ^{2}H and ^{33}S) relaxation rates have been reported for dimethylsulphone in solution.[576] The ^{2}H data were used to estimate the correlation time and the ^{17}O data thus provided the QCC, which was compared with the values obtained from measurements in a liquid crystalline solvent and with ab initio molecular-orbital (MO) calculations. Valentine *et al.*[577] have studied ^{17}O T_1 and T_2 data in urea as a function of pH, and discussed the effect of protonation on the relaxation rates. The same group have also reported several ^{17}O NMR investigations, including some relaxation data, on amino acids and peptides.[578-581] Linewidth and ^{17}O T_1 measurements in ^{17}O enriched enkephalins in aqueous and organic solutions have been reported.[582]

Several groups have reported ^{17}O relaxation studies on aromatic and heterocyclic compounds. Monti *et al.*[583] have studied substituted nitrobenzenes and found the ^{17}O linewidth to be strongly dependent on the substituent position. Delseth and Kintzinger[584] have studied ^{13}C and ^{17}O relaxation in cyclic ethers, ketones and lactones, and determined the QCCs using the dual spin probe method. A similar approach was taken in work on furan and tetrahydrofuran[585] and in a study of lactams.[573] Finally, Gerlt *et al.*[586] have reported variable-temperature ^{17}O linewidth studies on phosphate esters and adenine nucleosides.

I now discuss the work on ^{33}S. In spite of technical problems, this nucleus has attracted considerable attention. Work done with ^{33}S NMR has been recently reviewed.[587] and here I only include work that is relaxation oriented. Ancian *et al.*[242] have studied carbon disulphide in alkane solution using ^{33}S linewidths as a source of information on the rotational correlation time, to be combined with τ_{SR} from ^{13}C work. A dual spin probe study of ^{33}S relaxation and QCC in dimethylsulphone has been reported.[576] Larsson and Kowalewski[585] have reported a similar work on thiophene and tetrahydrothiophene while Ruessink *et al.*[588] have studied sulpholane in solution in a similar way. Sulpholane and related compounds were also studied by Hinton,[589] who reported the results of variable-temperature ^{33}S T_1 measurements. Sulphur

relaxation data and linewidths in organic and inorganic sulphates and related compounds in aqueous solution have been studied.[590,591] Finally, Crumrine and Gillece-Castro[592] have studied ^{33}S linewidths in solutions of sulphonic acids and sulphonate salts as a function of solvent composition and solute concentration.

The last group of papers to be reviewed here is concerned with quadrupolar relaxation of halogens nuclei. The work on covalently bonded halogens is scarce and most of it has already been mentioned in Sections 2.1 and 2.2. Here, I wish to mention the papers on organic solutes employing indirect measurements through ^{13}C scalar relaxation.[251,275,276] The work on halide ion NMR is usually grouped with the category "inorganic" (see Section 5.2 of Part 1) or "macromolecular" (see below). Here, I wish to mention an important early paper[593] on interactions between halide ions and organic cations containing charged nitrogen, phosphorus or sulphur, as well as two more recent papers on ^{35}Cl and ^{81}Br linewidth studies of anilinium and pyridinium salt solutions.[574,594]

2.6. Organic solutes in anisotropic solvents

In this brief section, I summarize the work on the relaxation of nuclei residing in small, organic molecules dissolved in liquid crystalline solvents. The field was recently reviewed.[595,596] The fact that the solvent is anisotropic affects the relaxation studies in three ways. First, the degeneracy of certain transitions is lifted; e.g. the system of three equivalents spins gives rise to a single line in the isotropic environment and to three lines in the anisotropic medium. Second, the symmetry equivalence of certain spectral densities vanishes. Third, other relaxation experiments, such as the Jeener–Broekaert, quadrupole echo and multiple-quantum experiments (see Section 3.4 of Part 1) become possible.

This section is organized as follows. First, studies involving five- and six-atom solute molecules, corresponding to very simple spin systems are discussed and then the discussion is continued roughly in the order of increasing molecular size of the compounds studied.

The deuteron relaxation in deuterochloroform was studied by using a combination of various relaxation techniques.[597] The spectral densities of motion at zero frequency, Larmor frequency and double Larmor frequency were determined. Another isotope modification of chloroform, $^{13}CHCl_3$, constitutes an AX spin system. The relaxation properties of this system in the nematic phase were reported.[598] The same paper also contains a discussion of the relaxation in the A_2 spin system, exemplified by $^{12}CH_2Cl_2$. Dichloromethane-d_2 is a two-deuteron system, characterized by a total of six auto- and cross-correlation spectral densities, all of which were determined in

temperature- and field-dependent measurements.[599] Poupko *et al.*[600] have reported additional ^1H measurements on the same system and on the $^{13}CH_2Cl_2$ species. The observed frequency dependence of the relaxation rates was interpreted using the slowly relaxing local structure model. Voigt and Jacobsen[601] have studied the relaxation properties of a system consisting of a spin-1 nucleus coupled to a spin-$\frac{1}{2}$ nucleus in the nematic phase, and used the data on still another isotopic species of dichloromethane ($CHDCl_2$) as an example. Another simple molecule that has frequently been studied in nematic solution is acetonitrile. Proton relaxation in the A_3 system has been studied using different spin perturbations.[602,603] The molecular dynamics was discussed; the rotational diffusion about the three-fold axis was not affected significantly by the liquid crystal, but the reorientation of the axis was dramatically slowed down as compared with that in the neat liquid. Black *et al.*[604] have studied the acetonitrile species enriched in ^{13}C at the methyl position (AX_3 spin system). The relaxation of the ^{13}C quartet was observed, following a variety of perturbations of the proton system. The results were consistent with the proton work mentioned above. The ^{13}C and ^{14}N relaxation (^{14}N T_1 was determined from the linewidth of the nitrile ^{13}C) in acetonitrile dissolved in a nematic solvent has also been reported under conditions of proton decoupling.[605] Deuteron relaxation in the partially oriented trideuteromethyl group of acetonitrile has been studied using multiple quantum spin–echo experiments.[606] Plomp *et al.*[607] have reported variable-field ^{14}N relaxation measurements on methyl isocyanide, CH_3NC, while Imbardelli and Chidichimo[608] have studied the molecular dynamics of iodomethane in the nematic phase by analysing proton linewidths.

Imbardelli *et al.*[609] have also reported a study of proton linewidths (and from those of the ^{14}N relaxation) in pyridine in nematic mesophase. Caniparoli *et al.*[610] have studied deuteron relaxation in several benzene derivatives dissolved in a lyotropic lamellar phase of a water–sodium dibutylphosphate mixture. Deuteron relaxation dispersion in deuterated toluene and *p*-xylene has been studied and the results interpreted in terms of a model in which the solute molecules undergo a small-step rotational diffusion in an ordering potential, with contributions from slow director fluctuations.[611] The temperature and frequency dependence of the spectral densities obtained from deuteron relaxation measurements on a highly ordered probe molecule, *p*-diethynylbenzene, in different mesophases have been presented.[612–614] The rotational dynamics of the probe molecule and the director fluctuations were discussed. In another paper from the same group,[615] the temperature- and frequency-dependent deuteron relaxation data were given for deuterated biphenyl in various mesophases. Finally, Plomp and Bulthuis[616] have reported frequency-dependent deuteron relaxation data on diphenylethyne in a nematic solvent; they had problems interpreting the results using the

rotational diffusion and director fluctuation model. More sophisticated theories of the effects of director fluctuations[8,9] have also been used to interpret this experimental data.

3. MACROMOLECULES AND AGGREGATES IN SOLUTION

This part of the survey is not meant to be comprehensive. Rather, it contains a selection of work, heavily biased towards physico-chemical (as opposed to biochemical) aspects of nuclear spin relaxation, reflecting the personal interests of the reviewer. Three topics are covered. In Section 3.1 the relaxation of nuclei residing in water molecules and in monoatomic ions (counterions to the charged macromolecules/aggregates, or added salt) in aqueous solutions of macromolecules and aggregates (such as micelles) is discussed. The remaining sections are devoted to the relaxation of nuclei resident in the aggregates (Section 3.2) and macromolecules (Section 3.3). In all three sections, the discussion is limited to macroscopically homogeneous, isotropic, liquid solutions. Thus, the work on gels, mesophases, suspensions, tissue, etc., is not covered.

3.1. Relaxation of ionic and water nuclei in aqueous systems

This section covers the work in which measurements were carried out on the low-molecular-weight environment of the macromolecules and aggregates rather than on the large species themselves. The influence of the macromolecules and aggregates on the dynamic behaviour of the solvent (usually water) is similar. The aggregates and the water-soluble macromolecules are often highly charged and the common, electrostatic interactions largely determine the static and dynamic properties of the ions. It seems natural, therefore, to collect in this section work on both types of system. The field has been subject to several reviews, among which I wish to mention the recent paper by Bryant[617] on the macromolecular solvation dynamics and that by Forsén *et al.*[618] on ion binding in biological systems.

This section is organized as follows. I begin by dealing with work on water nuclei, starting with general references and work concerned with aqueous solutions of uncharged polymers. I then proceed with a discussion of the work on aqueous solutions of synthetic linear polyelectrolytes, followed by micellar and related systems and protein solutions. Finally, the relaxation of nuclei in ions is discussed following a similar ordering.

The interpretation of the magnetic resonance data obtained from systems that are microscopically heterogeneous, such as aqueous solutions of macromolecules, is complicated. An important theoretical paper on the quadrupolar

relaxation of water nuclei (^{2}H and ^{17}O) has been published by Halle and Wennerström.[619] The authors presented a "two-step" model in which two components of motion of the water molecules were considered at the "interfacial" site: a fast anisotropic reorientation superimposed on a more extensive slow motion. The two-step model is both physically and operationally different from the approach of simply describing the motion in the interfacial ("bound") site as anisotropic reorientation. The interfacial water was allowed to undergo a rapid two-site exchange with the bulk water (discrete exchange model, DEM). A more sophisticated treatment of the transfer of water molecules between the interfacial region and the bulk ("continuous diffusion model", CDM) was proposed for the general case[620] and with a particular reference to the relaxation dispersion observed at low frequencies in the ^{17}O nuclei of water in colloidal systems.[621] Gore and coworkers[622] have proposed a method for separating the intra- and inter-molecular contributions to the water proton relaxation rate by means of comparisons with the ^{1}H relaxation rate, and applied it to the aqueous solutions with variable concentration of polyethylene glycol. The same authors have also studied another aspect of water nuclei relaxation in the same model system—the cross-relaxation of the water and methylene proton.[623] Deuteron and ^{17}O relaxation in aqueous solutions of the same polymer (denoted as polyethylene oxide) was also studied.[624] The results were interpreted using a two-site exchange ("two phase") model, with the bound site characterized by a simple anisotropic motion. Conti *et al.*[625] have studied the water proton T_1 over five decades of magnetic-field values (the so-called NMRD measurement) for solutions containing a more complicated uncharged polymer, polysaccharide glycogen. The data were interpreted in terms of the two-step model.

I now turn to water nuclei relaxation in the presence of ionizable polymers which, under certain pH conditions, form polyelectrolyte solutions. Halle and Piculell[626] have reported a ^{17}O relaxation study of aqueous solutions of poly(acrylic acid) (PAA) and poly(methacrylic acid) (PMA). The measurements were carried out at two resonance frequencies as a function of temperature, concentration and degree of dissociation. The results were interpreted in terms of the two-step model. The proton-exchange broadening of ^{17}O was also taken into consideration. Similar systems have been studied by Leyte and his group.[627,628] Mulder *et al.*[627] have reported relaxation rates of water nuclei (^{1}H, ^{2}H and ^{17}O) and polymer protons in concentrated aqueous solutions of different isotopic forms of PMA. The cross-relaxation between the polymer and water protons was found to be unimportant; the dynamic behaviour of the solvent molecules was discussed within the framework of the anisotropic rotation in the bound state. More recently, van Maarel *et al.*[628] have studied in a similar way the ^{2}H and ^{17}O relaxation in aqueous solutions

of PAA and poly(styrenesulphonic acid) as a function of polymer concentration.

I turn now to surfactant and related systems and again begin by citing ^{17}O relaxation studies employing the two-step model in the data analysis. Similar data have been reported by Halle and Carlström[629] on aqueous solutions of micelles composed of ionic surfactants of varying alkyl chain length, head group and counterion. The structural and dynamic information about the water–micelle interaction was derived. The anisotropic reorientation of water molecules on the micellar surface was typically 2–3 times slower than in pure water. Piculell[630] has studied water ^{17}O and ^{2}H relaxation rates in micellar solutions of alkyl-ammonium chloride. Frenot and coworkers[631] have studied ^{2}H and ^{17}O relaxation in D_2O solutions of alkylammonium chlorides with 8–14 carbon atoms in the aliphatic chain, and compared the two-step model with a model describing the water molecule motion in the vicinity of the head groups in terms of Woessner-type anisotropic reorientation model. The latter model led to more consistent interpretation. Deuteron relaxation of D_2O in solutions containing short-chain monosubstituted ammonium compounds was reported.[632] Belmajdoub *et al.*[633] have reported multinuclear studies of relaxation and diffusion for solvent bound to cetyltrimethylammonium bromide micelles in water and formamide. The ^{17}O relaxation in water in micellar solutions of nonionic detergents has also been measured.[634]

Some authors have studied water relaxation in inverted micelles, i.e. aggregates containing aqueous core, surrounded by surfactant molecules with their hydrophobic chains directed outwards, towards the nonaqueous solvent. Carlström and Halle[635] have reported ^{2}H and ^{17}O transverse and longitudinal relaxation rates for the AOT/D_2O/isooctane system (AOT is an anionic surfactant), as a function of droplet size, droplet volume fraction, temperature and resonance frequency. Different dynamic models were discussed. Llor and Rigny[636] studied water proton relaxation in water/AOT/cyclohexane systems while Maitra and Patanjali[637] reported similar studies on the same ternary system, with and without added cholesterol. Quist and Halle[638] also studied a similar system, but containing another hydrocarbon. They reported ^{2}H longitudinal and transverse relaxation rates at temperatures down to $-29°C$. The results provided evidence of the existence of reversed micelles with unfrozen cores. Finally, ^{1}H, ^{2}H and ^{17}O relaxation in the water inside inverse micelles in sodium diethylhexylphosphate/water/benzene system has also been studied.[639]

I now turn to protein solutions and begin by citing some important earlier work. Koenig *et al.*[640] have reported ^{1}H, ^{2}H and ^{17}O data for water in some protein solutions. The dispersion curves of the three nuclei were very similar, which indicated that whole water molecules (rather than exchanging protons)

were involved in the interaction. A larger series of ^1H and ^2H NMRD measurements on proteins of widely differing molecular weights was also reported[641] and the relation of the NMRD data to rotational correlation times of proteins discussed. Turning to the newer work, I begin with that on quadrupolar water nuclei. Halle and coworkers[642,643] have studied ^{17}O relaxation in several protein solutions. The data could be satisfactorily interpreted by the two-site DEM, together with the two-step model for the bound site. For deuterons, it was necessary to include a third site in the DEM. Baianu and coworkers[644] reported similar results for lysozyme solutions, while Kumosinski *et al.*[645] presented a ^2H relaxation study of water interactions with another protein. Gallier *et al.*[646] have studied ^2H and ^1H spin–spin and spin–lattice relaxation in a protein solution over a wide temperature range, down to well below freezing.

Among water proton relaxations studies, the NMRD work of the type mentioned above[640,641] is probably the most spectacular. Some typical data[641] are presented in Fig. 5. A large number of such measurements has been reported over the last decade for paramagnetic solutions and for tissues. Here, I mention only a few that fit within the limits of the present review. Conti[647] has reported such measurements in solutions of bovine fibrinogen, complemented by some T_2 data. The data were interpreted using a modification of the two-step model. The frequency dependence of the water proton relaxation

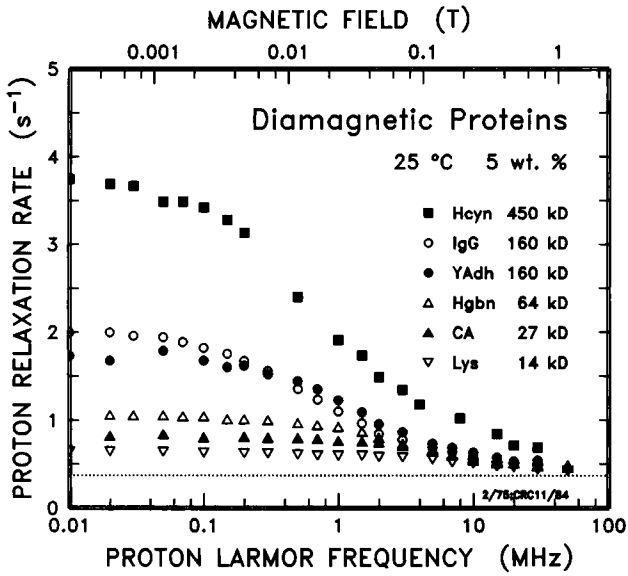

Fig. 5. Dispersion of the solvent-proton spin–lattice relaxation rate (at 25°C) in 50 mg ml^{-1} solutions of protein with a range of molecular weight. (····) The relaxation rate in the protein-free solvent. (After Hallenga and Koenig.[641])

rates in protein solutions was discussed.[648] Koenig *et al.*[649] have studied the cross-relaxation between the water and protein protons. More recently, the same group[650,651] studied the relaxation of water protons in calf lens homogenates (essentially concentrated protein solutions) and discussed in particular the cross-relaxation with the ^{14}N of the NH groups. Bryant and Jarvis[652] studied solvent proton NMRD in protein solutions in water and DMSO. The methyl protons in DMSO displayed a clear dispersion, which demonstrates that the effect is due to the dynamic coupling between water and protein motions rather than chemical exchange. Some other papers on proton relaxation should also be mentioned. Otting and Wüthrich[653] studied protein hydration in an aqueous solution at variable temperature by measuring (by means of NOESY and ROESY experiments) the NOE effect between protons of individual amino acids and water. Fullerton *et al.*[654] have investigated the effect of protein polymerization (docking) on the water proton T_1. Finally, ^1H relaxation has been employed to study the interaction of water with amino acids and proteins.[655]

Turning to the relaxation of nuclei of simple ions in macromolecular solution, I begin with systems containing synthetic polyelectrolytes. An important early paper on the field was published by van der Klink *et al.*[656] These authors pointed out that the polyelectrolyte solutions, containing quadrupolar nuclei in counterions, represented a complex case of a field gradient modulated both in magnitude and in direction and estimated the gradient by solving the Poisson–Boltzmann (PB) equation for a continuous charge distribution on the polyion. Such an approach, taken also more recently by Delville and coworkers,[657,658] has been criticized by Halle[659] who stressed the importance of the discrete nature of the charge distribution. Levij *et al.*[660,661] have studied the ^{23}Na relaxation in solutions of several polyelectrolytes as a function of concentration. They found the transverse relaxation in dilute solutions to be generally nonexponential, but were unable to explain the results theoretically. Similar, but less comprehensive, work has also been reported by Gunnarsson and Gustavsson.[662] The data of Levij *et al.*[660] were successfully interpreted by Halle *et al.*[659,663] The interpretation involved using the CDM approach combined with the self-consistent mean-field cell description of the equilibrium distribution and the description of translational diffusion of the ions based on the Smoluchowski equation. The counterion electric-field gradient enters the theory as a parameter. The magnitude of this parameter was recently studied[664] using molecular-dynamics simulations.

Van der Maarel *et al.*[665] have studied dilute aqueous polyacrylate solutions using ^{23}Na (and ^{13}C) relaxation in sodium ions enclosed by cryptands. In this case, no evidence of nonexponential relaxation could be obtained. Moreover, it was found that the polyion had only a moderate effect on the counterion rotational mobility. Van der Maarel *et al.*[666] also presented a combined study

of lithium counterions in polyelectrolyte solutions using neutron diffraction and the contribution to the ^{7}Li relaxation caused by DD interaction with ^{17}O in the hydration sphere. This study confirmed the conclusion about the limited influence of the polyion on the rotational motion. Barnes *et al.*[667] have also reported a combined neutron diffraction–nuclear relaxation study on an aqueous polymer solution, here using the ^{35}Cl relaxation rate and studying the influence of polyethyleneglycol on the hydration sphere of the chloride ion. Van Rijn *et al.*[668] have studied ^{23}Na relaxation in semidilute polyelectrolyte solutions as a function of salt concentration, polymer charge density and degree of polymerization. They correlated the ^{23}Na results with the relaxation behaviour of deuterons in selectively deuterated polymer chains. Linse *et al.*[669] have studied ^{25}Mg relaxation in the presence of polystyrenesulphonate. Urry and coworkers reported quadrupolar ion relaxation studies of interactions of alkali metal ions with gramicidin A incorporated in lysolecithin micelles and summarized the data in a review.[670] Finally, ^{35}Cl and ^{81}Br relaxation measurements of micellar solutions of hexadecyltrimethylammonium chloride and bromide have been described.[671]

I now turn to counterion nuclei relaxation in biopolymer systems and begin with nucleic acids. Bleam *et al.*[672,673] have reported ^{23}Na linewidth measurements on NaDNA systems as a function of temperature and as a function of the concentration of sodium and other ions. No evidence of a non-Lorentzian lineshape was found. The results were discussed in view of current theories of counterion binding to linear polyelectrolytes. Braunlin and Nordenskiöld[674] have presented a similar study of potassium binding to double-helical DNA using ^{39}K NMR, and found that the lineshape could not be fitted to a single Lorentzian. Non-Lorentzian lineshapes were also observed[675] in a study on interactions between DNA and Mg(II) using ^{25}Mg NMR. Braunlin *et al.*[676] have reported ^{43}Ca spin–lattice and linewidth studies of Ca(II)–DNA interactions. Under the conditions of their experiments, the lineshape was always Lorentzian and the spin–lattice relaxation always exponential. The longitudinal and transverse relaxation rates, however, were not equal.

Most of the metal-ion NMR studies of protein–metal interaction are judged to be too biochemically oriented to be included in this review. However, I wish to mention some papers on ^{23}Na in protein systems. Transverse and longitudinal ^{23}Na relaxation have been studied in solutions of plasma proteins and in some body fluids.[677] The authors were unable to resolve the magnetization decay curves into two exponentials and a procedure was proposed for the quantitative interpretation of the measured relaxation rates. Two papers have dealt with the methodological improvements facilitating the detection of multiexponential relaxation in protein solutions. For this purpose the use of a double-quantum filtered spectrum was proposed (see Section 3.4

of Part 1) and it was demonstrated that the two signal components in such a spectrum occurred in antiphase.[678] Rooney *et al.*[679] actually measured double-quantum spectrum (and double-quantum linewidth) of an isotropic protein solution, where the occurrence of the double-quantum line is directly related to biexponential relaxation.

Some additional papers on metal-nuclei relaxation in protein systems, where the metal is strongly bound to the protein, are mentioned in Section 3.3.

3.2 Relaxation of nuclei in amphiphilic molecules in aggregates

After covering the relaxation studies of the nuclei residing in the environment of aggregates and macromolecules, in this section work on micellar systems employing nuclear relaxation measurements on nuclei residing in the micelles themselves is reviewed. Also included are studies of inverted micellar systems. The field covered here has been subject to several reviews. I wish to mention in particular the comprehensive surveys by Chachaty[680] and by Lindman *et al.*[681]

^{13}C spin–lattice relaxation in micellar solutions is usually characterized by a T_1 of a magnitude that indicates extreme narrowing conditions. At the same time, the relaxation rates are not field independent and the NOE is not complete, though the DD mechanism clearly dominates. An important contribution to the understanding of relaxation phenomena in micellar systems has been presented by Wennerström *et al.*,[682] who formulated the so-called two-step model for ^{13}C relaxation in alkyl chains of micelle-forming amphiphiles. In the first step, the fast local motions average out most (but not all) of the DD interaction; the magnitude of the residual DD interaction at a particular site depends on the degree of local anisotropy and is characterized by an "order parameter". The residual is averaged out on a slower time-scale by motions of the aggregate itself. The two-step model is thus capable of providing both the dynamic information, in the form of the two correlation times, and the time-averaged information of the degree of the local order. This particular form of the two-step model is a development of earlier ideas[683] and is analogous to the model proposed for quadrupolar relaxation.[619] A very similar theory, known as the "model-free approach", was also developed in the context of biopolymers in solution.[684] Wennerström *et al.*[682] have employed their model to analyse ^{13}C T_1 measurements on sodium octanoate micelles and were able to relate the observed frequency dependence of the relaxation rate to the slow micellar motion.

Similar experiments and a similar interpretation have more recently been presented for other micellar and microemulsion systems.[185,685–689] The two-step model can also be applied to other nuclei residing in the amphiphiles, with ^{2}H being the most obvious candidate (compare Section 2.3). Söderman

et al.[690] have reported combined ^{2}H, ^{13}C and ^{14}N, multiple-field relaxation measurements on the micellar phase of a dodecyltrimethylammonium chloride–water system. They were able to show that the order parameters obtained from the relaxation measurements agree reasonably well with the order parameters obtained from static quadrupolar splittings for ^{2}H and ^{14}N in the liquid-crystalline phase of the same two-component system. They also proposed a "three-step model", a generalization allowing for the non-spherical shape of the micelles. Söderman and coworkers[691–694] have employed multiple-field deuteron relaxation measurements and the two-step (or three-step) model to aqueous micellar and microemulsion systems. A typical set of data, obtained for hexadecyltrimethylammonium chloride micelles[689] is shown in Fig. 6. Similar work has also been presented on micellar solutions in nonaqueous solvents.[695] Belmajdoub *et al.*[696–698] have reported multiple-field ^{13}C, ^{14}N and ^{1}H relaxation measurements for micellar systems in D_2O. The proton signals from the various methylene groups were unresolved and showed an exponential spin–lattice relaxation. Proton relaxation experiments, interpreted using the two-step model, have also been reported.[699] Combined frequency-dependent ^{13}C and ^{15}N relaxation mea-

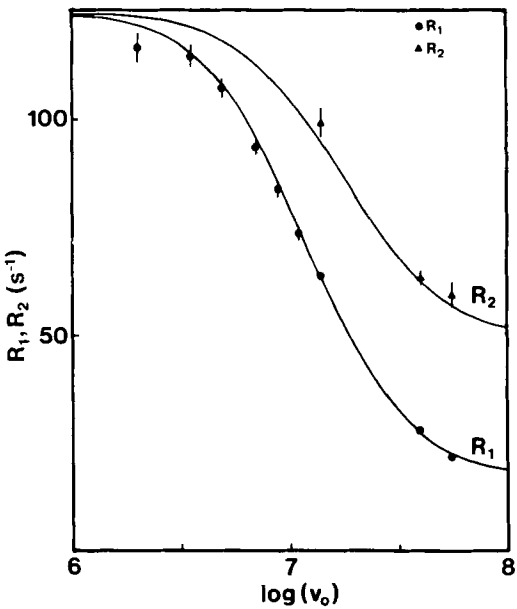

Fig. 6. Deuteron spin–lattice (●) and spin–spin (▲) relaxation rates as function of the logarithm of Larmor frequency (in Hz) for hexadecyltrimethylammonium chloride micelles. (Reproduced with permission from O. Söderman *et al.*[691])

surements on micellar solutions, interpreted using the two-step model have been presented.[700,701]

Two groups have presented related multinuclear, multiple-field relaxation measurements on micellar systems, including the data for organic counterions. Chachaty *et al.*[702] have studied micellar solutions of pyridinium octylhydrogen phosphate, using ^{1}H, ^{2}H, ^{13}C and ^{31}P relaxation measurements. Jansson *et al.*[703] have reported ^{2}H and ^{13}C relaxation data on decylammonium butanoate. The data on the butanoate ion indicated that it was strongly anchored at the micelle, with the hydrocarbon tail oriented towards the hydrocarbon core. Heatley[704] has studied ^{1}H and ^{13}C longitudinal and transverse relaxation as a function of resonance frequency for surfactant aerosol OT in methanol solution and in inverted microemulsions in benzene. Deuteron relaxation and the lineshape of deuteron coupled ^{13}C resonance at a single magnetic field has been reported.[705] These two experiments provide model-independent values of spectral densities at the deuteron Larmor frequency, ω_0, and at $2\omega_0$. The spectral densities obtained in this way were compared with the results of the two-step model with parameters from a fit to deuteron relaxation at three different fields and the agreement was excellent. Söderman and Stilbs[706] have demonstrated that the two-step model could be useful for ^{13}C relaxation studies at a single magnetic field, if both the T_1 and the NOE were determined and if one was satisfied with obtaining the relative (rather than absolute) order parameter profile for the alkyl chain. Similar work employing single-field ^{13}C T_1 and T_2 and ^{1}H spin–lattice relaxation measurements has also been reported.[707]

I turn now to other types of relaxation work on micellar systems. At almost the same time as the two-step model was presented,[682] Canet *et al.*[708] proposed a somewhat different theory for ^{13}C relaxation in micellar systems. The approach was essentially a modification of Woessner's anisotropic rotational diffusion model. It was applied by the same group[709,710] and by Faure *et al.*;[639] more recently, the same authors turned to the two-step model. Frequency-dependent ^{13}C T_1 measurements in a micellar system were also reported and the results interpreted using the concept of the distribution of correlation times.[711] Ueno and Kishimoto[712] and Matsushita *et al.*[713] have used the ^{13}C T_1 data measured as a function of concentration to study the micelle-formation phenomena. ^{13}C relaxation has been used to probe internal motions in unsaturated monomeric surfactants and their oligomeric analogues.[714]

Stark *et al.*[715] have reported ^{13}C relaxation measurements on nitrobenzene and aniline dissolved in micellar solutions, while perdeuterated *trans*-decalin, solubilized in a variety of micellar environments has been studied using ^{2}H relaxation.[716] Both groups analysed the data using the fully anisotropic rotational diffusion model and discussed the motional restrictions imposed by

the micellar environment as well as the applicability of the hydrodynamic approach. Somewhat similar measurements have also been reported for other systems, involving solubilization in micelles.[717,718]

Ulmius and Lindman[719] have studied ^{19}F relaxation in micelles consisting of fluorinated amphiphiles. The ^{19}F relaxation was found to arise partly from intermolecular DD interactions with water protons and was used to probe the water penetration into micelles. Boicelli *et al.*[720] have studied ^{31}P relaxation in phosphate ions in inverted micelles as a function of the pH, while ^{31}P relaxation in sodium dibutylphosphate solution, measured as a function of concentration, has been used to follow the aggregation phenomena.[721] ^{31}P relaxation measurements in micellar monoalkylphosphate solutions have been reported and the data analysed assuming anisotropic motion.[722]

Some authors have studied relaxation in multispin systems in micellar solution. Prestegard and Grant[723] have studied the width of different components of the ^{13}C multiplet of the methylene group. The difference between the inner and the outer lines (differential line broadening, DLB) was related to the cross-correlation spectral densities. A theory has been presented[724] for DLB for methyl carbon multiplet in micelles, under the motional conditions corresponding to the two-step model.[682] An experimental procedure and theoretical analysis for extraction of cross-correlation spectral densities for methyl groups has been reported.[725] The procedure involved, besides conventional ^1H spin–lattice and spin–spin relaxation experiments, the observation of relaxation-allowed transitions in double-quantum filtered proton spectra. The method was applied to deoxycholate micelles. Wong *et al.*[726] have reported a comprehensive investigation of the same system, employing multiple-field $^{13}CT_1$ ^{13}C DLB and ^1H multiple-quantum relaxation.

Proton relaxation in salicylate ion in viscoelastic micelles has been studied.[727] Nonselective inversion-recovery, linewidth and NOE measurement were presented and the rotational dynamics discussed. Two-dimensional NOE experiments as a tool for structural studies of micellar systems have been reported.[728,729] Finally, Nery *et al.*[730] have studied proton relaxation in binary systems D_2O–n-alkylammonium chloride ($n = 8$–14) as a function of temperature and concentration, while Zheliaskova and Derzhanski[731,732] have reported similar measurements in the micellar phase of the alkylphenylpolyethylene glycol–water system.

3.3. Relaxation of nuclei residing in macromolecules

In this section a selection of applications of nuclear spin relaxation studies on nuclei residing in macromolecules is presented. Several theory-oriented papers

of relevance to this section were mentioned in Section 2.4 of Part 1, while papers devoted to experimental methodology can be found throughout Section 3 of Part 1. In order to save space, I abstain as far as possible from referring to this work here.

The organization of this section is as follows. First, work on synthetic polymers is presented and then studies on proteins, nucleic acids and polysaccharides are discussed. Within each category of compounds, I include the dynamic as well as the structural aspects. The structural work often involves two-dimensional NOE measurements. I follow here the praxis of Section 2, i.e. of being restrictive in referring to the NOE studies. Thus, reports on NOESY spectra using a single mixing time are not included. Moreover, work considered to be primarily of biochemical interest is not covered.

Among recent monographs and review papers pertaining to this section, I wish to mention in particular a book on the NMR of proteins and nucleic acids[733] and a review on the relaxation and backbone motions of macromolecules in solution.[734] Among earlier reviews, the papers by Wright *et al.*[65] and by Jardetzky[735] should be mentioned.

I begin the discussion of the relaxation studies of synthetic polymers by citing a series of studies by Leyte and coworkers in which deuteron relaxation measurements were employed.[736-739] Mulder and coworkers[736,737] have studied methyl and methylene deuterated forms of poly(methacrylic acid) at several different magnetic field strengths and compared to the results of the analysis of the data using the anisotropic rotational diffusion model, the empirical multi-Lorentzian spectral density description, the model-free approach[684] and the damped diffusion model.[740,741] The anisotropic diffusion model was found to be preferable in terms of the number of parameters required to reproduce the experimental data. In two other papers from the same group,[738,739] a study of the main-chain dynamics of methylene deuterated sodium polyacrylate in aqueous solution was reported and different models compared. The role of electrostatic interactions and their implications for counterion relaxation were discussed.

A large number of authors have reported ^{13}C relaxation (T_1 and NOE) experiments, sometimes combined with proton relaxation studies. Levy *et al.*[742] reported early variable-frequency and variable-temperature $^{13}C\,T_1$ and NOE measurements on poly(n-alkylmethacrylate). The dynamic model used for the interpretation of the results included the distribution of the correlation times for the backbone and multiple internal rotations of the side chains. The same group later also presented a modified interpretation of the data.[260] Several groups have presented multiple-field ^{13}C measurements and interpreted the results using the models developed for 'flexible chains" (in the terminology of Heatley[734]), i.e. a model centered around the concerted conformational transitions in polymers. Bergmann and Schlothauer[743] have

studied in this way the copolymers of vinyl chloride and vinylidene chloride and used the so-called VJGM model (see Section 2.4 of Part 1) for interpreting the data. Model calculations of relevance to this work have been presented.[744] Ratto *et al.*[745] have presented variable-temperature, two-magnetic fields work on substituted polycarbonates in solution, they used the Hall–Helfand model and related the results to the properties of the monomer units. Chi-Cheng Hung *et al.*[746] have reported similar work on other synthetic polymers and compared the Hall–Helfand and Woessner-like approaches. Single-magnetic-field, variable-temperature ^{13}C experiments have been made on poly(2-hydroxyethylmethacrylate) and the data interpreted using the distribution of correlation times and VJGM models.[747] Bahar *et al.*[748] have presented a related dynamic model, based on the stochastic treatment of conformational transitions in a polymer, and applied it to the earlier ^{13}C and ^{1}H relaxation data on poly(ethyleneglycol) in a variety of solvents. The same polymer has been studied in aqueous solution using ^{13}C and ^{1}H relaxation.[749] The local polymer dynamics was described in terms of the reorientation of a small segment and internal motions within it. Rinaldi *et al.*[750] have presented a ^{13}C and ^{15}N spin–lattice relaxation study on poly(vinylamine) and poly(iminoethylene) in aqueous solution as a function of pH. The data were interpreted qualitatively in terms of effective correlation times. Equally qualitative was the work of Cole *et al.*[751] who compared their ^{13}C experiments on several copolymers and terpolymers and compared the NMR data with the results of dielectric relaxation studies.

Among proton relaxation work on synthetic polymers I wish to mention only three recent papers. Skolnick and Yarvis[752] have applied the damped-diffusion model to proton relaxation data of poly(vinylacetate) in toulene solution. Tabak[753] has reported spin–lattice and spin–spin relaxation studies as a function of magnetic field for solutions of poly(methylmethacrylate) and poly(styrene). The data were interpreted in terms of segmental dynamics. Usmanov and Sivergin[754] have reported similar measurements for another polymer solution and interpreted the data using the distribution of correlation times.

I now turn to the work on polypeptides and proteins in solution and begin with ^{13}C studies. Some of the work on ^{13}C is of primarily methodological interest. Dill and Allerhand[755] have studied ^{13}C relaxation in egg-white lysozyme treated as a rigid isotropic rotor.[755] They pointed out that, in systems outside of the extreme narrowing region, small errors in the assumed CH distances could lead to large errors in rotational correlation times, and proposed a methodology for estimating the distance from combined ^{13}C T_1 and NOE measurements in the vicinity of the minimum in the T_1 vs. τ_R curve. Jarvet[756] studied ^{13}C spin-lattice relaxation behaviour for carbonic anhydrase in aqueous solution. The relaxation of all α-carbons in the molecule

was found to be exponential, while a moderate nonexponentiality was observed for the CH_2 and CH_3 carbons. The results were also compared with the results of experiments made on a powder sample, where the relaxation process was severely nonexponential. The linewidth and the spin–lattice relaxation of the carbonyl carbon in a ^{13}C enriched protein has been reported.[757] The experiments were carried out as a function of temperature in a DMSO–water mixture. The relaxation rates were consistent with the CSA relaxation mechanism and varied with viscosity in a manner consistent with the hydrodynamics of a rigid body.

Some authors have interpreted ^{13}C relaxation measurements on polypeptides and proteins in terms of models for protein dynamics. Perly *et al.*[758] have reported ^{13}C and ^{1}H relaxation measurements on a polypeptide. The α-carbon relaxation was interpreted using a distribution-of-correlation-times model, while additional motions were allowed for the side chains. More recently, various "model-free" approaches have been applied. For bovine pancreatic trypsin inhibitor (BPTI) ^{13}C T_1, T_2 and NOE data at two magnetic fields have been reported.[759] The same protein was also studied by Fedotov.[760] Both groups used their own versions of the "model-free" method. The Lipari and Szabo[684] approach was selected in work on Gramicidin A in DMSO solution.[761] The order parameter was found to be approximately constant along the chain, while the short correlation time indicated that the internal motions became more rapid towards the N-terminus.

With regard to the proton relaxation (and cross-relaxation) work on polypeptides and proteins, the proton spin–lattice relaxation times of some resonances in chlorophyll a have been reported.[762] The nonselective inversion-recovery experiments were interpreted in terms of single-exponential relaxation processes for selected protons and the resulting "T_1" values were used as a structural tool. Torda and Norton[763] have reported a similar work on a natural polypeptide, employing ^{1}H measurements at several different fields and interpreting the results within the "model-free" approach.

Structural applications of the proton cross-relaxation by means of the two-dimensional NOE (NOESY) method have been discussed at length in recent books[20,733] as well as in numerous reviews, e.g. Refs 764–766. There is nothing I can add to these papers and I wish here only to mention some methodologically oriented work which could have been mentioned in Sections 3.3 and 3.5 of Part 1. Clore and Gronenborn[767] presented the theory of time-dependent transferred NOE for exchanging systems and applied it to a ligand–protein complex. Olejniczak *et al.*[768] have discussed the time evolution of proton NOE after a selective saturation, and its implications for determining internuclear distances. Lysozyme was used as an example. Mirau and Bovey[769] have studied an α-helical polypeptide using

two-dimensional NOE experiments (for ten different mixing times) and nonselective relaxation measurements. In this way, they were able to investigate both the reorientational dynamics and interatomic distances.

I turn next to relaxation studies of nuclei other than ^{13}C or ^{1}H in proteins. Individual transitions have been studied in the ^{31}P and ^{19}F spectra of glycogen phosphorylase, containing the fluorophosphate instead of the phosphate group.[770] The experiments provided the interference terms between the DD and the CSA interactions. This work[770] has been given a more general interpretation by Werbelow.[771] Some authors have studied the relaxation of metal nuclei residing in proteins. Andersson *et al.*[772] have reported spin–lattice and spin–spin relaxation measurements on ^{43}Ca bound to proteins parvalbumin, troponin C and calmodulin. Apparent relaxation rates (corresponding to the assumed single-exponential relaxation) were obtained. The analysis yielded both the rotational correlation times and the quadrupolar coupling constants. Ellis and coworkers[773] have presented a careful, multiple-magnetic-field investigation of ^{113}Cd relaxation and exchange kinetics in cadmium substituted calmodulin. Finally, Baltzer *et al.*[774,775] have reported relaxation data on ^{57}Fe in carbonylmyoglobin and ferrocytochrome c.

Next, I turn to the relaxation studies of nucleic acids. Several theory-oriented papers concerned with ^{13}C relaxation were mentioned in Section 2.4 of Part 1; I do not repeat the references here. I begin the discussion with studies involving nuclei other than protons. In an early paper, Bolton and James[776] reported ^{31}P (T_1, NOE, linewidth and off-resonance $T_{1\rho}$ at two magnetic fields) and ^{13}C T_1 and NOE studies in polynucleotides poly(A) and poly(I)–poly(C) and in calf thymus DNA. The ^{31}P relaxation was shown to be due to both the DD interaction with protons and to the CSA mechanism and the results were interpreted using a two-correlation-times model. Poly(A), enriched in ^{17}O, was also studied by using ^{17}O spin–lattice and spin–spin relaxation measurements.[777] Levy *et al.*[778] have studied nucleosome-length DNA fragments (120–160 base pairs) and reported ^{13}C T_1, T_2 and NOE measurements at four magnetic fields. The results were discussed only qualitatively. Borer *et al.*[779] also reported ^{13}C relaxation studies of shorter DNA fragments, while Schmidt *et al.*[780] investigated ^{13}C relaxation in transfer RNA, isotopically enriched at C-1 of ribose. The internal dynamics of the molecule was discussed using several models. More recently, some groups have studied the internal dynamics of nucleic acids using the "model-free" approach.[684] Schmidt *et al.*[781] have reported ^{13}C T_1 and NOE measurements at three magnetic fields on a ^{13}C enriched sample of transfer RNA. Similar measurements, also including the linewidths, on a synthetic oligonucleotide adopting a hairpin conformation, were given by Williamson and Boxer.[782] In another paper concerned with the same system,[783] the authors combined the ^{13}C data with ^{31}P T_1 and T_2 measurements.

We turn now to proton relaxation studies. Mirau and Bovey[784] have reported proton spin–lattice relaxation measurements, following nonselective, selective and biselective excitation, for imino protons in double-stranded RNA polymer, poly(rA)·poly(rU). The dipolar and exchange contributions to the measured rates were resolved. NOE studies of nucleic acids are quite numerous and were reviewed in the monographs mentioned above[20,733] and in a recent survey.[785] As in the case of low molecular-weight and protein studies, I wish to mention here only few papers that are either methodology oriented or actually follow the time course of the cross-relaxation phenomena by reporting variable-mixing-time two-dimensional NOE experiments. A quantitative complete relaxation matrix analysis of the NOE build-up after a selective inversion has been presented using poly(A) and poly(C) as examples[786] James and coworkers[787,788] have reported two-dimensional NOE studies with several mixing times on DNA octamer duplexes and interpreted the data in terms of molecular structure and dynamics. A similar system has also recently been studied by Boelens *et al.*[789] and used as a model compound for an iterative relaxation matrix approach to macromolecular structure determination. Finally, Yu-Sen Wang and Ikuta[790] have proposed a method to account for proton $T_{1\rho}$ in biomolecules in solution and applied it to oligodeoxynucleotides of *B* and *Z* type.

The last category of macromolelcules to be discussed here are the polysaccharides. The nucleus of choice here has been ^{13}C and the interpretation of the results has been qualitatative. Gagnaire *et al.*[791] have presented such data on polysaccharide nigeran and discussed the link between carbon relaxation and conformational analysis. $^{13}CT_1$ and NOE data have been reported on dextran and amylose in aqueous and DMSO solutions.[792] Qin-Ji Peng and Perlin[793] reported similar measurements on various starches. Finally, ^{13}C relaxation measurements have been used to study the interaction between another polysaccharide, heparin, and calcium ions.[794]

4. CONCLUDING REMARKS

Over the last decade, the field of nuclear magnetic relaxation has been highly active, showing a great deal of innovative ideas and a rapid evolution towards steadily more demanding applications. In these concluding remarks, I wish to summarize the most important developments of the 1980s (some of which have their roots in the 1970s), as well as to attempt to make some guesses on future developments. The order of various topics corresponds roughly to the consecutive sections of Parts 1 and 2 of the present review. I have chosen to present this discussion in general terms, without referring to individual papers.

In the field of relaxation theory, the development of the Liouville superoperator methods is judged as being very important and is likely to

continue, both in the context of treating complex dynamic situations and with the purpose of obtaining a more unified description of evolution, relaxation and exchange processes in two-dimensional experiments. Another development the importance of which I wish to emphasize, is the increased appreciation of the interference and cross-correlation phenomena, in particular the role of the combined DD–CSA and dipolar–quadrupolar interactions. Further theoretical as well as experimental contributions seem well motivated. In the area of spin relaxation and molecular dynamics, I feel that the use of simulations as a reference of analytical models is going to prove increasingly fruitful. Among the analytical models developed during the last decade, the conceptual simplicity of the two-step model or the "model-free" approach appears to be particularly valuable. Finally, the difficult area at the borderline of relaxation and chemical-exchange phenomena has undergone an important theoretical development, which is likely to continue.

The experimental methodology in the field of relaxation-related studies has been an important part of the recent avalanche-like progress of the NMR method in general. In particular, one should stress the importance of cross-relaxation phenomena and of the two-dimensional NOE experiment as a tool for their measurement. The areas of multiple-quantum (MQ) relaxation, MQ-filtered relaxation experiments, relaxation-allowed coherence transfer phenomena, etc., demonstrate the power of sophisticated pulse techniques in combination with elegant theoretical analysis. As mentioned above, the frontier between the theoretical relaxation work and the design of new experiments is likely to become even more diffuse. Finally, the continuing rapid development in advanced methods for the analysis of the relaxation data, both in terms of dynamic models and in terms of internuclear distances, should be emphasized.

The theoretical and experimental developments mentioned above have also been implemented in the field of applications. Turning to these, I wish first to mention the rapid accumulation of data on the relaxation of nuclei residing in water molecules in simple as well as complicated (macromolecular and colloidal) systems and the improved understanding thereof. The work on the magnetic nuclei available in water molecules, including the effects of isotopic substitution at one site in the molecule on the nuclear relaxation at another site, extensive variable-field measurements and improved theoretical models have been essential for this development. Magnetic relaxation studies are here a part of the broad effort to reach a better understanding of the physical details of interactions between water molecules and macromolecules, which is certainly going to progress rapidly.

The truly multinuclear era in relaxation measurements, which opened in the 1980s with advances in instrumentation, has obvious implications for the field denoted "inorganic applications". Among the main-group elements, a lot of

interesting chemistry has been reported, some of it involving the "dual spin probe" technique. In the field of transition metals, most of the work has been exploratory or routine. However, some sophisticated applications have also been reported, not least on the ^{113}Cd nucleus. Advanced nuclear relaxation work on metal-containing systems is very likely soon to expand in volume.

Relaxation studies of pure liquids and liquid mixtures, initiated in the 1960s, have remained a field of interest for many authors. Of particular interest are studies aimed at improving the understanding of molecular interactions and dynamics, including both temperature and pressure as experimental variables. Hopefully, the availability of accurate data of this type will stimulate the general progress in the area of the theory of liquids. Another related development involves combining NMR relaxation measurements with other techniques, e.g. Raman or Rayleigh light scattering, translational diffusion studies and molecular dynamics simulations.

In the area of measurements on organic solutes, I wish in particular to stress three developments, all of which are likely to flourish in the years to come. The availability of improved methods for the analysis of relaxation data at several sites of one molecule has enabled the elaborate characterization of the anisotropic motions of small and medium-sized molecules. Moreover, the development of both the instrumentation and models has made it possible to extend quantitatively relevant analysis (in terms of molecular dynamics) to large molecules and aggregates. Last, but not least, ^{1}H cross-relaxation measurements (sometimes combined with ^{13}C relaxation studies) have proved to be extremely fruitful in the study of the dynamics and structure of medium to large sized molecules in solution.

ACKNOWLEDGEMENTS

I wish to express my gratitude of the Swedish Natural Science Research Council for its continuing support of my research in the field of nuclear spin relaxation, without which the writing of this review would not be possible. My coworkers and my family are gratefully acknowledged for their support and patience during the more than one year which it took to prepare this work. Finally, I am indebted to Barbara Hessel for her skilful contribution to making the manuscript presentable.

REFERENCES

1. J. Kowalewski, *Annual Reports on NMR Spectroscopy*, Vol. 22 (ed. G.A. Webb), p. 307. Academic Press, London, 1990.

2. H. Weingärtner, in *Specialist Periodical Reports on NMR* , Vol. 18 (ed. G.A. Webb), p. 134. Royal Society of Chemistry, London, 1989.
3. S. Szymanski and G. Binsch, *J. Magn. Reson.*, 1989, **81**, 104.
4. Zheng-Yu Peng and Chien Ho, *J. Magn. Reson.*, 1989, **82**, 318.
5. E.R. Henry and A. Szabo, *J. Chem. Phys.*, 1985, **82**, 4753.
6. D. Canet, *Progr. NMR Spectrosc.*, 1989, **21**, 237.
7. H.J. Bender and M.D. Zeidler, *Ber. Bunsenges. Phys. Chem.*, 1971, **75**, 236.
8. R.L. Vold, R.R. Vold and M. Warner, *J. Chem. Soc., Faraday Trans. 2*, 1988, **84**, 997.
9. G. Van der Zwan and L. Plomp, *Liq. Cryst.*, 1989, **4**, 133.
10. T.E. Bull, *Chem. Phys.*, 1988, **121**, 1.
11. R. Uusvuori and M. Lounasmaa, *Magn. Reson. Chem.*, 1986, **24**, 1048.
12. M. Baldo and A. Grassi, *Magn. Reson. Chem.*, 1989, **27**, 533.
13. E. Belorizky and P.H. Fries, *Chem. Phys. Lett.*, 1988, **145**, 33.
14. K.V. Vasavada and J.I. Kaplan, *J. Magn. Reson.*, 1985, **64**, 32.
15. P.-O. Westlund and H. Wennerström, *J. Magn. Reson.*, 1989, **81**, 68.
16. K. Ichikawa, *J. Chem. Soc., Faraday Trans. 2*, 1986, **82**, 1913.
17. D. Canet, J. Brondeau and K. Elbayed, *J. Magn. Reson.*, 1988, **77**, 483.
18. J. Homer and J.K. Roberts, *J. Magn. Reson.*, 1987, **74**, 424.
19. N.R. Nirmala and G. Wagner, *J. Magn. Reson.*, 1989, **82**, 659.
20. D. Neuhaus and M.P. Williamson, *The Nuclear Overhauser Effect*. VCH, Weinheim, 1989.
21. J. Keeler, D. Neuhaus, and M.P. Williamson, *J. Magn. Reson.*, 1987, **73**, 45.
22. J. Keeler and F. Sanchez-Ferrando, *J. Magn. Reson.*, 1987, **75**, 96.
23. S.B. Landy and B.D.N. Rao, *J. Magn. Reson.*, 1989, **81**, 371.
24. H. Oschkinat, D. Limat, L. Emsley, and G. Bodenhausen, *J. Magn. Reson.*, 1989, **81**, 13. H. Oschkinat and W. Bermel, *J. Magn. Reson.*, 1989, **81**, 220.
25. L. Emsley and G. Bodenhausen, *J. Magn. Reson.*, 1989, **82**, 211.
26. N.H. Andersen, H.L. Eaton and Xiaonian Lai, *Magn. Reson. Chem.*, 1989, **27**, 515.
27. Zhao Dezheng, T. Fujiwara and K. Nagayama, *J. Magn. Reson.*, 1989, **81**, 628.
28. K.E. Kövér and G. Batta, *J. Magn. Reson.*, 1986, **69**, 344.
29. N. Müller, *J. Magn. Reson.*, 1989, **81**, 520.
30. S. Wimperis and G. Bodenhausen, *Mol. Phys.*, 1989, **66**, 897.
31. J.-M. Böhlen, S. Wimperis and G. Bodenhausen, *J. Magn. Reson.*, 1988, **77**, 589.
32. R.J.S. Brown, *J. Magn. Reson.*, 1989, **82**, 539.
33. H. Barkhuijsen, R. de Beer, W.M.M.J. Bovée and D. van Ormondt, *J. Magn. Reson.*, 1985, **61**, 465. H. Barkhuijsen, R. de Beer, and D. van Ormondt, *J. Magn. Reson.*, 1987, **73**, 553. J. Tang and J.R. Norris, *J. Magn. Reson.*, 1986, **69**, 180.
34. W. Denk, R. Baumann and G. Wagner, *J. Magn. Reson.*, 1986, **67**, 386.
35. T.A. Holak, J.N. Scarsdale and J.H. Prestegard, *J. Magn. Reson.*, 1987, **74**, 546.
36. E.T. Olejniczak, R.T. Gampe and S.W. Fesik, *J. Magn. Reson.*, 1989, **81**, 178.
37. V. Stoven, A. Mikou, D. Piveteau, E. Guittet and J.-Y. Lallemand, *J. Magn. Reson.*, 1989, **82**, 163.
38. D.M. LeMaster, L.E. Kay, A.T. Brünger and J.H. Prestegard, *FEBS Lett.*, 1988, **236**, 71
39. E.T. Olejniczak, *J. Magn. Reson.*, 1989, **81**, 392.
40. J. Fejzo, Z. Zolnai, S. Macura and J.L. Markley, *J. Magn. Reson.*, 1989, **82**, 518.
41. S.B. Landy and B.D.N. Rao, *J. Magn. Reson.*, 1989, **83**, 29.
42. M. Madrid, J.E. Mace and O. Jardetzky, *J. Magn. Reson.*, 1989, **83**, 267.
43. I. Ursu, M. Bogdan, F. Balibanu, P. Fitori, G. Mihailescu and D.E. Demco, *Mol. Phys.*, 1987, **60**, 1357.
44. F. Brunet, P. Rigny and J. Virlet, *Rev. Roum. Phys.*, 1988, **33**, 445.
45. J.R.C. Van der Maarel, *J. Magn. Reson.*, 1989, **81**, 92.

46. K. Ichikawa and T. Jin, *Chem. Lett.*, 1987, 1179.
47. I.S. Pronin and A.A. Vashman, *Zh Neorg. Khim.*, 1987, **32**, 603 (*Chem. Abs.*, 1987, 107:47040f).
48. M. Holz and A. Sacco, *Z. Phys. Chem. (Munich)*, 1987, **153**, 129.
49. G.W. Buchanan, R.A. Kirby, K. Bourque and C. Morat, *Can. J. Chem.*, 1988, **66**, 2204.
50. A. Delville, H.D.H. Stöver and C. Detellier, *J. Am. Chem. Soc.*, 1987, **109**, 7293.
51. T. Harazono, K. Tanaka and Y. Takeuchi, *Inorg. Chem.*, 1987, **26**, 1894.
52. E. Liepins, I. Zicmane and E. Lukevics, *J. Organomet. Chem.*, 1988, **341**, 315.
53. F. Sakai, H. Fujiwara and Y. Sasaki, *J. Organomet. Chem.*, 1986, **310**, 293.
54. S. Chapelle and P. Granger, *J. Magn. Reson.*, 1988, **76**, 1.
55. L. Helm, C. Ammann and A.E. Merbach, *Z. Phys. Chem. (Munich)*, 1987, **155**, 145.
56. R.T.C. Brownlee, B.P. Shehan and A.G. Wedd, *Aust. J. Chem.*, 1988, **41**, 1457; *Inorg. Chem.*, 1987, **26**, 2022.
57. R.T.C. Brownlee, M.J. O'Connor, B.P. Shehan and A.G. Wedd, *Aust. J. Chem.*, 1986, **39**, 931.
58. M. Findeisen, L. Kaden, B. Lorenz, S. Rummel and M. Wahren, *Inorg. Chim. Acta*, 1987, **128**, L15. M. Findeisen, L. Kaden, B. Lorenz and M. Wahren, *Inorg. Chim. Acta*, 1988, **142**, 3.
59. F.A. Cotton and R.L. Luck, *Inorg. Chem.*, 1989, **28**, 8.
60. Y. Masuda and H. Yamatera, *J. Phys. Chem.*, 1988, **92**, 2067.
61. S.M. Socol, S. Lacelle and J.G. Verkade, *Inorg. Chem.*, 1987, **26**, 3221.
62. G.M. Bodner and L. Bauer, *J. Organomet. Chem.*, 1982, **226**, 85.
63. D.D. McIntyre, A.W. Apblett, P. Lundberg, K.J. Schmidt and H.J. Vogel, *J. Magn. Reson.*, 1989, **83**, 377.
64. K. Miura, M. Tanaka, H. Fukui and H. Toyama, *J. Phys. Chem.*, 1988, **92**, 2390.
65. D.A. Wright, D.E. Axelson and G.C. Levy, in *Topics in Carbon-13 NMR Spectroscopy*, Vol. 3 (ed. G.C. Levy), Chap. 2. Wiley, New York, 1979.
66. R.T. Boeré and R.G. Kidd, *Annual Reports on NMR Spectroscopy*, Vol. 13, p. 319. Academic Press, London, 1983.
67. J. Jonas, *Acc. Chem. Res.*, 1984, **17**, 74.
68. E. Fukushima, A.A.V. Gibson and T.A. Scott, *J. Chem. Phys.*, 1979, **71**, 1531.
69. F. Li, J.R. Brookeman, A. Rigamonti and T.A. Scott, *J. Chem. Phys.*, 1981, **74**, 3120.
70. R.E. Wasylishen, *Can. J. Chem.*, 1987, **65**, 2077.
71. S.K. Garg, J.A. Ripmeester and D.W. Davidson, *J. Chem. Phys.*, 1980, **73**, 2005.
72. K.T. Gillen, J.H. Noggle and T.K. Leipert, *Chem. Phys. Lett.*, 1972, **17**, 505.
73. D.E. O'Reilly, E.M. Peterson and C.E. Scheie, *J. Chem. Phys.*, 1974, **60**, 1603.
74. M. Ohuchi, T. Fujito and M. Imanari, *J. Magn. Reson.*, 1979, **35**, 415.
75. B.A. Pettitt and R.E. Wasylishen, *Chem. Phys. Lett.*, 1979, **63**, 539.
76. H. Radkowitsch, F.X. Prielmeier, E.W. Lang and H.-D. Lüdemann, *Physica*, 1986, **139–140B**, 96.
77. E.W. Lang, F.X. Prielmeier, H. Radkowitsch and H.-D. Lüdemann, *Ber. Bunsenges. Phys. Chem.*, 1987, **91**, 1017.
78. E.W. Lang, F.X. Prielmeier, H. Radkowitsch and H.-D. Lüdemann, *Ber. Bunsenges. Phys. Chem.*, 1987, **91**, 1025.
79. C.R. Lassigne and E.J. Wells, *J. Magn. Reson.*, 1977, **26**, 55.
80. M. Yanagisawa and O. Yamamoto, *Bull. Chem. Soc. Jpn.*, 1979, **52**, 2147.
81. M. Schwartz, *Chem. Phys. Lett.*, 1980, **73**, 127.
82. W.T. Huntress, Jr., *J. Phys. Chem.*, 1969, **73**, 103.
83. D.L. VanderHart, *J. Chem. Phys.*, 1974, **60**, 1858.
84. Lian-Pin Hwang, *Mol. Phys.*, 1984, **51**, 1235.
85. M. Rabii, *J. Chem. Phys.*, 1985, **83**, 4972.
86. J. DeZwaan and J. Jonas, *J. Chem. Phys.*, 1975, **62**, 4036.

87. H.S. Sandhu, *J. Magn. Reson.*, 1978, **29**, 563.
88. A.A. Rodrigues, S.J.H. Chen and M. Schwartz, *J. Magn. Reson.*, 1987, **74**, 114.
89. T.M. Vardag and H.-D. Lüdemann, *Chem. Phys.*, 1988, **128**, 527.
90. M. Besnard, J. Lascombe and H. Nery, *J. Phys.*, 1980, **41**, 723.
91. K.T. Gillen and J.E. Griffiths, *Chem. Phys. Lett.*, 1972, **17**, 359.
92. K. Tanabe, *Chem Phys.*, 1978, **31**, 319.
93. O. Yamamoto and M. Yanagisawa, *Chem. Phys. Lett.*, 1978, **54**, 164.
94. P. Linse, S. Engström, and B. Jönsson, *Chem. Phys. Lett.*, 1985, **115**, 95.
95. K.-L. Oehme, F. Seifert, G. Rudakoff, W. Carius, W. Hölzer and O. Schröter, *Chem. Phys.*, 1985, **92**, 169.
96. A. Brodka, B. Stryczek, L. Nikiel and R. Wrzalik, *Mol. Phys.*, 1988, **65**, 619.
97. N.K. Gaisin and Kh.Z. Khusainov, *Teor. Eksp. Khim.*, 1987, **23**, 504.
98. J. Homer and E.R.V. Cedeno, *Tetrahedron*, 1983, **39**, 2847.
99. D.E. O'Reilly, E.M. Peterson and D.L. Hogenboom, *J. Chem. Phys.*, 1972, **57**, 3969.
100. K. Tanabe, *Chem. Phys. Lett.*, 1981, **83**, 397.
101. T.T. Bopp, *J. Chem. Phys.*, 1967, **47**, 3621.
102. T.E. Bull and J. Jonas, *J. Chem. Phys.*, 1970, **53**, 3315.
103. T.E. Bull, *J. Chem. Phys.*, 1975, **62**, 222.
104. B.M. Braun and M. Holz, *Z. Phys. Chem. (Munich)*, 1983, **135**, 77.
105. D.E. Woessner, B.S. Snowden and E.T. Strom, *Mol. Phys.*, 1968, **14**, 265.
106. P.-O. Westlund and R.M. Lynden-Bell, *J. Magn. Reson.*, 1987, **72**, 522.
107. T.K. Leipert, J.H. Noggle and K.T. Gillen, *J. Magn. Reson.*, 1974, **13**, 158.
108. E. von Goldammer, H.-D. Lüdemann and A. Müller, *J. Chem. Phys.*, 1974, **60**, 4590.
109. T. Bien, M. Possiel, G. Döge, J. Yarwood and K.E. Arnold, *Chem. Phys.*, 1981, **56**, 203.
110. H.J. Böhm, R.M. Lynden-Bell, P.A. Madden and I.R. McDonald, *Mol. Phys.*, 1984, **51**, 761.
111. T.M. Plantenga, H.A. Lopes Cardozo, J. Bulthuis and C. MacLean, *Chem. Phys. Lett.*, 1981, **81**, 223.
112. G. Parry Jones, A. Bradbury and P.A. Bradley, *Mol. Cryst. Liq. Cryst.*, 1979, **55**, 143.
113. Shaw-Guang Huang and M.T. Rogers, *J. Chem. Phys.*, 1986, **85**, 401.
114. S. Kawanishi, T. Sasuga and M. Takehisa, *J. Phys. Soc. Jpn.*, 1980, **48**, 1307; 1980, **48**, 1311.
115. S. Kawanishi, T. Sasuga and M. Takehisa, *J. Phys. Soc. Jpn.*, 1981, **50**, 3080.
116. S. Kawanishi, T. Sasuga and M. Takehisa, *J. Phys. Soc. Jpn.*, 1982, **51**, 1579.
117. S. Kawanishi, T. Sasuga and M. Takehisa, *J. Phys. Chem.*, 1981, **85**, 1271.
118. J.P. Kintzinger and J.M. Lehn, *Mol. Phys.*, 1971, **22**, 273.
119. D. Schweitzer and H.W. Spiess, *J. Magn. Reson.*, 1974, **15**, 529.
120. B. Stryczek, *J. Mol. Struct.*, 1986, **143**, 297.
121. E.J. Pedersen, R.R. Vold and R.L. Vold, *Mol. Phys.*, 1978, **35**, 997.
122. T. Eriksen and E.J. Pedersen, *Mol. Phys.*, 1984, **53**, 1411.
123. R. Rzanny, K.-L. Oehme, G. Rudakoff, W. Hölzer, W. Carius and O. Schröter, *Z. Phys. Chem. (Leipzig)*, 1985, **266**, 849.
124. W. Carius, O. Schröter, K.L. Oehme, E. Kluk and A. Kocot, *Acta Phys. Polon.*, 1984, **A65**, 519.
125. M. Besnard, J.C. Lassegues, A. Lichanot and H. Nery, *J. Phys.*, 1984, **45**, 487.
126. D.E. Woessner and B.S. Snowden Jr., *Adv. Mol. Relax. Proc.*, 1972, **3**, 181.
127. H.W. Spiess, D. Schweitzer and U. Haeberlen, *J. Magn. Reson.*, 1973, **9**, 444.
128. D.J. Wilbur and J. Jonas, *J. Chem. Phys.*, 1975, **62**, 2800.
129. H. Versmold, *J. Chem. Phys.*, 1980, **73**, 5310.
130. T.E. Bull, *J. Chem. Phys.*, 1979, **70**, 571.
131. A. Tancredo, P.S. Pizani, C. Mendonca, H.A. Farrach, C.P. Poole, Jr., P.D. Ellis and R.A. Byrd, *J. Magn. Reson.*, 1978, **32**, 227.

132. P.S. Pizani, A. Tancredo, C. Mendonca, H.A. Farrach and C.P. Poole, Jr., *Chem. Phys. Lett.*, 1980, **70**, 112.
133. Dilin Xie, Jinshan Wang, Liang Chen and Yuxian Hu, *Gaodeng Xuexiao Huaxue Xuebao*, 1985, **6**, 447 (*Chem. Abst.* 1985, 103 214660j).
134. M.A. Hamza, G. Serratrice, M.-J. Stebe and J.-J. Delpuech, *Adv. Mol. Relax. Inter. Proc.*, 1981, **20**, 199.
135. Th. Bluhm, *Mol. Phys.*, 1984, **52**, 1335.
136. Th. Bluhm, *J. Magn. Reson.*, 1984, **60**, 91.
137. S. Shimokawa, *Ber. Bunsenges. Phys. Chem.*, 1986, **90**, 126.
138. E. Rössler and H. Sillescu, *Chem. Phys. Lett.*, 1984, **112**, 94.
139. C.G. Beguin and R. Dupeyre, *J. Magn. Reson.*, 1981, **44**, 294.
140. J. Kowalewski and A. Ericsson, *J. Phys. Chem.*, 1979, **83**, 2044.
141. Th. Dries, F. Fujara, M. Kiebel, E. Rössler and H. Sillescu, *J. Chem. Phys.*, 1988, **88**, 2139.
142. E. Arndt and J. Jonas, *J. Phys. Chem.*, 1981, **85**, 463.
143. I. Artaki and J. Jonas, *Mol. Phys.*, 1985, **55**, 867.
144. I. Artaki and J. Jonas, *J. Chem. Phys.*, 1985, **82**, 3360.
145. Buem Chan Min, Seihun Chang, Kook Joe Shin and Jo Woong Lee, *Bull. Korean Chem. Soc.*, 1985, **6**, 354.
146. A.M. Sazonov, *Zh. Fiz Khim.*, 1987, **61**, 1053.
147. H. Versmold, *Ber. Bunsenges. Phys. Chem.*, 1980, **84**, 168.
148. M.S. Ansari and H.G. Hertz, *Z. Phys. Chem (Munich)*, 1983, **137**, 187.
149. H.G. Hertz, *Progr. NMR Spectrosc.*, 1983, **16**, 115.
150. T. Eguchi, G. Soda and H. Chihara, *Mol. Phys.*, 1980, **40**, 681.
151. T. Frech and H.G. Hertz, *Ber. Bunsenges. Phys. Chem.*, 1985, **89**, 948.
152. C. Dugue, J. Emery and R.A. Pethrick, *Mol. Phys.*, 1980, **41**, 703.
153. S.L. Whittenburg, S.J. McKinnon, V.K. Jain and R.F. Evilia, *J. Phys. Chem.*, 1988, **92**, 4236.
154. F. Noack and G. Preissing, *Z. Naturforsch., Teil A*, 1969, **24**, 143.
155. J.P. Kintzinger and M.D. Zeidler, *Ber. Bunsenges. Phys. Chem.*, 1973, **77**, 98.
156. M. Elwenspoek, *Mol. Phys.*, 1979, **37**, 689.
157. M. Wolfe and J. Jonas, *J. Chem. Phys.*, 1979, **71**, 3252.
158. T.L. James, G.B. Matson, I.D. Kuntz and R.W. Fisher, *J. Magn. Reson.*, 1977, **28**, 417.
159. P. Bendel, *J. Magn. Reson.*, 1981, **42**, 364.
160. A.M. Aparkin and V.A. Daragan, *Izv. Akad. Nauk SSSR*, 1987, 778.
161. W. Suchanski and P.C. Canepa, *J. Magn. Reson.*, 1979, **33**, 389.
162. J.D. Halliday, P.E. Bindner and S. Padamshi, *Can. J. Chem.*, 1984, **62**, 1258.
163. V.A. Daragan, I.V. Zlokazova, N.K. Gaisin and H.Z. Khusanov, *Teor. Eksp. Khim.*, 1981, **17**, 587.
164. B. Ancian, B. Tiffon and J.-E. Dubois, *Chem. Phys.*, 1983, **74**, 171.
165. V.A. Daragan, A. Dias Ruano and I.V. Edneral, *Teor. Eksp. Khim.*, 1982, **18**, 485.
166. D.W. Aksnes and K. Ramstad, *Magn. Reson. Chem.*, 1987, **25**, 534.
167. B.A. Pettitt, J.S. Lewis, R.E. Wasylishen, W. Danchura and E. Tomchuk, *J. Magn. Reson.*, 1981, **44**, 508.
168. T. Hasebe and S. Ohtani, *J. Chem. Soc., Faraday Trans.*, 1, 1988, **84**, 187.
169. D.W. Aksnes, K. Ramstad and O.P. Bjoerlykke, *Magn. Reson. Chem.*, 1987, **25**, 1063.
170. D.W. Aksnes, K. Ramstad and O.P. Bjoerlykke, *Magn. Reson. Chem.*, 1988, **26**, 1086.
171. D.W. Aksnes and K. Ramstad, *Acta Chem. Scand., Ser. A*, 1987, **41**, 1.
172. S. Mooibroek and R.E. Wasylishen, *Can. J. Chem.*, 1985, **63**, 2926.
173. S. Mooibroek, R.E. Wasylishen, J.B. Macdonald, C.I. Ratcliffe and J.A. Ripmeester, *Can. J. Chem.*, 1988, **66**, 734.
174. B.I. Geller, V.A. Daragan and I.V. Zlokazova, *Zh. Fiz. Khim.*, 1980, 3008.

175. W. Storek, *Chem. Phys. Lett.*, 1983, **98**, 267.
176. K.M. Larsson, J. Kowalewski and U. Henriksson, *J. Magn. Reson.*, 1985, **62**, 260.
177. H.-H. Grapengeter, R. Kosfeld and H.W. Offergeld, *Colloid Polym. Sci.*, 1980, **258**, 1104.
178. J. Kowalewski and E. Berggren, *Magn. Reson. Chem.*, 1989, **27**, 386.
179. T.C. Moore, W.D. McCormick and C.G. Wade, *J. Phys. Chem.*, 1985, **89**, 3936.
180. A. Ejchart, P. Oleski and K. Wroblewski, *Pol. J. Chem.*, 1985, **59**, 845.
181. A. Petr, G. Grossmann, G. Klose, T. Ahlnäs and T. Götze, *J. Magn. Reson.*, 1986, **67**, 231.
182. Z. Pajak and E. Szczesniak, *Ber. Bunsenges. Phys. Chem.*, 1979, **83**, 980.
183. T. Hasebe, N. Nakamura and H. Chihara, *Bull. Chem. Soc. Jpn.*, 1980, **53**, 896.
184. H. Richter and M.D. Zeidler, *Mol. Phys.*, 1985, **55**, 49.
185. T. Ahlnäs, G. Karlström and B. Lindman, *J. Phys. Chem.*, 1987, **91**, 4030.
186. J.F. Martin, R.L. Vold and R.R. Vold, *J. Magn. Reson.*, 1983, **51**, 164; *J. Chem. Phys.*, 1984, **80**, 2237.
187. D.M. Quinn, *Biochemistry*, 1982, **21**, 3548.
188. G.S. Ginsburg, D.M. Small and J.A. Hamilton, *Biochemistry*, 1982, **21**, 6857. D.H. Croll, D.M. Small and J.A. Hamilton, *J. Chem. Phys.*, 1986, **85**, 7380.
189. M.D. Zeidler, in *Water. A Comprehensive Treatise*, Vol. 2 (ed. F. Franks), Chap. 10. Plenum Press, New York, 1973.
190. E. von Goldammer and H.G. Hertz, *J. Phys. Chem.*, 1970, **74**, 3734.
191. M. Woznyi, E.W. Lang and H.-D. Lüdemann, *J. Phys., Colloq., Ser. C*, 1984, **7**, 45, 179.
192. L.S. Podenko, A.G. Zavodovskii and V.F. Blashchanitsa, *Zh. Fiz. Khim.*, 1987, **61**, 1650.
193. K. Hallenga, J.R. Grigera and H.J.C. Berendsen, *J. Phys. Chem.*, 1980, **84**, 2381.
194. T. Bjorholm and J.P. Jacobsen, *J. Magn. Reson.*, 1980, **39**, 237.
195. D. Lankhorst, J. Schriever and J.C. Leyte, *Chem. Phys.*, 1983, **77**, 319.
196. E.S. Baker and J. Jonas, *J. Phys. Chem.*, 1985, **89**, 1730.
197. B. Blicharska, T. Frech and H.G. Hertz, *Z. Phys. Chem. (Munich)*, 1984, **141**, 139. T. Frech and H.G. Hertz, *Z. Phys. Chem. (Munich)*, 1984, **142**, 43.
198. J. Kowalewski and H. Kovacs, *Z. Phys. Chem. (Munich)*, 1986, **149**, 49.
199. H. Kovacs, J. Kowalewski and A. Maliniak, *Acta Chem. Scand., Ser. A*, 1987, **41**, 471.
200. B.C. Gordalla and M.D. Zeidler, *Mol. Phys.*, 1986, **59**, 817.
201. B.M. Braun and M. Holz, *J. Solution Chem.*, 1983, **12**, 685.
202. M.I. Burgar, T.E.St. Armour and D. Fiat, *J. Phys. Chem.*, 1981, **85**, 502.
203. M. Holz and A. Sacco, *Mol. Phys.*, 1985, **54**, 149.
204. K.-D. Merboldt and J. Frahm, *Ber. Bunsenges. Phys. Chem.*, 1986, **90**, 614.
205. N. Ito and T. Kato, *J. Phys. Chem.*, 1984, **88**, 801.
206. B. Parbhoo and O.B. Nagy, *J. Mol. Struct.*, 1988, **177**, 393.
207. S.J. Richardson, I.C. Baianu and M.P. Steinberg, *J. Food Sci.*, 1987, **52**, 806.
208. G. Carlström and B. Halle, *J. Chem. Soc., Faraday Trans. 1*, 1989, **85**, 1049.
209. A. Yoshino, T. Yoshida and K. Takahashi, *Magn. Reson. Chem.*, 1989, **27**, 344.
210. H.G. Hertz, A. Kratochwill and H. Weingärtner, *Proc. Ind. Acad. Sci., Chem. Sci.*, 1985, **94**, 337.
211. C.K. Finter and H.G. Hertz, *Z. Phys. Chem. (Munich)*, 1986, **148**, 75; *J. Chem. Soc., Faraday Trans. 1*, 1988, **84**, 2735.
212. H. Leiter, K.J. Patil and H.G. Hertz, *J. Solution Chem.*, 1983, **12**, 503. H. Leiter, C. Albayrak and H.G. Hertz, *J. Mol. Liq.*, 1984, **27**, 211.
213. G.R. Smith and B. Ternai, *Aust. J. Chem.*, 1983, **36**, 493.
214. S.A. Mikhailenko and V.V. Yakuba, *Ukr. Fiz. Zh. (Russ. Ed.)*, 1981, **26**, 784 (*Chem. Abs.* 95:15603j).
215. M.A. Suhm, K.J. Müller and H. Weingärtner, *Z. Phys. Chem. (Munich)*, 1987, **155**, 101.

216. M. Cebe, D. Kaltenmeier and H.G. Hertz, *Z. Phys. Chem. (Munich)*, 1984, **140**, 181. E. Cebe and M. Cebe, *Chim. Acta Turc.*, 1984, **12**, 315 (*Chem. Abs.*, 1986, 105:114554a).
217. Z. Pajak, L. Latanowicz and K. Jurga, *Ber. Bunsenges. Phys. Chem.*, 1980, **84**, 769; 1983, **87**, 143.
218. W. Koch, H. Leiter and S. Mal, *Z. Phys. Chem. (Munich)*, 1983, **136**, 89.
219. H.G. Hertz and M. Holz, *Z. Phys. Chem. (Munich)*, 1983, **136**, 81.
220. A. Kratochwill, *Z. Phys. Chem. (Wiesbaden)*, 1980, **120**, 165.
221. M. Cebe, D. Kaltenmeier and H.G. Hertz, *J. Chim. Phys.*, 1984, **81**, 7.
222. M. Cebe, *Fen Fak. Derg., Ser. A*, 1984, **7**, 39 (*Chem. Abs.* 1984, 101:47482c).
223. W. Koch and H.G. Hertz, *Z. Phys. Chem (Wiesbaden)*, 1982, **130**, 139.
224. W. Koch, H. Leiter and H.G. Hertz, *J. Solution Chem.*, 1981, **10**, 419.
225. B.P. Nikolaev, *Khim. Fiz.*, 1984, **3**, 1511.
226. H.M. Ratajczak and J.A. Ladd, *J. Mol. Liq.*, 1984, **29**, 97; 1989, **40**, 135.
227. J.P. Jacobsen, *J. Magn. Reson.*, 1980, **41**, 240.
228. H. Kovacs, J. Kowalewski, A. Maliniak and P. Stilbs, *J. Phys. Chem.*, 1989, **93**, 962.
229. T. Tokuhiro, *J. Chem. Soc., Faraday Trans. 2*, 1988, **84**, 1793.
230. H. Leiter, S. Mal and H.G. Hertz, *Z. Phys. Chem. (Munich)*, 1983, **136**, 101.
231. H.G. Hertz, T. Wild and H. Weingärtner, *Z. Phys. Chem. (Munich)*, 1984, **140**, 71.
232. B. Blicharska, H.G. Hertz and H. Versmold, *J. Magn. Reson.*, 1979, **33**, 531. T. Frech and H.G. Hertz, *J. Mol. Liq.*, 1985, **30**, 237.
233. A. Loewenstein, *Adv. Nucl. Quadr. Reson.*, 1983, **5**, 53.
234. H. Saito, H.H. Mantsch and I.C.P. Smith, *J. Am. Chem. Soc.*, 1973, **95**, 8453.
235. J.P. Jacobsen and K. Schaumburg, *J. Magn. Reson.*, 1977, **28**, 191.
236. O. Söderman, *J. Magn. Reson.*, 1986, **68**, 296.
237. F.W. Wehrli, in *Topics in Carbon-13 NMR Spectroscopy*, Vol. 2 (ed. G.C. Levy), Chap. 6. Wiley, New York, 1976.
238. J.B. Lambert, R.J. Nienhuis and J.W. Keepers, *Angew. Chem., Intl. Ed. Engl.*, 1981, **20**, 487.
239. K.E. Kövér and G. Batta, *Progr. NMR Spectroscopy.*, 1987, **19**, 223.
240. A. Dölle and Th. Bluhm, *Progr. NMR Spectrosc.*, 1989, **21**, 175.
241. I.C.P. Smith, in *NMR of Newly Accessible Nuclei* Vol 2, (ed. P. Laszlo). Academic Press, New York, 1983.
242. B. Ancian, B. Tiffon and J.-E. Dubois, *Chem. Phys. Lett.*, 1979, **65**, 281.
243. B. Ancian, B. Tiffon and J.-E. Dubois, *J. Magn. Reson.*, 1979, **34**, 647.
244. R.R. Vold, R.L. Vold, and N.M. Szeverenyi, *J. Chem. Phys.*, 1979, **70**, 5213.
245. B.C. Nishida, R.L. Vold and R.R. Vold, *J. Phys. Chem.*, 1986, **90**, 4465.
246. R.V. Gregory, M.R. Asdjodi, H.G. Spencer, A.L. Beyerlein and G.B. Savitsky, *J. Chem. Phys.*, 1984, **81**, 4790.
247. M.R. Asdjodi, R.V. Gregory, G.C. Lickfield, H.G. Spencer, J.W. Huffman and G.B. Savitsky, *J. Chem. Phys.*, 1987, **86**, 1653.
248. M.T. Chenon, J.M. Bernassau, C.L. Mayne and D.M. Grant, *J. Phys. Chem.*, 1982, **86**, 2733.
249. M.T. Chenon, J.M. Bernassau and C. Coupry, *Mol. Phys.*, 1985, **54**, 277.
250. A.A. Rodrigues, A.F.T Chen and M. Schwartz, *J. Mol. Liq.*, 1988, **37**, 117.
251. V. Mlynarik, *J. Magn. Reson.*, 1985, **61**, 333.
252. G.C. Levy and J.T. Bailey, *Org. Magn. Reson.*, 1980, **13**, 403.
253. H. Nery, D. Canet, W.M.M.J. Bovée and J. Vriend, *Mol. Phys.*, 1981, **42**, 683.
254. K. Seidman, J.F. McKenna, S.E. Emery, G.B. Savitsky and A.L. Beyerlein, *J. Phys. Chem.*, 1980, **84**, 907.
255. M.S. Brown, D.M. Grant, W.J. Horton, C.L. Mayne and G.T. Evans, *J. Am. Chem. Soc.*, 1985, **107**, 6698.
256. P. Dais, V. Gibb, G.A. Kenney-Wallace and W.F. Reynolds, *Chem. Phys.*, 1980, **47**, 407.

257. L.M. Sweeting and E.D. Becker, *J. Phys. Chem.*, 1984, **88**, 6075.
258. V.A. Daragan and E.E. Ilina, *Izv. Akad. Nauk SSSR, Ser. Khim.*, 1988, 1277.
259. V.A. Daragan and E.E. Ilina, *Izv. Akad. Nauk SSSR, Ser. Khim.*, 1988, 1281.
260. G.C. Levy, P.L. Rinaldi, J.J. Dechter, D.E. Axelson and L. Mandelkern, *ACS Symp. Ser.*, 1980, **142**, 119.
261. K.L. Williamson, N.V. Reo and T.R. Stengle, *J. Am. Chem. Soc.*, 1985, **107**, 4162.
262. J.B. Lambert and R.J. Nienhuis, *J. Am. Chem. Soc.*, 1980, **102**, 6659.
263. K.F. Kuhlmann and D.M. Grant, *J. Chem. Phys.*, 1971, **55**, 2998. T.D. Alger, D.M. Grant and R.K. Harris, *J. Phys. Chem.*, 1972, **76**, 281. J.R. Lyerla, Jr. and D.M. Grant, *J. Phys. Chem.*, 1972, **76**, 3213.
264. M. Kakihana, M. Kotaka and M. Okamoto, *J. Phys. Chem.*, 1983, **87**, 3510.
265. A. Ericsson, J. Kowalewski, T. Liljefors and P. Stilbs, *J. Magn. Reson.*, 1980, **38**, 9.
266. A. Gryff-Keller and L. Poppe, *J. Chem. Soc., Perkin Trans. 2*, 1985, 603.
267. D. Wallach and W.T. Huntress Jr., *J. Chem. Phys.*, 1969, **50**, 1219.
268. V.A. Daragan, I.V. Zlokazova and I.V. Edneral, *Teor. Eksp. Khim.*, 1980, **16**, 752.
269. M.M. Fuson and J.H. Prestegard, *J. Chem. Phys.*, 1982, **76**, 1539.
270. G. Jaccard, S. Wimperis and G. Bodenhausen, *Chem. Phys. Lett.*, 1987, **138**, 601.
271. H. Sterk and M. Mittelbach, *J. Magn. Reson.*, 1985, **62**, 175.
272. H. Sterk, J. Kalcher and G. Kollenz, *Z. Phys. Chem. (Wiesbaden)*, 1979, **118**, 151.
273. D.P. Kelly, D.R. Leslie and R.A. Craig, *J. Magn. Reson.*, 1983, **52**, 480.
274. V. Mlynarik, *Org. Magn. Reson.*, 1981, **17**, 178.
275. V. Mlynarik, *Org. Magn. Reson.*, 1984, **22**, 164.
276. S. Hayashi, K. Hayamizu and O. Yamamoto, *J. Magn. Reson.*, 1980, **37**, 17.
277. J. Brunn, C. Beck, R. Radeglia and Z. Srank, *Z. Chem.*, 1980, **20**, 62.
278. C.P.J. Vuik, Misbah ul Hasan and C.E. Holloway, *J. Chem. Soc., Perkin Trans. 2*, 1979, 1214.
279. Chin Yu and G.C. Levy, *Org. Magn. Reson.*, 1984, **22**, 131.
280. G.C. Levy, T. Pehk and E. Lippmaa, *Org. Magn. Reson.*, 1980, **14**, 214.
281. K. Laihia, M. Pitkänen and K. Schulze, *Finn. Chem. Lett.*, 1986, **13**, 65.
282. M. Pitkänen, K. Laihia, F.K. Velichko and B.D. Lavrukhin, *Magn. Reson. Chem.*, 1987, **25**, 717.
283. S. Ng, *Org. Magn. Reson.*, 1983, **21**, 50.
284. A. Okubo, H. Kawai, T. Matsunaga, T. Chuman, S. Yamazaki and S. Toda, *Tetrahedron Lett.*, 1980, **21**, 4095.
285. J.M. Bernassau and M. Fetizon, *Tetrahedron*, 1981, **37**, 2105.
286. G.N. Ranadive, P.S.R. Anjaneyulu and A.K. Lala, *Ind. J. Chem. B*, 1981, **20**, 910.
287. R.V. Hosur and G. Govil, *Org. Magn. Reson.*, 1981, **17**, 71.
288. N.R. Dando, H.S. Gold and C. Dybowski, *Org. Magn. Reson.*, 1983, **21**, 467.
289. N.R. Dando, C. Dybowski and H.S. Gold, *J. Phys. Chem.*, 1983, **87**, 3094.
290. F. Coletta, G. Moro and P.L. Nordio, *Mol. Phys.*, 1987, **61**, 1259.
291. F. Coletta, A. Ferrarini and P.L. Nordio, *Chem. Phys.*, 1988, **123**, 397.
292. H. Nery and D. Canet, *J. Magn. Reson.*, 1981, **42**, 370.
293. H. Nery, D. Canet, F. Toma and S. Fermandjian, *J. Am. Chem. Soc.*, 1983, **105**, 1482.
294. B. Parbhoo and O.B. Nagy, J. Phys. Chem., 1985, **89**, 239.
295. Y. Van Haverbeke, R.N. Muller and L. Vander Elst, *J. Phys. Chem.*, 1984, **88**, 4978.
296. L. Pogliani, N. Niccolai and C. Rossi, *Spectrosc. Lett.*, 1984, **17**, 159.
297. E. Gaggelli, G. Valensin, G. Adembri, A.M. Celli, M. Scotton and A. Sega, *J. Chem. Soc., Perkin Trans. 2*, 1988, 1139.
298. Y. Inoue and Y. Miyata, *Bull. Chem. Soc. Jpn.*, 1981, **54**, 809.
299. Y. Inoue, Fu-Hua Kuan and R. Chujo, *Bull. Chem. Soc. Jpn.*, 1987, **60**, 2539.

300. H.E. Bleich, J.A. Glasel, M. Latina and J. Visintainer, *Biopolymers*, 1979, **18**, 2849.
301. K.D. Kopple, Yu-Sen Wang, A. Go Cheng and K.K. Bhandary, *J. Am. Chem. Soc.*, 1988, **110**, 4168.
302. O.W. Howarth and L. Yun Lian, *J. Chem. Soc., Perkin Trans. 2*, 1982, 263.
303. N. Niccolai, C. Rossi, P. Mascagni, P. Neri and W.A. Gibbons, *Biochem. Biophys. Res. Commun.*, 1984, **124**, 739.
304. P. Mascagni, A. Prugnola, W.A. Gibbons and N. Niccolai, *J. Chem. Soc., Perkin Trans. 2*, 1986, 1015.
305. S. Berger, F.R. Kreissl, D.M. Grant and J.D. Roberts, *J. Am. Chem. Soc.*, 1975, **97**, 1805.
306. M.S. Brown, C.L. Mayne, D.M. Grant, T.C. Chou and E.L. Allred, *J. Phys. Chem.*, 1984, **88**, 2708.
307. T. Iwaoka, H. Kuwano, S. Maramatsu, R. Endo, Y. Nakada, J. Ide and M. Kondo, *Agric. Biol. Chem.*, 1981, **45**, 1381.
308. M. Costas, D. Patterson and D.F.R. Gilson, *J. Phys. Chem.*, 1984, **88**, 6056.
309. Chin Yu, C.L. Demoulin and G.C. Levy, *Magn. Reson. Chem.*, 1985, **23**, 952.
310. R. Jost and J. Sommer, *C.R. Hebd. Seances Acad. Sci., Ser. C*, 1980, **290**, 173.
311. C. Pattaroni and J. Lauterwein, *Magn. Reson. Chem.*, 1987, **25**, 745.
312. D.E. Axelson and C.E. Holloway, *Can. J. Chem.*, 1980, **58**, 1679.
313. M.E. Moseley, *Chem. Script.*, 1980, **16**, 28.
314. P. Stilbs and M.E. Moseley, *J. Magn. Reson.*, 1979, **33**, 209.
315. H. Beierbeck, R. Martino and J.K. Saunders, *Can. J. Chem.*, 1980, **58**, 102.
316. J. Kowalewski and T. Liljefors, *Chem. Phys. Lett.*, 1979, **64**, 170.
317. R.H. Newman, *J. Magn. Reson.*, 1982, **47**, 138.
318. J.M. Bernassau, M. Fetizon and J.A. Pinheiro, *J. Phys. Chem.*, 1986, **90**, 1051.
319. J.P. Zahra, B. Waegell, R. Faure and E.J. Vincent, *Org. Magn. Reson.*, 1982, **18**, 185.
320. K.F. Kuhlmann, D.M. Grant and R.K. Harris, *J. Chem. Phys.*, 1970, **52**, 3439.
321. R.E. Wasylishen and B.A. Pettitt, *Can. J. Chem.*, 1977, **55**, 2564.
322. B. Ancian, B. Tiffon and J.-E. Dubois, *J. Chem. Phys.*, 1981, **74**, 5857.
323. B. Ancian and B. Tiffon, *J. Chem. Soc., Faraday Trans. 2*, 1984, **80**, 1067.
324. J. Brondeau, D. Canet, C. Millot, H. Nery and L. Werbelow, *J. Chem. Phys.*, 1985, **82**, 2212.
325. H. Beierbeck, R. Martino and J.K. Saunders, *Can. J. Chem.*, 1979, **57**, 1224.
326. H. Sterk and E. Maier, *Adv. Mol. Relax. Inter. Proc.*, 1982, **22**, 17.
327. H. Sterk and E. Maier, *Adv. Mol. Relax. Inter. Proc.*, 1982, **23**, 247.
328. R. Gerhards, W. Dietrich, G. Bergmann and H. Duddeck, *J. Magn. Reson.*, 1979, **36**, 189.
329. W.A. Mellink and R. Kaptein, *Org. Magn. Reson.*, 1980, **13**, 279.
330. H. Beierbeck, J.W. Easton, J.K. Saunders and R.A. Bell, *Can. J. Chem.*, 1982, **60**, 1173.
331. G.C. Levy, A. Kumar and D. Wang, *J. Am. Chem. Soc.*, 1983, **105**, 7536.
332. J. Bastard, J.M. Bernassau, Do Khac Duc, M. Fetizon and E. Lesueur, *J. Phys. Chem.*, 1986, **90**, 3936.
333. J.M. Bernassau, M. Fetizon, I. Hanna and J.A. Pinheiro, *J. Phys. Chem.*, 1986, **90**, 3941.
334. M.P. Murari, R. Murari and W.J. Baumann, *Magn. Reson. Chem.*, 1985, **23**, 243.
335. R.K. Harris and R.H. Newman, *Mol. Phys.*, 1981, **43**, 1069.
336. W. Kolodziejski and P. Laszlo, *Helv. Chim. Acta*, 1985, **68**, 1193.
337. D.J. Craik, W. Adcock and G.C. Levy, *Magn. Reson. Chem.*, 1986, **24**, 783.
338. G.C. Levy, D.J. Craik, B. Nordén, M.T. Phan Viet and A. Dekmezian, *J. Am. Chem. Soc.*, 1982, **104**, 25.
339. A. Dölle and Th. Bluhm, *J. Chem. Soc., Perkin Trans 2*, 1985, 1785.
340. A. Dölle and Th. Bluhm, *Mol. Phys.*, 1986, **59**, 721.
341. P.W. Rabideau, W.K. Smith and B.D. Ray, *Magn. Reson. Chem.*, 1989, **27**, 191.

342. G.C. Levy, J.D. Cargioli and F.A.L. Anet, *J. Am. Chem. Soc.*, 1973, **95**, 1527.
343. A.M. Gladkii, V.A. Daragan and I.V. Edneral, *Khim. Fiz.*, 1985, **4**, 506 (*Chem. Abs.*, 1985, 102:230732u). V.A. Daragan and E.E. Ilina, *Izv. Akad. Nauk SSSR, Ser. Khim.*, 1987, 782.
344. K.-L. Oehme and G. Rudakoff, *Z. Phys. Chem.* (*Leipzig*), 1986, **267**, 513.
345. A. Maitra, *Colloids Surf.*, 1988, **32**, 149.
346. G. Rudakoff and K.-L. Oehme, *Acta Phys. Polon. A*, 1980, **57**, 865.
347. M.A. Hamza, G. Serratrice and J.-J. Delpuech, *Org. Magn. Reson.*, 1981, **16**, 98.
348. D.H. Lee and R.E.D. McClung, *Chem. Phys.*, 1987, **116**, 101.
349. E. Königsberger and H. Sterk, *J. Chem. Phys.*, 1985, **83**, 2723.
350. A.F.T. Chen, S.P. Wang and M. Schwartz, *Magn. Reson. Chem.*, 1988, **26**, 675.
351. S.P. Wang, A.F.T. Chen and M. Schwartz, *Mol. Phys.*, 1988, **65**, 689.
352. T.C. Farrar, B.R. Adams, G.C. Grey, R.A. Quintero-Arcaya and Qihui Zuo, *J. Am. Chem. Soc.*, 1986, **108**, 8190.
353. R. Benn, *J. Magn. Reson.*, 1984, **59**, 164.
354. H. Sterk and E. Königsberger, *J. Phys. Chem.*, 1986, **90**, 916.
355. V. Mlynarik, *Coll. Chech. Chem. Commun.*, 1983, **48**, 984.
356. Tao Ji, Xiuwen Han, Guobao Cheng and Jiehan Hu, *Bopuxue Zazhi*, 1984, **1**, 345 (*Chem. Abs.*, 1986, 105:208362p).
357. L.M. Jackman, J.C. Trewella and R.C. Haddon, *J. Am. Chem. Soc.*, 1980, **102**, 2519.
358. J.J. Ford, W.A. Gibbons and N. Niccolai, *J. Magn. Reson.*, 1982, **47**, 522.
359. N. Niccolai, L. Pogliani, E. Tiezzi and C. Rossi, *Nuovo Cim., Ser D.*, 1984, **3**, 993.
360. N. Niccolai, A. Prugnola, P. Mascagni, C. Rossi, L. Pogliani and W.A. Gibbons, *Spectrosc. Lett.*, 1987, **20**, 307.
361. M.J. Shapiro and A.D. Kahle, *Org. Magn. Reson.*, 1979, **12**, 235.
362. R.S. Norton, *Org. Magn. Reson.*, 1981, **17**, 37.
363. K.E. Malterud and T. Anthonsen, *Acta Chem. Scand., Ser. B*, 1987, **41**, 6.
364. S.S. Al-Showiman, H.M. Al-Hazimi and I.M. Al-Najjar, *J. Chem. Soc. Pak.*, 1981, **3**, 69.
365. J.B. Lambert, R.J. Nienhuis and R.B. Finzel, *J. Phys. Chem.*, 1981, **85**, 1170.
366. R. Dupeyre and C. Beguin, *J. Chim. Phys.*, 1981, **78**, 365.
367. P.J.A. Ribeiro-Claro, C.F.G.C. Geraldes and J.J.C. Teixeira-Dias, *J. Magn. Reson.*, 1987, **71**, 132.
368. P.J.A. Ribeiro-Claro, A.M. Amorim da Costa and J.J.C. Teixeira-Dias, *J. Raman Spectrosc.*, 1987, **18**, 497.
369. Jo Woong Lee, Chull-Hyung Cho, Seong-Kyu Park, Byung-Wook Jo, Bong-Oh Ro and Sung-Hyu Choe, *Bull. Korean Chem. Soc.*, 1987, **8**, 73.
370. N.M. Azancheev, A.I. Maklakov and V.V. Zykova, *Zh. Strukt. Khim.*, 1981, **22**, 50.
371. S. Andersson, R.E. Carter and T. Drakenberg, *Acta Chem. Scand., Ser. B*, 1980, **34**, 661.
372. S. Andersson, R.E. Carter and T. Drakenberg, *Acta Chem. Scand., Ser. B*, 1984, **38**, 579.
373. J. Huet and D. Zimmermann, *Nouv. J. Chim.*, 1983, **7**, 29.
374. A. Makriyannis and J.J. Knittel, *Tetrahedron Lett.*, 1979, 2753.
375. A. Makriyannis and S. Fesik, *J. Am. Chem. Soc.*, 1982, **104**, 6462. J.J. Knittel and A. Makriyannis, *J. Med. Chem.*, 1981, **24**, 906.
376. M. Akiyama, T. Watanabe and M. Kakihana, *J. Phys. Chem.*, 1986, **90**, 1752.
377. O.D. Vetrov, V.A. Daragan and I.V. Edneral, *Khim. Fiz.*, 1982, 1490 (*Chem. Abs.* 1983, 99:146476a).
378. G. Rudakoff and K.-L. Oehme, *Z. Chem.* (*Leipzig*), 1982, **22**, 188.
379. R.E. London and M.A. Phillippi, *J. Magn. Reson.*, 1981, **45**, 476.
380. P. Dais, *Magn. Reson. Chem.*, 1987, **25**, 141.
381. R.K. Harris and R.H. Newman, *Mol. Phys.*, 1985, **54**, 1021.

382. J.D. Korp, I. Bernal and G.E. Martin, *J. Cryst. Mol. Struct.*, 1981, **11**, 11.
383. P. Dais, *Magn. Reson. Chem.*, 1989, **27**, 61.
384. R.S. Norton and R.J. Wells, *Tetrahedron Lett.*, 1980, **21**, 3801.
385. R.S. Norton, K.D. Croft and R.J. Wells, *Tetrahedron*, 1981, **37**, 2341.
386. V. Leon, J. Espidel and R.A. Bolivar, *Org. Magn. Reson.*, 1983, **21**, 766.
387. V.G. Berezhnoi and A.N. Niyazov, *Izv. Akad. Nauk Turkm. SSR, Ser. Fiz.-Tekh., Khim. Geol. Nauk*, 1980, 120 (*Chem. Abs.*, 1981, 94:14709r).
388. T.D. Alger, W.D. Hamill, Jr., R.J. Pugmire, D.M. Grant, G.D. Silcox and M. Solum, *J. Phys. Chem.*, 1980, **84**, 632.
389. D.M. Lamb, S.T. Adamy, K.W. Woo and J. Jonas, *J. Phys. Chem.*, 1989, **93**, 5002.
390. V.G. Berezhnoi and A.N. Niyazov, *Izv. Akad. Nauk Turkm. SSR, Ser. Fiz.-Tekh., Khim. Geol. Nauk*, 1981, 88 (*Chem. Abs.*, 1981, 94:1738325).
391. A. Ericsson and J. Kowalewski, *Chem. Phys.*, 1981, **60**, 387.
392. R.K. Harris and R.H. Newman, *Mol. Phys.*, 1979, **38**, 1315.
393. N.K. Wilson, *Magn. Reson. Chem.*, 1985, **23**, 12.
394. R.E. Wasylishen, B.A. Pettitt and W. Danchura, *Can. J. Chem.*, 1977, **55**, 3602.
395. J.-J. Delpuech, B. Benayada, D. Nicole and P. Tekely, *J. Magn. Reson.*, 1989, **81**, 288.
396. A. Gryff-Keller and L. Poppe, *Magn. Reson. Chem.*, 1985, **23**, 150.
397. T.D. Alger, M. Solum, D.M. Grant, G.D. Silcox and R.J. Pugmire, *Anal. Chem.*, 1981, **53**, 2299.
398. I.D. Campbell, R. Freeman and D.L. Turner, *J. Magn. Reson.*, 1975, **20**, 172.
399. W.B. Smith, *Org. Magn. Reson.*, 1981, **17**, 151.
400. Y. Van Haverbeke, A. Maquestiau, R.N. Muller and L. Vander Elst, *Spectrochim. Acta, Part A*, 1980, **36**, 627.
401. L.D. Hall and M. Yalpani, *Org. Magn. Reson.*, 1981, **16**, 60.
402. H.P. Hopkins and S.Z. Ali, *J. Phys. Chem.*, 1980, **84**, 203.
403. H.P. Hopkins and S.Z. Ali, *J. Phys. Chem.*, 1980, **84**, 2814.
404. W.J.P. Blonski, F.E. Hruska and T.A. Wildman, *Org. Magn. Reson.*, 1984, **22**, 505.
405. J. Guillerez, B. Tiffon, B. Ancian, J. Aubard and J.-E. Dubois, *J. Phys. Chem.*, 1983, **87**, 3015.
406. B. Tiffon, J. Guillerez and B. Ancian, *Magn. Reson. Chem.*, 1985, **23**, 460.
407. E.J. Pedersen, R.L. Vold and R.R. Vold, *Mol. Phys.*, 1980, **41**, 811.
408. T. Wamsler, J.T. Nielsen, E.J. Pedersen and K. Schaumburg, *J. Magn. Reson.*, 1981, **43**, 387.
409. A. Maliniak, J. Kowalewski and I. Panas, *J. Phys. Chem.*, 1984, **88**, 5628.
410. A. Maliniak and J. Kowalewski, *J. Phys. Chem.*, 1986, **90**, 6330.
411. A. Maliniak, A. Laaksonen, J. Kowalewski and P. Stilbs, *J. Chem. Phys.*, 1988, **89**, 6434.
412. D.J. Craik, G.C. Levy and A. Lombardo, *J. Phys. Chem.*, 1982, **86**, 3893.
413. R. Uusvuori and M. Lounasmaa, *Org. Magn. Reson.*, 1984, **22**, 286.
414. P. Dais and G. Fainos, *Can. J. Chem.*, 1986, **64**, 560.
415. Yu.Yu. Samitov and R.Kh. Sadykov, *Teor. Eksp. Khim.*, 1986, **22**, 603.
416. N. Platzer, *Org. Magn. Reson.*, 1978, **11**, 350.
417. H. Fujiwara, T. Takagi, M. Sugiura and Y. Sasaki, *J. Chem. Soc., Perkin Trans. 2*, 1983, 903.
418. I.V. Edneral, *Teor. Eksp. Khim.*, 1983, **19**, 429.
419. K.J. Friesen and B.J. Blackburn, *Can. J. Chem.*, 1984, **62**, 1618.
420. I.M. Al-Najjar and H.B. Amin, *Spectrochim. Acta, Part A*, 1987, **43**, 1307.
421. H. Duddeck and M. Kaiser, *Spectrochim. Acta, Part A*, 1985, **41**, 913.
422. L. Vander Elst, Y. Van Haverbeke, A. Maquestiau and R.N. Muller, *Magn. Reson. Chem.*, 1987, **25**, 16.
423. C. Rossi and N. Niccolai, *Chem. Phys. Lett.*, 1987, **142**, 418.
424. H. Sterk and H. Gruber, *J. Am. Chem. Soc.*, 1984, **106**, 2239.

425. M. Sugiura, T. Sai, N. Takao and H. Fujiwara, *J. Chem. Soc., Perkin Trans. 2*, 1983, 907.
426. M. Baldo, K.J. Irgolic, M. Nicolini, G.C. Pappalardo and V. Viti, *J. Chem. Soc., Faraday Trans. 2*, 1983, **79**, 1633.
427. K.E. Kövér, G. Batta and Z. Madi, *J. Magn. Reson.*, 1986, **69**, 538.
428. K.E. Kövér and G. Batta, *J. Magn. Reson.*, 1987, **73**, 512.
429. C.H. Womack, R.T. Gampe Jr., B.K. Lemke, K.N. Sawhney, T.L. Lemke and G.E. Martin, *J. Heterocycl. Chem.*, 1982, **19**, 1105.
430. T.P. Pitner, J.F. Whidby and W.B. Edwards, III, *J. Am. Chem. Soc.*, 1980, **102**, 5149.
431. V.B. Rozhnov, *Izv. Akad. Nauk Kaz. SSR, Ser. Khim.*, 1987, 75.
432. D.W. Aksnes and T.A. Holak, *Org. Magn. Reson.*, 1981, **17**, 285. D.W. Aksnes and K. Ramstad, *Magn. Reson. Chem.*, 1985, **23**, 253.
433. M. Jay and G.E. Martin, *J. Heterocycl. Chem.*, 1982, **19**, 241.
434. B. Stoddart and M. Hooper, *Magn. Reson. Chem.*, 1989, **27**, 241.
435. Y. Takeuchi, *Heterocycles*, 1981, **15**, 1147.
436. D. Kaplan and G. Navon, *Org. Magn. Reson.*, 1981, **17**, 79.
437. G.E. Martin, D.N. Srivasta, J.A. Matson and A.J. Weinheimer, *Steroids*, 1983, **41**, 637.
438. C. Erk, *Appl. Spectrosc.*, 1986, **40**, 100.
439. P.D.J. Grootenhuis, E.J.R. Sudhölter, C.J. van Staveren and D.N. Reinhoudt, *J. Chem. Soc., Chem. Commun.*, 1985, 1426.
440. P.D.J. Grootenhuis, J. van Eerden, E.J.R. Sudhölter, D.N. Reinhoudt, A. Roos, S. Harkema and D. Feil, *J. Am. Chem. Soc.*, 1987, **109**, 4792.
441. E. Kleinpeter, M. Gäbler, W. Schroth, J. Mattinen and K. Pihlaja, *Magn. Reson. Chem.*, 1988, **26**, 387.
442. M. Baldo, A. Grassi, L. Guidoni, M. Nicolini, G.C. Pappalardo and M. Viti, *Spectrochim. Acta, Part A*, 1982, **38**, 1253.
443. N. Niccolai, C. Rossi, V. Brizzi and W.A. Gibbons, *J. Am. Chem. Soc.*, 1984, **106**, 5732.
444. N. Niccolai, C. Rossi, P. Mascagni, W.A. Gibbons and V. Brizzi, *J. Chem. Soc., Perkin Trans. 1*, 1985, 239.
445. C. Rossi, A. Casini, M.P. Picchi, F. Laschi, A. Calabria and R. Marcolongo, *Biophys. Chem.*, 1987, **27**, 255.
446. E. Gaggelli, N. Marchettini and G. Valensin, *J. Chem. Soc., Perkin Trans 2*, 1987, 1707.
447. E. Gaggelli, N. Marchettini, A. Sega and G. Valensin, *Magn. Reson. Chem.*, 1988, **26**, 1041.
448. K.-A. Kovar and D. Linden, *Arch. Pharm.* 1983, **316**, 834.
449. A. Grassi, B. Perly and G.C. Pappalardo, *Chem. Phys.*, 1989, **130**, 335.
450. G.C. Pappalardo, L. Radics, M. Baldo and A. Grassi, *J. Chem. Soc., Perkin Trans 2*, 1985, 955.
451. K. Izumi, *Agric. Biol. Chem.*, 1987, **51**, 1725.
452. A.S. Serianni and R. Barker, *J. Magn. Reson.*, 1982, **49**, 335.
453. P. Dais and A.S. Perlin, *Carbohydr. Res.*, 1987, **169**, 159.
454. A. Allerhand, D. Doddrell and R. Komoroski, *J. Chem. Phys.*, 1971, **55**, 189.
455. K. Bock and R.U. Lemieux, *Carbohydr. Res.*, 1982, **100**, 63.
456. A. Allerhand and M. Dohrenwend, *J. Am. Chem. Soc.*, 1985, **107**, 6684.
457. D.C. McCain and J.L. Markley, *Carbohydr. Res.*, 1986, **152**, 73.
458. D.C. McCain and J.L. Markley, *J. Am. Chem. Soc.*, 1986, **108**, 4259.
459. D.C. McCain and J.L. Markley, *J. Magn. Reson.*, 1987, **73**, 244.
460. H. Kovacs, S. Bagley and J. Kowalewski, *J. Magn. Reson.*, 1989, **85**, 530.
461. P. Dais and A.S. Perlin, *Can. J. Chem.*, 1983, **61**, 1542.
462. P. Dais and A.S. Perlin, *Magn. Reson. Chem.*, 1988, **26**, 373.
463. N. Marchettini, S. Ulgiati and C. Rossi, *Magn. Reson. Chem.*, 1989, **27**, 223. N. Marchettini, L. Pogliani, C. Rossi and S. Ulgiati, *Spectrosc. Lett.*, 1987, **20**, 81.

464. A. Neszmelyi, A. Liptak, P. Nanasi and J. Szejtli, *Acta Chim. Hung.*, 1983, **113**, 431.
465. K. Matsuo, *Macromolecules*, 1984, **17**, 449.
466. J. Breg, D. Romijn, J.F.G. Vliegenthart, G. Strecker and J. Montreuil, *Carbohydr. Res.*, 1988, **183**, 19.
467. C. Rossi, *J. Chem. Phys.*, 1986, **84**, 6581.
468. C. Rossi, N. Marchettini, L. Pogliani, F. Laschi and N. Niccolai, *Chem. Phys. Lett.*, 1987, **136**, 506.
469. C. Rossi, N. Niccolai and F. Laschi, *J. Phys. Chem.*, 1987, **91**, 3903.
470. R.S. Norton, R.P. Gregson and R.J. Quinn, *J. Chem. Soc., Chem. Commun.*, 1980, 339.
471. R.P. Gregson, R.J. Quinn and R.S. Norton, *J. Carbohydr. Nucleosides Nucleotides*, 1981, **8**, 345.
472. A. Neszmelyi, V. Zsoldos-Mady, A. Messmer and I. Pinter, *Acta Chim. Hung.*, 1983, **113**, 423.
473. J.H. Noggle and R.E. Schirmer, *The Nuclear Overhauser Effect*. Academic Press, New York, 1971.
474. R.L. Vold and R.R. Vold, *Progr. NMR Spectrosc.*, 1978, **12**, 79.
475. T. Raj, B. Borah, R.M. Riddle and R.G. Bryant, *J. Solution Chem.*, 1981, **10**, 741.
476. G.R. Smith and B. Ternai, *Aust. J. Chem.*, 1983, **36**, 2227.
477. J. Homer and E.R.V. Cedeno, *J. Chem. Soc., Faraday Trans. 2*, 1984, **80**, 375.
478. B. Blicharska, *Acta Phys. Polon., Ser. A*, 1986, **70**, 127.
479. P.S. Hubbard, *J. Chem. Phys.*, 1970, **52**, 563.
480. E. Haslinger and R.M. Lynden-Bell, *J. Magn. Reson.*, 1978, **31**, 33 (Erratum, *J. Magn. Reson.*, 1980, **38**, 189).
481. E. Haslinger and W. Robien, *J. Am. Chem. Soc.*, 1980, **102**, 1237.
482. V.S. Dimitrov and J.A. Ladd, *Magn. Reson. Chem.*, 1985, **23**, 529.
483. N. Niccolai and E. Tiezzi, *J. Phys. Chem.*, 1979, **83**, 3249.
484. N. Niccolai, V. Garsky and W.A. Gibbons, *J. Am. Chem. Soc.*, 1980, **102**, 1517.
485. N. Niccolai, M.P. Miles and W.A. Gibbons, *Biophys. Biochem. Res. Commun.*, 1979, **91**, 157.
486. K. Mizuno, T. Takagi, Y. Ikeda and Y. Shindo, *J. Chem. Soc., Faraday Trans. 1*, 1989, **85**, 1099.
487. G. Valensin, T. Kushnir and G. Navon, *J. Magn. Reson.*, 1982, **46**, 23.
488. G. Valensin, V. Dive, A. Lai, A. Yiotakis and F. Toma, *J. Chem. Soc., Faraday Trans. 2*, 1989, **85**, 293.
489. H. Kessler, A.G. Klein, R. Obermeier and M. Will, *Liebigs Ann. Chem.*, 1989, 269.
490. M.D. Bruch, J.H. Noggle and L.M. Gierasch, *J. Am. Chem. Soc.*, 1985, **107**, 1400.
491. Mei-chang Kuo, T. Drakenberg and W.A. Gibbons, *J. Am. Chem. Soc.*, 1980, **102**, 520.
492. N. Niccolai, L. Pogliani, C. Rossi, P. Corti and W.A. Gibbons, *Biophys. Chem.*, 1984, **20**, 217.
493. L.D. Hall, K.F. Wong and H.D.W. Hill, *J. Chem. Soc., Chem. Commun.*, 1979, 951.
494. W.M.M.J. Bovée, J. Vriend, J.A. Peters, J.M.A. Baas and B. Van de Graaf, *Mol. Phys.*, 1980, **41**, 933.
495. L.D. Colebrook and L.D. Hall, *Org. Magn. Reson.*, 1983, **21**, 532.
496. G.A. Morris, *J. Magn. Reson.*, 1980, **41**, 185.
497. L. Abis, E. Dalcanale, A. Du vosel and S. Spera, *J. Org. Chem.*, 1988, **53**, 5475.
498. R.E. Stark, R.L. Vold and R.R. Vold, *J. Magn. Reson.*, 1979, **33**, 421.
499. A. Kratochwill, R.L. Vold and R.R. Vold, *J. Chem. Phys.*, 1979, **71**, 1319.
500. P.E. Balonga, C. Vasques, R.H. Contreras, V.J. Kowalewski and D.G. de Kowalewski, *J. Magn. Reson.*, 1984, **59**, 58.
501. F. Tabak and G. Bingöl, *J. Mol. Liq.*, 1988, **37**, 263.
502. W.J. Chazin and L.D. Colebrook, *Magn. Reson. Chem.*, 1985, **23**, 597.
503. J. Homer and E.R.V. Cedeno, *J. Chem. Soc., Faraday Trans. 2*, 1983, **79**, 1021.
504. R. Dupeyre and C. Beguin, *J. Chim. Phys.*, 1981, **78**, 577.

505. R. Rowan III, P.H. Mazzocchi, C.A. Kanagy and M. Regan, *J. Magn. Reson.*, 1980, **39**, 27.
506. D.J. Craik, R.M. Drew, I. Kyratzis, I.D. Rai and J.A. Weigold, *Aust. J. Chem.*, 1986, **39**, 2049.
507. J.M. Bruce, F. Heatley, R.G. Ryles and J.H. Scrivens, *J. Chem. Soc., Perkin Trans. 2*, 1980, 860.
508. L.I. Kruse, C.W. DeBrosse and C.H. Kruse, *J. Am. Chem. Soc.*, 1985, **107**, 5435.
509. B. Tiffon and J.S. Lomas, *Org. Magn. Reson.*, 1984, **22**, 29.
510. E. Gaggelli, N. Marchettini and G. Valensin, *Magn. Reson. Chem.*, 1987, **25**, 970.
511. A. Sega, M. Ghelardoni, V. Pestellini, L. Pogliani and G. Valensin, *Org. Magn. Reson.*, 1984, **22**, 649.
512. P. Bigler, *J. Magn. Reson.*, 1987, **75**, 162.
513. T. Yonemitsu, K. Tsutsumi and N. Takiguchi, *Kyushu Sangyo Daigaku Kogakubu Kenkyu Hokoku*, 1984, **21**, 25 (*Chem. Abs.*, 1987, 107:39036u).
514. D.L. Ashley, E.R. Barnhart, D.G. Patterson, Jr. and R.H. Hill, Jr., *Anal. Chem.*, 1988, **60**, 15.
515. A. Kratochwill and R.L. Vold, *J. Magn. Reson.*, 1980, **40**, 197.
516. C. Rossi, L. Pogliani, F. Laschi and N. Niccolai, *J. Chem. Soc., Faraday Trans. 1*, 1983, **79**, 2955.
517. M. Sugiura, N. Takao, S. Ueji and H. Fujiwara, *J. Chem. Soc., Perkin Trans. 2*, 1985, 83.
518. M. Sugiura, N. Takao and H. Fujiwara, *Magn. Reson. Chem.*, 1988, **26**, 1051.
519. T. Ade, A. Hermann, V. Hoffmann and J. Weiss, *J. Mol. Struct.*, 1988, **177**, 367.
520. E. Haslinger, H. Kalchhauser and W. Robien, *J. Mol. Liq.*, 1984, **28**, 223.
521. H. Haruyama, S. Sato, K. Kawazoe and M. Kondo, *Chem. Pharm. Bull.*, 1987, **35**, 957.
522. R.Kh. Sadykov, E.N. Klimovitskii, Yu. Yu. Samitov and B.A. Arbuzov, *Izv. Akad. Nauk SSSR, Ser. Khim.*, 1983, 2497.
523. G.B. Young and T.L. James, *J. Am. Chem. Soc.*, 1984, **106**, 7986.
524. M.A. Khadim, L.D. Colebrook and L.D. Hall, *J. Heterocycl. Chem.*, 1980, **17**, 651.
525. S. Peiris and L.D. Colebrook, *Org. Magn. Reson.*, 1984, **22**, 228.
526. J. Hennig and H.-H. Limbach, *J. Am. Chem. Soc.*, 1984, **106**, 292.
527. D. Kaplan and G. Navon, *J. Chem. Soc., Perkin Trans. 2*, 1981, 1374.
528. N. Niccolai, H.K. Schnoes and W.A. Gibbons, *J. Am. Chem. Soc.*, 1980, **102**, 1513.
529. F. Heatley, L. Akhter and R.T. Brown, *J. Chem. Soc., Perkin Trans. 2*, 1980, 919.
530. N.M. Szeverenyi, A.A. Bothner-By and R. Bittner, *J. Chem. Phys.*, 1980, **84**, 2880.
531. W.J. Chazin, L.D. Colebrook and J.T. Edward, *Can. J. Chem.*, 1983, **61**, 1749.
532. H. Haruyama and M. Kondo, *Chem. Pharm. Bull.*, 1987, **35**, 170.
533. W.J. Chazin and L.D. Colebrook, *Can. J. Chem.*, 1986, **64**, 2220.
534. P. Berntsson and R.E. Carter, *Acta Pharm. Suec.*, 1981, **18**, 221.
535. P. Dais and A.S. Perlin, *Adv. Carbohydr. Chem. Biochem.*, 1987, **45**, 125.
536. L.D. Hall and H.D.W. Hill, *J. Am. Chem. Soc.*, 1976, **98**, 1269.
537. K. Bock, L.D. Hall and C. Pedersen, *Can. J. Chem.*, 1980, **58**, 1916.
538. K. Bock, L.D. Hall and C. Pedersen, *Can. J. Chem.*, 1980, **58**, 1923.
539. P. Dais, T.K.M. Shing and A.S. Perlin, *Carbohydr. Res.*, 1983, **122**, 305.
540. P. Dais, T.K.M. Shing and A.S. Perlin, *J. Am. Chem. Soc.*, 1984, **106**, 3082.
541. A.G. Avent and R. Freeman. *J. Magn. Reson.*, 1980, **39**, 169.
542. J.R. Everett and J.W. Tyler, *J. Chem. Soc., Perkin Trans. 2*, 1988, 325.
543. M. Guéron, J.L. Leroy and R.H. Griffey, *J. Am. Chem. Soc.*, 1983, **105**, 7262.
544. E.R. Andrew and R. Gaspar Jr., *Chem. Phys. Lett.*, 1988, **146**, 184.
545. E.R. Andrew and R. Gaspar Jr., *Chem. Phys. Lett.*, 1988, **147**, 551.
546. M. Witanowski, L. Stefaniak and G.A. Webb. *Annual Reports on NMR Spectroscopy*, Vol. 18, p. 1. Academic Press, London, 1986.
547. G.C. Levy and R.L. Lichter, *Nitrogen-15 Nuclear Magnetic Resonance Spectroscopy*. Wiley, New York, 1979.
548. J.B. Lambert and D. Stec III, *Org. Magn. Reson.*, 1984, **22**, 301.

549. J.P. Marchal, J. Brondeau and D. Canet, *Org. Magn. Reson.*, 1982, **19**, 1.
550. J. Kowalewski and G.A. Morris, *J. Magn. Reson.*, 1982, **47**, 331.
551. D. Marion, C. Garbay-Jaureguiberry and B.P. Roques, *J. Am. Chem. Soc.*, 1982, **104**, 5573.
552. D. Marion, C. Garbay-Jaureguiberry and B.P. Roques, *J. Magn. Reson.*, 1983, **53**, 199.
553. C.G. Beguin and R. Dupeyre, *J. Flourine Chem.*, 1981, **17**, 205.
554. G.C. Levy, J.D. Cargioli, P.C. Juliano and T.D. Mitchell, *J. Am. Chem. Soc.*, 1973, **95**, 3445.
555. C.T.G. Knight, *J. Non-Cryst. Solids*, 1988, **104**, 151.
556. Yi-Ming Pai, W.P. Weber and K.L. Servis, *J. Organomet. Chem.*, 1985, **288**, 269.
557. R. Kosfeld, C. Kreuzburg and R. Krause, *Makromol. Chem.*, 1988, **91**, 4030.
558. N.J. Koole, A.J. de Koning and M.J.A. de Bie, *J. Magn. Reson.*, 1977, **25**, 375.
559. R.K. Harris and E.M. McVicker, *J. Chem. Soc., Faraday Trans. 2*, 1976, **72**, 2291.
560. J.B. Robert, M.C. Taieb and J. Tabony, *J. Magn. Reson.*, 1980, **38**, 99.
561. K. Ramarajan, M.H. Herd and K.D. Berlin, *Phosphorus Sulfur*, 1981, **11**, 199.
562. R.K. Nanda, A. Ribeiro, T.S. Jardetzky and O. Jardetzky, *J. Magn. Reson.*, 1980, **39**, 119.
563. P. Bendel and T.L. James, *J. Magn. Reson.*, 1982, **48**, 76.
564. M. Christensen and J.P. Jacobsen, *Magn. Reson. Med.*, 1988, **7**, 197.
565. I.L. Claeys and F.H. Arnold, *AIChE J.*, 1989, **35**, 335.
566. B. Tiffon, B. Ancian and J.-E. Dubois, *J. Chem. Phys.*, 1981, **74**, 6981.
567. B. Tiffon and B. Ancian, *J. Chem. Phys.*, 1982, **76**, 1212.
568. H. Kovacs, J. Kowalewski and A. Maliniak, *Chem. Phys. Lett.*, 1988, **152**, 427.
569. J.D. Halliday, P.E. Bindner and S. Padamshi, *Can. J. Chem.*, 1985, **63**, 2975.
570. Jae-Ryun Suhr, Chang-Ju Yoon, Seong-Gu Ro and Young-Sang Choi, *Bull. Korean Chem. Soc.*, 1987, **8**, 230.
571. V.F. Galat and E.V. Titov, *J. Mol. Struct.*, 1988, **174**, 303.
572. J.M. Robert and R.F. Evilia, *Anal. Chem.*, 1988, **60**, 2035.
573. J.-P. Marchal and D. Canet. *J. Chem. Soc., Faraday Trans. 2*, 1982, **78**, 435.
574. J. Ogino, H. Suezawa, and M. Hirota, *Chem. Lett.*, 1983, 889.
575. B. Tiffon, B. Ancian and J.-E. Dubois, *Chem. Phys. Lett.*, 1980, **73**, 89.
576. A. Loewenstein and D. Igner, *J. Phys. Chem.*, 1988, **92**, 2124.
577. B. Valentine, T.E. St. Amour and D. Fiat, *Org. Magn. Reson.*, 1984, **22**, 697.
578. B. Valentine, T. St. Amour, R. Walter and D. Fiat, *J. Magn. Reson.*, 1980, **38**, 413.
579. A. Steinschneider and D. Fiat, *Int. J. Peptide Protein Res.*, 1984, **23**, 591.
580. B. Valentine, A. Steinschneider, D. Dhawan, M.I. Burgar, T. St. Amour and D. Fiat, *Int. J. Peptide Protein Res.*, 1985, **25**, 56.
581. A. Steinschneider, B. Valentine, M.I. Burgar and D. Fiat, *Magn. Reson. Chem.*, 1985, **23**, 104.
582. C. Sakarellos, I.P. Gerothanassis, N. Birlirakis, T. Karayannis, M. Sakarellos-Daitsiotis and M. Marraud, *Biopolymers*, 1989, **28**, 15.
583. D. Monti, F. Orsini and G. Severini Ricca, *Spectrosc. Lett.*, 1986, **19**, 505.
584. C. Delseth and J.-P. Kintzinger, *Helv. Chim. Acta*, 1982, **65**, 2273.
585. K.M. Larsson and J. Kowalewski, *Acta Chem. Scand., Ser. A*, 1986, **40**, 218.
586. J.A. Gerlt, P.C. Demou and S. Mehdi, *J. Am. Chem. Soc.*, 1982, **104**, 2848.
587. J.F. Hinton, *Annual Reports on NMR Spectroscopy*, Vol. 19, p. 1. Academic Press, London, 1987.
588. B.H. Ruessink, W.J. van der Meer and C. MacLean, *J. Am. Chem. Soc.*, 1986, **108**, 192.
589. J.F. Hinton, *J. Magn. Reson.*, 1984, **59**, 469 (Erratum, *J. Magn. Reson.*, 1985, **62**, 356).
590. P.S. Belton, I.J. Cox and R.K. Harris, *J. Chem. Soc., Faraday Trans. 2*, 1985, **81**, 63.
591. P.P. Mahendroo and A.D. Sherry, *Magn. Reson. Chem.*, 1985, **23**, 503.
592. D.S. Crumrine and B. Gillece-Castro, *J. Org. Chem.*, 1985, **50**, 4408.
593. H. Wennerström, B. Lindman and S. Forsén, *J. Phys. Chem.*, 1971, **75**, 2936.
594. H. Suezawa, T. Kodama, J. Ogino and M. Hirota, *Chem. Lett.*, 1984, 1645.

595. R.R. Vold, in *Nuclear Magnetic Resonance of Liquid Crystals* (ed. J.W. Emsley), p. 253. Reidel, Dordrecht, 1985.
596. R.L. Vold and R.R. Vold, *Isr. J. Chem.*, 1983, **23**, 315.
597. R.R. Vold and R.L. Vold, *J. Chem. Phys.*, 1977, **66**, 4018.
598. J.M. Courtieu, C.L. Mayne and D.M. Grant, *J. Chem. Phys.*, 1977, **66**, 2669.
599. R.L. Vold, R.R. Vold, P. Poupko and G. Bodenhausen, *J. Magn. Reson.*, 1980, **38**, 141.
600. R. Poupko, R.L. Vold and R.R. Vold, *J. Phys. Chem.*, 1980, **84**, 3444.
601. J. Voigt and J.P. Jacobsen, *J. Chem. Phys.*, 1983, **78**, 1693.
602. J.M. Courtieu, N.T. Lai, C.L. Mayne, J.M. Bernassau and D.M. Grant, *J. Chem. Phys.*, 1982, **76**, 257.
603. J. Courtieu, C.L. Mayne, D.M. Grant and J.M. Bernassau, *J. Magn. Reson.*, 1982, **48**, 346.
604. E.P. Black, J.M. Bernassau, C.L. Mayne and D.M. Grant, *J. Chem. Phys.*, 1982, **76**, 265.
605. H.A. Lopes Cardozo, J. Bulthuis and C. MacLean, *J. Magn. Reson.*, 1979, **33**, 27.
606. D. Jaffe, R.R. Vold and R.L. Vold, *J. Magn. Reson.*, 1982, **46**, 475.
607. L. Plomp, A.C. Loman and J. Bulthuis, *J. Chem. Phys.*, 1986, **84**, 6591.
608. D. Imbardelli and G. Chidichimo, *Chem. Phys. Lett.*, 1987, **134**, 96.
609. D. Imbardelli, G. Chidichimo and M. Longeri, *Chem. Phys. Lett.*, 1987, **135**, 319.
610. J.-Ph. Caniparoli, Th. Bredel, C. Chachaty and J. Maruani, *J. Phys. Chem.*, 1989, **93**, 797.
611. L. Plomp, M. Schreurs and J. Bulthuis, *J. Chem. Phys.*, 1988, **88**, 5202.
612. W.H. Dickerson, R.R. Vold and R.L. Vold, *J. Phys. Chem.*, 1983, **87**, 166.
613. L.S. Selwyn, R.L. Vold and R.R. Vold, *J. Chem. Phys.*, 1984, **80**, 5418.
614. L.S. Selwyn, R.R. Vold and R.L. Vold, *Mol. Phys.*, 1985, **55**, 287.
615. P.R. Luyten, R.R. Vold and R.L. Vold, *J. Phys. Chem.*, 1985, **89**, 545.
616. L. Plomp and J. Bulthuis, *Liq. Cryst.*, 1988, **3**, 927.
617. R.G. Bryant, *Stud. Phys. Theor. Chem.*, 1988, **38**, 683.
618. S. Forsén, T. Drakenberg and H. Wennerström, *Quart. Rev. Biophys.*, 1987, **19**, 83.
619. B. Halle and H. Wennerström, *J. Chem. Phys.*, 1981, **75**, 1928.
620. B. Halle, *Mol. Phys.*, 1984, **53**, 1427.
621. B. Halle and L. Piculell, *J. Chem. Soc., Faraday Trans. 1*, 1986, **82**, 415.
622. J.C. Gore, M.S. Brown, J. Zhong and I.M. Armitage, *J. Magn. Reson.*, 1989, **83**, 246.
623. J.C. Gore, M.S. Brown and I.M. Armitage, *Magn. Reson. Med.*, 1989, **9**, 333.
624. J. Breen, D. Huis, J. de Bleijser and J.C. Leyte, *J. Chem. Soc., Faraday Trans. 1*, 1988, **84**, 293.
625. S. Conti, G.J. Béné and P. Magnin, *Helv. Phys. Acta*, 1988, **61**, 66.
626. B. Halle and L. Piculell, *J. Chem. Soc., Faraday Trans. 1*, 1982, **78**, 255.
627. C.W.R. Mulder, J. Schriever, W.J. Jesse and J.C. Leyte, *J. Phys. Chem.*, 1983, **87**, 2342.
628. J.R.C. Van der Maarel, D. Lankhorst, J. de Bleijser and J.C. Leyte, *Macromolecules*, 1987, **20**, 2390.
629. B. Halle and G. Carlström, *J. Phys. Chem.*, 1981, **85**, 2142.
630. L. Piculell, *J. Phys. Chem.*, 1985, **89**, 3590.
631. M.P. Frenot, H. Nery and D. Canet, *J. Phys. Chem.*, 1984, **88**, 2884. M.P. Bozonnet-Frenot, J.P. Marchal and D. Canet, *J. Phys. Chem.*, 1987, **91**, 89.
632. R. Bhanumathi and S.K. Vijayalakshamma, *Ind. J. Chem., Ser. A*, 1985, **24**, 727.
633. A. Belmajdoub, J.C. Boubel and D. Canet, *J. Phys. Chem.*, 1989, **93**, 4844.
634. J. Kamegai and T. Kurosaki, *Chem. Express*, 1987, **2**, 85.
635. G. Carlström and B. Halle, *Langmuir*, 1988, **4**, 1346, *J. Phys. Chem.*, 1989, **93**, 3287.
636. A. Llor and P. Rigny, *J. Am. Chem. Soc.*, 1986, **108**, 7533.
637. A. Maitra and P. Patanjali, *Colloids and Surfaces*, 1987, **27**, 271.
638. P.-O. Quist and B. Halle, *J. Chem. Soc., Faraday Trans 1*, 1988, **84**, 1033.
639. A. Faure, A.M. Tistchenko, T. Zemb, and C. Chachaty, *J. Phys. Chem.*, 1985, **89**, 3373.
640. S.H. Koenig, K. Hallenga and M. Shporer, *Proc. Natl. Acad. Sci. USA*, 1975, **72**, 2667.

641. K Hallenga and S.H. Koenig, *Biochemistry*, 1976, **15**, 4255.
642. B. Halle, T. Andersson, S. Forsén and B. Lindman, *J. Am. Chem. Soc.*, 1981, **103**, 500.
643. L. Piculell and B. Halle, *J. Chem. Soc., Faraday Trans. 1*, 1986, **82**, 401.
644. T.S. Lioutas, I.C. Baianu and M.P. Steinberg, *Arch. Biochem. Biophys.*, 1986, **247**, 68; L.T. Kakalis and I.C. Baianu, *ibid.*, 1988, **267**, 829.
645. T.F. Kumosinski, H. Pessen, S.J. Prestrelski and H.M. Farrell Jr., *Arch Biochem. Biophys.*, 1987, **257**, 259.
646. J. Gallier, P. Rivet and J. de Certaines, *Biochim. Biophys. Acta*, 1987, **915**, 1.
647. S. Conti, *Mol. Phys.*, 1986, **59**, 449.
648. H.E. Rorschach and C.F. Hazlewood, *J. Magn. Reson.*, 1986, **70**, 79.
649. S.H. Koenig, R.G. Bryant, K. Hallenga and G.S. Jacob, *Biochemistry*, 1978, **17**, 4348.
650. S.H. Koenig, *Biophys. J.*, 1988, **53**, 91.
651. C.F. Beaulieu, J.I. Clark, R.D. Brown III, M. Spiller and S.H. Koenig, *Magn. Reson. Med.*, 1988, **8**, 45; C.F. Beaulieu, R.D. Brown III, J.I. Clark, M. Spiller and S.H. Koenig, *ibid.*, 1989, **10**, 362.
652. R.G. Bryant and M. Jarvis, *J. Phys. Chem.*, 1984, **88**, 1323.
653. G. Otting and K. Wüthrich, *J. Am. Chem. Soc.*, 1989, **111**, 1871.
654. G.D. Fullerton, M.F. Finnie, K.E. Hunter, V.A. Ord and I.L. Cameron, *Magn. Reson. Imag.*, 1987, **5**, 353.
655. N.G. Vostrikova, V.P. Denisov, Yu. M. Petrusevich and O.P. Revokatov, *Vestn. Mosk. Univ., Ser. 3: Fiz., Astron.*, 1986, **27**, 76.
656. J.J. van der Klink, L.H. Zuiderweg and J.C. Leyte, *J. Chem. Phys.*, 1974, **60**, 2391.
657. A. Delville, H. Gilboa and P. Laszlo, *J. Chem. Phys.*, 1982, **77**, 2045.
658. A. Delville and P. Laszlo, *Biophys. Chem.*, 1983, **17**, 119.
659. B. Halle, D. Bratko and L. Piculell, *Ber. Bunsenges. Phys. Chem.*, 1985, **89**, 1254.
660. M. Levij, J. de Bleijser and J.C. Leyte, *Chem. Phys. Lett.*, 1981, **83**, 183.
661. M. Levij, J. de Bleijser and J.C. Leyte, *Chem. Phys. Lett.*, 1982, **87**, 34.
662. G. Gunnarsson and H. Gustavsson, *J. Chem. Soc., Faraday Trans. 1*, 1982, **78**, 2901.
663. B. Halle, H. Wennerström and L. Piculell, *J. Phys. Chem.*, 1984, **88**, 2482.
664. P. Linse and B. Halle, *Mol. Phys.*, 1989, **67**, 537.
665. J.R.C. Van der Maarel, D. Van Duijn, J. de Bleijser and J.C. Leyte, *Chem. Phys. Lett.*, 1987, **135**, 62.
666. J.R.C. Van der Maarel, D.H. Powell, A.K. Jawahier, L.H. Leyte-Zuiderweg, G.W. Neilson and M.C. Bellisent-Funel, *J. Chem. Phys.*, 1989, **90**, 6709.
667. A.C. Barnes, J.E. Enderby, J. Breen and J.C. Leyte, *Chem. Phys. Lett.*, 1987, **142**, 405.
668. C.J.M. van Rijn, A.J. Maat, J. de Bleijser and J.C. Leyte, *J. Phys. Chem.*, 1989, **93**, 5284.
669. P. Linse, H. Gustavsson, B. Lindman and T. Drakenberg, *J. Magn. Reson.*, 1981, **45**, 133.
670. D.W. Urry, *Bull. Magn. Reson.*, 1987, **9**, 109.
671. H. Fabre, N. Kamenka, A. Khan, G. Lindblom, B. Lindman and G.J.T. Tiddy, *J. Phys. Chem.*, 1980, **84**, 3428.
672. M.L. Bleam, C.F. Anderson and M.T. Record Jr., *Proc. Natl. Acad. Sci USA*, 1980, **77**, 3085.
673. M.L. Bleam, C.F. Anderson and M.T. Record Jr., *Biochemistry*, 1983, **22**, 5418.
674. W.H. Braunlin and L. Nordenskiöld, *Eur. J. Biochem.*, 1984, **142**, 133.
675. D.M. Rose, C.F. Polnaszek and R.G. Bryant, *Biopolymers*, 1982, **21**, 653.
676. W.H. Braunlin, T. Drakenberg and L. Nordenskiöld, *Biopolymers*, 1987, **26**, 1047.
677. H. Shinar and G. Navon, *Magn. Reson. Med.*, 1986, **3**, 927.
678. J. Pekar and J.S. Leigh Jr., *J. Magn. Reson.*, 1986, **69**, 582.
679. W.D. Rooney, T.M. Barbara and C.S. Springer Jr., *J. Am. Chem. Soc.*, 1988, **110**, 674.
680. C. Chachaty, *Progr. NMR Spectrosc.*, 1987, **19**, 183.
681. B. Lindman, O. Söderman and H. Wennerström, *Ann. Chim. (Rome)*, 1987, **77**, 1.

682. H. Wennerström, B. Lindman, O. Söderman, T. Drakenberg and J.B. Rosenholm, *J. Am. Chem. Soc.*, 1979, **101**, 6860.
683. H. Wennerström, G. Lindblom and B. Lindman, *Chem. Scripta*, 1974, **6**, 97.
684. G. Lipari and A. Szabo, *J. Am. Chem. Soc.*, 1982, **104**, 4546.
685. T. Ahlnäs, O. Söderman, C. Hjelm and B. Lindman, *J. Phys. Chem.*, 1983, **87**, 822.
686. H. Walderhaug, O. Söderman and P. Stilbs, *J. Phys. Chem.*, 1984, **88**, 1655.
687. O. Söderman and H. Walderhaug, *Langmuir*, 1986, **2**, 57.
688. J. Carnali, B. Lindman, O. Söderman and H. Walderhaug, *Langmuir*, 1986, **2**, 51.
689. M. Jansson, Puyong Li and P. Stilbs, *J. Phys. Chem.*, 1987, **91**, 5279.
690. O. Söderman, H. Walderhaug, U. Henriksson and P. Stilbs, *J. Phys. Chem.*, 1985, **89**, 3693.
691. O. Söderman, U. Henriksson and U. Olsson, *J. Phys. Chem.*, 1987, **91**, 116.
692. O. Söderman, G. Carlström, U. Olsson and T.C. Wong, *J. Chem. Soc., Faraday Trans 1*, 1988, **64**, 4475.
693. U. Olsson, P. Ström, O. Söderman and H. Wennerström, *J. Phys. Chem.*, 1989, **93**, 4572.
694. O. Söderman, D. Canet, J. Carnali, U. Henriksson, H. Nery, H. Walderhaug and T. Wärnheim, *Surfactant Sci. Ser.*, 1987, **24**, 145.
695. K.P. Das, A. Ceglie, M. Monduzzi, O. Söderman and B. Lindman, *Progr. Colloid Polymer Sci.*, 1987, **73**, 167.
696. A. Belmajdoub, B. Diter and D. Canet, *Chem. Phys. Lett.*, 1986, **131**, 426.
697. A. Belmajdoub, J. Brondeau, J.C. Boubel and D. Canet, *Chem. Phys. Lett.*, 1987, **140**, 389.
698. A. Belmajdoub, K. ElBayed, J. Brondeau, D. Canet, I. Rico and A. Lattes, *J. Phys. Chem.*, 1988, **92**, 3569.
699. F. Heatley, Hoon Hong Teo and C. Booth, *J. Chem. Soc., Faraday Trans. 1*, 1984, **80**, 981.
700. O. Söderman, G. Carlström, M. Monduzzi and U. Olsson, *Langmuir*, 1988, **4**, 1039.
701. T.C. Wong, K. Ikeda, K. Meguro, O. Söderman, U. Olsson and B. Lindman, *J. Phys. Chem.*, 1989, **93**, 4861.
702. C. Chachaty, T. Ahlnäs, B. Lindström, H. Nery and A.M. Tistchenko, *J. Colloid Interf. Sci.*, 1988, **122**, 406.
703. M. Jansson, Puyong Li, U. Henriksson and P. Stilbs, *J. Phys. Chem.*, 1989, **93**, 1448.
704. F. Heatley, *J. Chem. Soc., Faraday Trans. 1*, 1989, **85**, 917.
705. P. Stilbs, O. Söderman and H. Walderhaug, *J. Magn. Reson.*, 1986, **69**, 411.
706. O. Söderman and P. Stilbs, *Chem. Phys. Lipids*, 1986, **41**, 117.
707. J.F. Ellena, R.N. Dominey and D.S. Cafiso, *J. Phys. Chem.*, 1987, **91**, 131.
708. D. Canet, J. Brondeau, H. Nery and J.P. Marchal, *Chem. Phys. Lett.*, 1980, **72**, 184.
709. D. Canet, J.P. Marchal, H. Nery, B. Robin-Lherbier and J.M. Cases, *J. Colloid Interf. Sci.*, 1983, **93**, 241.
710. J.P. Marchal, D. Canet, H. Nery, B. Robin-Lherbier and J.M. Cases, *J. Colloid Interf. Sci.*, 1984, **99**, 349.
711. C.A. Martin and L.J. Magid, *J. Phys. Chem.*, 1981, **85**, 3938.
712. M. Ueno and H. Kishimoto, *J. Phys. Chem.*, 1983, **87**, 850.
713. K. Matsushita, Y. Terada, T. Yoshida and H. Okabayashi, *Z. Naturforsch., Teil A*, 1983, **38**, 1149.
714. B. Durairaj and F.D. Blum, *Langmuir*, 1989, **5**, 370.
715. R.E. Stark, M.L. Kasakevich and J.W. Granger, *J. Phys. Chem.*, 1982, **86**, 335.
716. P. Stilbs, H. Walderhaug and B. Lindman, *J. Phys. Chem.*, 1983, **87**, 4762.
717. O.P. Yablonskii, V.V. Volynets, V.P. Konovalova and V.L. Tsaylingold, *Kolloidn. Zh.*, 1988, **50**, 404.
718. W. Abraham, T.M. Harris and D.J. Wilson, *Sep. Sci. Technol.*, 1987, **22**, 2269.

719. J. Ulmius and B. Lindman, *J. Phys. Chem.*, 1981, **85**, 4131.
720. C.A. Boicelli, F. Conti, M. Giomini and A.M. Giuliani, *Spectrochim. Acta, Part A*, 1982, **38**, 299.
721. S. Belaid and C. Chachaty, *J. Colloid Interf. Sci.*, 1982, **86**, 277.
722. Y. Chevalier and C. Chachaty, *Colloid Polym. Sci.*, 1984, **262**, 489.
723. J.H. Prestegard and D.M. Grant, *J. Am. Chem. Soc.*, 1978, **100**, 4664.
724. Lian-Pin Hwang, Pei-Lein Wang and T.C. Wong, *J. Phys. Chem.*, 1988, **92**, 4753.
725. L.E. Kay and J.H. Prestegard, *J. Am. Chem. Soc.*, 1987, **109**, 3829.
726. T.C. Wong, Pei-Lein Wang, Der-Ming Duh and Lian-Pin Hwang, *J. Phys. Chem.*, 1989, **93**, 1295.
727. F.A.L. Anet, *J. Am. Chem. Soc.*, 1986, **108**, 7102.
728. J.J.H. Nusselder, J.B.F.N. Engberts, R. Boelens and R. Kaptein, *Recl. Trav. Chim. Pays-Bas*, 1988, **107**, 105.
729. E. Kolehmainen, *Magn. Reson. Chem.*, 1988, **26**, 760.
730. H. Nery, J.P. Marchal, D. Canet and J.M. Cases, *J. Colloid Interf. Sci.*, 1980, **77**, 174.
731. A. Zheliaskova and A. Derzhanski, *Liq. Cryst.*, 1988, **3**, 833.
732. A.I. Derzhanski and A.G. Zheliaskova, *Dokl. Bolg. Akad. Nauk*, 1988, **41**, 21.
733. K. Wüthrich, *NMR of Proteins and Nucleic Acids*. Wiley, New York, 1986.
734. F. Heatley, *Annual Reports on NMR Spectroscopy*, Vol 17, p. 179. Academic Press, London, 1986.
735. O. Jardetzky, *Acc. Chem. Res.*, 1981, **14**, 291.
736. C.W.R. Mulder, J. Schriever and J.C. Leyte, *J. Phys. Chem.*, 1985, **89**, 475.
737. C.W.R. Mulder and J.C. Leyte, *J. Phys. Chem.*, 1985, **89**, 1007.
738. C.J.M. van Rijn, W. Jesse, J. de Bleijser and J.C. Leyte, *J. Phys. Chem.*, 1987, **91**, 203.
739. C.J.M. van Rijn, J. de Bleijser and J.C. Leyte, *Macromolecules*, 1987, **20**, 1248.
740. J. Skolnick and R. Yaris, *Macromolecules*, 1982, **15**, 1041 (*Erratum, Macromolecules*, 1983, **16**, 491).
741. J. Skolnick and R. Yaris, *Macromolecules*, 1983, **16**, 266.
742. G.C. Levy, D.E. Axelson, R. Schwartz and J. Hochmann, *J. Am. Chem. Soc.*, 1978, **100**, 410.
743. H. Bergmann and K. Schlothauer, *Acta Polym.*, 1988, **39**, 694.
744. M. Knörgen, K. Schlothauer and R. Radeglia, *Acta Polym.*, 1987, **38**, 111.
745. J.A. Ratto, P.T. Inglefield, R.A. Rutowski, K.-L. Li, A.A. Jones and A.K. Roy, *J. Polym. Sci. Ser. B*, 1987, **25**, 1419.
746. Chi-Cheng Hung, J.H. Shibata, A.A. Jones and P.T. Inglefield, *Polymer*, 1987, **28**, 1062.
747. Seok Heon Oh, Ryong Ryoo and Mu Shik Jhon, *J. Polym. Sci., Ser. A*, 1989, **27**, 1383.
748. I. Bahar, B. Erman and L. Monnerie, *Macromolecules*, 1989, **22**, 2396.
749. J. Breen, D. van Duijn, J. de Bleijser and J.C. Leyte, *Ber. Bunsenges. Phys. Chem.*, 1986, **90**, 1112.
750. P.L. Rinaldi, Chin Yu and G.C. Levy, *Macromolecules*, 1981, **14**, 551.
751. R.H. Cole, S.A. Chambers, A.H. Fawcett, L.C. Waring and P. Windsor, IV, *J. Mol. Liq.*, 1987, **36**, 167.
752. J. Skolnick and R. Yaris, *Macromolecules*, 1982, **15**, 1046.
753. F. Tabak, *J. Mol. Liq*, 1988, **39**, 137.
754. S.M. Usmanov and Yu. M. Sivergin, *Zh. Fiz. Khim.*, 1988, **62**, 1888.
755. K. Dill and A. Allerhand, *J. Am. Chem. Soc.*, 1979, **101**, 4376.
756. J. Jarvet, *Eesti NSV Tead. Akad. Toim. Fuus., Mat.*, 1988, **37**, 67.
757. B. Tobias and J.L. Markley, *J. Magn. Reson.*, 1986, **69**, 381.
758. B. Perly. C. Chachaty and A. Tsutsumi, *J. Am. Chem. Soc.*, 1980, **102**, 1521.

759. O. Jardetzky, A.A. Ribeiro and R. King, *Biochem. Phys. Res. Commun.*, 1980, **92**, 883. A.A. Ribeiro, R. King, C. Restivo and O. Jardetzky, *J. Am. Chem. Soc.*, 1980, **102**, 4040.
760. V.D. Fedotov, *Teubner-Texte Phys.*, 1986, **9**, 262 (*Chem. Abs.*, 1987, 107:23976q).
761. G.E. Hawkes, Lu-Yu Lian, E.W. Randall, K.D. Sales and E.H. Curzon, *Eur. J. Biochem.*, 1987, **166**, 437.
762. R.P.H. Kooyman and T.J. Schaafsma, *J. Am. Chem. Soc.*, 1984, **106**, 551.
763. A.E. Torda and R.S. Norton, *Biopolymers*, 1989, **28**, 703.
764. G.M. Clore and A.M. Gronenborn, *Protein Eng.*, 1987, **1**, 275.
765. R. Kaptein, R. Boelens, R.M. Scheek and W.F. van Gunsteren, *Biochemistry*, 1988, **27**, 5389.
766. K. Wüthrich, *Science*, 1989, **243**, 45.
767. G.M. Clore and A.M. Gronenborn, *J. Magn. Reson.*, 1983, **53**, 423.
768. E.T. Olejniczak, P.M. Pousen and C.M. Dobson, *J. Magn. Reson.*, 1984, **59**, 518.
769. P.A. Mirau and F.A. Bovey, *J. Am. Chem. Soc.*, 1986, **108**, 5130.
770. S.G. Withers, N.B. Madsen and B.D. Sykes, *J. Magn. Reson.*, 1985, **61**, 545.
771. L.G. Werbelow, *J. Magn. Reson.*, 1987, **71**, 151.
772. T. Andersson, T. Drakenberg, S. Forsén, E. Thulin and M. Svärd, *J. Am. Chem. Soc.*, 1982, **104**, 576.
773. P.D. Ellis, P.P. Yang and A.R. Palmer, *J. Magn. Reson.*, 1983, **52**, 254.
774. L. Baltzer, E.D. Becker, R.G. Tschudin and O.A. Gansow, *J. Chem. Soc. Chem. Commun.*, 1985, 1040.
775. L. Baltzer, *J. Am. Chem. Soc.*, 1987, **109**, 3479.
776. P.H. Bolton and T.L. James, *J. Phys. Chem.*, 1979, **83**, 3359.
777. M. Petersheim, V.W. Miner, J.A. Gerlt and J.H. Prestegard, *J. Am. Chem. Soc.*, 1983, **105**, 6357.
778. G.C. Levy, P.R. Hilliard, L.F. Levy, R.L. Rill and Inners, *J. Biol. Chem.*, 1981, **256**, 9986.
779. P.N. Borer, N. Zanatta, T.A. Holak, G.C. Levy, J.H. Van Boom and A.H.J. Wang, *J. Biomol. Struct. Dyn.*, 1984, **1**, 1373.
780. P.G. Schmidt, T. Playl and P.F. Agris, *Biochemistry*, 1983, **22**, 1408.
781. P.G. Schmidt, H. Sierzputowska-Gracz and P.A. Agris, *Biochemistry*, 1987, **26**, 8529.
782. J.R. Williamson and S.G. Boxer, *Nucl. Acids Res.*, 1988, **16**, 1529.
783. J.R. Williamson and S.G. Boxer, *Biochemistry*, 1989, **28**, 2819.
784. P.A. Mirau and F.A. Bovey, *J. Magn. Reson.*, 1987, **71**, 201.
785. A.M. Gronenborn and G.M. Clore, *Progr. NMR Spectrosc.*, 1985, **17**, 1.
786. W. Massefski, Jr. and P.H. Bolton, *J. Magn. Reson.*, 1985, **65**, 526.
787. N. Jamin, T.L. James and G. Zon, *Eur. J. Biochem.*, 1985, **152**, 157.
788. T.L. James, E.-I. Suzuki, N. Pattabiraman and G. Zon, *Bioact. Mol.*, 1987, **3**, 503.
789. R. Boelens, T.M.G. Koning, G.A. van der Marel, J.H. van Boom and R. Kaptein, *J. Magn. Reson.*, 1989, **82**, 290.
790. Yu-Sen Wang and S. Ikuta, *J. Am. Chem. Soc.*, 1989, **111**, 1243.
791. D. Gagnaire, S. Perez and V. Tran, *Makromol. Chem.*, 1984, **185**. J. Briand and L.D. Hall, *J. Magn. Reson.*, 1989, **82**, 180.
792. K. Matsuo, *Macromolecules*, 1984, **17**, 449.
793. Qin-Ji Peng and A.S. Perlin, *Carbohydr. Res.*, 1987, **160**, 57.
794. P. Dais, Qin-Ji Peng and A.S. Perlin, *Carbohydr. Res.*, 1987, **168**, 163.

NMR of Coals and Coal Products

WOLFGANG MEILER and REINHARD MEUSINGER

Sektion Physik, Universität Leipzig, Linnéstr. 5,
O-7010 Leipzig, Federal Republic of Germany

1. INTRODUCTION

The complete molecular structure of coal is one of the unsolved secrets of nature. The origin of coal is well known, and knowledge exists on the physical and chemical coalification processes that occur in organic matter. Unfortunately, the large number of parameters involved in the geochemical evolution of coal leads to a very complicated situation with respect to the variety of coals. Today many complementary analytical methods play an important role in the systematic and extensive investigation of coals.

Of the various analytical methods available, NMR spectroscopy has proved to be of special importance in coal research. Different NMR techniques allow the structure of coal and coal products to be investigated in a direct and nondestructive way. Moreover, besides the investigation of pit coal, extracts and a variety of coal-derived materials, measurements made on samples in connection with technological coal conversion and refinement processes are also possible. The application of NMR techniques to the study of fossil carbonaceous materials is of interest from the standpoint of both basic theoretical and applied research.

It is not possible to give here a complete review of the entire field of coal

ANNUAL REPORTS ON NMR SPECTROSCOPY
VOLUME 23 ISBN 0-12-505323-1

Copyright © 1991 Academic Press Limited
All rights of reproduction in any form reserved

research by NMR methods without neglecting important details of the experimental methods, the theoretical background, and the extensive range of coal chemistry. Therefore, we review a limited number of articles which are connected with topical studies in this field of research. In addition, we demonstrate the application of NMR techniques to brown coals from westelbian coalfields near Leipzig.

This chapter is divided into the following sections:

(i) a short survey is given of the origin and composition of coals and of the processing technologies of coal conversion;
(ii) a few general remarks are given on the application of NMR techniques to coal research together with some experimental details;
(iii) a section is devoted to NMR experiments carried out on coals with regard to studying the carbon network, the proton system (including the water content), and the heteroatoms; and
(iv) the applicability of NMR techniques in the field of physical and chemical treatment of coals and of the investigation of coal-derived products are described (to appear in a future volume of *Annual Reports on NMR Spectroscopy*).

Besides the well-established methods like solid-state NMR measurements, new applications, e.g. ^{13}C single-pulse NMR investigations of compound systems and ^{1}H NMR self-diffusion studies, are presented.

2. COAL: ORIGIN, COMPOSITION AND PROCESSING

2.1. Origin of fossil fuels and systems of coal classification

Plants are the source of coal and the other fossil fuels such as bitumen, mineral pitch and mineral oil. Life began on earth about 3000 million years ago. The oldest coals arose from algae and other primitive vegetation living at that time, but the quantity of this material was limited. About 400 million years ago, in Devonian times, coal began to form in abundance. Today coal of different origin, composition and coalification rank can be found in all continents.

The importance of the coalification process is briefly discussed here with particular emphasis on the complicated and integrated chemical and physical processes. With regard to a deeper understanding and the geophysical and geological aspects the reader is referred to the literature.[1-5]

The coalification process undergone by the plant material is divided into two phases: the biochemical and geochemical coalification periods. The biochemical coalification period is characterized by the decomposition of the plants, the reduction of cellulose and lignin, and the formation of humic acids. The swamps reformed and deposits of peat were formed. The influence

of the pressure caused by sand or other sediments led to the formation of lignite or soft brown coals. Such processes led to the large middle German brown coal deposits situated west and east of the River Elbe.

The geochemical coalification period is characterized by chemical changes in the low-rank coals (brown coals and lignites), caused by geological processes at the higher temperatures and pressure at depths of a few thousand metres below the earth's surface. The chemical changes that occurred consist in an increased carbon content of the material, a reduction in the hydrogen and the oxygen content, and likewise the content of volatile substances, the disappearance of lignine, molecular changes in bituminous substances, and the transformation of humic acids into insoluble substances. The physical processes involved a reduction in volume and water content.[3] With increasing coalification, the differences between different materials equalized. In extreme forms like anthracite and pure carbon graphite, no reference whatsoever to the source material could be found.

With the industrial revolution in Europe in the 19th century, detailed fuel classification became necessary. A survey of the different classifications has been given.[1] Based on the heterogeneity of coals and their distinct exploitation, many different classification parameters have been used. The first systems classified the coals according to the residue left on heating[6] or according to the oxygen content.[7] The latter system was the first in the history of coal research and application in which the elementary composition of coal was used for classification purposes.

Since coals consist mainly of carbon, hydrogen, oxygen and, in lower concentrations, sulphur and nitrogen (and only traces of many other elements[8]), it was more or less obvious that the classification should be based on an elementary analysis. This classification is also useful for many NMR investigations. Unfortunately, however, the relations between the elementary composition and the technological properties of coal with respect to its use as a fuel and as a basic material for the manufacture of gas, coke and chemicals, are very complicated. Therefore some further classification parameters for the direct characterization of coals, such as the calorific value (heat of combustion), volatile matter content, moisture content and swelling index, were used. International coal-classification systems exist for hard coals and brown coals.[9-17] Furthermore, brown coals can also be classified according to their visual appearance.[18] A possible simplified scheme of coal classification is presented in Fig. 1.

2.2. Physical and chemical methods in coal research

The individual composition of a particular coal results from its specific geochemical evolution. These geochemical processes condition the wide

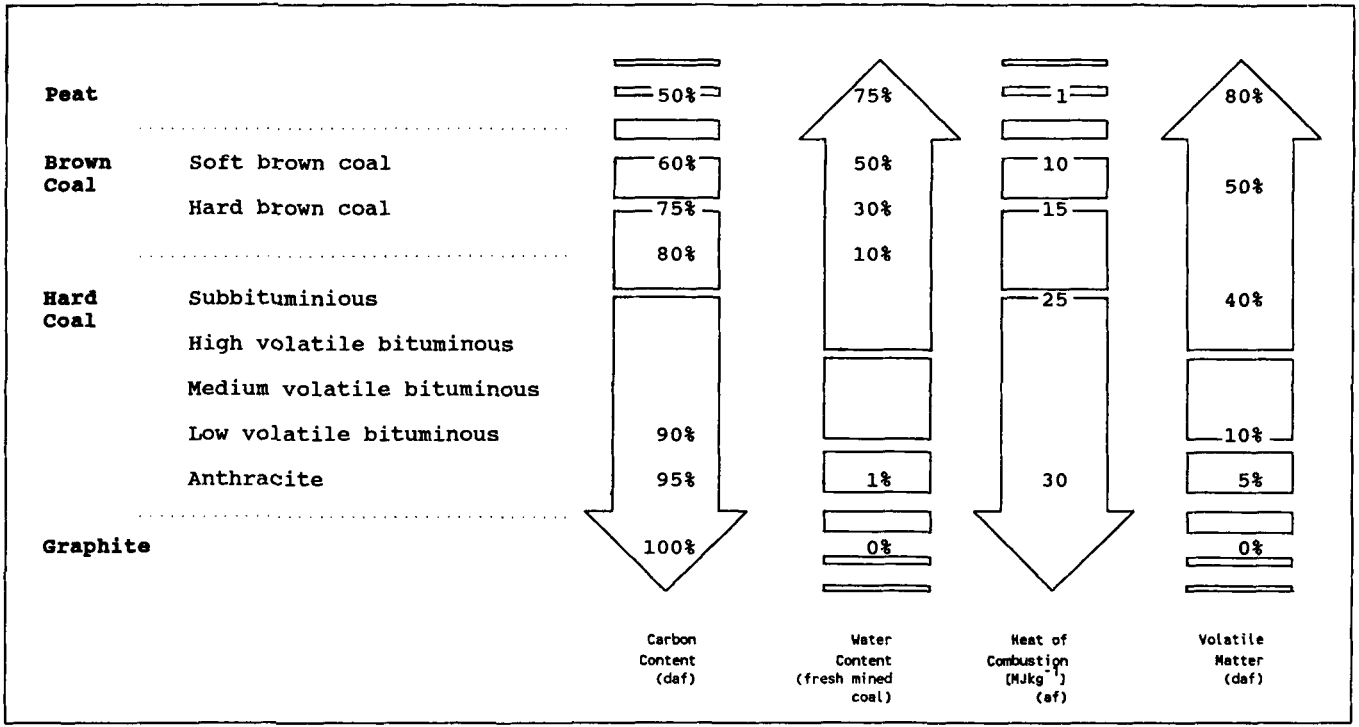

Fig. 1. Incomplete scheme of the classification of materials by increasing degree of coalification (the denotation of hard coals follows the US National Classification, values are rounded and differ for distinct parameters in the literature). daf, Dried ash free; af, ash free.

differences in the organic as well as the mineral matter composition and lead to an essentially insoluble material. Almost the whole spectrum of analytical techniques is applicable to the investigation of the chemical and physical properties of coals.[19-22] A complete representation of all the analytical methods would require too much space and is, therefore, not given here. However, a short survey of some spectroscopic methods, including NMR techniques,[23] is given. Besides NMR, other methods are used to investigate the absorption or transmission of radiation in coal and coal products.

2.2.1. Electron spin resonance

Like atomic nuclei with non-zero spin, unpaired electrons possess a magnetic moment. In this way, the microwave absorption on applying an external magnetic field is observable. The concentration of unpaired electrons can be detected, which is related to, for example, the number of free radicals in coals and coal-derived liquids. It is important to note that free radicals determine the reactivity of the coal surface and the duration of constancy of coal-derived oils.[24-28]

2.2.2. Infra-red spectroscopy

Infra-red (IR) spectroscopic methods have found a wide range of application in coal research.[19] In the frequency range 3500–400 cm^{-1} IR radiation reflects the excitation of bond deformations in hydrocarbons. Because solid coal shows no optical transmissivity, it is necessary to produce thin coal sections, usually KBr discs which contain a few milligrams of coal per gram of KBr. Therefore, the identification of specific bond types and direct information about the chemical structure of the organic matter and the water in coal is possible. New developments concern the use of Fourier transform IR (FTIR) spectroscopy.[29-33] This technique allows rapid signal detection and computerized treatment of the spectra. The detection of diffuse reflected IR radiation[34,35] allows the investigation of powdered-coal samples. Using this technique, the quantitative determination—often a problem in IR spectroscopy—of the total water content of coal is possible.[36] The method investigates the IR band of the combination vibration of water molecules in the near-IR region and utilizes an interior standard in the coal itself.

2.2.3. Ultraviolet–visible spectroscopy

Ultraviolet-visible spectroscopy measures the light absorption which leads to transitions of electrons between orbitals (bonding and nonbonding) from ground states to higher energy levels. Optical fluorescence spectroscopy is

used to observe the inverse effect. These techniques have proved to be of little use on the investigation of coal and coal products.

2.2.4. X-ray diffraction spectroscopy

X-ray diffraction spectroscopy is a powerful technique used to determine the structure of crystalline substances. Amorphous substances, such as coal, produce continuous spectra in which only more or less broad maxima appear. Because of this, clear information about atomic arrangements, the macromolecular constitution or porosity is difficult to obtain.

2.2.5. Mössbauer spectroscopy

Mössbauer spectroscopy allows the investigation of iron compounds in coals and coal products. This is of special importance if iron phases (in brown coals especially iron sulphides) play an important role in catalytic coal processing techniques.[23,37–41]

2.2.6. Mass spectrometry

Mass spectrometry is a very suitable technique for determining the molecular composition of complex mixtures. However, the method requires the volatilization of the sample. Therefore mass spectroscopy is more applicable to coal-derived products than to solid coals. New developments in this field are high-resolution mass spectrometry (HR-MS) and the coupling of gas chromatography and mass spectrometry (GC-MS). For the investigation of solid coals, thermal decomposition (pyrolysis) in vacuum followed by GC-MS or field-ionization MS[42] was developed.

2.3. Model concepts of coal composition

Although it is very difficult to determine the structure of coal, this fundamental knowledge is necessary if insight into its behaviour in conversion processes is to be gained. At present some problems exist in the complete understanding of the molecular "architecture" of coal. The use of a combination of analytical techniques is necessary to characterize the elemental composition, molecular structure, porosity, amount of volatile products, etc. Thus several attempts have been made to develop coal models. These models are predominantly related to hard coals.[43–57] In the literature some reservations exist about the utility of such molecular-structure models. This is not surprising, since in formulating such models many assumptions are necessary. However, ^{13}C

cross-polarization (CP) magic-angle spinning (MAS) NMR spectra in particular provide a lot of detailed information, e.g. about the existence of special structural groups including oxygen containing groups. It is important to note that there are problems associated with the direct determination of the oxygen content of coals and of the oxygen containing structural groups. The general ideas concerning coal structure today result in multicomponent concepts. The components differ in molecular size and mobility. The use of the two-component system, in which "guest" molecules are included in pores of the insoluble "host" structure, is widespread. An impression of this model is given in Fig. 2.

The host structure should consist of a three-dimensional cross-linked macromolecular network. A certain similarity exists between the molecular structure of coals and that of polymers.[58,59]

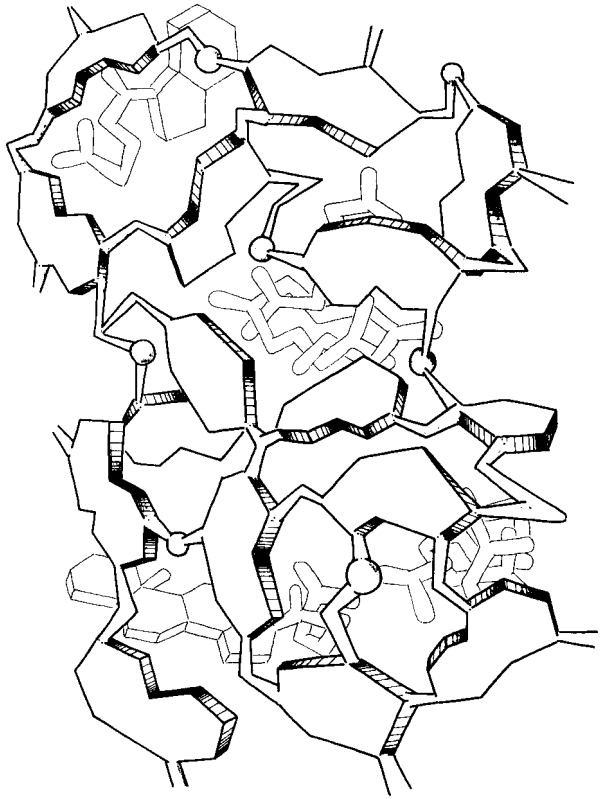

Fig. 2. Presentation of the two-component structure of coal. Aromatic units are connected by aliphatic chains and ether bridges (circles). Smaller molecules, e.g. aliphatic compounds, are embedded in this network.

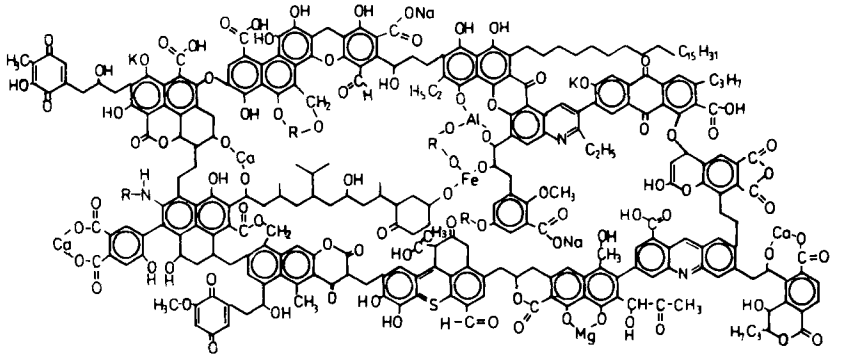

Fig. 3. Proposed structural unit of Rheinische Braunkohle, comprising $C_{270}H_{240}N_3S_1O_{90}$. (Reproduced with permission from Hüttinger and Michenfelder.[61])

It can be assumed that the structure of lignites and brown coals also represents a complicated system with regard to the mobility and interconnection of the molecular and macromolecular parts of coals.[60] A proposed two-dimensional structural unit of a brown coal[61] is shown in Fig. 3. This structural unit has been developed from the results of elemental analysis, pyrolysis experiments and titration studies. The model has been successfully applied to explain the pyrolysis and hydropyrolysis behaviour of Rheinische Braunkohle.

The present state of the discussion about coal structure is summarized in two debates published in *Fuel*: "The concept of a mobile or molecular phase within the macromolecular network of coals"[62] and "Molecular structure of coals".[42] These articles depend essentially on results of NMR measurements.

2.4. Processing technologies in coal chemistry

Coals of different rank are used in the chemical industry as energy sources as well as raw materials. They are characterized by their many possible uses: hard coals, cokes, pulverized brown coal and brown coal briquettes as solid fuels (physical coal processing);[63–65] coal gasification[66] and coal liquefaction in processes to form engine fuels and chemical raw materials (chemical coal processing).[67–75] Precious substances were obtained in extraction procedures. The generation of gas from coal enables the production of many chemicals.[66]

In the field of the production of chemicals from fossil materials, the consumption of mineral oil and gas exceeds the use of coal. However, the geological reserves of coal are much higher than the stocks of oil and gas.

Since the reserves of fossil carbonacious materials are irreplaceable, the development of new and improved processes to produce chemicals and fuels from coal will play an increasing role in the future.

The conversion of coal to liquid fuels[76–78] is brought about either by synthesis or by degradation. In synthesis processes, the coal is broken down by gasification to the gas. In degradation, some of the chemical structures from the initial state of the coal matter are present in the products. The degradation as well as the synthesis processes originated largely in Germany. Petrol derived from coal played an important role during World War II.[79]

New technical developments, especially for the increased use of brown coals, are concerned with gasification by the fluidized-bed technique, liquefaction and pyrolysis at low temperature, liquefaction at reduced pressure, novel low severity processes for coal liquefaction and liquefaction by coprocessing,[80] e.g. the common liquefaction of coal powder, bitumen and residue oil, respectively.

3. NMR IN COAL RESEARCH

3.1. Historical development

Detailed information on the history of the use of NMR methods can be found in the literature.[19,81] A review of so-called "firsts" in NMR investigations of coals and coal derivatives is presented by Retcofsky *et al.*[81]

Obviously, ^{1}H broad-band NMR measurements on coals were the first applications in the field of NMR.[82–84] The introduction of line-narrowing techniques (magic angle spinning and multiple-pulse dipolar decoupling) led to significantly reduced ^{1}H NMR linewidths for coals.[85] The combinations of the two averaging techniques is widely used today and is known as CRAMPS (combined rotation and multiple-pulse spectroscopy).[86] However, in comparison with ^{13}C NMR studies, the investigation of solid-coal samples using ^{1}H NMR is of less significance.

The first broad-band ^{13}C NMR spectra of coals were published in 1971.[87] These studies were supplanted by developments in the enhancement of sensitivity and line resolution; the first publications appeared in 1976 (cross polarization, CP)[88] and 1977 (cross-polarization magic-angle spinning, CP-MAS)[89,90] (cf. Ref. 81).

Modifications of the CP-MAS technique with regard to the suppression of spinning side bands, especially at higher magnetic fields, and with regard to distinguishing between carbon atoms with different numbers of directly bonded hydrogen atoms or different thermal mobilities have been developed in recent years (see Section 3.2).

The history of the NMR study of liquid and soluble coal constituents with

regard to process products closely parallels that of petroleum and other liquids. The first published account appeared in 1959.[91] In 1960 the classic paper by Brown and Ladner[92] was published in which the authors developed a set of formulae (the so-called Brown–Ladner equations) for deducing information about the carbon distribution from ^{1}H NMR measurements. These high-resolution measurements allow deeper insight into the molecular structure of the variety of coal-derived compounds. The high-resolution ^{13}C NMR technique was introduced much later.[93] Today, quantitative ^{13}C NMR measurements[94] yield information about parameters such as functional-group distribution, aromaticity, heterogeneity of the sample composition, degree of condensation of aromatic rings and medium chain lengths.

With the development of modern sensitive high-field NMR spectrometers in recent years, other nuclei in coals and coal products were studied. Examples are ^{23}Na, ^{27}Al, ^{29}Si and ^{33}S NMR of solid-coal samples and ^{17}O NMR studies of coal-derived liquids. Chemical modifications of the coal surface and coal products allow the determination of distinct functionalities, for instance the observation of ^{119}Sb NMR signals in treated coal-derived liquids. Examples of such heteroatom studies are outlined below.

3.2. Experimental: sample preparation and NMR facilities

In solid-state MAS-NMR experiments coals, solid coal products and residues mainly were usually measured in pulverized form. In most cases, defined particle-diameter fractions of dried and grained coal were used.

Sometimes, especially in the investigation of mixtures of coals and solvents, MAS experiments are not possible because of the mobility of some parts of the sample. These systems can be measured without sample spinning or with slow rotation frequencies, as in standard high-resolution NMR experiments on liquid samples. If relatively definite conditions are necessary, e.g. for self-diffusion measurements of solvents in coals or for the study of distinct water contents in the pore systems of coal, the preparation of evacuated sealed-off samples of degassed coals including the desired amount of molecules is useful.

The quantitative determination of the amount of observed coal matter is still a problem. To solve this problem, the use of intensity standards, such as adamantane or poly(dimethylsiloxane) (PDMS), in the coal samples is helpful.

The quantitative determination of average parameters of liquid samples in ^{13}C NMR investigations requires the use of relaxation reagents, e.g. Cracac. The addition of a few milligrams of this substance to the sample lead to

an essentially equal spin–lattice relaxation behaviour of the different molecular groups and to acceptable measuring times.

Our own ^{13}C and ^{1}H high-resolution, diffusion and relaxation measurements were performed using the following spectrometers:

(i) MSL 300, BRUKER Physik Karlsruhe; high-field spectrometer HFS 270, operating at 270 MHz ^{1}H NMR frequency, built at the Physics Department of the University, Leipzig;
(ii) double-resonance spectrometer UDRIS, operating at 90 MHz ^{1}H NMR frequency, also built in Leipzig; and
(iii) The self-diffusion measurements were carried out using the NMR pulse spectrometer FEGRIS built at the Physics Department of the University Leipzig. Operating at a ^{1}H NMR frequency of 60 MHz, this device allows application of pulsed magnetic field gradients up to 20 T m^{-1} with a duration of 5 ms maximum and with rise and fall times of the order of 10 μs.

3.3. Typical methods and problems of NMR in coal research

In this section a brief summary is given of the application of some ^{13}C as well as ^{1}H NMR methods to the investigation of the structural properties and dynamic processes of coal systems. Selected methodological problems are discussed.

3.3.1. Solid-state ^{13}C NMR techniques

In solid-state NMR studies of organic materials, ^{13}C is often the most favourable nucleus to observe since its spectra provide the most direct structural information (relative numbers of carbon atoms in various functional groups), and are experimentally easy to obtain with a good signal-to-noise ratio and good resolution.

Although the application of rapid sample spinning around the so-called magic angle between the external magnetic field and the sample axis is today routine, a large part of the chemical information is lost with MAS because no knowledge about the anisotropy of the chemical-shift tensor is available.[95] The available information about the principal solid-state ^{13}C NMR techniques used for coals is summarized in Table 1.[94]

Solid-state ^{13}C NMR spectroscopy has become an important tool for investigating the structure of coal by combining the cross-polarization (CP) technique with high-power proton decoupling and MAS.[89,90] The pulse programme is shown in Fig. 4(a).

Table 1. Summary of the principal solid-state ^{13}C NMR techniques for coals. (Reproduced with permission from Snape *et al.*[94])

Name	Use	Notes
High-power decoupling	Removal of ^{1}H–^{13}C dipolar interactions of several kHz	Dipolar interactions are much larger than scalar coupling. Therefore more power needed than for decoupling in solution-state ^{13}C NMR
Magic-angle spinning (MAS)	Removal of chemical-shift anisotropy (CSA); > 100 ppm broadening for aromatic peaks	Sample spun at speeds of > 2 kHz at an angle of 54°44′ to the magnetic field
Cross-polarization (CP)	To avoid long relaxation delays required for normal free induction decay (FID) methods	Magnetization transferred from ^{1}H to ^{13}C under Hartmann–Hahn conditions. Four-fold sensitivity improvement, variable CP time often used to determine maximum intensities of aromatic and aliphatic bands
Dynamic nuclear polarization (DNP)	To increase sensitivity	Magnetization transferred from unpaired electrons to ^{13}C spins via ^{1}H spins if required. About 100-fold sensitivity improvement

Spectral-editing techniques TOSS and PASS pulse sequences	Removal of spinning sidebands in high-field spectra	Pulse sequences modulate phase of sidebands, but loss of intensity is unavoidable
Variable CP time	Resolution of protonated carbons	Observed at short contact times
Dipolar dephasing	Separation of tertiary and quaternary aromatic C peaks; and aliphatic C peaks due to mobile (CH_3 and alkyl CH_2) groups from more rigid CH_2 and CH groups	Dipolar decoupling removed for about 50 μs after CP
Sideband analysis	Resolution of bridgehead, nonbridgehead and tertiary aromatic carbons	Relative intensities of sidebands used in high-field spectra

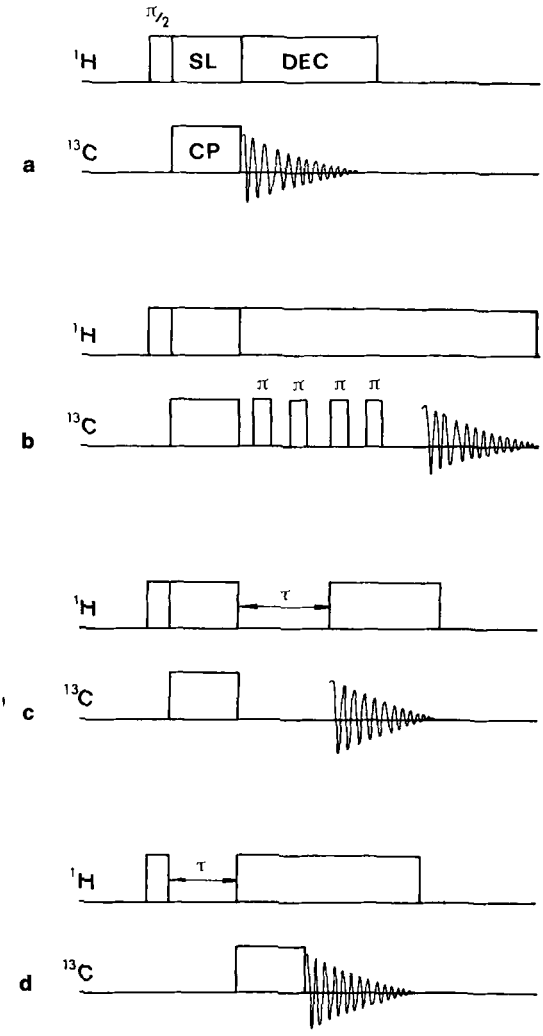

Fig. 4. Pulse programmes used in solid-state NMR experiments (^1H–^{13}C double-resonance spectroscopy). (a) Cross-polarization (CP) (SL, spin locking; DEC, decoupling); (b) CP with total suppression of spinning sidebands (CP TOSS); (c) dipolar dephasing (DD); (d) proton mobility sequence (PMS).

Figure 4(b) shows the same programme with additional (4 or 6) rotation-synchronized 180° pulses for the suppression of spinning sidebands, especially at higher magnetic fields (> 2.3 T). For lower field strengths in MAS experiments, no spinning sidebands were observed. These spinning sidebands

arise if the MAS frequency is lower than the highest chemical-shift anisotropies in the spectra. Various techniques for the suppression of spinning sidebands (e.g. total suppression of spinning sidebands (TOSS) and phase-altered spinning sidebands (PASS)) have been established.[96–100]

However, spinning sideband suppression results in a change in the intensity of the peaks, depending on their anisotropies and the rotational frequency. Hence it is not possible to derive in a straightforward way from the line intensities in such spectra the true concentration of structural groups and, consequently, the coal characterization parameters such as aromaticity (f_a). If the tensor parameters are known[95,101] the dependence of the isotropic peak intensity on the rotational frequency can be evaluated.[102] The method of calculating spinning sidebands.[103,104] has been extended to the calculation of intensities in MAS spectra where the spinning sidebands are suppressed by a sequence of four ideal 180° pulses.[96] It has been shown that the exact computation of intensities in MAS-TOSS-NMR spectra is possible and can be simplified by an approximation where only terms with a single spinning frequency are considered. This allows a simple estimation of the anisotropy parameter to be obtained from the dependence of the intensities on the spinning rate. Conversely, it is possible to recover the true intensities in such spectra from the anisotropy. The method has been verified by experimental determining the dependence of the TOSS intensities of the ^{13}C NMR lines of glycine and poly(styrene) on the spinning frequency.[101]

A typical ^{13}C CP-MAS-TOSS-NMR spectrum of a brown coal lithotype Schleenhain (brown) is shown in Fig. 5(a). If the resolution of the spectra is relatively poor, a computer-aided line deconvolution leads to intensities of well-known ^{13}C NMR line positions for the structural groups of coals. The ^{13}C CP-MAS-TOSS-NMR spectrum of a brown coal from the Schlabendorf (eastelbian) deposit without (experimental) and with the exact computation of intensities (TOSS correction)[105] is shown in Fig. 6(a). The dependence of the experimentally determined aromaticity, f_a,

$$f_a = \frac{C_{ar}}{C_{total}} \tag{1}$$

on the MAS frequency, f_{rot}, is shown in Fig. 6(b).[105] Figures 4(c) and 4(d) show two modifications of the conventional CP technique with respect to the observation of special parts of the ^{13}C NMR signal. Signal differentiation via dipolar dephasing[106,107] (DD, Fig. 4(c)) can also be done in combination with the TOSS technique (DD-TOSS[108]).

Depending on the duration of the decoupling gap (dipolar dephasing period τ or t_{DD}) the observable signal intensities of different carbon types become smaller with different rates for CH_3, CH_2/CH and for quaternary carbon

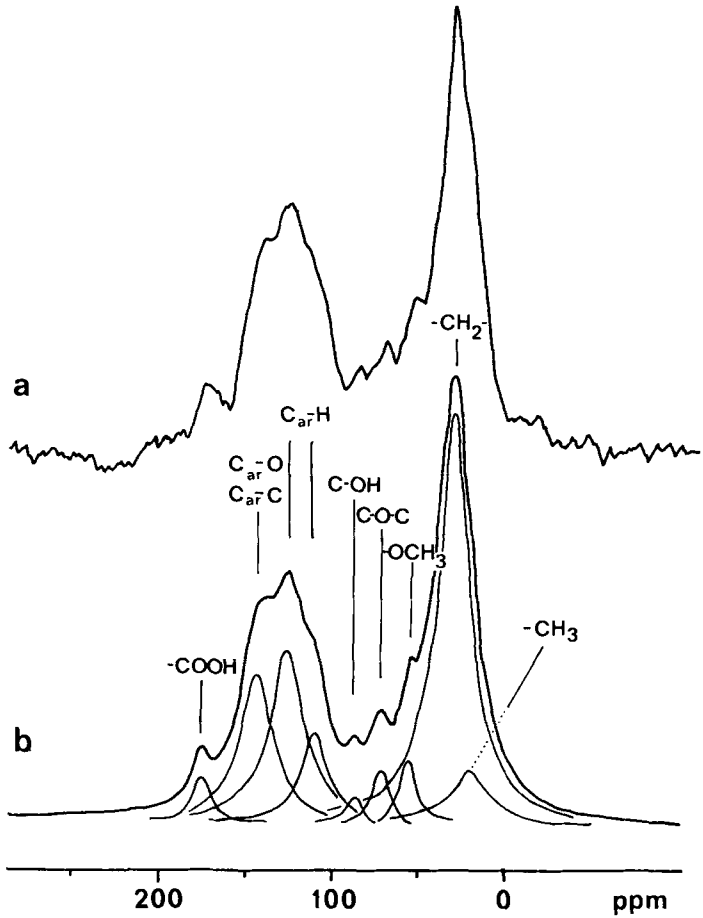

Fig. 5. ^{13}C CP-MAS-TOSS-NMR spectra of the lithotype Schleenhain (brown, westelbian), resonance frequency 75.48 MHz. (a) Experimental spectrum; (b) line decomposition with respect to typical ^{13}C NMR line positions of coal structural groups.

(C_{quart}) groups (the method does not allow discrimination between CH_2 and CH groups). The signal intensities for the individual dipolar dephasing times can be fitted to determine the amount of the different carbon types. However, this method is time consuming and severe overlapping of the signals impairs the accuracy of determination of the intensities. Therefore, a method was developed[109–111] in which only two spectra for two dipolar dephasing times (e.g. 0 and 60 μs) were recorded. The first spectrum contains the ordinary

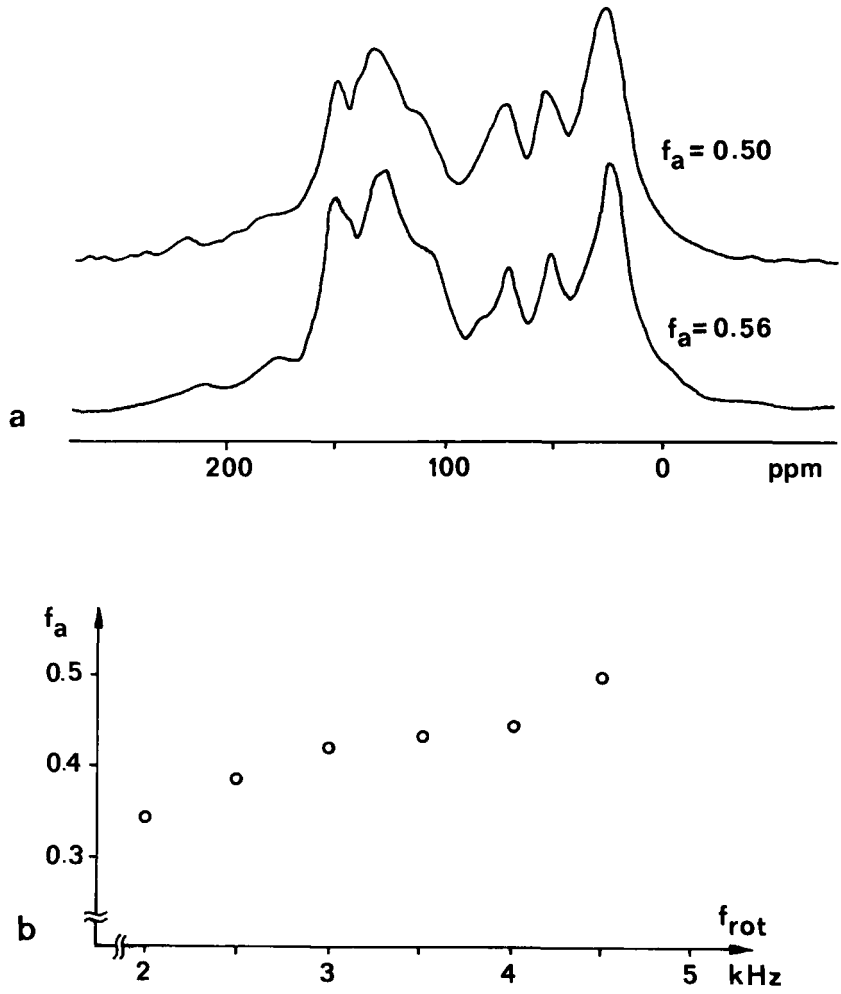

Fig. 6. ^{13}C CP-MAS-TOSS-NMR investigations of the brown coal Schlabendorf (eastelbian). Resonance frequency 75.48 MHz, CP mixing time 3 ms. (a) Experimental spectrum,. aromaticity $f_a = 0.50$ and TOSS-corrected spectrum, aromaticity $f_a = 0.56$, MAS frequency 4.5 kHz. (b) Dependence of aromaticity, f_a, on the MAS frequency.

spectrum with all signals, while the second one contains only signals of C_{quart} atoms and of CH_3 groups. The magnetization of strongly dipolar coupled CH_2 and CH carbon atoms decays in the decoupling gap and the signals were eliminated completely. By calculating the difference spectrum, the CH_2/CH subspectrum is generated.

The second modification is the proton mobility sequence (PMS, Fig. 4(d)).[112,113] The transverse relaxation time T_2 depends on the mobility of the spin-bearing nuclei described quantitatively by the correlation time τ_C.[114] The first experiments performed on coals using PMS were ^{1}H NMR studies separating the free induction decay into usually two components.[115–117] The component with the shorter decay constant can be described by a Gaussian function and has been connected with the rigid component of the coal. The other component follows a slowly decaying exponential function and has been related to the mobile component. Experiments have been performed in which deuterated solvents were added to the sample, leading to swelling of the coal; a significant enhancement of the mobilization of hydrogen-bearing species was found.[115,117] The PMS method was developed in order to distinguish between rigid and mobile hydrogen atoms bonded to either aromatic or aliphatic carbon atoms. This separation is performed indirectly via an analysis of the ^{13}C NMR spectrum using a modification of the conventional CP experiment.[118] After the 90° pulse in the ^{1}H channel a variable delay time, τ, is inserted (Fig. 4(d)). During τ, the above-mentioned fast Gaussian and slower exponential decays take place for the proton magnetization of the rigid and mobile components, respectively. The remaining proton magnetization is then transferred via CP to the carbon system—for short contact times primarily to the directly bonded carbon atoms. The analysis of the signal intensities in the aromatic and aliphatic regions of the ^{13}C NMR spectrum as a function of the delay time, τ, should yield values for the relative concentrations of the rigid and mobile species.

At this point the following question should be asked: Is the amount of magnetization independent of molecular mobility? This question must be answered if a quantitative determination of the rigid and mobile components is to be made. However, the answer is by no means obvious, since the CP technique was introduced to enhance the signal intensity in rigid solids.

It has been shown, by both a general theoretical treatment and experiments on a system containing species of definite mobility, that the efficiency of CP decreases dramatically with increasing molecular motion.[119] The theoretical treatment is based on a general "short" correlation time theory for a system of dipolar coupled ^{1}H and ^{13}C spins under the influence of a constant magnetic field, B_0, and the corresponding two resonant radiofrequency field.[120] Below a critical value of τ (τ_c) which is of the order of some 10 μs, the NMR signal intensity is strongly reduced. This result has been confirmed quantitatively by measurements performed on a molecular system where the correlation time of the thermal motion could be determined unambiguously and varied over a large interval. Acetone molecules adsorbed in the well-defined cavity system of a zeolite NaX at different temperatures represent the model system studied.[119] The methods of NMR also find wide application in the field of the

investigation of adsorbed molecules.[121] From the ^1H NMR relaxation measurements an absolute value of $\tau_c = 3.2\,\mu s$ at $T = 240 \pm 5\,K$ (minimum of $T_{2,eff}$) and an apparent activation energy of $14 \pm 1\,kJ\,mol^{-1}$ was derived for the correlation time of the adsorbed acetone molecules. Therefore, within the temperature range from 150 K up to room temperature, τ_c covers the range from 2×10^{-4} to 1×10^{-6} s.

In the careful phase- and baseline-corrected ^{13}C NMR spectra at the lowest temperatures (150 and 168 K) the anisotropy of both the carbonyl and the methyl ^{13}C NMR shifts could be observed. In order to find the maximum value for the intensity of the ^{13}C CP-NMR signals at each temperature, the contact time was varied between 30 μs and 8 ms. The maxima appeared at contact times of 1 and 2 ms for the methyl and carbonyl carbons, respectively. In comparison with ^{13}C single-pulse NMR spectra (direct excitation of the ^{13}C spin system, see below) one can see a dramatic decrease in the efficiency of the CP method even to values of less than 1, which means that the single-pulse signal intensity is larger than that of a CP experiment. Hence, from both theoretical and experimental studies it follows that any NMR method which is based on magnetization transfer by CP is not suitable for determining quantitatively the concentration of components of very different mobility in a sample.[119] The results of the PMS method must be used with care since it underestimates or even neglects the amount of mobile components in coal. Possibly some of the unexpected and surprising results of studies possibly originate in these methodical questions, e.g. that most of the protons in the detected "mobile components" should be bonded to aromatic structures. However, extracts from coals of various ranks contain predominantly aliphatic hydrogen.[122,123]

Besides these methodical problems further aspects influence the accurate quantitative ^{13}C NMR measurement of coals, e.g. the correct determination of carbon aromaticity, f_a. The problems of carbon counting are discussed in the literature.[94,95,124–129] Significant errors can arise in ^{13}C CP-MAS-NMR measurements of coal parameters like aromaticity due to the unfortunate spin dynamics of coals. The amount of magnetization transfer from abundant ^1H to dilute ^{13}C spins during the CP period varies considerably for different carbon atom types. Two opposite physical processes determine the transfer of magnetization. The decay of polarization in the proton spin system occurs at a rate determined by a time constant $T_{1\rho}$ (H). The process of magnetization transfer to the ^{13}C spins is related to the strengths of the C–H dipole–dipole interactions of the different carbon atoms and follows a rate governed by a time constant T_{CH}. If $T_{1\rho}$ (H) is smaller than the time necessary for the most weakly coupled carbons to cross polarize, the bands of these carbon atoms will be reduced in intensity. The extreme case for such carbon atoms is that the bands become lost in the noise.

Quantitative ^{13}C NMR measurements require the understanding of a number of essential relaxation mechanisms that occur in the sample. The situation can be extremely complex in CP measurements of coals where several, sometimes competing, relaxation mechanisms occur. The relaxation times of these processes are T_{CH}, $T_1(H)$, $T_{1\rho}(H)$ and $T_{1\rho}(C)$.[94] Besides the spin dynamics, other complicating factors impair quantitative measurements for the routine determination of coal parameters, such as MAS effects on the resonance line intensities,[130,131] sample heterogeneity (existence of maceral domains in coal matter) and, to some extent, paramagnetic species in high concentration.[132–135] There is a consensus in the literature[94] that significant errors can arise in NMR measurements of aromaticity and structural-group intensity. The values of unseen carbon cited in the literature differ, by as much as about 50% for bituminous coals. Because of the heterogeneous distribution of paramagnetic and ferromagnetic species in fossil fuels, the observed carbons are not always representative of the actual functional group distribution.

Further information, full experimental details and explanations of pulse programmes and investigational methods of the solid-state NMR of coals and related model compounds can be found elsewhere.[118,136–142]

In concluding this section, we give some remarks[94] on the solid-state CP MAS measurements of coals at higher magnetic field (> 2.3 T). It has been proven that, in many cases, no substantial improvement in resolution is obtained by using higher magnetic fields since the main line-broadening effects in a typical ^{13}C CP-MAS-NMR experiment on coal are heterogeneous. The sensitivity enhancement at higher magnetic fields is largely negated by the smaller sample volumes used for high-speed rotors. As pointed out above, at higher magnetic fields the interference of MAS with the CP process is a serious problem.[142–144] Besides sideband suppression (see above), other techniques have been described in the literature, such as the use of MAS during the detection period, whereas the CP period is carried out while the sample is static (magic-angle hopping)[145,146] or by spinning the sample at an angle at which the spinning modulation of the dipole interactions is attenuated or eliminated.[143]

3.3.2. Solid-state ^1H NMR measurements

The study of coal structure using solid-state ^1H NMR methods has typically been limited by the occurrence ^1H–^1H homonuclear dipole–dipole interactions. The line broadening caused in this way dominates the chemical-shift effects. Therefore, broad-band ^1H NMR spectra contain a relatively low amount of information. The ^1H NMR investigations of coals have focussed on spin–lattice (T_1) and spin–spin (T_2) measurements (see below). To overcome this situation, the combination of pulse sequences for averaging ^1H–^1H

homonuclear dipole–dipole interaction, e.g. MREV-8[147,148] and BR 24[149] and MAS have been used.

This CRAMPS technique led to a poor resolution of the aromatic and aliphatic ranges of the proton chemical shifts in the ^{1}H NMR spectra of some bituminous coals,[150] unless higher magnetic fields were applied.[151] To obtain further detailed information with respect to the determination of the aromatic and aliphatic contributions of the mobile and immobile components in coal, the CRAMPS technique is coupled with ^{1}H dipolar dephasing experiments.[152,153]

3.3.3. Liquid-state NMR methods in coal system investigation

The methods described in this section are characterized by low-power decoupling field strengths which allow the removal of weak spin–spin interactions. For some applications (broad bands) to solid samples and to coal solvent multicomponent systems no decoupling was used.

Figure 7 presents pulse programmes, the direct excitation of the spin system by a single pulse (SP; Bloch decay measurements, Fig. 7(a)), low-power ^{1}H–^{13}C broad-band decoupling during the whole experiment (the ^{13}C NMR signals are ^{1}H decoupled and enhanced in intensity by the nuclear Overhauser effect (NOE), Fig. 7(b)), the inverse gated decoupling technique (decoupling of the signals only, Fig. 7(c)), and the gated decoupling technique (coupled spectrum with NOE, Fig. 7(d)).

With regard to the application to coal-derived liquids, we refer to the well-known methods of high-resolution ^{1}H and ^{13}C NMR spectroscopy described in the literature.[153–163] The NMR spectra of coal-derived liquids and mineral oils are characterized by a large number of individual lines corresponding to their heterogeneous composition. The analysis and structure determination of individual components of coals and coal-derived liquid mixtures remains in the background: the isolation of individual components of these liquids has proved complicated and the concentration of individual components is often too low with respect to the sensitivity of NMR.

The aims of NMR investigations are to determine:

(i) the average molecular parameters;
(ii) the average molecule construction; and
(iii) the functional groups present.[154]

Quantitative aspects of ^{13}C and ^{1}H NMR of crude-oil, petroleum and coal liquefaction products have been described,[164] and procedures for determining the optimum instrumental parameters to be used in quantitative Fourier-transform NMR (e.g. acquisition time, flip angle, pulse delay, solvent and relaxation reagent) are outlined. It has been shown that digital correction of

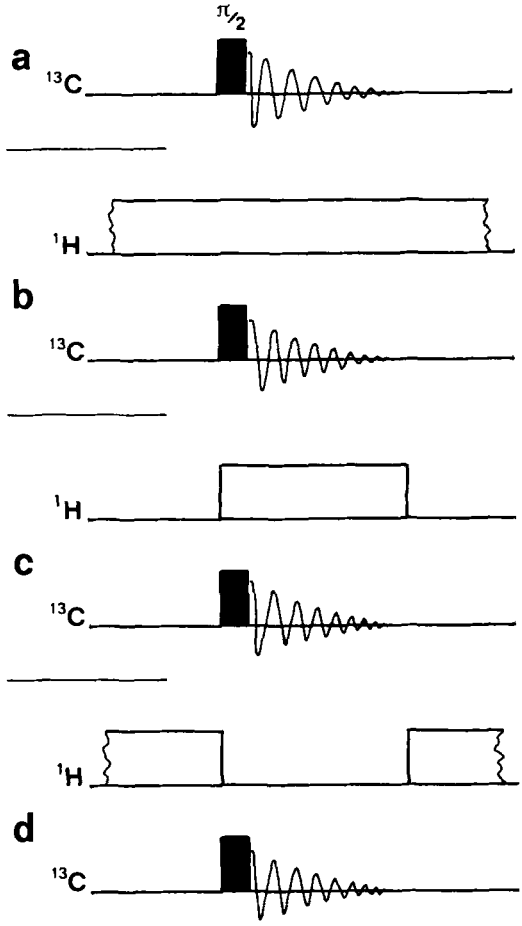

Fig. 7. Pulse programmes used in NMR experiments of liquids (^{13}C NMR; ^{1}H–^{13}C double-resonance spectroscopy). (a) Single pulse direct excitation (SP). (b) Broad-band (low power) decoupling (BB). (c) Inverse gated decoupling (IGATED); the ^{13}C NMR signals are only ^{1}H broad-band decoupled. (d) Gated decoupling (GATED); the ^{13}C NMR signals are enhanced by the nuclear Overhauser effect (NOE).

the signal improves the accuracy of quantitative measurements by up to ca. 1%.[164] ^{13}C NMR multipulse sequences for the analysis of coal and petroleum products are applied with respect to the discrimination between the four possible types of CH_x groups ($x = 0, 1, 2$ or 3).[165]

Examples of suitable pulse sequences for detecting subspectra are the polarization-transfer methods INEPT (insensitive nuclei enhanced by

polarization transfer)[166] and DEPT[167] (distortionless enhancement by polarization transfer). Other methods are based on the observation of spin echos, PCSE[168,169] (partially coupled spin echo) and Doddrell's[170] pulse sequence.[165]

In the following some explanations relative to low-power single-pulse excitation with parameters typical of liquid-state spectroscopy are presented. The advantages of this technique compared with high-power solid-state and MAS measurements are the distinctly lower cost of the experiment and the possibility of measuring solid and powdered coal samples as well as coal–solvent multicomponent systems. By choosing appropriate values for the dwell time and the beginning of the signal-acquisition, spectra without phase and baseline distortions can be obtained.[171,172] The ^{13}C NMR lines in these spectra originate mainly from carbons with weak dipole–dipole interaction (carbons which are not directly bound to protons, methyl groups or mobile species).

In contrast, it can be shown that $\equiv CH$ and $-CH_2-$ groups are considerably understated in the observed intensity. Further complications in definite structural-group determination can arise from the superposition of line-broadening effects caused by dipole–dipole interaction and anisotropy of chemical shielding;[173] for example, the relatively narrow line of a methyl group compared with the broad signal of a methylene group, $-O-CH_3$ (e.g. solid dimethylsulfon).

Using the direct excitation of the ^{13}C spins the considerable spin–lattice relaxation times of different carbon atoms (e.g. aromatic groups) determine the intensity distribution within the spectrum. This situation is depicted in Fig. 8. In order to calibrate broad-line spectra and to make an intensity determination, a standard is applied. A piece of poly(dimethylsiloxane) (PDMS, silicone rubber) within the coal powder or coal solvent system leads to a relatively sharp ^{13}C NMR line at 0 ppm.[174] This substance possesses a short T_1 of ^{13}C nuclei and a stable molecular structure with respect to possible chemical reactions. Quantitative measurements can be carried out using this internal standard and data obtained from an elemental analysis. It seems reasonable to assume that up to 80% of the carbon atoms in the coal were observed for repetition times of greater than 30 s, but the corresponding measuring times are considerably longer. The measuring time can be reduced if small amounts of relaxation reagents are added in a suitable way to the coals.[175] The result of so doing is given in Fig. 9 which shows equal spectra for pure brown coal and the same coal with 2 mass% of $CuSO_4$.

If the $CuSO_4$ content is too high, the "visibility" of carbon atoms decreases in the spectra. For example, a content of 6 mass% of $CuSO_4$ leads to only ca. 60% of the carbon atoms being observed. In this it is important to note that an equal decrease is observed in all the ^{13}C NMR lines.

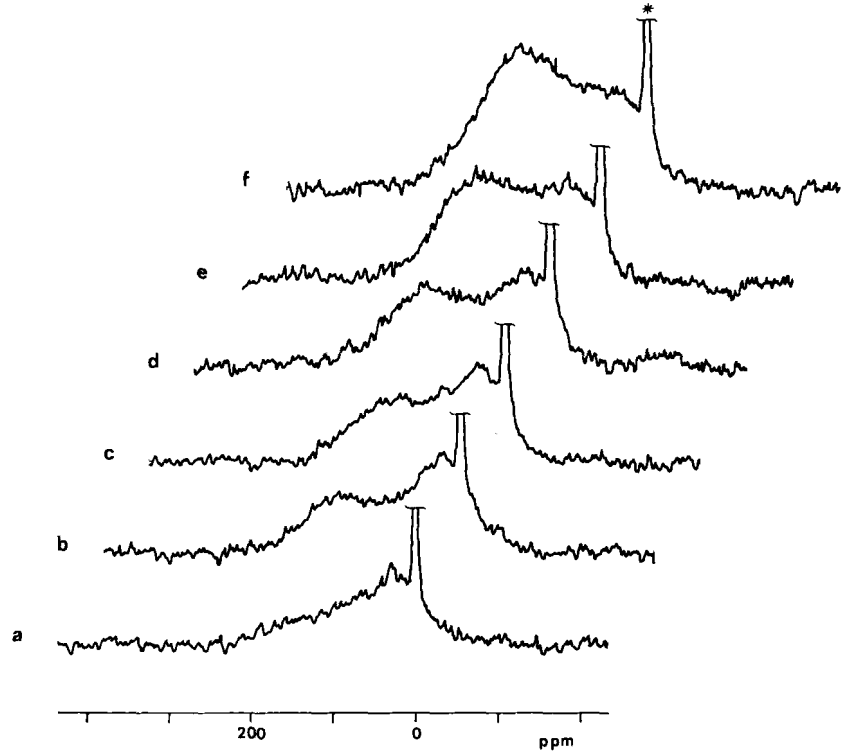

Fig. 8. ^{13}C SP-NMR spectra of brown coal Schleenhain I as a function of repetition time (recycle delay). Resonance frequency 75.48 MHz; * denotes the intensity standard poly(dimethylsiloxane) (PDMS). Repetition times (in seconds): (a) 2; (b) 5; (c) 10; (d) 20; (e) 30; (f) 100.

For some routine ^{13}C SP-NMR measurements uniform conditions, including relatively short repetition times, i.e. the aromatic region of the spectrum is underestimated, were used. Figure 10 shows the results of the investigation of brown coal lithotypes. It can be seen from these spectra that the value of the aromaticity obtained with ^{13}C SP-NMR differs significantly. The fossil resin retinite is, as might be expected, the substance containing the highest amount of aliphatic structures.

A necessary condition for the appearance of a nuclear Overhauser enhancement (NOE) is high molecular mobility. It seems likely, therefore, that experiments corresponding to the pulse programmes shown in Fig. 7 are suitable for the determination of mobile portions in coal systems. From the difference between the GATED spectrum and the SP spectrum without decoupling one can conclude that at least ca. 5% of the aromatic carbons and

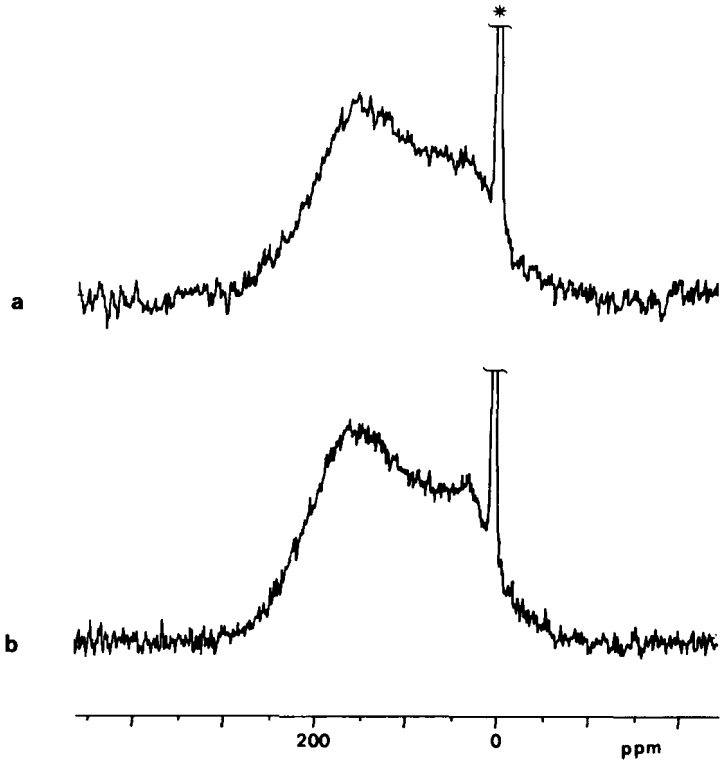

Fig. 9. ^{13}C SP-NMR spectra of brown coal Schleenhain I (westelbian). Resonance frequency 75.48 MHz; * denotes the intensity standard poly(dimethylsiloxane) (PDMS). (a) Repetition time 100 s, 500 scans (corresponding a measuring time of 14 h). (b) Two mass% of $CuSO_4$ was added to the sample used in (a); repetition time 5 s, 500 scans (corresponding a measuring time of 0.7 h).

30% of the aliphatic carbons are Overhauser sensitive.[171] The value for the aliphatic carbons cannot be totally explained in terms of rotating methyl groups and points to structures of different mobilities being present in the coal (cf. Fig. 11).

3.3.4. Proton spin relaxation

^1H NMR pulse techniques especially for the observation of transverse relaxation (spin–spin, T_2), have been described in the literature.[176–178] In these papers a complete analysis of the time-domain signal of the transverse magnetization was not undertaken, so that only the total hydrogen content of the sample was determined. An analysis of the free induction decay (FID)

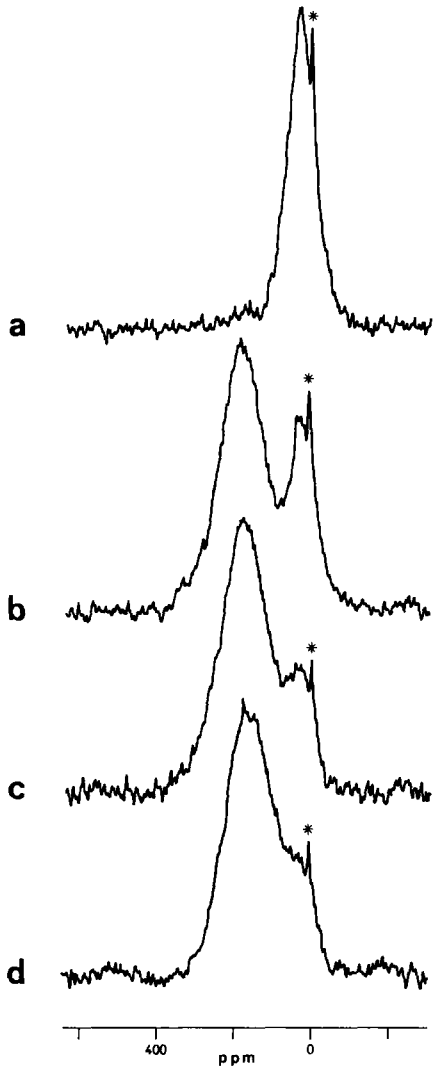

Fig. 10. ^{13}C SP-NMR spectra of lithotypes of brown coal Merseburg-East (westelbian). Resonance frequency 75.48 MHz, repetition time 5 s, 1000 scans; * denotes the intensity standard poly(dimethylsiloxane) (PDMS). (a) Retinite (fossile resin); (b) yellow coal; (c) brown coal; (d) black coal lithotype.

signal of wet coal samples in combination with a gravimetric analysis of the water loss on drying the sample allows the water content to be determined.[179] Besides the quantity of water, the percentage of hydrogen in the macromolecular network of the coals may also be determined. Previous studies of the

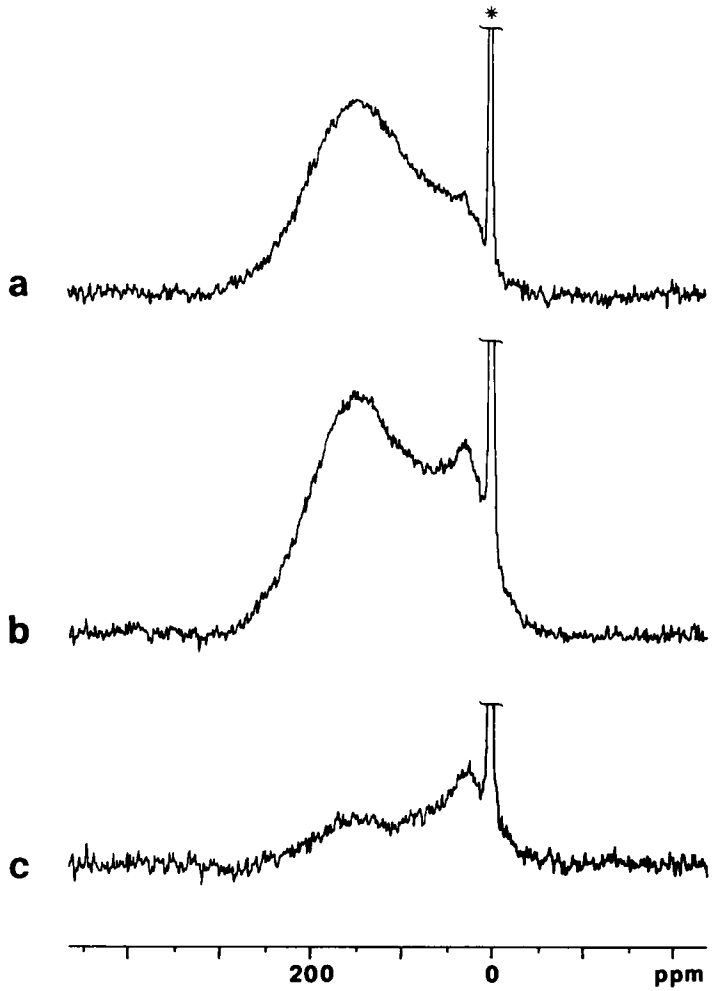

Fig. 11. ^{13}C NMR spectra of brown coal lithotype Schleenhain brown (westelbian) for the determination of the NOE. Resonance frequency 75.48 MHz; repetition time 30 s; * denotes the intensity standard poly(dimethylsiloxane) (PDMS). (a) Single pulse (SP), without decoupling; (b) GATED decoupling; (c) difference between (b) and (a), showing the NOE signal enhancement in the aliphatic and aromatic regions of the spectrum.

decomposition of FIDs of protons have revealed the existence of mobile and immobile components.[42,117,180,181] The FID signal has been detected using a 90° pulse of the solid echo. The observation of two or more damping constants may reflect the composition as well as the mobility of the components of all the protons in the sample. The proton free induction decay of an untreated wet

coal can be approximated with sufficient accuracy by the sum of a slowly decaying Lorentzian (exponential) component and a rapidly decaying Gaussian component:

$$F(t) = A_1 \exp(-t/T_{21}) + A_s \exp(-t^2/T_{2s}^2) \quad (2)$$

In many cases a decomposition into two Gaussian and one exponential function is also possible:[182]

$$F(t) = A_1 \exp(-t/T_{21}) + A_m \exp(-t^2/T_{2m}^2) + A_s \exp(-t^2/T_{2s}^2) \quad (3)$$

The rapidly decaying Gaussian function (indicated by the subscript s) obviously belongs to protons in the macromolecular skeleton of the coals. The second Gaussian decay (indicated by subscript m) is characterized by a small relative fraction ($\leqslant 10\%$) and represents less-mobile water molecules, whereas the exponential decay is due to protons of relatively mobile water in the brown coals.[182] It is possible that the protons in mobile parts of the macromolecular structure of coals also contribute to the fraction "m"; this has been observed in particular in some high-rank coals.[62,183] In a solvent-saturated coal, a third component of Lorentzian type has been observed.[117,181] Because of the diversity of the chemical structure of coals and the large variety of motions, the physical as well as the chemical interpretation of coal systems in terms of the ^{1}H NMR FID is not evident.[42]

Previous studies of ^{1}H longitudinal (spin–lattice, T_1) relaxation as a function of temperature have revealed the existence of at least two components with different mobility in coals.[184] In a recent study on a set of 13 coals of various ranks, T_1 relaxation measurements were carried out.[42,185] The relaxation curves of 11 coals were analysed in terms of a weighted sum of two exponentials. It was observed that fast-relaxing protons are more abundant in low-rank coals than in high-rank coals. This component represents the molecular part of the coal structure and the largest fractions of the protons in the molecular component of coal are found in two lignites, for which this part amounts to 50%.[42,185]

An interesting application of ^{1}H relaxation measurements is their use in *in situ* thermal-analysis studies. Thermal transformations in coals and related organic materials using specially designed high-temperature NMR probes were obtained. Transverse as well as spin–lattice relaxation measurements allowed insight to be gained into the thermal behaviour of different mobile coal components in pyrolysis experiments.[186–189]

3.3.5. Measurement of diffusion processes

A fashionable way of observing the molecular mobility of water in coals, in mixtures of coal with organic solvents, and of coal constituents is to use the

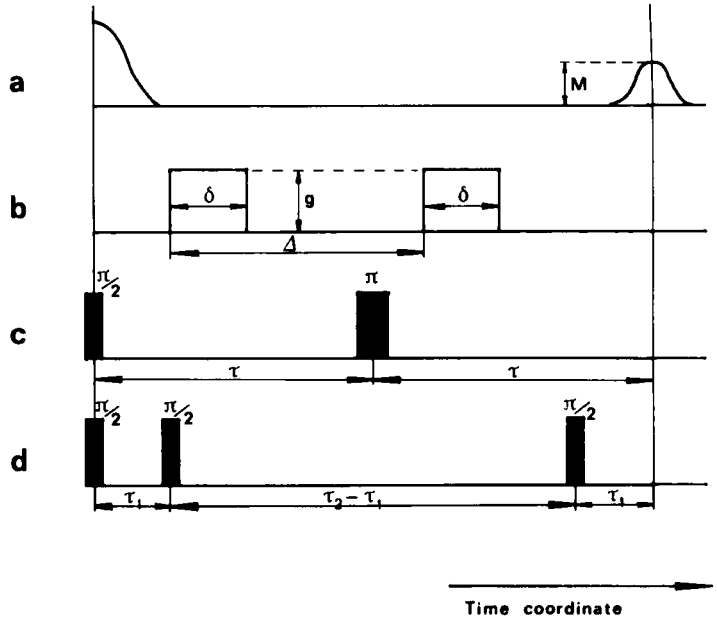

Fig. 12. Pulse scheme for estimating self-diffusion coefficients by NMR methods. Observed NMR signal (a) and applied pulsed field gradients (b) for NMR self-diffusion measurements with the primary spin-echo sequence (c) or with the stimulated spin-echo pulse sequence (d).

NMR pulsed field gradient technique.[190–192] In this method, molecular migration is studied by following the precessional phases of the considered nuclear spins (usually ^1H) during their translational motion within a space-dependent magnetic field. Some details about the theoretical background of this method are given in the following. Figure 12 illustrates the pulse sequence of the NMR pulsed field gradient technique. The NMR spin-echo brought about by a sequence of two radiofrequency pulses ($\pi/2$ and π, in the case of the primary spin echo) or of three radiofrequency pulses ($\pi/2$, $\pi/2$ and $\pi/2$, in the case of the stimulated spin-echo) as a function of an additionally applied inhomogeneous magnetic field, the "pulsed field gradients", can be seen. The signal attenuation may be represented by the relation

$$\psi(\Delta, \delta, g) = \exp\{-\gamma^2 \delta^2 g^2 D(\Delta - \delta/3)\} \tag{4}$$

where γ denotes the gyromagnetic ratio of the nuclei considered, D is the self-diffusion coefficient of the molecular species under study, and δ, Δ, and g are the width, separation, and intensity of the field gradient pulses, respectively (cf.

Fig. 12). The self-diffusion coefficient is related to the molecular mean-square displacement $\langle r(\Delta)^2 \rangle$ during the time between the two gradient pulses (observation time, Δ) by the Einstein equation

$$\langle r^2(\Delta)^2 \rangle = 6D\Delta \tag{5}$$

In the case of the primary spin-echo, its intensity without field gradients is determined by the transverse nuclear magnetic relaxation time, T_2. For the rigid constituents T_2 is so short ($\leqslant 100\,\mu s$) that the observed signal is due only to the mobile phase of the sample. In the stimulated spin-echo sequence, the signal attenuation is due to the longitudinal nuclear magnetic relaxation time T_1, rather than to T_2. Since, in general, $T_1 > T_2$, it is often advantageous to apply the stimulated rather than the primary spin-echo radiofrequency pulse sequence.[192]

3.3.6. Two-dimensional NMR

In NMR spectroscopy, two-dimensional methods offer new insight into the structure of molecular systems. Especially in solution-state NMR spectroscopy, many methods exist which provide more specific information.[160,162] Most standard two-dimensional NMR methods are not directly applicable to organic solids for a number of reasons, the main one being the strong dipolar coupling among the abundant protons. Applications of two-dimensional NMR methods to coals[193] and solid polymers,[194] which with great care can be used as model systems with respect to some properties of coals, can be found in the literature.

In principle, the time-scheme of two-dimensional solid-state NMR spectroscopy is identical to that of high-resolution two-dimensional NMR spectroscopy of liquids (see Fig. 13). During the preparation method, the spin system of the sample is brought into a well-defined state. In the evolution period (t_1 denotes the length of time), the spin system develops under the influence of nuclear spin interactions. In a fixed mixing period the nuclear magnetization is mixed between different resonances. The FID is recorded

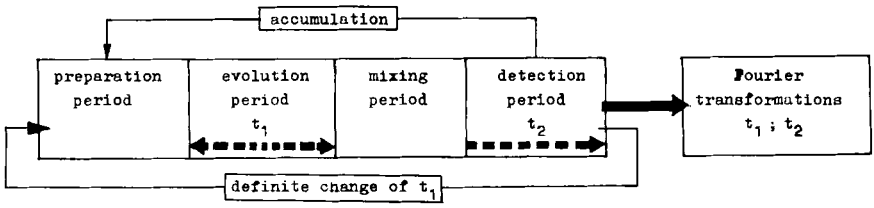

Fig. 13. Time-scheme of two-dimensional NMR experiments.

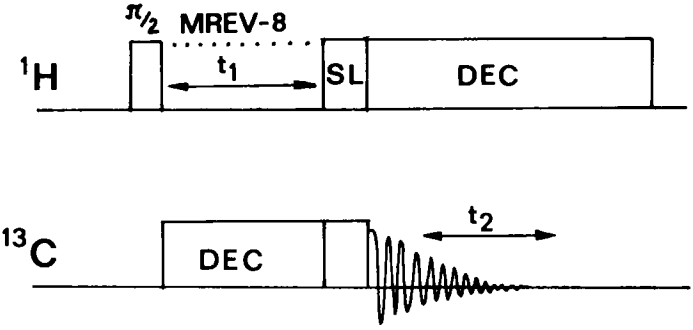

Fig. 14. Pulse programme used in ^{1}H–^{13}C solid-state heteronuclear shift-correlation method.

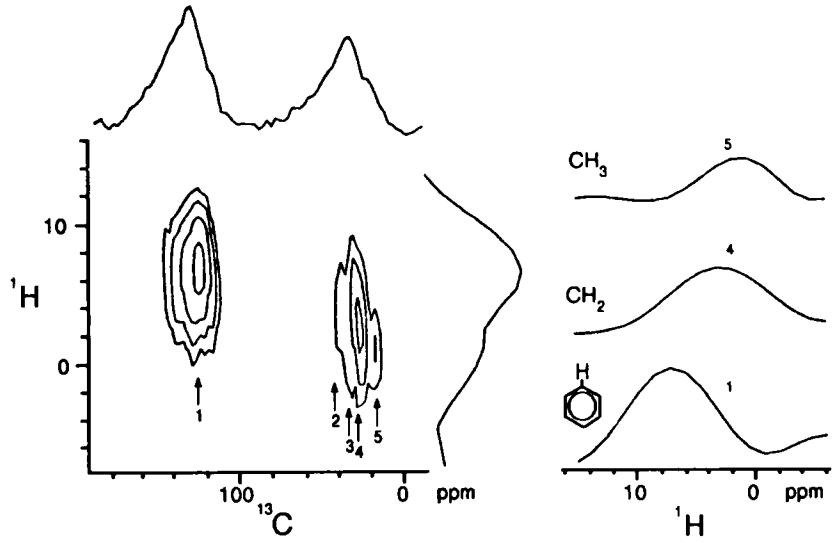

Fig. 15. Contour plot of the ^{13}C–^{1}H chemical-shift correlation spectrum for an Illinois No. 6 coal. The trace at the top is the ^{13}C CP-MAS spectrum of the carbons detected in this experiment. The total proton spectrum detected indirectly with this method is given along the right-hand side. The proton spectra on the far right corresponds to particular ^{13}C chemical shifts as indicated by the numbers 1–5. (Reproduced with permission from Zilm and Webb.[193])

during the subsequent detection period (t_2). After this experiment, a different evolution time t_1 is applied. The two-dimensional NMR spectrum is produced by two successive Fourier transformations after t_2 and t_1. With respect to the possible nuclear spin interactions which determine the resonance frequencies

on both axes of the two-dimensional NMR spectrum, there are many two-dimensional NMR methods for static as well as rotating samples. These methods can be used to investigate molecular structure and order. Furthermore, the study of dynamic processes in solids (e.g. chemical exchange) in possible. A review of the methods used to investigate the structure and dynamics of solid polymers has been given by Blümich and Spiess.[194] As an example, the pulse sequence for the detection of a $^{1}H-^{13}C$ solid-state heteronuclear shift correlation spectrum is given in Fig. 14. The contour plot of the $^{1}H-^{13}C$ chemical-shift correlation spectrum for the Illinois No. 6 coal is shown in Fig. 15.[193]

REFERENCES

1. D.W. van Krevelen, *Coal*. Elsevier, Amsterdam, 1961.
2. R.A. Meyers (ed.), *Coal Structure*. Academic Press, New York, 1982.
3. H. Pätz, J. Roscher and A. Seifert, *Kohle—ein Kapitel aus dem Tagebuch der Erde*. Teubner, Leipzig, 1986.
4. H.H. Schobert, *J. Chem. Educ.*, 1989, **66**, 242, 290.
5. J. Butler, H. Marsh and F. Goodarzi, *Fuel*, 1988, **67**, 269.
6. G..J.B. Karsten, *Arch. Bergbau*, 1826, **12**, 3.
7. V. Regnault, *Ann. Mines*, 1837, **12**, 161.
8. H.J. Gluskoter, R.R. Ruch, W.G. Miller, R.A. Cahill, G.B. Dreher and J.K. Kuhn, *Circ.-Ill. State Geol. Surv.*, 1977, **499**, 1.
9. *International Classification of Hard Coals by Type*. United Nations, Geneva, 1956.
10. *International System of Classification of Coals (Heat of Combustion* $< 5700 \pm 60$ *kcal/kg, ash free)*. ECE of the United Nations, Geneva, 1958.
11. E. Stach, M.Th. Mackowsky, M. Teichmüller, G.H. Taylor, D. Chandra and R. Teichmüller (eds), *STACH's Textbook of Coal Petrology*. Gebr. Borntraeger Verlag, Berlin, 1975.
12. M. Teichmüller, *Fortschr. Geol. Rheinld. u. Westf.*, 1974, **24**, 65.
13. A. Hollerbach, *Techn. Mitteilungen*, 1982, **75**, 94.
14. E. Künstner, E. Sontag and M. Süss, *Z. angew. Geol. (Berlin)*, 1980, **26**, 298.
15. W. Gothan, K. Pietzsch and W. Petraschek, *Braunkohle*, 1927, **26**, 669.
16. K. Hafner and E. Rammler, *Bergbautechnik*, 1968, **18**, 32.
17. M. Süss, *Z. angew. Geol. Berlin*, 1986, **32**, 29.
18. H. Bode, *Z. Berg-, Hütten- u. Salinenwesen im preuß. Staate*, 1932, **80**, 172.
19. N. Berkowitz, *The Chemistry of Coal*. Elsevier, Amsterdam, 1985.
20. M.J. McIntosh, *Fuel*, 1976, **55**, 59.
21. C. Karr (ed.), *Analytical Methods for Coal and Coal Products*, Vols. I–III. Academic Press, New York, 1978.
22. M.A. Elliot (ed.), *Chemistry of Coal Utilization*, Secondary Supplementary Volume. Wiley, New York, 1981.
23. L. Petrakis and J.P. Fraissard (eds), *Magnetic Resonance—Introduction, Advanced Topics and Applications to Fossil Energy*. Reidel, Dordrecht, 1984.
24. T.G. Fowler and K.D. Bartle, Carbon, 1987, **25**, 709.
25. S. Schlick, M. Narayana and L. Kevan, *Fuel*, 1986, **65**, 873.
26. S. Duber, H.M. Wachowska and A.B. Wieckowski, *Fuel*, 1987, **66**, 1069.

27. S. Duber and A.B. Wieckowski, *Fuel*, 1982, **61**, 433.
28. G. Klepel, D. Landgraf, H. Metz and B. Milsch, *Freiberger Forschungshefte*, 1988, **A781**, 121.
29. P.B. Tooke and A. Grint, *Fuel*, 1983, **62**, 1003.
30. P.R. Solomon and R.M. Carangelo, *Fuel*, 1988, **67**, 949.
31. P.C. Painter, M. Sobkowiak and J. Youtcheff, *Fuel*, 1987, **66**, 973.
32. T. Zerlia, *Fuel*, 1985, **64**, 1310.
33. M. Starsinic, Y. Otake, P.L. Walker, Jr. and P.C. Painter, *Fuel*, 1984, **63**, 1002.
34. O. Ito, H. Seki and M. Iino, *Fuel*, 1988, **67**, 573.
35. S.A. Fysh, D.A.J. Swinkels and P.M. Fredericks, *Appl. Spectrosc.*, 1985, **39**, 356.
36. H. Pfeifer, B. Staudte, W. Meiler and U. Zscherpel, Verfahren zur Bestimmung des absoluten Wassergehaltes in Feststoffen, Patent No. DD 271569.
37. C. Michalk, K. Knese, W. Böhlmann and R. Meusinger, *Erdöl Erdgas, Kohle*, in press.
38. H. Mehner, H. Berndt, D. Radeck and R. Heinrich, *Chem. Technol.*, 1988, **40**, 397.
39. P.A. Montano, *Magn. Res. Rev.*, 1982, **7**, 175.
40. P.S. Cook and J.D. Castrion, *Fuel*, 1987, **66**, 669.
41. A.S. Bommanavar and P.A. Montano, *Fuel*, 1982, **61**, 523.
42. F. Derbyshire, A. Marzec, H.-R. Schulten, M.A. Wilson, A. Davis, P. Tekely, J.-J. Delpuech, A. Jurkiewicz, C.E. Bronnimann, R.A. Wind, G.-E. Maciel, R. Narayan, K. Bartle and C. Snape, *Fuel*, 1989, **68**, 1091.
43. P.H. Given, *Fuel*, 1960, **39**, 147.
44. W.H. Wiser, *Ann. Chem. Soc. Symp. Ser.*, 1978, **71**, 29.
45. J.H. Shinn, *Fuel*, 1984, **63**, 1187.
46. A. Volborth (ed.), *Coal Science and Chemistry*. Elsevier Science Publishers B.V., Amsterdam, 1987.
47. M.E. Bailey, *J. Chem. Educ.*, 1974, **51**, 446.
48. H.H. Oelert and L. Lenart, *Chem. in unserer Zeit*, 1975, **9**, 183.
49. N.D. Rusanova, *Chim. Tverd. Topl.*, 1978, **6**, 3.
50. J.W. Larsen and E.W. Kuemmerle, *Fuel*, 1976, **55**, 162.
51. K.-D. Gundermann, *Kohlenveredelung*, 1986, **102**, 100.
52. H. Hewel-Bundermann and H. Jüntgen, *Kohlenveredelung*, 1988, **104**, 124.
53. S.K. Bhatia, *AIChE J.*, 1987, **33**, 1707.
54. N. Berkowitz, *Adv. Chem. Ser.*, 1988, **217**, 217.
55. M.W. Haenel, G. Collin and M. Zander, *Erdöl, Erdgas, Kohle*, 1989, **105**, 71, 131.
56. D.P. Mahojan, *Powder Technol.*, 1984, **40**, 1.
57. K.-D. Gundermann, K. Hümke, E. Emrich and U. Rollwage, *1987 International Conference on Coal Science* (ed. J.A. Moulijn *et al.*). Elsevier, Amsterdam, 1987.
58. M. Weller and C.A. Wert, *Fuel*, 1984, **63**, 891.
59. C.A. Wert and M. Weller, *J. Appl. Phys.*, 1982, **53**, 6505.
60. K.-H. Rentrop, *Chemische und physikalische Charakterisierung der Kohle*, Freib. Forschungsheft A 668. Dt. Verlag für Grundstoffindustrie, Leipzig, 1982.
61. K.J. Hüttinger and A.W. Michenfelder, *Fuel*, 1987, **66**, 1164.
62. P.H. Given, A. Marzec, W.A. Barton, L.J. Lynch and B.C. Gerstein, *Fuel*, 1986, **65**, 155.
63. E. Rammler and H.-J. v. Alberti, *Technologie und Chemie der Braunkohlenverwertung*, Dt. Verlag f. Grundstoffindustrie, Leipzig, 1962.
64. H. Krug and W. Nauendorf, *Braunkohlenbrikettierung*, Dt. Verlag f. Grundstoffindustrie, Leipzig, 1984.
65. D. Effenberger and K.-E. Militzer, *Energietechnik*, 1988, **38**, 241.
66. J. Keller and A. Brandl, *Erdöl Erdgas, Kohle*, 1989, **105**, 88.
67. D. Merrick and R.M. Davidson, *Erdöl Ergas, Kohle*, 1989, **105**, 67.

68. B.O. Strobel, *Erdöl Erdgas, Kohle*, 1989, **105**, 75.
69. B.O. Strobel, *Erdöl Erdgas, Kohle*, 1988, **104**, 524.
70. H. Teggers, *Braunkohle*, 1987, **39**, 154.
71. M.W. Haenel, G. Collin and M. Zander, *Erdöl Erdgas, Kohle*, 1989, **105**, 71, 131.
72. A.G. Gribat, *Erdöl Erdgas, Kohle*, 1986, **102**, 412.
73. P. Speich, *Energiewirtschaft. Tagesfragen*, 1984, **34**, 1.
74. P. Speich, *Braunkohle*, 1985, **37**, 377.
75. D. Osteroth, *Naturwissenschaften*, 1987, **74**, 257.
76. J. Gibson, *Chem. Br.*, 1980, **16**, 26.
77. M. Janardanarao, *J. Sci. Ind. Res.*, 1984, **43**, 436, 649.
78. S. Nowak, *Chem. Technol.*, 1986, **38**, 47.
79. A.N. Stranges, *Fuel Proc. Technol.*, 1987, **16**, 205.
80. W. Dolkemeyer, U. Lenz and K.-A. Theis, *Erdöl Erdgas, Kohle*, 1989, **105**, 79.
81. H.L. Retcofsky, K.D. Rose and F.P. Miknis, *Symposium on Magnetic Resonance of Heavy Ends*. American Chemical Society, Miami Beach Meeting, 1985.
82. P.C. Newman, L. Pratt and R.E. Richards, *Nature*, 1955, **175**, 645.
83. C.L.M. Bell, R.E. Richards and R.W. Yorke, *Brennst. Chem.*, 1958, **39**, 530.
84. R.A. Friedel, *J. Chem. Phys.*, 1959, **31**, 280.
85. B.C. Gerstein, C. Chow, R.G. Pembleton and R.C. Wilson, *J. Phys. Chem.*, 1977, **81**, 565.
86. B.C. Gerstein and C.R. Dybowski, *Transient Techniques in NMR in Solids*. Academic Press, New York, 1985.
87. H.L. Retcofsky and R.A. Friedel, *Anal. Chem.*, 1971, **43**, 485.
88. D.L. Vander Hart and H.L. Retcofsky, *Fuel*, 1976, **55**, 202.
89. J. Schaefer and E.O. Stejskal, *J. Am. Chem. Soc.*, 1976, **98**, 1031.
90. V.J. Bartuska, G.E. Maciel, J. Schaefer and E.O. Stejskal, *Fuel*, 1977, **56**, 354.
91. R.A. Friedel, *J. Chem. Phys.*, 1959, **31**, 280.
92. J.K. Brown and W.R. Ladner, *Fuel*, 1960, **39**, 87.
93. R.A. Friedel and H.L. Retcofsky, *Chem. Ind.*, 1966, 455.
94. C.E. Snape, D.E. Axelson, R.E. Botto, J.J. Delpuech, P. Tekely, B.C. Gerstein, M. Pruski, G.E. Maciel and M.A. Wilson, *Fuel*, 1989, **68**, 547.
95. D.E. Wemmer, A. Pines and D.D. Whitehurst, *Phil. Trans. R. Soc. London, Ser. A*, 1981, **300**, 15.
96. W.T. Dixon, J. Schaefer, M.D. Sefczik, E.O. Stejskal and R.A. McKay, *J. Magn. Reson.*, 1982, **49**, 341.
97. W.T. Dixon, *J. Chem. Phys.*, 1982, **77**, 1800.
98. M.A. Hemminga, P.A. de Jager, K.P. Datema and J. Breg, *J. Magn. Reson.*, 1982, **50**, 508.
99. M.A. Hemminga and P.A. de Jager, *J. Magn. Reson.*, 1982, **51**, 339.
100. D.P. Raleigh, E.T. Olejniczak, S. Vega and R.G. Griffin, *J. Magn. Reson.*, 1987, **72**, 238.
101. B. Maess, Diploma thesis, Karl-Marx University, Leipzig, 1987.
102. F. Engelke, B. Maess and D. Fenzke, *J. Magn. Reson.*, 1989, **84**, 441.
103. E. Lippmaa, M. Alla and T. Tuherm, in *Magnetic Resonance and Related Phenomena*, Proceedings, XIXth Congress. Ampere, Heidelberg, 1976, p. 113.
104. J. Herzfeld and A.E. Berger, *J. Chem. Phys.*, 1980, **73**, 6021.
105. F. Engelke, A. Germanus, W.-D. Hoffmann, W. Meiler, R. Meusinger, D. Michel, H.-E. Müller and H. Pfeifer, *Proceedings, 2nd Conference on Carbochemistry, Rostock*, 1988, **2**, 337.
106. M. Alla and E. Lippmaa, *Chem. Phys. Lett.*, 1976, **37**, 260.
107. S.J. Opella and M.H. Frey, *J. Am. Chem. Soc.*, 1979, **101**, 5854.
108. I. Kasüschke and R. Gerhards, *Erdöl Kohle-Erdgas-Petrochem. Brennstoff-Chem.*, 1986, **39**, 141.
109. L.B. Alemany, D.M. Grant, T.D. Alger and R.J. Pugmire, *J. Am. Chem. Soc.*, 1983, **105**, 6697.
110. D.P. Murphy, T.J. Cassady and B.C. Gerstein, *Fuel*, 1984, **61**, 1233.

111. D.P. Murphy, B.C. Gerstein, V.L. Weinberg and T.F. Yen, *Anal. Chem.*, 1982, **54**, 522.
112. P. Tekely, D. Nicole, J. Brondeau and J.-J. Delpuech, *J. Phys. Chem.*, 1986, **90**, 5608.
113. P. Tekely, D. Nicole, J.-J. Delpuech, L. Julien and C. Bertho, *Energy Fuels*, 1987, **1**, 121.
114. A. Abragam, *The Principles of Nuclear Magnetism.* Clarendon Press, Oxford, 1961.
115. T. Yokono and Y. Sanada, *Fuel*, 1978, **57**, 334.
116. A. Jurkiewicz, A. Marzec and N. Pislewski, *Fuel*, 1982, **61**, 647.
117. W.A. Barton, L.J. Lynch and D. Webster, *Fuel*, 1984, **63**, 1262.
118. A. Pines, M.G. Gibby and J.S. Waugh, *J. Chem. Phys.*, 1973, **59**, 569.
119. D. Schulze, H. Ernst, D. Fenzke, W. Meiler and H. Pfeifer, *J. Phys. Chem.*, 1990, **94**, 3499.
120. H. Ernst, D. Fenzke and H. Pfeifer, *Ann. Phys. (Leipzig)*, 1981, **38**, 257.
121. H. Pfeifer, W. Meiler and D. Deininger, Nuclear Magnetic Resonance of Organic Compounds Adsorbed in Porous Solids, in *Annual Reports on NMR Spectroscopy*, Vol. 15 (ed. G.A. Webb), p. 15. Academic Press, London, p. 291.
122. A. Grint, S. Mehani, M. Trewhalla and M.J. Crook, *Fuel*, 1985, **64**, 1355.
123. S.R. Moinelo, A. Garcia, J. Bermejo and R. Menndez, *J. Mol. Struct.*, 1986, **143**, 545.
124. D.E. Axelson, *Solid State Nuclear Magnetic Resonance of Fossil Fuels.* Multiscience, Montreal, 1985.
125. R.E. Botto, R. Wilson and R.E. Winans, *Energy Fuels*, 1987, **1**, 173.
126. F.P. Miknis, M. Sullivan, V.J. Bartuska and G.E. Maciel, *Org. Geochem.*. 1981, **3**, 19.
127. R.L. Dudley and C.A. Fyfe, *Fuel*, 1982, **61**, 651.
128. P.D. Murphy. T.J. Cassady and B.C. Gerstein, *Fuel*, 1982, **61**, 1233.
129. M.J. Sullivan and G.E. Maciel, *Anal. Chem.*, 1982, **54**, 1615.
130. P. Ollivier and B.C. Gerstein, *Carbon*, 1984, **22**, 409.
131. D.E. Axelson, *Fuel*, 1987, **66**, 195.
132. E.W. Hagaman, R.R. Chambers and M.C. Woody, *Anal. Chem.*, 1986, **58**, 387.
133. T. Yoshida, Y. Maekawa and T. Fujito, *Anal. Chem.*, 1983, **55**, 388.
134. K.J. Packer, R.K. Harris, A.M. Kenwright and C.E. Snape, *Fuel*, 1983, **62**, 999.
135. R. Wind, M.J. Duezvestijn, C. Van der Lugt, J. Schmidt and H. Vriend, *Fuel*, 1987, **66**, 876.
136. M.E.A. Cudby, *Eur. Spectrosc. News*, 1988, **78**, 18.
137. R. Voelkel, *Angew. Chem., Int. Ed. Engl.*, 1988, **27**, 1468.
138. M.A. Wilson and A.M. Vassallo, *Org. Geochem.*, 1985, **8**, 299.
139. D.C. Van der Hart and A.M. Garroway, *J. Chem. Phys.*, 1979, **71**, 2773.
140. L.B. Alemany, D.M. Grant, T.D. Alger and R.J. Pugmire, *J. Am. Chem. Soc.*, 1983, **105**, 6697.
141. L.B. Alemany, D.M. Grant, R.J. Pugmire and L.M. Stock, *Fuel*, 1984, **63**, 513.
142. M.A. Wilson, A.M. Vassallo and N.J. Russell, *Org. Geochem.*, 1983, **5**, 35.
143. M. Sardashti and G.E. Maciel, *J. Magn. Reson.*, 1987, **72**, 467.
144. E.O. Stejskal, J. Schaefer and J.S. Waugh, *J. Magn. Reson.*, 1977, **28**, 105.
145. N.M. Szeverenyi, A. Bax and G.E. Maciel, *J. Magn. Reson.*, 1985, **61**, 448.
146. R.C. Zeigler, R.A. Wind and G.E. Maciel, *J. Magn. Reson.*, 1988, **79**, 299.
147. W.K. Rhim, D.D. Elleman and R.W. Vaughan, *J. Chem. Phys.*,, 1973, **59**, 3740.
148. P. Mansfield, M.J. Orchard, D.C. Stalker and K.H.B. Richards, *Phys. Rev., Ser. B*, 1973, **7**, 90.
149. D.P. Burum and W.K. Rhim, *J. Chem. Phys.*, 1979, **71**, 944.
150. L.M. Ryan, R.E. Taylor, A.J. Pfaff and B.C. Gerstein, *J. Chem. Phys.*, 1980, **72**, 508.
151. G. Scheler, U. Haubenreisser and H. Rosenberger, *J. Magn. Res.*, 1981, **44**, 134.
152. C.E. Bronniman, B.L. Hawkins, M. Zhang and G.E. Maciel, *Anal. Chem.*, 1988, **60**, 1743.
153. A. Jurkiewicz, C.E. Bronnimann and G.E. Maciel, *Fuel*, 1989, **68**, 872.
154. L. Petrakis and D. Allen, *NMR for Liquid Fossil Fuels.* Elsevier, Amsterdam, 1987.
155. H. Dreeskamp, H. Kluge and I. Koch, *Anwendung neuer Techniken der ^{13}C-NMR-Spektroskopie in der Analytik der für den Bereich der Kohlechemie typischen Stoffe.* DGMK-Bericht 324, Hamburg, 1985.
156. H. Günther, *NMR-Spektroskopie (NMR Spectroscopy).* Georg Thieme, Stuttgart, 1983.

157. C. Dybowski and R.L. Lichter (eds), *NMR Spectroscopy Techniques.* M. Dekker, New York, 1987.
158. C.J. Turner, *Prog. in NMR Spectrosc.*, 1984, **16**, 311.
159. W. McFarlane and D.S. Rycroft, Multiple resonance, in *Annual Reports on NMR Spectroscopy*, vol. 16 (ed. G.A. Webb), p. 293. Academic Press, London, 1985.
160. R. Benn and H. Günther, *Angew. Chem., Int. Ed. Engl.*, 1983, **22**, 350.
161. G.A. Morris, *Magn. Reson. Chem.*, 1986, **24**, 371.
162. R.R. Ernst, G. Bodenhausen and A. Wokaun, *Principles of Nuclear Magnetic Resonance in One and Two Dimensions.* Oxford University Press, Oxford, 1987.
163. L.D. Field and S. Sternkell (eds), *Analytical NMR.* Wiley, Chichester, 1989.
164. J.-J. Delpuech, in *Magnetic Resonance—Introduction, Advanced Topics and Applications to Fossil Energy* (ed. L. Petrakis and J.P. Fraissord), p. 351. Reidel. Dordrecht, 1984.
165. R. Gerhards, in *Magnetic Resonance—Introduction, Advanced Topics and Applications to Fossil Energy* (ed. L. Petrakis and J.P. Fraissard), p. 377. Reidel, Dordrecht, 1984.
166. G.A. Morris and R. Freeman, *J. Am. Chem. Soc.*, 1979, **101**, 760.
167. D.M. Doddrell, D.T. Pegg and M.R. Bendall, *J. Magn. Reson.*, 1982, **48**, 323.
168. D.W. Brown, T.T. Nakashima and D.L. Rabenstein, *J. Magn. Reson.*, 1981, **45**, 302.
169. C. Le Cocq and J.Y. Lallemand, *J. Chem. Soc., Chem. Commun.*, 1981, 150.
170. M.R. Bendall, D.M. Doddrell and D.T. Pegg, *J. Am. Chem. Soc.*, 1981, **103**, 4603.
171. D. Schulze, J. Witt, W. Meiler, R. Meusinger and H. Pfeifer, *Int. Conf. Coal Structure*, Jadwisin, 1989 and MARECO, Reinhardsbrunn, 1989.
172. D. Schulze, J. Witt, W. Meiler, R. Meusinger and H. Pfeifer, *3. Tagung Carbochemie*, Rostock, 1990.
173. J. Witt, in preparation.
174. D. Fenzke, D. Schulze and J. Witt, unpublished.
175. D. Schulze, W. Meiler and H. Pfeifer, in preparation.
176. S.D. Robertson, F. Cuncliffe, C.S. Fowler and I.J. Richter, *Fuel*, 1979, **58**, 770.
177. M. Bouquet, *Fuel*, 1985, **64**, 226.
178. B.C. Gerstein and R.G. Pambleton, *Anal. Chem.*, 1977, **49**, 75.
179. N.G. Cutmore, B.D. Sowerby and L.J. Lynch, *Fuel*, 1986, **65**, 34.
180. A. Jurkiewicz, A. Marzec and N. Pislewski, *Fuel*, 1982, **61**, 647.
181. B. Kamienski, M. Pruski and B.C. Gerstein, *Energy Fuels*, 1987, **1**, 45.
182. R. Graebert and D. Michel, *Fuel*, 1990, **69**, 826.
183. A. Marzec, A. Jurkiewicz and N. Pislewski, *Fuel*, 1983, **62**, 996.
184. A. Jurkiewicz, S. Idziak and N. Pislewski, *Fuel*, 1987, **66**, 1066.
185. R.A. Wind, A. Jurkiewicz and G.E. Maciel, *Fuel*, 1989, **68**, 1189.
186. L.J. Lynch, D.S. Webster and W.A. Barton, *Adv. Magn. Res.*, 1988, **12**, 385.
187. L.J. Lynch and D.S. Webster, *Fuel*, 1979, **58**, 235.
188. D.S. Webster and L.J. Lynch, *Fuel*, 1981, **60**, 549.
189. L.J. Lynch, D.S. Webster, N.A. Bacon and W.A. Barton, in *Magnetic Resonance—Introduction, Advanced Topics and Applications to Fossil Energy* (ed. L. Petrakis and J.P. Fraissard), p. 617. Reidel, Dordrecht, 1984.
190. J. Kärger, H. Pfeifer and W. Heink, *Adv. Magn. Res.*, 1988, **12**, 1.
191. B.C. Gerstein, in *Magnetic Resonance—Introduction, Advanced Topics and Applications to Fossil Energy.* (ed. L. Petrakis and J.P. Fraissard) p. 409. Reidel, Dordrecht, 1984.
192. R. Meusinger, F. Dennhardt, J. Kärger, W. Meiler and H. Pfeifer, *Fuel*, 1990, **69**, 12.
193. K.W. Zilm and G.G. Webb, *Fuel*, 1988, **67**, 707.
194. B. Blümich and H.W. Spiess, *Angew. Chem., Int. Ed. Engl.*, 1988, **27**, 1655.

A continuation of this chapter, with respect to an application report, will be appearing in a future volume of *Annual Reports on NMR Spectroscopy.*

Index

Elements are entered under their abbreviations eg. Co (cobalt), with cross-references where necessary

This Page Intentionally Left Blank